Memoirs of an Effort to Unlock

THE MYSTERY OF SEVERE STORMS

During the 50 Years, 1942-1992

Mt. Fuji photographed by Ted Fujita from JAL 105 at 9:18 a.m. 31 May 1989

Tetsuya Theodore Fujita

Charles E. Merriam
Distinguished Service Professor Emeritus

THE UNIVERSITY OF CHICAGO

The Mystery of Severe Storms

強力な嵐の神秘

Printed in the United States of America

Published by the Wind Research Laboratory
Department of Geophysical Sciences
The University of Chicago

WRL Research Paper Number 239

Library of Congress Catalog Card Number 92-64168

National Technical Information Service (NTIS) PB 92-182021

This book was written in appreciation of the cooperation and support to the author's research during the past 50 years performed both in Japan and in the United States. A very limited number of copies were printed and distributed to the contributors in October 1992. It may be possible for others to obtain copies if available. Please write to:

本書は、日本とアメリカで行った著者の研究に協力および援助された方々に進呈するために出版したもので、非売品です。再版はしませんが、余分があれば、一般の希望者にも配布できますので、ご連絡下さい。

Office of Prof. T. T. Fujita
Department of Geophysical Sciences
The University of Chicago
5734 Ellis Avenue
Chicago, Illinois 60637

F O R E W O R D

This year marks the 50th anniversary of my research on meteorology which I started in 1942 before becoming a faculty of Meiji College of Technology in 1943. Throughout the past one half century, my hobby was to observe, measure and analyze data on damaging winds and their parent clouds, in an attempt to unlock the mystery of small but violent airflows which escape detection by conventional wind-measuring devices. Fortunately, my hobby was identical to my occupation under two single employers, the first in Japan and the second in the United States. Commemorating this Golden Anniversary, I looked back at my research history, uncovering numerous research results which have not been published in color.

The purpose of this book is to summarize my lifetime research with color diagrams and pictures in appreciation of the financial supports provided by the Governments of Japan and the United States and the moral support of individual scientists in both countries. I recall that I was able to walk on a series of stepping stones marked "good luck" ever since I was fished out of postwar Japan to the University of Chicago by Professor Horace R. Byers, my fatherly mentor professor.

Although I regret that I had no chance to orbit around the earth in a manned spacecraft, I was fortunate to have flown repeatedly over and around thunderstorm tops by high-altitude research Lear Jet. I was thrilled by a supersonic flight across the Atlantic in the cockpit of Air France Concorde. At low latitude, on the other hand, I flew in Cessna over 40,000 km above the swaths of tornadoes in search of the damage caused by unidentified winds. The starburst patterns of uprooted trees found in forests led me to hypothesize the downburst/microburst winds which initiated a controversy lasting from the late 1970s to the 1980s. By classifying numerous damage photographs taken from low-flying aircraft, the Fujita Tornado Scale (F scale) was devised in 1971. It is a six-point intensity scale pegged to the windspeed.

I wish to express my sincere appreciation to Meiji College of Technology and its successor, the Kyushu Institute of Technology, for educating me in my student and junior faculty years in Japan and to the Department of Geophysical Sciences of the University of Chicago for stimulating and assisting my research activities under generous supports of various government agencies. Upon reaching the mandatory retirement age of 70, the transition from the pre-retirement to the post-retirement research was so smooth that I did not even realize it. Thanks to the University Administration and to Frank Richter, the Department Chairman for permitting me to continue uninterrupted research during my emeritus years.

October 1992

Tetsuya Theodore Fujita

Professor Emeritus
The University of Chicago

序　　文

北九州市小倉に生れ、南にそびえる貫山のかなたに青い鳥を求めて山歩きをしている時、美しい鍾乳洞を発見したのが昭和１４年。その後、サイエンスに興味を持って、明治専門学校に入学。機械工学を専攻したが、地質学の教授に師事して地形図と投影画法を学んだ。その後、衝撃の力と題する卒論でオシログラフや高速写真機を使いながら、物理学教室の助手となり、昭和１８年の９月に卒業。ひきつづき母校の物理学教室に残って、助教授になった。

終戦後間もなく、長崎と広島の原爆被害の現地調査をした際、爆風による被害が、爆心からスターバースト状に拡がっていたのが印象的であった。渡米後、昭和４９年に起った、史上最悪のたつまきの爪跡をセスナ機で調査中に見たのが、それもスターバースト状に吹き倒された森の大木で、それは長崎で知った爆風被害の縮図のようで、強力な下降気流が地面に激突して起る新型の強風によるものと推定した。その概念を、ニューヨーク空港での墜落事故の原因に適用して、その風をダウンバースト、小型で強い風をマイクロバーストと命名し、航空気象界に賛否の論争を引きおこした。その後、マイクロバーストによる航空事故が次々に発生したため、航空局がマイクロバーストの早期探知に尽力したので、事故は激減し、マイクロバーストの重要性が世界的に認められる様になった。

一方、世界中のたつまきの７５パーセントが発生するアメリカに、その強さを表わすスケールが無い事に気付き、風速を基準にした、たつまきの藤田スケールを昭和４６年に試作し、さらに多数の航空写真を低空から撮ってスケールを改良した。今ではアメリカで発生するすべてのたつまきの強さが藤田スケールで表わされている。

昭和１８年に明治専門学校の助教授になってから今年は５０年目に当り、その間、私の趣味は一貫して嵐の観測と研究であり、それが又私の職業でもあった。言い換えれば、私は強風を伴う嵐と結婚してきた様なもので、嵐の神秘を空と宇宙から観測して楽しみ、又嵐の爪跡をさがし求めて全米を、時には日本をもかけめぐった。今年はその金婚式を記念して、この回顧録をまとめ、金表紙の本とし、私の研究に協力して下さった方々に贈る事にした。又、長年月にわたって、私の研究の為に多額の研究費を支出し、最新の観測装置を提供して下さった日本政府とアメリカ政府に謝意を表したいと思う。

平成４年１０月

シカゴ大学名誉教授

藤　田　哲　也

Table of Contents　　目　次

The most important letter I received in my life

THE UNIVERSITY OF CHICAGO
CHICAGO 37 · ILLINOIS
DEPARTMENT OF METEOROLOGY

January 30, 1951

Dr. Tetsuya Fujita
Kyushu Institute of Technology
Tobata City, Japan

Dear Dr. Fujita:

I have looked over your paper "Micro-analytical Study of Thunder-Nose," and note that in view of the fact that you were not familiar with the work of the U. S. Thunderstorm Project on this subject your conclusions are highly valuable and really represent an independent discovery of some of the factors derived from our work. In particular you deserve credit for noting the importance of the thunderstorm downdraft and outflowing cold air.

Under separate cover I am sending you a copy of the book "The Thunderstorm" which is the principal report of the Thunderstorm Project carried out under my direction. I wish particularly that you would take note of the information about entrainment of air in the updraft. This concept has had a profound effect in modifying all our thinking about the thermodynamics of the thunderstorm and must be incorporated in considerations of all forms of convective clouds. Perhaps you should also refer to the original articles on this subject by Stommel and Austin in the Journal of Meteorology. The references to these articles are given in the thunderstorm report.

Dr. Nagata, the director of the Geophysical Institute of Tokyo University was our guest in Chicago two weeks ago. I told him about your work and we had some discussion about the possibility of making use of the U.S. Air Force radar photographs in studies such as yours. It would not be necessary for the Japanese to go near the radar equipment if they could only get sequences of photographs of the radarscopes during thunderstorm or squall line occurrences. I will be in Washington next week and plan to discuss this matter with the Commanding General of the Air Weather Service.

Sincerely yours,

Horace R. Byers, Chairman
Department of Meteorology

HRB:EP

Chapter One

Dawn of Mesometeorology

1.1 Early Mesoanalysis Performed in Japan

Because Japan was isolated during the Second World War, I was not able to identify the scale applicable to the fine structure of squall line, thunder nose, etc., which have not been analyzed in Japan. Without proper references available to me in 1947-50, I simply identified the small-scale analysis as "microanalytical study."

On the other side of the Pacific Ocean, weather radars began depicting precipitation cells, emphasizing the scale of radar echoes and their environment. In 1951, the late Dr. Ligda of Texas A & M recognized a scale too large to be observed from a single station, yet too small to appear on a synoptic chart. He designated the phenomena of this size as "mesometeorological."

After coming to the University of Chicago as a visiting research associate (1953-55), I worked with Dr. Morris Tepper of the U.S. Weather Bureau located at 24th and M Streets NW, in Washington, D.C. After frequent visits to his Severe Storms Unit, we finalized the "mesoanalysis" technique which I had started in 1947 in Japan under the name of "microanalysis." As our mesoanlysis began revealing previously unknown weather systems, such as mesohighs and mesocyclones, the new field of mesometeorology was born inside the red brick building at 24th and M.

Time-Space Conversion

Late in the afternoon of 17 July 1948, while I was sitting in the living room of my birthplace, I heard a distant thunder which warned me of an approaching thunderstorm. Grabbing a pencil and paper, I rushed to the rooftop where I began recording the direction of cloud-to-ground lightning and the time between the flash and subsequent thunder. During the 1 hr 30 min observation period, the storm moved from left to right without approaching my house.

The location of the 33 lightning flashes plotted on a local map of Kitakyushu (Fig. 1.1-1) showed that the storm moved from the other side of Sarakura mountain toward the sea in a northeasterly direction. An x-t diagram was produced by selecting the vector x in the direction of the minimum scatter of the lightning locations on the diagram.

After determining the motion vector, a method of time-scale conversion was developed in an attempt to separate the lightnings into three groups identified by A, B, and C. It is likely that the individual group denotes the size and position of thunderstorm cores.

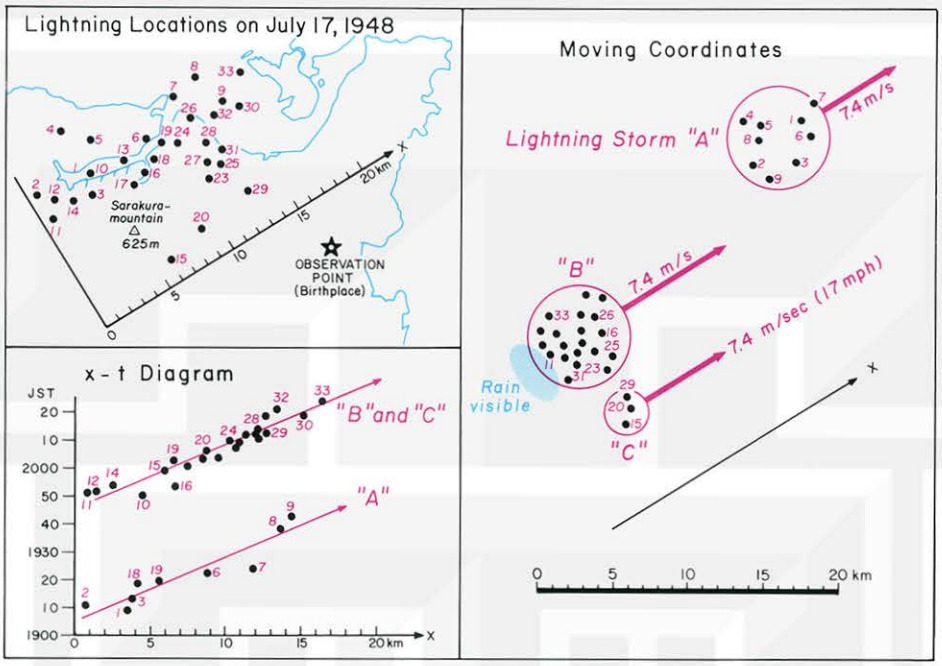

Fig. 1.1-1 Three areas of lightning flashes observed on 17 July 1948 from the roof of my birthplace house. A method of time-space conversion was used. From Fig. 21 by Fujita (1951a).

The Seburiyama Thunderstorm

This thunderstorm of 24 August 1947 was observed at the Seburiyama mountaintop station. The station was a frame structure equipped with gust recorder, microbarograph, hygrothermograph, etc. Due to lightning hazards, the entire observation was made inside the station.

In order to perform the post-storm analysis, I collected the weather reports and recorded traces from 30 stations in western Japan which were used to produce microscale maps of the pressure field associated with the thunder nose.

Hourly microanalysis charts between 1000 and 1800 local time (Refer to Fig. 1.1-2) reveal that the parent system of the thunder nose was a small (mesoscale) thunderstorm high which moved across the northern tip of the island of Kyushu (For 10-min interval charts, refer to Fig. 6.2-24). There were a number of similar small highs over the island, indicating that such miniature highs should be rather common phenomena.

Although no references were found in Japan at that time, I thought that a significant divergence of horizontal winds must be induced by such a thunderstorm high. Based on the expected divergence and nonhydrostatic pressure inside the thunder nose, a model of a thunderstorm with a downward current inside was produced (Refer to Section 6.2). When I sent a copy of the paper describing the thunderstorm model to Professor Byers of the University of Chicago, he appreciated the model. I did not realize the fact that he had operated the Thunderstorm Project, discovering the downdraft.

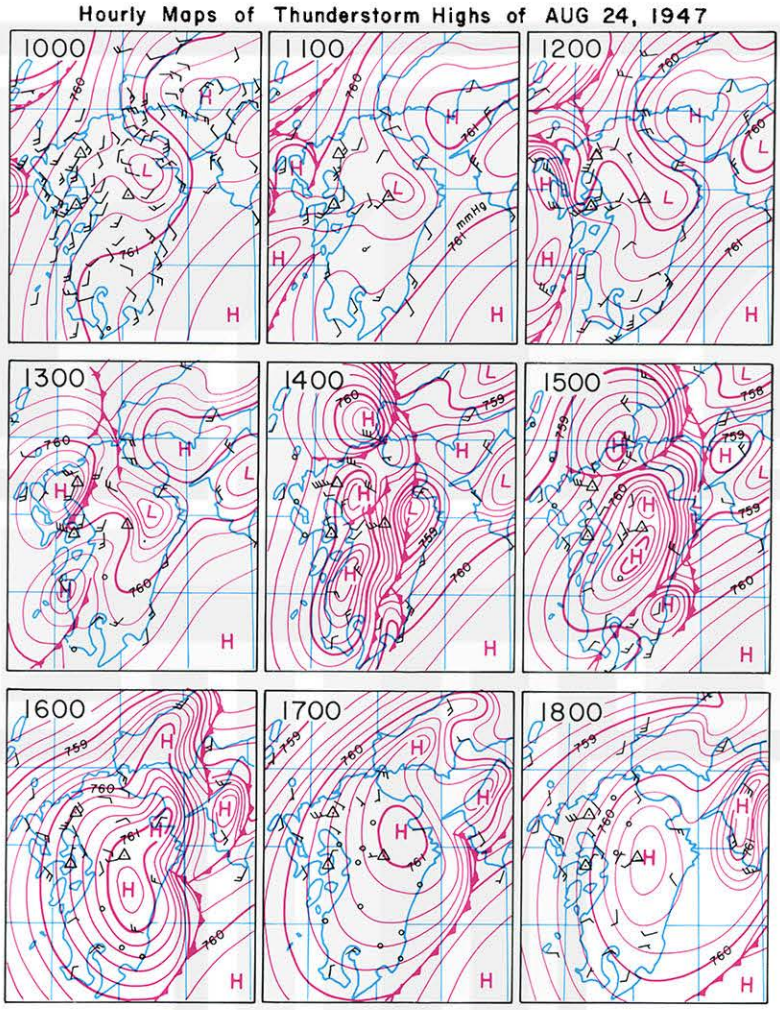

Fig. 1.1-2 Hourly maps of the thunderstorm highs of 24 August 1947. Recorded traces from 30 stations were used for the time-space conversion. From Fig. 11 by Fujita (1951a).

Solar Eclipse Mesonet

An 88% solar eclipse was predicted to occur at Kitakyushu on 9 May 1948. In order to determine the effect of the reduced solar radiation upon surface wind and temperature, I designed and operated a solar eclipse network (Mesonet) in cooperation with Kokura High School I graduated from in 1939.

98 volunteers, consisting of my students, friends, and relatives manned the 46 stations shown in Fig. 1.1-3. These stations were distributed inside a 600^2 km area. Because no private cars were available at that time, we had to use public transportation, leaving home before sunrise. I stayed at the top of the 625-m (2,050') Sarakurayama mountain overlooking the network.

Although it was a rather primitive network, observed winds depicted an outflow of the shallow cold air induced by the solar eclipse. A case study of the data is presented in Section 6.2.

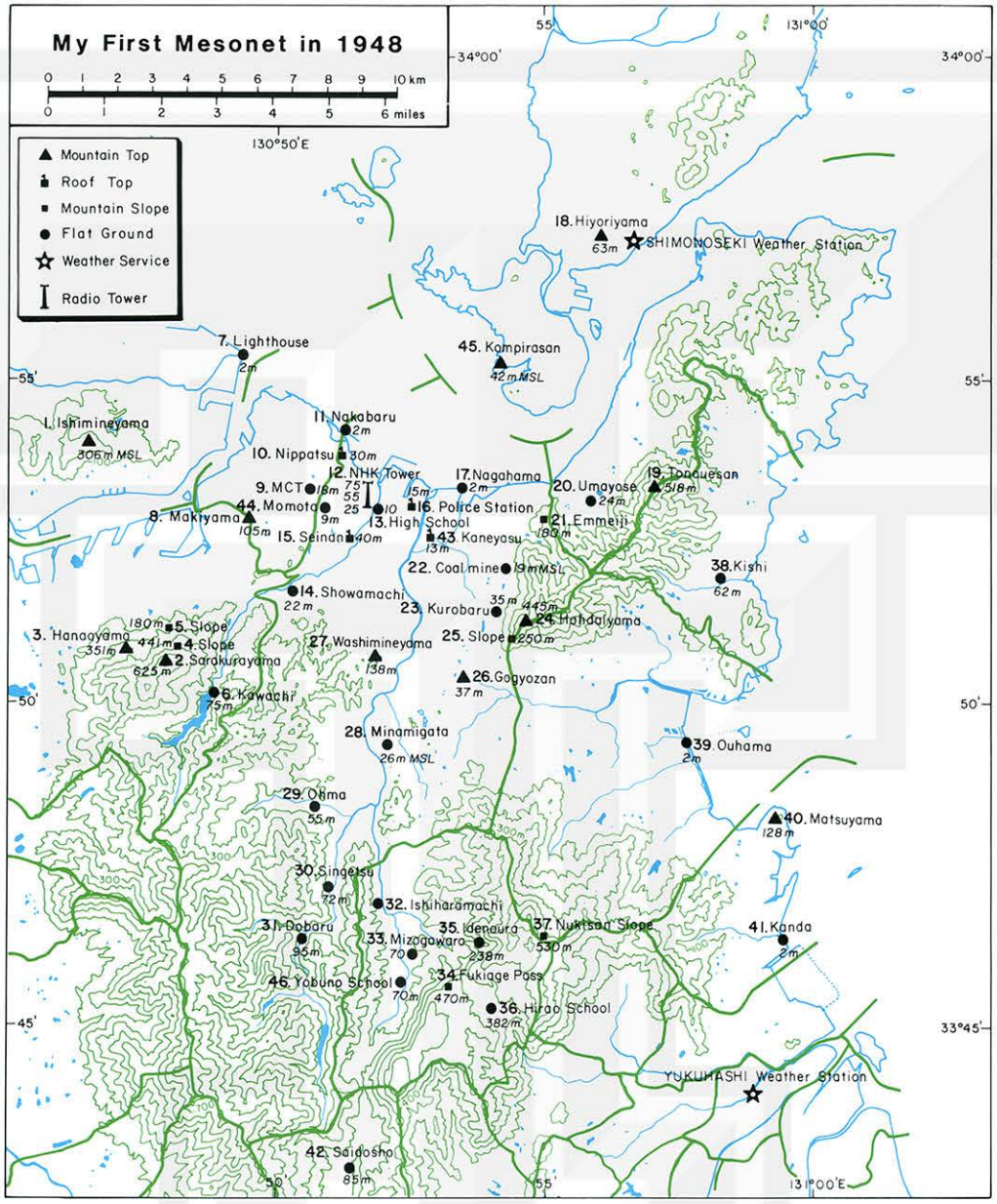

Fig. 1.1-3 The Solar Eclipse Mesonet of 9 May 1948 consisting of 46 surface stations operated by 98 volunteers. Stations were placed at various heights ranging between near sea-level and 625-m mountaintop. One of the NHK radio towers was used to measure wind and temperature at 1 m, 30 m, and 50 m levels.

Microanalysis of Cold Front

On 26 September 1948 an intense cold front characterized by a significant pressure rise swept across northern Kyushu. Operational synoptic maps, however, showed little evidence of the tight pressure gradient at the front. In an attempt to analyze the microstructure of both wind and pressure fields, recorded traces of pressure, temperature, rainfall, and wind were collected from all available weather stations. These records were reduced into time

sections with time increasing from right to left which is the direction opposite from the traveling motion of the frontal system (See examples in Figs. 1.1-4 through 7).

Under the assumption that the pressure field translates on Lagrangian coordinates moving with the front, the time section converted into space section was placed at each station in Fig. 1.1-8. It should be noted that the isobars on a microanalysis map must satisfy not only the pressure value measured at the station but also its spatial variation obtained by the time-space conversion.

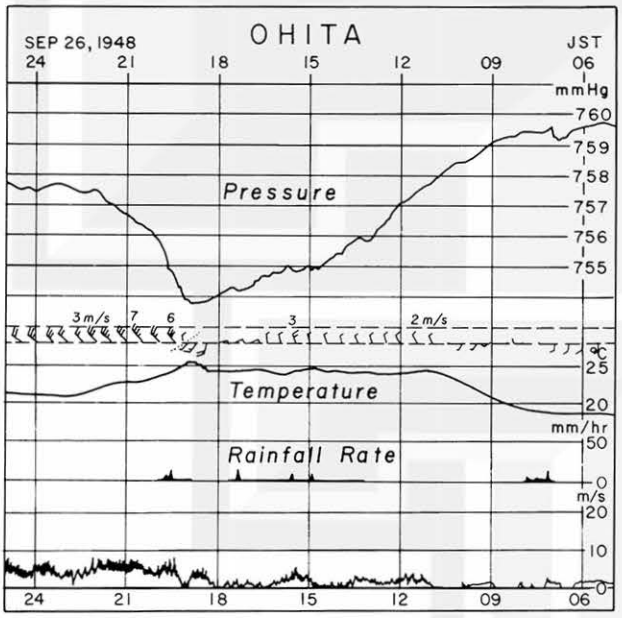

Fig. 1.1-4 Traces from Ohita, Kyushu.

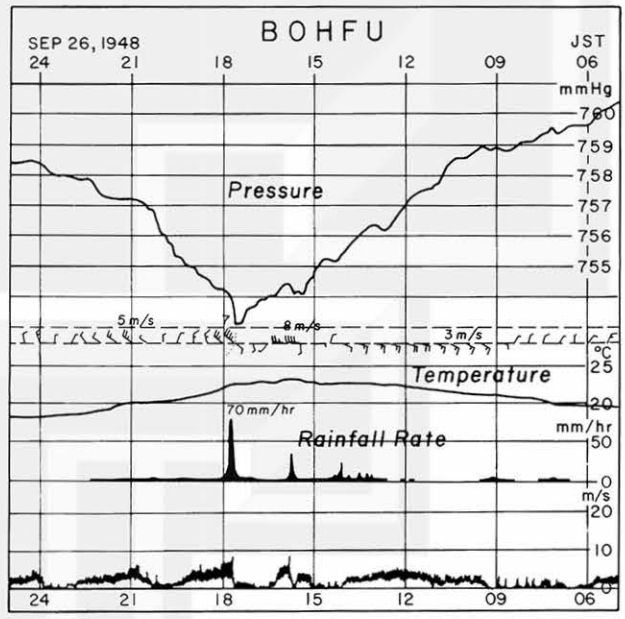

Fig. 1.1-6 Traces from Bohfu, Honshu.

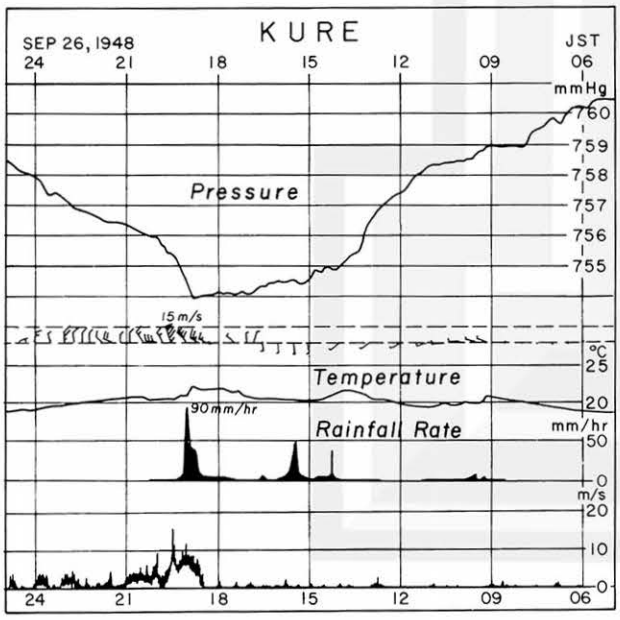

Fig. 1.1-5 Traces from Kure, Honshu.

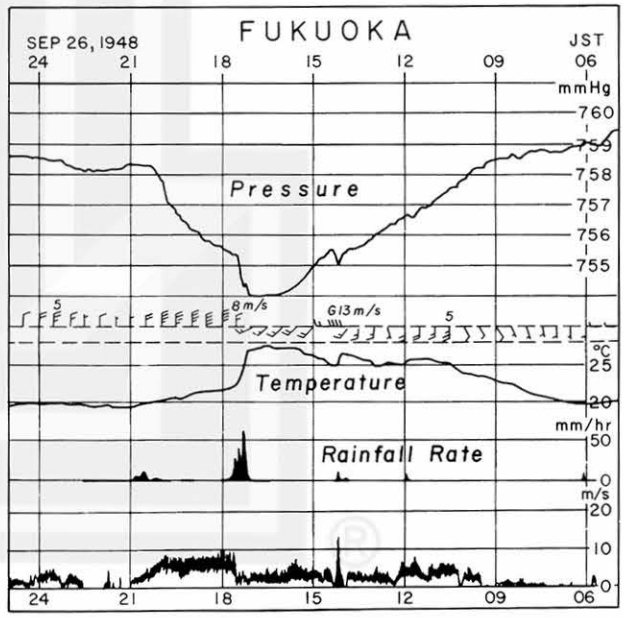

Fig. 1.1-7 Traces from Fukuoka, Kyushu.

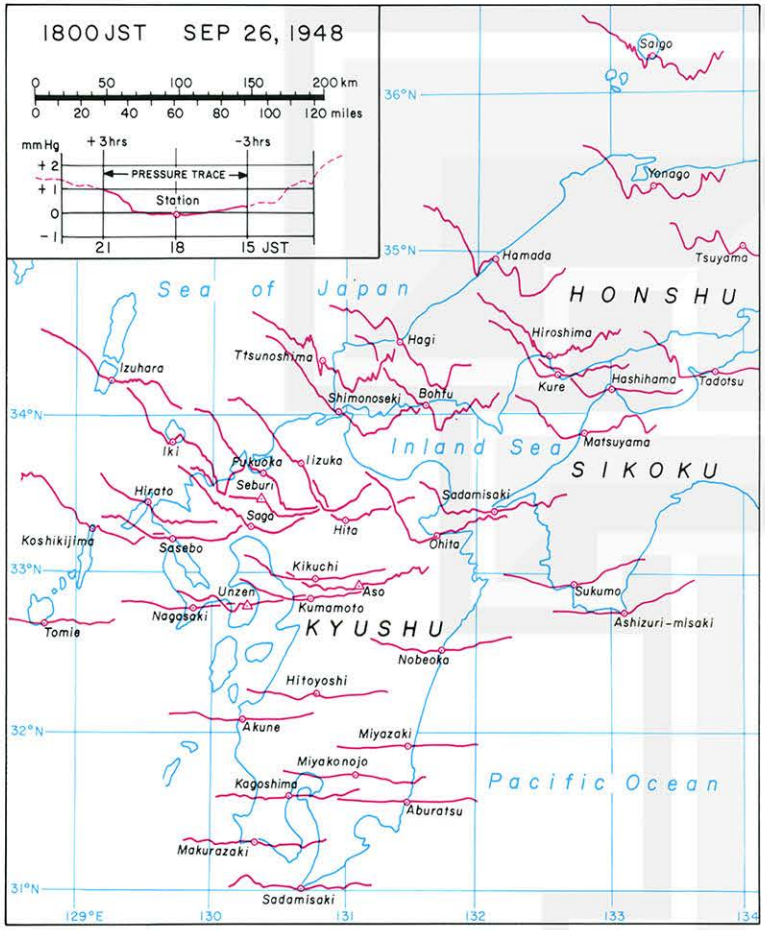

Fig. 1.1-8 Space sections of the barograph from 42 stations in western Japan on 26 September 1948.

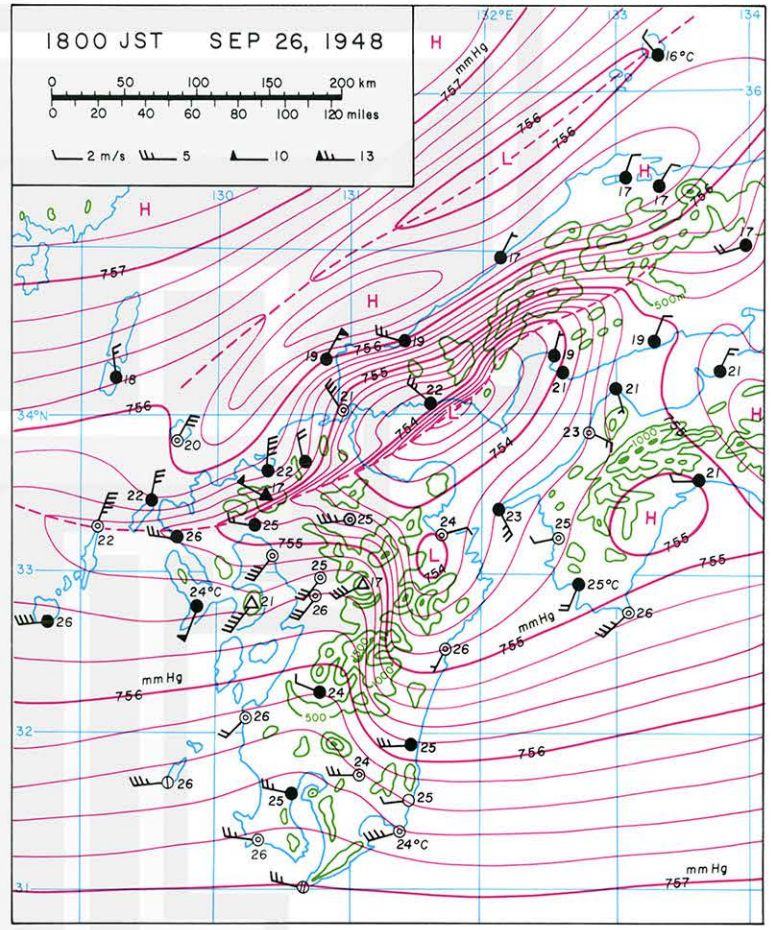

Fig. 1.1-9 My early mesoanalysis of the squall line of 26 September 1948.

Figure 1.1-9 shows the microscale map at 1800 JST analyzed with 0.2 mm Hg contours. The main features of the cold front are the tight pressure gradient and near 90° crossing angle of the winds on the cold-air side of the advancing cold front. The geostrophic windspeed at the steepest pressure gradient is in excess of 120 m/s. Both wind direction and speed at the front indicate that winds are far from geostrophic and advective in nature.

1.2 Joint Research with U.S. Weather Bureau

While at the University of Chicago (1953-55) as a visiting research associate, I worked with Dr. Morris Tepper of the U.S. Weather Bureau at Washington, D.C. At that time, he was collecting barograph traces from the Pressure-Jump Network placed in the west-central Midwest. The preliminary objective of the network was to pursue the proposed mechanism of tornado formation at the intersection of two pressure-jump lines.

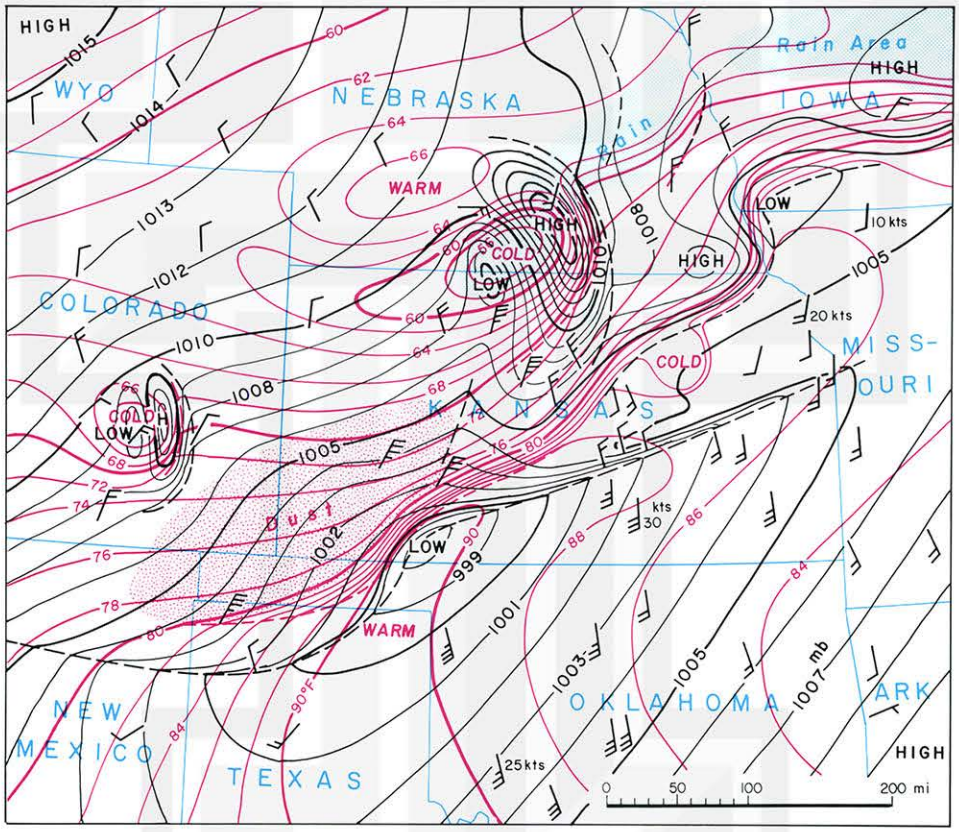

Fig. 1.2-1 Mesoanalysis of a squall line over the Midwest at 0200 CST 25 June 1953. This map reveals that a pressure-jump line does not always coincide with a line of temperature drop. Fujita et al (1956).

Microanalysis to Mesoanalysis

During my frequent visits to his Severe Storms Research Unit, we decided to identify our subsynoptic analysis as "MESOANALYSIS." This term is more suitable than microanalysis in view of a possible confusion with microclimate and micrometeorology.

Our landmark paper, "Mesoanalysis" coauthored by Fujita, Newstein, and Tepper (1956) was published in color as Weather Bureau Research Paper 39. Shown in Fig.

1.2-1 is a simplified version of the hourly maps from the paper. The map reveals a number of mesoscale systems, such as a pressure-jump line, thunderstorm highs (mesohighs), temperature and pressure fronts, which are smoothed out in most operational synoptic analysis.

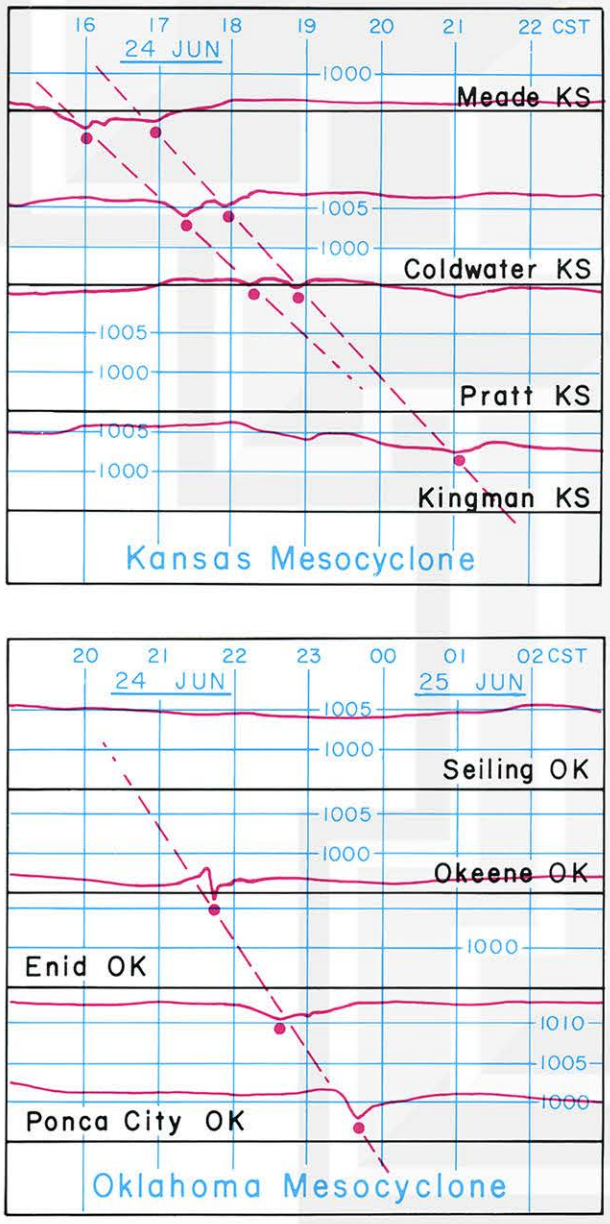

Fig. 1.2-2 Two x-t diagrams showing the movement of the Kansas and Oklahoma mesocyclones of 24 June 1953. From Fujita et al (1956).

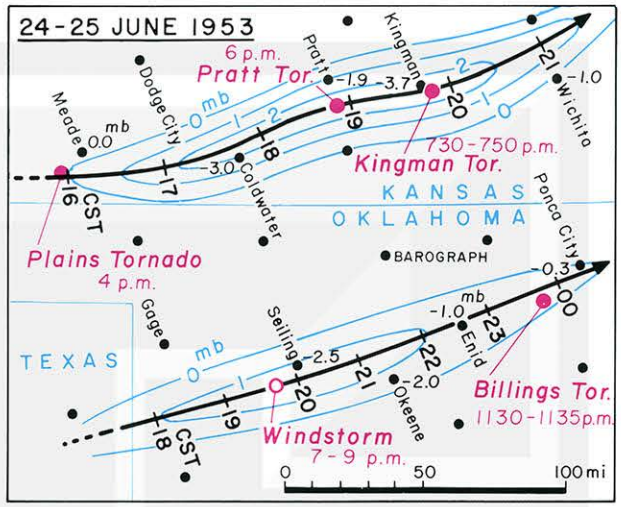

Fig. 1.2-3 Pressure drops caused by two mesocyclones in Fig. 1.2-2.

Mesocyclone Identified

Based on the time-space continuity of barograph traces from the Pressure-Jump Network, we also analyzed a number of miniature cyclones similar to those termed "tornado cyclone" by Brooks in 1949. Some cyclones induced tornado(es) while others did not. Because these cyclones may or may not spawn tornado, we call the cyclone "MESOCYCLONE," which is the genetic term of the intense mesoscale low-pressure system.

Figure 1.2-2 presents barograph traces affected by two mesocyclones of 24 June 1953, the one in southern Kansas and the other in northern Oklahoma. The maximum pressure drop (pressure deficit) by these mesocyclones was -3.7 mb at Kingman (See Fig. 1.2-3). Tornadoes were reported from near Meade, Pratt, and Kingman located along the path of the Kansas mesocyclone. On the other side of the state line, the Oklahoma mesocyclone spawned one tornado and a windstorm on its path.

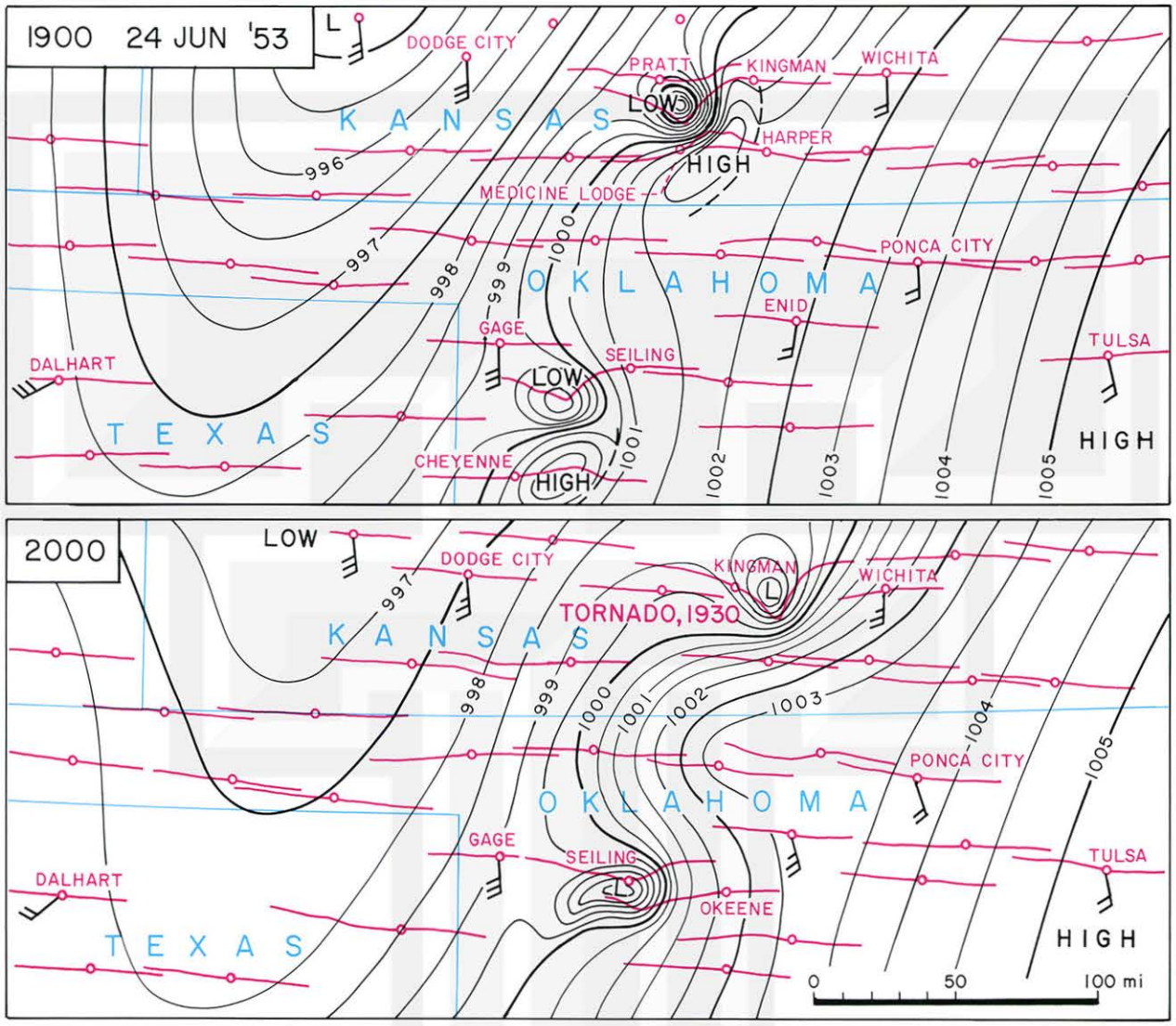

Fig. 1.2-4 Mesosynoptic surface maps of two mesocyclones in Fig. 1.2-3 at 1900 and 2000 CST 24 June 1953. The Kansan mesocyclone induced three tornadoes; the Plains tornado at 1600 CST, the Pratt tornado at 1900 CST, and the Kingman tornado at 1930-1950 CST. The Oklahoma mesocyclone induced a windstorm at Seiling and tornadoes at Billings at 2330-2335 CST. This analysis suggested strongly that mesocyclones are potential inducers of tornadoes. After Fujita et al (1956).

Hourly mesoanalysis maps of these mesocyclones at 1900 and 2000 CST revealed their horizontal extent of 30 to 40 miles accompanied by the tight core circulations (Refer to Fig. 1.2-4). It is also seen that each mesocyclone at 1900 CST was associated with a small thunderstorm high, suggesting that the mesocyclone was located on the northwest side of a large thunderstorm. Our cooperative mesoanalysis of pressure-jump lines resulted in a conclusion that the mesocyclone is an important inducer of tornadoes.

Mesohigh Defined

The term "mesohigh" introduced by Fujita, Newstein, and Tepper (1956) denotes the mesoscale high pressure system which had been regarded as the "noise" in synoptic maps. A mesohigh beneath a thunderstorm is a localized high pressure generated by a dome of cold air and by the dynamic pressure of a downdraft descending to the ground.

A large mesohigh accompanied by a group or a line of thunderstorms is a conglomerate of the cold domes induced by individual thunderstorms.

The excess pressure of a mesohigh superimposed upon undisturbed pressure field can be obtained by subtracting the undisturbed pressure graphically (See Fig. 1.2-5). Gradient of excess pressure is very large along the advancing edge, called pressure-surge line or pressure-jump line. When excess pressure is larger than 5 mb, the leading edge of a mesohigh appears like an active cold front. Some analysts connect the synoptic front with the leading edge of a mesohigh front, thus creating a bulge of a cold front.

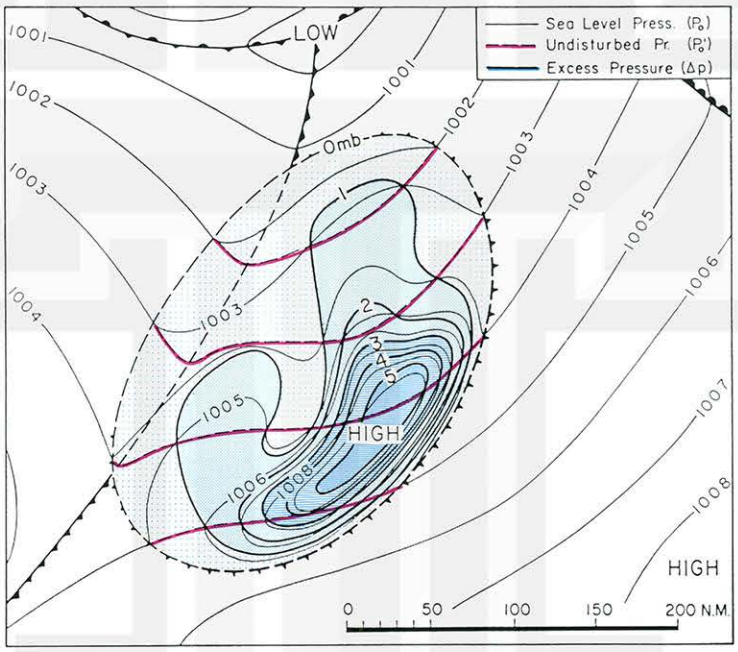

Fig. 1.2-5 Separation of the excess pressure of a squall-line mesosystem of 4 June 1953 over the Midwest. From Fujita (1959b).

Without foreseeing the need for the research on mesoscale meteorology in the United States in the 1960s and beyond, I started a pilot analysis of microscale disturbances in Japan in 1947.

Thanks are due to Professor Horace R. Byers for fishing me out of postwar Japan to apply the microanalysis technique for better understanding of Midwestern squall lines and thunderstorms. Thanks are also due to Dr. Morris Tepper of the U.S. Weather Bureau for conducting our joint research in the 1950s, which resulted in the identification of MESOMETEOROLOGY by creating the following terms; "mesohigh," "mesolow," "mesocyclone," "wake depression," and "mesosystem."

Chapter Two

Tornadoes

In my childhood days in Japan, we were told that four fearful things are, in the order of fear, Zishin, Kaminari, Kaji, Oyaji (Earthquake, Lightning, Fire, and Father), because Japan is the land of earthquakes which occur without warning. An equivalent fear in the Midwest could be Tornado, Lightning, Fire, and Crime except for those who sit on the New Madrid Fault.

After coming to the United States, I was fascinated by the power and the behavior of the tornado. The Gross National Product (GNP) of U.S. tornadoes in recent years is 750 per year, while the estimated Gross International Product (GIP) of global tornadoes is 1,000 per year. In other words, 75% of the tornadoes on the planet earth have been produced in the United States. Furthermore, U.S. produces over 90% of the violent (F4 and F5) tornadoes in the world.

2.1 Long Term Variation of U.S. Tornadoes True or False ?

United States Prorated by Tornado Deaths (1916 - 1989)

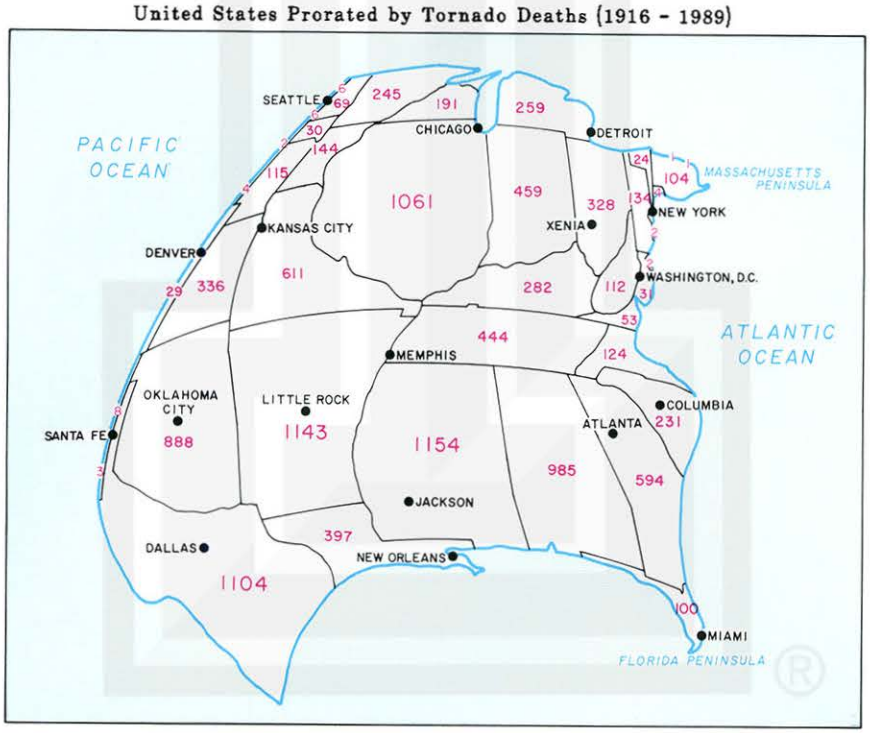

Fig. 2.1-1 A distorted shape of the United States obtained by prorating the area of each state in proportion to the number of tornado deaths.

During the 75 years since 1916, 11,944 persons were killed by U.S. tornadoes. Due to the tornado activities centered in the Midwest, the shape of the United States is severely distorted (Fig. 2.1-1) if the area of each state was prorated by tornado deaths. Because of the rare occurrence of killer tornadoes to the west of the Rockies, both Denver, Colorado and Santa Fe, New Mexico are seen on the west coast.

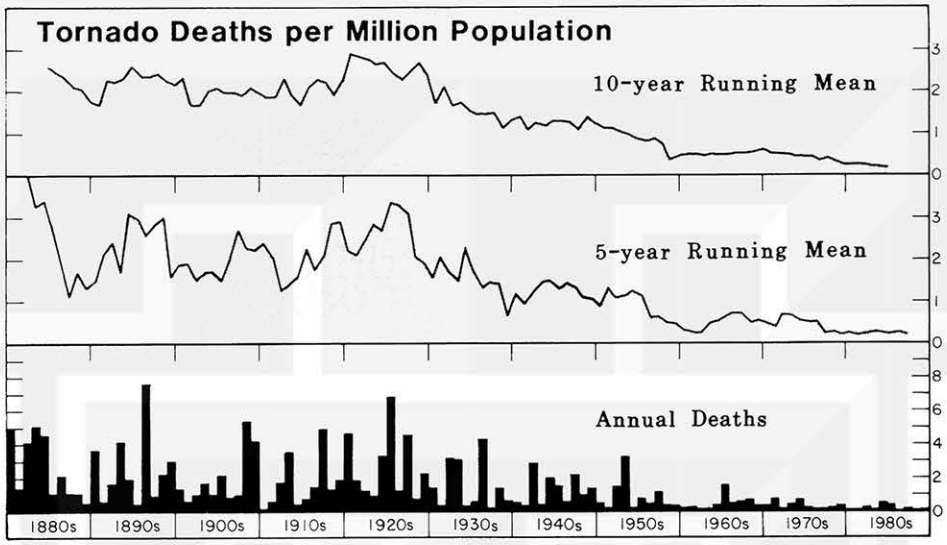

Fig. 2.1-2 Annual tornado deaths per million population of the United States. Deaths in early years (1890-1915) were supplied by Mr. Tom Grazulis, a dedicated tornado researcher and producer of a 16-mm movie "The Tornado: Approaching the Unapproachable."

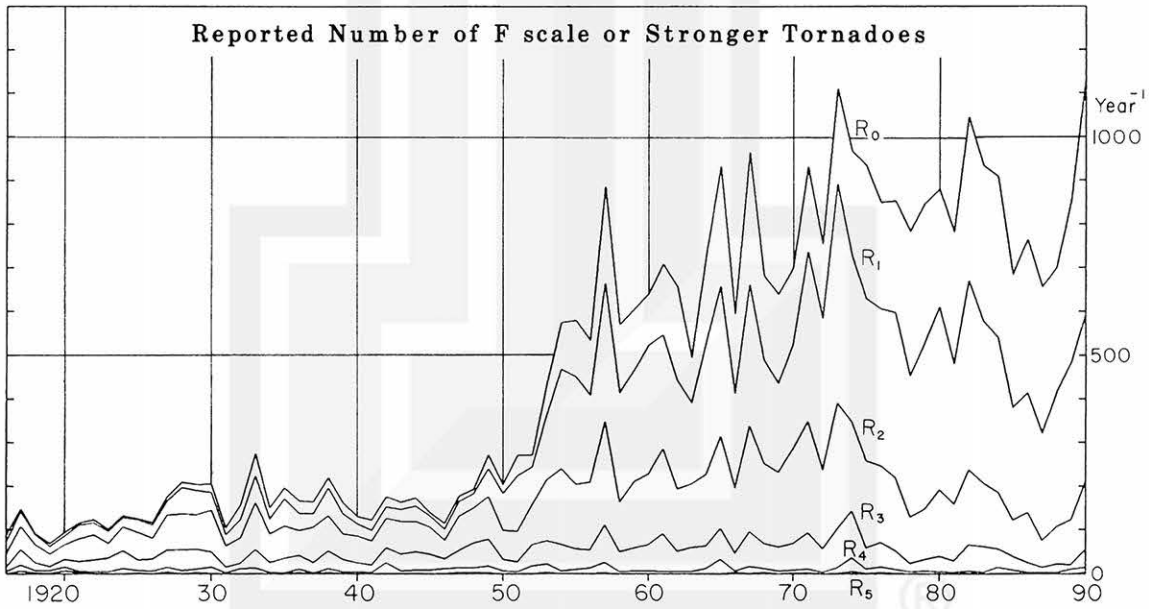

Fig. 2.1-3 Number of tornadoes confirmed and reported in the United States between 1916 and 1990. This chart was produced by counting tornado occurrences by cumulative F scales (Table 2.1-1). The top line denotes the number of F0 or stronger tornadoes, and the bottom line, F5 tornadoes only.

The long-term tornado deaths per million population decreased during the past 110 years. The trend of decrease, however, can be divided into four periods, dark period (1880-1919), learning period (1920-1952), awareness period (1953-1974), and effective warning period (1975-present). It is unlikely that the general public in the dark period knew the tornado hazards. After the Super-outbreak tornadoes of 3-4 April 1974, people in tornado areas began paying serious attention to tornado watches and warnings, thus bringing tornado deaths down significantly (Fig. 2.1-2).

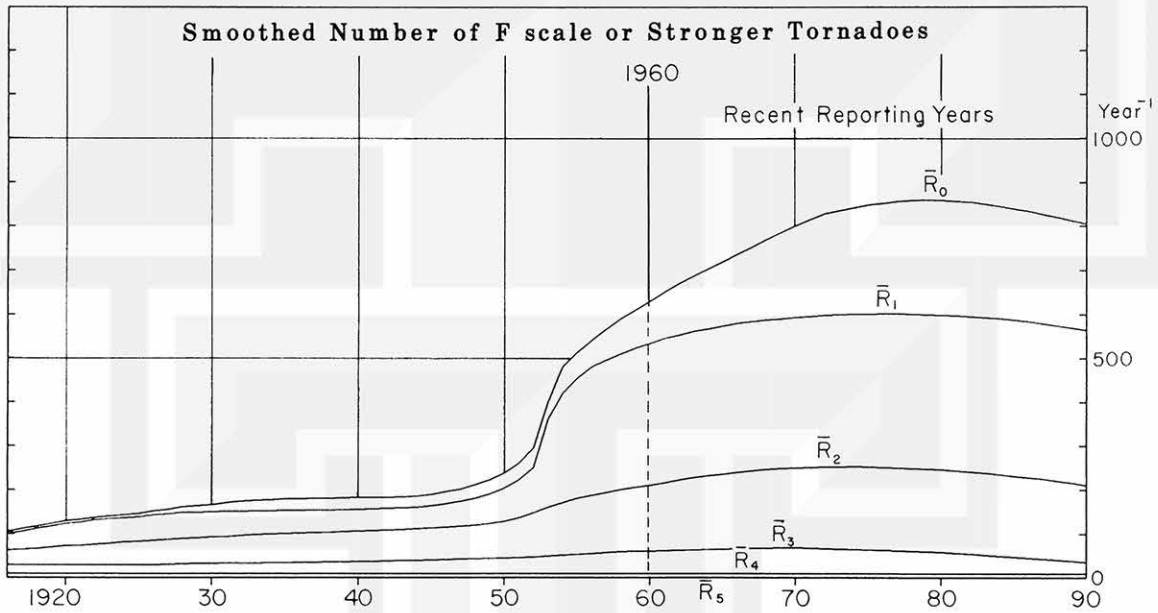

Fig. 2.1-4 Smoothed curves of the cumulative number of tornadoes in Fig. 2.1-3. As in the previous figure, the top curve denotes the smoothed number of F0 or stronger tornadoes. Other curves show the number of F1 or stronger, F2 or stronger, etc.

The number of U.S. tornadoes began increasing rapidly in the 1950s (Fig. 2.1-3). However, most increases were attributed to the detection efficiency of F2 or weaker tornadoes. In an attempt to visualize the overall trend of the increase, numbers of annual tornadoes in Fig. 2.1-3 were smoothed into five curves of cumulative tornadoes, F0-F5, F1-F5, ... , and F5 (Fig. 2.1-4).

In determining the distribution of U.S. tornadoes during the 1916-1989 period and their breakdown into the seven decades, 1920s, 30s, 40s, ... , and 80s, eight path maps were generated by computer in two colors, F0-F2 in blue and F3-F5 in red (Fig. 2.1-5). These maps show clearly that the number of blue-colored tornadoes were insignificant until the 1940s. After the 1950s, the number increased rapidly, overshadowing F3-F5 tornadoes printed in red.

The foregoing evidence shows that the number of tornadoes must be normalized to the most reasonable number determined by the best guess. Without knowing the theoretical means of computing the best-guess number applicable to the 74-year period, it was assumed that the number averaged over the recent 30 reporting years is the best-guess number. These numbers were computed as functions of the cumulative F scales, F0-F5, F1-F5, F2-F5, etc., and tabulated in Table 2.1-1.

The normalization was done by computing the quotient, the smoothed numbers (Fig. 2.1-4) divided by the best-guess numbers

Tornadoes in 1916-1989 (74yrs)

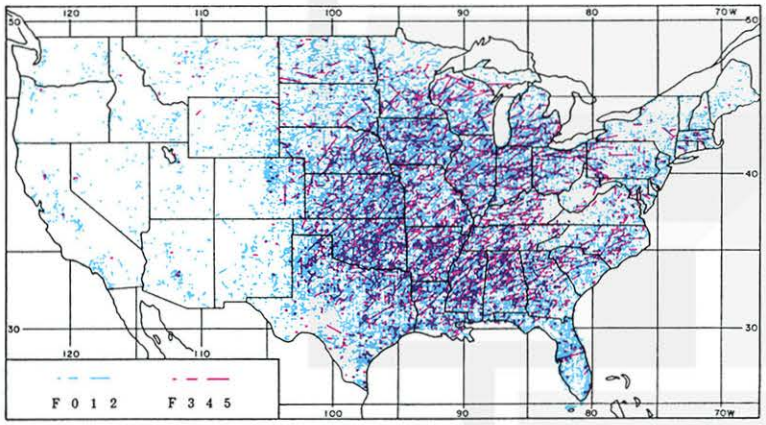

Fig. 2.1-5a Computer-plotted paths of all U.S. tornadoes during the 74-year period, 1916-1989. Paths of F0, F1, and F2 tornadoes are shown in blue while those of F3, F4, and F5, in red.

Tornadoes in 1920-1929 (10yrs)

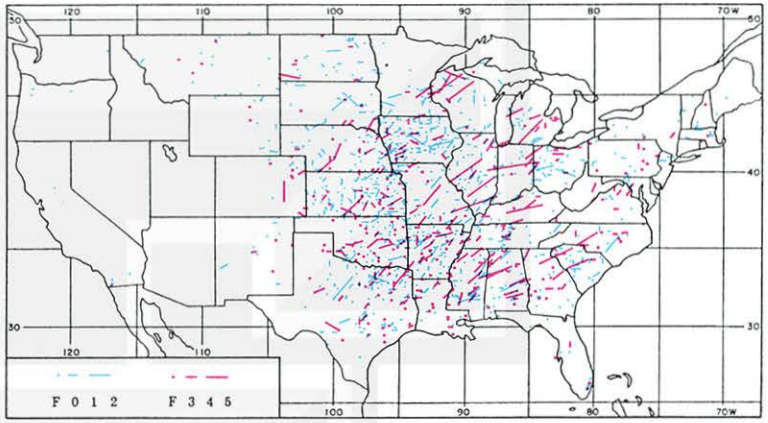

Fig. 2.1-5b Paths of tornadoes in the 1920s. The most significant tornado in this decade was the Tri-state tornado of 18 March 1925, killing 695.

Tornadoes in 1930-1939 (10yrs)

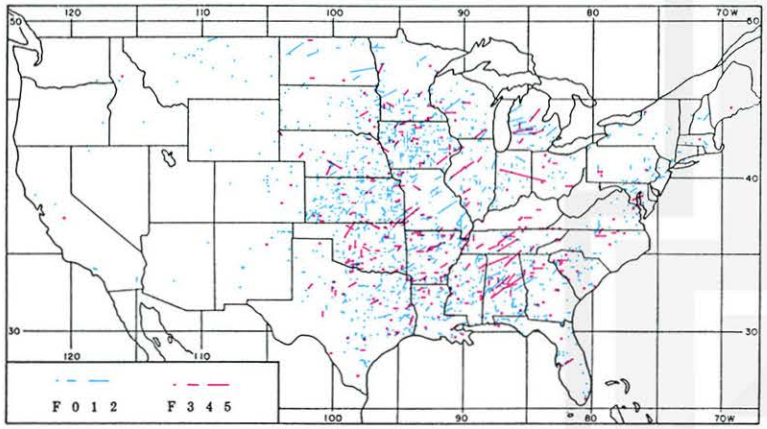

Fig. 2.1-5c Paths of tornadoes in the 1930s. 321 killed by Alabama tornadoes of 21 March 1932. 216 died at Tupelo, Mississippi on 5 April 1936 and 203 at Gainesville, Georgia on 6 April 1936.

Tornadoes in 1940-1949 (10yrs)

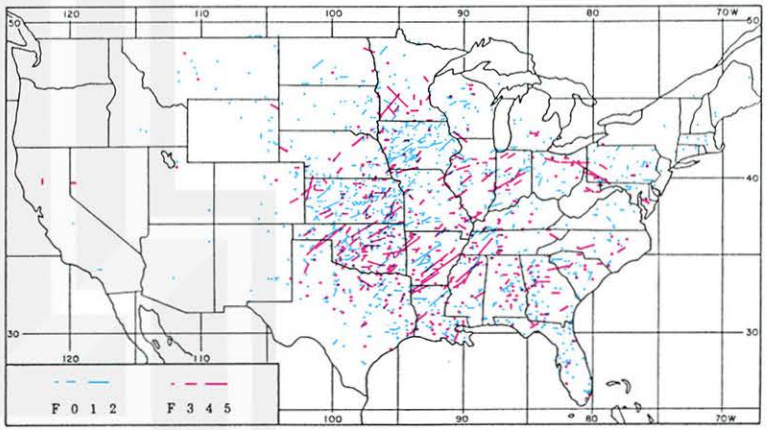

Fig. 2.1-5d Path of tornadoes in the 1940s. On 23 June 1944, a number of tornadoes moving northwest to southeast killed 153 in the Ohio to Maryland area. 167 killed on 9 April 1947 in the Texas to Kansas area.

Tornadoes in 1950-1959 (10yrs)

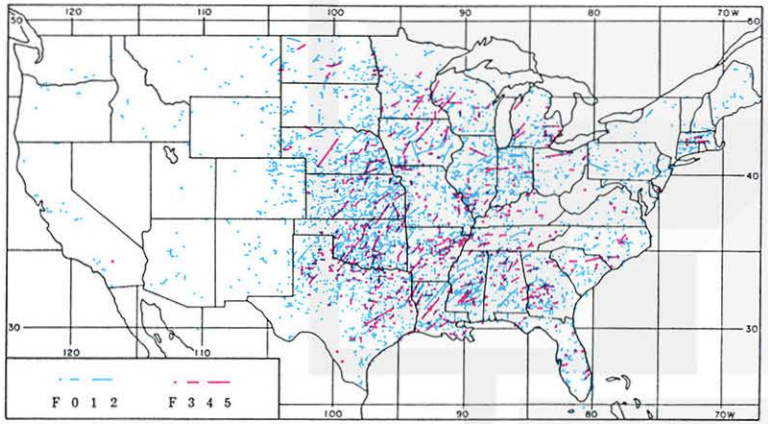

Fig. 2.1-5e Paths of tornadoes in the 1950s. On 21-22 March 1952, 208 killed in Arkansas to Tennessee, 114 on 11 May 1953 at Waco, Texas, and 116 on 8 June 1953 at Flint and Lakeport, Michigan.

Tornadoes in 1960-1969 (10yrs)

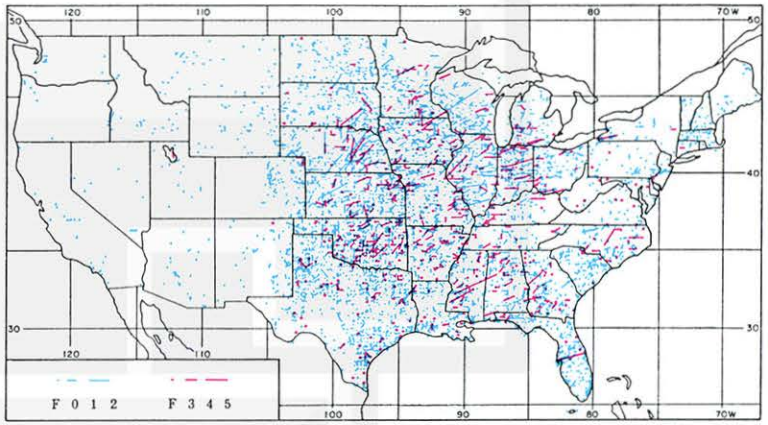

Fig. 2.1-5f Paths of tornadoes in the 1960s. The Palm-Sunday tornadoes of 11 April 1965 killed 271 in the northern Midwest. Fujita and his associates conducted an extensive aerial survey and photography.

Tornadoes in 1970-1979 (10yrs)

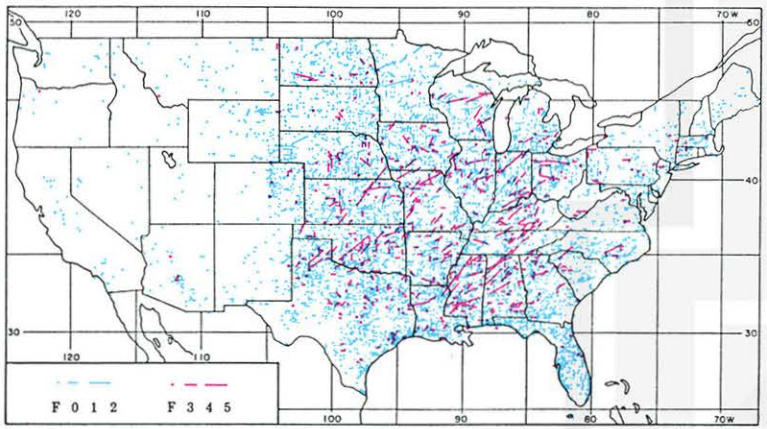

Fig. 2.1-5g Paths of tornadoes in the 1970s. The Super-outbreak tornadoes of 3-4 April 1974 killed 315. Fujita, Greg Forbes, along with others, made aerial damage surveys of practically all tornadoes.

Tornadoes in 1980-1989 (10yrs)

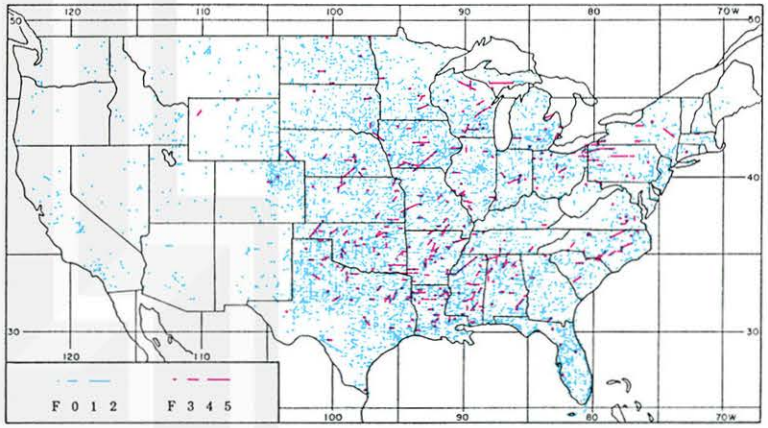

Fig. 2.1-5h Paths of the 1980 tornadoes. Upper Midwest tornadoes of 7 June 1984 left behind a total path length of 594 miles, the U.S.-Canada tornadoes on 31 May 1985, 510 total miles.

(Table 2.1-1). The quotients computed annually for cumulative F-scale tornadoes were used as multipliers to prorate the numbers of the reported tornadoes into the best-guess numbers. As expected, the prorated numbers of tornadoes eliminated the effect of the artificial increase in the 1950s, resulting in a uniform distribution of the cumulative F-scale tornadoes throughout the statistical period, 1916-1989 (Fig. 2.1-6).

Cumulative F scales	Averaged Numbers
F5	1.2 tornadoes
F5 + F4	10.0
F5 + F4 + F3	59.6
F5 + F4 + F3 + F2	238.6
F5 + F4 + F3 + F2 + F1	584.7
F5 + F4 + F3 + F2 + F1 + F0	796.7

Table 2.1-1 The definition of cumulative F-scale tornadoes and their occurrence numbers averaged over the recent 30 years, 1960-89. Annual number of tornadoes, except F4 and F5, were normalized to these averaged numbers in compensating for unreported tornadoes in early years.

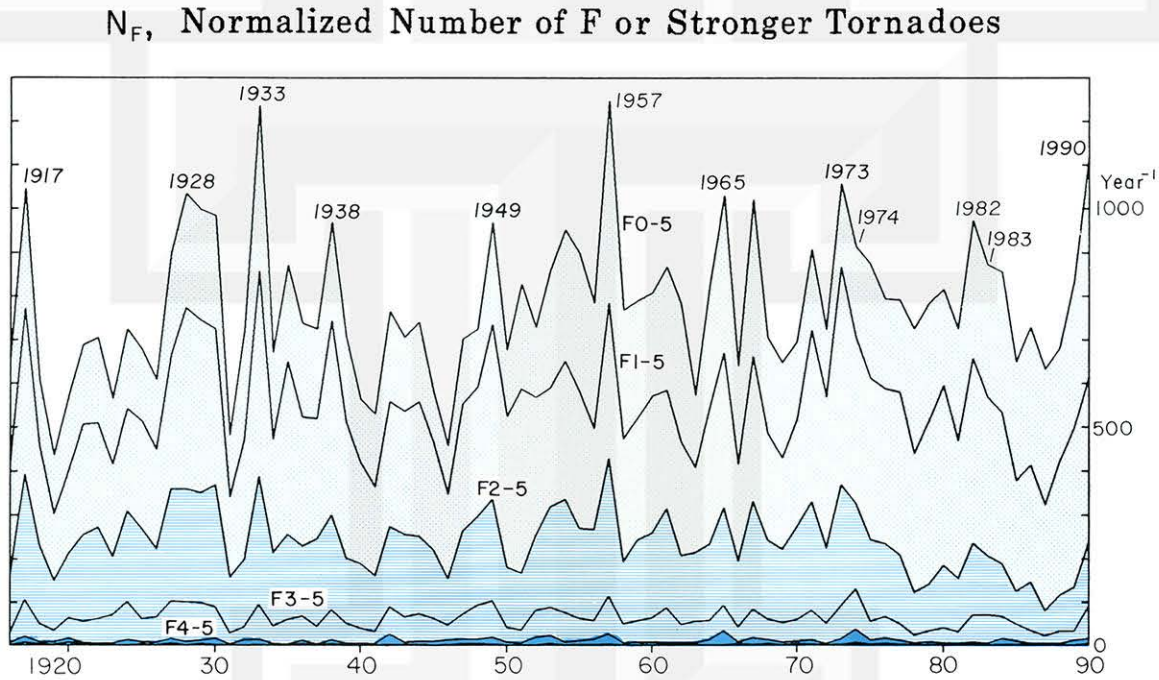

Fig. 2.1-6 Normalized number of tornadoes by cumulative F scales, F0 to F5, F1 to F5, F2 to F5, etc. Number of F2 or stronger tornadoes is shaded dark blue. It is seen that the normalization increased the numbers of early tornadoes.

Tornado Activity Number

Annual tornado activities vary from year to year. In expressing their long-term variation, it is necessary to assign an activity number for each year. In 1991, the **Tornado Activity Number (TAN)** was defined as the F-scale weighted number of tornadoes in each year. The weighting function was chosen as the F-th power of 3, which increases from 1 to 243 when the F-scale increases from F0 to F5. In other words, the TAN denotes the equivalent number of F5 tornadoes which would induce the total effect of the annual tornadoes with mixed F scales.

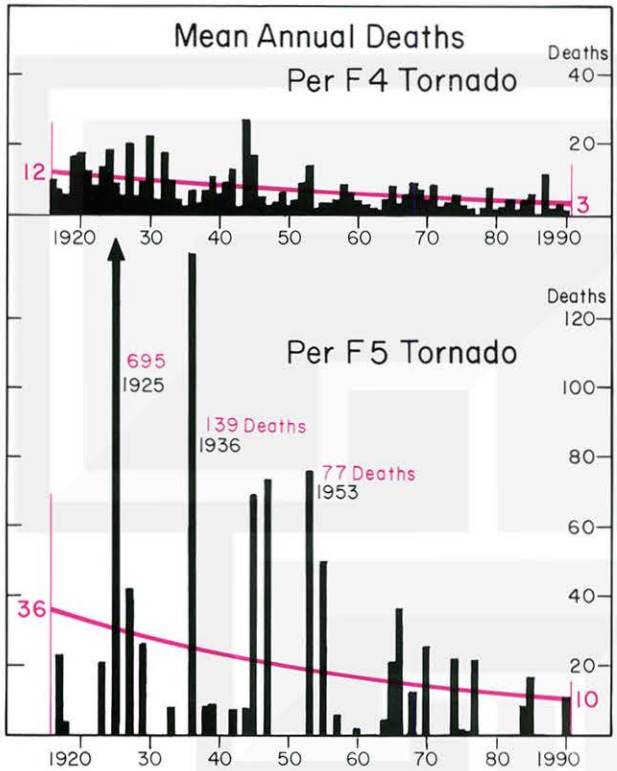

Fig. 2.1-7 The 74-year trend of the annual deaths caused by F4 and F5 tornadoes, respectively. On the average, deaths by an F5 tornado are three times larger than those by an F4 tornado.

Because F4 and F5 tornadoes in early years were often confirmed as long-track tornadoes, their numbers were modified according to the deaths caused by individual tornadoes (Fig. 2.1-7).

The TAN between 1916 and 1990 (Fig. 2.1-8) shows a dozen or more spikes. An initial attempt of relating the annual TAN with sunspots and El Niño failed, because peak-day tornadoes such as Tri-state (1925), Palm Sunday (1965), Jumbo Outbreak (1974), and others dominate TAN (Fig. 2.1-8).

On the other hand, the TAN excluding one peak-tornado day of the year results in a relatively low-spike variation. So far, no positive or negative correlation with other climatological parameters has been found. During the past two decades, however, tornado activities expressed by TAN are relatively low because of unknown reason(s).

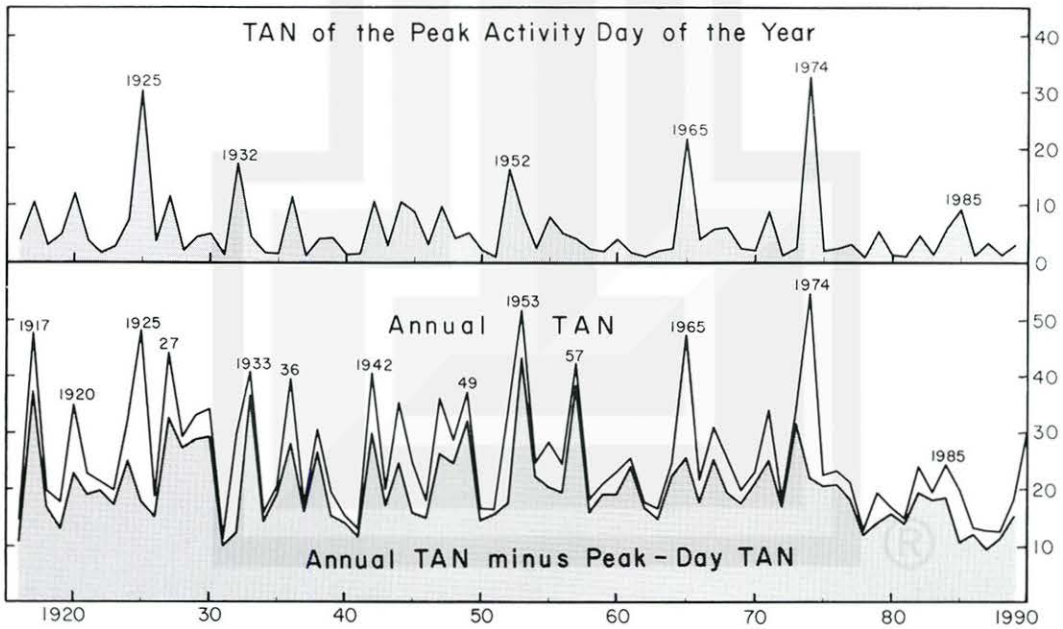

Fig. 2.1-8 Tornado Activity Number (TAN) of the peak activity day of each year (above) and the annual TAN with and without the peak activity day (below).

Tornadoes in January

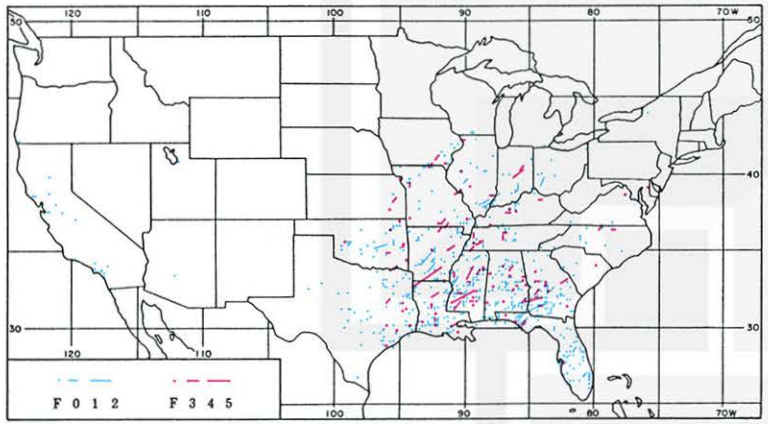

Fig. 2.1-9a January tornadoes are seen in the southern states centered in Georgia and Mississippi.

Tornadoes in February

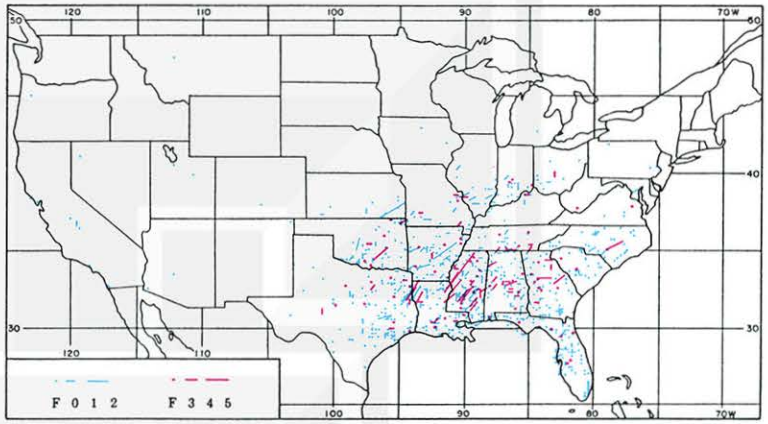

Fig. 2.1-9b February tornadoes often occur in Mississippi while their northern limit extends from Texas to southern Illinois to Maryland.

Tornadoes in March

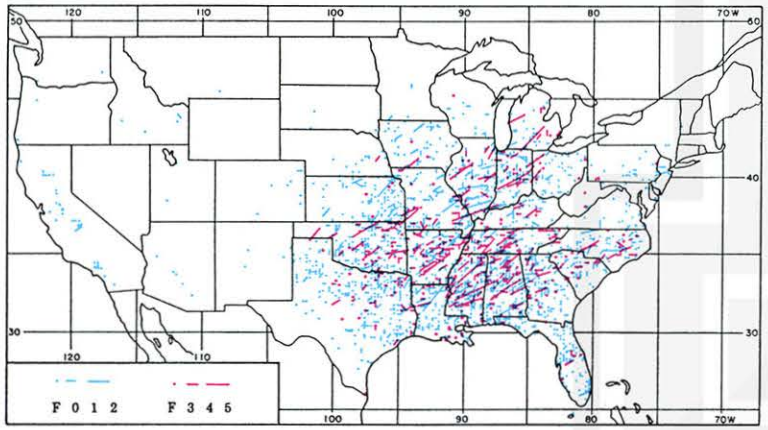

Fig. 2.1-9c March tornadoes spread quickly northward to the Minnesota-Michigan line with their activity center located along the Mississippi Valley.

Tornadoes in April

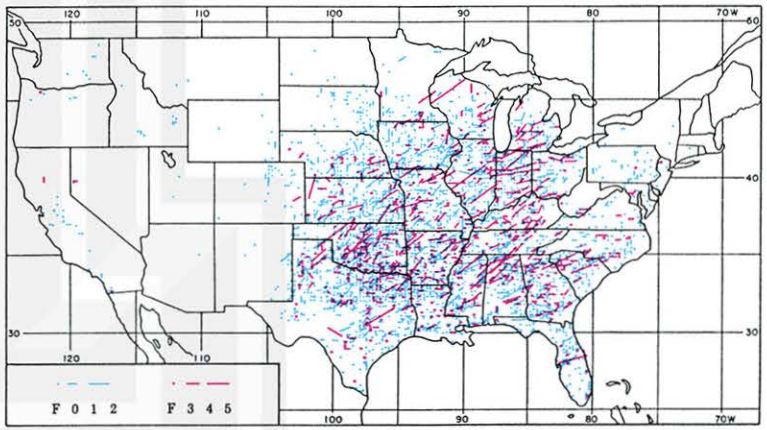

Fig. 2.1-9d Areas of April tornadoes cover the entire Midwest. There are two activity centers, the one over Oklahoma and the other over Indiana. They are located on both sides of the Mississippi River.

Tornadoes in May

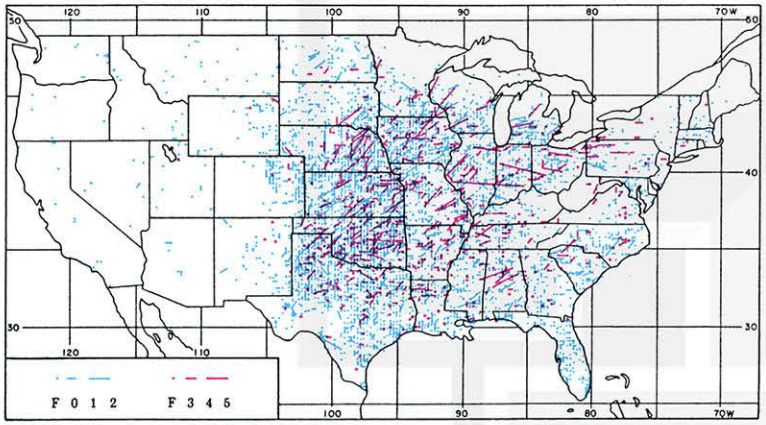

Fig. 2.1-9e May tornadoes are centered over the western Midwest extending from Oklahoma to Kansas to Iowa. Tornado activities decrease in the area east of the Mississippi River.

Tornadoes in June

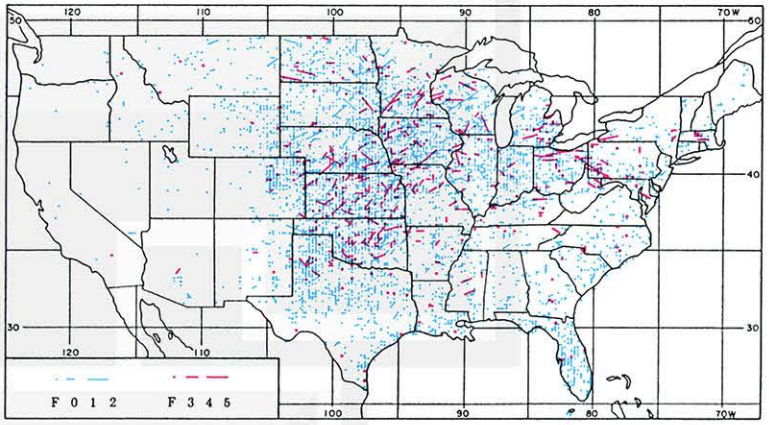

Fig. 2.1-9f Concentration of June tornadoes is seen in the northwestern Midwest north of the line extending from the Texas-Oklahoma border to southern Illinois to Maryland, which signifies the northwestern boundary of the Bermuda High.

Tornadoes in July

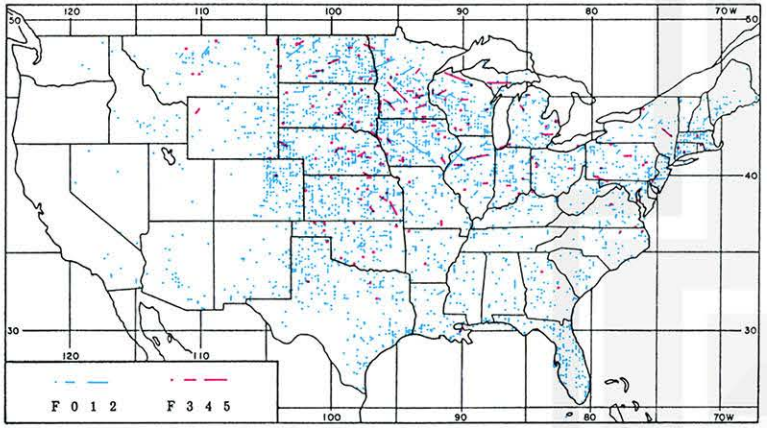

Fig. 2.1-9g Activity center of July tornadoes move farther to the northwest as the boundary of the Bermuda High advances north and northwest.

Tornadoes in August

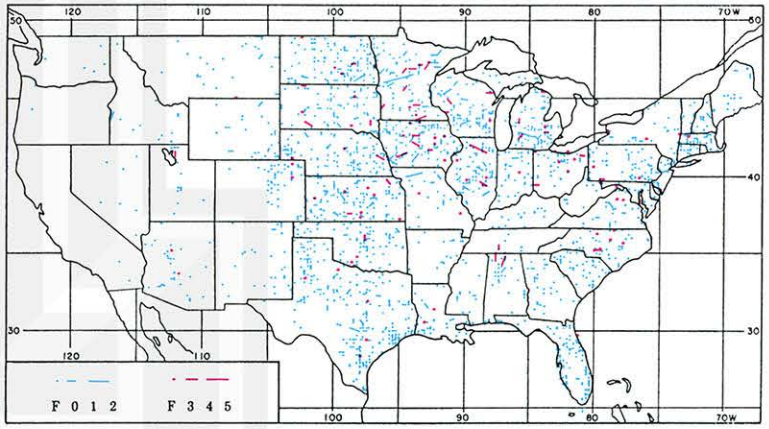

Fig. 2.1-9h August tornadoes are scattered over the western and northern Midwest. The southern boundary of tornado activities is clearly identifiable.

Tornadoes in September

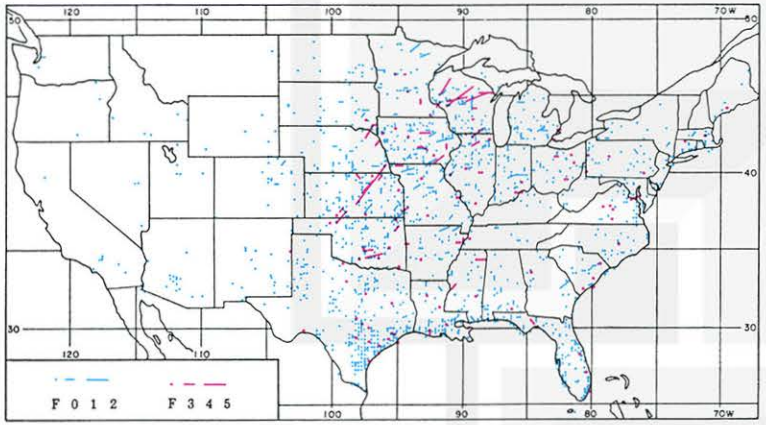

Fig. 2.1-9i September tornadoes are located to the northwest of the line extending from Oklahoma to Ohio. Meanwhile, hurricane-induced tornadoes occur along the Gulf Coast.

Tornadoes in October

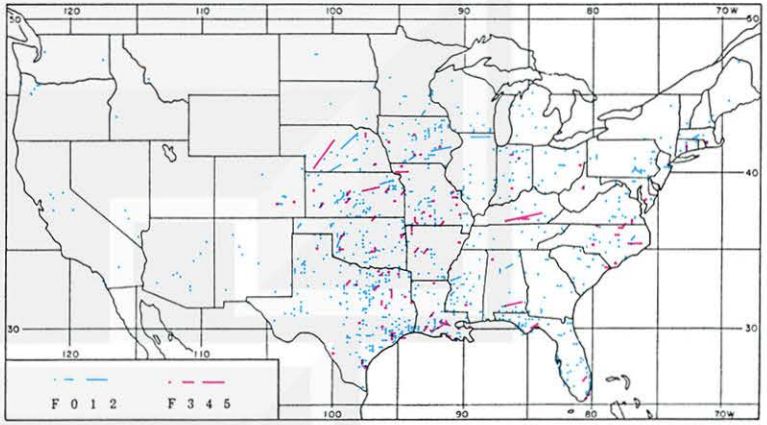

Fig. 2.1-9j October tornadoes are scattered over the area east of the Mississippi River, but their activities are insignificant.

Tornadoes in November

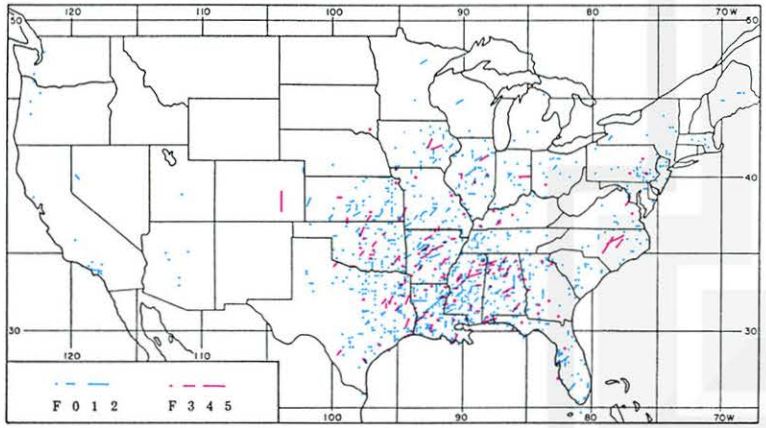

Fig. 2.1-9k November tornadoes are active in the states bordering Mississippi and Alabama. Wide-spread tornadoes could occur in these states.

Tornadoes in December

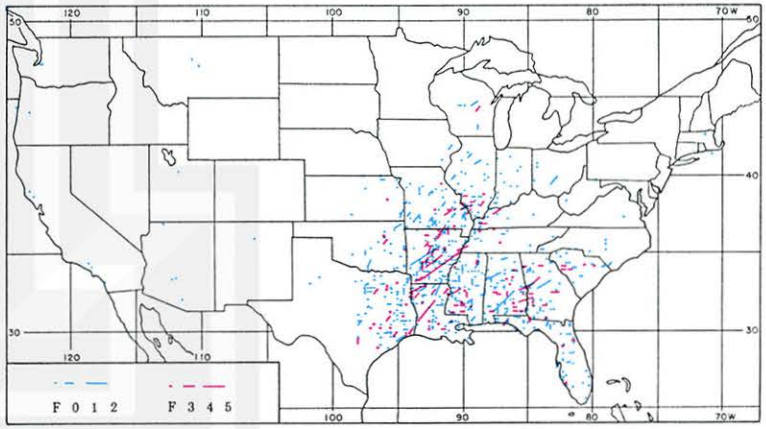

Fig. 2.1-9l December tornadoes are seen predominantly in the Mississippi Valley and Gulf states.

2.2 Fargo Tornado of 20 June 1957

Late in the afternoon of June 20, Fargo, ND was visited by a violent tornado, killing 10 persons and injuring 103 others. Over 1,300 homes in Fargo were damaged or completely destroyed. Fortunately, the city received an advanced tornado warning initiated by the motorists eastbound on US-10, a major east-west highway through Fargo.

What these motorists saw was a very large swirling cloud traveling east toward Fargo at 20 mph. Because its appearance was an oversized tornado, most cars overtook the cloud to give a first-hand report to the Fargo Police Department. When the approaching tornado was announced by radio and television, a large number of people with cameras anxiously waited for the arrival of the tornado. This was why an extraordinary number of high-quality pictures were available in the Fargo area.

In fact, the swirling cloud was not a tornado, but it was a rotating thunderstorm which spawned 5 tornadoes in series along US-10 between Buffalo, ND and Dale, MN. The rotating cloud traveled 70 miles in 3 hr 45 min at 18.7 mph or 30 km/hr. The Fargo Tornado was the third one in the series.

Citizen's Cooperation in Collecting Tornado Pictures

After learning from Mr. Ferguson Hall of the U.S. Weather Bureau, Washington, D.C., that an unusual number of tornado pictures were taken in the Fargo area, Dr. Byers told me to undertake a photogrammetric study of both tornado funnel and parent clouds. Thereafter, I worked with Mr. Dewey Bergquist, a WDAY-TV weatherman in Fargo. Through repeated announcements on TV, he informed citizens of the need for tornado pictures in determining the size, windspeed, and structure of the unusual tornado.

Within one to two months, a total of 150 cloud pictures were obtained; two photos from Absaraka, 13 from West Fargo, 114 from Fargo, 13 from Moorhead, and 8 from Dilworth. In addition, five movie films were received; one from Wheatland, 3 from Fargo, and 1 from Moorhead. It took about two years before completing a rather complicated photogrammetry performed with new techniques. At the conclusion of the research, it was decided to publish every single photo contributed by photographers because they were eager to find out how other pictures looked like and how they were put together in determining tornado parameters such as dimensions, windspeeds, structures, etc.

A Detailed Analysis of Fargo Tornado of June 20, 1957, Fujita (1960a) was printed by the U.S. Government Printing Office as U.S. Weather Bureau Research Paper No. 42 for distribution, costing only 45 cents per copy. I was told that most of the 3,000 copies printed were purchased by the Fargo-area residents.

Triangulation of Tornado

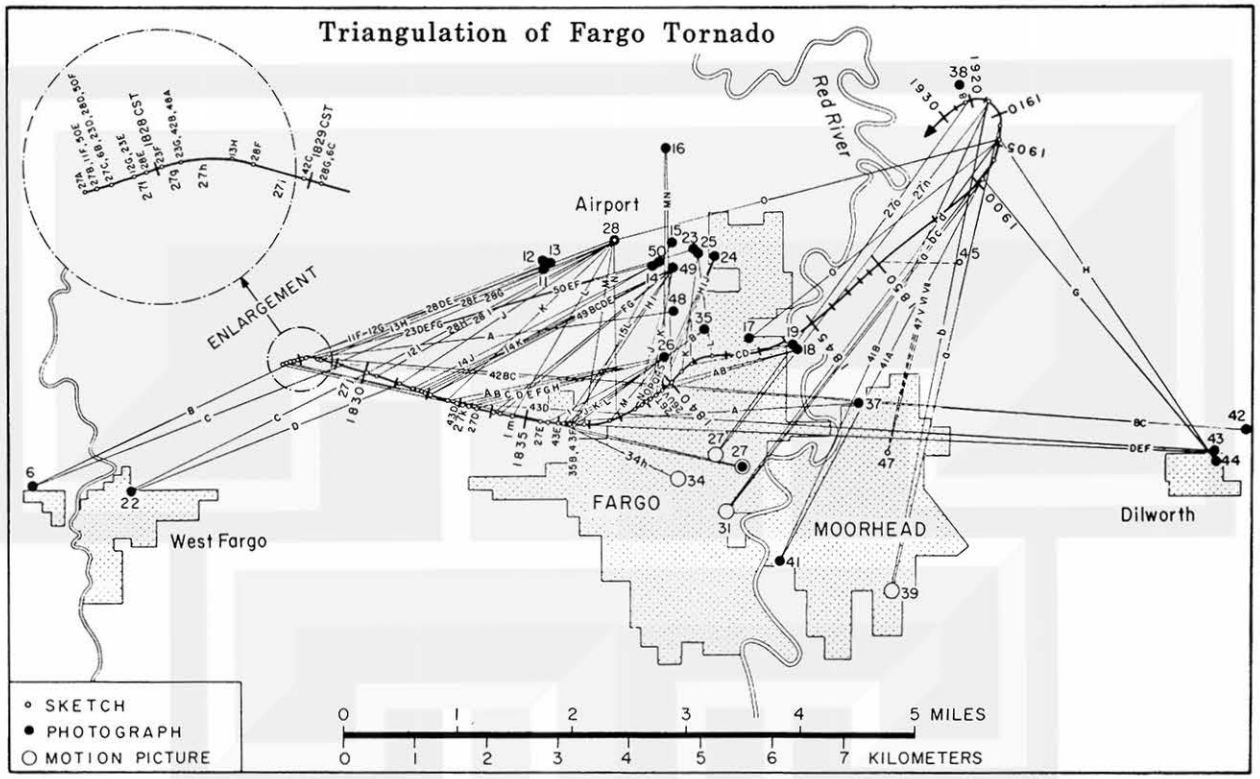

Fig. 2.2-1 Determination of the path of the Fargo tornado based on the triangulation of funnel clouds. To determine the touchdown location, 118 photos taken from different sites were used. Simultaneous photos were selected by matching the size and shape of the funnel clouds.

The 53 photographic sites used by the 30 photographers listed in Fujita (1960a) were visited with Bergquist one by one for determining the exact azimuth angles on each photograph.

After determining the azimuths, the center azimuths viewed from different sites were used in triangulating the successive positions of the tornado center on the ground (Fig. 2.2-1). Thereafter, the effective focal length and the distance from site to tornado were used in reducing tornado pictures into a unique print size.

A sequence of 14 pictures (Fig. 2.2-2) reveals the fast descent of the funnel cloud from the cloud base to the ground in less than 30 seconds. After the touchdown, the funnel diameter increased rapidly until 1828.8 CST when the base of the funnel just above the ground began disappearing. At 1829.6 there was a clear space beneath the sheared-off funnel. Shortly thereafter, the funnel turned into a huge cone surrounded by a thick debris cloud encircling the base of the funnel near the ground. At 1836.2 the funnel was on the west edge of Fargo.

Triangulation of Rotating Cloud

Making use of the method of triangulating the tornado funnel, the center of the rotating cloud was determined accurately in estimating the path of the rotation center. Under the assumption of uniform translational motion, cloud positions at one-minute intervals were marked on the path line (Fig. 2.2-3).

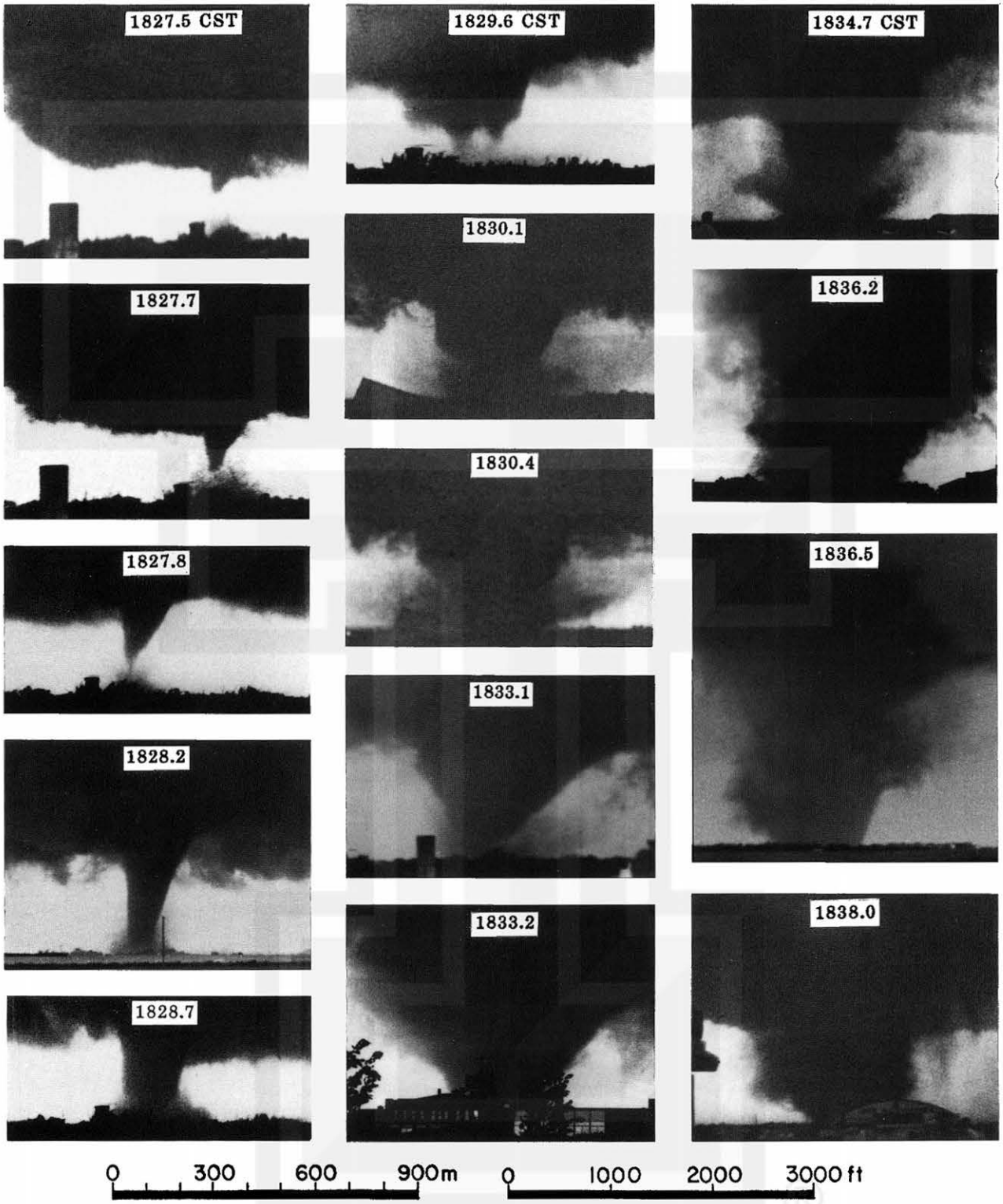

Fig. 2.2-2 Fourteen size-adjusted pictures of the Fargo tornado, which were selected from 75 pictures in Fujita (1960a). These pictures show the rapid growth of the tornado funnel.

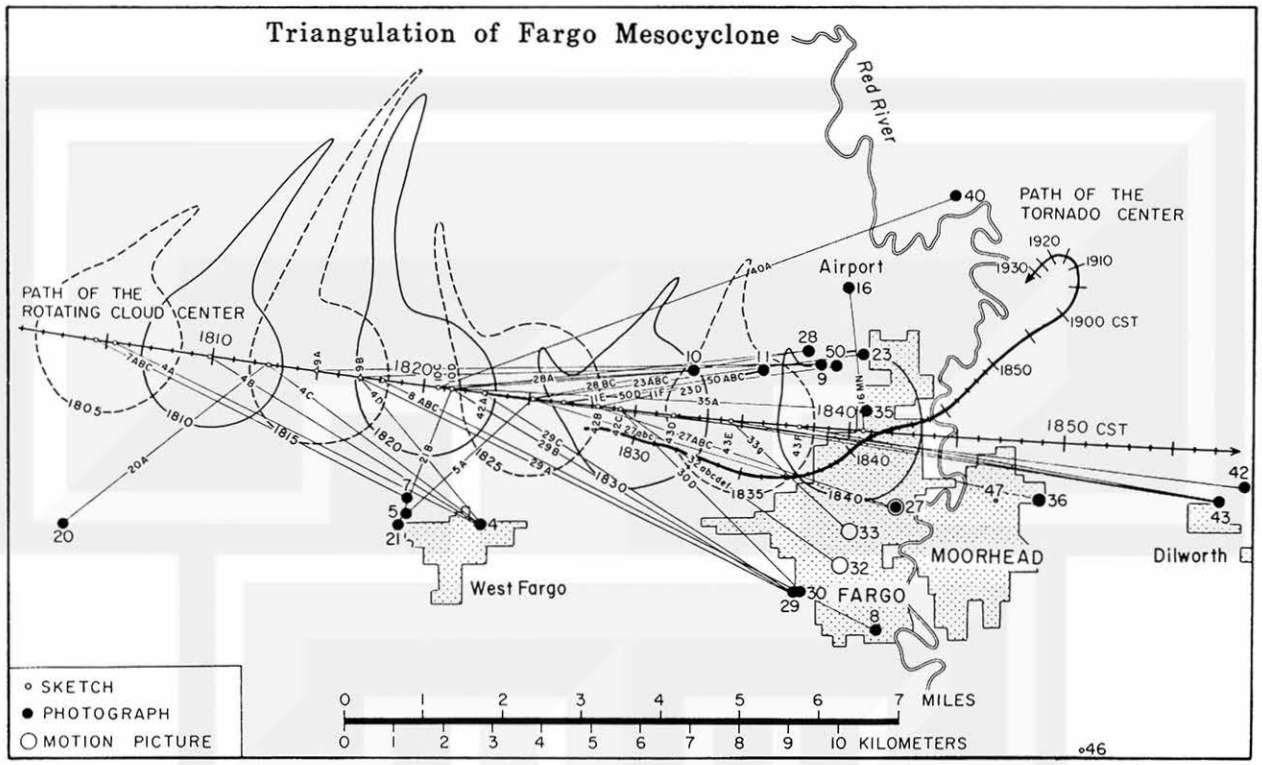

Fig. 2.2-3 Long-range triangulation of the rotating cloud accompanied by a long tail cloud which extended toward the northerly direction. The initial tail cloud disappeared at 1830 CST, being taken over by a new one which was rather short in length.

The combination of the time-dependent locations of the tornado and the center of the rotating cloud suggested strongly that the funnel aloft of the Fargo Tornado appeared first at 1827.5 CST (Fig. 2.2-2) 0.5 km to the south of the rotation center of the parent cloud.

Size-normalized pictures (Fig. 2.2-4) looking, more or less, toward the west revealed that the Fargo Tornado at 1837 was located beneath the edge of the depressed cloud base which I called the rotating **wall cloud.**

Movement of Collar and Wall Clouds

Shown in Fig. 2.2-5 are views of the wall cloud at 1826 CST, 1.5 min before the funnel cloud began descending from the depressed base of the wall cloud. Apparently, the wall cloud was located where the near-ground moist air swirled up into the rotating thunderstorm. The vertical motion at the right-hand (north) edge of the wall cloud computed from the movie imagery at 0.4-sec intervals were 70 ft/sec at 3,000 ft, and 35 ft/sec at 1,500 ft, characterized by a constant convergence of 2.3×10^{-2} sec.

The movie also revealed that the vertical motion on the left-hand (south) side was relatively small. In other words, the funnel cloud of the Fargo Tornado formed to the south of the rotation center, where the vertical motion of the wall cloud was relatively weak. I was not able to explain the reason at that time.

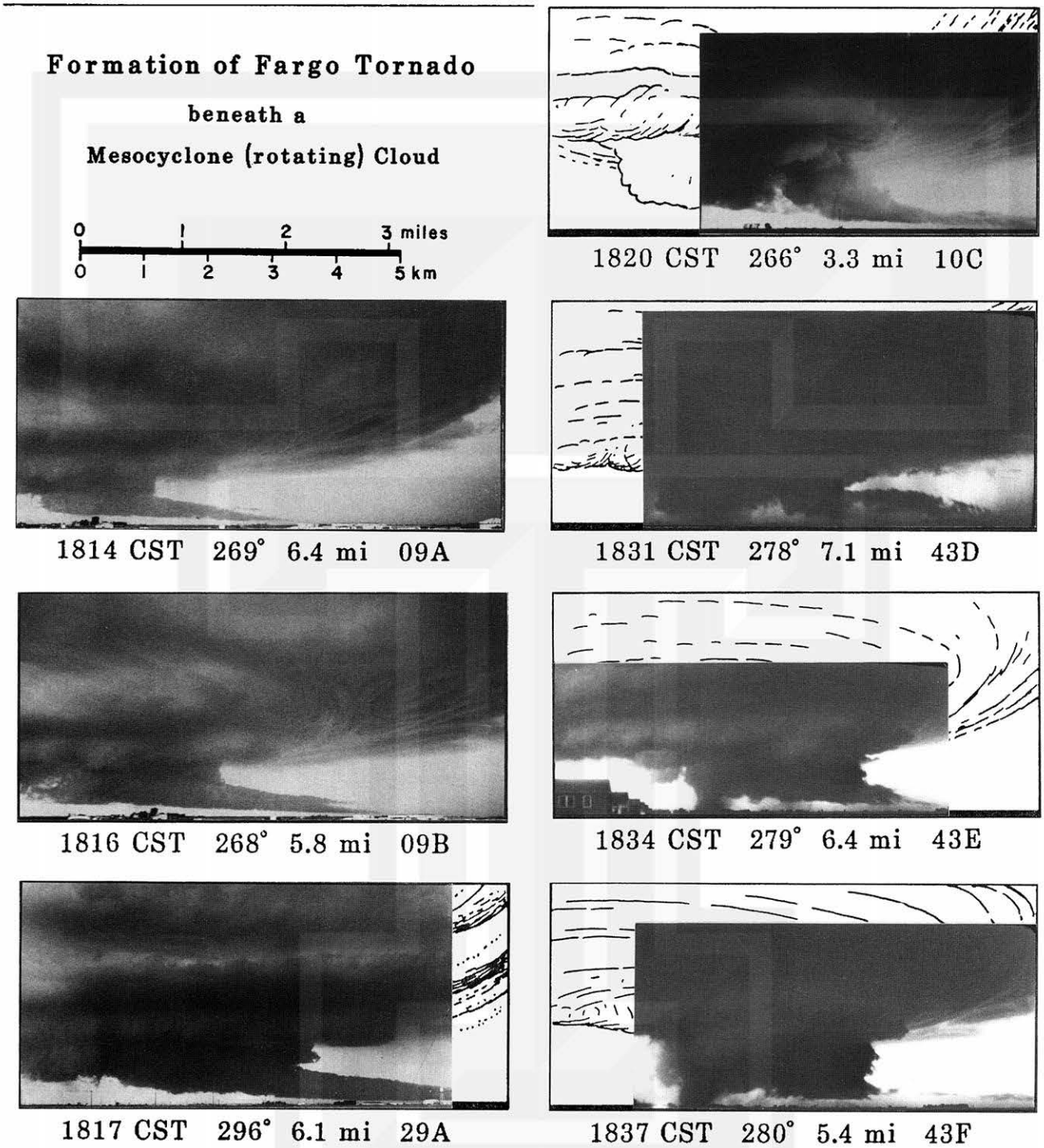

Fig. 2.2-4 Evolution of the parent cloud of the Fargo tornado. At 1815 CST, 12 min before the tornado formation, the cloud was characterized by a small but well-defined wall cloud and a long tail cloud to the right (north). After touchdown, the tornado axis tilted, pushing the tornado on the surface directly beneath the south edge of the wall cloud.

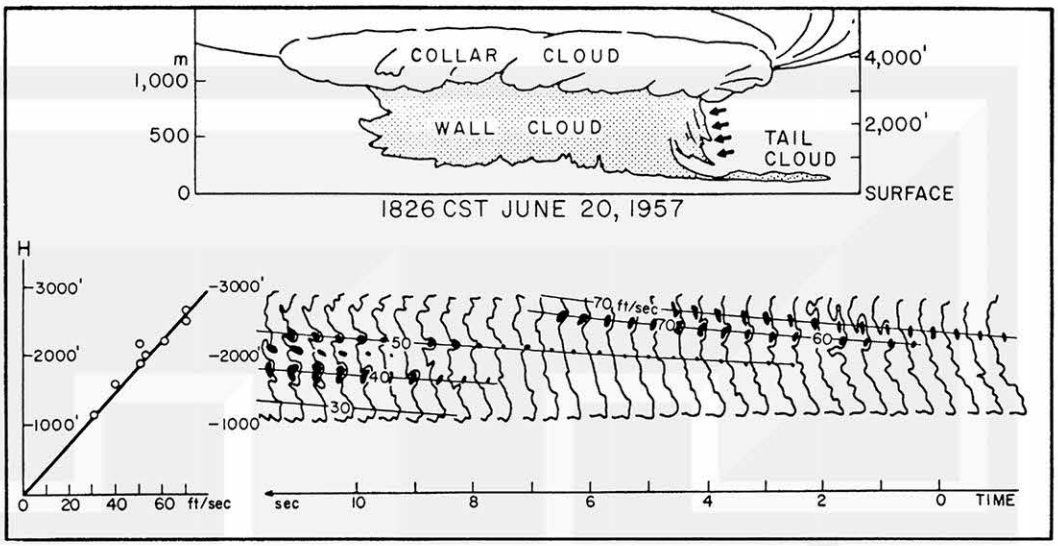

Fig. 2.2-5 The base of the rotating cloud characterized by collar, wall, and tail clouds. Although the wall cloud was located where the moist air on the ground rose into the rotating cloud, the vertical motion on the right side was very large, reaching 70 ft/sec at the collar cloud base.

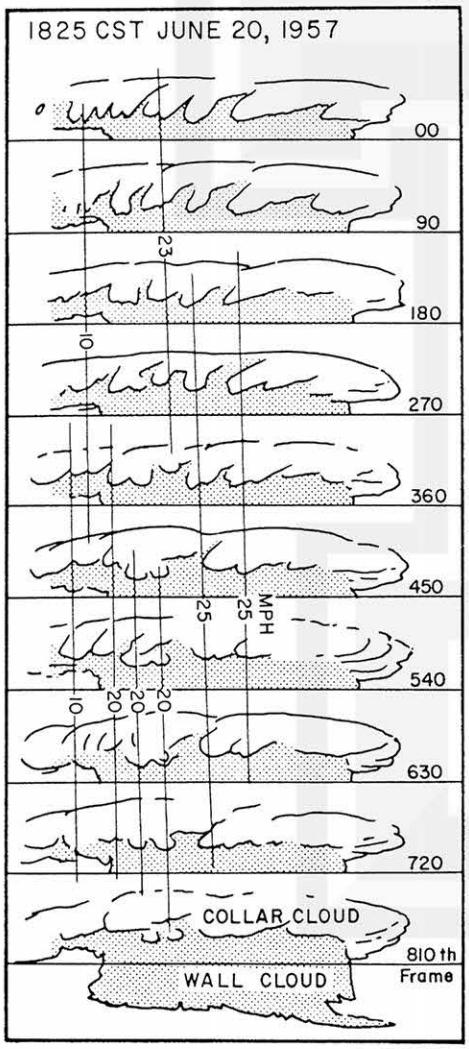

Fig. 2.2-6 Rotation rate of the collar cloud determined by the time-motion analysis of a movie film. Apparently, the rotation rate increased upward within the depth of the collar cloud.

One or two **tail clouds** were seen on the strong vertical motion side of the wall cloud where the cloud base was very low. The **collar cloud** (Fig. 2.2-5) was a ring-shaped cloud which encircled the rotating wall cloud where it was connected to the base of the large swirling cloud at 4,000 ft (1.2 km).

The 810-frame movie of the collar cloud (Fig. 2.2-6) showed clearly that the collar cloud was rotating at 10 to 25 mph (15 to 40 km/hr) tangential speed. There was a vertical shear within the 1,800 ft (550 m) depth of the ring. The top of the ring was rotating faster than the base of the ring.

2.3 Palm Sunday Tornadoes, 1965

The Palm Sunday outbreak of 36 tornadoes occurred on 11 April 1965 in the six midwestern states of Iowa, Wisconsin, Illinois, Michigan, Indiana, and Ohio where 253 persons were killed. In order to survey as many tornadoes as possible before cleanup, I decided to use Cessna aircraft.

The aerial survey performed on April 12, 13, 16, and 19, flying 7,500 miles revealed interesting evidence of tornadoes. Although a number of long-track tornadoes were reported initially, most long tracks consisted of several short tracks produced by a series of family tornadoes spawned by a parent cloud, mesocyclone, or hook echo. A family of six, L-1 through L-6, was the largest in number (Fig. 2.3-1).

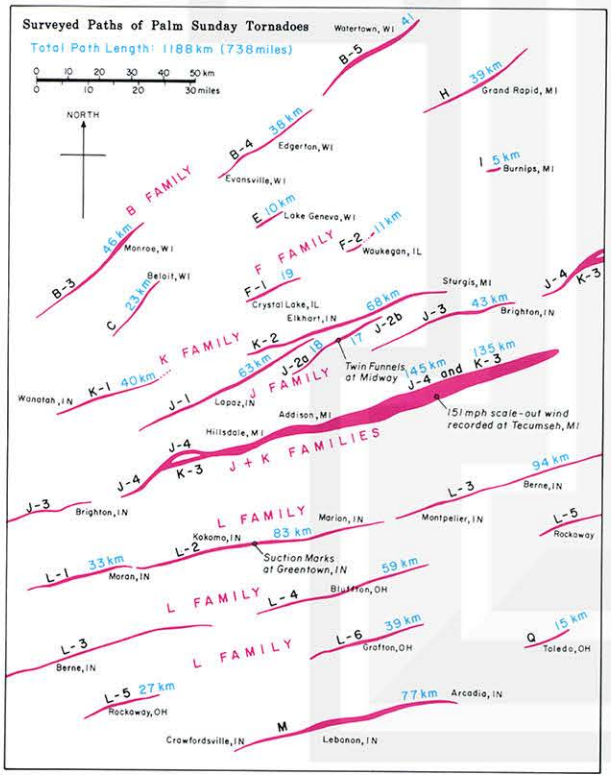

Fig. 2.3-1 A composite map of the Palm Sunday tornadoes surveyed by the Fujita group.

Cycloidal Ground Marks

Fig. 2.3-2 Cycloidal marks which I photographed with 135 mm telephoto lens. Since 1953, these marks were assumed as lines of scratches.

Cycloidal marks in open fields have been regarded as scratch marks. My telephoto pictures of the cycloidal marks, 10 miles east of Kokomo, Indiana suggested, however, that they consist of debris, rather than scratches (Fig. 2.3-2). However, I was not able to visit the site on the ground. Two years later in 1967, this evidence was confirmed in Illinois.

Interacting Tornadoes

After completing the aerial survey, I visited the site of Mr. Paul Huffman's twin-funnel picture southeast of Elkhart, Indiana. It was suggested that the single funnel tornado was split into two funnels while passing over the Midway Trailer Court.

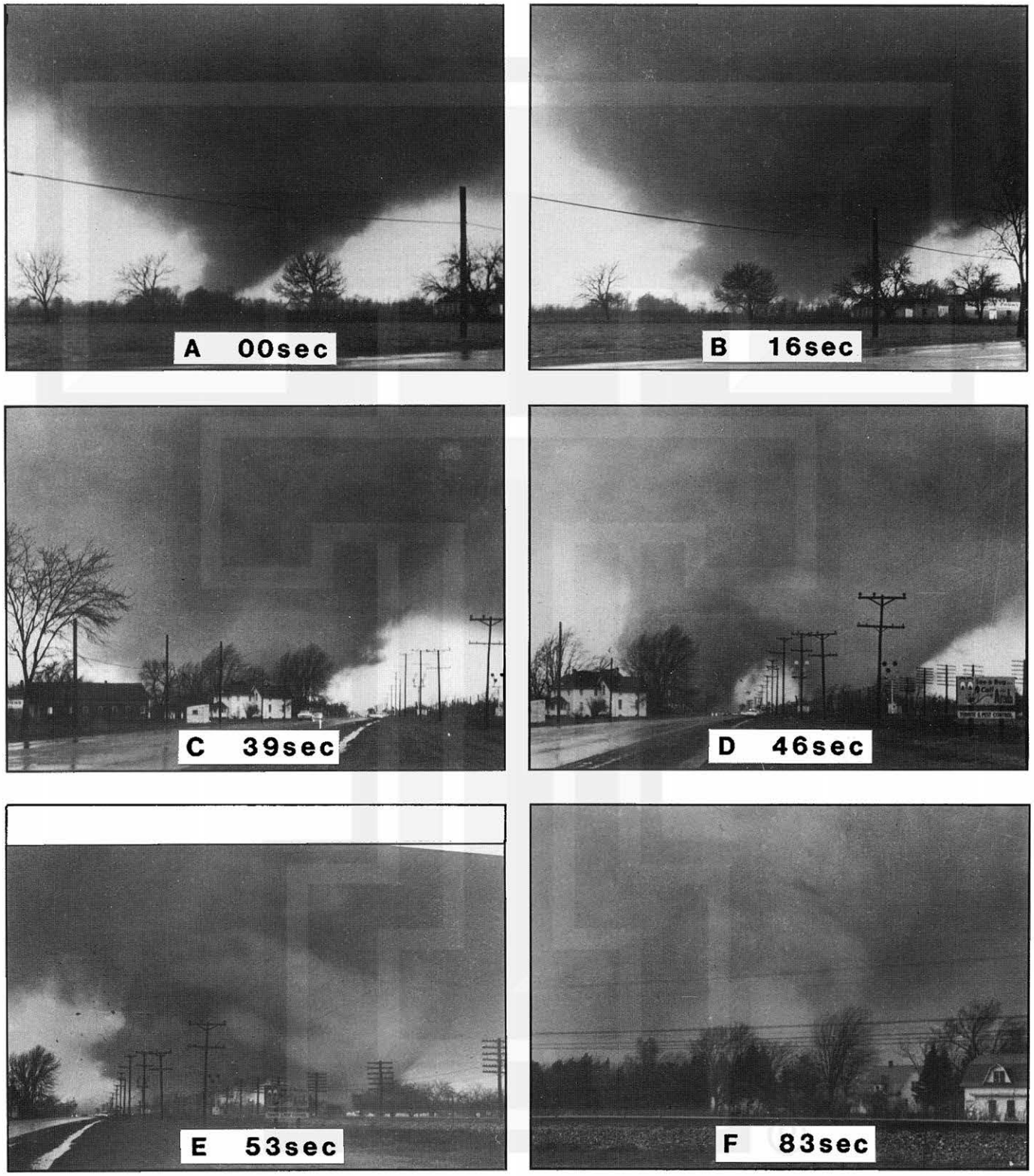

Fig. 2.3-3 Six pictures of the Midway tornado as it moved across U.S. Highway 33. Courtesy of Mr. Paul Huffman, staff photographer of the Elkhart Truth, with whom I surveyed his picture site and azimuth angles for photogrammetric study.

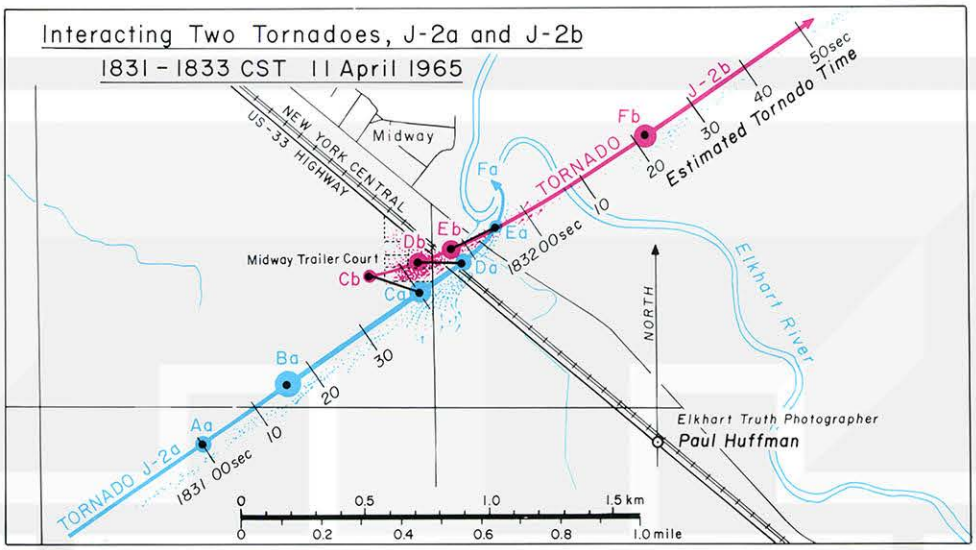

Fig. 2.3-4 Paths of two tornadoes, J-2a and J-2b at positions A (1831+00sec), B (+16sec), C (+39sec), D (+46sec), E (+53sec), and F (+83sec). The new tornado formed at Cb and rotated around the old one which disappeared at Fa.

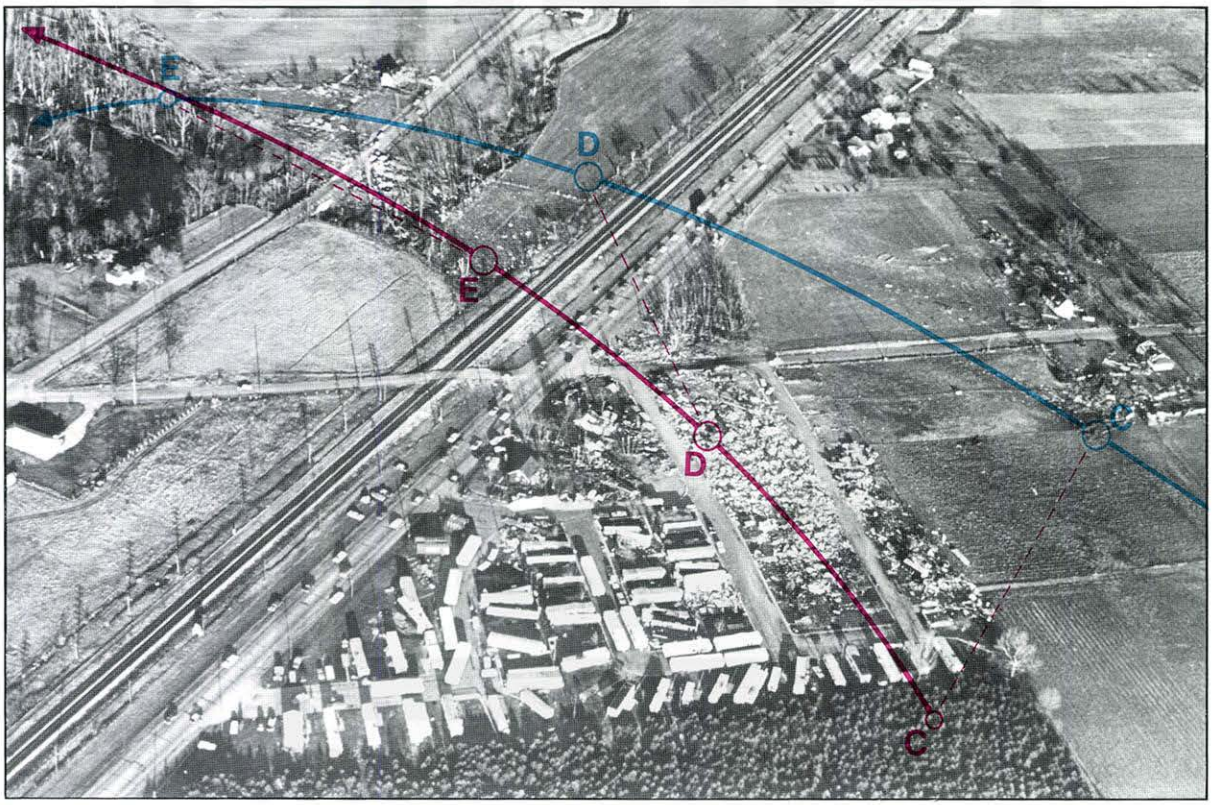

Fig. 2.3-5 Paths of two tornadoes at their positions C, D, and E superimposed upon the aerial photograph which I took on 13 April 1965.

Since then, I studied the Hesston-Goessel tornado of 13 March 1990 in Kansas (p45) finding that the movement of the twin funnels and that of the Kansas tornadoes were very similar to each other. Based on the new knowledge gained 25 years later, the twin funnels in Huffman's picture were changed to two interacting tornadoes or "**binary tornadoes**" (p46).

Highest Windspeed Recorded

In 1971, when I was working on the tornado scale pegged to the damage-causing windspeeds, I tried to collect wind traces recorded at or near confirmed damage locations. Due to the fact that most anemometers do not survive in extreme winds, the 150+ mph peak gust (Fig. 2.3-6) is the highest windspeed known to me.

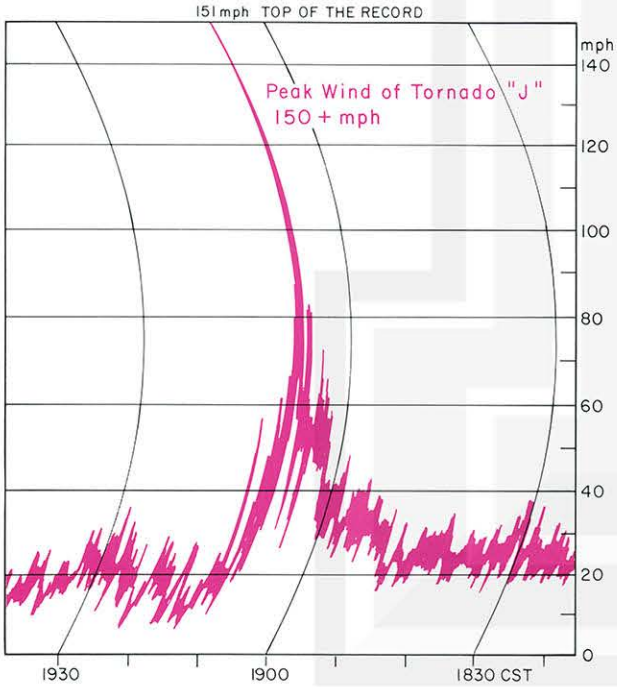

Fig. 2.3-6 The 150+ mph peak wind recorded by the Tecumseh, Michigan Health Study, the University of Michigan. Although the top line was 150 mph, the wind trace extended to 151 mph.

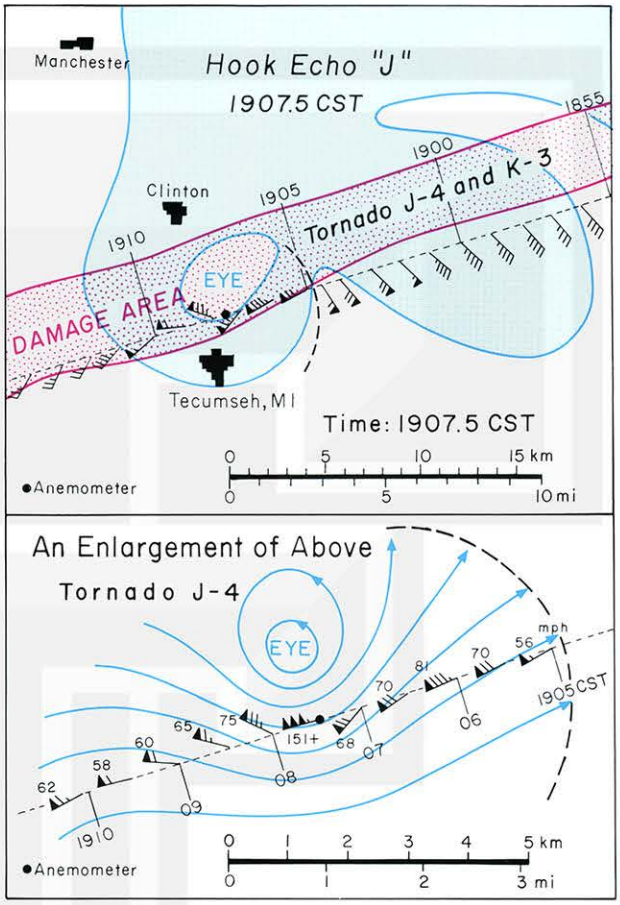

Fig. 2.3-7 Time-space conversions of the recorded winds in relation to the mesocyclone/hook echo "J". The 151+ mph wind was recorded at the south edge of the estimated F1 to F2 damage.

Fortunately, I flew by Cessna over the anemometer site at the Tecumseh airport on 13 April, two days after the recording, confirming that the damage around the anemometer was no more than F2 (113-157 mph). A subsequent analysis of the recorded winds in relation to the hook echo "J" revealed that the peak gust was by mesocyclone, rather than tornado, which left behind a 5-km wide swath of F2 damage.

2.4 The Fujita Tornado Scale

In scaling the intensity of tornadoes, I connected the upper end of Beaufort Scale (B12) or 73 mph with the lower end of Mach Number (M1) or 738 mph into 12 non-linear steps. Taking into consideration the recorded peak winds and corresponding damage, I assumed that tornado windspeeds can be expressed by the 6-point scale, F0 to F5. The Fujita Tornado Scale was thus devised. Fujita (1971b).

For determining the F scale, we have to estimate the f-scale damage of any structure with a damage. Then we select the F scale as a combination of f scales and structure types (Fig. 2.4-1).

Along with the definition of the F-scale windspeeds, corresponding damages were photographed and compiled into an F-scale damage chart of strong framehouse for which the damage scale and the windspeed scale are identical (Fig. 2.4-2). Produced also is an F-scale damage of cornfields which cover large areas in the Midwest (Fig. 2.4-3).

THE FUJITA TORNADO SCALE

Damage f scale		Little Damage	Minor Damage	Roof Gone	Walls Collapse	Blown Down	Blown Away
		f0	f1	f2	f3	f4	f5
Windspeed F scale		17 m/s – 32	32 – 50	50 – 70	70 – 92	92 – 116	116 – 142
		F0	F1	F2	F3	F4	F5
		40 mph – 73	73 – 113	113 – 158	158 – 207	207 – 261	261 – 319
To convert f scale into F scale, add the appropriate number							
Weak Outbuilding	-3	f3	f4	f5	f5	f5	f5
Strong Outbuilding	-2	f2	f3	f4	f5	f5	f5
Weak Framehouse	-1	f1	f2	f3	f4	f5	f5
Strong Framehouse	0	F0	F1	F2	F3	F4	F5
Brick Structure	+1	-	f0	f1	f2	f3	f4
Concrete Building	+2	-	-	f0	f1	f2	f3

Fig. 2.4-1 The Fujita tornado scale (F scale) pegged to damage-causing windspeeds. The extent of damage expressed by the damage scale (f scale) varies with both windspeed and the strength of structures.

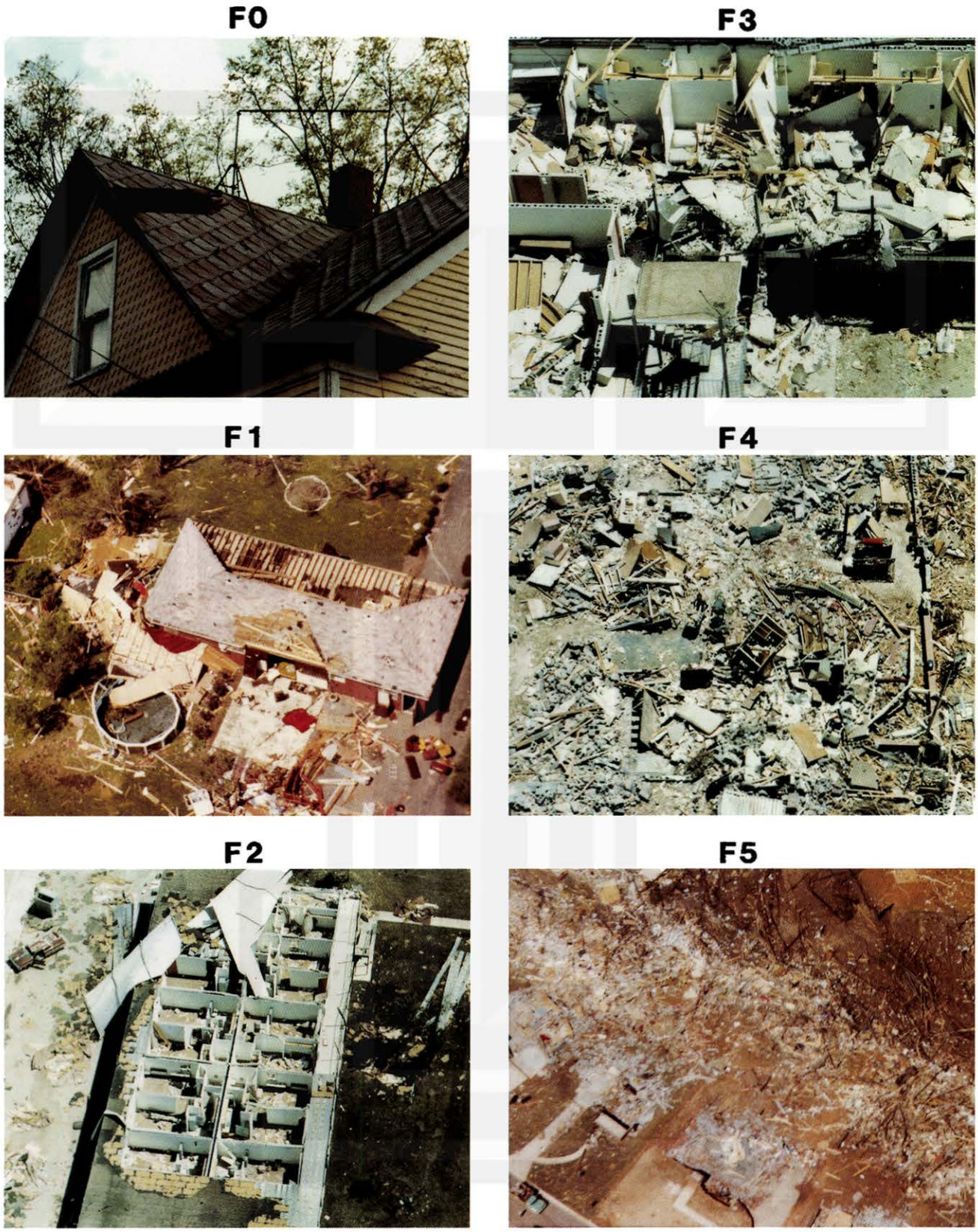

Fig. 2.4-2 A collection of F-scale damage pictures applicable to strong framehouses. Weak houses and outbuildings will receive f-scale damage larger than the F-scale pegged to the windspeed.

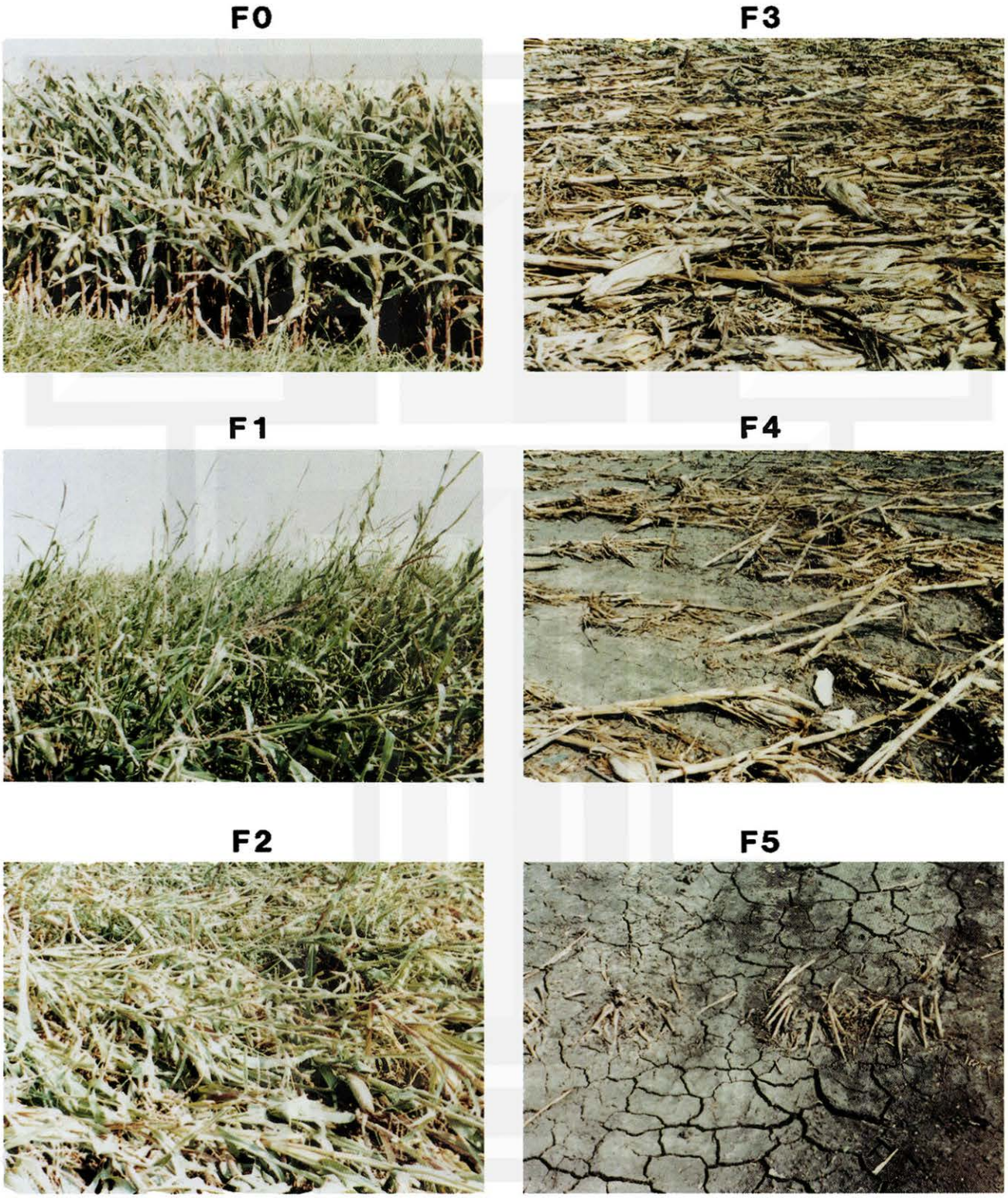

Fig. 2.4-3 Estimated F-scale winds corresponding to the cornfield damage caused by the Plainfield, Illinois tornado of 28 August 1990. Most corn crops return to normal after F0 or F1 wind. The F5 wind will wipe out the crops extending above the ground.

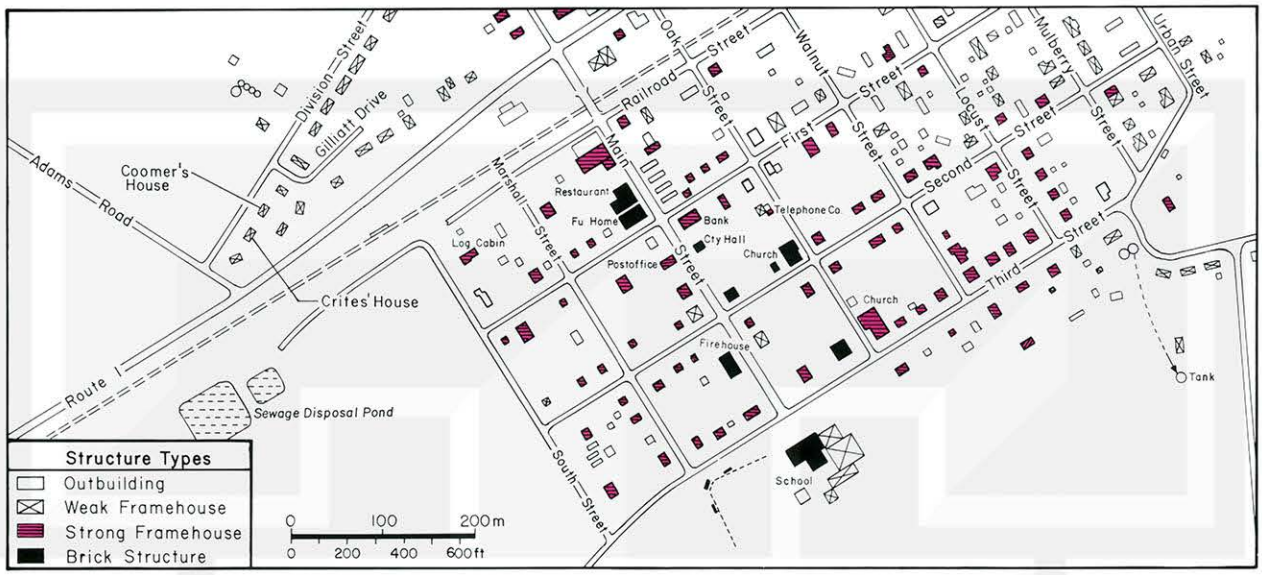

Fig. 2.4-4 Distribution of structures in Allendale, Illinois before the 7 January 1989 tornado. Pre-tornado structure types were determined with the help of local residents who could recall the types of original structures.

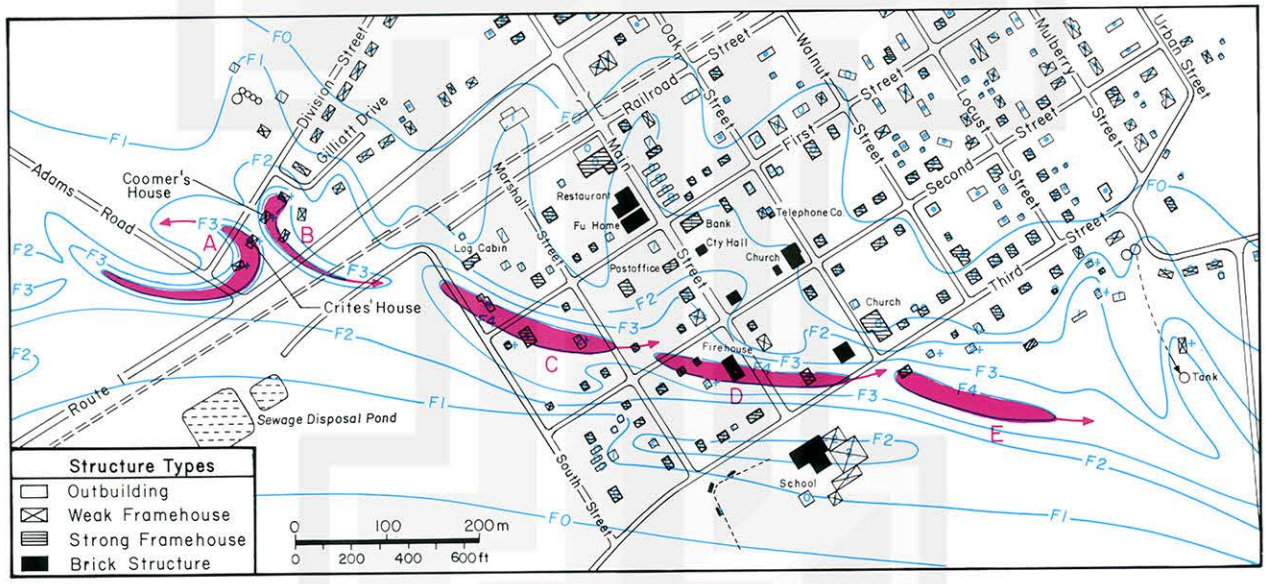

Fig. 2.4-5 F-scale, not f-scale, contour lines obtained by assessing the F scale of each structure in town by combining the structure type with the f-scale damage received.

Test estimates of F scale were made after the Allendale, Illinois tornado of 7 January 1989. First, the structure types before the tornado were determined (Fig. 2.4-4). Then the proper F scale of each structure was obtained by correcting the effects of structure types (Fig. 2.4-5).

Of interest are two suction vortices, A and B, which lifted two houses into two different directions, the one toward the west and the other, toward the east. These examples show that tornado winds are highly variable within a short distance both in wind direction and speed, necessitating the use of all types of structures in mapping the F-scale wind pattern.

2.5 Selected U.S. Tornadoes

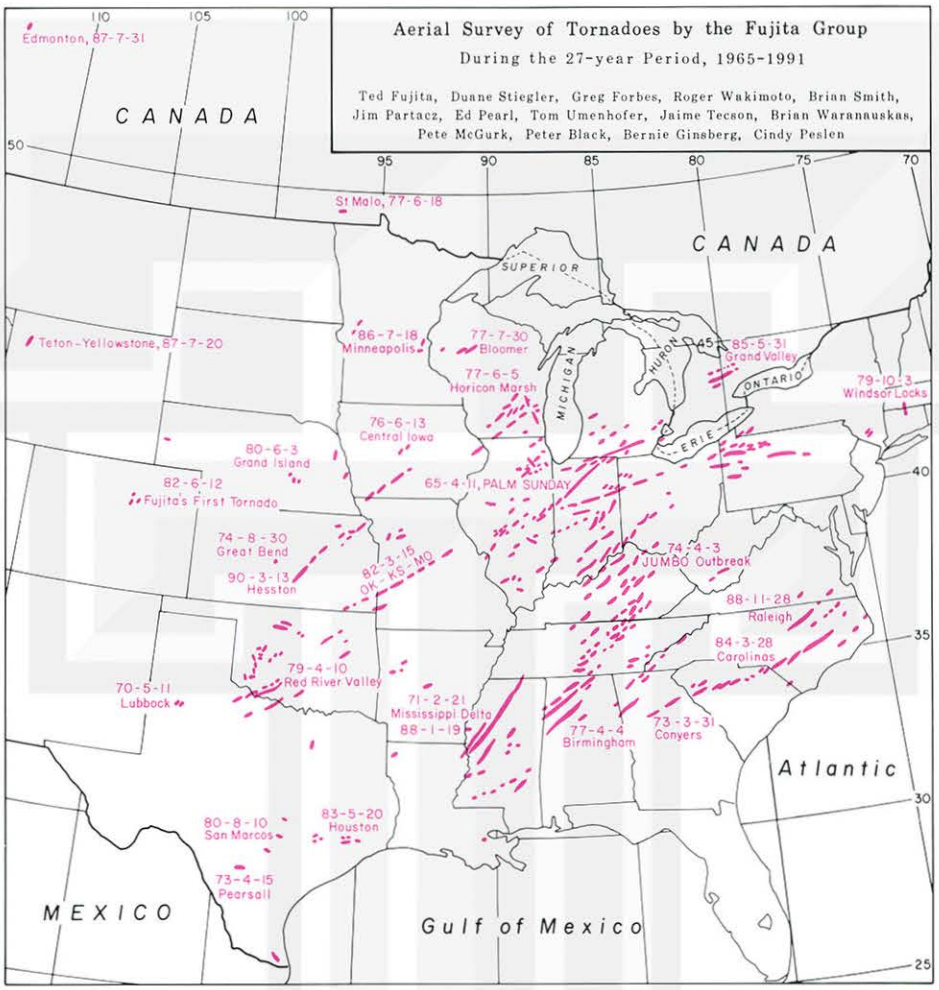

Fig. 2.5-1 Damage paths of tornadoes surveyed by the Fujita group mostly from low-flying Cessna aircraft. Over 300 damage swaths were flown over.

Suction Vortex Hypothesis

High-quality aerial photos taken from low-flying aircraft over the damage swaths of more than 300 tornadoes revealed the existence of ground marks generated by small swirling winds. In general, a large swirl, acting like a small hurricane, blows objects while a small swirl lifts objects. In other words, a large swirl acts like a blower and a small swirl, like a sucker. A tornado behaves either like blower or sucker or their combination.

On the basis of the cycloidal ground marks photographed from the air and on the ground (Fig. 2.5-2), I concluded in 1971 that a cycloidal mark can be produced by a small but strong vortex, the **Suction Vortex,** as it orbits around the core of a tornado (Fig. 2.5-3). No matter how strong a vortex might be, it does not lift the debris at

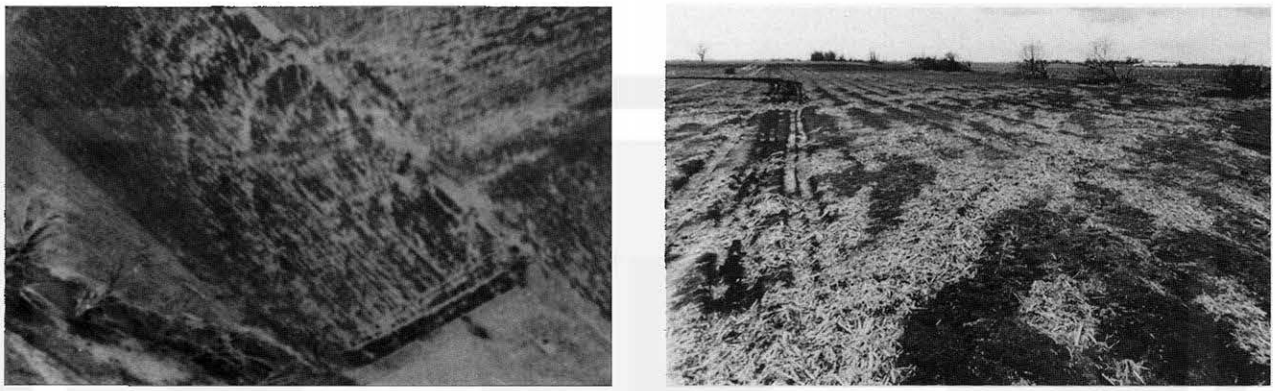

Fig. 2.5-2 An aerial photograph of cycloidal marks (left) of the Barrington, Illinois tornado of 21 April 1967 and its close-up view on the ground.

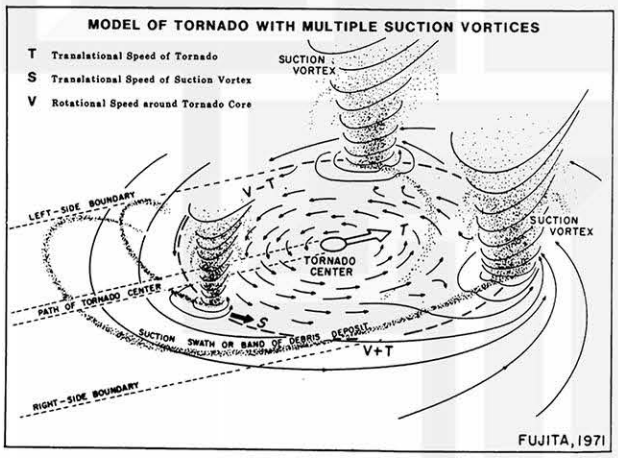

Fig. 2.5-3 A model of tornado with suction vortices around its core. This hypothetical model was produced based solely on the geometric shape and characteristics of cycloidal marks which consist of litter/debris. It is assumed that a small but strong vortex will collect debris, but it will leave behind the debris on the ground at the vortex center.

the ground where vertical motion is zero. Some meteorologists did not believe my story until vortex pictures became available (p286).

An excellent example of an effort of a small tornado trying to pull up a tree in an open field (Fig. 2.5-4) was recorded by a video taken from a helicopter of KARE-TV. The tree was in an upright position while resisting the vertical winds acting as a sucker.

The geometric shape of the ground marks of an orbiting suction vortex can be used in computing the orbital speed of the vortex. Based on the orbital geometry (Fig. 2.5-5), the intensity of the Goessel tornado was rated F5. As seen in this example, aerial photographs of the specific damage is important in assessing the nature of tornado winds.

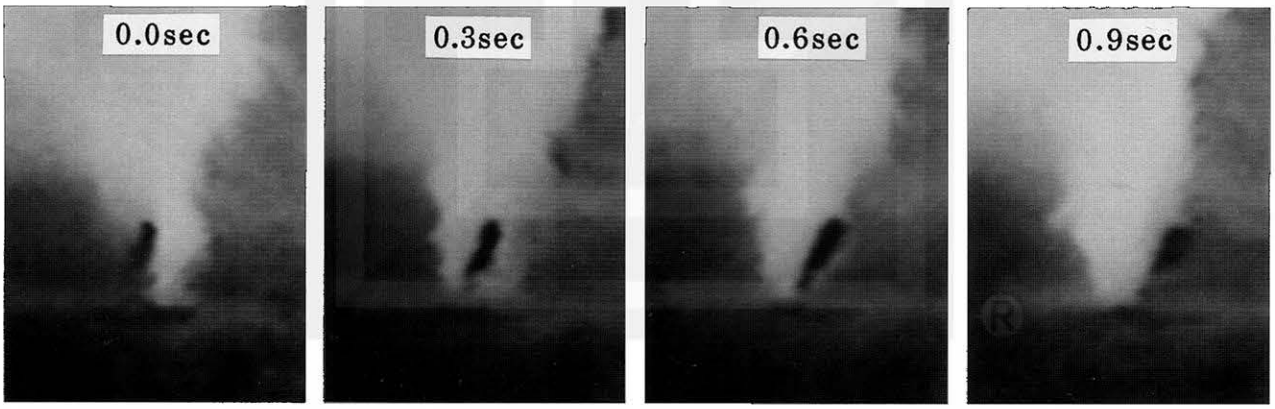

Fig. 2.5-4 Four frames of the video provided by Mr. Paul Douglas, chief meteorologist, News 11 of Minneapolis showing the helicopter view of the Minneapolis tornado of 18 July 1986.

Fig. 2.5-5 Goessel Tornado of 13 March 1990 (left) photographed by Doug Nelson and the cycloidal marks (right) produced by the tornado. Aerial photograph by Duane Stiegler.

Fig. 2.5-6 Liftoff point of the Magnet, Nebraska tornado of 6 May 1975. After taking the aerial photo (right) Ted Fujita visited the liftoff point on the ground (left).

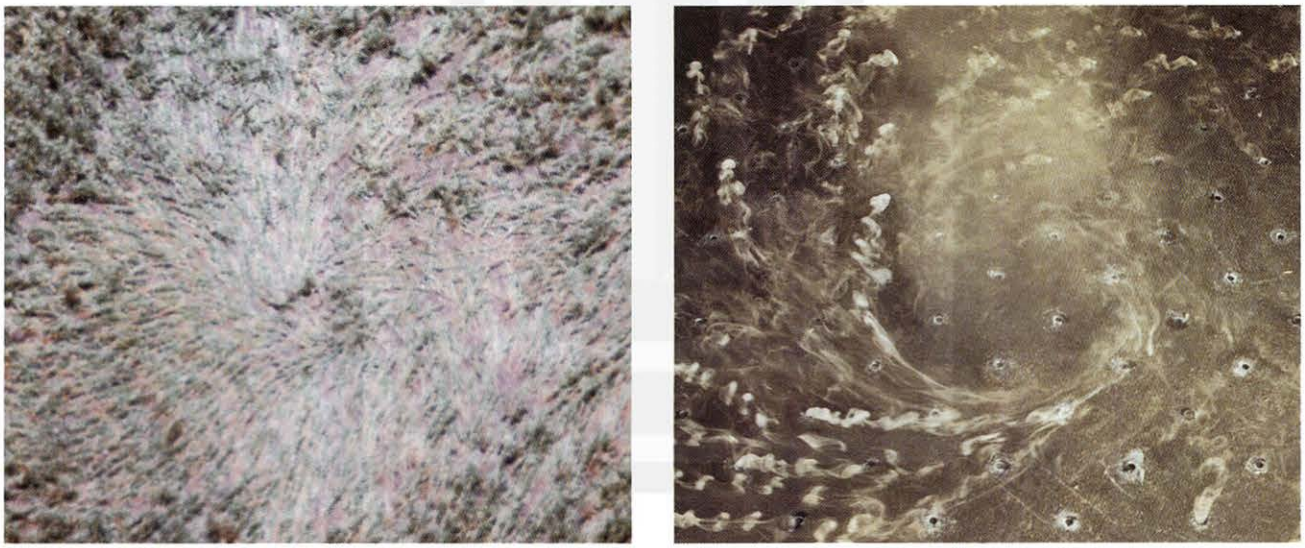

Fig. 2.5-7 A small eye of a stationary suction vortex (left) and my laboratory model of a small vortex with a calm eye inside.

JUMBO OUTBREAK TORNADOES of 3-4 April 1974

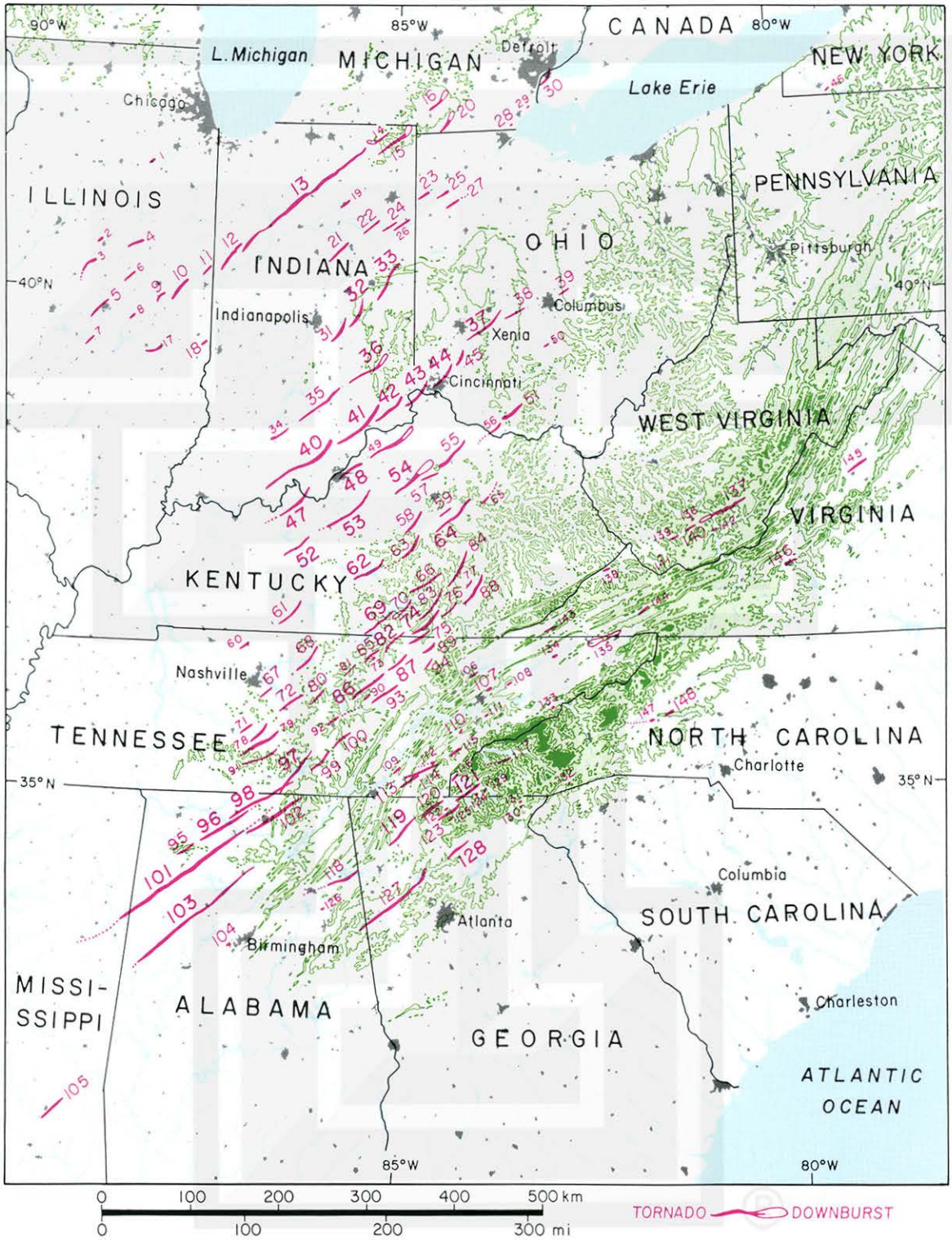

Fig. 2.5-8a Paths of the Jumbo (Super) outbreak of 148 tornadoes on 3-4 April 1974. After the initial path map was completed in 1974, some tornadoes were reassessed as damaging downbursts.

Jumbo Outbreak Tornadoes, 1974

This unusual outbreak has been identified as (1) "**Superoutbreak**" which denotes a large number of damaging tornadoes, and (2) "**Jumbo Outbreak**" because the date of the onset in 1974 (74) in the 4th month on the 3rd day (4+3=7) can be memorized as the numerals of the 747 Jumbo Jet which implies a jumbo-size outbreak.

The outbreak started at 1210 CST on the 3rd of April and ended at 0520 CST on the 4th, after 17 hrs and 10 min. In the wake of the 148 tornadoes, 315 persons were killed, injuring 5,484 others. The total composite path length was 2,584 miles (4,180 km). In visualizing the extent of the outbreak, paths of the 148 tornadoes (Fig. 2.5-8a) were superimposed upon the map of Japan in the identical scale (Fig. 2.5-8b). Should an outbreak of this magnitude occur in Japan, the aftermath of the storm could create a national disaster.

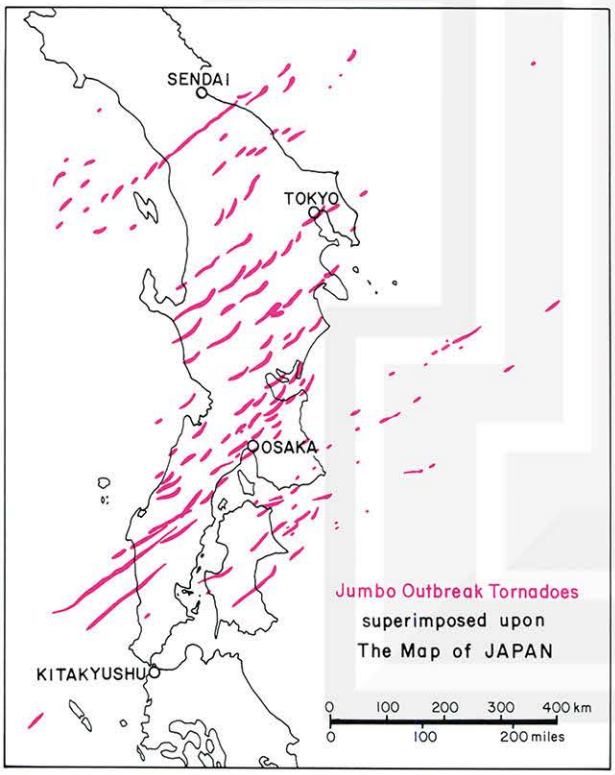

Fig. 2.5-8b Jumbo outbreak of 148 tornadoes superimposed upon the same-scale map of Japan.

Immediately after the outbreak, I initiated a jumbo-scale, fact-finding aerial survey and photography over the 13 states and Windsor, Canada. The participants and their organizations at that time were Fujita, Forbes, Pearl, Tecson, Pasken, LaPlaca, and Sereno (my group at U. of Chicago), Golden and Lemon (NSSL), McCarthy (U. of Oklahoma), and Shanahan (S&W Engineering Corp.). Without the cooperative efforts of these dedicated individuals, the extent of the worst outbreak in recent memory could not have been documented with success. Some of the data/analyses are presented in this book (pp280-283, 287, and 288).

Pearsall Tornado, 1973

The Pearsall, Texas tornado of 15 April 1973 moved across I-35, 90 miles north of the Mexican border at 1720 CST. While U.S. cars were waiting on shoulders, two cars from Mexico drove into the dark cloud on the highway. Of the 8 occupants, 5 were killed instantly.

During my damage survey, I have never seen such a brutal destruction of cars by an F4 tornado. Passenger seats were stripped off steel frames and individual tires and springs were scattered all over the peanut field. Even axles were broken into several pieces.

From helicopter, I found cycloidal marks in wheat fields, which were made visible by the sunlight scattering from the leaves of blown down wheat. The forward-scattering light was strongest while back-scattering was insignificant. I took six pictures to demonstrate the change in the view of cycloidal marks from bright to dark (Fig. 2.5-9). In taking pictures of cycloidal marks in cornfields, we have to choose the best direction of view relative to the sun. Otherwise, one will see nothing from the air.

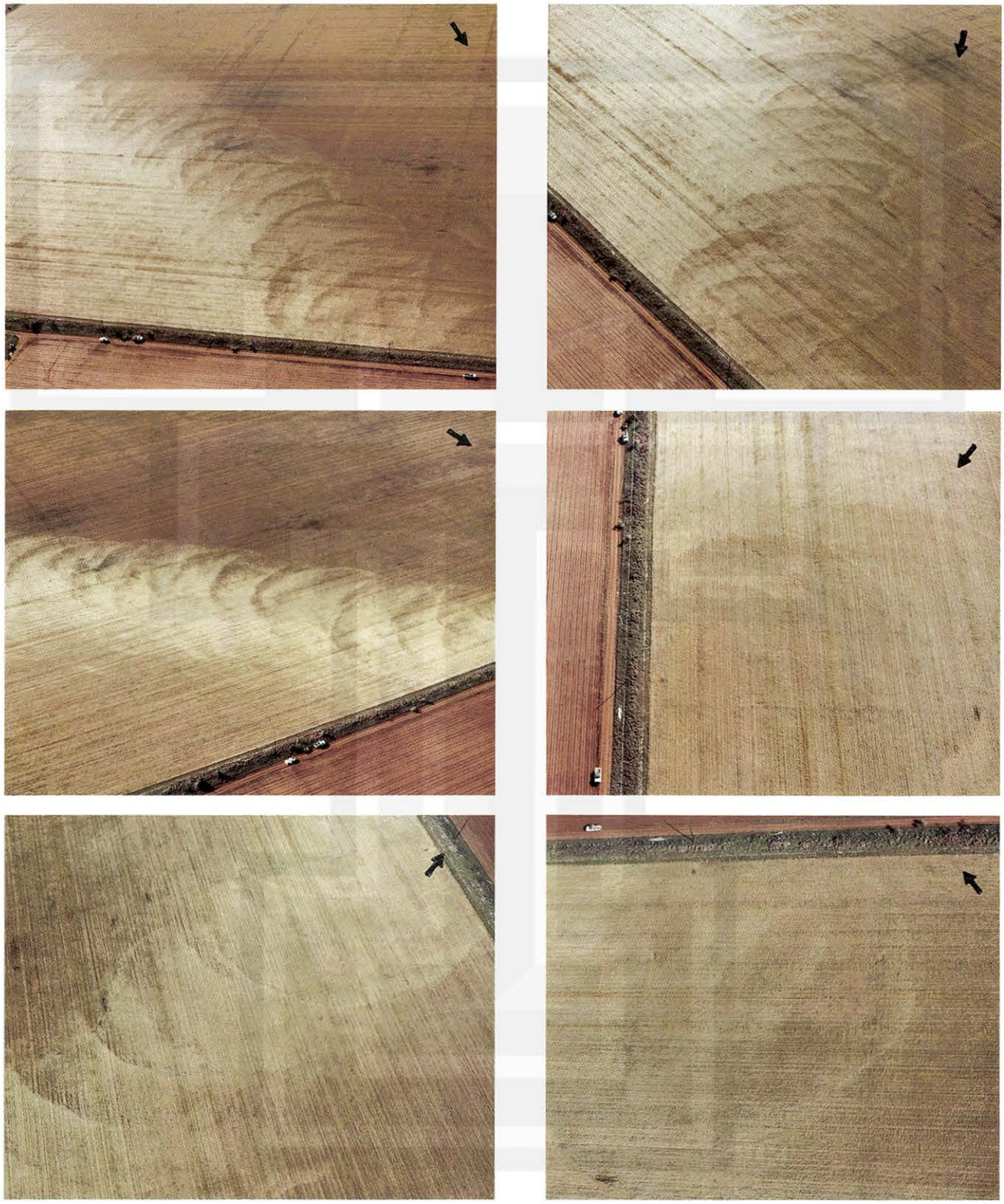

Fig. 2.5-9 Suction vortex marks in the wheat field after the Pearsall, Texas tornado of 15 April 1973 photographed by Ted Fujita from six different directions. An arrow in each picture shows the direction of sunlight.

Bossier City Tornado, 1978

The Bossier City, Louisiana tornado of 3 December 1978 traveled 6.8 miles (11 km) from Bossier City toward the northeast. The F4 tornado at 0150 CST lifted a number of heavy objects. A car was thrown into a house, killing two sisters while asleep in bed.

A three-men team consisting of Dr. Robert Abbey then with the Nuclear Regulatory Commission, Prof. James McDonald of Texas Tech University and myself arrived at Shreveport on the day after the tornado to survey the damage. At Meadowview Elememtary School, six I-beams, B through G, each weighing 700 lbs (320 kg) became airborne (Fig. 2.5-10). I-beam D (Fig. 2.5-13) stuck into the ground at 23° angle while others flew 60 m to 370 m (200' to 1200'). It is hard to believe that an I-beam could fly such a distance without a portion of the roof attached.

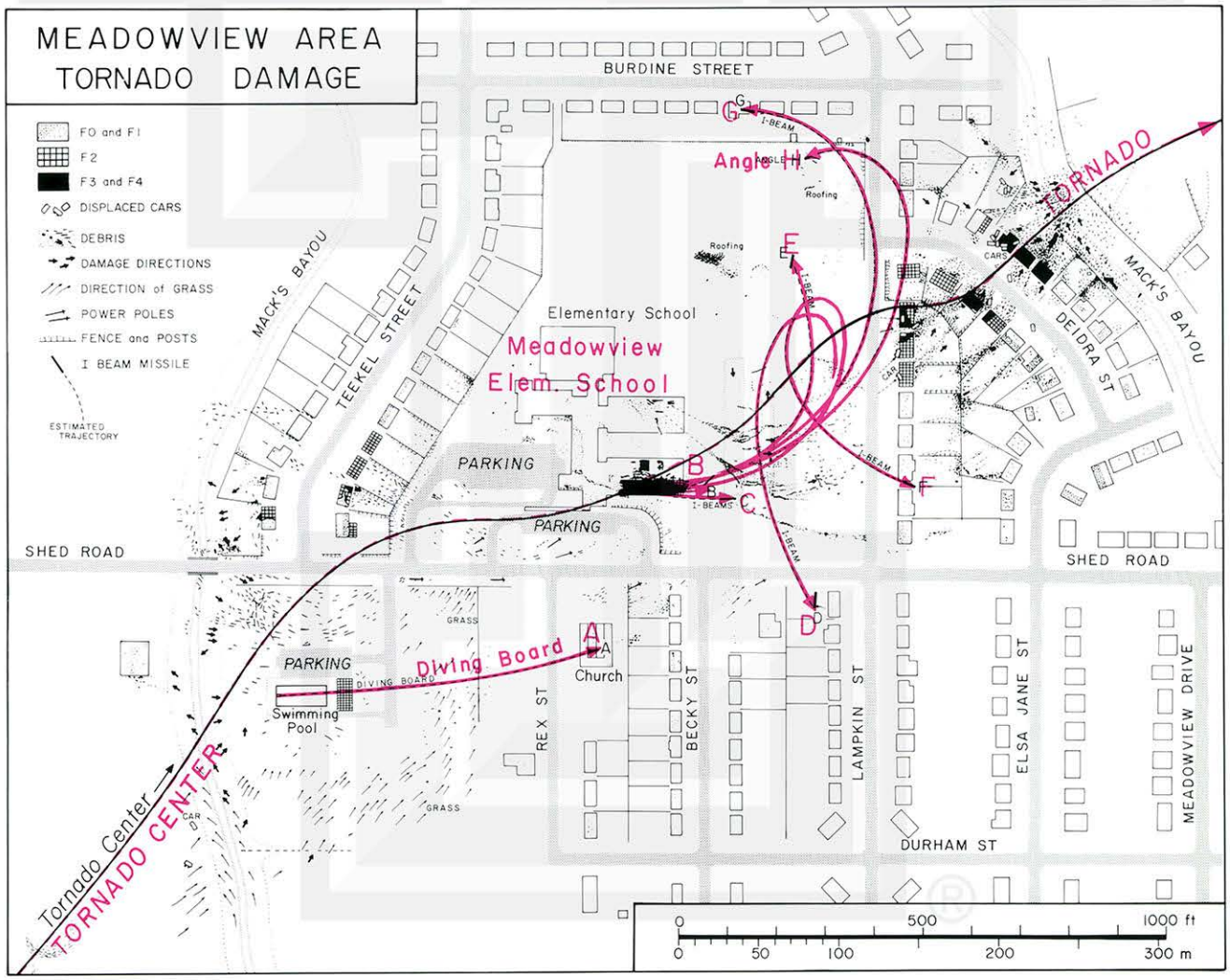

Fig. 2.5-10 Estimated trajectories of the six steel I beams which became airborne during the Bossier City, Louisiana tornado as it passed over the Meadowview Elementary School.

Fig. 2.5-11 Meadowview Elementary School where the six I-beams originated.

Fig. 2.5-12 Three girls studying in the school yard after the tornado.

Fig. 2.5-13 I-beam "D" stuck in the backyard of a house on Lampkin Street.

Fig. 2.5-14 Bob Abbey (left) and Ted Fujita (right) hanging on the steel I-beam to test its strength in supporting our weights. It did not move even a millimeter.

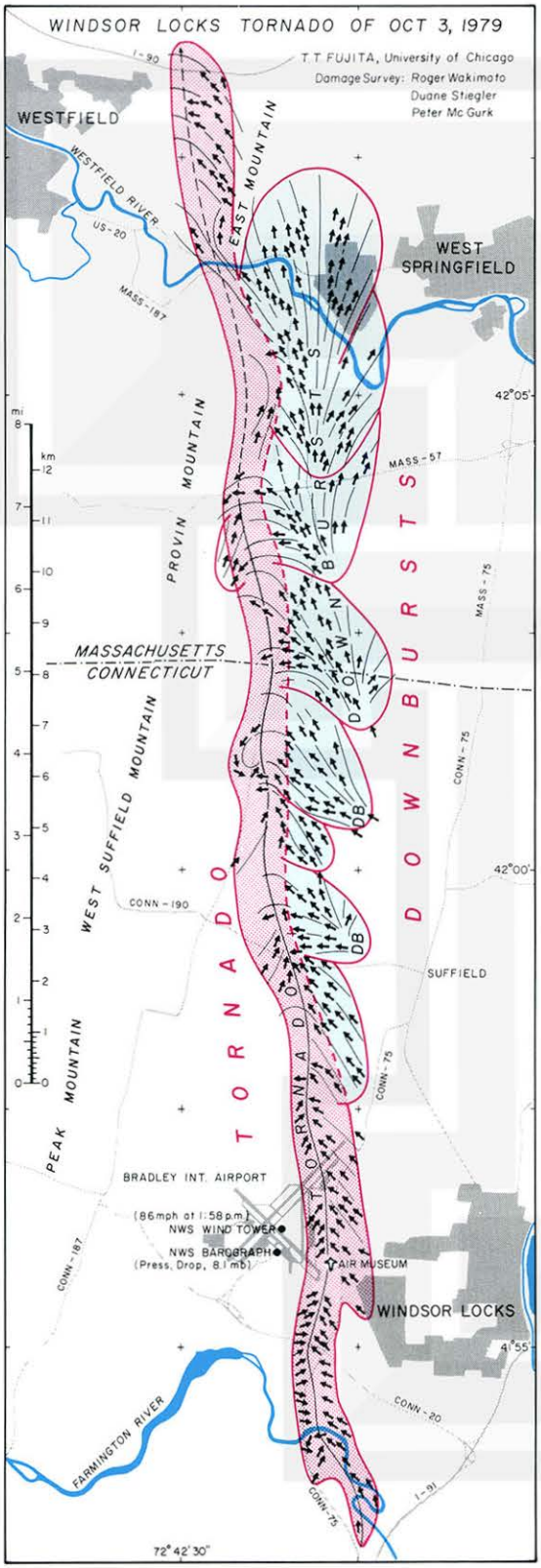

Fig. 2.5-15 A series of microbursts/downbursts descended on the right side of the tornado.

Windsor Locks Tornado, 1979

The Windsor Locks tornado of 3 October 1979 was surveyed from the air and ground by my staff members, Roger Wakimoto, Duane Stiegler, and Peter McGurk. The tornado moved north across the Connecticut-Massachusetts state line. The most interesting damage pattern was a series of seven downburts (microbursts) descended on the east side of the tornado (Fig. 2.5-15). The damage pattern implies that each microburst forced the tornado center to deviate to the left (west), while adding cyclonic angular momentum to the tornado circulation.

A scene of interacting tornado and microburst was videotaped (Fig. 2.8-6) by Mr. Mike Phelps on 12 April 1991 near Lincoln, Nebraska. My analysis (Fig. 2.8-5) of the Mobara, Japan tornado also shows the weakening and reintensification of the tornado vortex as it was interacting with the microburst(s) descended on the right (east) side of the tornado.

Grand Island Tornadoes, 1980

The Grand Island, Nebraska tornadoes were very unusual because they consisted of seven tornadoes which rotated either clockwise or counterclockwise. The WSR-57 radar at Grand Island photographed tornado echoes which were combined with damage swaths to determine the movements of the seven tornadoes during the 2 hrs and 45 min period between 1945 and 2230 CST (Fig. 2.5-16).

The old section of the city was damaged by an anticyclonic tornado while the new southeast section, by a cyclonic tornado which shrunk from 1.5 miles initial diameter to 0.7 mile while intensifying from F2 to F4.

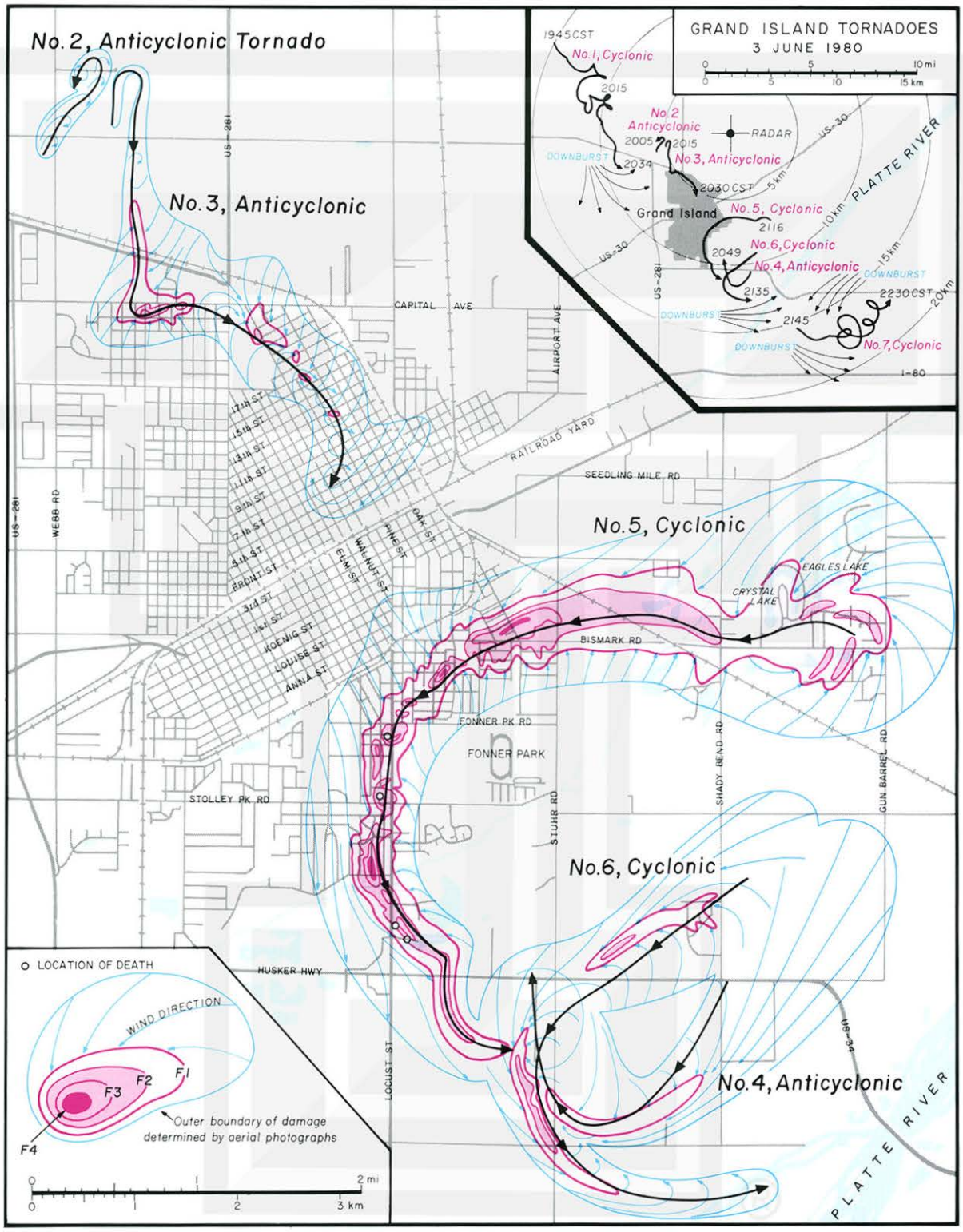

Fig. 2.5-16 The Grand Island, Nebraska tornado of 3 July 1980 consisting of 4 cyclonic and 3 anticyclonic tornadoes. In addition, 4 downbursts occurred while tornadoes were in progress. These were the most complicated tornadoes I ever surveyed.

Central Kansas Tornado(es), 1990

The Central Kansas tornado of 13 March 1990, extending from Pretty Prairie to 12 miles northeast of Dwight was confirmed as a long-track tornado with 110-mile path length. Duane Stiegler's aerial survey performed two days after the tornado suggested the existence of a 10-mile gap in the path between Hillsboro and Pilsen across Marion Reservoir. The gap was also confirmed by the video by Mrs. Denise Bina, showing the dissipation of the funnel followed by the touchdown of a new tornado near Pilsen. The long-track tornado was divided into the 60-mile long Hesston tornado (F4) and the 47-mile long Dwight tornado (F2).

Later, we received a video by KSNW-TV taken from I-135, two miles northwest of Hesston, showing two separate funnels simultaneously. An examination of the video frames raised a suspicion that a new tornado formed before the Hesston tornado ended on the east side of I-135. While Duane and I were thinking about two simultaneous tornadoes, a dedicated tornado chaser Jon Davies, president of Harvester Co., Ltd at Pratt, Kansas drove around the suspected areas of two concurrent tornadoes, mapping the path of the Hesston tornado merging to the path of a developing new tornado (Jon's letter to Fujita dated 23 March 1990).

Early in Summer 1990, I sent Duane again to the merger area northeast of Hesston to photograph the damage found by Jon and to take panoramic photographs at the sites of videos showing two tornadoes simultaneously. After his return to Chicago,

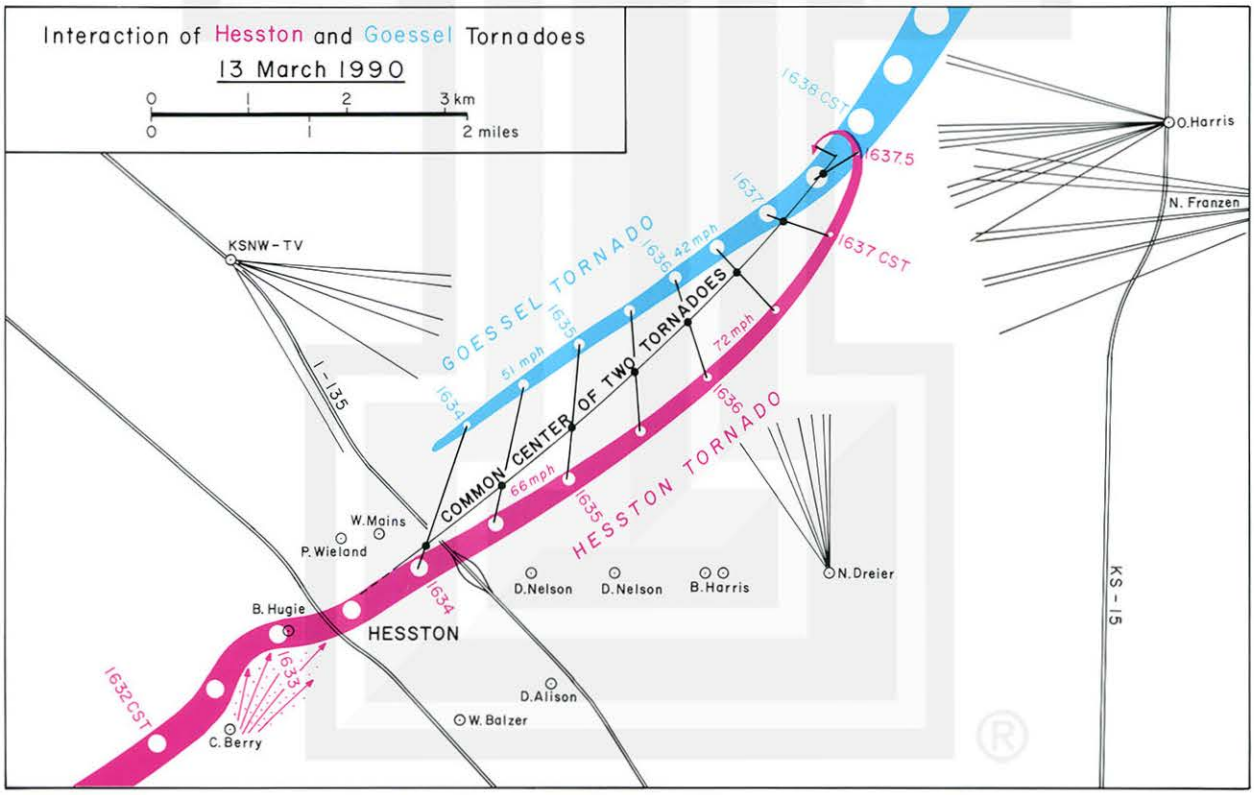

Fig. 2.5-17 Hesston and Goessel tornadoes which rotated around the common center. Radial lines from photographic sites denote azimuths of tornadoes used in triangulating interacting tornadoes moving like binary stars. Based on this analysis, the twin funnels of the Midway tornado of 11 April 1965 were reanalyzed (pp28 and 29).

we performed detailed photogrammetric analyses of the two interacting Hesston (old) and Goessel (new) tornadoes.

It was concluded that the new tornado formed on the east side of I-135 at 1634 CST while the old one was approaching I-135. The two tornadoes began interacting like binary stars, rotating around their common center. Two tornadoes interacting inside the circulation fields of each other may be called "**binary tornadoes.**" It is seen that the Hesston tornado was moving at 72 mph while the new tornado slowed down to only 42 mph due to their interaction.

The Goessel tornado intensified as it moved northeast, generating semi-circular ground marks on both sides of KS-15 while traveling at 40 to 45 mph. The intensity of the tornado estimated from the geometric shape of the cycloidal marks was F5.

Mystery of Cycloidal Marks

In 1971, I proposed that cycloidal marks in cornfields (Fig. 2.5-3) are the loci of sub-tornado vortices which rotate around the core of the tornado, calling the vortex, the "**suction vortex.**"

Some meteorologists did not agree with my concept on the ground that they have not seen a picture of a tornado with small funnel clouds rotating around the parent tornado. On the other hand, historian-type meteorologists found early tornado pictures with multiple funnels, stating, in effect, "Fujita's suction vortex is nothing new, because they were photographed long before his time."

While ignoring these contradictory comments, I waited for a chance of seeing a picture of tornado swirling directly above the cycloidal ground marks seen in aerial photograph. Thanks to Duane Stiegler for taking excellent aerial photographs of cycloidal marks of the Goessel tornado and to Doug Nelson, a dedicated tornado chaser who photographed the huge funnel of the Goessel tornado as it was swirling above the cycloidal marks (Fig. 2.5-5).

My photogrammetric comparison of ground marks and the Goessel tornado in action revealed that the orbiting suction vortices are identifiable only as pleats of the huge funnel on the ground (p37), not as the individual funnel clouds hanging from the base of the parent tornado. The Wichita Falls tornado (p286) was characterized by multiple funnels of suction vortices. However, their winds on the ground were too weak and diffused to generate the cycloidal marks seen in cornfields (p36) and in wheat fields (p40).

In other words, the suction vortices while generating cycloidal marks are so strong that they are hidden inside the dust and funnel clouds of the parent tornado. I have not yet seen other pictures showing cycloidal marks and generating tornado together. Until the mystery of the suction vortex is solved, the generation mechanism of the ground marks by suction vortices will remain as my brainchild.

Plainfield Tornado, 1990

The initial plan of including the Plainfield tornado in this book has been changed, because it will be published in the forthcoming Proceedings of Tornado Symposium III.

2.6 Fujita's First Tornado Observation

On 12 June 1982 during the JAWS Project, I observed for the first time in my life three tornadoes beneath a suspicious cloud I spotted from the CP-3 site (Fig. 2.6-4). Immediately thereafter, three Doppler radars and King Air began collecting multiple data on the tornadoes (Figs. 2.6-1, 2, 3, 5, 6, and 7). Tornado No. 2 was the largest and the best. It was detected by CP-4 PPI as a reflectivity eye (Fig. 2.6-10) and by CP-3 RHI as a huge pumpkin, 1200 m in diameter (Fig. 2.6-11). The maximum Doppler velocity by RHI scan with the 150 m x 500 m scan volume at the range of the tornado was approaching 20 m/s at 500 m AGL. However, the tornado at

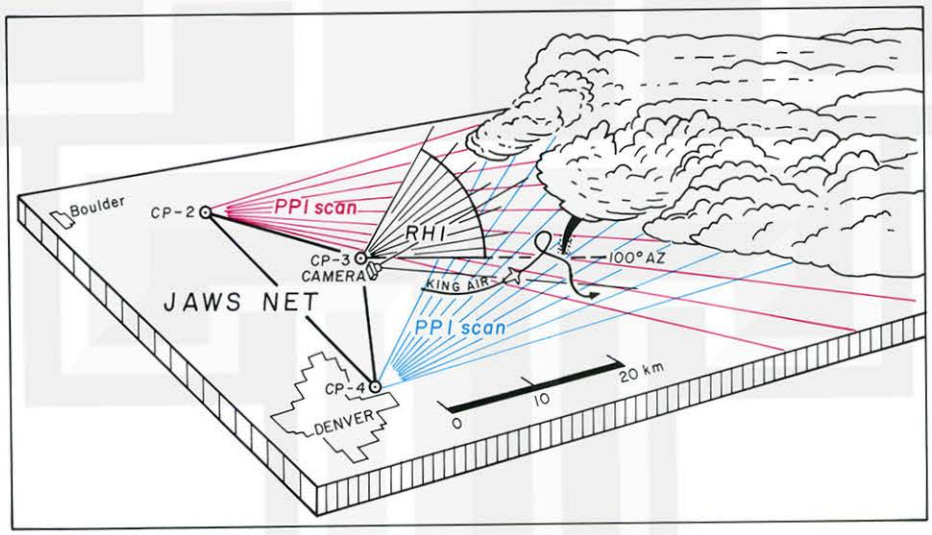

Fig. 2.6-1 Schematic diagram showing Fujita's first observation of tornadoes on 12 June 1982 during the JAWS Project.

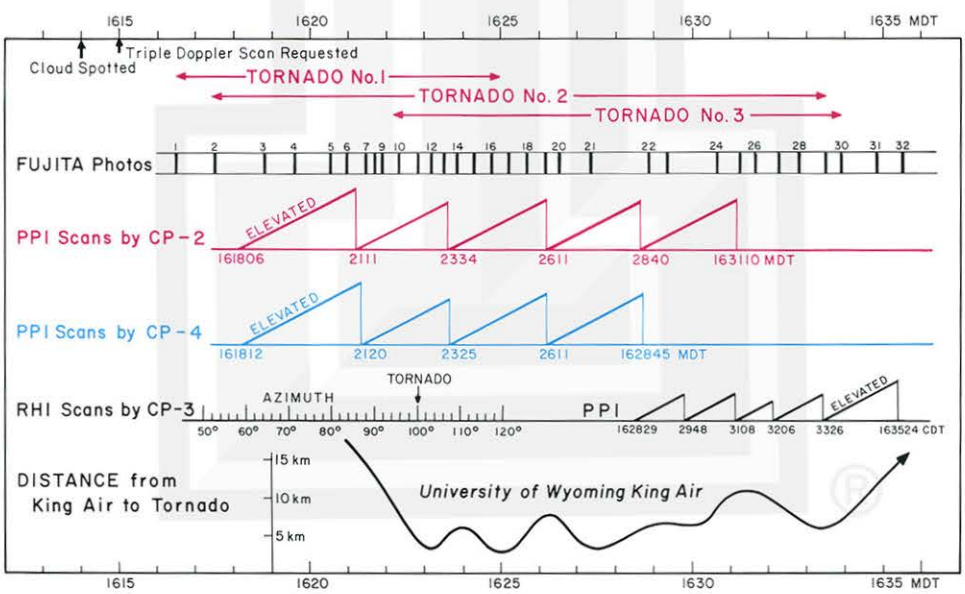

Fig. 2.6-2 Three tornadoes were scanned by NCAR's three Doppler radars and photographed by Fujita from the CP-3 Doppler radar site where he spotted a suspicious cloud at 1614 MST. King Air flew very close to Tornado No. 2.

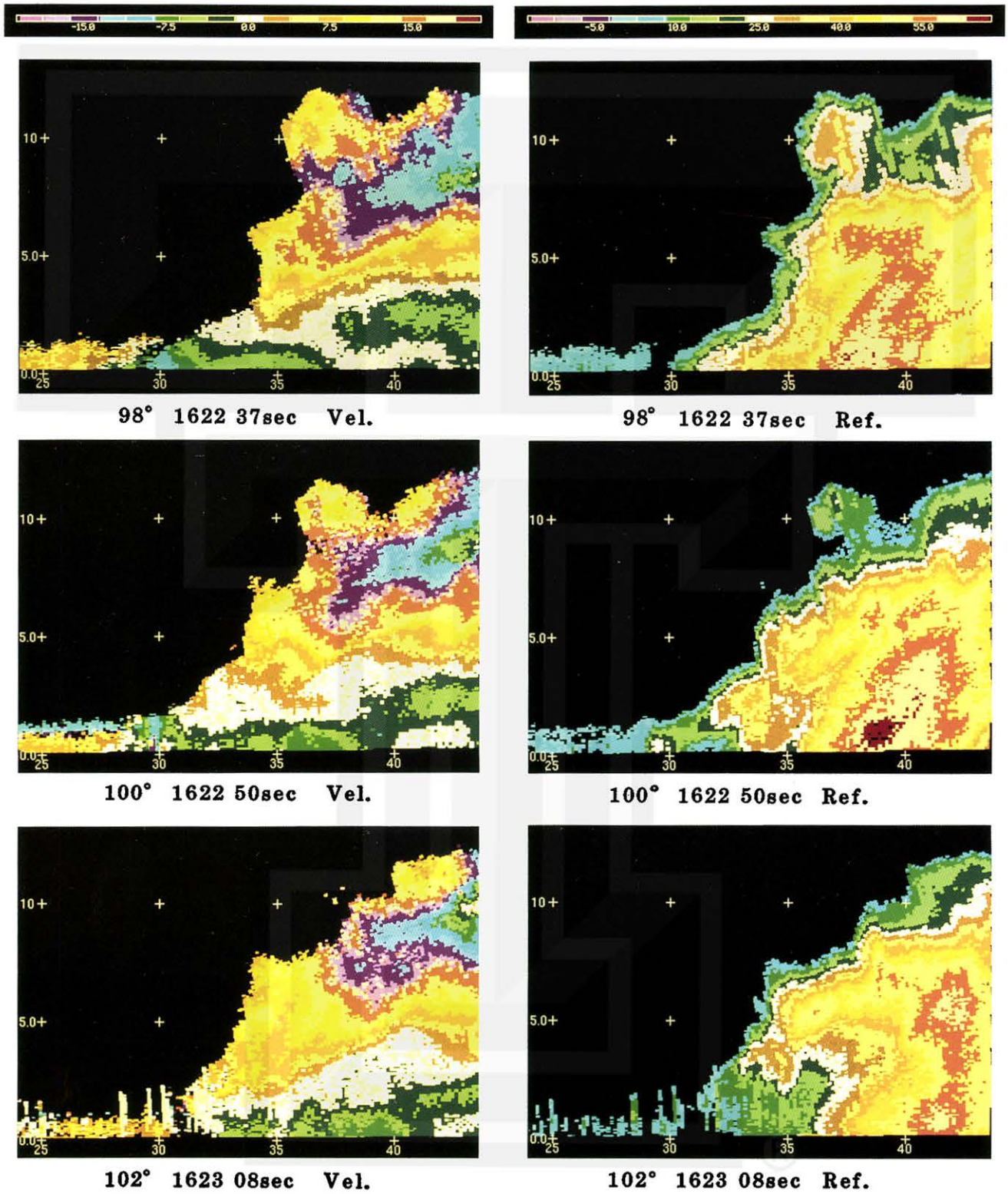

Fig. 2.6-3 Three RHI cross sections of Fujita's first tornado observed on 12 June 1982 using JAWS equipment. The center of the tornado on the ground was at 100° azimuth and 29.5 km range.

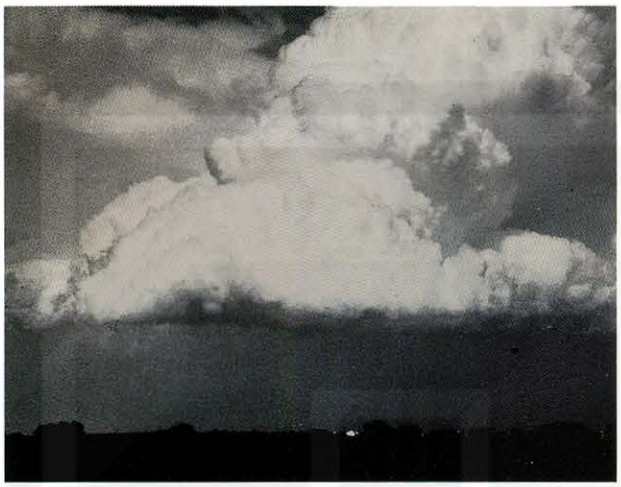

Fig. 2.6-4 A cumulus tower with tilted axis at azimuth 68°. Photo by Ted at 1618 MDT 12 June 1982.

Fig. 2.6-5 Tornadoes No. 1 (left) and No. 2 (center) photographed by Ted at 1621 40 sec.

Fig. 2.6-6 Tornado No. 2 at 1622 MDT photographed by Prof. Kerry Emanuel from the King Air.

Fig. 2.6-7 Tornadoes No. 2 (left) and No. 3 at 1629 57 sec photographed by Mr. Wayne Sand.

Fig. 2.6-8 Side of the gravel road north of the Wagner farm eroded by Tornado No. 2.

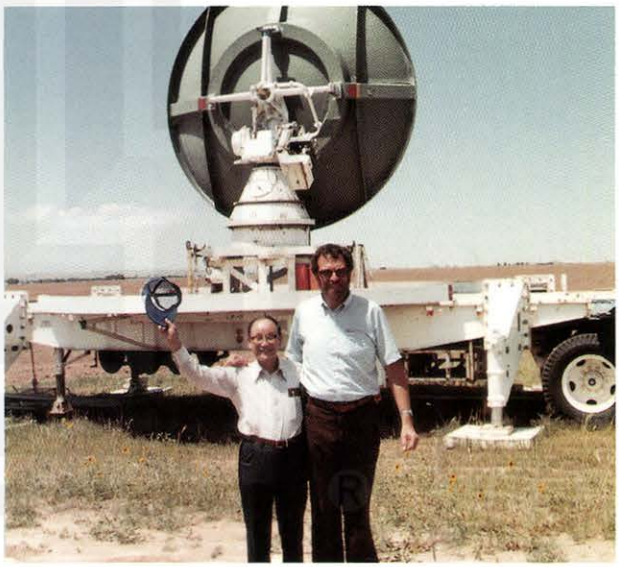

Fig. 2.6-9 Happy Ted Fujita after observing his first tornado and being greeted by John McCarthy.

the RHI scan time eroded the gravel road with estimated F2 winds (Fig. 2.6-8), suggesting that the Doppler velocity was too low to be realistic due to large-volume averaging.

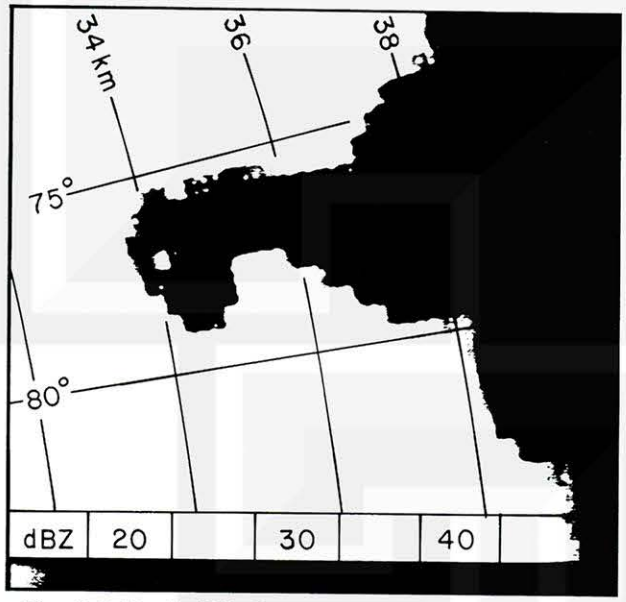

Fig. 2.6-10 A PPI photograph of Tornado No. 2 at 161852 MDT taken by CP-4 with 4.0° elevation angle at 2.4 km AGL at the range of the tornado.

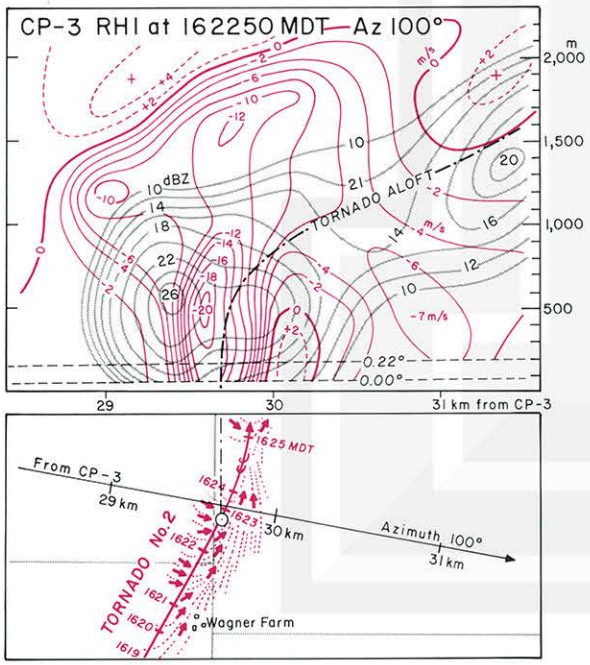

Fig. 2.6-11 Detailed analysis of relfectivity (dBZ) and Doppler velocity (m/s) along the 100° azimuth 100 m north of the tornado center.

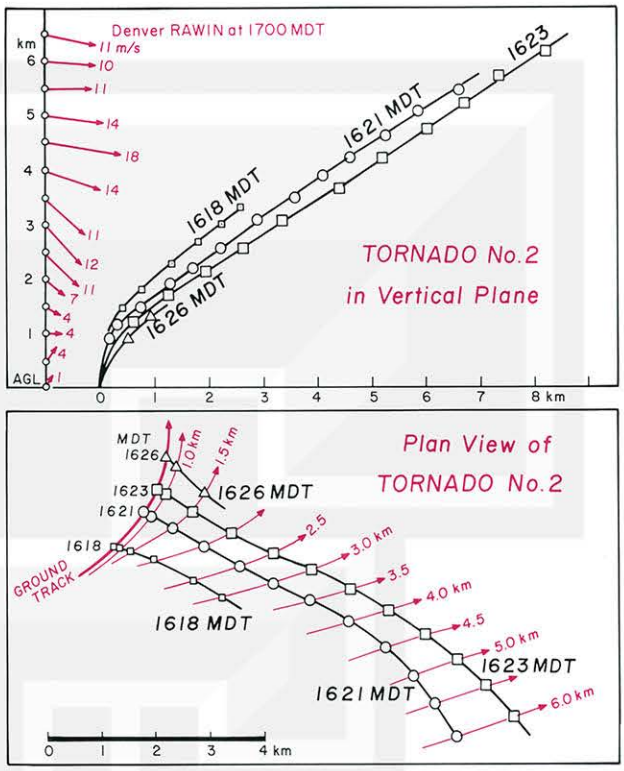

Fig. 2.6-12 The vortex axis of Tornado No. 2 projected on both vertical and horizontal planes.

Of interest is the evolution of the vortex axis of Tornado No. 2 which extended up to 6 km AGL into the cloud (Fig. 2.6-12 upper). Apparently, the tilt of the vortex axis increased from the first detection at 1618 MDT to the last, at 1626 MDT. The tilt was probably caused by the 10 to 18 m/s westerlies between 4 and 6 km AGL seen in the Denver RAWIN at 1700 MDT.

The plan view of the vortex axis (Fig. 2.6-12 lower) reveals the northeast to northerly movement of the tornado on the ground. However, the axis above the 2 km AGL moved eastward, suggesting that the axis incloud was displaced gradually by the vortex-level airflow. In other words, **Tornado No. 2 formed inside the near-ground boundary layer outside the cloud,** maintaining its vertical axis at the surface. The axis stretched into higher levels while interacting with incloud airflows. This preliminary research as of 30 June 1992 will be completed with Jim Wilson of NCAR.

2.7 Selected Canadian Tornadoes

Rosa Tornado of 18 June 1977

This rare tornado lifted a house off its foundation, killing two persons. Requested by the Winnipeg Weather Office, I visited the St. Malo area to conduct an aerial survey.

It was an F4 tornado spawned by an isolated thunderstorm in satellite pictures (Figs. 2.7-1 and 3). Located along the center line of the damage swath were several swirl patterns of uprooted trees commonly seen in the wake of a slow-moving, large tornado. As the tornado crossed Highway 59, it blew off a section of the pavement.

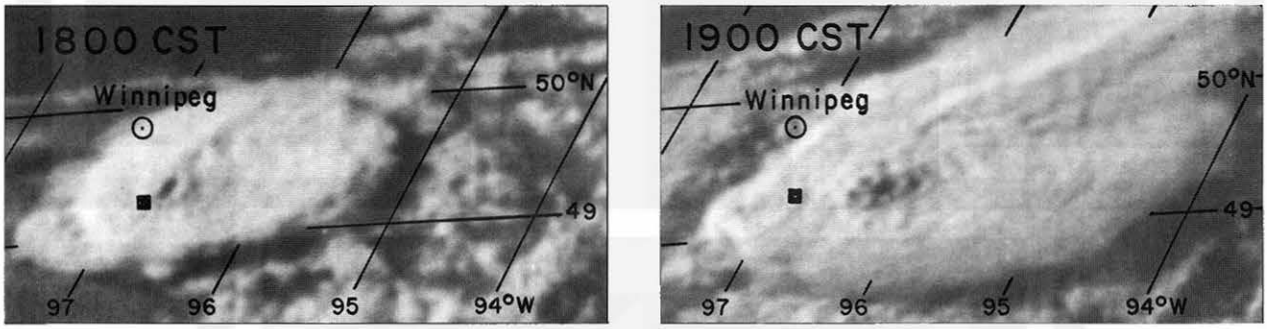

Fig. 2.7-1 Visible images of GOES showing the Rosa tornado cloud at 1800 CST and 1900 CST located to the south-southeast of Winnipeg, Canada on 18 June 1977.

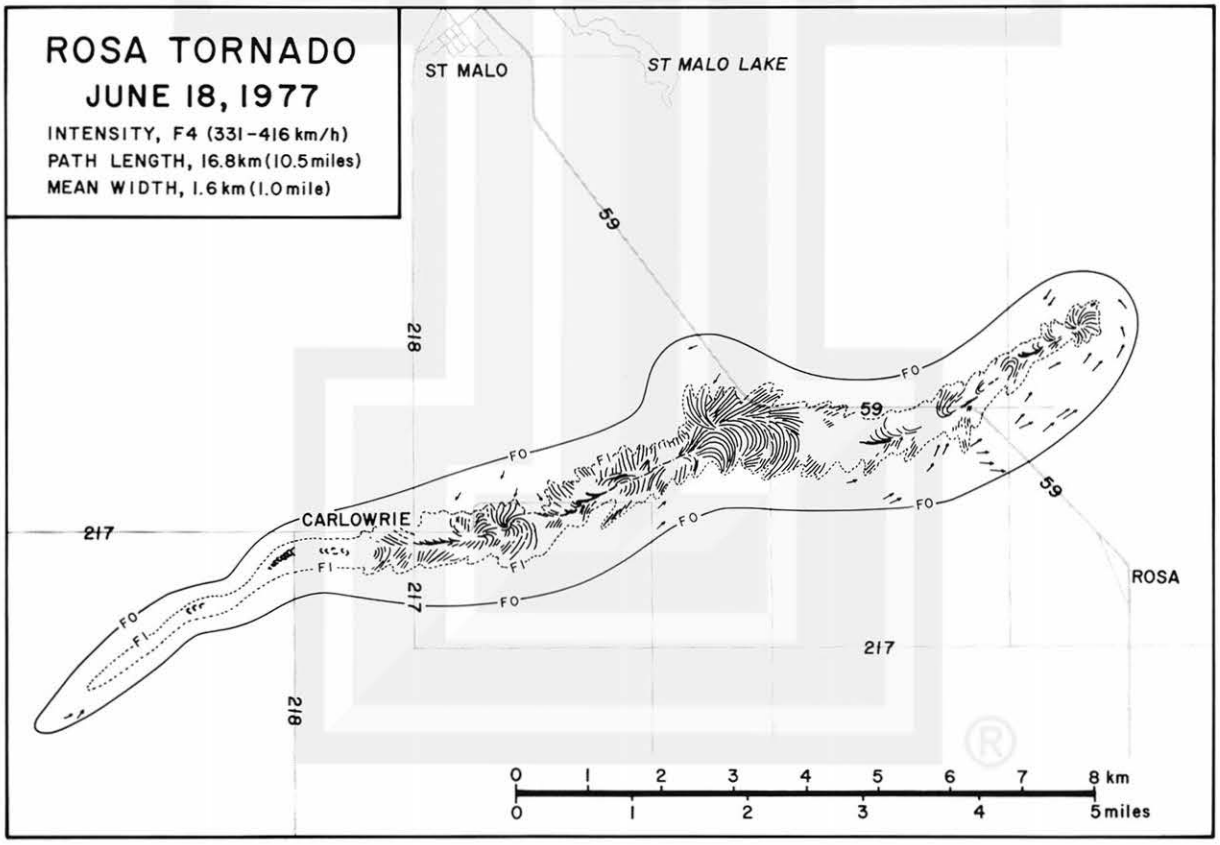

Fig. 2.7-2 The 16-km path of the Rosa tornado (F4). The asphalt pavement on Highway 59 two miles northwest of Rosa was blown off. Aerial survey and mapping by Ted Fujita.

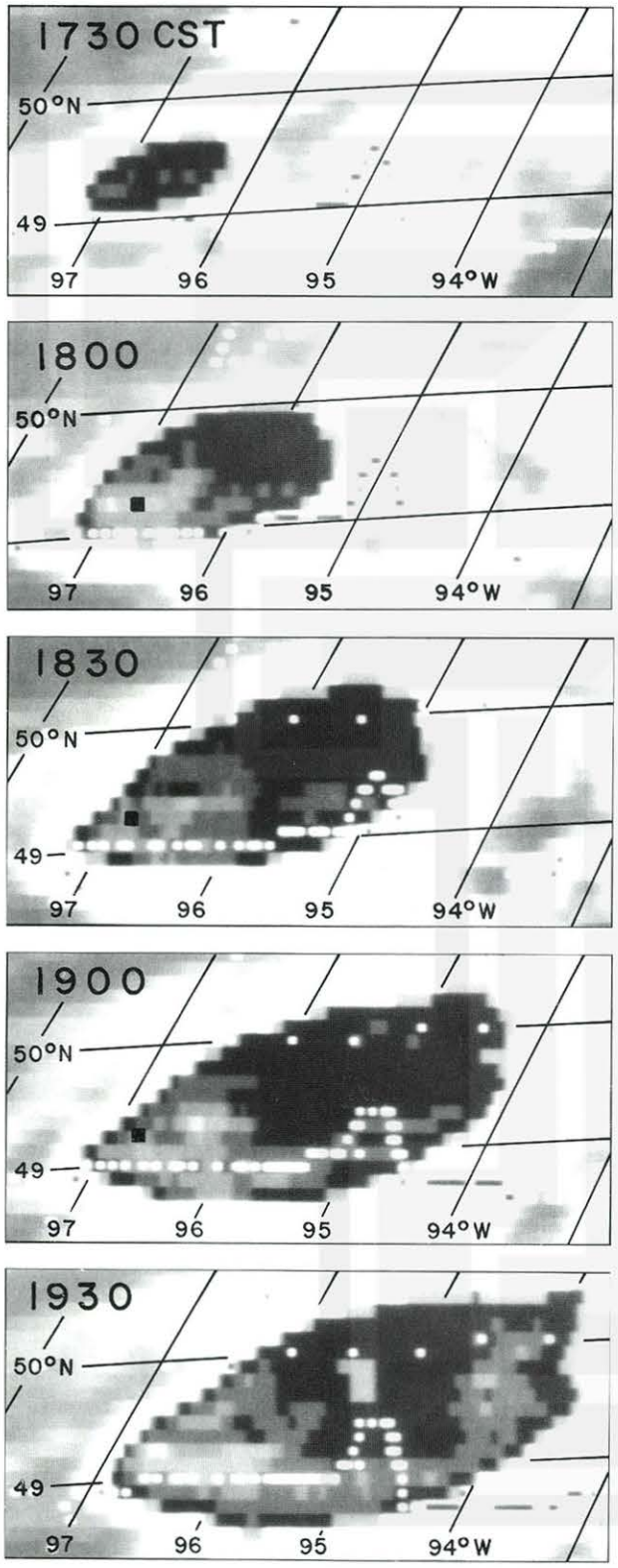

Fig. 2.7-3 Five infrared pictures at 30-min intervals taken by GOES on 18 June 1977. Painted square denotes the Rosa tornado.

Edmonton Tornado of 31 July 1987

This tornado was surveyed by Brian Smith of my staff then, and rated as F4. The damage path was 23-mile long and one half mile wide on the average. Although the highest F-scale damage was near the 11 path miles, most deaths occurred at the trailer park near the end of the path.

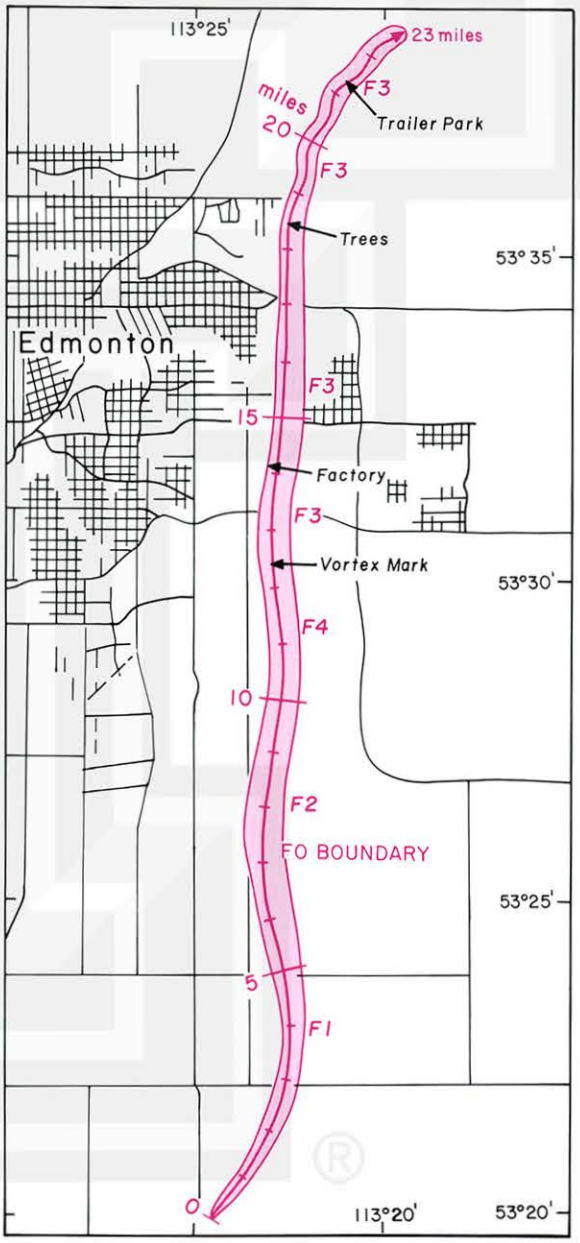

Fig. 2.7-4 The 37-km (23-mi) swath of the Edmonton, Canada tornado of 31 July 1987.

Fig. 2.7-5 A vortex mark in the field at 12.4 path miles in Fig. 2.7-4.

Fig. 2.7-6 An F3 damage of the factory at 14.1 path miles.

Fig. 2.7-7 Damaged trees on the river bank at 18.4 path miles.

Fig. 2.7-8 A trailer park at 21.3 path miles. All pictures were taken by Brian Smith.

2.8 Selected Japanese Tornadoes

Fig. 2.8-1 The Tokyo tornado of 24 May 1964 which left behind a 5-km path in Setagaya. Courtesy of Mr. Takashi Ohkami.

Fig. 2.8-2 Strength of an invisible waterspout a moment after its landing on the coast of Japan Sea. Courtesy of the Yomiuri Newspaper.

Although Japan is not yet collecting tornado data systematically, Professors Yasushi Mitsuta and Hatsuo Ishizaki of Kyoto University and Prof. Yukio Omoto of the University of Osaka Prefecture collected nationwide tornado data, finding the occurrences of 5 to 35 tornadoes a year. These frequencies prorated to the area of the contiguous United States are 80 to 700 a year.

On the average, tornadoes in Japan are weaker than U.S. tornadoes, rarely reaching the F4 intensity and no F5 storm has been confirmed. Due to high density of population, tornado hazards in cities and suburban areas became a concern.

Before coming to the United States, I surveyed the Yanagawa tornado of 29 September 1947 (p194). After moving to the U.S., I studied three more Japanese tornadoes, the Omiya tornado (F3) of 7 July 1971, publishing a paper by Fujita, Watanabe, Tsuchiya, and Shimada (1972c), and the Tokyo tornado of 28 February 1978, reported by Fujita (1978b), which hit a 10-car subway train while crossing the Arakawa bridge. Two cars overturned and 3 derailed, injuring 21 passengers. Presented in this book are the results of my analysis of the Mobara tornado of 11 December 1990.

On 23 June 1985, an F2 tornado occurred in Kokura Section of Kitakyushu City, 5 km northwest of my birthplace, the residence of my brother Sekiya. Mr. Okabe, a photographer of the Yomiuri Newspaper was on his way to shopping when he saw numerous roofing tins and tiles flying around an approaching dark cloud. After he took the picture (Fig. 2.8-3), he had to move his car 100 m (300') to avoid the oncoming tornado.

Japan is a land of earthquakes and heavy rainfall. Although weak tremors do not damage structures, they loosen tiles on the roofs, causing rain leaks. As a result, tin roofs became popular and they use eaves and/or extended tin roofs in order not to get wet in rain. Naturally, extended tin roofs are vulnerable to tornado winds which swirl and rise violently.

Several days after the tornado, I called my brother to request his damage survey by car and on foot. According to his house-to-house survey map (Fig. 2.8-4), the tornado moved through densely-populated areas. A monorail track, the Nippo mainline, and its branch line were in the 3.2-km path of the F2 tornado. In the wake of the Kokura tornado, 277 houses were damaged and one woman was injured as she was blown off the ground and hit by a piece of lumber.

Fig. 2.8-3 Picture of the Kokura tornado at 1432 JST taken by Mr. Koji Okabe. Courtesy of Seibuhonsha of the Yomiuri Newspaper.

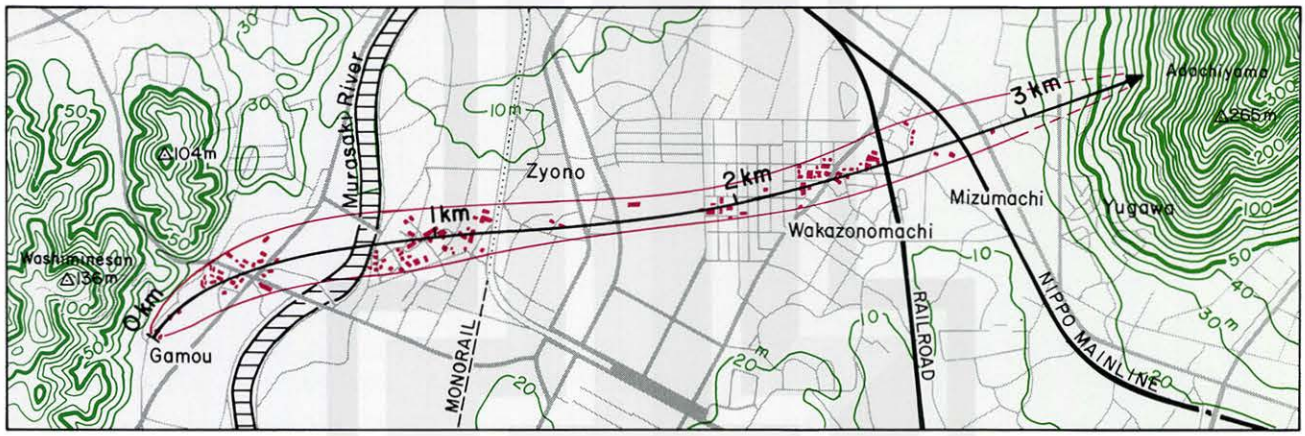

Fig. 2.8-4 The 3.2-km path of the Kokura tornado of 23 June 1985 surveyed by my brother, Sekiya Fujita.

Mobara Tornado of 11 December 1990

The City of Mobara located 60 km southeast of Tokyo was visited by an F4 tornado, one of the worst storms in post-war Japan. The tornado occurred after dark in winter, 3 weeks before New Year's Day, damaging 1,000 houses and injuring 60 persons.

On the day after the tornado, Japanese National Television (NHK) called me requesting for an independent study of

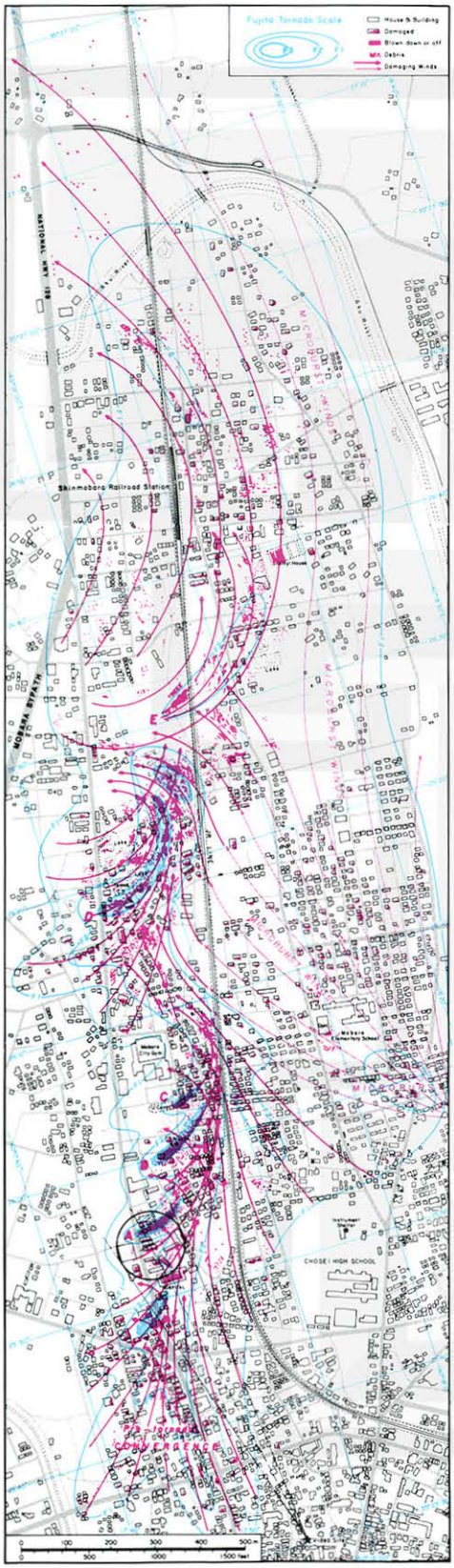

Fig. 2.8-5 Damage areas of the Mobara tornado of 11 December 1990 extending from the west of downtown Mobara to the north of the Shinmobara Railroad Station.

Fig. 2.8-6 An interaction between a tornado and a microburst on 12 April 1991 near Lincoln, Nebraska. The original video frames by Mr. Mike Phelps were printed backward to match viewing directions.

the storm based on my experience and method being used in studying U.S. tornadoes. They provided me with a video taken from a helicopter flown early next morning. Based on the enlarged video frames, I determined the damage directions of trees, debris, and structures, concluding that the Mobara tornado moved toward the north-northeast while a microburst (small downburst) descended to the ground on the east side of the tornado (Fig. 2.8-5).

When the tornado was undercut by the microburst winds, the initial course of the tornado deviated toward the left while passing between Mobara City Gymnasium and the JR railroad. As microburst winds weakened, the tornado redeveloped into a large vortex with its center near National Highway 128.

The first evidence of the tornado-microburst interaction was confirmed in the Windsor Locks tornado of 3 October 1979 (p43). On April 12, 1991, a video of the interaction phenomenon was obtained in Nebraska (Fig. 2.8-6).

Funnel Motion computed from Video

Five video frames showing the funnel cloud illuminated by a lightning flash was taken from a house 740 m to the south-southeast of the funnel (Fig. 2.8-7). The motion of the funnel cloud was computed at WRL, using the repetition movie technique. Computed velocities showed 93 m/s (208 mph) at 120-m AGL. The strongest vertical velocity was 61 m/s (136 mph) at 90-m AGL on the left edge of the funnel, while velocities on the right edge were horizontal (Fig. 2.8-8).

It has been known that a suction vortex which orbits around the core of a tornado forms where vertical motion is very large. When the video in lightning was taken, the left edge of the funnel was moving

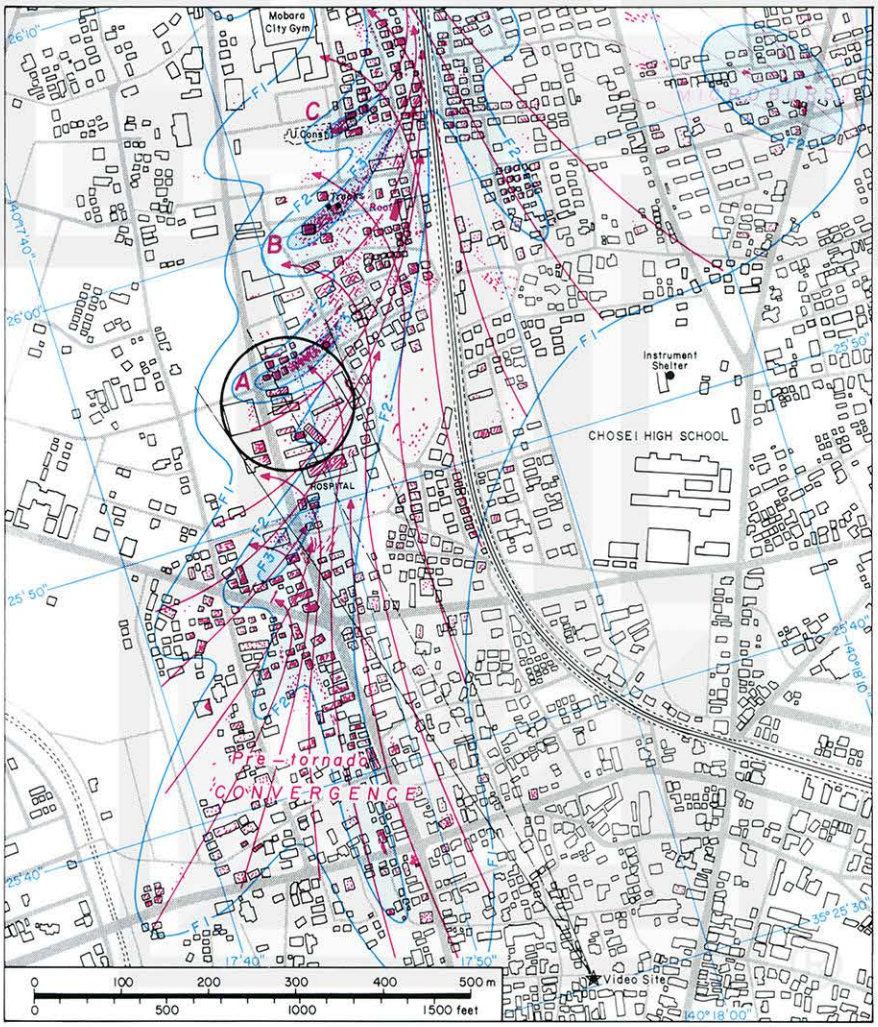

Fig. 2.8-7 The Mobara tornado after its touchdown. Five frames in the video by Mr. Sasaki show a large funnel illuminated by lightning. The funnel on the ground just to the north of Kimizuka Hospital is shown by a circle.

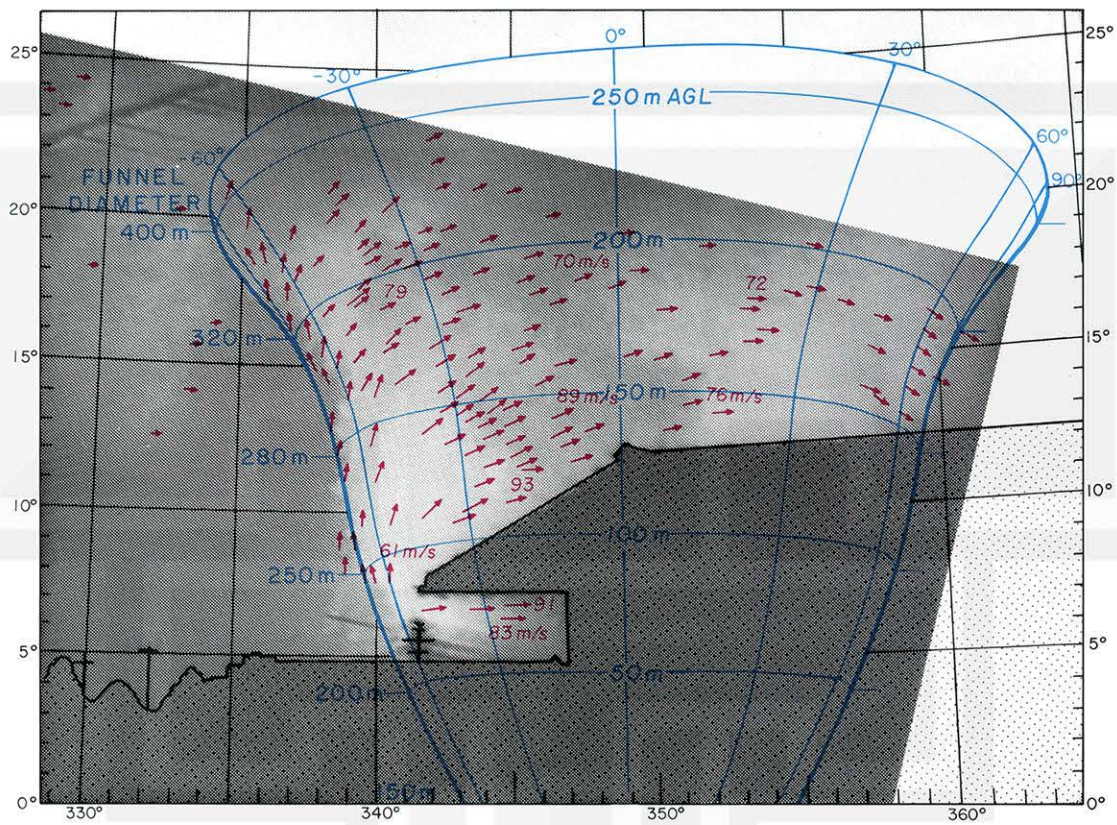

Fig. 2.8-8 Motion of the funnel cloud from the 5 frames of the video by Mr. Kazumi Sasaki. Ground photogrammetry was performed by Mr. Kazuo Watanabe who visited the site for me to take angular measurements.

north along Highway 128 northwest of Kimizuka Hospital where Suction Vortex A developed. After formation, the vortex moved east while picking up cars and depositing debris along its path (Fig. 2.8-9). As expected, the suction vortex moved along the south edge of the funnel cloud for a short distance and disappeared on the west edge of the funnel where no vertical motion existed.

Records of Peak Winds

The Tokyo Electric Power Company located in the inflow region of the tornado in its formation stage, recorded a 30 m/s peak wind (Fig. 2.8-10). The peak was followed by a gradual decrease in wind as the tornado moved away.

The 31 m/s and 20 m/s peak winds at Mobara Agricultural High School were caused by the two pulses of microbursts which descended far to the east of the major tornado (Fig. 2.8-11). The distance of the High School from the tornado was 1.9 km toward the east, which was too far to record the tornado winds.

Suction Vortex B identified in Fig. 2.8-7 formed 250 m south of City Gymnasium where a house at B was lifted off its foundation and broken up into pieces by estimated F4 winds. After leveling the house, the vortex picked up 10-ton and 5-ton trucks parked on the curbside and threw them into a front yard and an open lot, respectively (Fig. 2.8-13). Vortex C formed at the construction site south of the Gymnasium, where a number of reinforced steel rods were bent down, some to the ground.

Some think, by mistake, that a car is the safe place to stay in a tornado. On 27 April 1967, many motorists stopped at red traffic light at Oak Lawn near Chicago were killed by an F4 tornado. At Wichita Falls, Texas on 10 April 1979, those who were waiting in cars parked at a shopping center died when an F4 tornado picked up their cars like match boxes.

Fig. 2.8-9 Autos and debris deposited in the path of Suction Vortex A shown in Fig. 2.8-7. Aerial photo courtesy of the Mainichi Newspaper.

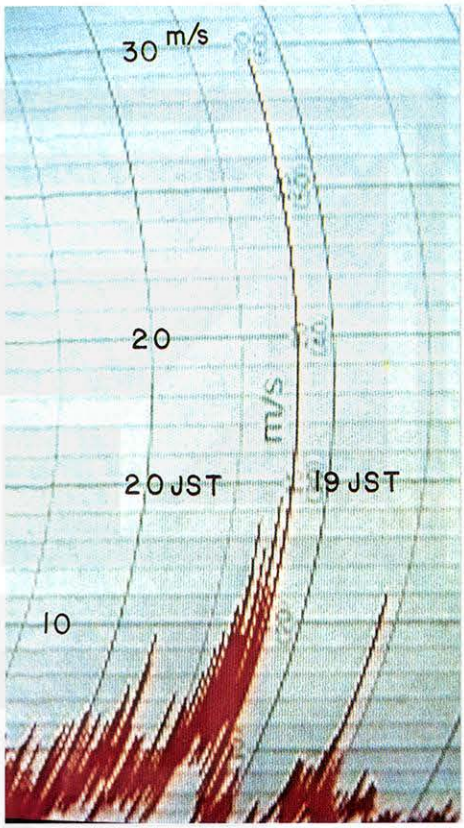

Fig. 2.8-10 Windspeeds recorded by the Tokyo Electric Power Company.

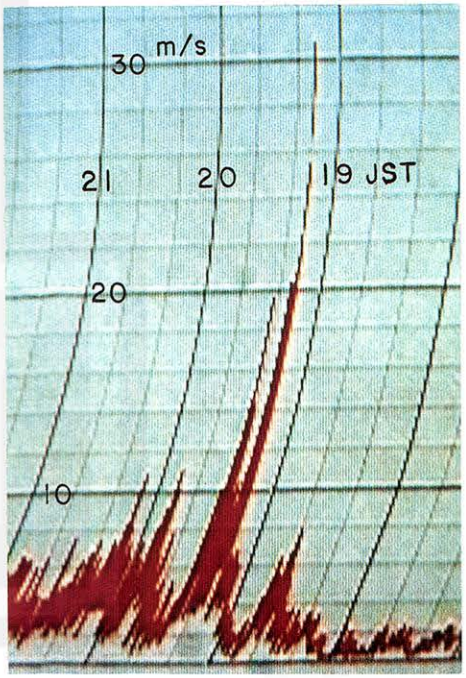

Fig. 2.8-11 Gust-recorder trace from Mobara Agricultural High School provided by NHK.

An Artist's View of the Mobara Nocturnal Tornado

Fig. 2.8-12 An artist's view of the Mobara nocturnal tornado painted by Mrs. Toshiko Arai, wife of the Japanese ambassador to the Philippines. She developed a special method of painting the wind effects for this book.

Fig. 2.8-13 The path of Suction Vortex B which lifted a house off its foundation at B.

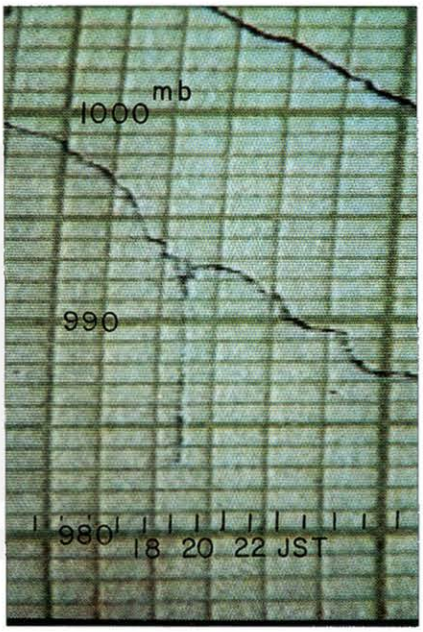

Fig. 2.8-14 A 10-mb pressure drop recorded at Chosei High School.

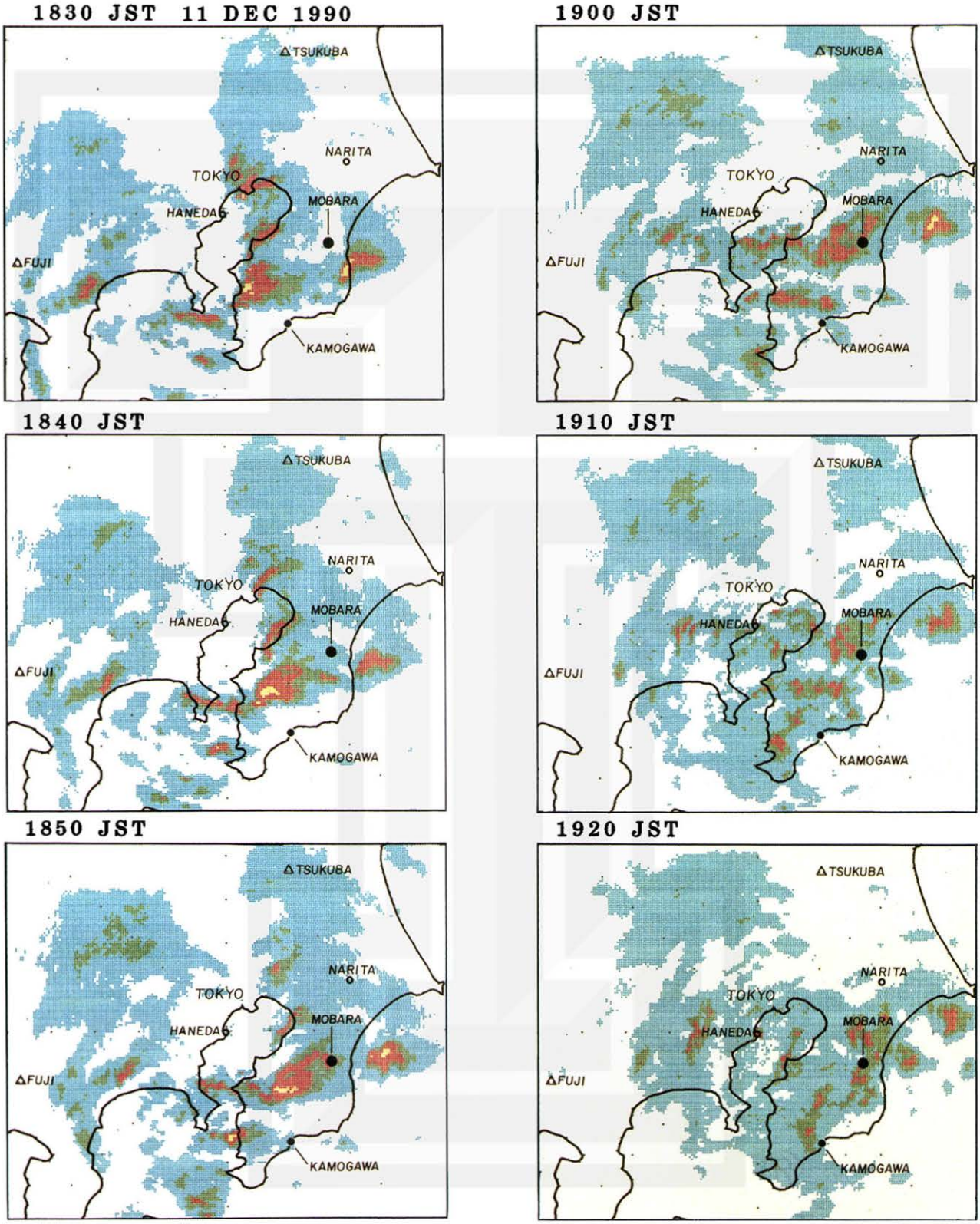

Fig. 2.8-15 Six pictures taken by the Haneda airport radar on 11 December 1990 between 1830 and 1920 JST. Estimated time of the Mobara tornado was 1914-1918 JST. It should be noted that three distinct hook echoes are clearly visible at 1840. The one over Tokyo produced the Haneda microbursts (p126). The one to the northwest of Kamogawa was moving toward Mobara. Courtesy of Japan Air Lines.

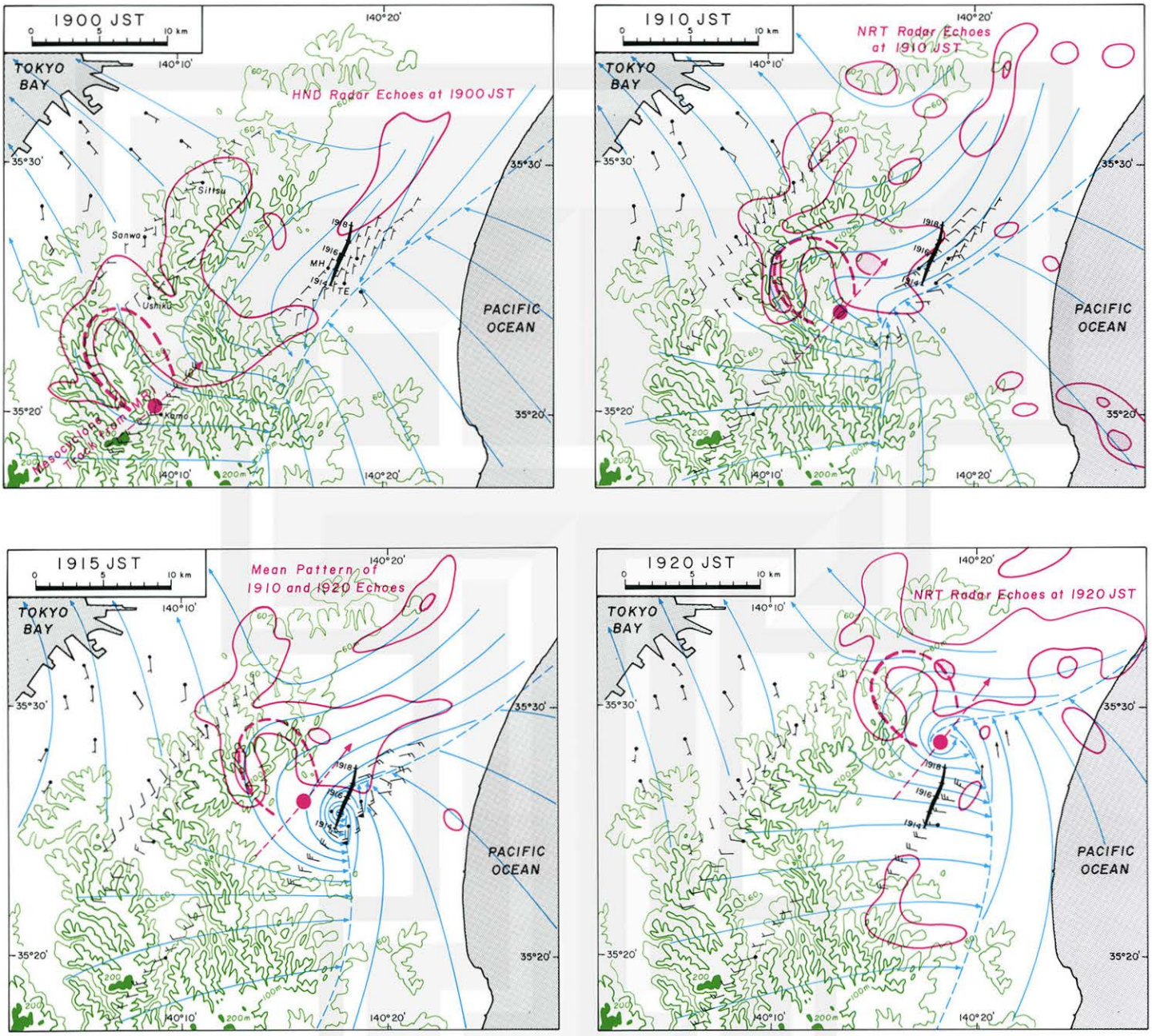

Fig. 2.8-16 Four mesoanalysis maps showing the distribution of radar echoes, surface winds, streamlines, and mesocyclone centers estimated from the Doppler velocity measured by MRI at Tsukuba.

As revealed by the asymetric pressure change before and after the pressure drop by the tornado proper (Fig. 2.8-14), the Mobara tornado formed inside the pressure field of the mesocyclone, but not necessarily near the cyclone center. Four mesoanalysis maps (Fig. 2.8-16) show the existence of large, horseshoe echo, but its relationship with the mesocyclone is not clear. It is likely that the tornado formed in the inflow region, 3 miles from the mesocyclone center.

Chapter Three

Cloud Truth Experiments

Since the successful launch of the first Television and Infrared Observation Satellite (TIROS I) on 1 April 1960, weather observations in the United States entered the space age. The conventional cloud observation made while looking up changed into the looking-down observation from outer space. I received my first NASA grant in October 1962 to determine the precise location of clouds in satellite pictures and to perform the interpretation of clouds depicted by visible and infrared imagery. In achieving the goal, I conducted a number of cloud-truth experiments from both ground and aircraft while weather satellites took pictures at 2 to 15 minute rapid-scan intervals.

3.1 Ground-based Photography

Haleakala Experiment with ATS I

In 1967, the Applications and Technology Satellite (ATS I) was placed above the equator in the Central Pacific Ocean to conduct the Line Islands Experiment on and around Palmyra, Fanning, and Christmas Islands. The experiment was coordinated by Dr. Walter Orr Roberts, director of NCAR at that time. He presented the certificates with his signature and silhouette of palm trees and a research aircraft on one of the Line Islands to all participants (Fig. 3.1-1).

Fig. 3.1-1 The design on the bottom of the certificate presented to the participants of the Line Islands Experiment signed by the late Dr. Walter Orr Roberts.

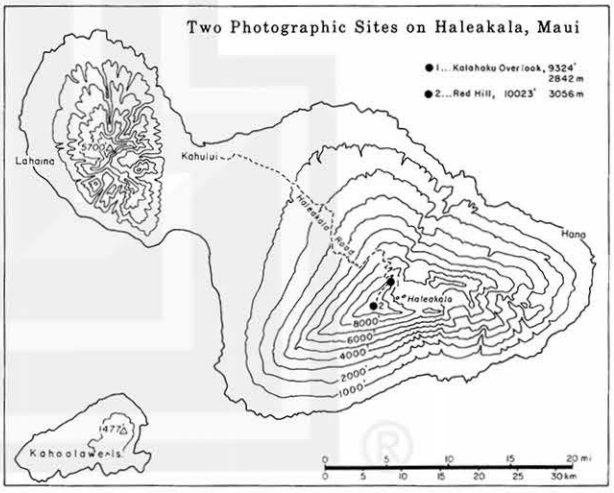

Fig. 3.1-2 Two photographic sites on the Haleakala Volcano for taking infrared pictures in March and April 1967.

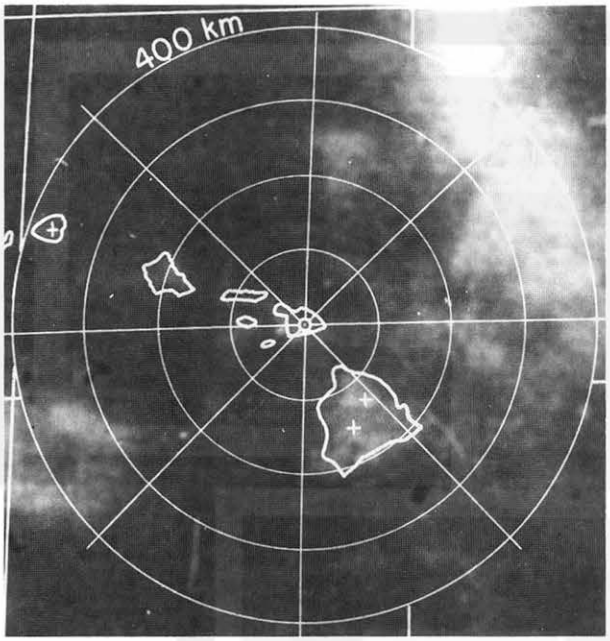

Fig. 3.1-3 An ATS I picture at 1649 HST 29 March 1967. The concentric circles around Haleakala show the ranges at 100 km intervals.

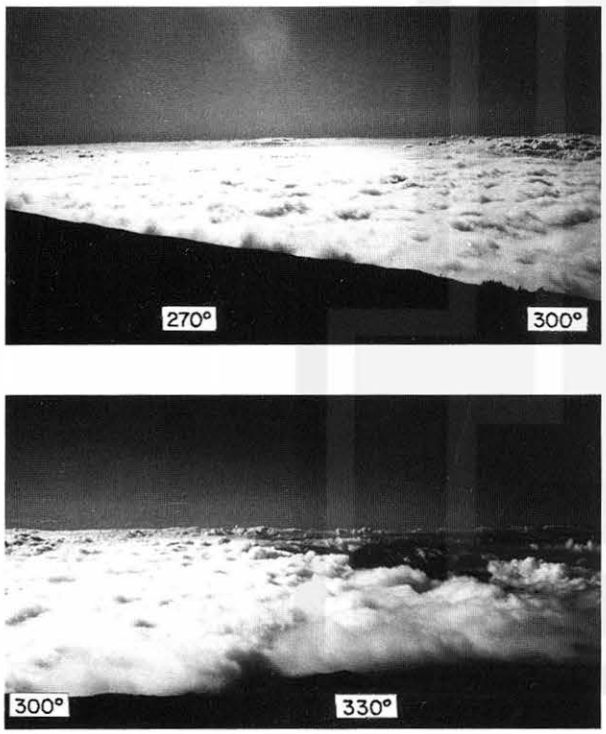

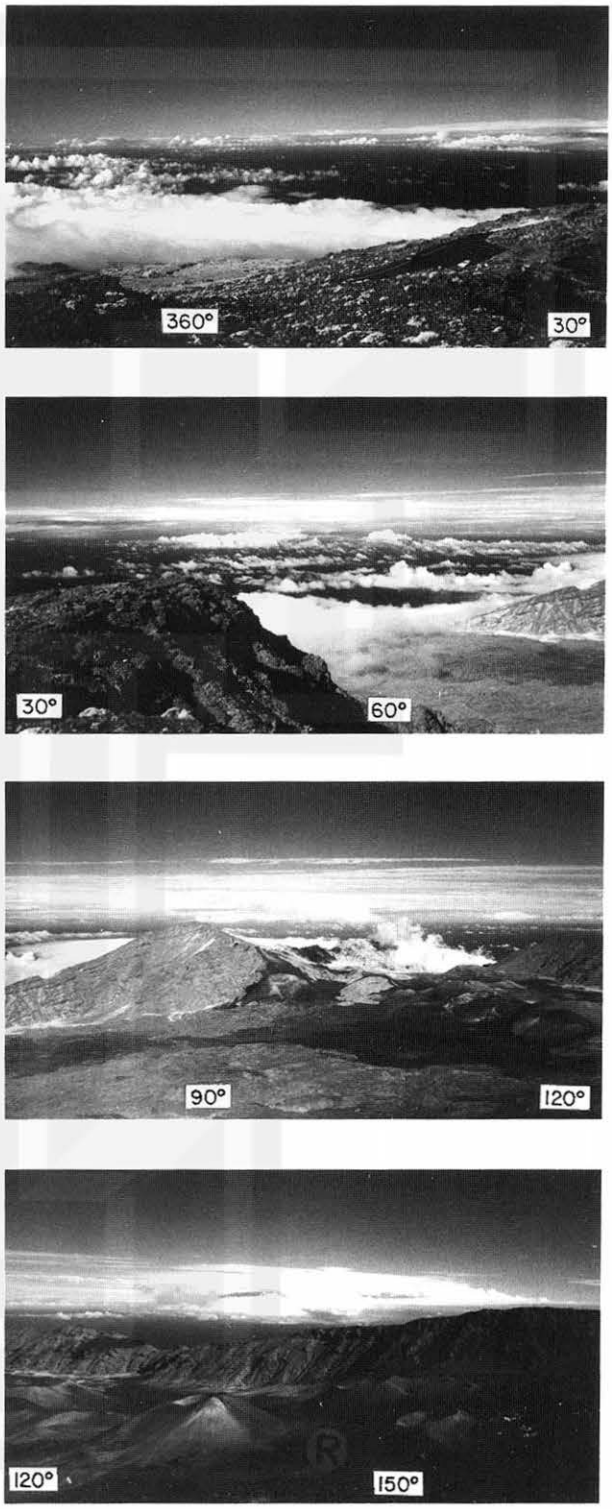

Fig. 3.1-4 Cloud truth panoramic pictures taken from the Kalahaku site at 1640 HST, several minutes in advance of the ATS I picture in Fig. 3.1-3.

My research group took near-infrared pictures of clouds from two camera sites, 9,324' (2,842 m) Kalahaku Overlook and 10,023' (3,056 m) Red Hill, the highest spots on Haleakala Volcano on Maui Island (Fig. 3.1-2), Hawaii. Due to high elevation of the photographic sites and relatively low tops of tradewind cumuli, we could photograph middle and high clouds all around the volcano as far as 300 to 400 km (Fig. 3.1-3).

An example of panoramic photos at 1640 HST (Fig. 3.1-4) reveal that middle and high clouds north through southeast were the extensive cloud mass in the ATS I picture at 1649 HST. Seen to the southeast between 135° and 170° azimuths are Mauna Kea and Mauna Loa surrounded by convective clouds.

A number of analytical studies relating satellite and ground photographs concluded that the interpretation of satellite imagery can be improved significantly by combining these photos taken simultaneously. It was also found that the top of Haleakala provided us with excellent views. The sites were approachable from Kahului via narrow but paved road all-the-way to the mountaintop.

Barbados Experiment

with ATS III

ATS III above the equator in Brazil became available in November 1967. Although the satellite transmitted color imagery only on 19 November 1967, B & W pictures in high quality were available for a long time thereafter. In July 1969, I conducted a cloud-truth experiment with my staff members, Vincent Ankus and Dorothy Bradbury.

The objectives of the experiment were to develop the methods of stereoscopic computations of clouds based on two whole-sky cameras and to determine the nature of the convective clouds tracked by ATS III for cloud-wind computations. Due to high altitude of cirrus clouds (Fig. 3.1-5) over the tropical island of Barbados at 13°N, tracking of high clouds on whole-sky photos turned out to be easy. It was also found that even a small segment of cirrus clouds could be followed 15 to 20 minutes while cumuliform clouds were undergoing rapid changes within several minutes.

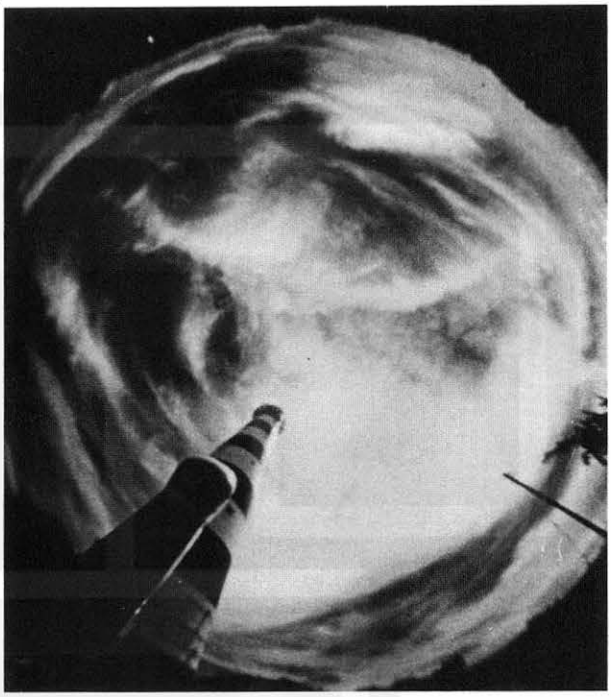

Fig. 3.1-5 A whole-sky picture from the lighthouse site at the end of the 2-mile baseline. This photo was taken at 1725 LST 26 July 1969.

A telephoto camera was used in following rapidly-changing convective clouds, a group of which was tracked by satellite. As expected, the group consisted of a number of updraft cells at different stages of growth. When the updraft weakened, the cloud top drifted away, resulting in the separation of the cloud top and the base (Fig. 3.1-6).

Unexpectedly, we encountered hazy, low visibility situations in which no usable pictures of distant clouds could be taken. Examination of ATS III pictures revealed the extensive areas of dust clouds originated in Sahara and advanced westward across the entire width of the Atlantic taking several days.

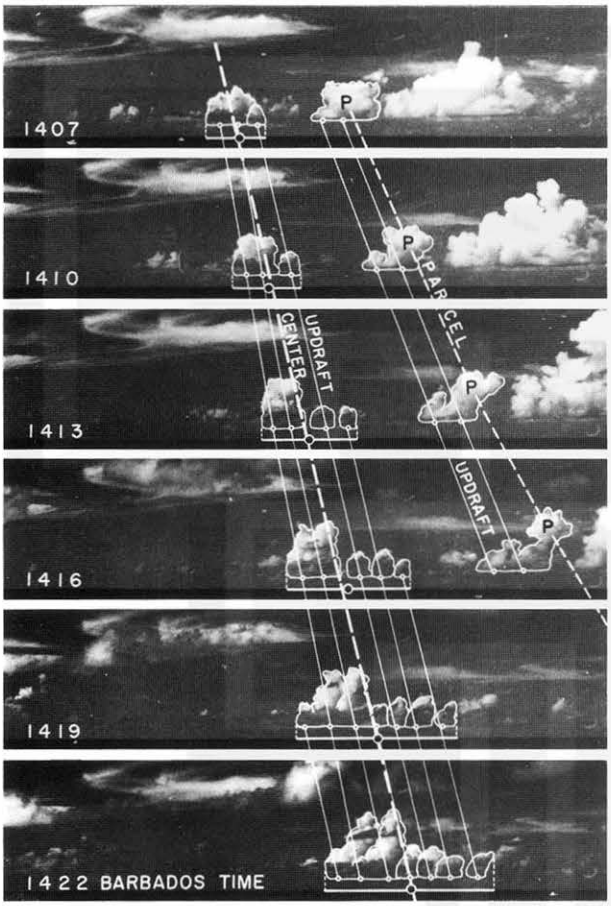

Fig. 3.1-6 Groups of cumuli, smallest clouds to be tracked by ATS III during the Barbados Experiment in July 1969.

Towering Cumuli in Florida

The view of the towering cumuli over southern Florida is spectacular. However, most clouds at later stages are often obstructed by small clouds on the foreground hiding the clear boundaries of growing turrets.

On 22 March 1972, the day of the 82 kts (42 m/s) westerlies at 11 km level over south Florida, Mr. Ron Holle of the Environmental Research Laboratory of NOAA took a 16 mm time-lapse movie of towering cumuli from the University of Miami at Coral Gables, Florida. During

Movie of Towering Cumuli

1649-1702 EST, 22 March 1972

by Ron Holle

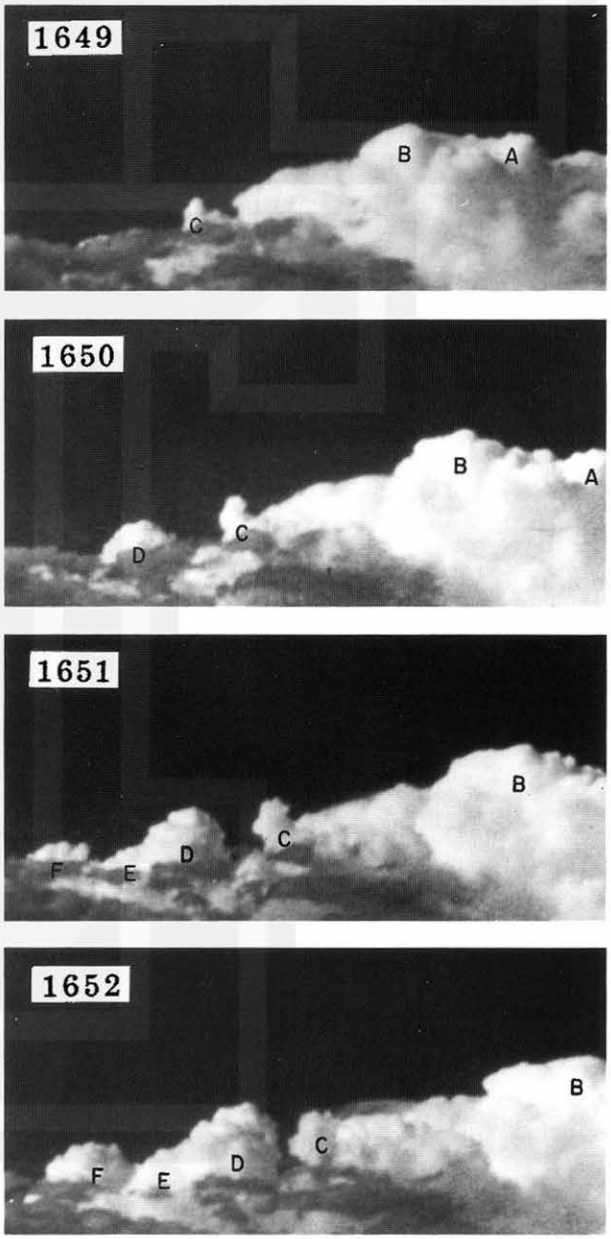

Fig. 3.1-7 Continued to next page.

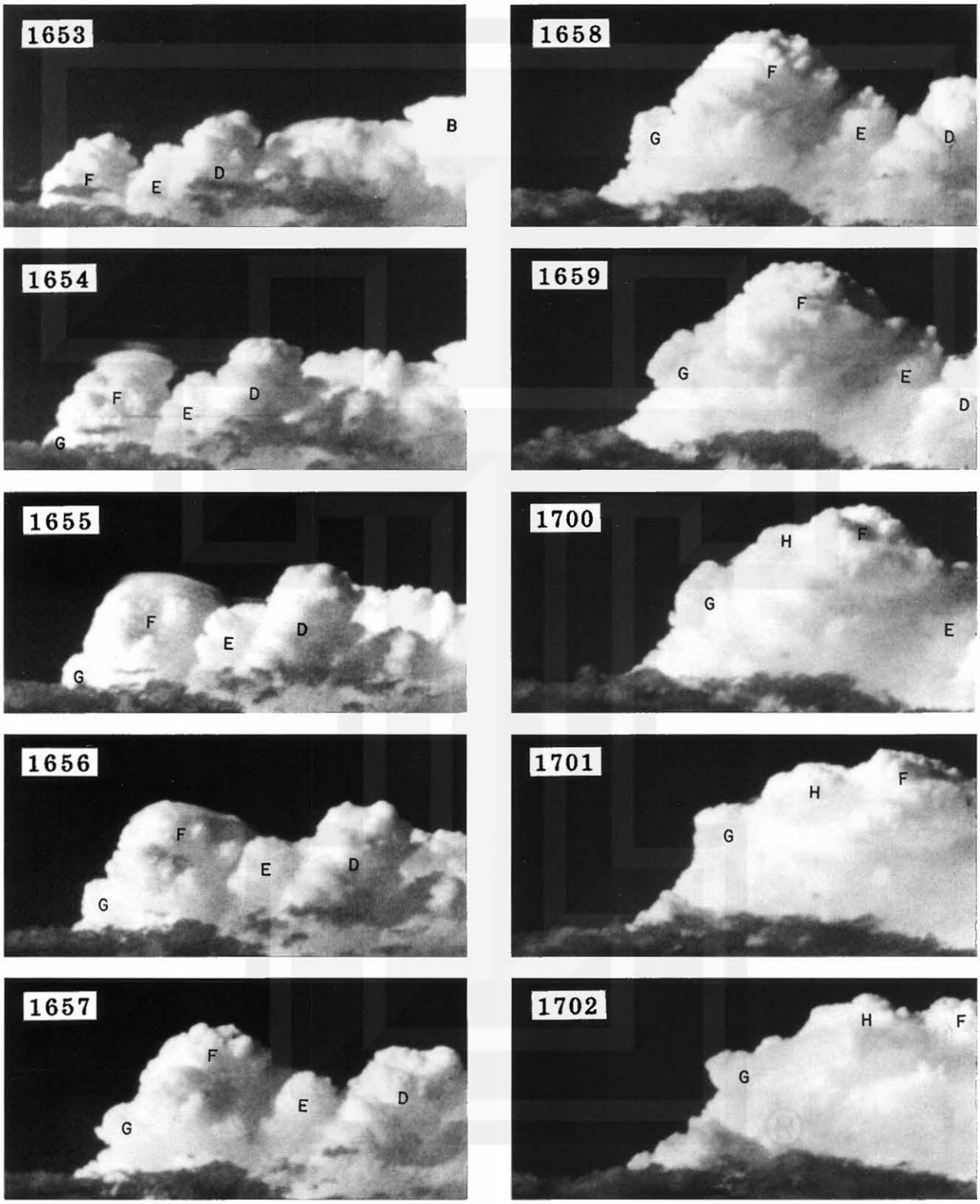

Fig. 3.1-7 Pictures of growing cumulus clouds at one-minute intervals selected from Ron Holle's time-lapse movie taken at 3-sec intervals.

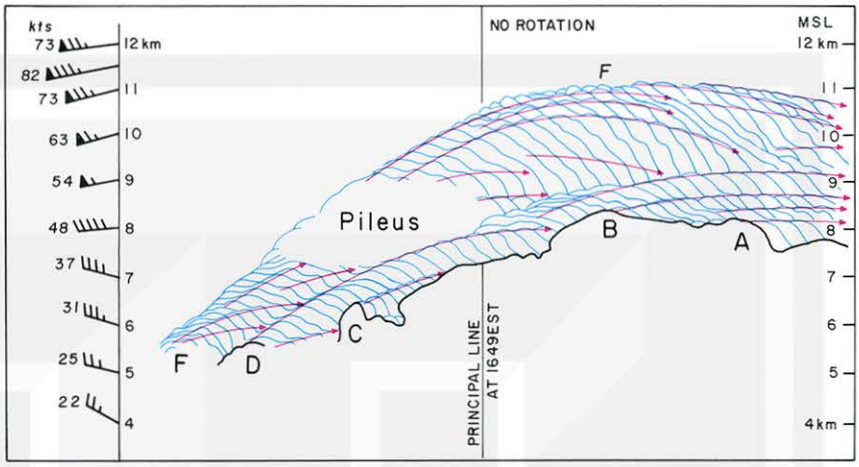

Fig. 3.1-8 Outer boundaries of the cumulus clouds in the movie drawn at 6-sec intervals. The principal line of the movie frame was kept constant.

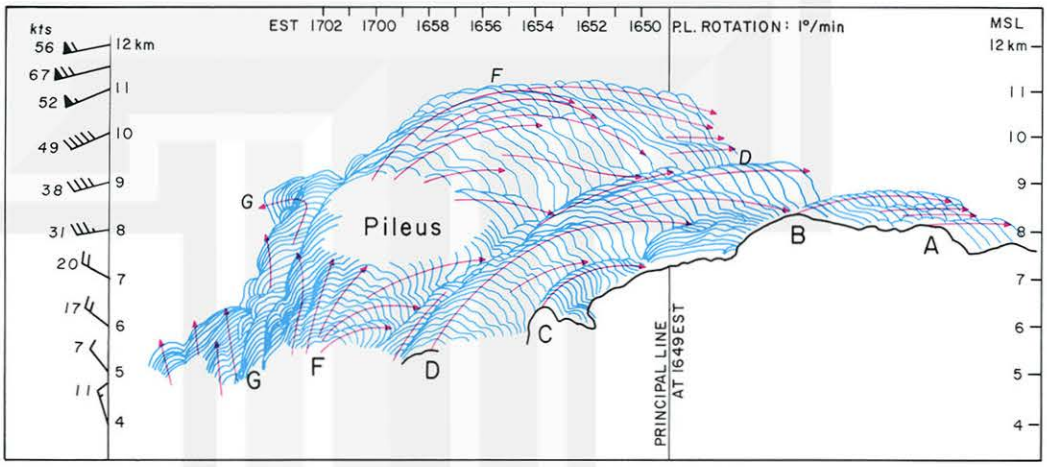

Fig. 3.1-9 Outer boundaries of the same clouds drawn by rotating the principal line from right to left at the rate of one degree per minute.

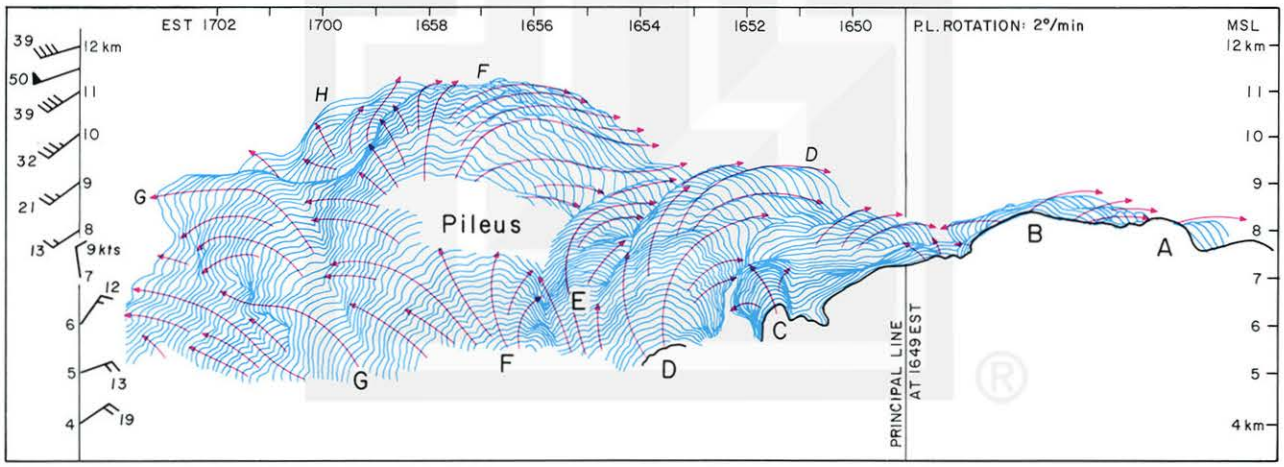

Fig. 3.1-10 Outer boundaries of the same clouds drawn by rotating the principal line at the rate of two degrees per minute.

my visit to Miami at a later date, Ron showed me his impressive time-lapse movie taken at 3 sec intervals.

After spending intermittent 20 years since then, his movie, along with additional data he collected, was analyzed by developing various photogrammetric techniques. For overviewing the growth of the turrets during the 13 min movie period, frames at one minute intervals (every 20th frame) were enlarged, identifying individual turrets with letters, A through H (Fig. 3.1-7). A fast-growing turret F induced a pileus cloud as it penetrated a humid layer between 7 and 9 km MSL.

At first, the cloud boundaries at 0.2-min intervals (every fourth frame) were enlarged and traced by eliminating the boundaries hidden behind the earlier boundaries. The composite boundaries revealed trajectories of the humps located at the tops of small updrafts, 200 to 400 m in diameter. During the pileus-forming stage, these humps were not visible (Fig. 3.1-8). This analysis shows that the humps were pushed downwind constantly as they rose and fell during the evolution.

In an attempt to generate the hump trajectories on coordinates which move downwind in the direction of the turret movement, cloud boundaries at 0.2 min intervals were traced by shifting successive movie frames from right to left at the rate of one degree per minute. In other words, the principal line of the movie was rotated to slow down the left to right movement of the turrets. In effect, the composite boundaries thus created, would generate hump trajectories under hypothetical westerlies 15 kts weaker than the actual winds (Fig. 3.1-9).

A 2-degree rotation per minute is expected to generate the coordinates moving left to right at the mean motion of the turrets. Results show that the westerlies were, in effect, reduced by 32 kts, from 82 to 50 kts, resulting in the turrets with near vertical axis (Fig. 3.1-10). Meanwhile, the westerlies at 7 km MSL was reduced to zero, and turret F became the most significant cloud with strong divergence near the tropopause at 10.5 km (34,000') MSL. Turret G on the left side of F was pushed toward the upwind side, while turret D on the other side, toward the right, indicating that a large turret could influence the growth of small ones in the vicinity.

This cloud-truth analysis performed with Ron revealed that turrets below the tropopause undergo both rising and drifting motions, inducing strong divergence near the tropopause. On the other hand, a turret top overshooting into the stratosphere descends abruptly, instead of spreading, killing the updraft which had created the overshooting cloud. This subject will be discussed in depth in Section 3.2.

CHAMEX 1988

at Cape Hatteras

As the resolution of satellite imagery increased during the 1970s and 80s, both man and machine began tracking a large number of target clouds accurately. In view of the fact that some clouds are good targets while others are not, the question of the accuracy of cloud winds became an important issue among users. First of all, it is not possible to find clouds which move precisely with the environmental winds. Furthermore, winds in the real atmosphere vary with height, necessitating accurate height assignment to each satellite-tracked wind.

To meet these requirements, I proposed the CHAMEX (Cloud Height And Motion EXperiment) in which clouds are tracked independently by both satellites and stereoscopic cameras operated simultaneously. Meanwhile, conventional balloons were used in determining the vertical distribution of winds and humidity which are hard to determine by either cameras or satellites in cloudy skies.

The first CHAMEX was conducted for a period of four days, 19-22 September 1988 at Cape Hatteras, North Carolina. The specific location was selected on the coastline with relatively cold ocean temperature which would suppress the development of low clouds in daylight hours, allowing us to take low, middle, and high clouds from the ground. The existence of the NWS rawinsonde station at Cape Hatteras was also the major decision factor.

Four whole-sky cameras were placed on two separate baselines, cameras A and B on 1,790 m (1.11 mi) distance for triangulating middle and high clouds and cameras C and D on 200 m (0.12 mi) distance for low clouds. These photographic sites were placed inside the Cape Hatteras National Seashore in the vicinity of the campground (Fig. 3.1-11).

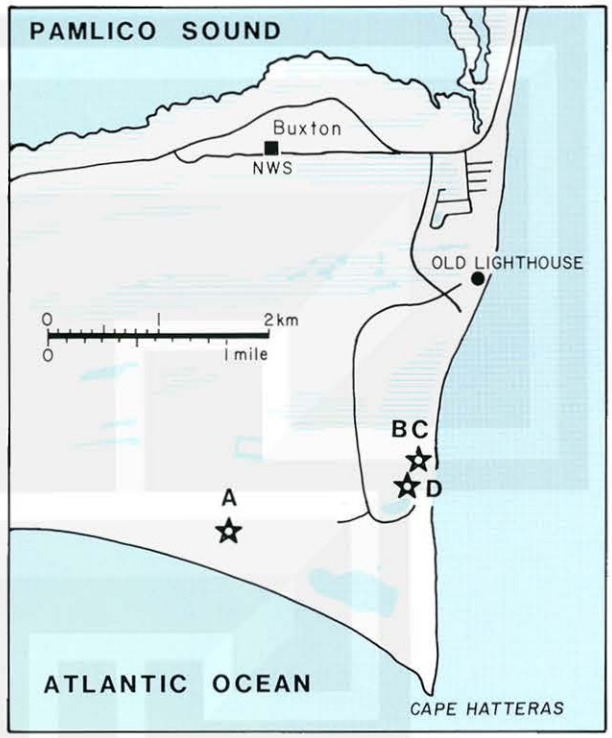

Fig. 3.1-11 Four photographic sites used in the CHAMEX Cape Hatteras Experiment, 19 to 22 September 1988. Baseline lengths used were 1,790 m from A to B and 200 m from C to D. Cameras B and C were colocated.

Unlike industrial cities, Cape Hatteras provided us with excellent photographic sites, enabling us to obtain clear pictures of clouds all-the-way to the horizon (Fig. 3.1-12). It should be noted that a whole-sky camera takes pictures while looking straight up; whereas, a satellite photographs while in the looking-down attitude. In order to match up satellite and whole-sky photos for comparison purposes, we have to print whole-sky pictures backward. On a backward print, the east horizon is on the right-hand side when the north is placed at the top.

Three-hourly soundings revealed the descent of moist layers, from 400 mb to the ground from the 19th to the 20th, and 350 mb to 500 mb on the 21st to the 22nd (Fig. 3.1-13). Corresponding to these descents, high clouds in whole-sky pictures dried up. It was also found that most middle clouds were located at the base of the moist layer, obtaining the middle-cloud winds close to the rawin winds at the height of the moisture base.

Q and A

Question: Ted, who drafted the large number of color diagrams used in this book?

Answer: I did every one of them. During the past 10 to 20 years, I drafted color-separated figures in making slides for meetings. They were combined into B & W figures for my publications and technical reports. Meanwhile, I kept the original drawings, hoping that they can be used in my memoirs printed in color.

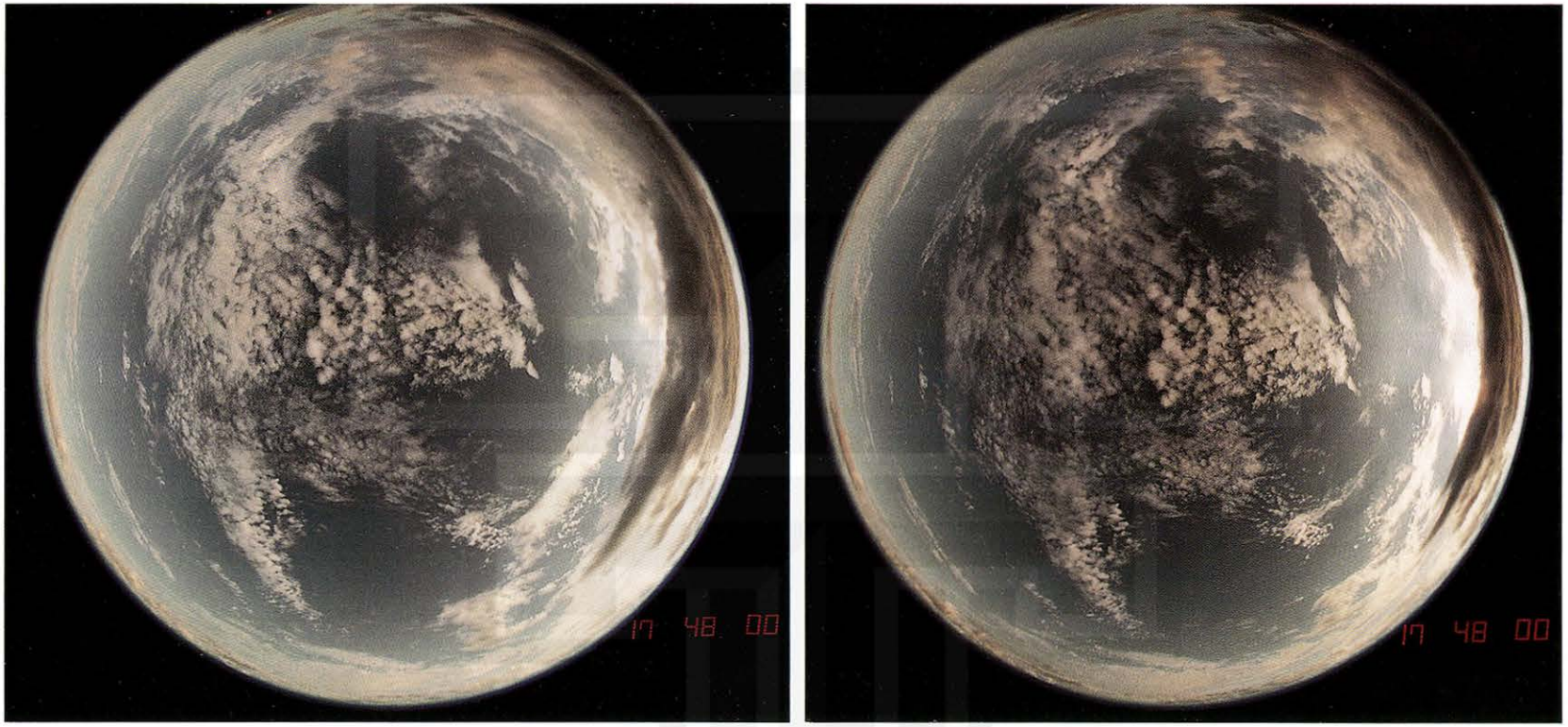

Fig. 3.1-12 Whole-sky images of cameras A (left) and B (right) taken simultaneously at 17h 48m 00s 20 September 1988. On these pictures, printed normally, top is north and west is on the right side.

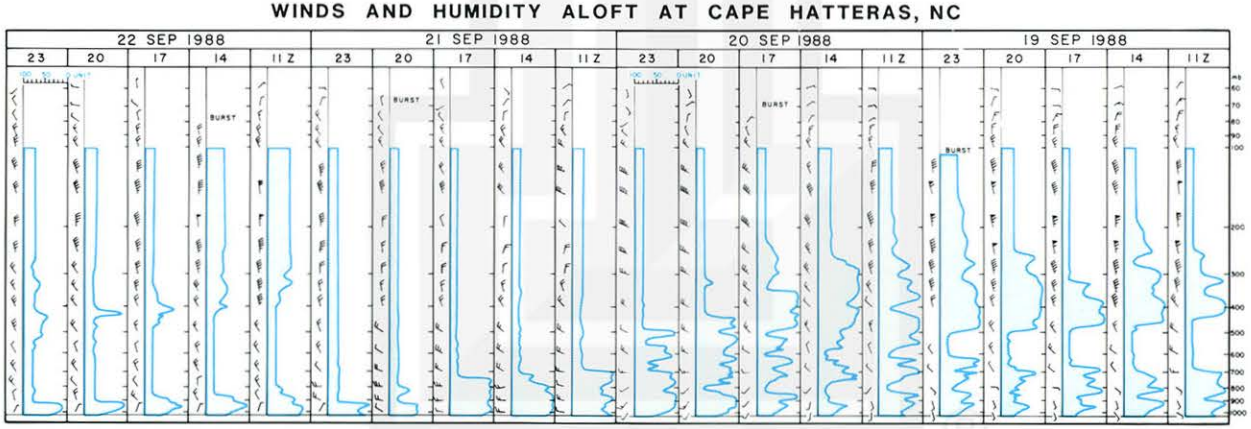

Fig. 3.1-13 Winds and humidity aloft depicted by a series of 3-hourly soundings taken during daylight hours, 11 to 23 GMT (07 to 19 EDT).

CHAMEX 1989

at Key West

CHAMEX 1989 was conducted at Key West, Florida, placing four whole-sky cameras along the south coasts of Key West (Cameras A and B), Stock Island (Camera C), and Boca Chica Key (Camera D). Unlike the Cape Hatteras Experiment, all cameras were lined up so that multiple baseline lengths can be utilized in triangulating clouds at various heights and distances. Instead of using color film, dark red (R3) filters were used to penetrate haze and to increase the cloud/background contrast. These two changes improved significantly the speed and the quality of my stereoscopic analyses, making use of backward-printed B & W pictures.

One miscalculation which I made was the size of the Keys as measured by the heat island effects of the shallow water less than 2 m in depth. Apparently, the extensive shallow waters around the Keys heat up every afternoon, inducing numerous towering cumuli over the heat-island waters. Almost every afternoon, we had to cover the whole-sky lenses during passing showers and uncover them immediately after the end of each rain. While I was overseeing the entire experiment, the cameras were attended by four staff members, Duane Stiegler, Jim Partacz, Joe Skowronek, and David Rexroth. They hated the frequent and short showers that moved over the camera sites.

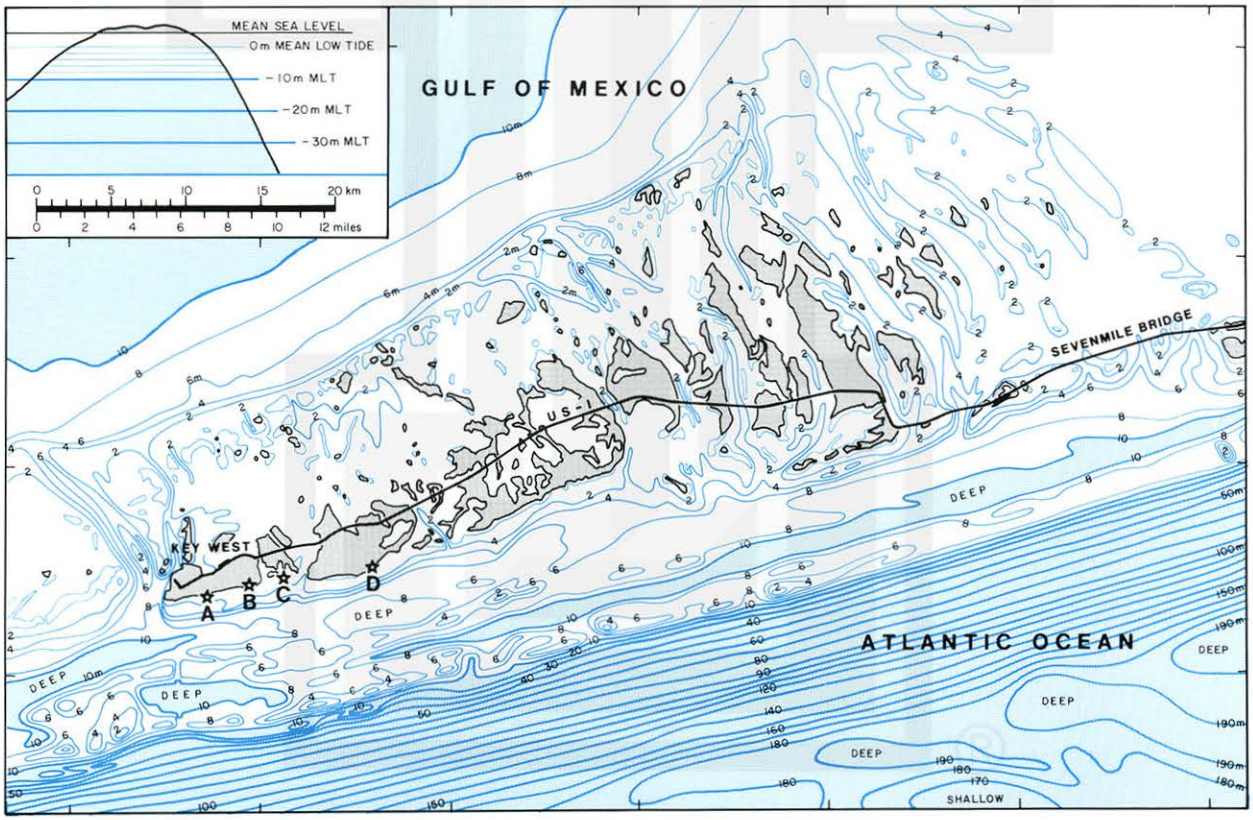

Fig. 3.1-14 Four camera sites used for the CHAMEX Key West in 1989. In order to avoid convective clouds, sites were placed along the south coast. Baseline distances were 3,000 m (A to B), 2,240 m (B to C), and 6,100 m (C to D).

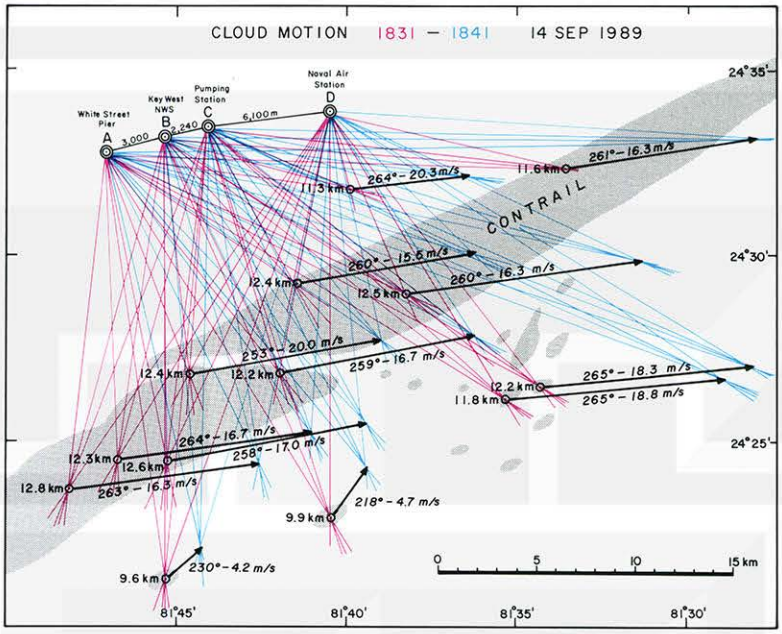

Fig. 3.1-15 Triangulation of a condensation trail photographed by four whole-sky cameras operated in stereoscopic mode. Both heights and motions of the contrail and nearby clouds were computed. Time: 1831 to 1841 GMT (10 min).

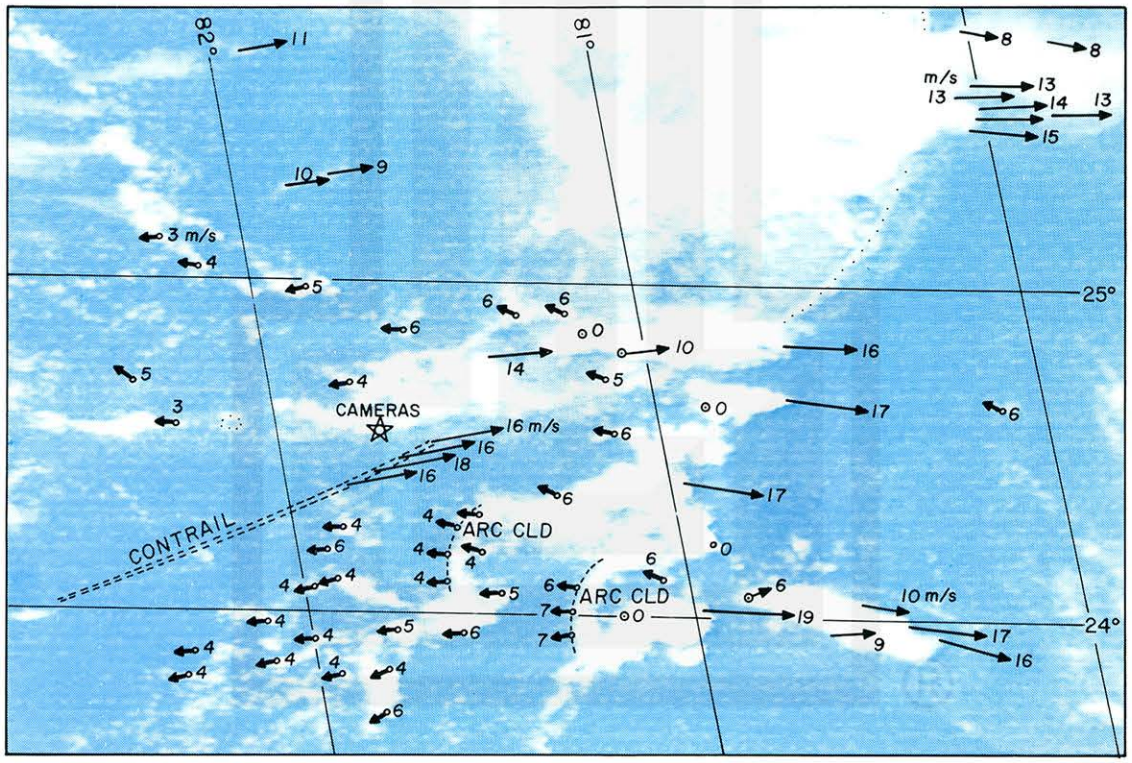

Fig. 3.1-16 Cloud-motion winds computed from the 5-min pictures taken during the 20-min period, 1841-1901 GMT 14 September 1989. Motions of the contrail in Figs. 3.1-15 and 16 computed independently by different methods were very close.

Although no special sounding was released during the Key West CHAMEX, a strip chart recorder was used for obtaining the recorder record of each scheduled sounding. Double parachutes were attached to slow down the descending speed after the burst. Almost all dual parachutes worked very well, obtaining both humidity and temperature records during the ascent and the descent.

Of a number of case studies reported by Fujita (1991a), stereoscopic computations of the height and motion of a 500-m wide contrail are very interesting. The whole-sky imagery showed a number of small cells embedded inside the contrail and trackable stereoscopically. The mean velocity of these cells was 16.9 m/s from 259° with their average height of 12.4 km or 40,600' MSL (Fig. 3.1-15).

An independent tracking of the contrail was done by using four 5-min GOES pictures taken during a 20-min period. At first, I followed the contrail in the direction perpendicular to the line of the contrail. Later, my eyes began following the large cells embedded inside the contrail, obtaining finally the mean speed of 16.5 m/s (Fig. 3.1-16) which is very close to the stereoscopic speed. No estimate of the contrail height was made from the satellite imagery.

The Key West CHAMEX produced an important bridge connecting satellite imagery with terrestrial photographs for better understanding the satellite-tracked cloud winds. It was confirmed that a field of view of high clouds in a single whole-sky picture extends as far as 100 km, approximately one-degree arc of the planet earth.

Space Shuttle Atlantis

2 August 1991

During my photographic experiment at Cocoa Beach in Florida as a part of Project CAPE, Space Shuttle Atlantis was launched on 2 August 1991 from the Kennedy Space Center, giving us a golden opportunity in studying the deformation of the plume left behind by the Atlantis rocket. Along with Jim Partacz of WRL, Susie and I were at NASA's viewing area, 11.85 km (7.36 mi) south of the launch pad.

While the event was photographed by telephoto cameras, a whole-sky camera was set up to record the plume at 2.5-min intervals for one hour between 1100 and 1200 EDT. The liftoff took place at 11h 02m 07s (110207 EDT) under perfect weather conditions (Fig. 3.1-17).

The first whole-sky picture at 110230 caught the rocket at 1.6 km MSL. The second picture at 110500 showed that the plume ended at 47 km MSL while Atlantis already passed the 70 km altitude. The plume at 8 to 13 km began bending toward the west (left), pushed by the easterly jet at 12 km MSL (Fig. 3.1-18).

When Atlantis penetrated the thin layer of cirrus clouds at 12 km, a long shadow of the plume was photographed by both whole-sky and telephoto cameras (Fig. 3.1-19). Approximately 20 seconds later, another distinct shadow appeared at 21 km MSL in the stratosphere. It is likely that the shadow was not on clouds but on the volcanic ashes from the Pinatubo volcano which erupted on 15 June 1991.

Preliminary tracking of the plume was very interesting and informative. The heights of the tracer plume were first determined by combining the tracks of the tracers with the height of the flight track given at one-second intervals. The computed plume winds as a function of height revealed the existence of two layers of weak winds in the stratosphere at 15 km and 40 km (Fig. 3.1-20).

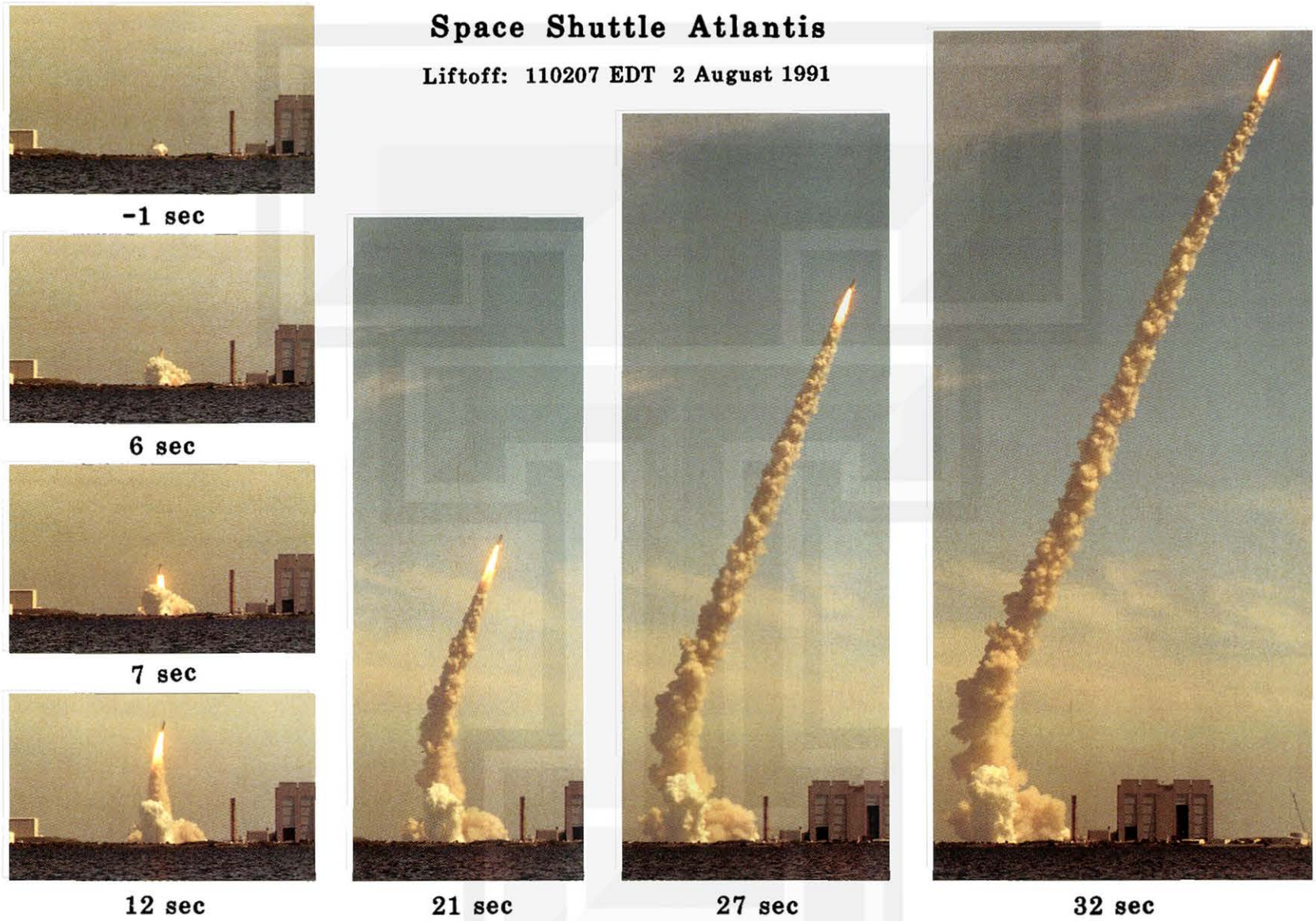

Fig. 3.1-17 A sequence of pictures taken from the NASA viewing area 11.85 km (7.36 mi) to the south of the launch pad of Space Shuttle Atlantis. Photos by Jim Partacz of WRL. Time shown below each picture denotes the seconds after the liftoff, at 11h 02m 07s Eastern Daylight Time.

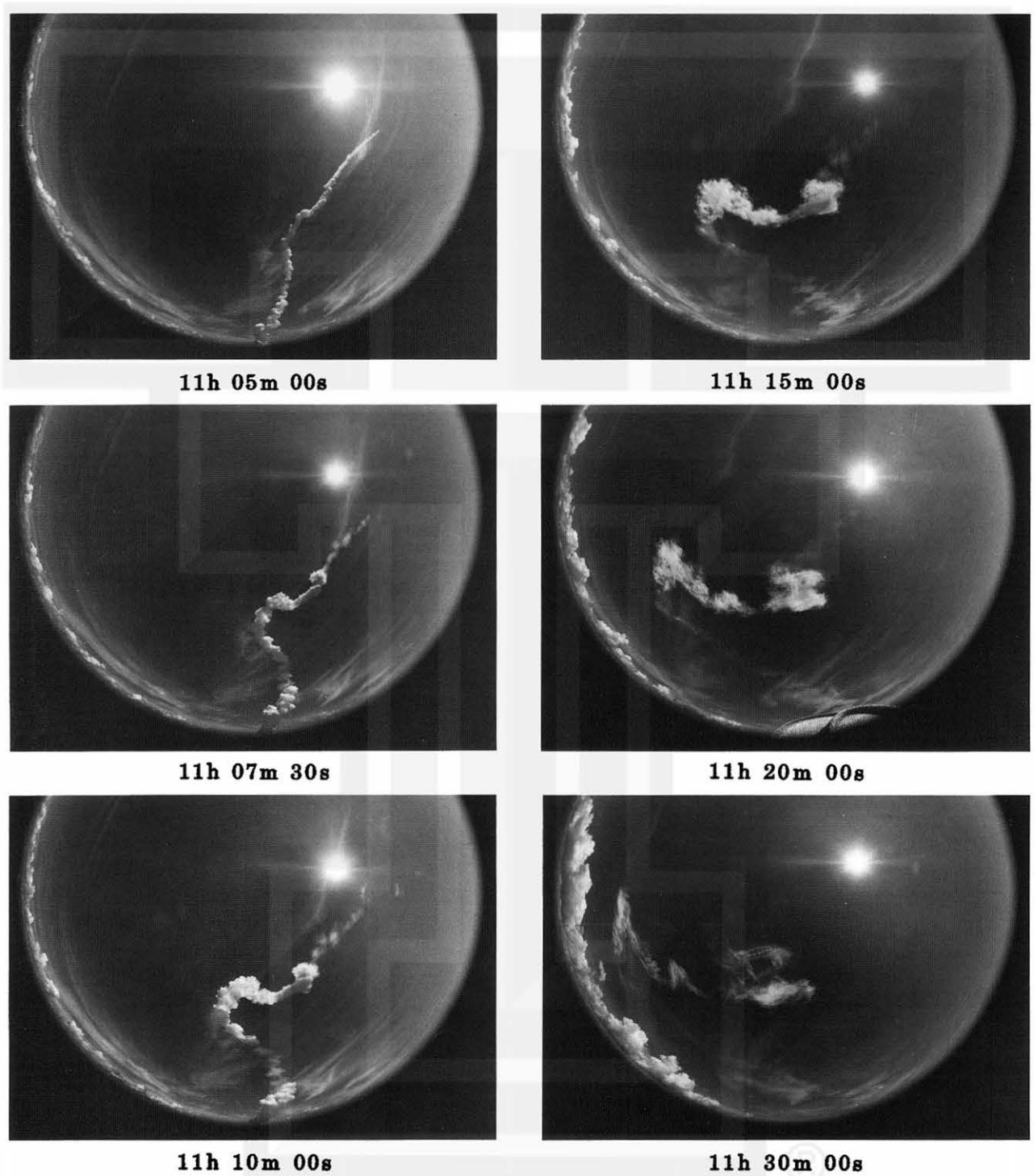

Fig. 3.1-18 Six whole-sky pictures selected from a sequence of pictures taken at 2.5 minute intervals between 1100 and 1200 EDT. The height of the plume in the first picture (upper left) taken 3 min after liftoff was 48 km (157,500') MSL. Photos by Ted Fujita.

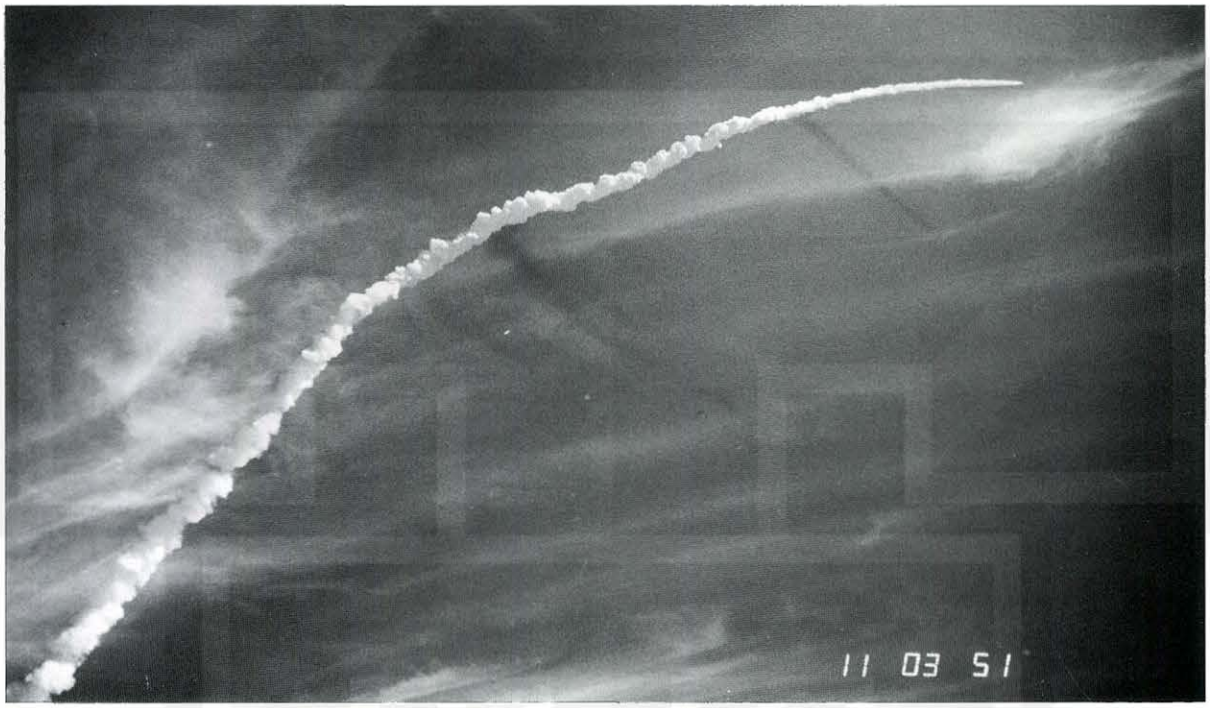

Fig. 3.1-19 Plume of Atlantis at 110351 EDT, showing the shadow of the plume at 21 km MSL on the thin layer of the ashes from the Pinatubo volcano.

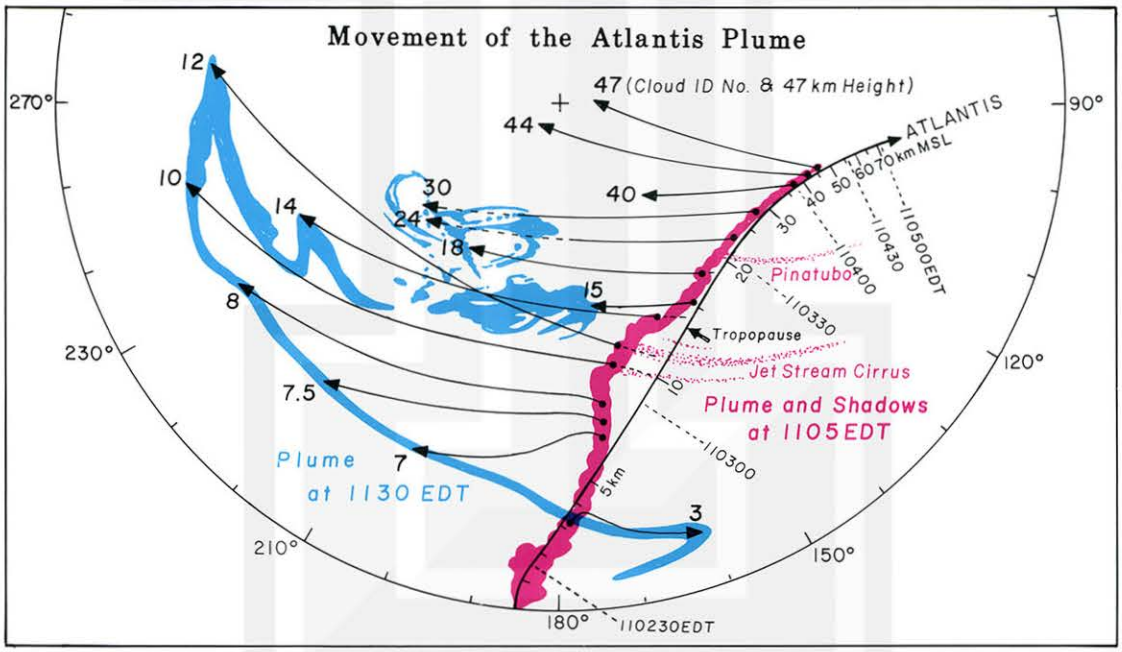

Fig. 3.1-20 Trajectories of the plume during the 25-minute period between 1105 EDT (plume in red) and 1130 EDT (distorted plume in blue). The flight path of Atlantis is shown along with its height in km and time in ETD.

NCAR's three Doppler radars, CP-2, 3, and 4 detected the plume which, somehow, backscattered both 5 cm and 10 cm microwaves (Fig. 3.1-21). This subject is being studied jointly with Jim Wilson of NCAR by combining the Doppler radar data with the whole-sky imagery obtained concurrently.

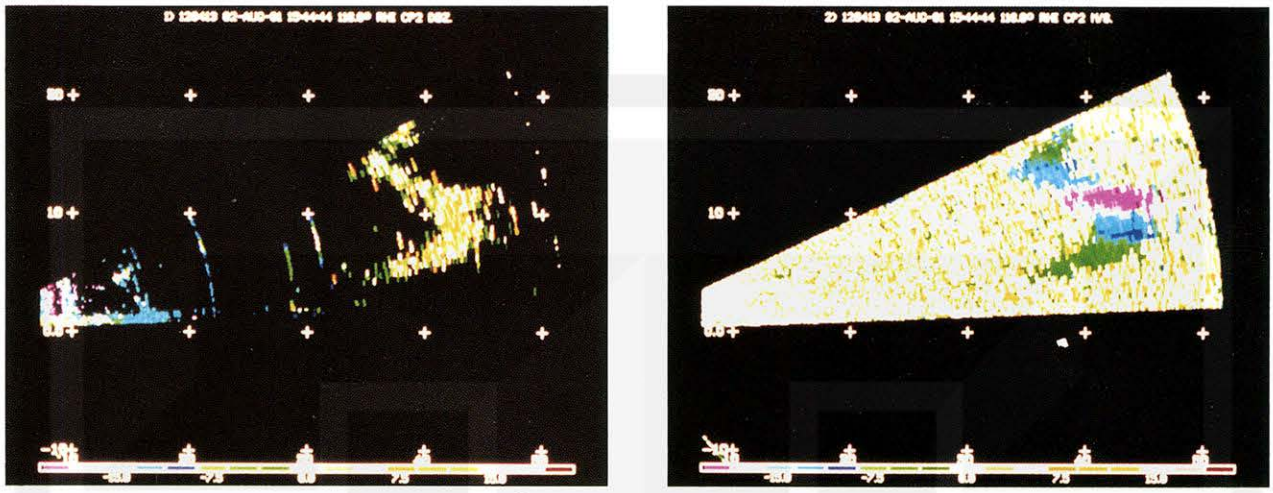

CP-2 116°AZ RHI at 11h 44m 44s

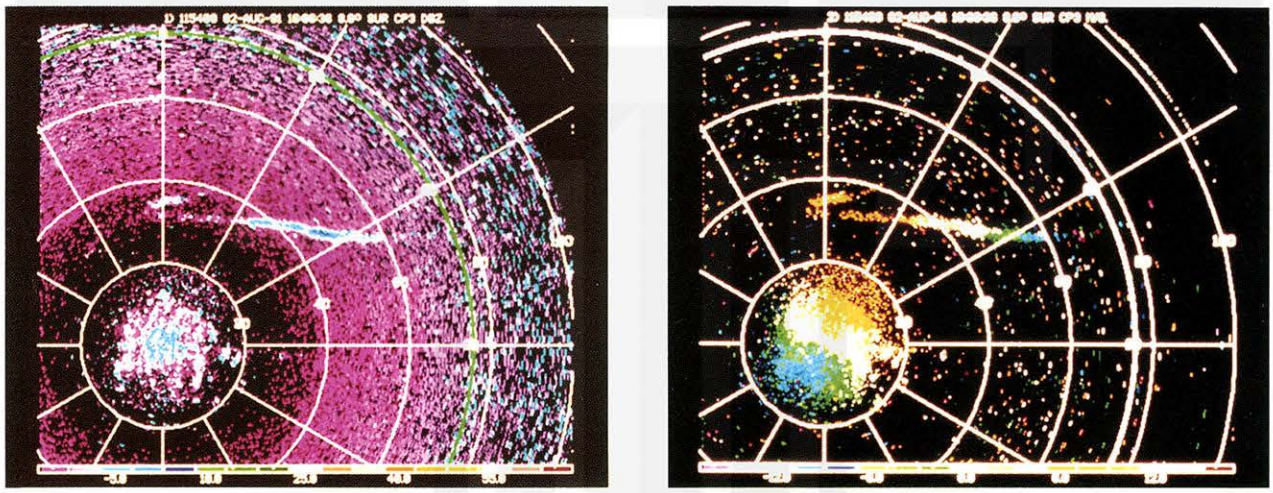

CP-3 8.0°EL PPI at 12h 06m 36s

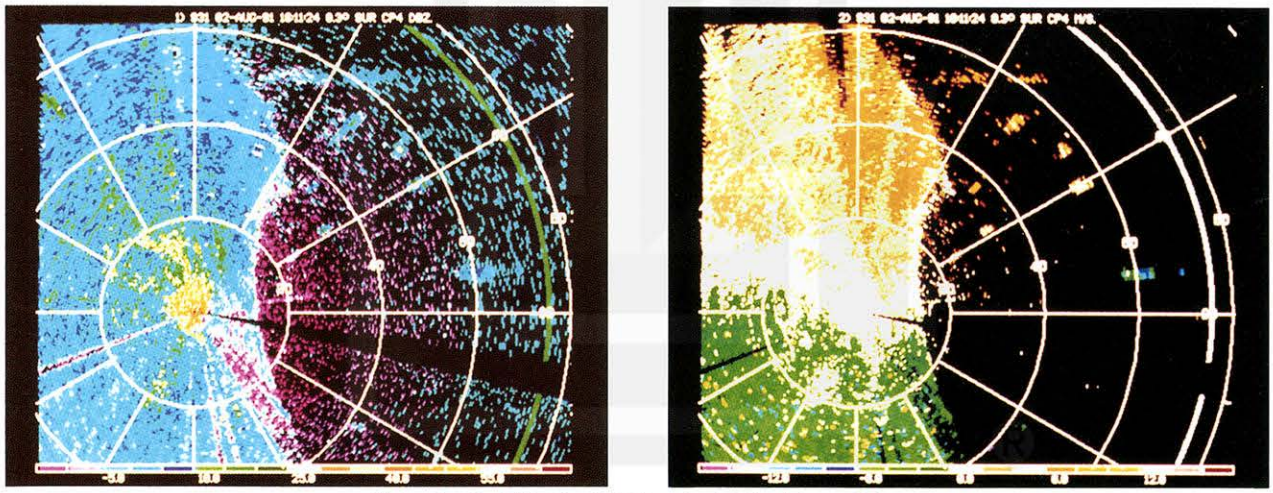

CP-4 0.3°EL PPI at 12h 11m 24s

Fig. 3.1-21 Reflectivity and velocity of the plume of Atlantis depicted by NCAR's three Doppler radars, CP-2, CP-3, and CP-4. These Doppler radars recorded the plume signatures long after the visible plume disappeared completely. Photos by Jim Wilson of NCAR.

3.2 Aerial Photographic Experiment

With rare exceptions of using stratospheric balloons, most thunderstorm tops are observed from the surface of the earth. Mt. Everest, the highest point on the earth is 8,850 m (29,028') which is only one half of the maximum height of severe thunderstorms over the Midwestern United States.

During the past 30 years, tall and extensive anvil clouds were photographed by satellite, revealing the existence of the convective clouds which overshoot into the stratosphere above the anvil surface. The clouds, called overshooting tops, are identified in high-resolution satellite pictures, but their temporal and spatial resolutions are not high enough to determine the nature of the clouds.

Supported by NASA and NOAA, I conducted aerial photographic experiments over the Midwest, making use of DC-6, P-3, Lear Jet, etc., in an attempt to improve the interpretation of satellite data.

Overshooting Clouds

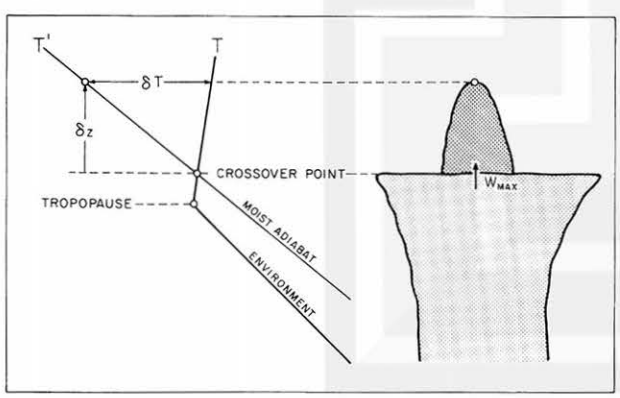

Fig. 3.2-1 Schematic diagram showing that the kinetic energy required to overshoot against the negative buoyancy is proportional to the square of the overshooting height.

Unlike convective clouds in the troposphere, those clouds which overshoot into the stratosphere above the anvil top must rise against the enormous negative buoyancy encountered above the crossover point (Fig. 3.2-1). Due to the fact that an overshooting dome is under the influence of two major opposing forces, the upward momentum of updraft and the downward force of negative buoyancy, the cloud top rises and sinks repeatedly within a very short time.

The incloud temperature of an active overshooting top is usually far below -40°C,

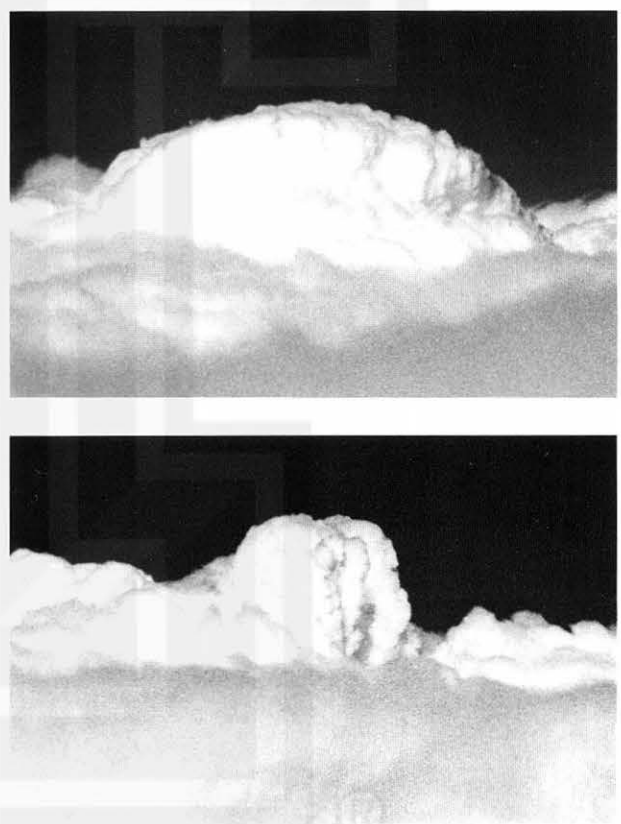

Fig. 3.2-2 An overshooting dome (above), the "Stone Mountain" and the overshooting cliff (below), the "Devil's Tower" with a rudder on the cliff. Photos were taken on 12 May 1972 over southwest Texas at 1708 CST from Lear Jet flying at 50,000', 30 km from the clouds.

the critical temperature of the spontaneous nucleation. Consequently, the hydrometeors in an overshooting top should already be frozen. On the other hand, the close-up view of the cloud in rising stage often gives an impression of a water cloud (Fig. 3.2-2).

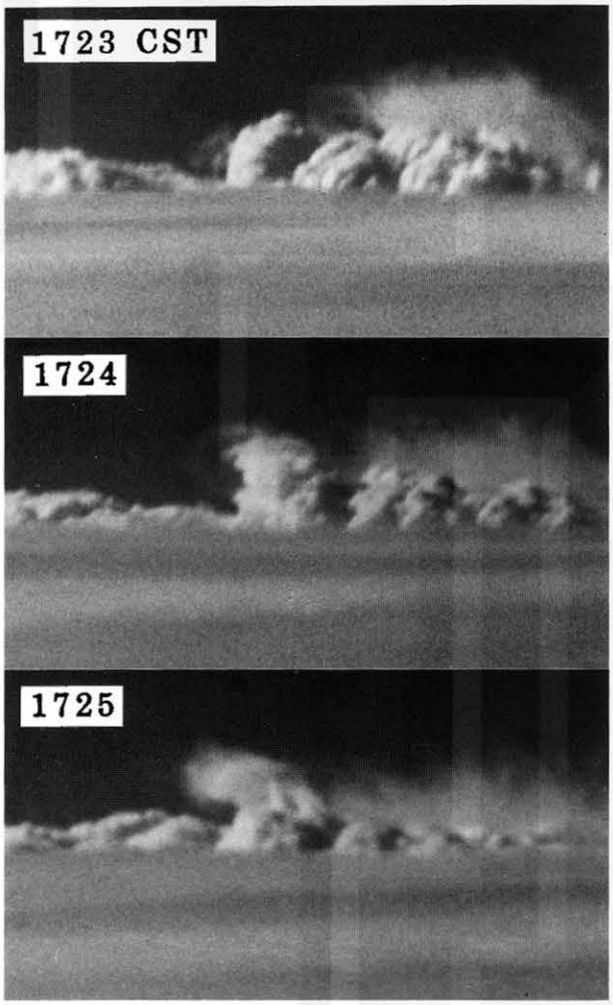

Fig. 3.2-3 Glaciation of an overshooting dome on 13 May 1972 over west-central Texas. Photos from Lear Jet flying at 45,000', 160 km from the cloud.

At numerous occasions, while flying in research Lear Jet, I witnessed glaciation of overshooting tops. Glaciation in cloud physics is the sudden transformation of supercooled droplets into ice crystals. If an overshooting top below the critical temperature of -40°C consists entirely of ice particles, it should not glaciate again. Three photographs (Fig. 3.2-3) taken at one-minute intervals, however, reveal a rapid glaciation of the dome top into hairy streaks curling from the top to the side of the dome. Two minutes later, the top half of the dome glaciated into a fuzzy cloud drifting away from the dome top.

In spite of the photographic evidence of glaciation, it is unlikely that an overshooting dome consists solely of supercooled hydrometeors. By definition of glaciation, on the other hand, it is hard to visualize that the frozen hydrometeors inside the dome glaciate again into a fuzzy-looking ice cloud.

Another strange and noteworthy phenomenon I observed and photographed was the accelerated glaciation of the dome triggered by the anvil-top cirrus as it moved over the dome top. The impression I received was a seeding of water cloud by cirrus (ice crystal) cloud at the dome top.

In determining the rapid rise and sink of overshooting tops, I took a number of Super-8 movies at one-half second intervals while standing in research Lear Jet. The most difficult thing was to hold the movie camera steadily while flying around thunderstorms in moderate turbulence. In producing a time-series display, movie frames at 10-sec intervals were enlarged and arranged (Fig. 3.2-4). The picture sequence shows the existence of domes (1 to 4 km in diameter) and turrets (less than 1 km in diameter).

The vector motion of the dome boundaries were computed to infer the incloud airflow, which gave rise to the computed cloud-motion vectors (Fig. 3.2-5). In general, the rising motion of a dome turns into sinking motion within one to three minutes. During my 12 years of Lear-Jet Experiment, I have never seen an overshooting cloud in steady state. Rapid scan pictures at 5-min intervals often fail to retain the continuity of fast-changing overshooting domes.

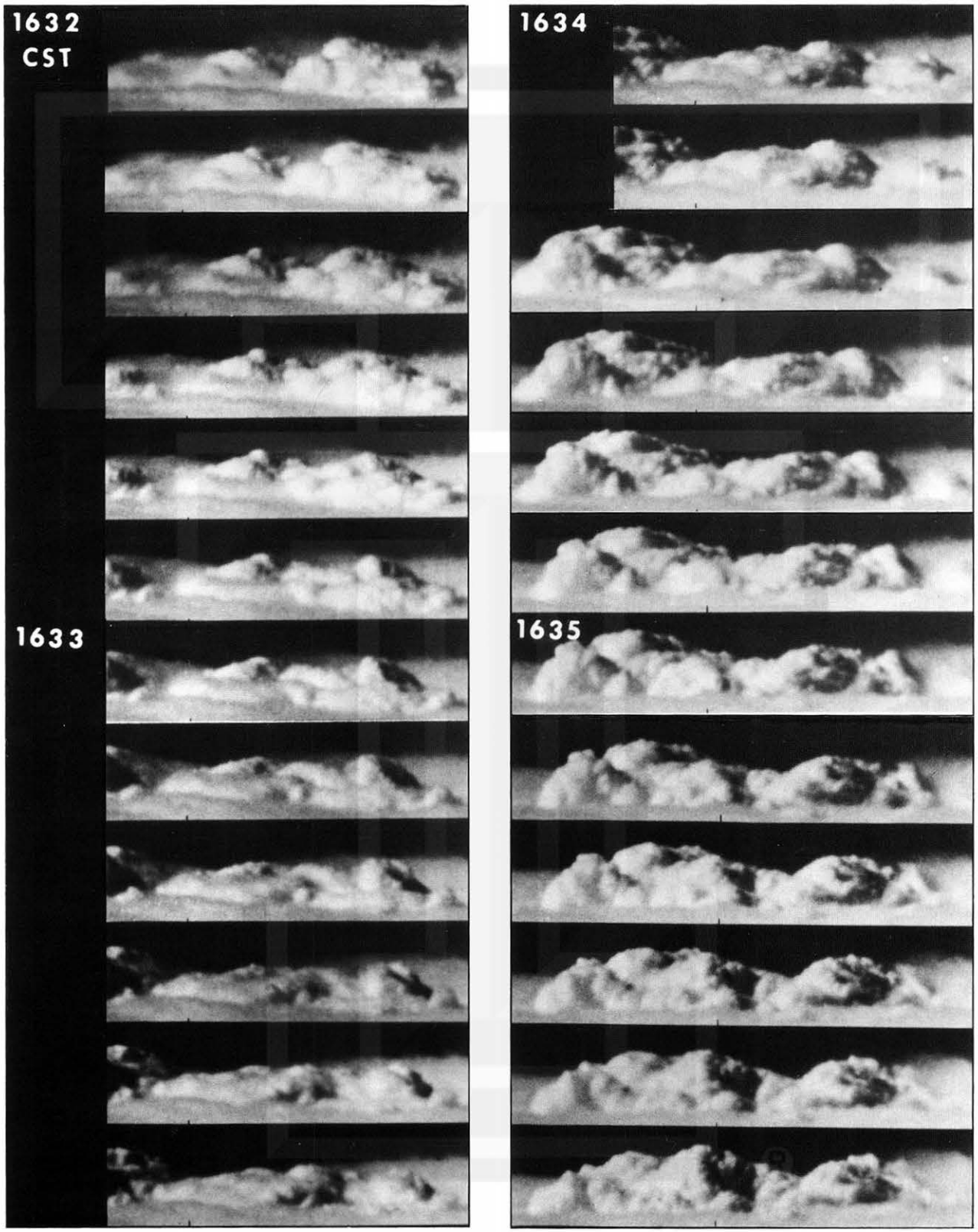

Fig. 3.2-4 A sequence of 10-sec interval pictures enlarged from Fujita's Super-8 movie taken at two frames per second. Overshooting clouds on 12 May 1972 were located at 27.2°N and 98.7°W, 100 to 110 km to the north of the Lear Jet at 47,000'.

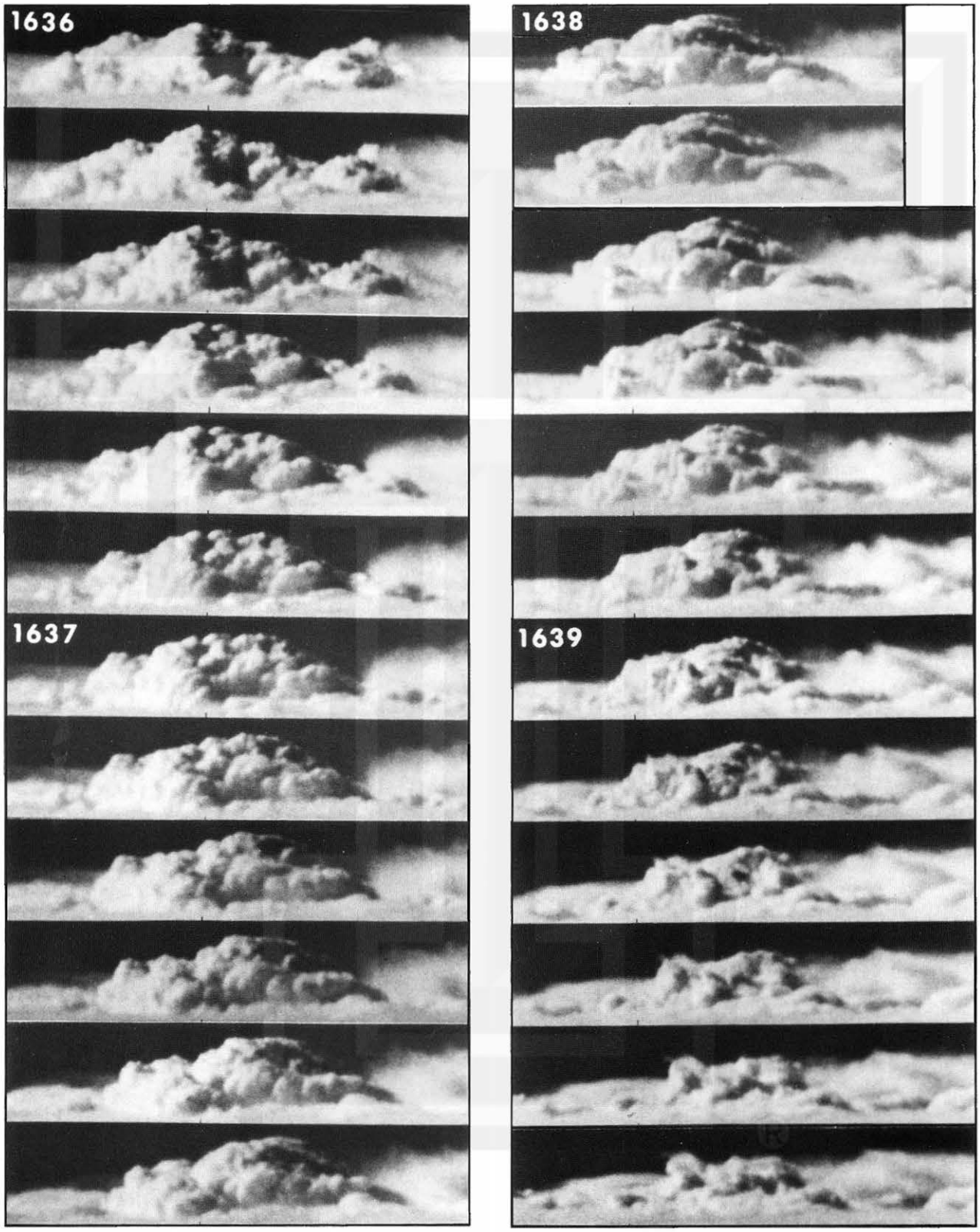

Fig. 3.2-4 ——Continued——

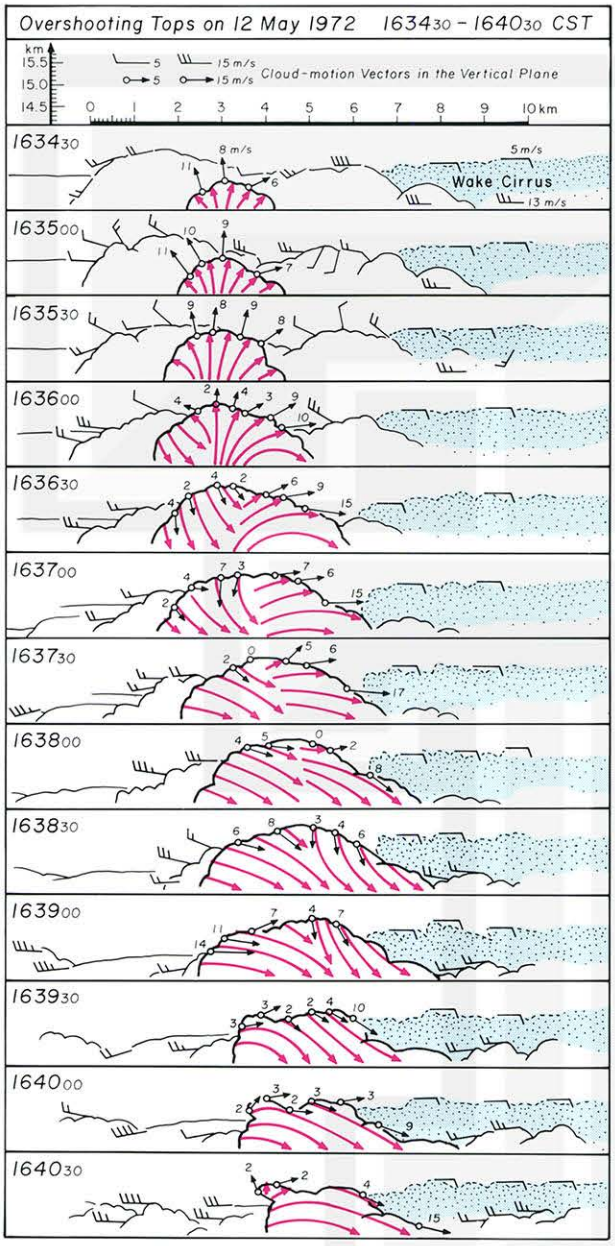

Fig. 3.2-5 The internal airflow of an overshooting cloud in Fig. 3.2-4 estimated from the motion vectors of dome-cloud boundaries. This diagram shows a rapid change of a rising dome into a sinking dome. As seen in this example, I have not witnessed cloud parcels from overshooting clouds descending into the stratosphere. Instead, parcels always sink into the anvil clouds.

Collapse and Splashout

The foregoing evidence reveals that an overshooting top sinks rapidly into the anvil cloud which obscures the sinking motion taking place beneath the anvil top visible from high altitude aircraft. I found, however, a rare case of an overshooting top collapsing at the edge of an anvil, allowing me to compute the sinking and spreading motions as fast as 20 m/sec (Fig. 3.2-6).

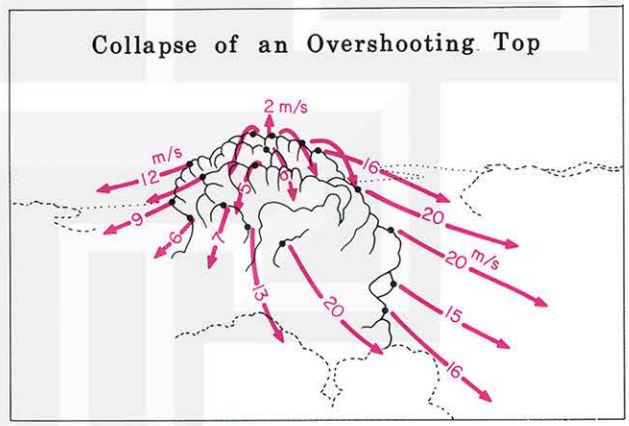

Fig. 3.2-6 Motion vectors of a collapsing dome on 12 May 1972. Vectors were computed from the picture sequence in Fig. 3.2-7.

The picture sequence used for computing the velocity field shows a dramatic expansion of the collapsing cloud beneath the anvil-top level (Fig. 3.2-7). When such sinking and expanding motions take place abruptly inside an anvil cloud, the induced motion field will be analagous to that created by a huge rock thrown into a pond. Simplified consequences will be a rapid escape of the anvil-top materials from the collapsing area outward. If the top sinks far below the anvil surface, anvil materials will splash up into the stratosphere like a huge fountain at the anvil top.

A model of the collapse and splashout I had in mind consisted of sinking stage, morning-glory stage, and fountain stage

A Collapsing Dome over Texas on 12 May 1972

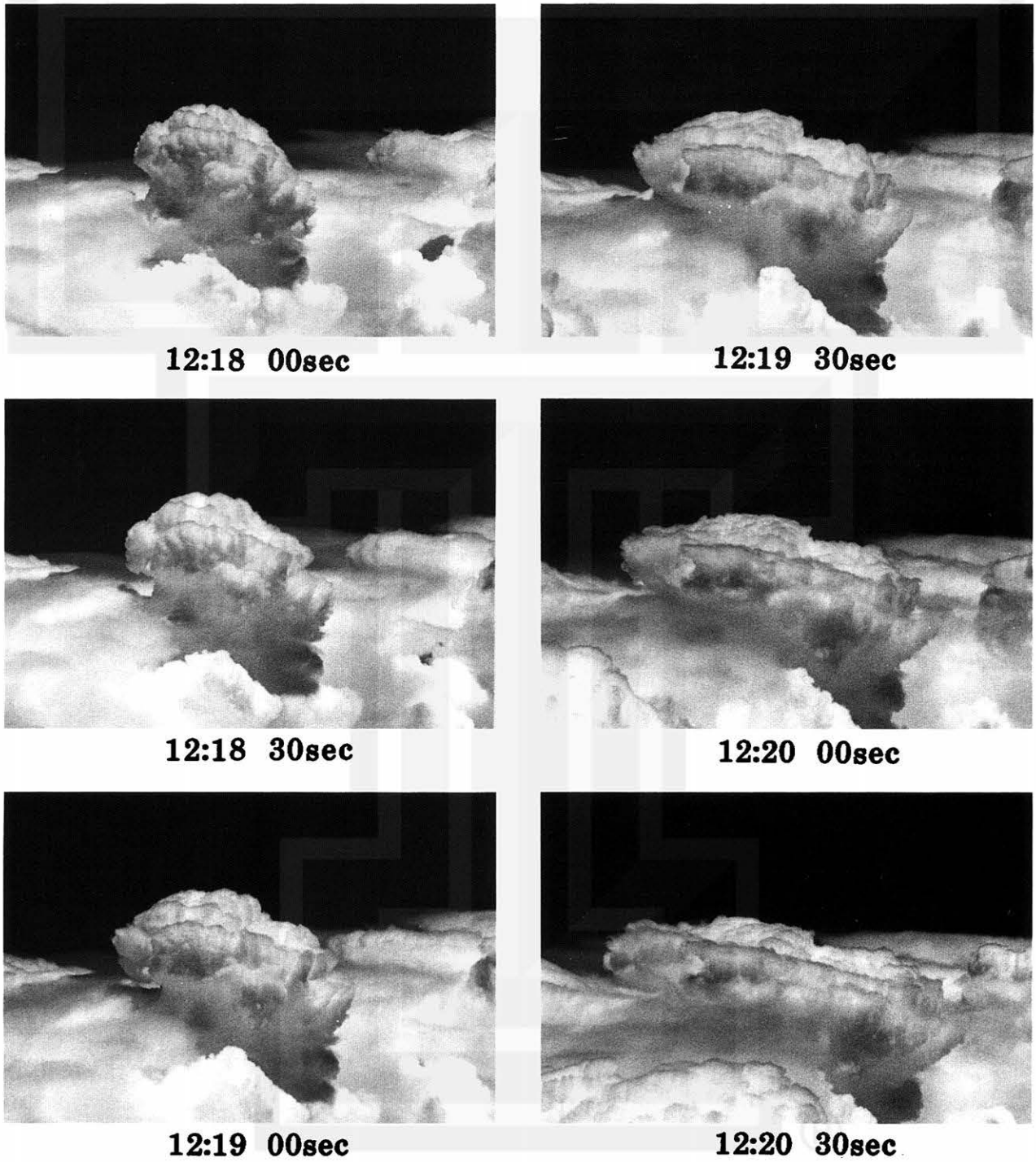

Fig. 3.2-7 Time sequence pictures of an overshooting dome on 12 May 1972 over Cotulla, Texas taken during the sinking and expanding stages of the cloud found at the edge of the anvil cloud. The distance to the cloud was 85 km from the Lear Jet at 47,200'. Picture times in CST.

(Fig. 3.2-8). During the Lear-Jet Experiment in 1972-83, I searched extensively for the evidence of these three stages. On 6 May 1973, I was delighted to find a sinking dome at 180 km NNW of San Antonio, Texas. The cloud in the early sinking stage spotted at 1850 CST turned into morning-glory stage. Although my flight altitude of 50,000' was not high enough to overview the splashout phenomenon, the event I witnessed was good enough to infer the collapse and splashout processes (Fig. 3.2-9).

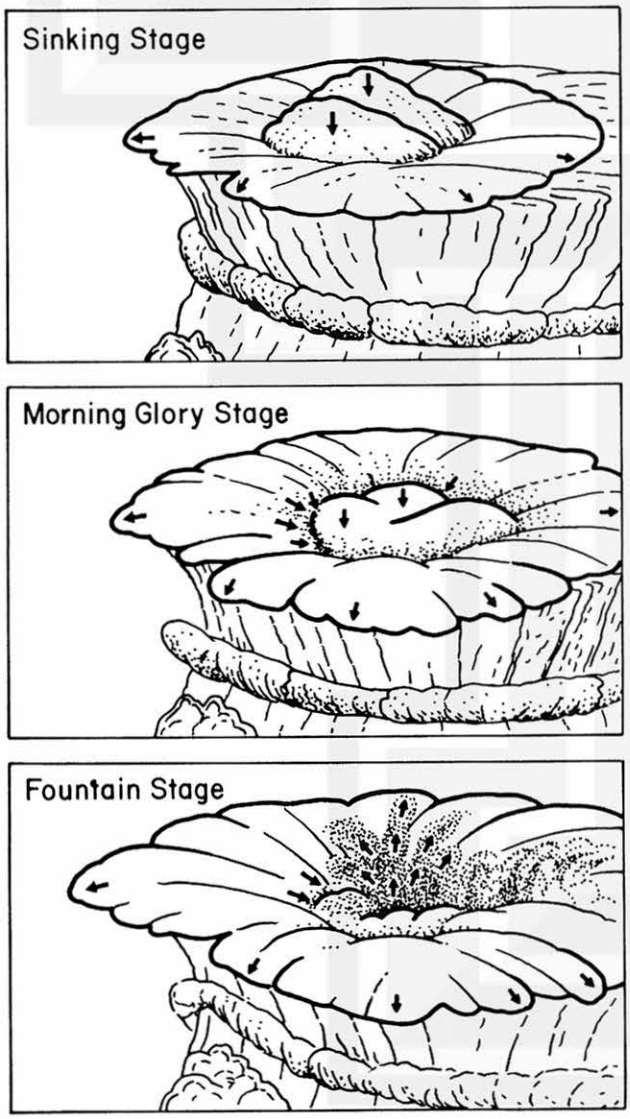

Fig. 3.2-8 A conceptual model of the three stages of the collapse and splashout processes expected to occur at an anvil top when an overshooting dome sinks rapidly into the anvil cloud.

The first picture at 1850 CST shows the early sinking stage of an overshooting dome surrounded by the thin layer of the anvil surface escaping from the base of the sinking dome. As the dome sank, the escaping motion accelerated, resulting in a significant spillout edge of the anvil surface (rim of morning glory) at 1851 CST. Thirty seconds later, the top of the dome disappeared into the anvil, reaching the morning-glory stage.

Thereafter, the rim of morning glory kept expanding for two minutes while small pieces of cirrus clouds bubbled up from where the dome had disappeared. No fountain stage was reached before the photographic sequence ended at 1853 30s CST.

The fountain stage was found and photographed during my final Lear-Jet Experiment over western Kansas in 1983. Shortly after seeing the collapse of an overshooting dome into an anvil top, a large fountain of cirrus formed suddenly (Fig. 3.2-10) to the west of our Lear Jet flying at 45,000'. At the conclusion of the experiment, I was pleased to confirm the three stages of "collapse and splashout" taking place above the anvil top rarely seen by man from close ranges.

Although I had seen a number of strange phenomena during my Lear-Jet Experiments, I never expected to witness a smoking cloud, somewhat like the cigarette smoke rings I used to see at Times Square in New York City. At 1736 CST on 12 May 1972, I found a pair of smoke rings off the west edge of an extensive anvil cloud at 47,000' over Rio Grande, 80 km WNW of Brownsville, Texas. The maximum westerly jet at 42,600' was 94 kts (48 m/s) and the wind at the smoke-ring height was 100 kts. The smoke rings were moving away from the parent anvil top. I am still puzzled on how to explain the mechanism of the smoke rings which were moving against the strong headwind at 47,000' over the Texas-Mexico border.

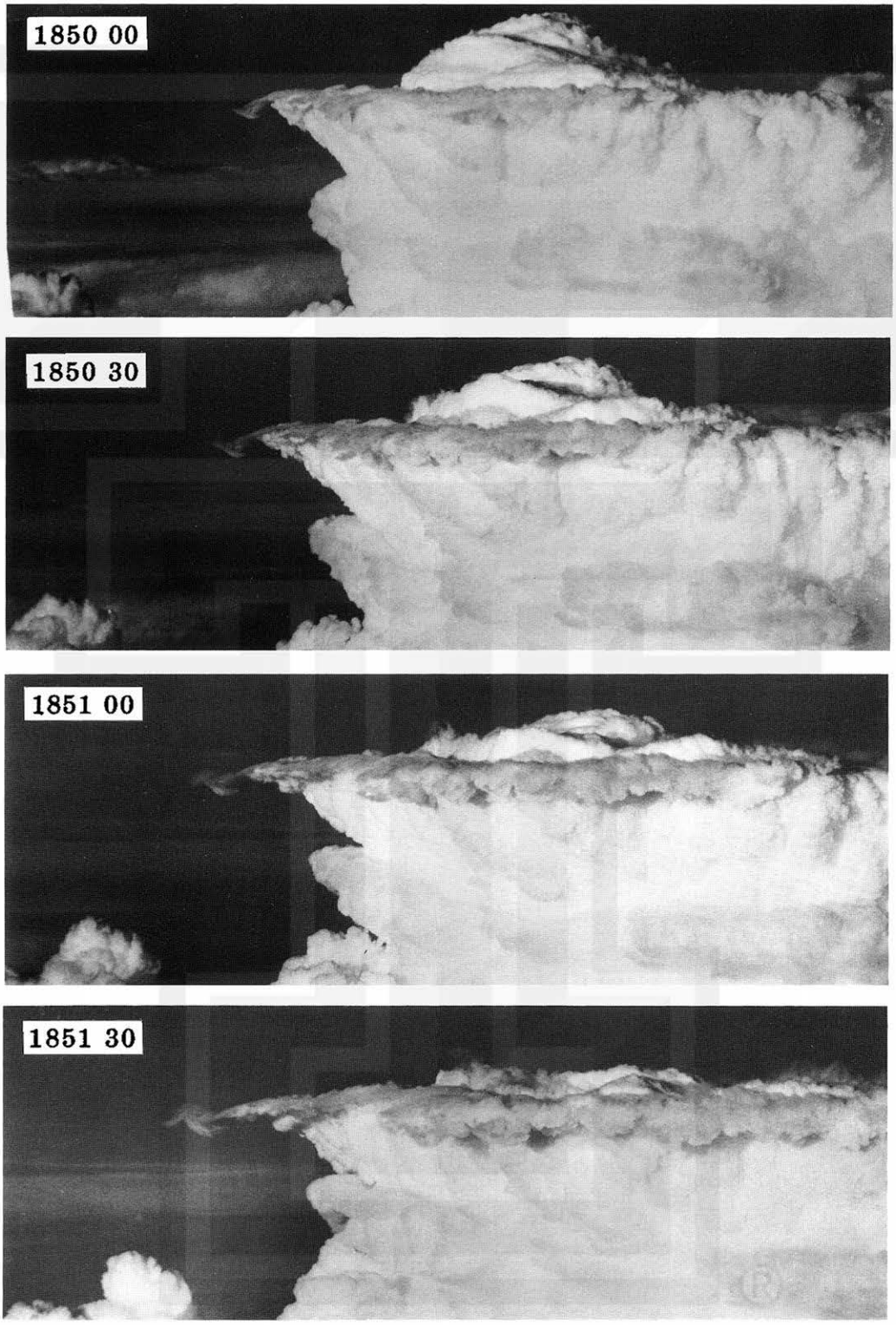

Fig. 3.2-9a Collapse and splashout motions photographed on 6 May 1973 in southwestern Texas from Lear Jet flying at 50,000'. The first picture at 1850 00s CST shows the onset stage of the splashout.

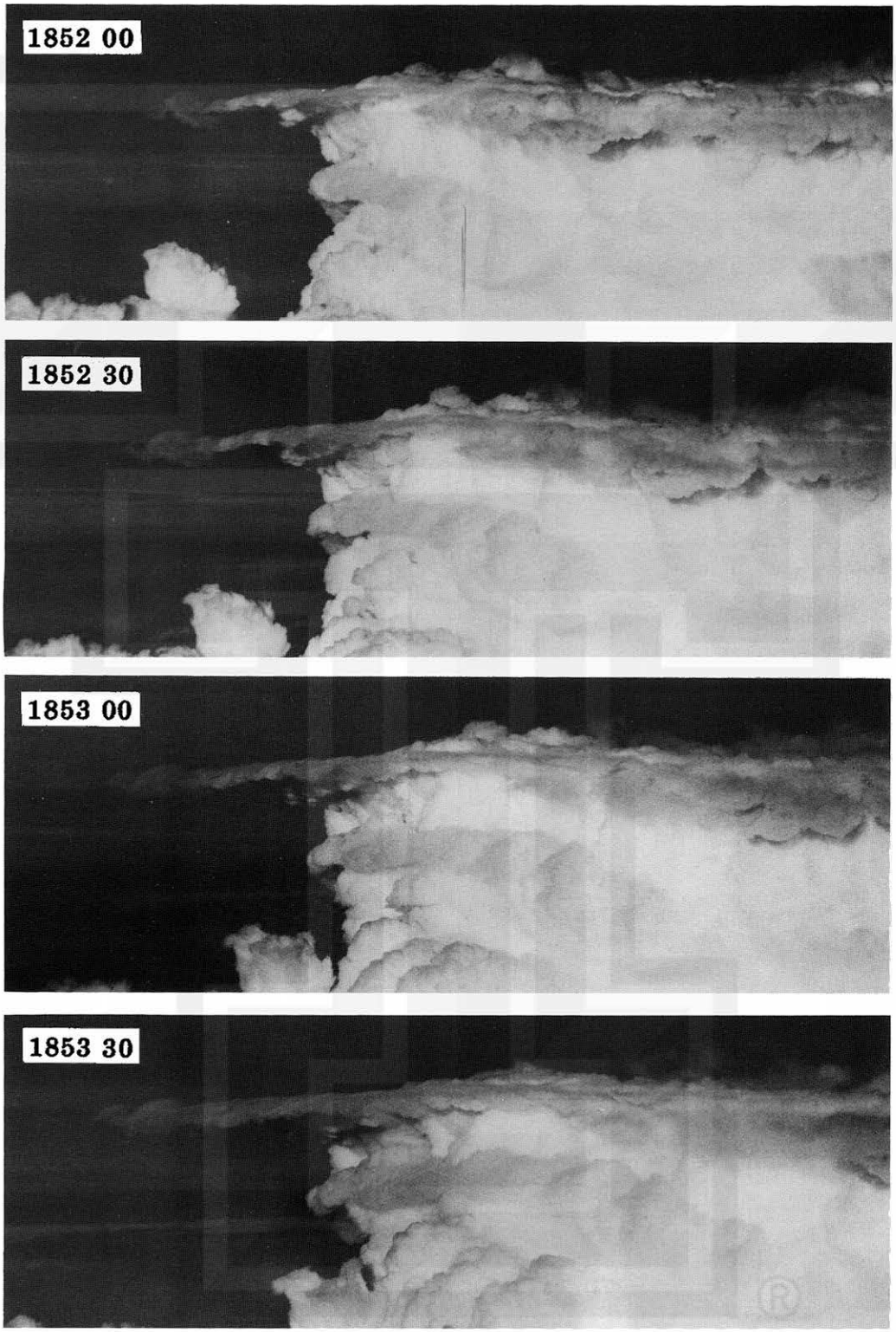

Fig. 3.2-9b The splashout cloud at the anvil surface was moving upwind, inducing both wave and vortex motions as it extended out upwind from the parent anvil top.

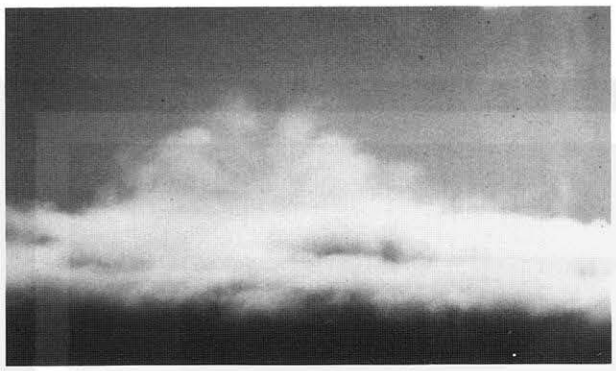

Fig. 3.2-10 The fountain stage of the anvil top photographed at 1750 30s CST 25 August 1983 over western Kansas. It was the last day of my Lear-Jet Experiment which began in 1972.

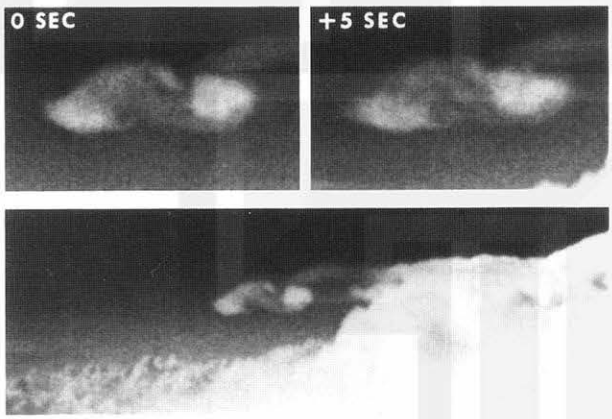

Fig. 3.2-11 A pair of smoke rings at 1736 CST on 12 May 1972 photographed from Lear Jet flying at 47,000' over the Rio Grande. The picture was taken looking northeast.

Anvil Top Cold Front

The top of a large anvil cloud is colder than its environment, acting as a "Little Antarctica" with high albedo and cold surface temperature. I expected that an extensive anvil surface generates katabatic winds blowing against the relatively weak westerlies inside the lowermost stratosphere (Fig. 3.2-12).

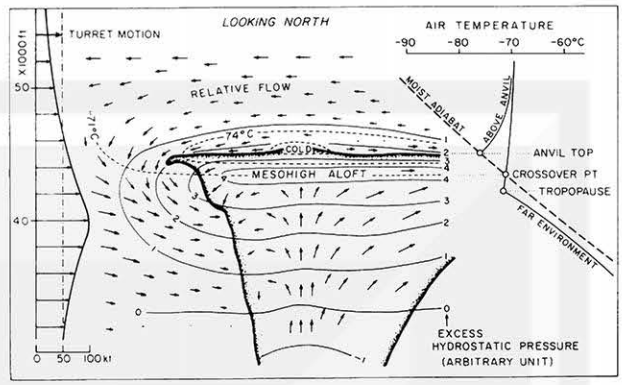

Fig. 3.2-12 A schematic model of a high-pressure area expected to form over an extensive anvil cloud acting as a Little Antarctica.

On 13 May 1972, during a continuous photographic mission over west-central Texas, an anvil-top cold front was found and photographed. The parent anvil cloud was 470 km long and 240 km wide (290 mi and 150 mi) and the head of the anvil with overshooting activities inside was

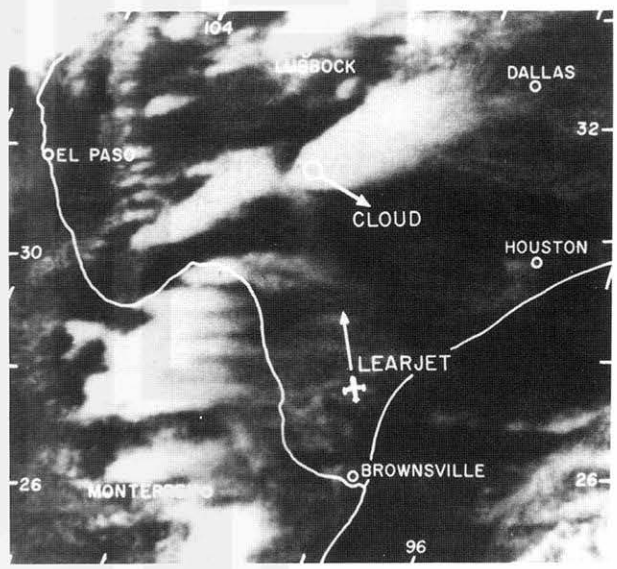

Fig. 3.2-13 A satellite picture of the anvil cloud over western Texas at 1537 CST on 13 May 1972.

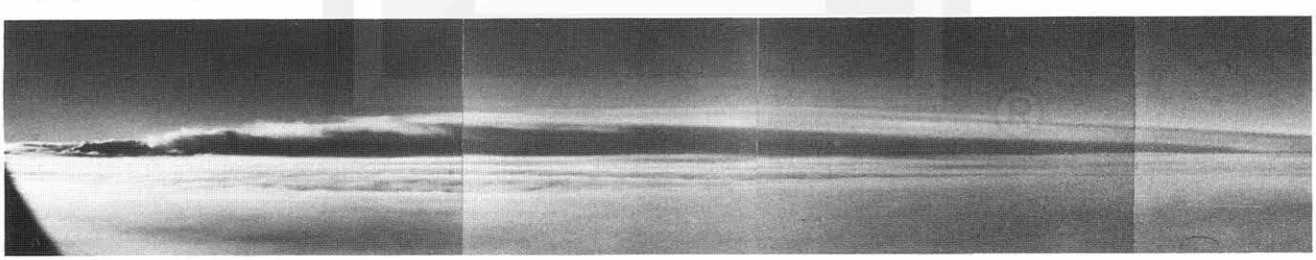

Fig. 3.2-14 A panoramic picture of the anvil cloud in Fig. 3.2-13 taken at 1901 CST. The anvil-top cirrus was 1.5 to 2 km thick, extending 200 to 300 km to the northeast.

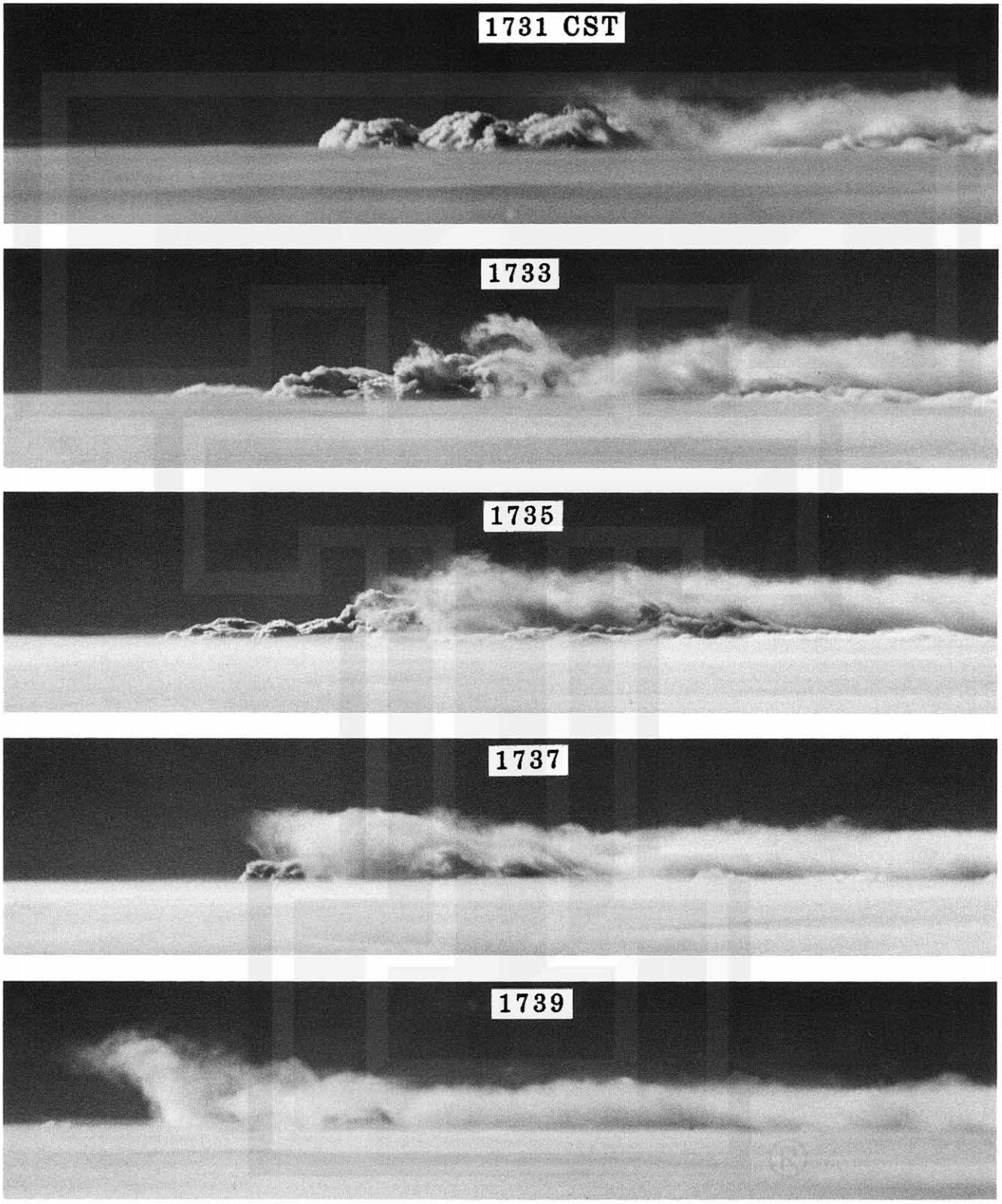

Fig. 3.2-15 An anvil-top cold front of May 1972 made visible by the stratospheric cirrus cloud moving west (left) at 87 km/hr or 54 mph relative to overshooting tops. Shortly after these pictures were taken, the fast moving cirrus topped by Kelvin-Helmholtz waves reached far to the west of the parent anvil cloud. It is likely that the K-H waves could cause severe CAT after becoming invisible. Pictures were taken from research Lear Jet at 45,000' over San Antonio, Texas.

moving toward the southeast (Fig. 3.2-13). The anvil cloud was topped by a long stream of cirrus, 1.5 to 2 km thick and 400 km (250 mi) long. It was one of the longest anvil-top cirrus seen from Lear Jet in 1972 (Fig. 3.2-14).

A strange movement of the anvil-top cirrus was first noticed shortly before 1830 CST when a wedge, resembling to the cold-frontal slope, began pushing toward the west (left in pictures). The computed westward speed was 87 km/hr (54 mph) relative to the overshooting domes in the picture sequence (Fig. 3.2-15). It should be noted that the tilt of the cirrus streaks toward the left indicates the faster movement of the cirrus at higher altitudes.

The tilt of the frontal surface, 30° at 1731 CST increased to 60° at 1733, and to an overhang tilt of 110° at 1735. In the final picture at 1739 CST, the top of cirrus cloud jumped up to 2.8 km (9,100') above the anvil surface characterized by an overhang tilt of 130°, suggesting the violent nature of the newly-identified front above the anvil surface.

This finding could be important for the air safety of high-altitude aircraft. The anvil-top cirrus could cause a short-lived severe turbulence which could be encountered by one aircraft, but not by the others following. The turbulence cannot be detected by airborne radars, and may not always be recognizable by pilots flying in thin cirrus clouds. What we should do is not to fly within 3 km above the anvil top while staying away from the upwind edge of an extensive anvil cloud.

Mesocyclone Thunderstorm

On 21 April 1961, a mesocyclone cloud 120 km southwest of Kansas City, Missouri (Fig. 3.2-16) was studied by flying three aircraft at high level, 40-45,000' (B57), middle level, 20,000' (DC-6), and low level,

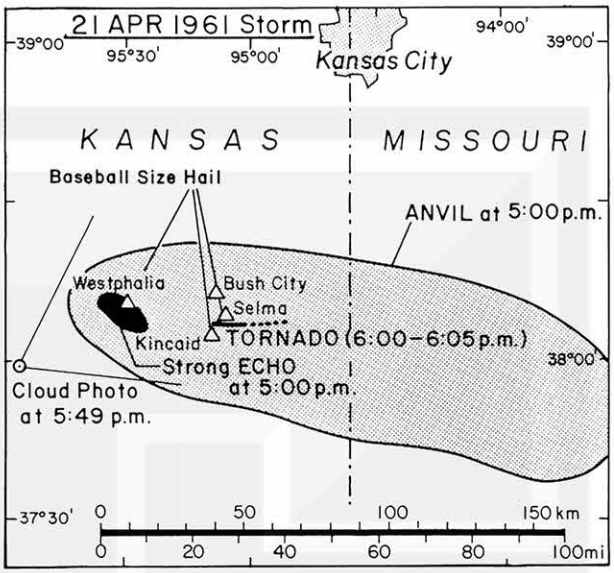

Fig. 3.2-16 The rotating thunderstorm of 21 April 1961 to the southwest of Kansas City, Missouri. The cloud spawned the Selma tornado rated F3.

3,000' (B26). The core of the thunderstorm viewed from the direction perpendicular to the cloud motion tilted 33° from the vertical (Fig. 3.2-17).

The thunderstorm at 1747 CST, looking northwest, was a rotating thunderstorm characterized by swirling low clouds and overshooting tops (Fig. 3.2-18) visible from the DC-6. While three levels were flown, the Kansas City WSR 57 radar photographed the mesocyclone echo which produced the Selma tornado at 1800-1805 CST, 10 to 15 min after I took the picture.

High-level Flight

The B-57 made three loops, 1,000' to 3,000' above the anvil top (Fig. 3.2-19). During the first loop, when overshooting tops were still insignificant, 40,300' to 41,000' were not influenced by minor overshooting activities at 1545-1602 CST.

When the second loop was flown at 1600-1630 CST, time of the Selma tornado,

the flight level was increased to 41,600'-43,000' in order to top the anvil. The flight-level winds were distorted significantly by large and tall overshooting domes. The difluence angle of the impinging winds on the upwind side was as large as 110° due to obstruction. On the downwind-side of the dome area, a confluence angle of 30° with 108 kts windspeed was measured at 43,000'. The aircraft winds clearly reveal the existence of severely-distorted obstacle flow at the flight level.

The third loop was flown at 1613-1645 CST after the Selma tornado had lifted. The flight level was further increased to 42,800'-45,000' in topping the anvil. The obstacle flow on the upwind side remained unchanged, while the wake flow became unstable in both time and space. These

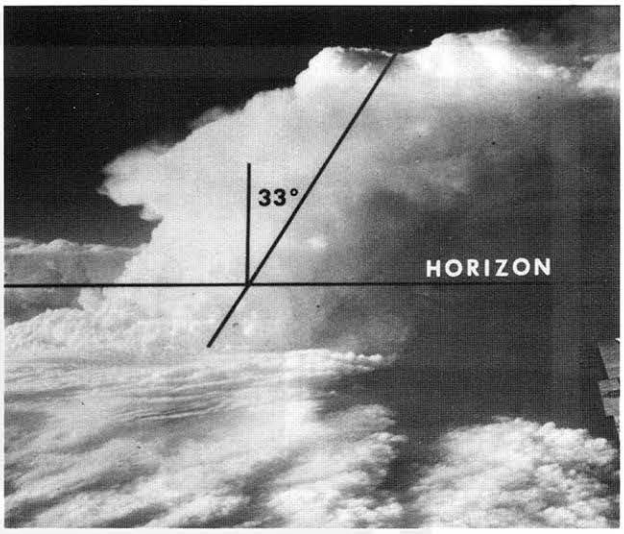

Fig. 3.2-17 Tilted cloud axis of the mesocyclone thunderstorm of 21 April 1961 looking north. Photo by Fujita at 1753 12s CST from DC-6.

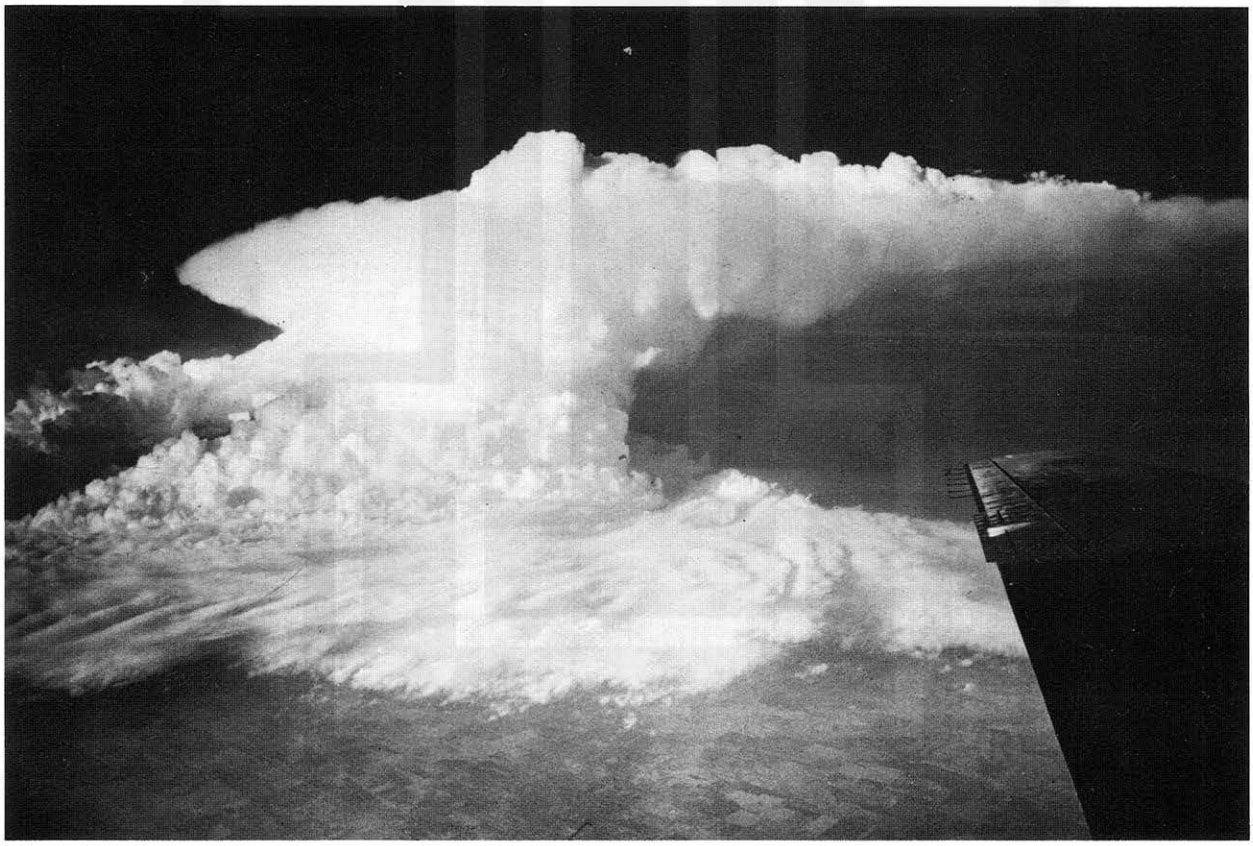

Fig. 3.2-18 The total view of the mesocyclone (rotating) thunderstorm of 21 April 1961 photographed by Fujita from DC-6 at 1749 58s CDT, looking toward the 312° azimuth.

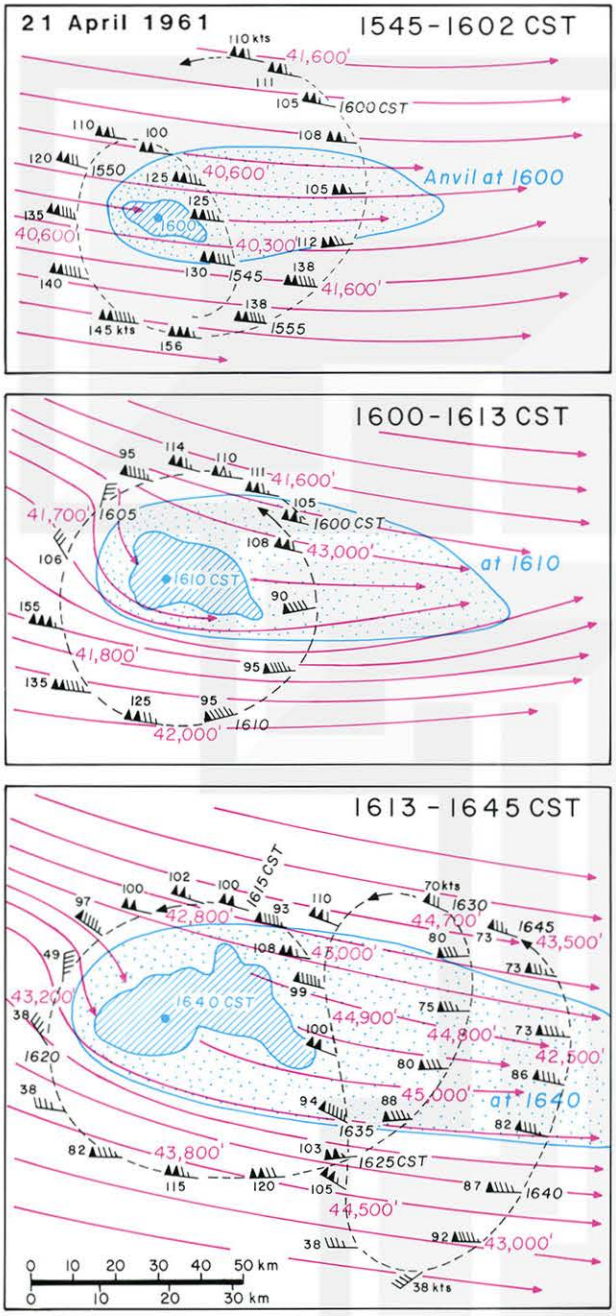

Fig. 3.2-19 Three loops around the overshooting domes of the 21 April 1961 thunderstorm flown by B-57 to determine the anvil-top winds to be affected by the obstructing domes.

three loop flights above the anvil top revealed a significant obstacle flow during intense overshooting activities. The obstacle flow was most pronounced when the Selma tornado was on the ground.

Middle-level Flight

The composite winds at 20,000' flown between 1620 and 1820 CST revealed a pronounced obstacle flow evidenced by a 40° difluence angle on the upwind side. Due to the rotation of the thunderstorm, the maximum wind on the right was 78 kts (40 m/s) which was 25 kts (13 m/s) faster than that on the left side. Apparently, the high winds on both sides of the updraft were caused by the acceleration of the airflow while going around the updraft core.

There was a very slow, 38 kts (20 m/s) wake flow on the downwind side of the updraft core. It is seen that the center of the slow winds deviated far to the left of the expected straight-line wake. The cyclonic shift of the slow winds is probably due to the rotation of the storm core (Fig. 3.2-20).

Low-level Flight

While I was directing the middle-level DC-6, Dr. Chester Newton directed the low-level flight, encountering severe turbulence beneath the rotating updraft. However, the results he obtained were very significant and rewarding. The composite wind map (Fig. 3.2-20) shows the 40 to 45 kts (20 to 23 m/s) inflow from the south to the updraft region. On the other side of the updraft, windspeed dropped to almost zero, suggesting that practically 100% of the inflow air was consumed by the rotating updraft.

The maximum vorticity and convergence at low level were 0.001 sec^{-1} and 0.017 sec^{-1}, respectively. This magnitude of convergence inside a 1-km deep layer would induce a 17 m/s (56 fps) updraft at the top of the inflow layer. Meanwhile, the vorticity of the inflow winds was large enough to generate and maintain the mesocyclone thunderstorm which spawned the Selma tornado, rated F3.

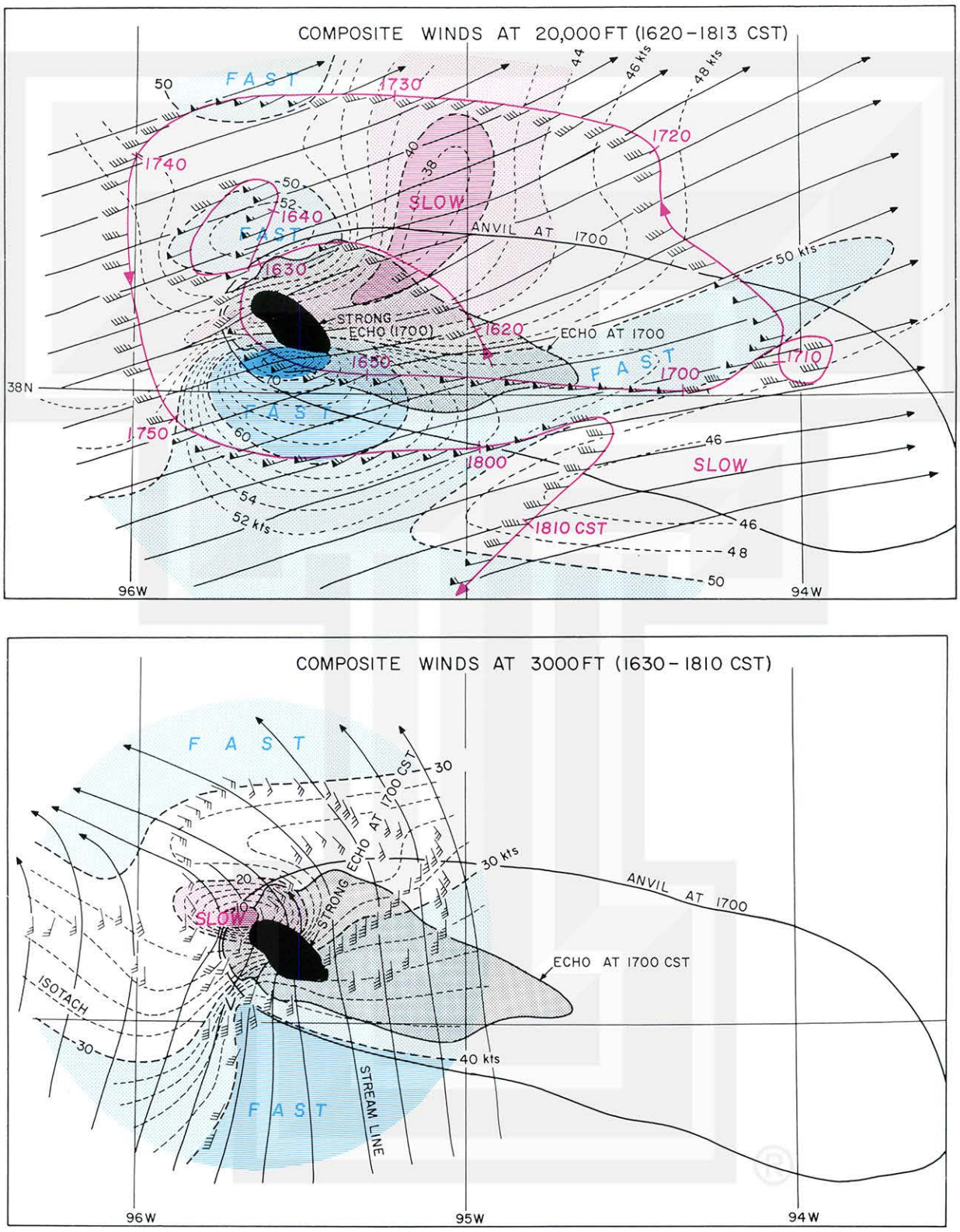

Fig. 3.2-20 The wake flow behind the 21 April 1961 thunderstorm obtained by plotting DC-6 winds along the flight path relative to the major echo (above). Significant convergence and vorticity fields at the flight level beneath the cloud base. Chester Newton directed the B-26 flight encountering severe turbulence (below).

Tornado Cloud Flyover

Along with Greg Forbes, Tom Umenhofer, and Duane Stiegler, a research Lear Jet took off Chicago's Midway Airport on 23 February 1977 toward Mississippi in an attempt to intercept a tornado-producing thunderstorm. The day in winter was chosen foreseeing a possible flyover because we cannot top a spring thunderstorm. While approaching Jackson, Mississippi above high overcast, I saw an active dome cloud and a sinking cloud top with benign appearance. Both clouds were identified later on a satellite picture (Fig. 3.2-21).

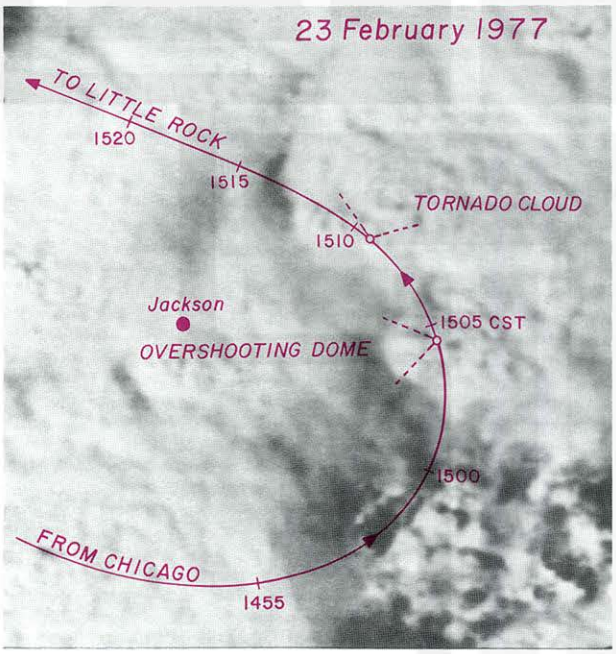

Fig. 3.2-21 The path of our Lear Jet which flew over the tornado-producing thunderstorm of 23 February 1977. Satellite picture at 1500 CST.

The top of the overshooting dome (Fig. 3.2-22) photographed at 1504 CST was weird but no storm on the ground was reported. Very soon, we received a radio message from Jackson Weather Service that a doughnut-shaped echo was seen beneath the cloud we were flying over. I asked the pilot to fly over the southwest edge of the cloud to take slant pictures.

At 1509, a horseshoe crater was seen atop the benign-looking cloud (Fig. 3.2-23). Several minutes later, an F3 tornado was on the ground. At 1550 CST, the second tornado (F4) touched down from the same cloud.

Fig. 3.2-22 A weird-looking overshooting dome which did not produce confirmed damage on the ground. Photo at 1504 CST 23 February 1977.

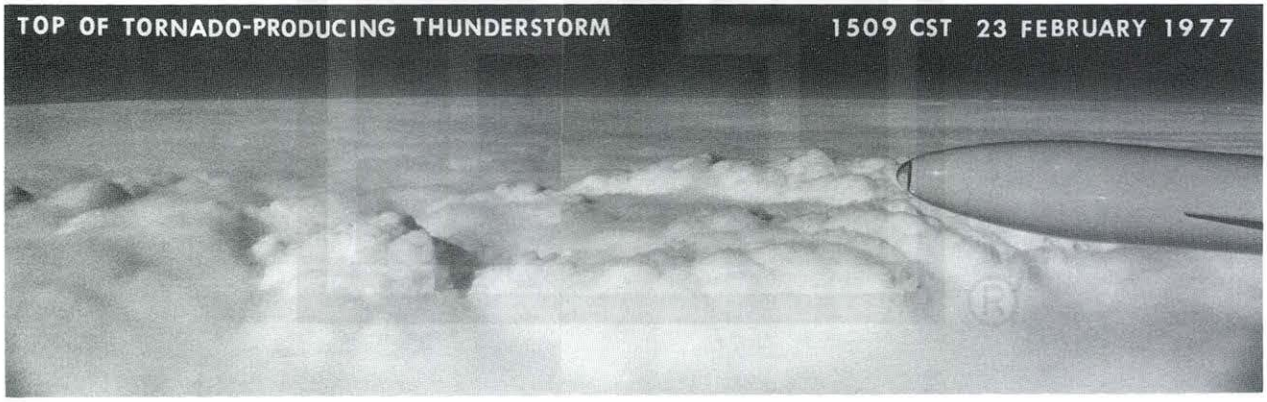

Fig. 3.2-23 A horseshoe crater found atop the doughnut-echo thunderstorm which spawned F3 and F4 tornadoes in succession.

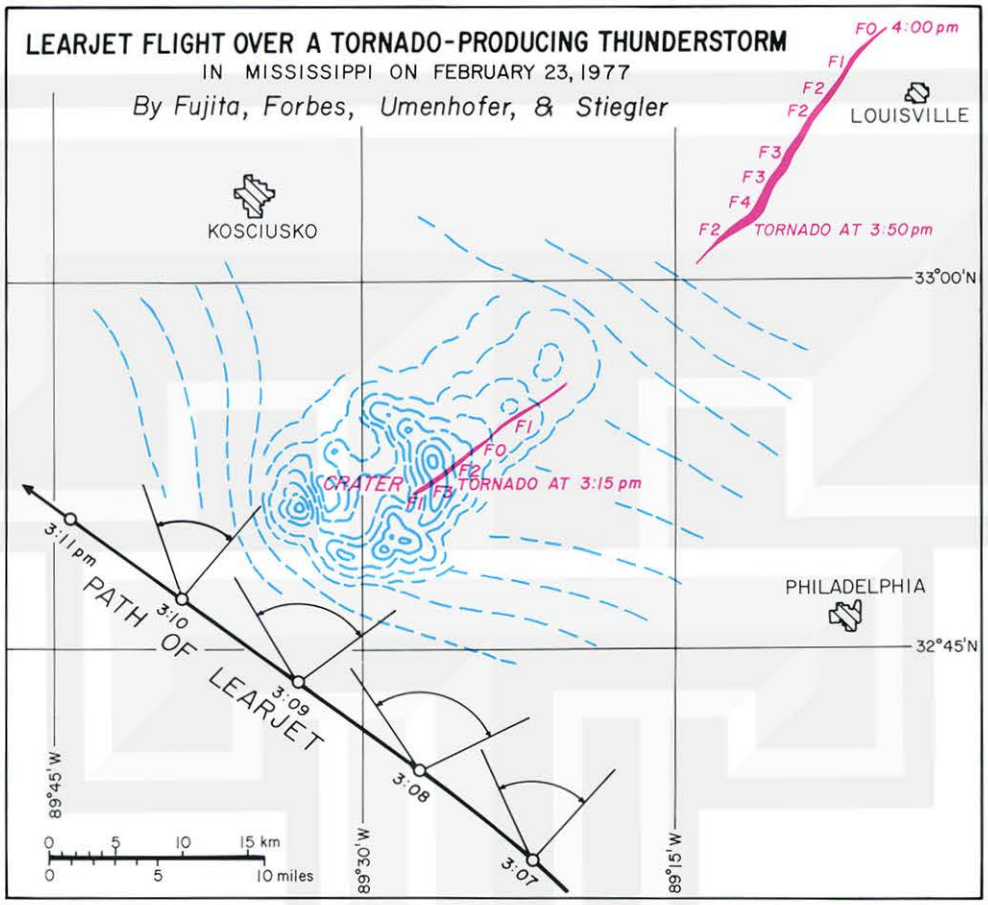

Fig. 3.2-24 Path of the Lear Jet during flyover when four pictures were taken at 1-min intervals. Intensities of two tornadoes were determined by the post-storm survey of the storm damage.

3.3 Interpretation of Anvil Top Warming

Since 1983, when the warm IR temperature atop severe thunderstorms was pointed out by McCann, there has been a mini-controversy on the cause of the warming.

Three possible causes proposed were: (1) warm and low emissivity cirrus in the stratosphere originated at or near the anvil surface in the wake region, (2) warm temperature of overshooting and descending parcels with large mixing along semi-steady state trajectories, and (3) depressed warm anvil surface in the wake region. By putting together the photographic evidence of my Lear Jet experiments, I concluded that (3) is the major contributor to the warming, followed by (1) and possibly (2). There are other opinions, however.

A significant wake of altostratus (Fig. 3.3-1) reveals that the flow was made visible by a veil cloud cascading down into the convective wake. Another picture of a wake at anvil top shows a cascade of anvil cirrus toward the depressed anvil surface which extends downwind into the wake region (Fig. 3.3-2). This type of picture is rare, because a wake region is usually covered with thick wake cirrus in the stratosphere.

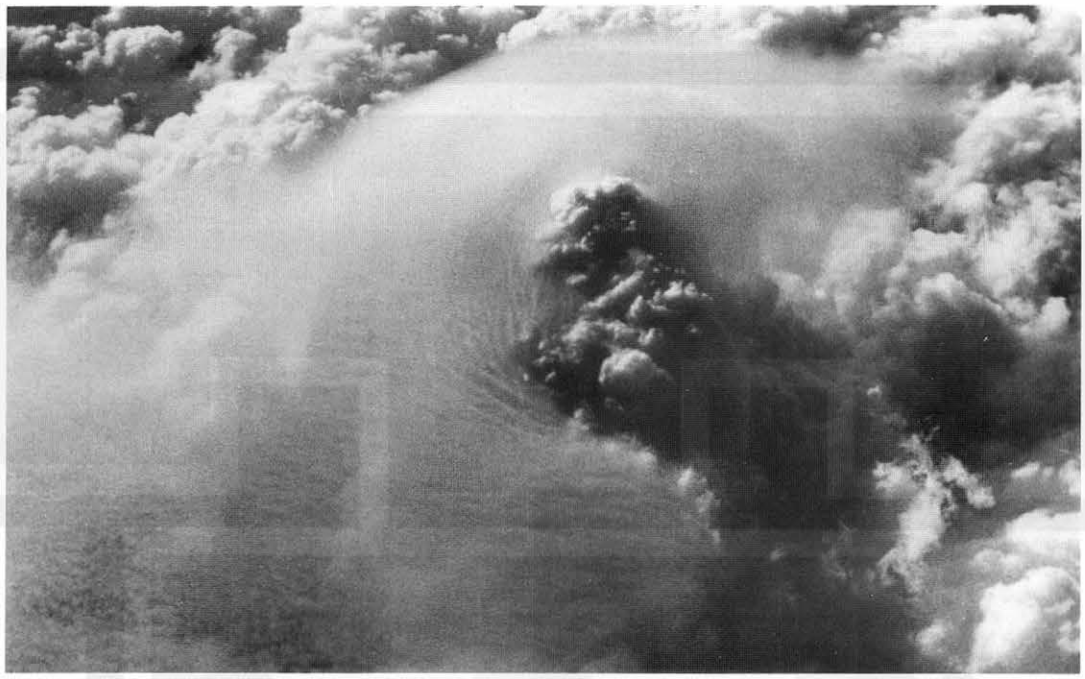

Fig. 3.3-1 An obstacle flow made visible by a veil of altostratus cloud blocked by towering cumuli over Missouri at 1525 CST 14 April 1973. The veil cloud was moving around the convective towers while cascading down on the wake side of the obstructed flow. Photo by Fujita from research Lear Jet.

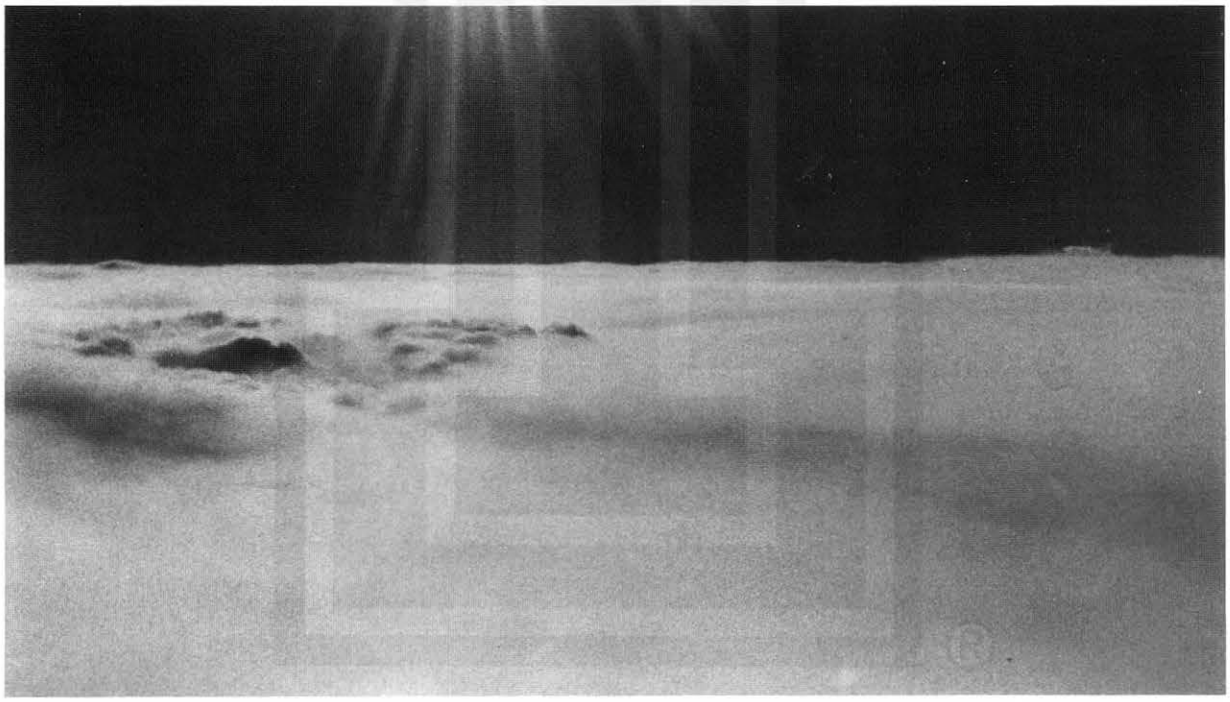

Fig. 3.3-2 A depressed anvil surface in the wake of the convective towers at 1630 CST on 4 April 1977 over western Alabama. The anvil surface, obstructed by a number of convective towers, was cascading down into the wake region, resulting in a depressed anvil surface. Photo by Fujita from research Lear Jet.

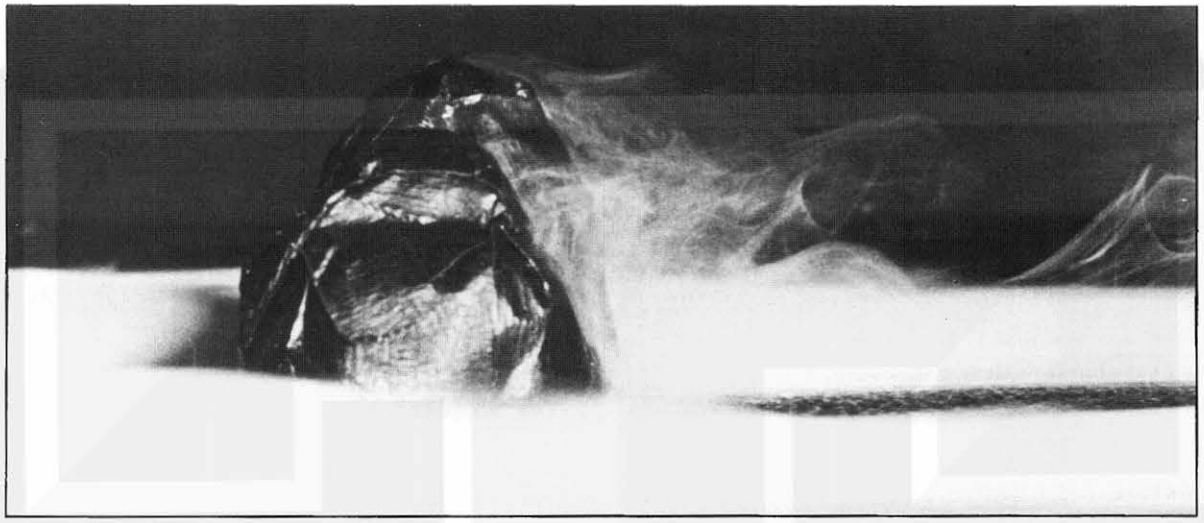

Fig. 3.3-3 A laboratory model of a simplified wake flow of dry-ice smoke impinging upon an obstructing rock. Seen in the wake region are depressed dry-ice surface and dry-ice smoke rising on the wake-side slope of the rock.

In an attempt to visualize the blocking effect, an obstacle was placed inside the stream of cold dry ice (Fig. 3.3-3). As expected, the dry-ice surface in the wake was depressed, exposing the solid surface underneath, while the smoke of cold dry ice kept rising on the wake-side slope of the obstructing rock. In the real atmosphere, a windshear reversal at the tropopause will transport the smoke upwind, passing over the obstructing cloud top.

Based on the Lear Jet photographs of the stratospheric cirrus, a model of an extensive wake effect was produced (Fig. 3.3-4). In warm seasons, the wake cirrus often rises above overshooting domes. It is likely that infrared radiation penetrates down 1 to 2 km into the wake cirrus, detecting the mixture of cloud and background temperature which is warmer than the temperature of overshooting domes.

Extensive time-motion and stereoscopic measurements of the 2 May 1979 thunderstorm over Oklahoma revealed the 16.6 km or higher tops of wake cirrus. Nevertheless, the IR temperature of these high tops are considerably warmer than the dome cloud located outside the wake region (Fig. 3.3-5).

On the basis of the 3-aircraft measurements of the mesocyclone cloud (Figs. 3.2-19 and 20), the wake flow could extend from the anvil top down to the middle level. It is also unlikely that a clear-cut boundary of the suppressed anvil surface exists. Consequently, the IR sensor will integrate the radiance from deep layers inside a convective wake.

An important aspect of the satellite-tracked cloud winds is the difference between cirrus and anvil winds at different heights. The anvil winds are measured by tracking cloud features embedded inside the anvil, while the cirrus winds are obtained by following small cloud elements. Unless these two types of winds at different heights are analyzed with extreme care, one might obtain fictitious circulations atop the convective region (Fig. 3.3-5).

Early in January 1992, a conclusive analysis of a time sequence of wake effects was obtained in cooperation with Mr. Ralph Anderson of NESDIS in Washington, D.C. A detailed analysis of the overshooting tops of the 1 June 1990 storm evidenced that an overshooting top at 1840 CST was 5°C colder than the anvil top around the cloud (Fig. 3.3-6). Five minutes later at 1845, a warm wake began forming on the downwind side of the dome.

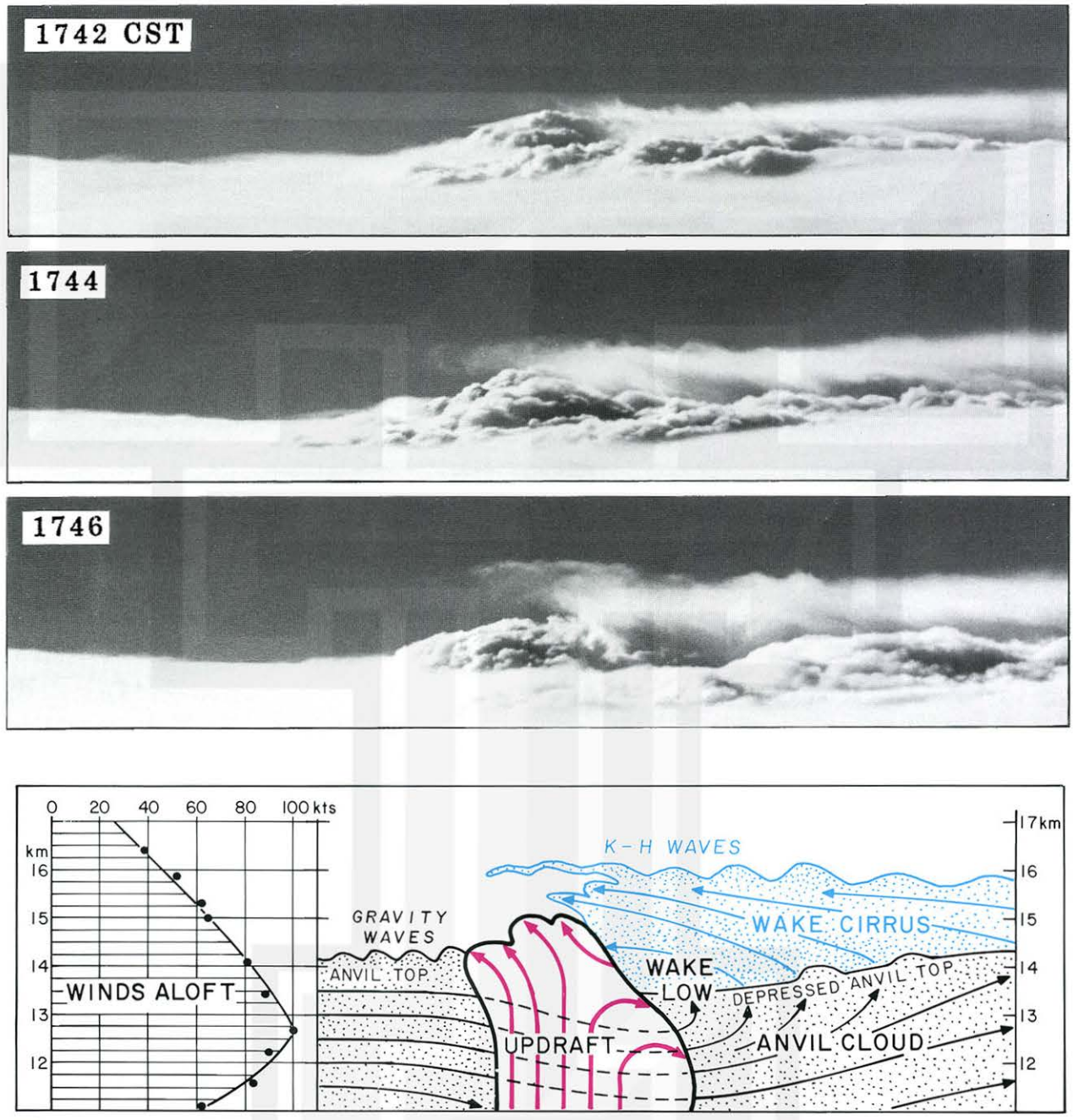

Fig. 3.3-4 A model of the wake flow induced by the updraft core beneath an overshooting dome. The wake cirrus rises from the depressed anvil into the stratosphere. The maximum height of the cirrus is often higher than that of overshooting domes. Photos taken on 12 May 1972 are actual examples of the phenomena.

The warming continued to 1855 when a stratospheric cirrus (S.Ci) suddenly formed inside the warm wake. The S.Ci enhanced the temperature of the wake. In 1990 and 1910 pictures, wake effects increased along with the S.Ci coverage, resulting in an enclosed warm area (Fig. 3.3-7).

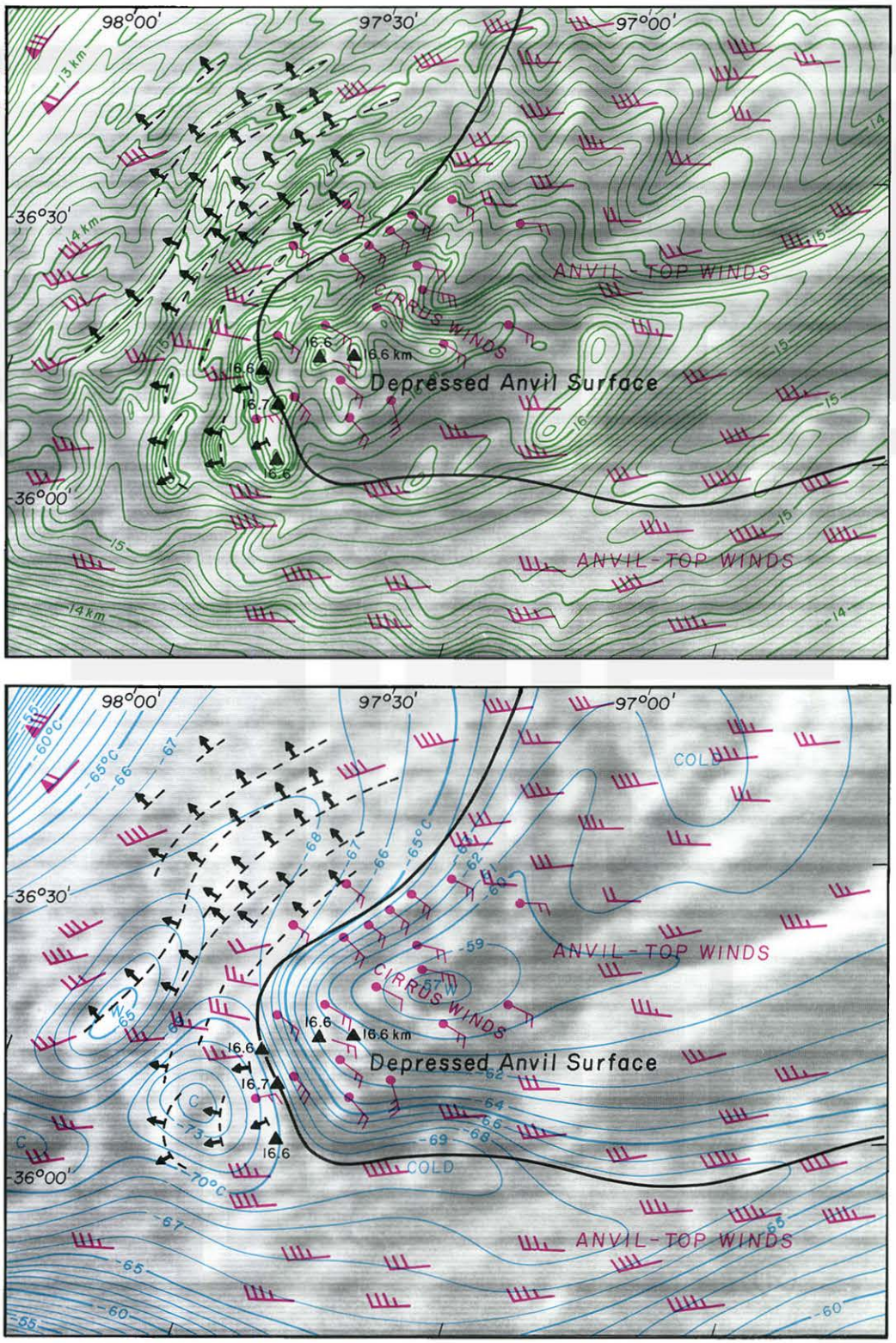

Fig. 3.3-5 Stereoscopic height contours (above) and IR isotherms (below) of the Oklahoma thunderstorm of 2 May 1979 at 1850 CST. Anvil-top winds are shown with standard wind symbols and wake cirrus winds, by red circles. Dashed lines with arrows are gravity waves.

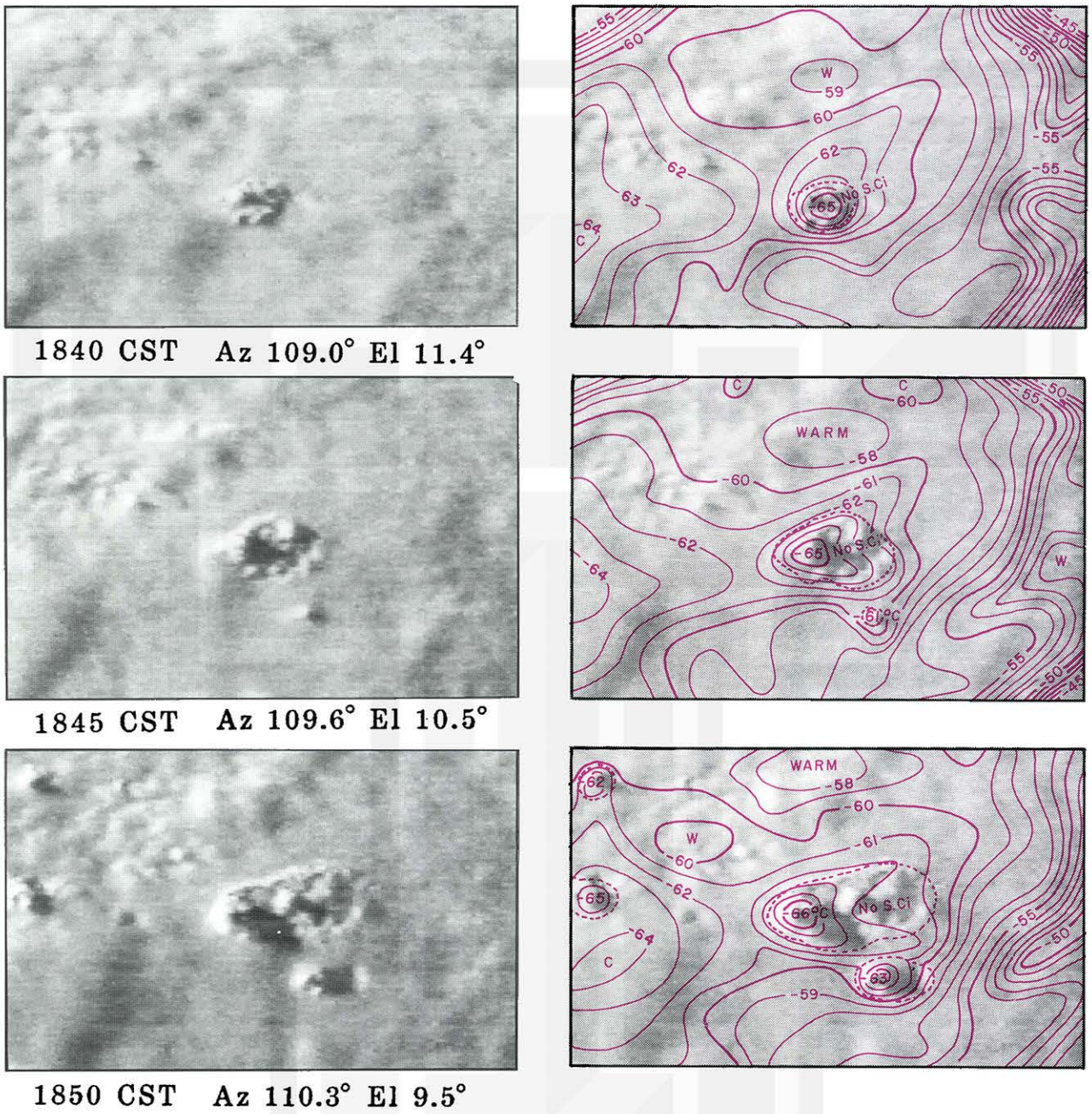

Fig. 3.3-6 Photographs and superimposed IR isotherms of the Texas Panhandle thunderstorm of 1 June 1990. Az and El denote the azimuth and elevation angles of the shadow vector at each picture time. No wake cirrus is seen in these pictures.

My research has concluded that the anvil-top warming begins with the suppression of the anvil inside the wake. After an anvil-top cirrus begins to rise inside the wake, an accumulation of the stratospheric cirrus will further enhance the warming. Because the tops of the warm cirrus are often higher than the overshooting tops outside the wake, anvil-top temperatures and cloud heights in wake regions are virtually unrelated.

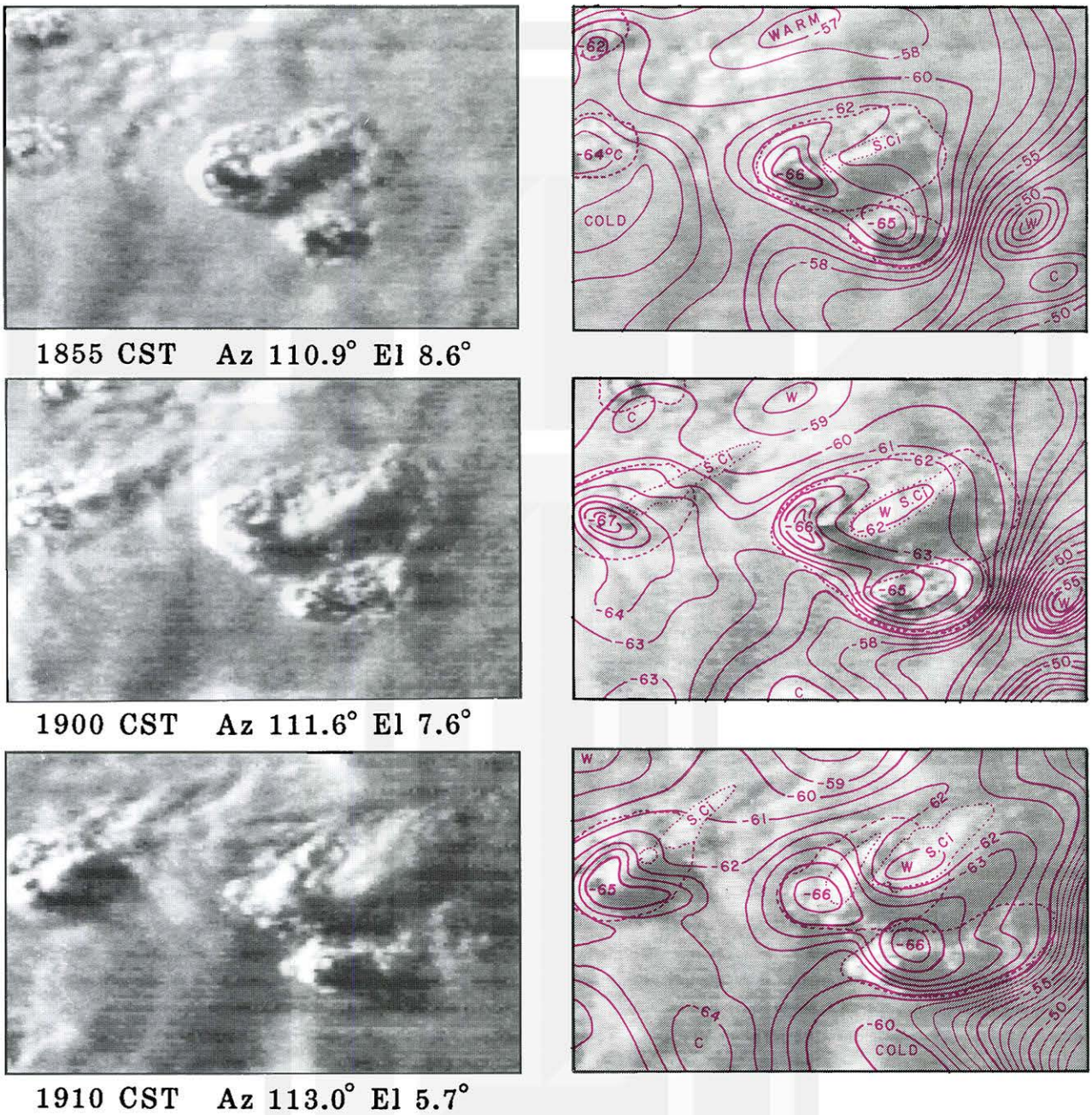

Fig. 3.3-7 Photographs and IR isotherms of the 1 June 1990 thunderstorm after the formation of the wake cirrus. Apparently, the stratospheric cirrus (S.Ci) is contributing to the additional warming of the wake region detected by satellite.

Fig. 3.3-8a The Lear Jet used in the 1970s for photographing anvil-top phenomena from high altitudes.

Fig. 3.3-8b An outside view from my photographic window on the left side of the aircraft.

Fig. 3.3-8c From left: Bill Shenk (NASA), Ted Fujita (U of C), Pilot, Co-pilot, Ed Pearl (U of C) who flew together for six days, 10-15 May 1972. Due to fuel line freeze, the right engine failed while over Rio Grande. We descended quickly to the Brownsville, Texas airport.

Fig. 3.3-8d In 1974, we conducted an extensive cloud-truth mission using dual Lear Jet and several Cessnas. The group became so large that it was nicknamed the "Fujita Air Force." Jim Purdom (NESDIS) investigated convective initiations for his Ph.D. thesis.

Chapter Four

Downburst Controversy

The Eastern 66 accident on 24 June 1975 at John F. Kennedy Airport, New York left behind 122 deaths and a ripple of questions on the wind that existed at the accident time. After an extensive meso-analysis of the weather events in and around the airport, I called the mysterious wind the **"Downburst."** In response to the requests for my research paper (Reference 1976a, page 279), 1,700 copies were printed in March 1976.

While receiving letters and phone calls in appreciation of my identification of the new wind from airlines and pilot associations, I also began receiving newspaper clippings from around the United States and Canada stating, in effect, that Fujita claims he identified his new wind, the downburst. Critics think, however, that I am renaming the wind already known for years or that I am dreaming of a superficial wind which was never detected by radar or anemometer.

This type of controversy is nothing new in the field of science. In generalizing the nature of the dispute, I wish to review the most significant controversy on the concept of the **Continental Drift proposed by Wegener** back in 1912 first. The **Downburst Controversy Section** describes the chronological events based on my recollections, publications, and letters received during the 18-year period, 1975 through 1992.

4.1 Historical Controversies

Wegener's Continental Drift

Back in 1940 when I worked under Prof. Matsumoto (p177), I read a masterbook, Das Antlitz der Erde by Austrian geologist Eduard Suess. Since then, I became interested in Alfred Wegener, German astronomer/meteorologist/geologist born in Berlin on 1 November 1880. He received his PhD in 1904. In 1912, Wegener worked out his startling interpretation of the shape of the continents on both sides of the Atlantic which were broken apart in the geological past and drifted to the present positions.

During the 1920s, on the basis of gravity measurements, Wegener proposed that continental rocks **SIAL** (density 2.70) are lighter than basaltic sea-floor rocks **SIMA** (2.95). He then assumed that the continent would plastically float on the heavier sea-floor rocks under the isostatic principle, maintaining a balance in the vertical direction. He assumed also that a continent could move horizontally over an extremely long geological time scale.

In 1922, Wegener completed his paper **On the Origin of Continents and Oceans** by adding detailed distribution of the fossils on both sides of the Atlantic Ocean. The paper, translated into five languages, was distributed worldwide. However, the weakest point of his theory was the identification of the force capable of moving individual continents slowly but steadily in various directions. Consequently, his paper received cool reception internationally.

In 1924, Harold Jeffreys, a prominent English geophysicist argued forcefully that the gravitational force is so strong that it cannot and will not move continents horizontally no matter how long it took in geological time.

Because of Jeffreys' prestige and the rejection of the horizontal force, the concept of Wegener's continental drift was killed in 1928 when Wegener was 48 years old. In Winter 1930, desperate and disappointed on his lifetime work on the drift, Wegener undertook an expedition in Greenland and was found dead in snow and ice.

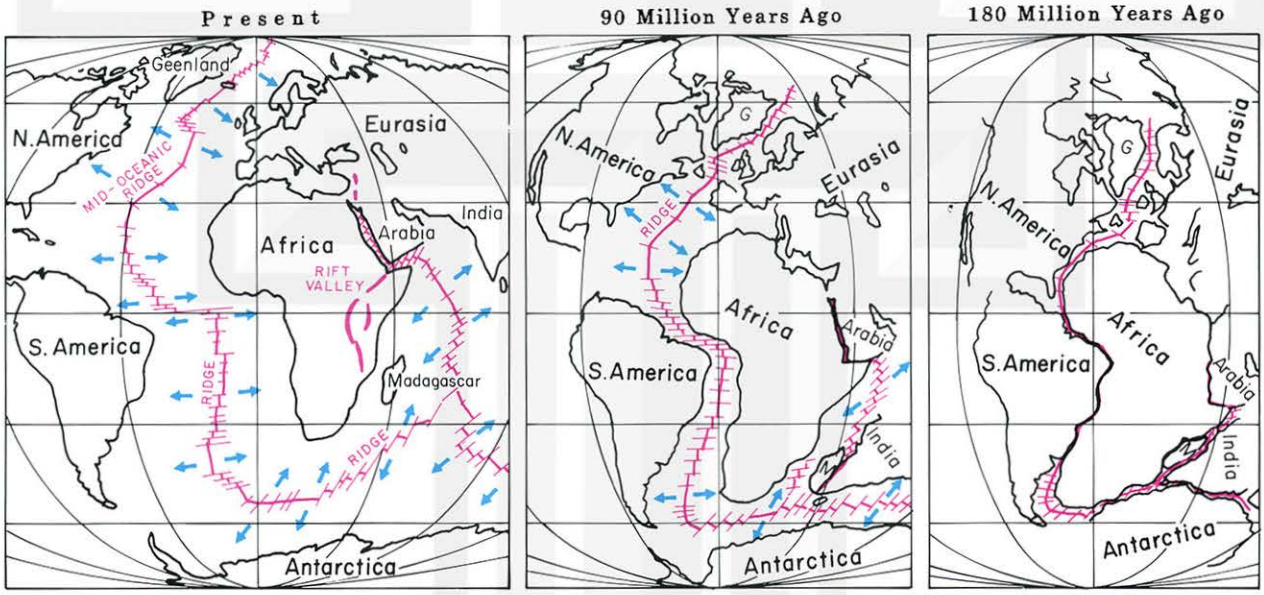

Fig. 4.1-1 Maps of the continents used in determining the paleoclimate maps in the "Paleoclimate" course taught jointly by Ted Fujita and Fred Ziegler. Distribution of paleocontinents is very similar to those produced by Wegener.

Morley's Sea-floor Spreading

Ever since Wegener's Continental Drift was rejected, geophysicists saw clearly the existence of the oceanic ridge along the centerline of the Atlantic Ocean. In 1960, 30 years after Wegener's tragic death, an idea of the **Sea-Floor Spreading** began. It was assumed that the sea floor is generated continuously along the axis of the mid-oceanic ridge and moves away from the spreading center.

Because of the outward movement of the generated sea floor, the farther the distance from the spreading center, the older the sea floor. Imaginative geophysicists thought that the high-temperature magma is magnetized by the earth's magnetic field as it rises and cools off below the Curie point. In other words, the spreading floor will carry along characteristic magnetic signatures, normal, zero, and reversal for millions of years (Fig. 4.1-2).

A controversy in publishing the paper on this important subject occurred in 1963 according to a book, **Dark Side of the Earth** by Robert Wood published in 1985. Lawrence Morley of the Canadian Geological Survey obtained an exciting result of the striped magnetic anomalies which reversed every million years. In February 1963, he sent a short paper to Nature. Two months later, he was informed that Nature had no room to print his paper. Immediately thereafter, he sent the paper to the Journal of Geophysical Research. Approximately six months later in late September 1963, his paper was turned down by a referee on the ground that Morley's speculation is good for cocktail parties, not for scientific aegis.

On 6 September 1963, however, Englishmen E. T. Vine and D. H. Mattews managed to publish a similar paper in Nature. Although I am a meteorologist, I concur with geophysicists that the independent discovery of the magnetic signatures by Vine, Mattews, and Morley was an important quantum leap in redeveloping Wegener's Continental Drift into the **Plate Tectonics.**

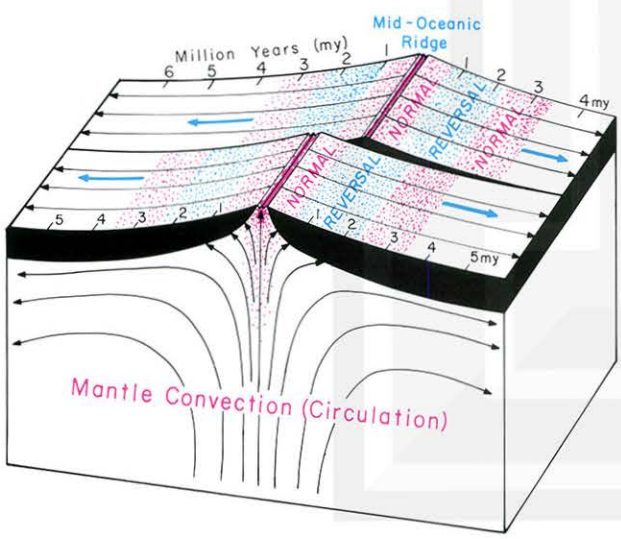

Fig. 4.1-2 Schematic diagram of magnetic signatures generated along the spreading center. The discovery of this phenomena reactivated Wegener's Continental Drift.

Downburst Controversy

The Eastern 66 accident at the John F. Kennedy (JFK), New York airport which triggered this controversy occurred on 24 June 1975. I did not imagine that windshear was the probable cause of the accident until Mr. Homer Mouden of Eastern Airlines sent me the basic data on the accident. Shortly before the Christmas recess in 1976, I decided to undertake an independent analysis of the probable windshear.

I suspected initially that the wind system in question could be very small in size. To update my knowledge of small-scale damaging winds likely to escape detection by an airport anemometer, I examined the collection of my aerial photographs taken after the tornado outbreak of 3-4 April 1974, known as Super- or Jumbo-outbreak.

Very soon, I found mysterious starburst patterns of uprooted trees caused probably by rare downdrafts which descended near the ground and burst out violently. Such a damage-causing downdraft might be extremely rare but it could happen, I thought.

At this point, I talked to Dr. Byers who was in charge of the Thunderstorm Project in Florida and Ohio in 1946-47. After listening to my concept of the damage-causing downdraft, he suggested that I call the wind system **"Downburst,"** because it consists of both **down and outburst** airflows each of which will endanger aircraft operations. He told me, "I have never seen such a small starburst wind during the Thunderstorm Project, because we did not look for that type of wind 30 years ago."

Encouraged by his comment, along with the evidence of the outburst damage, 0.5 to 5 km in diameter, three downbursts were located near the approach end of Runway 22L. They occurred during the 18-min period (1544-1602 EDT) when 11

aircraft landed prior to the accident at 1605 EDT. I was amazed to find that some aircraft experienced practically no windshear while others encountered strong crosswind or tail wind shear, depending upon their locations relative to the downburst center. Eastern 66 flew into the dead center of **Microburst 3** and crashed. Figures 4.1-3 to 5 are from Fujita (1976a) and (1985a).

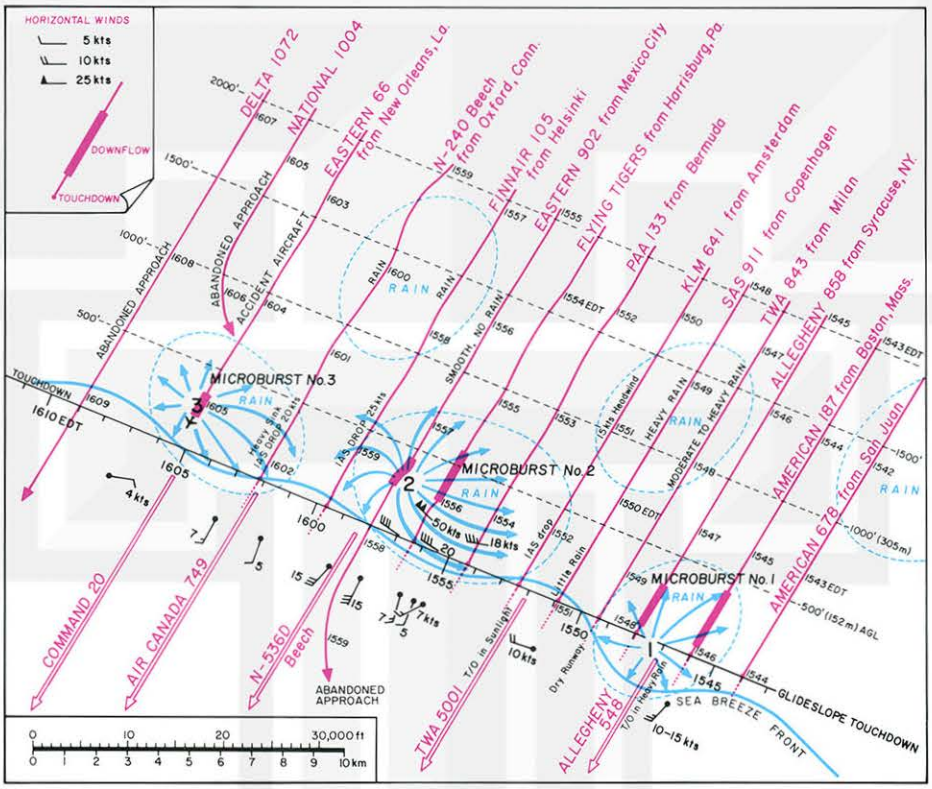

Fig. 4.1-3 Three small downbursts (microbursts) descended near the approach end of Runway 22L of JFK on 24 June 1975. These microbursts touched down one after another, 7 to 10 minutes apart. From Fujita (1976a and 1985a).

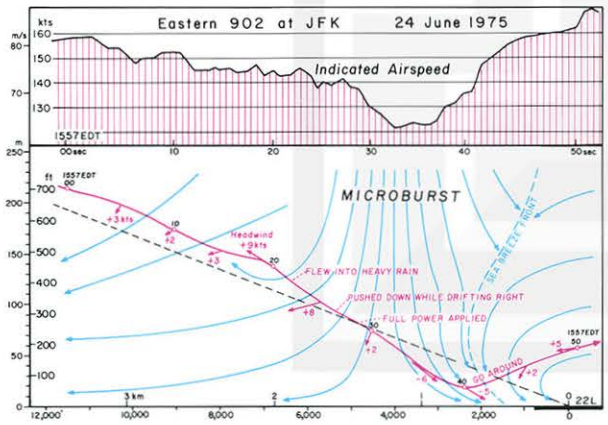

Fig. 4.1-4 Flight path of Eastern 902 attempted to land 7 min before Eastern 66. The aircraft was pushed toward right.

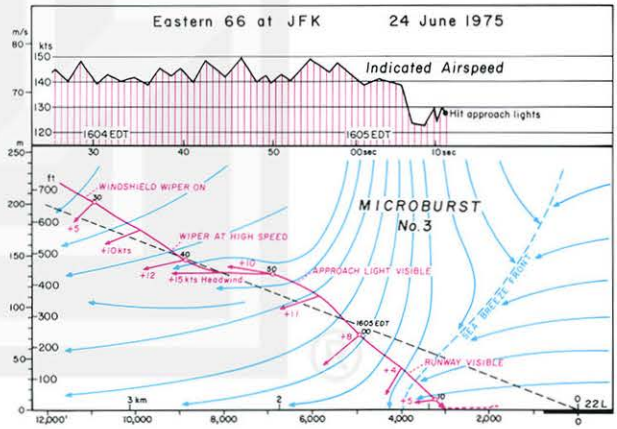

Fig. 4.1-5 Eastern 66 encountered strong head winds upon entering a shower. Very soon the head wind changed into a strong downflow.

In February 1976, I completed a research paper (Fujita 1976a) and 1,700 copies were printed foreseeing an application to air safety. Thereafter, I began receiving a large number of newspaper clippings from the United States and Canada. Many newspapers reported meteorologists' views that my downburst was actually the downdraft which has been known for decades.

Some airline pilots, on the contrary, informed me that they had experienced both vertical - wind and tailwind shears while flying through innocuous showers. I had to send a large number of copies to airlines and pilots, necessitating the second printing of 800 copies in September 1976. Meanwhile, more meteorologists criticized my concept on the ground that I am confused with the gust front and that the downburst was nothing but a new name given to the well-known gust-front phenomenon.

The criticism led to several sleepless nights. However, I did not want to abandon the downburst concept because of my belief and of increasing support from pilots who had experienced dangerous flights through downburst windshear which did not appear to behave like gust fronts. I felt seriously that I will have to detect downburst winds by Doppler radar being used by the National Center for Atmospheric Research (NCAR) at Boulder, Colorado.

NIMROD Experiment

Early in Autumn 1976, I called Dr. Clifford Murino, Director of Atmospheric Technology Division (ATD) of NCAR, now past president of UCAR, asking for the use of three Doppler radars for detecting the controversial downburst winds. After listening to my problem, he decided to come to Chicago to design with me a microburst-detection project in the western suburbs of Chicago. Very soon, Vin Lally of NCAR suggested the project name **Northern Illinois Meteorological Research On Downburst** with acronym, **NIMROD.** Nimrod in the Bible is referred to as a mighty hunter, the best name for hunting downbursts.

The **First Planning Meeting of NIMROD** was held late in Autumn 1976 at the University of Chicago participated by Drs. Cliff Murino and Bob Serafin, Manager of the Field Observing Facility (FOF) then, Director of NCAR now. It was decided that Murino and Serafin would provide me with their professional opinion in detecting downburst for the first time by Doppler radar. Serafin was confident in detecting the bursting wind at very low altitudes. Thereafter, I sent an application for the use of NCAR's three Doppler radars, CP-2, CP-3, and CP-4 along with 27 Portable Automated Mesonet stations (PAM).

Early in 1977, I visited the National Science Foundation at Washington, D.C. to answer their questions on my proposed experiment in the western suburbs of Chicago including the O'Hare airport. Dr. Ron Taylor, Program Director of Meteorology expressed his supportive views. I began driving on a paved highway leading to the destination - **Downburst.**

In spite of the occasional rumble of anti-downbursters, I felt very happy, now that I will be able to hunt for the mysterious winds, being guided by three prominent scientists. When I was preparing the manuscript of the 104-page "Manual of Downburst Identification for Project NIMROD," I received simultaneously two awards, **Admiral Luis de Florez Flight Safety Award** and **Aviation Week & Space Technology Distinguished Service Award** on 21 September 1977 at Ottawa, Canada. It was a great honor to receive these two awards from the Flight Safety Foundation (pp266-267).

After 15 April 1978, the first day of the experiment, I worked day and night with NCAR's Jim Wilson, radar meteorologist then, senior scientist now. On 29 May 1978 (Jim's 41st birthday), we made vertical (RHI) scans of a small but intense downburst for the first time by Doppler radar. In view of its small size, we called the storm **"Microburst."** Jim and I were excited after confirming a 31 m/s (69.4 mph) wind blowing straight toward us at very low altitude,

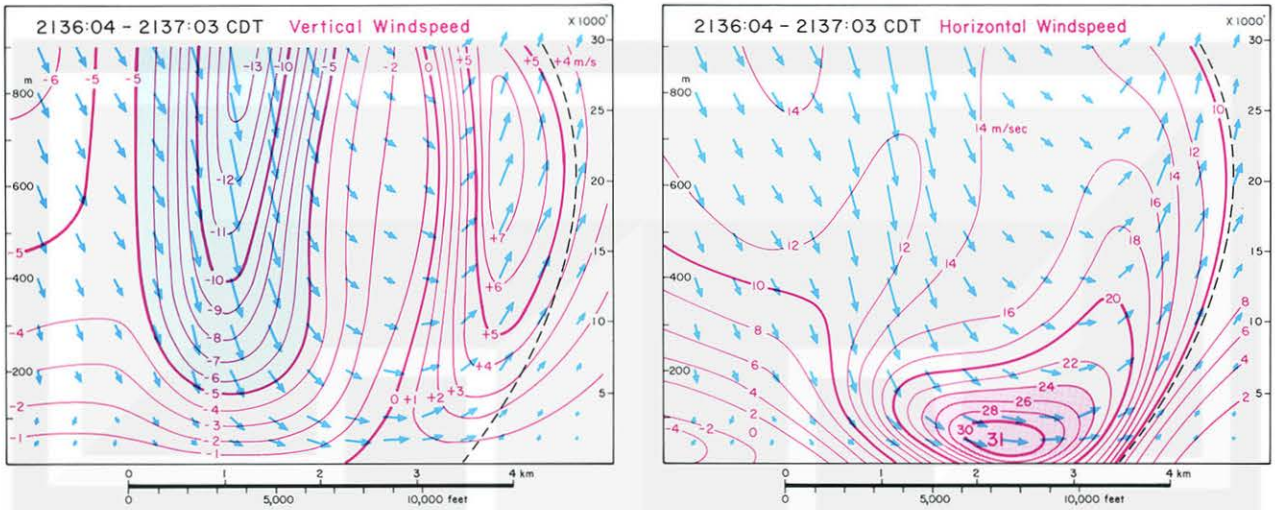

Fig. 4.1-6 Vertical cross section of the Yorkville microburst scanned by CP-3 Doppler radar at 9:36 p.m. on 29 May 1978 during NIMROD.

less than 30 m (100') above the ground (Fig. 4.1-6).

In spite of successful detections of downburst/microbursts by NIMROD, the meteorological community was still divided, in opinion, into bursters and anti-bursters. Those who were convinced of the danger of microburst windshear became concerned about the sustained controversy which could confuse pilots in making decisions. In an attempt to clarify the nature of the dispute, Susan West conducted an opinion poll by calling meteorologists and published her article, **Are Downbursts Just a Lot of Hot Air?** in the 17 March 1979 issue of Science News. I was informed later that several leading scientists mentioned in her article began supporting my hypothesis and surveyed downburst winds and damage.

Thereafter, I presented a paper, **Objective, Operation, and Results of Project NIMROD** before the 11th Conference on Severe Local Storms in October 1979 (Fujita 1979c), hoping for an end of the controversy.

JAWS Experiment

On 18 April 1980, at the conclusion of the 19th Radar Meteorology Conference at Miami Beach, three NCAR scientists, Bob Serafin, John McCarthy, Jim Wilson, and I sat around a dinner table at the Carillon Hotel to discuss a plan for conducting a microburst windshear experiment in the Denver area under dry environment.

Several weeks later, Vin Lally again came up with an attractive acronym, **JAWS (Joint Airport Wind Shear)** Project which later was changed to **Joint Airport Weather Studies,** because windshear problems have already been solved by the Windshear Office which was being closed.

Design of Airport Anemometers

On 9 July 1982, during the JAWS Project (15 May-8 August), PAA 759 failed to take off at the New Orleans airport. I learned later that the airport had 4 anemometers with the 5th one being installed. My analysis (Fujita 1983a) published on 12 January 1983 revealed that a microburst descended close to the center anemometer. It spread out quickly while the accident aircraft was accelerating on Runway 10. The aircraft hit a tree located near the east anemometer

which did not detect the less than one-minute old microburst, only 2 miles in diameter (Fig. 4.1-7).

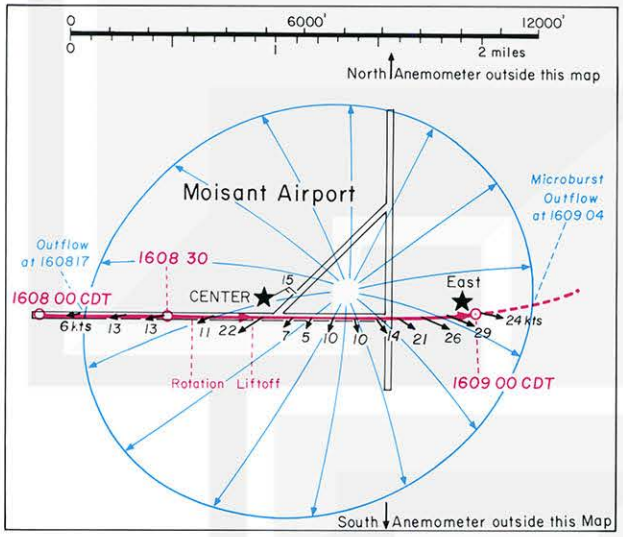

Fig. 4.1-7 The PAA 759 microburst on 9 July 1982 at Moisant Airport, New Orleans, Louisiana. This microburst intensified very rapidly while the aircraft was climbing above Runway 10.

After the New Orleans accident, the National Research Council established two panels to report on **Low-Altitude Wind Shear and its Hazard to Aviation.** It was published by the National Academy Press in 1983. After receiving the report, I felt personally that it did not emphasize strongly the immediate need for the accurate detection of microbursts. The term **"microburst"** was not used in the headline words of the 21 conclusions in pp70-84. Furthermore, the microburst was not discussed positively in the 19 recommendations in pp85-89. The reaction to the emphasis of the report for reducing microburst-related accidents may vary according to readers. I wished that the report could have focused the issue on the microburst windshear which is most difficult to detect and flyout safely.

I became less convinced about the effectiveness of 5 to 10 anemometers in detecting microbursts for avoidance purposes. On 4 May 1983, I wrote a letter to an agency requesting for the design history of the anemometer network known as **LLWSAS** or **LLWAS.** I received the requested information on 27 May 1983, indicating

20 April 1976, 21 letters were sent to the personnel in four agencies, suggesting the use of a 90%-solving detection system already available, instead of solving 99% of the problems taking 10 to 20 years from that time.

30 July 1976, the distribution of the seven anemometers for Runway 22L of the JFK airport was proposed (Fig. 4.1-8). Anemometer locations were determined based solely on a model of gust front. [The downburst windshear in my JFK report distributed in March 1976 was not taken into consideration].

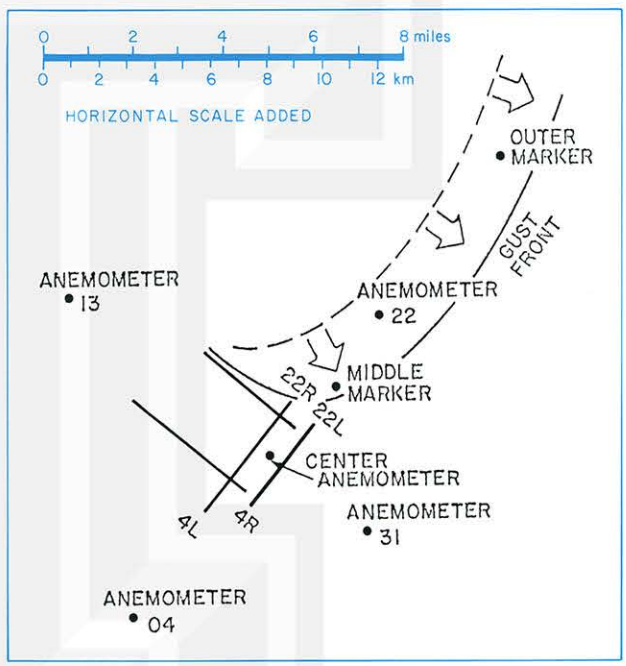

Fig. 4.1-8 A network of six anemometers for Runway 22L of JFK. The design was based on an approaching gust front rather than microburst.

DFW Airport Accident

A couple of years later on 2 August 1985, the Delta 191 accident occurred at the Dallas-Fort Worth (DFW) airport. I made an analysis of the aircraft performance to determine the size of the windshear in relation to the six anemometers

surrounding the runway area (Fig. 4.1-9). The result indicated that the aircraft entered the 1 min-old microburst, contacting the ground 60 sec later when the microburst was 3.3 miles in diameter. Due to its small size, none of the 6 anemometers encircling the runway area was affected by the microburst wind until after the accident.

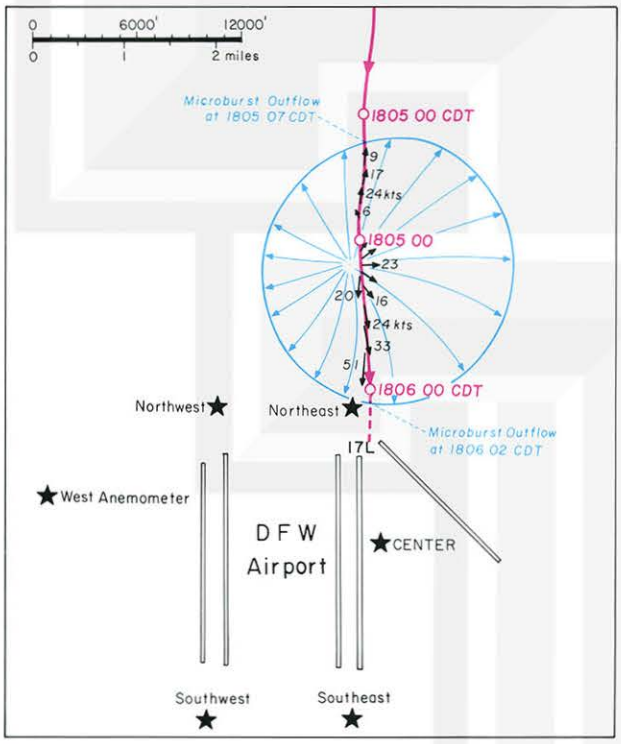

Fig. 4.1-9 The Delta 191 microburst which escaped detection by the six anemometers encircling the runway area. The microburst touched down outside the airport and expanded quickly into the runway area.

Late in August 1991, I submitted a paper by Fujita and Brian Smith, my former student, to an editor of the Proceedings of Tornado Symposium III. On 25 September 1991, the editor sent me a comment by a reviewer/referee stating, **"Myself and others have felt, since the late 1970's, that there were factors of embarrassment, frustration, and professional jealousy in some early criticism. Here was a phenomenon that had literally hit prominent meteorologists in the face for a lifetime and they failed to recognize it as a unique discrete phenomenon."**

Concluding Remarks

Unlike the tragic ending to Wegener's dispute, the downburst controversy which began in 1976 subsided gradually while I am still active as professor emeritus at the University of Chicago. Fortunately, I have been supported morally and financially by a large number of prestigious scientists. As early as Autumn 1976, Drs. Cliff Murino (ATD) and Bob Serafin (FOF) of NCAR assisted me in designing the wind-truth NIMROD experiment in the Chicago suburbs. Since then NCAR, along with NSF, played a decisive role in advancing various methods of downburst/microburst detection. Without their generous support, the controversy could have continued during my lifetime or even beyond.

Dry and Wet Microbursts

Dry Microburst

Three weeks after the termination of NIMROD on 1 July 1978, Cliff Murino told me, "Ted, NIMROD should not be your only experiment. Come to Colorado to see for yourself if we have microburst in Colorado or not."

On 27 July 1978, Cliff drove me to the National Hail Research Experiment (NHRE) site at Grover, 130 km northeast of NCAR. Shortly before reaching the site, I saw a dry microburst descending from a high cloud base. As soon as I got out of the car, I took one picture at 1530 MDT and the next, two minutes later (Fig. 4.1-10). Although I had visited Colorado many times, these were the first pictures I ever took, because I did not know what microbursts looked like.

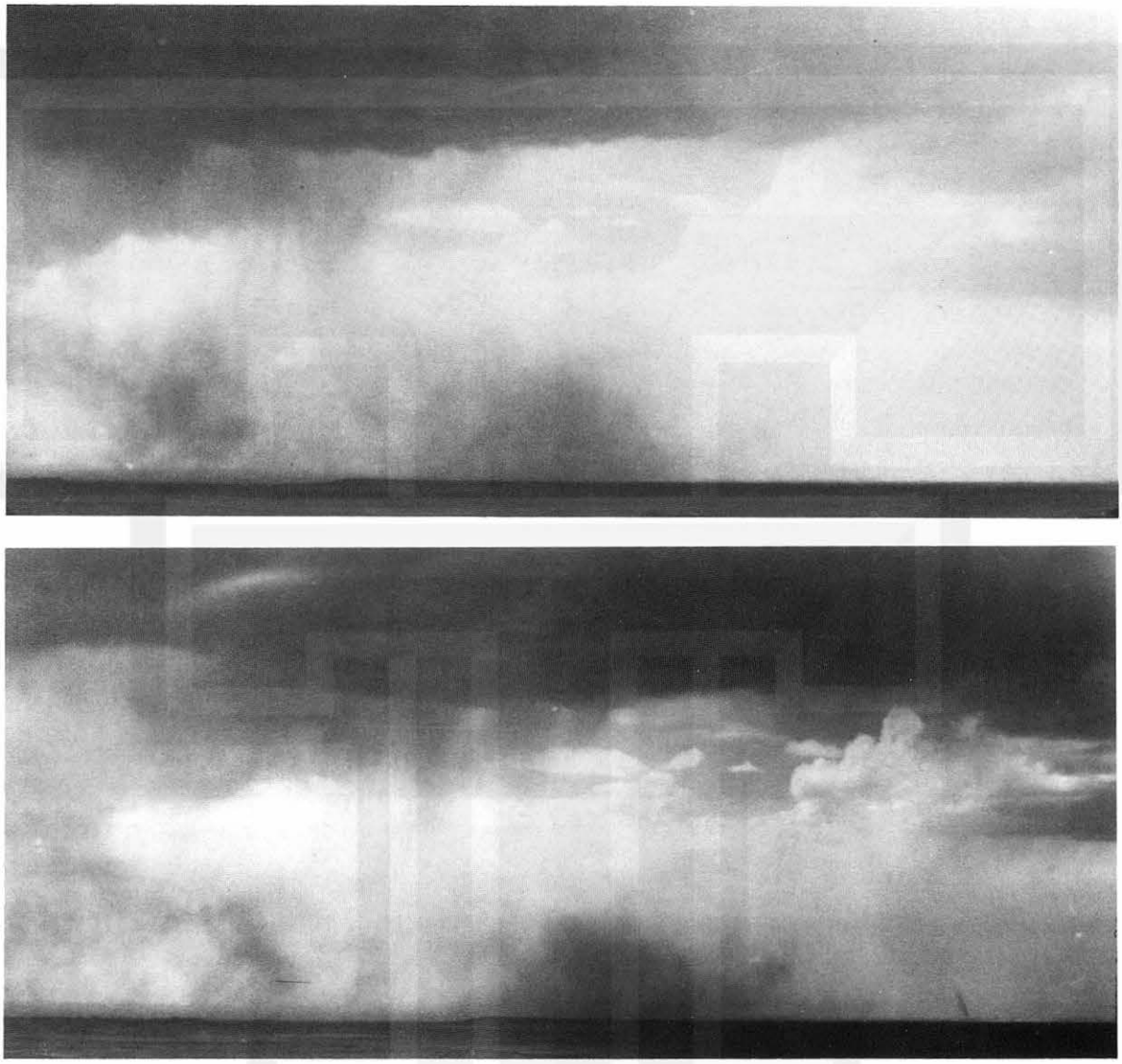

Fig. 4.1-10 Two pictures of a dry microburst I took with Cliff Murino on 27 July 1978 at 1530 (above) and 1532 MDT (below) from 1 km southwest of Grover, Colorado. The second picture shows a large dust devil formed on the leading edge of the outflow on the right side.

Wet Microburst

After photographing my first dry microburst in Colorado, I made a laboratory model of microbursts. First, steady-state downflows were brought down to the surface with a line of dry-ice smokes. However, they never produced microburst-like winds. Then I introduced a pulsed downward flow from above. It induced an outburst wind surrounded by a vortex ring (Fig. 4.1-11) each time after the head made contact with the surface. Unlike dry microburst, a descending head does not evaporate fast enough to generate additional negative buoyancy. If this is the case, detection of transient microburst by anemometers or Doppler radar will be harder than that of steady-state downflow. The Monrovia microburst (p120-124) is an example.

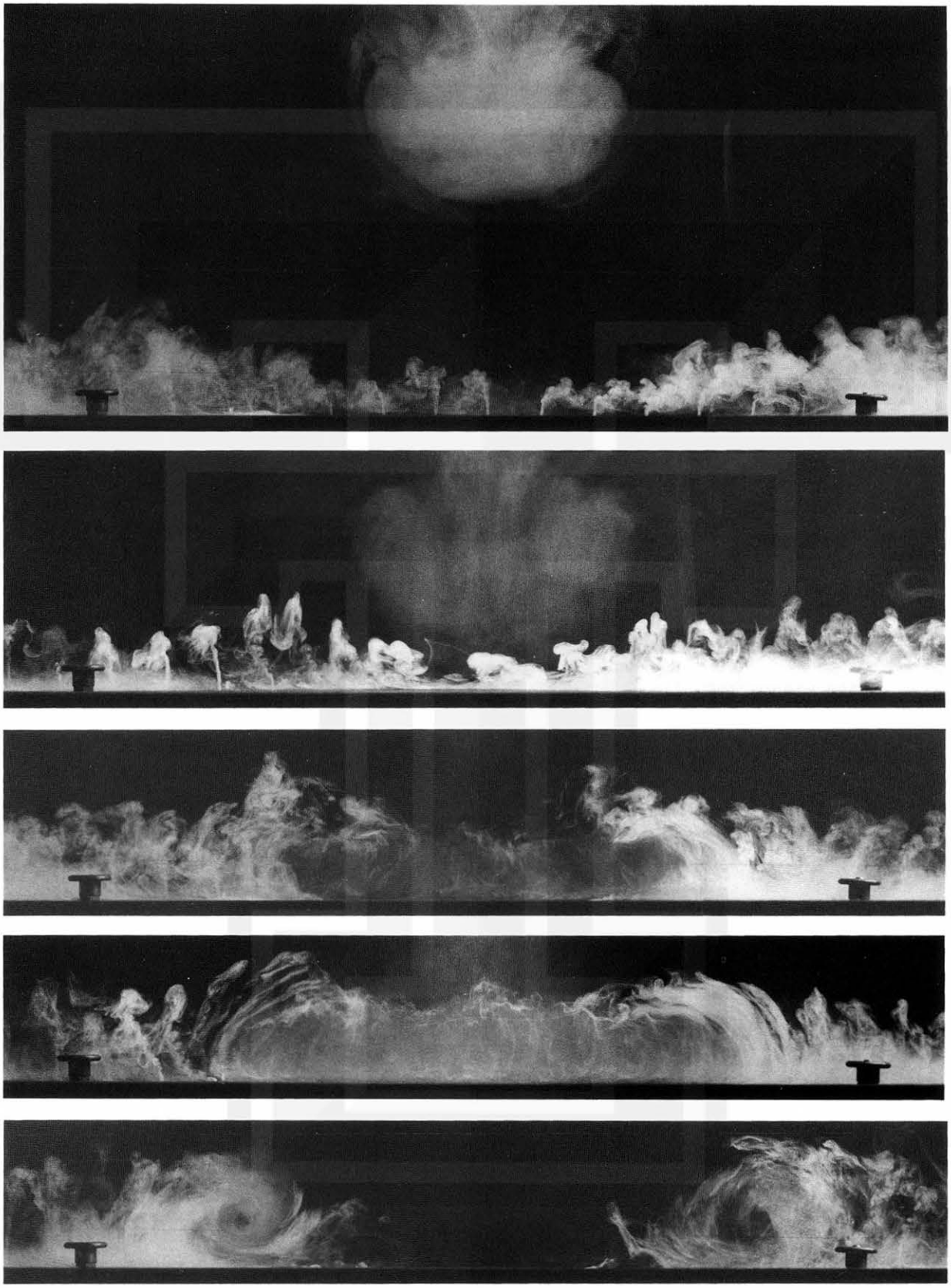

Fig. 4.1-11 Five stages of a laboratory model microburst. From top: 1. Midair stage, 2. Contact stage, 3. Outflow stage, 4. Outburst stage, and 5. Ring-vortex stage. Most aircraft accidents occurred in stages 4 and 5.

JAWS 1982 and the Tenth Anniversary 1992

Fig. 4.1-12 JAWS CP-2 Doppler radar in June 1982 with dark storm clouds in the background.

Fig. 4.1-14 The tenth anniversary **Toast/Kampai** at NCAR on 19 June 1992. From left: Rit, Jim, Roger, Ted, Bob, and John.

Fig. 4.1-13 Cutting the JAWS cake on 10 July 1982 during the mid-Project picnic at Boulder.

Fig. 4.1-15 Cutting the JAWS tenth anniversary cake following the Toast/Kampai.

Fig. 4.1-16 JAWS reunion party in Bob Serafin's garden on 20 June 1992. From left: Rit Carbone, Walt Dabberdt, John McCarthy, Bob Serafin, Roger Wakimoto, Ted Fujita, Jim Wilson, Akira Kasahara, and their spouses.

4.2 Nagasaki and Hiroshima Atom Bombs

The Hiroshima atom bomb exploded at 0815 JST on 6 August 1945, burning the city within 2 km radius of Ground Zero into ashes (Fig. 4.2-1). Three days later on the 9th at 1102 JST, the second bomb exploded (Fig. 4.2-2) over the Urakami Section of Nagasaki (Fig. 4.2-3). In September 1945, I visited Nagasaki first, then Hiroshima to witness, among other things, the effects of the shock wave on trees and structures.

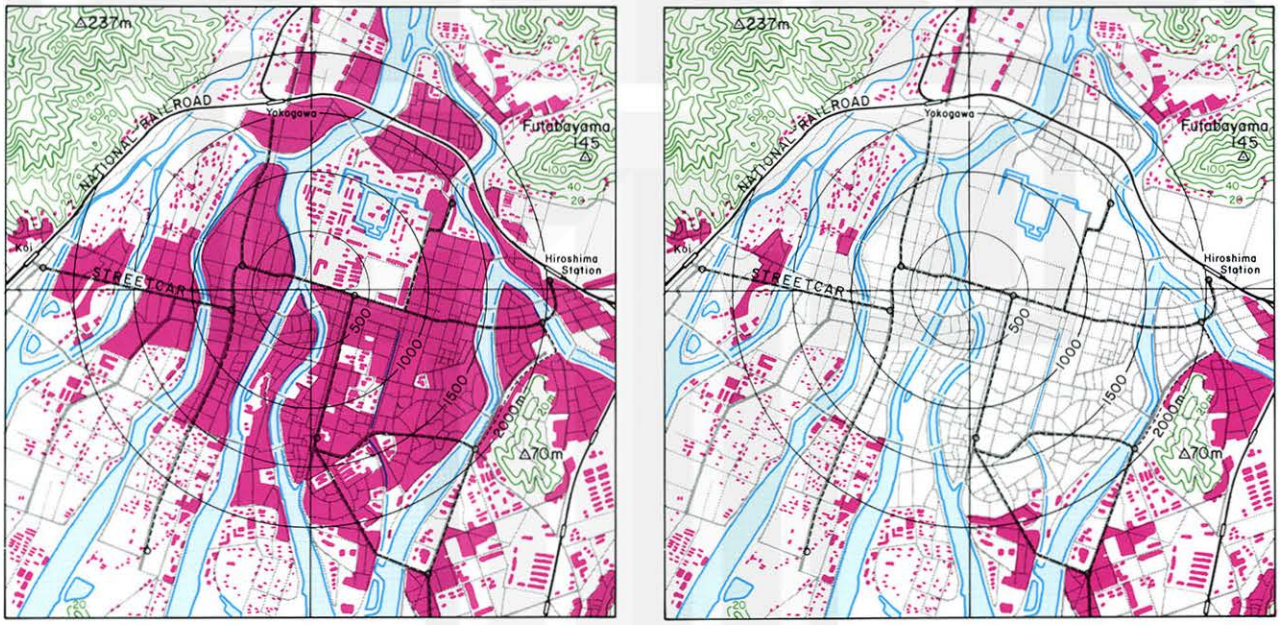

Fig. 4.2-1 City of Hiroshima before (left) and after the atom bomb on 6 August 1945. Late in September 1945, I visited the city staying at a small inn near the Koi railroad station to investigate the damage on foot.

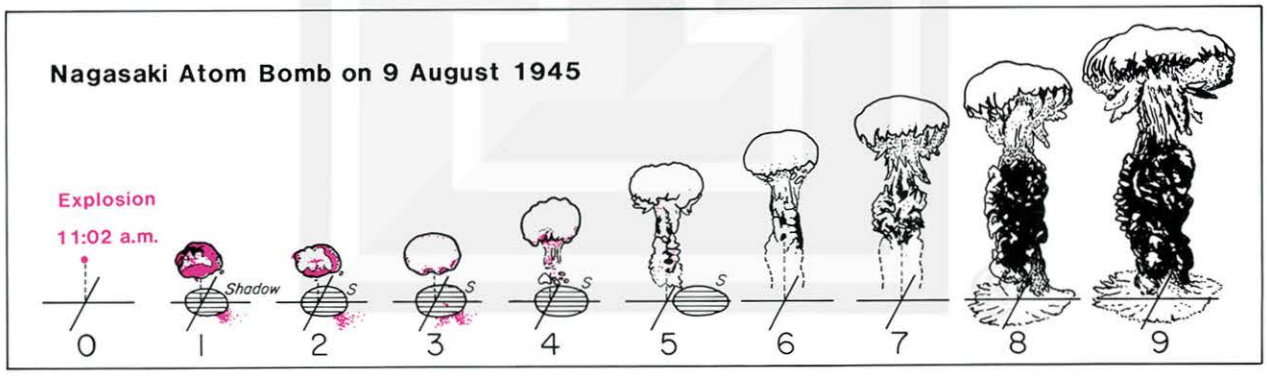

Fig. 4.2-2 Explosion of the Nagasaki atom bomb reconstructed from a 16-mm movie taken by the USAF.

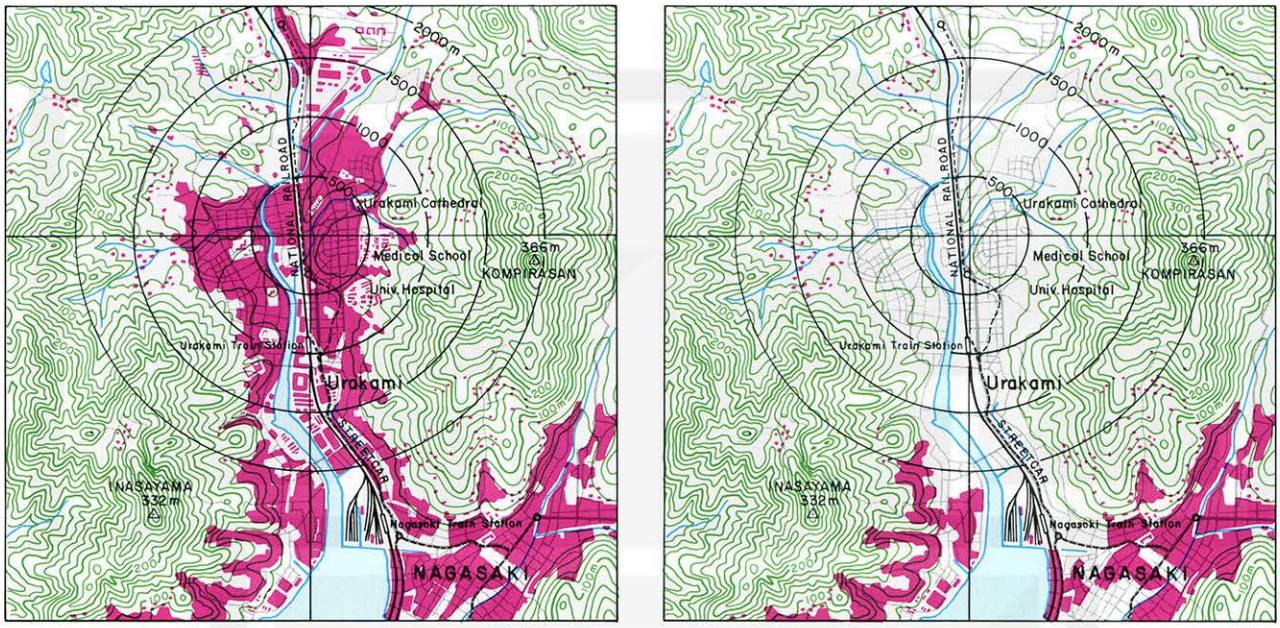

Fig. 4.2-3 City of Nagasaki before (left) and after the atom bomb on 9 August 1945. In September, I visited the area staying at the undamaged section of the city near the lower right corner of the map.

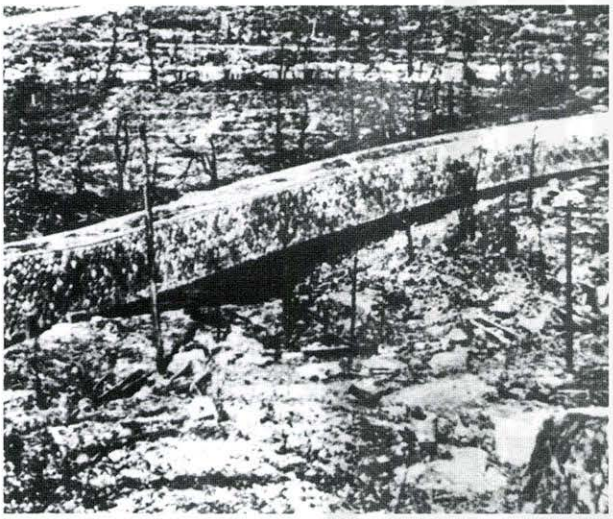

Fig. 4.2-4 A view of the Ground Zero area with blackened trees left standing after the shock wave which descended from above.

Fig. 4.2-5 Bamboo (above) and pine (below) forests flattened by the outburst force of the shock wave.

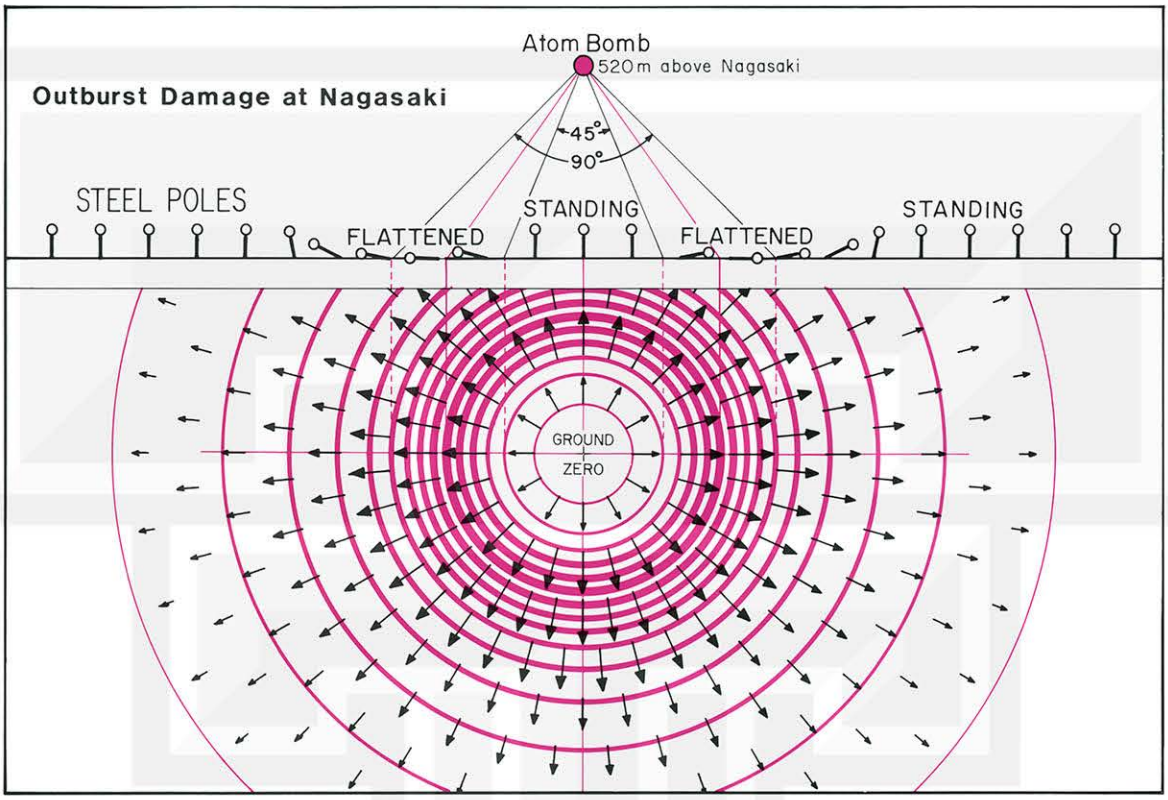

Fig. 4.2-6 Outburst forces induced by the shock wave as it hit the ground. The strongest force was estimated between the 300-m to 600-m ranges from Ground Zero. The Urakami Cathedral was located near the 500-m range (p181-184).

Within the 100- to 150-m range of Ground Zero, blackened trees, large and small, were left standing (Fig. 4.2-4). At the 300- to 600-m range, trees were broken off in horizontal directions away from Ground Zero in a giant starburst pattern (Figs. 4.2-5 and 6).

Starburst damage of Trees

In the United States

After coming to the United States, I photographed from low-flying Cessna a large number of damage areas in the wake of tornadoes. Unexpectedly, I came across starburst patterns of uprooted trees.

For instance, an aerial photograph of a Wisconsin forest (Fig. 4.2-7) suggests that strong winds descended to the ground surface, uprooting trees in a starburst pattern. Assuming that an aircraft cannot fly through this type of winds, I identified the wind as **downburst** during my research on the Eastern 66 accident.

On 1 July 1978, Mr. Mike Smith of Wichita, Kansas took beautiful pictures of a microburst in action and sent them to me (Fig. 4.2-8). Meanwhile, I took aerial photographs of the starburst damages of a cornfield in Indiana (Fig. 4.2-9), a forest in Wisconsin (Fig. 4.2-10), etc. On the basis of these pictures, I presumed that damage-causing downbursts (microbursts) have been occurring in various parts of the United States.

Fig. 4.2-7 Trees in northern Wisconsin blown down by the 4 July 1977 microburst which descended literally to the ground surface. Local residents thought that the area was hit by several tornadoes. They were microbursts, instead.

Fig. 4.2-8 One of the six pictures in a series taken in Wichita, Kansas on 1 July 1978. Courtesy of Mr. Mike Smith of WeatherData, Inc.

Fig. 4.2-9 An overall view of a starburst damage of a cornfield near Gessie, Indiana on 30 September 1977.

Fig. 4.2-10 A small but intense microburst at Bloomer, Wisconsin on 30 July 1977. All aerial photos were taken by Ted Fujita prior to the NIMROD experiment in 1978.

4.3 Monrovia Microburst

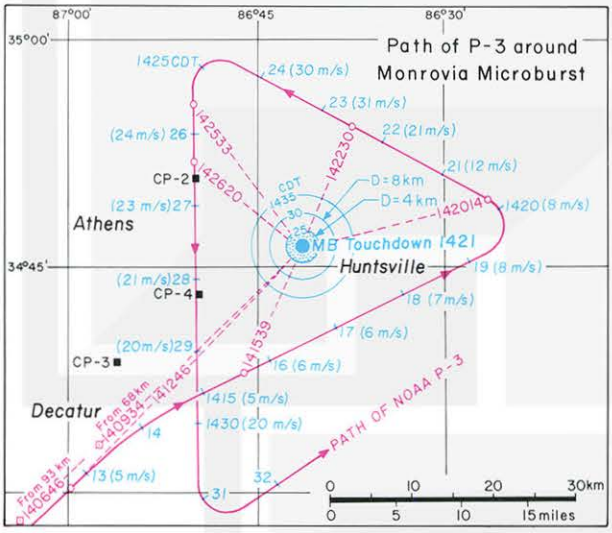

Fig. 4.3-1 A triangular path of NOAA P-3 at 500 mb pressure altitude. A rare view of the Monrovia cloud in growing, microburst, and decaying stages was witnessed by Mr. Saburo Onodera, a meteorologist of Japan Air Lines on board the P-3.

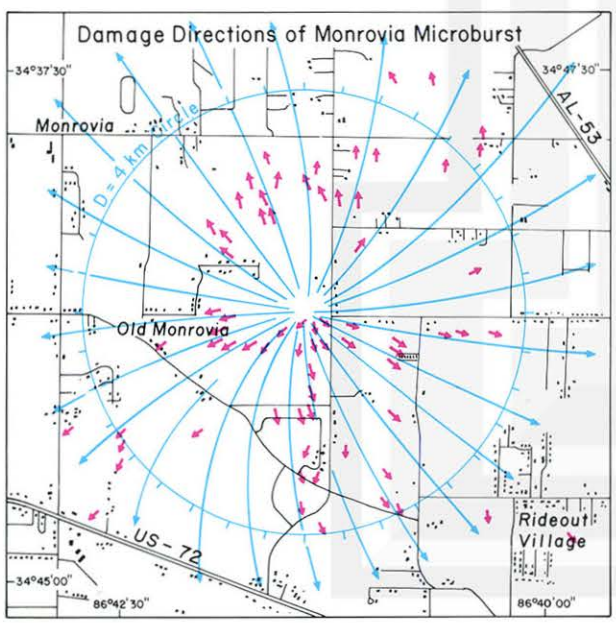

Fig. 4.3-2 Damage directions of the Monrovia microburst. A circle of 4 km in diameter shows the upper limit of the microburst dimension.

The Monrovia microburst occurred on 20 July 1986 during the **Microburst and Severe Thunderstorm (MIST)** Experiment (June and July 1986). Unusual data of the microburst cloud was obtained by NCAR's CP-2, CP-3, and CP-4 and a NOAA P-3. The aircraft was made available by Dr. C. B. (Gus) Emmanuel to support my microburst research. Gus, then the Director of NOAA/OAO in Miami, was convinced that my research will contribute to the safety of NOAA's hurricane flights over the Atlantic Ocean.

During the MIST experiment, I directed the P-3 in search of microburst clouds. On 20 July, while holding over northwest of Birmingham, I saw a towering cumulus near Huntsville. Simultaneously, Roger Wakimoto detected a fast-growing echo on the CP-4 display. We agreed immediately to work on the cloud. While approaching the cloud in northeast heading, I took the first picture at 140646 CDT from 93 km away (Fig. 4.3-1).

Thereafter, I completed three flight legs in a triangle with the cloud at the center. Next day, Greg Forbes and I surveyed the area beneath the cloud, obtaining a beautiful starburst pattern (Fig. 4.3-2) which resembles my laboratory model of microburst (Fig. 4.3-3).

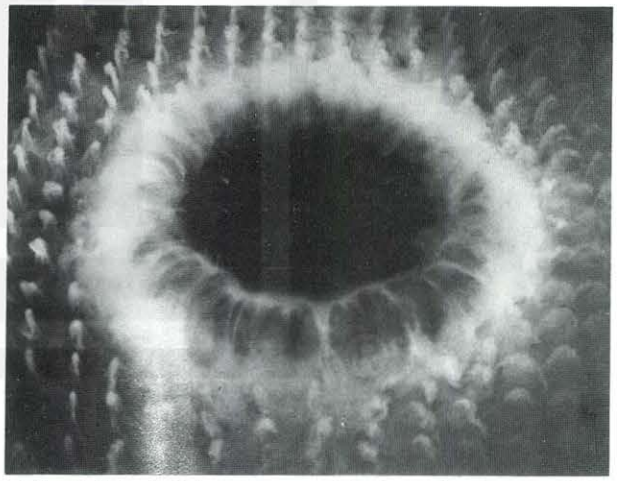

Fig. 4.3-3 A laboratory model of a microburst which resembles the Monrovia microburst.

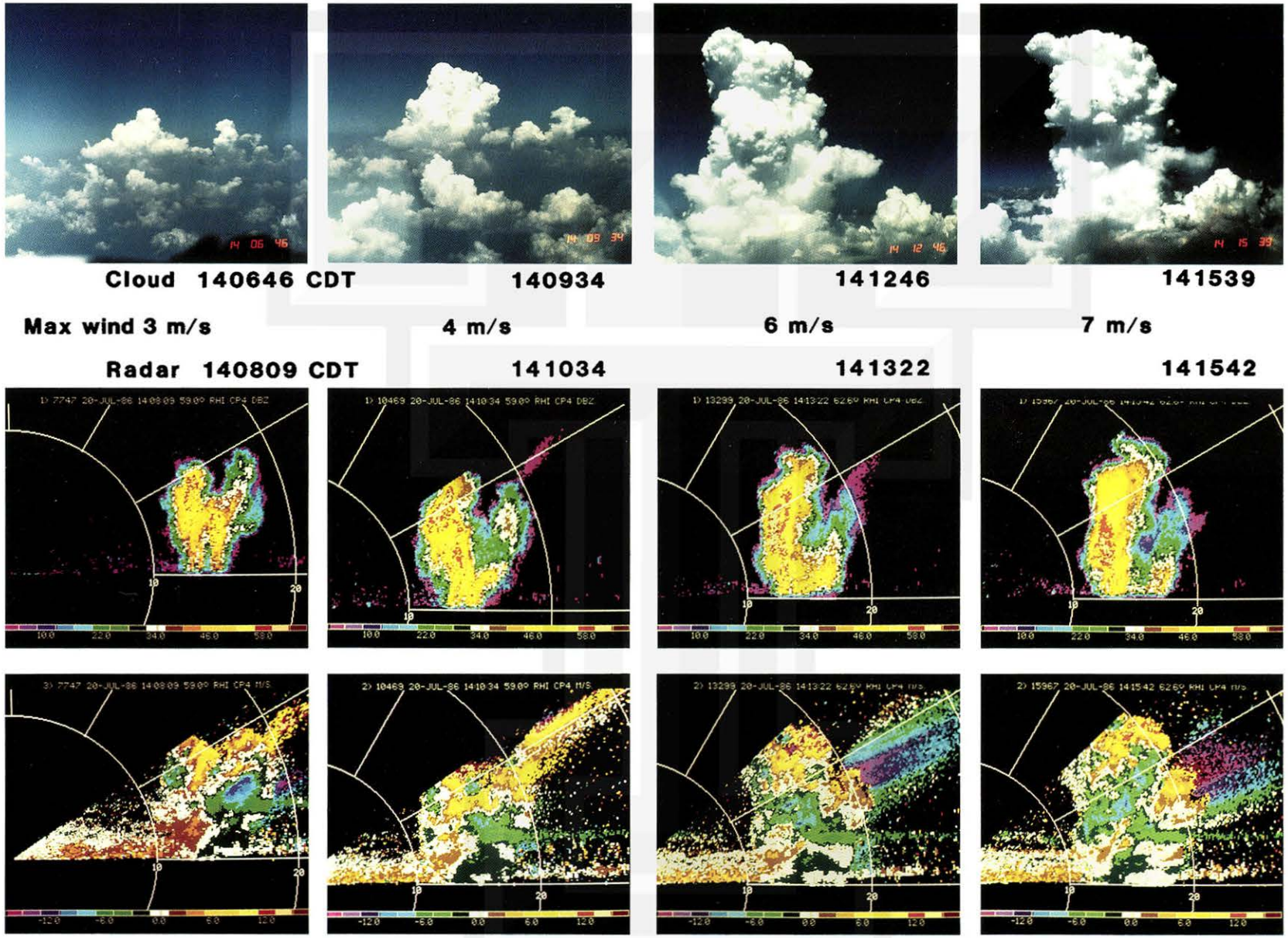

Fig. 4.3-4 The Monrovia cloud on 20 July 1986 in its pre-anvil stage. At 140646 and 140934 CDT, the cloud was in towering-cumulus stage and Doppler velocities were characterized by a yellow-colored flare, indicationg that large particles near the echo top were being carried upward. At 141322 CDT, the color of the flare velocity changed into red, suggesting that particles began falling.

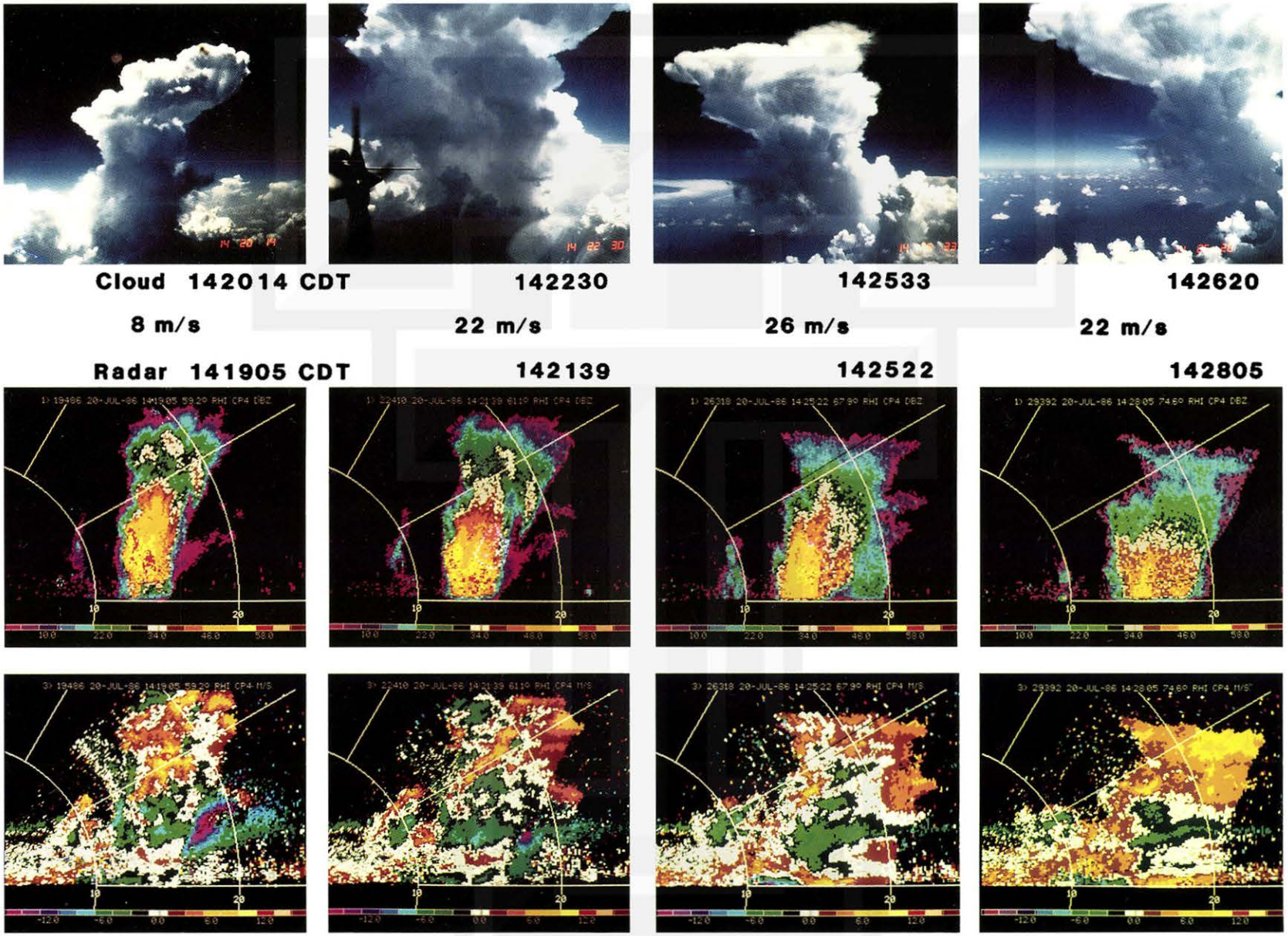

Fig. 4.3-5 The Monrovia cloud at the peak microburst stage. The cloud shape, however, does not imply a strong microburst in progress. At 141905 CDT when the high-reflectivity, flare-causing echo descended, the area of the apparent flare velocity became very small.

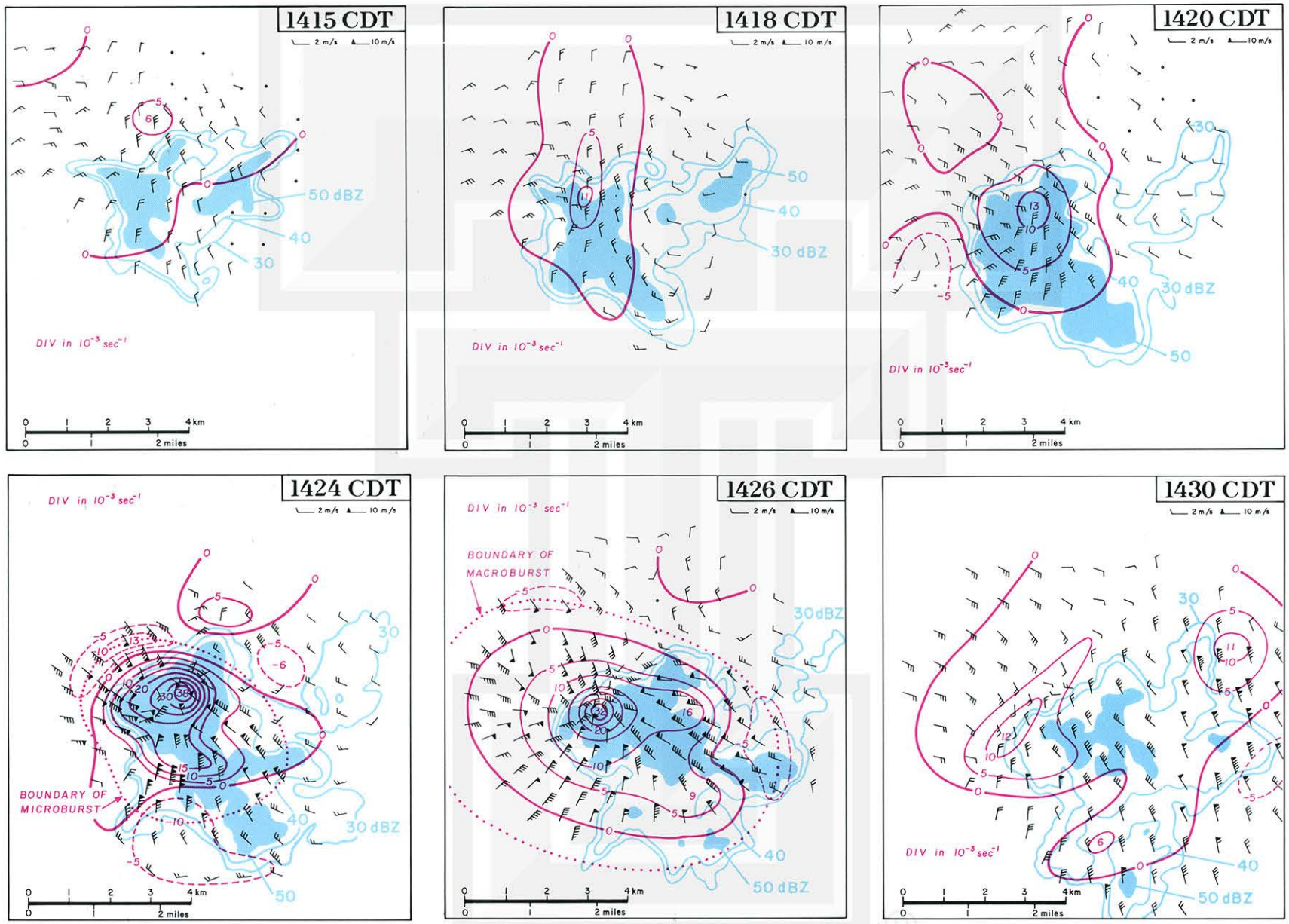

Fig. 4.3-6 Dual Doppler winds computed from CP-2 PPI and CP-4 RHI scans for the 15-min period, before, during, and after the Monrovia microburst of 20 July 1986. The maximum divergence measured at 1424 CDT was 0.038 per second which would induce a 19 m/s downflow at 500 m AGL. At 1425 CDT, the microburst expanded into a macroburst.

Shown in Figs. 4.3-4 and 5 are a chronological sequence of Roger's RHI scans showing reflectivity (middle) and Doppler velocity (bottom) and my cloud pictures taken within 3 sec to 105 sec of the radar scan time. My dual Doppler winds revealed that microburst winds began shortly after 1420 CDT when the P-3 was flying toward the northwest on the second leg. The peak wind occurring at 1423 was 31 m/s (Fig. 4.3-6).

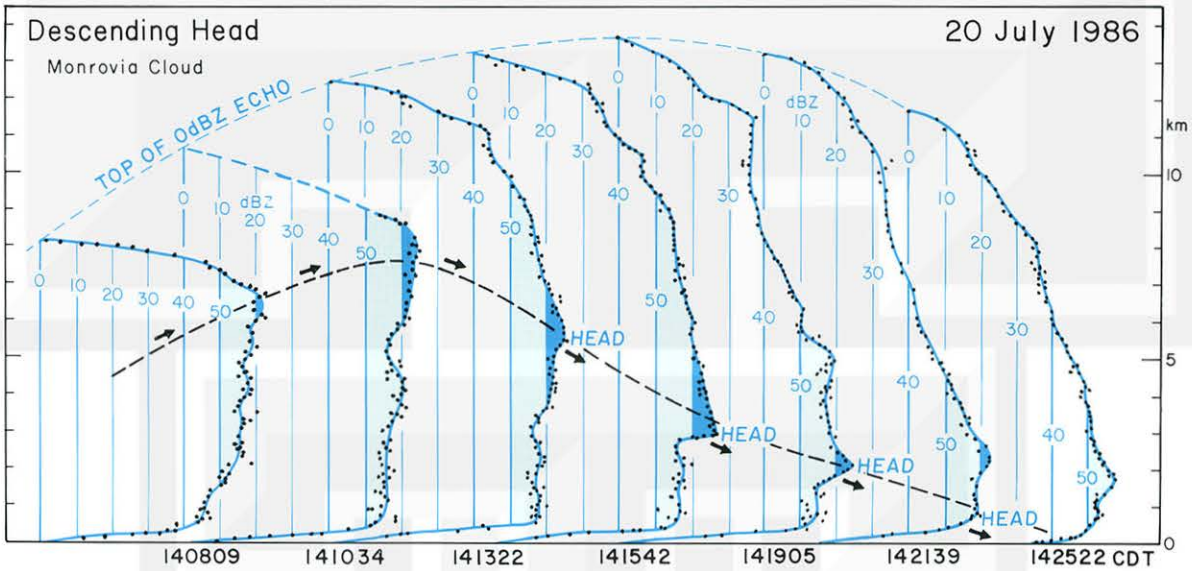

Fig. 4.3-7 Time sequence of reflectivity showing a rapid fall of the high-reflectivity (60+ dBZ) core which started 10 min before the onset of the microburst.

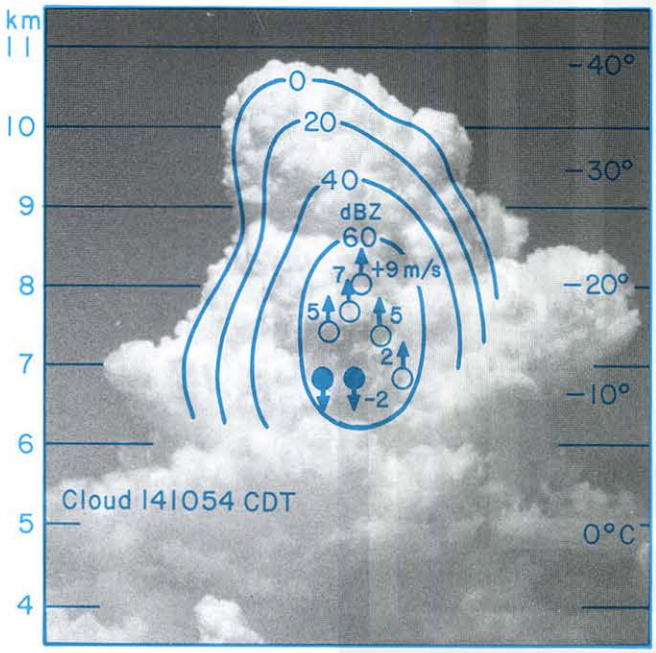

Fig. 4.3-8 CP-4 reflectivity at 141034 CDT superimposed upon the cloud picture taken at 141054 from the P-3. High-reflectivity particles were rising at 2 to 9 m/s.

Descent of Reflectivity Core

When vertical distributions of the reflectivity of each RHI scan were arranged into a time sequence (Fig. 4.3-7) a rapid fall of the 60 dBZ core became evident. The **falling core,** somewhat like the head of microburst (p112), began falling from about 8 km MSL and reached the ground at 1421 when microburst winds began.

The position of the core at 141034 CDT relative to the cloud picture at 141054 CDT suggests an accumulation of large particles near the 50-dBZ echo top (Fig. 4.3-8). It is likely that the downflow descended along with the head of high-reflectivity core, because microburst winds started when the core reached the ground.

Use of Apparent Flare Velocity

Jim Wilson and I called the Doppler radar signatures of both reflectivity and velocity fields in clear air behind the Monrovia cloud the **flare.** In 1988, Jim published a paper on flare, emphasizing the reflectivity and I worked on the application of the flare velocity, publishing a paper by Fujita and Black (1988a).

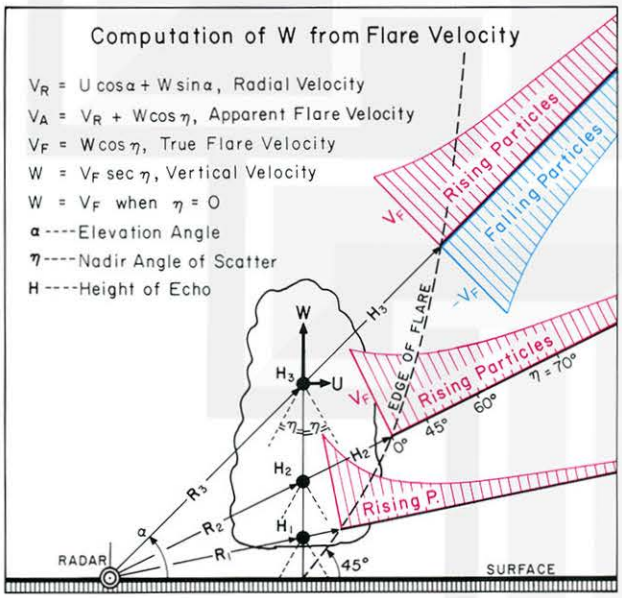

Fig. 4.3-9 A diagram showing the flare echo appearing in the clear area behind a high-reflectivity cloud. Doppler velocity of flare echo (apparent flare velocity) can be used in computing the vertical motion of the flare-causing particles.

A set of simple equations indicates that the velocity displayed by the flare echo, the **apparent flare velocity** is the sum of the radial velocity and the **true flare velocity.** The true flare velocity begins at the R+H range from radar and extends outward (Fig. 4.3-9).

Due to the cosine effect of the nadir angle of scatter, the true flare velocity decreases from the edge of the flare outward as the nadir angle increases from 0° to 90°. Because the function of the velocity decrease is known, the true flare velocity at H+R can be computed mathematically.

After computing these vertical velocities, the Monrovia cloud was lined up into a time sequence (Fig. 4.3-10), finding that high-reflectivity particles were transported upward at 3 to 9 m/s by a strong updraft inside the Monrovia cloud in its towering cumulus stage. Upon reaching just beneath the echo top at 141034 EDT, the high-reflectivity core began falling fast.

At 141539 CDT, my cloud photograph showed a significant constriction of the cloud tower (Fig. 4.3-11). This **constriction phenomenon** suggests a large-scale entry of dry air into the tower. The 1300 CDT sounding at Redstone Arsenal indicates layers of dry air above the 5.2-km MSL.

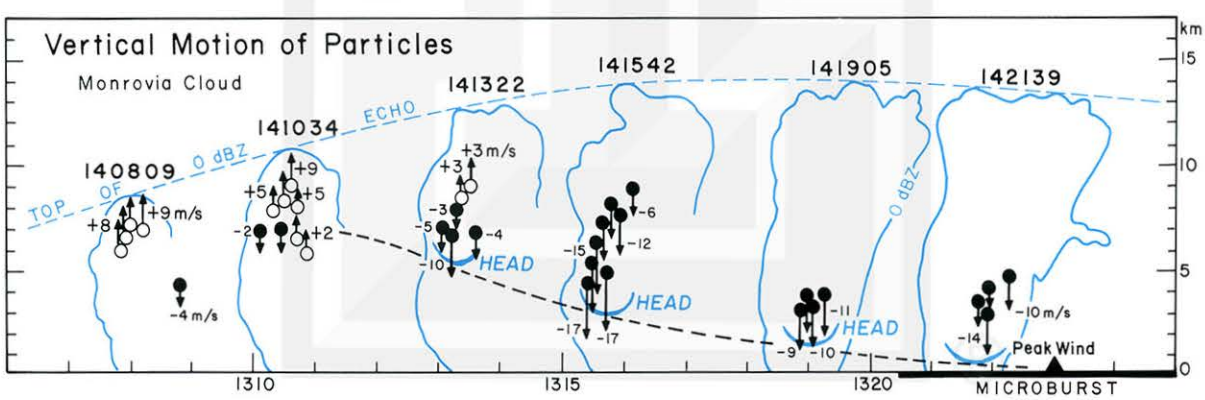

Fig. 4.3-10 Vertical velocity of the flare-causing particles. During the towering-cumulus stage, 140809-141034, particles were rising fast. Suddenly, particles began falling fast, reaching the ground with heavy rain, small hail, and microburst winds (see also Fig. 4.3-7).

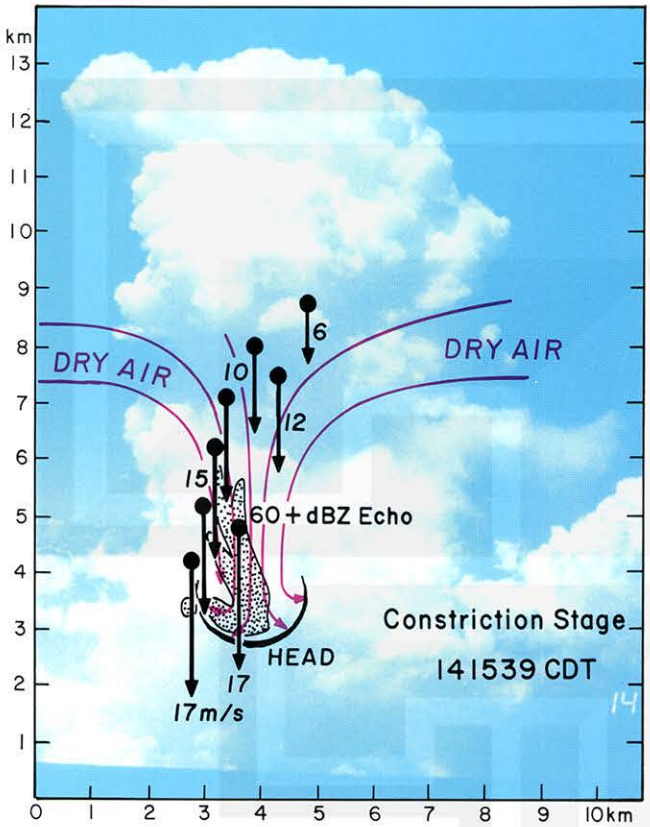

Fig. 4.3-11 The constriction stage of the Monrovia cloud depicted by combining the cloud photo at 141539 CDT and CP-4 echoes at 141542. Vertical velocities of flare-causing particles were computed from apparent flare velocities in Fig. 4.3-9.

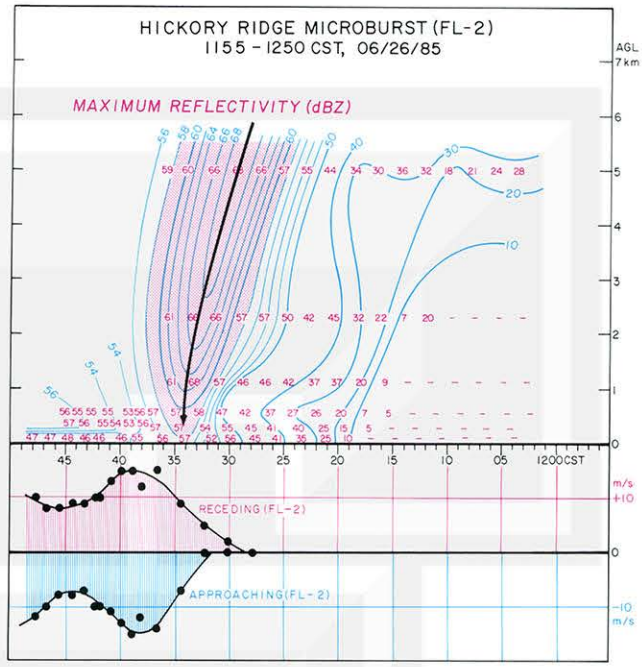

Fig 4.3-12 Time cross section of the Hickory Ridge microburst of 26 June 1985 inside the FLOWS Memphis, Tennessee network.

Recommendation of Convection Termination Studies

Convection initiation is important in the short-range forecast (0 to 6 hrs) of storms. For warning aircraft on microburst hazards, on the other hand, the usual lead time is extremely short (0 to 10 min). This research on the Monrovia microburst, along with my study on the Hickory Ridge (Fig. 4.3-11) and Dogwood Road microbursts on 26 June 1985 in the FLOWS Memphis Network, evidenced that a high-reflectivity core began falling about 10 min in advance of each microburst.

In view of my assessment that not a single detection system by itself can be used in warning microburst hazards without cry wolf or giving a false sense of security, I wish to propose an experiment to establish a physical relationship between the **falling core** and **microburst intensity.** Results of the proposed experiment on **Convection Termination** will lead us to the design of a **Falling Core Detection Radar (FCDR),** a 5-cm radar placed 10 to 20 km from an airport.

The following three systems will be used for a microburst watch followed by warning, similar to tornado watch and warning:

Watch by	**FCDR**	3-10	min leadtime
Warning by	**TDWR**	0-3	min leadtime
Warning by	**LLWAS**	0-1	min leadtime

I expect that the accuracy of FCDR can be improved for issuing warnings instead of just watches.

4.4 Microbursts at Haneda Airport, Japan

On 11 December 1990, four anemometers at the Haneda airport recorded the peak winds within the same minute. They were caused by two microbursts which descended inside a mesoscale pressure dome (Fig. 4.4-1). At the time of the peak wind, a 1-mb pressure drop was recorded.

A detailed mesoanalysis revealed that both microbursts were rotor microbursts connected by a common axis of rotation located on the front side of the outflow (Fig. 4.4-2). The traces of the peak winds appeared as sharp as needles pointing upward (Fig. 4.4-3). Although rotor microbursts are rare in Japan, as well as in the United States, they could occur anywhere. It was fortunate that the airport was closed during the short time of the microburst.

My cooperative observation of the Monrovia microburst with Onodera (Fig. 4.3-1) stimulated the air-safety concern of Japan Air Lines. In response to the need for exchanging ideas, Mr. Rikuro Nakayama, Director of Flight Operations Department promoted my visits to Tokyo for meetings with airline pilots and air-safety experts.

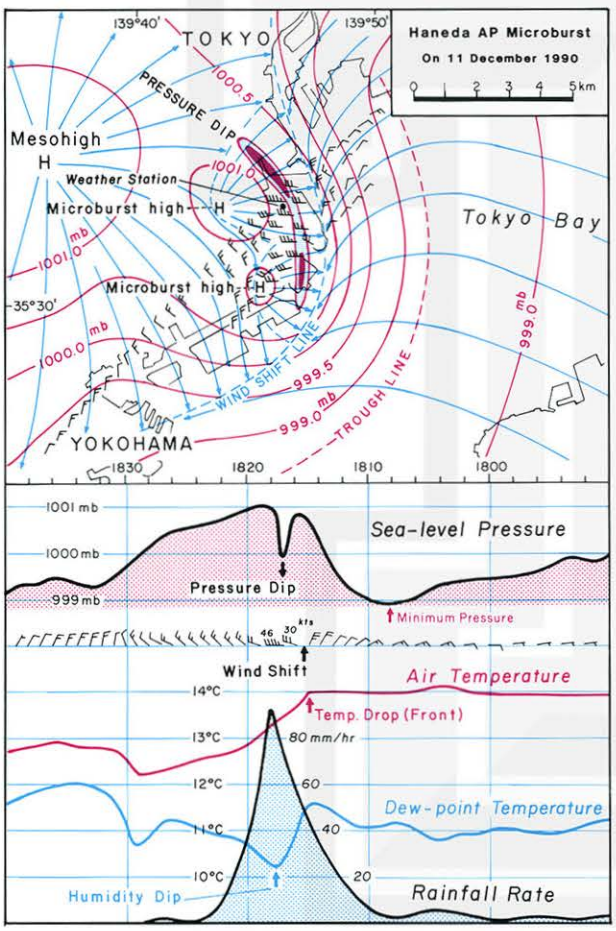

Fig. 4.4-1 A mesoanalysis of two microbursts at the Haneda airport (above) and four traces recorded at JMA station at Haneda. The pressure dip was caused by the rotor not by winds.

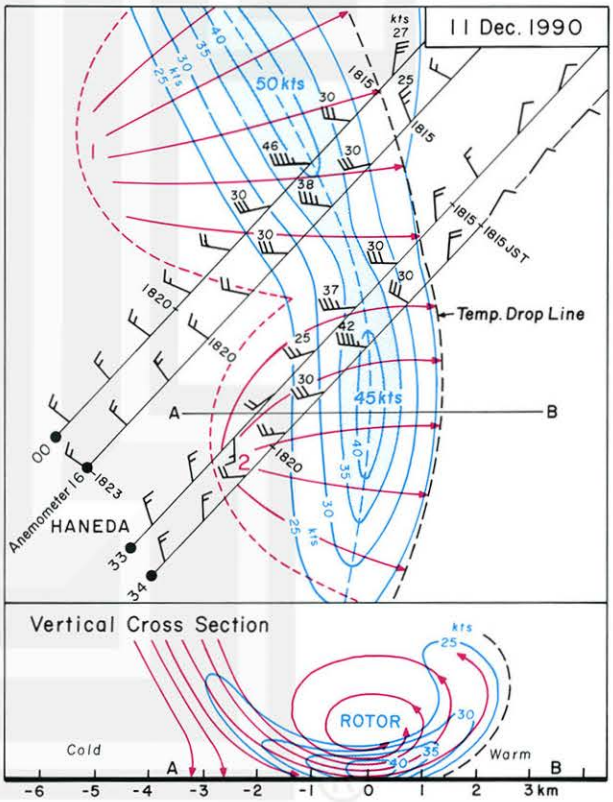

Fig. 4.4-2 Two rotor microbursts depicted by four anemometers; 00, 16, 33, and 34 of the Haneda airport. The highest winds of rotors 1 and 2 were 50 and 45 kts, respectively.

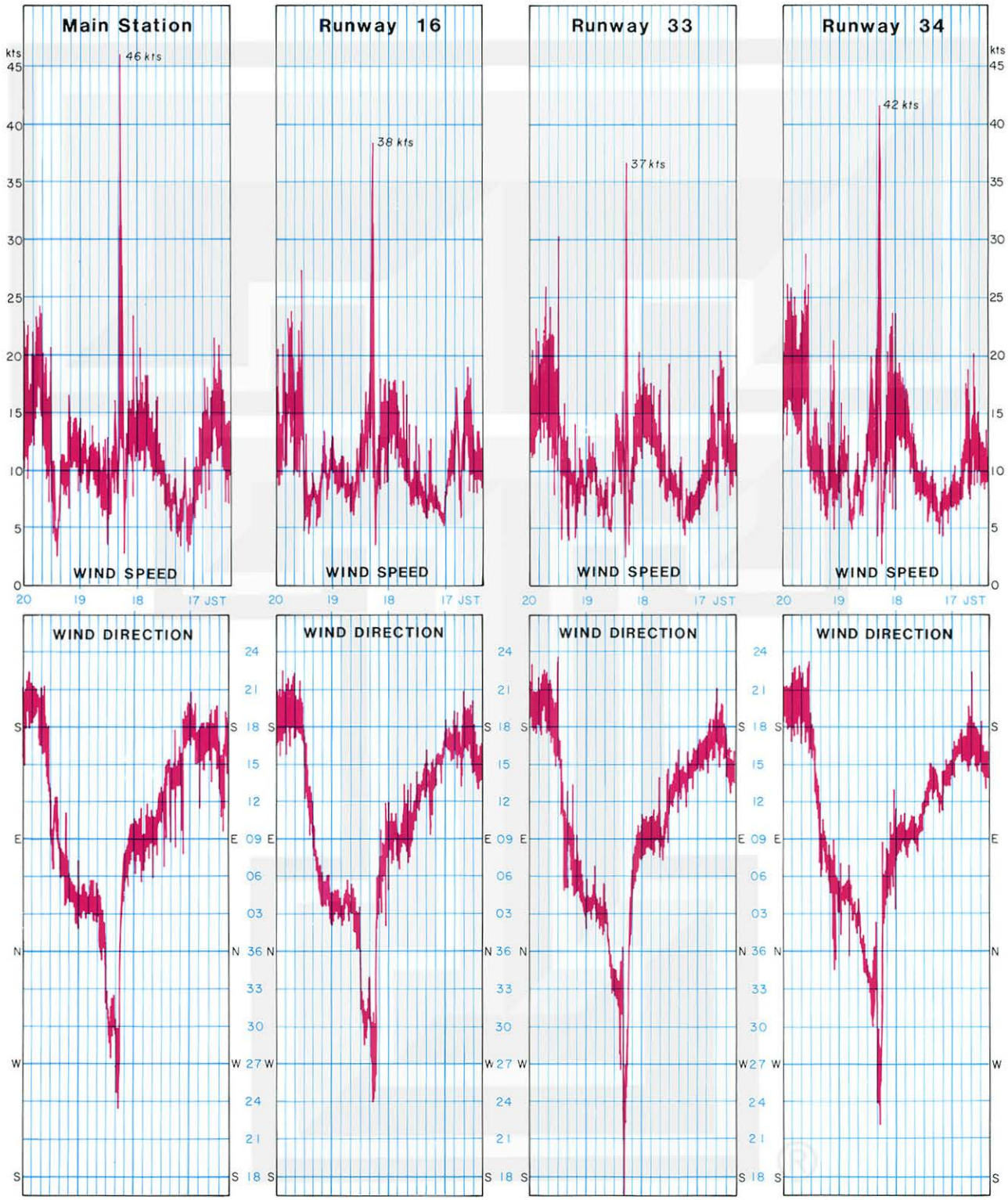

Fig. 4.4-3 Anemometer traces recorded by four anemometers at the Haneda airport on 11 December 1990. Although these traces look alike, a detailed mesoanlysis depicted the existence of two rotor microbursts.

Fig. 4.4-4 A group picture taken in 1989 at the office of Mr. Sakuraba. Seen behind his desk from left are Messrs. Akira Honne, Haruhiko Iwashita, Tetsuya T. Fujita, Kunietsu Sakuraba, Saburo Onodera, and Nobuo Murakami.

Fig. 4.4-5 A group picture of the participants to the wind-shear seminar at Japan Air Lines in 1988. Back row from left are Messrs. Junichiro Kobayashi, Akira Honne, Haruhiko Iwashita, Nobuo Murakami, Shinichi Kitamura, Seisho Aragaki, and Saburo Onodera. Front row from left are Messrs. Hidemaro Nagano, Tetsuya T. Fujita, Kozo Ninomiya, and Masahiro Yasuda.

On 19 October 1986, Mr. Tsuneo Maruyama, Senior Vice-President, along with Mr. Nakayama and I met in Chicago to discuss and complete a long-range plan of our cooperation on aviation meteorology emphasizing wind shear (Figs. 4.4-4 and 5).

Fig. 4.4-6 The main anemometer (00) at Haneda. Photo by Onodera in 1991.

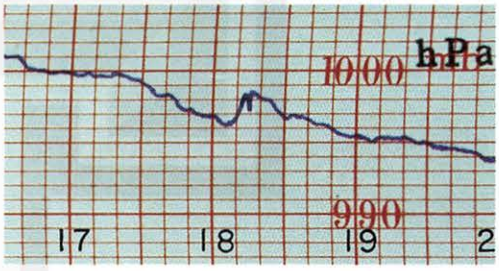

Fig. 4.4-7 A color photo of the pressure dip in Fig. 4.4-1.

Fig. 4.4-8 Ted Fujita trying desperately to fly out of the JFK microburst in a JAL simulator, crashing twice. Photo by Onodera on 18 May 1988.

Chapter Five

Satellites and Cyclones

5.1 Use of Weather Satellites

Cloud Motion Winds

The first geostationary satellite ATS-I was launched on 6 December 1966, allowing us to take pictures of clouds from a fixed location relative to the rotating earth. The spin scan camera on board the satellite was so stable that we could determine accurately the cloud motion relative to the earth surface.

After participating in the Line Islands Experiment in 1967, I became interested in computing the motion of high, middle, and low clouds in an attempt to estimate winds at cloud heights.

Because clouds, when observed in very small scale, form and evaporate rather continuously, we cannot expect that a cloud drifts precisely with the environmental winds. Convective clouds, in particular, could move in unexpected direction and speed. However, the motion of stratified clouds is often close to the wind at the cloud height.

Based on the five ATS-I pictures on 9 June 1968 taken at 24-min intervals, cirrus motions over the Pago Pago area were obtained for comparing cloud motions with rawin winds aloft (Fig. 5.1-1).

Results were encouraging because, as expected, small cirrus clouds tracked were spiraling out from an extensive cluster of high clouds. Quantitatively, computed motion vectors agreed very well with the upper-air soundings from four stations located inside the area of the wind analysis (Fig. 5.1-2).

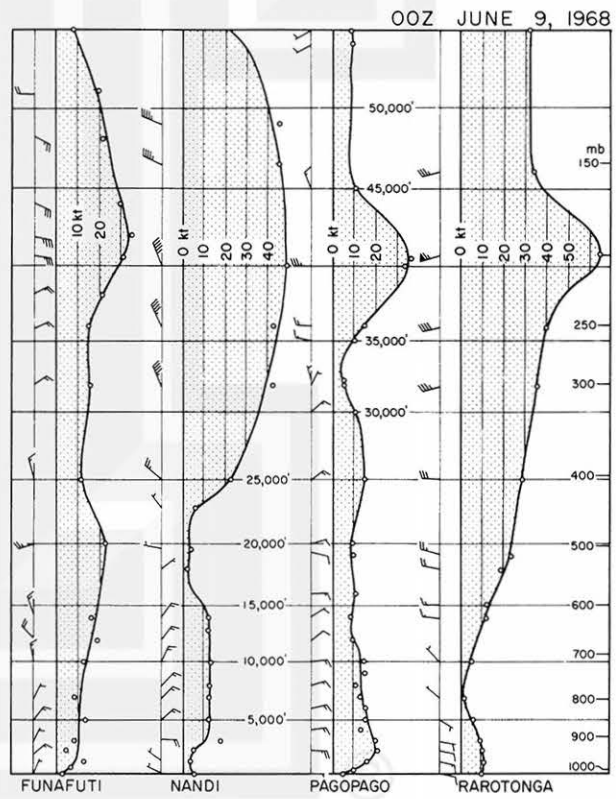

Fig. 5.1-1 Four soundings at 00 GMT 9 June 1968 for evaluating the cloud winds computed by ATS-I pictures over the Pacific.

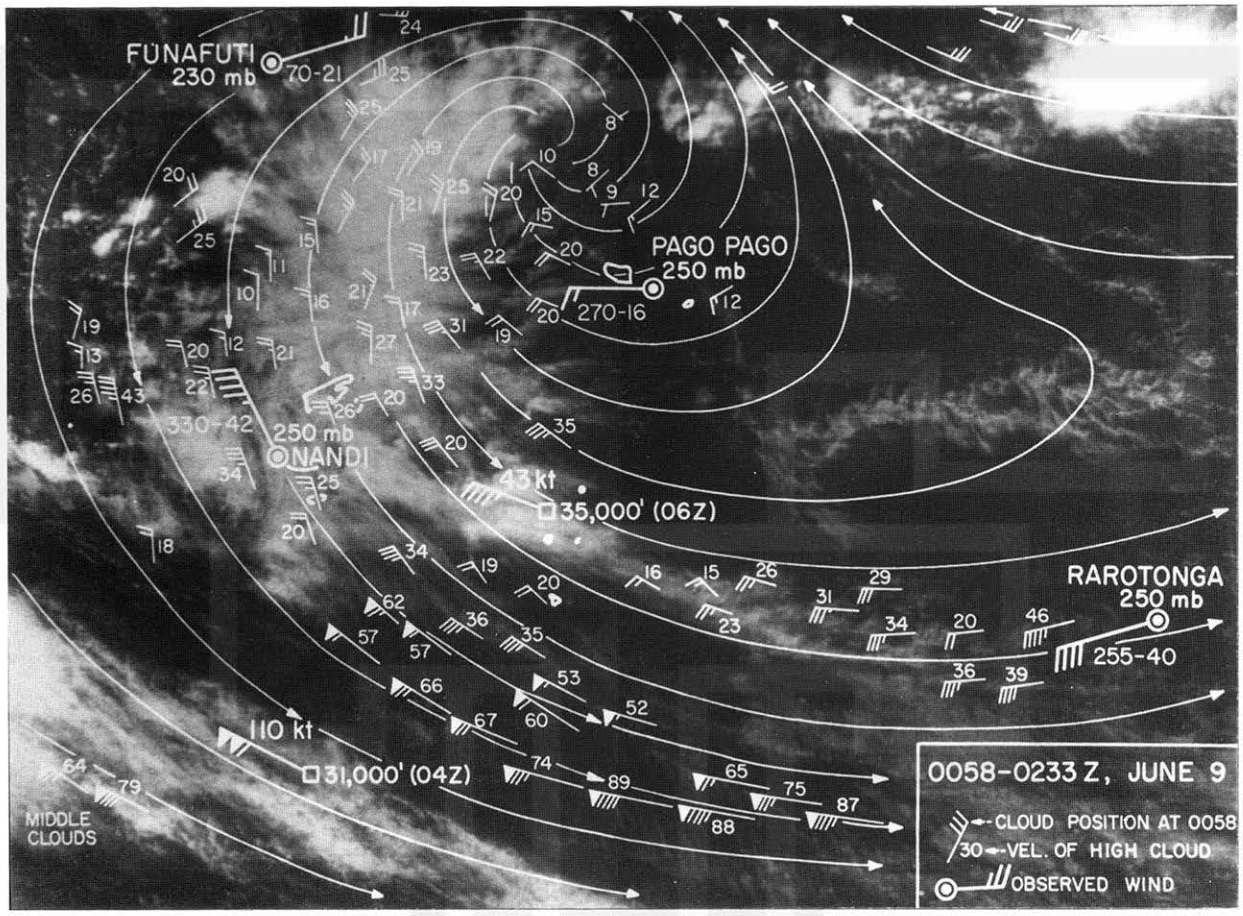

Fig. 5.1-2 Cloud winds (in kts) computed from five ATS-I pictures taken at 0058, 0122, 0145, and 0233 GMT on 9 June 1968. Total tracking time: 95 min and mean picture interval: 24 min.

The First Color Movie of The Planet Earth

The spin scan color camera was operated on board the ATS-III geostationary satellite launched on 5 November 1967. The first sequence of 34 color pictures were transmitted back to the earth on 19 November 1967.

As shown in Figs. 5.1-3, 4 and 5, the color camera generated 34 breathtaking views of the earth at 30-min intervals. Making use of the animation movie camera, the first color movie of the planet earth was produced in my photo laboratory. The movie shows the sunrise terminator sweeping across the disc, turning the earth into full earth. Then, the sunset terminator gradually moves from east to west, resulting into a dark planet.

The color movies also shows selected local areas to reveal mesoscale features of clouds and the background in color. The movie was made to project at 24 frames per second. It was found that the best viewing sequence is to take two frames per picture during the forward motion followed by one frame per picture for the return motion to create a repetition of slow forward, quick return motions.

ATS III Pictures on 19 November 1967 for the First Color Movie of the Planet Earth

by

Prof. Verner E. Suomi, U. of Wisconsin
Prof. Robert J. Parent, U. of Wisconsin
Prof. Tetsuya T. Fujita, U. of Chicago

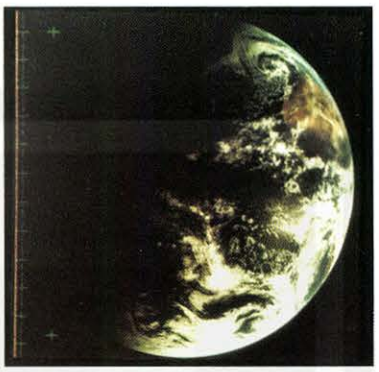

7:00 a.m.

3:30 a.m

5:30 a.m.

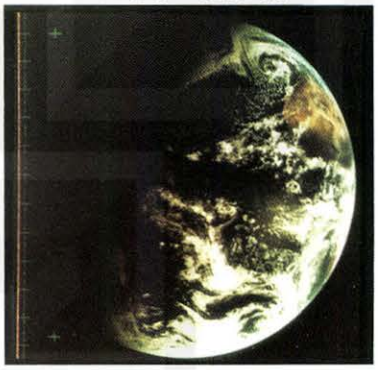

7:30 a.m.

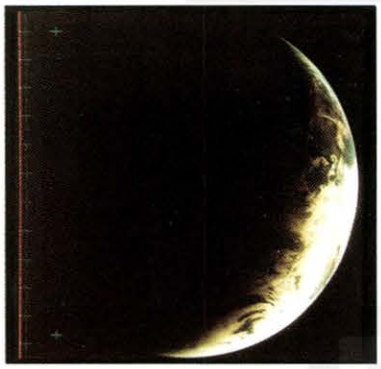

4:00 a.m.

6:00 a.m.

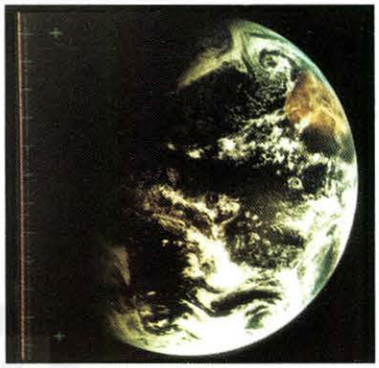

8:00 a.m.

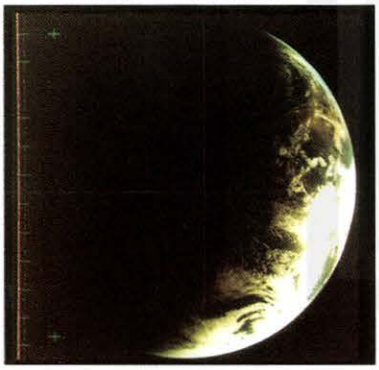

5:00 a.m.

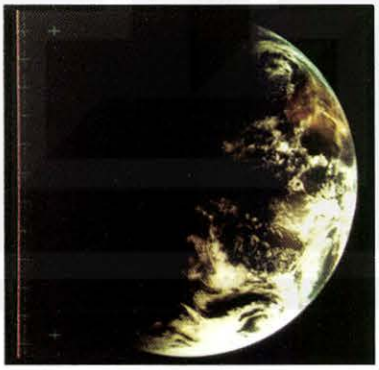

6:30 a.m.

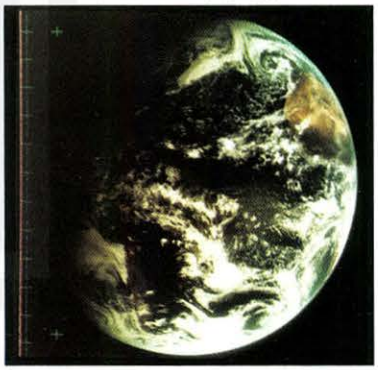

8:30 a.m.

Fig. 5.1-3 First color pictures of the earth taken by the Applications and Technology Satellite (ATS III). The spin-scan multicolor camera was invented by Professors Suomi and Parent of the University of Wisconsin.

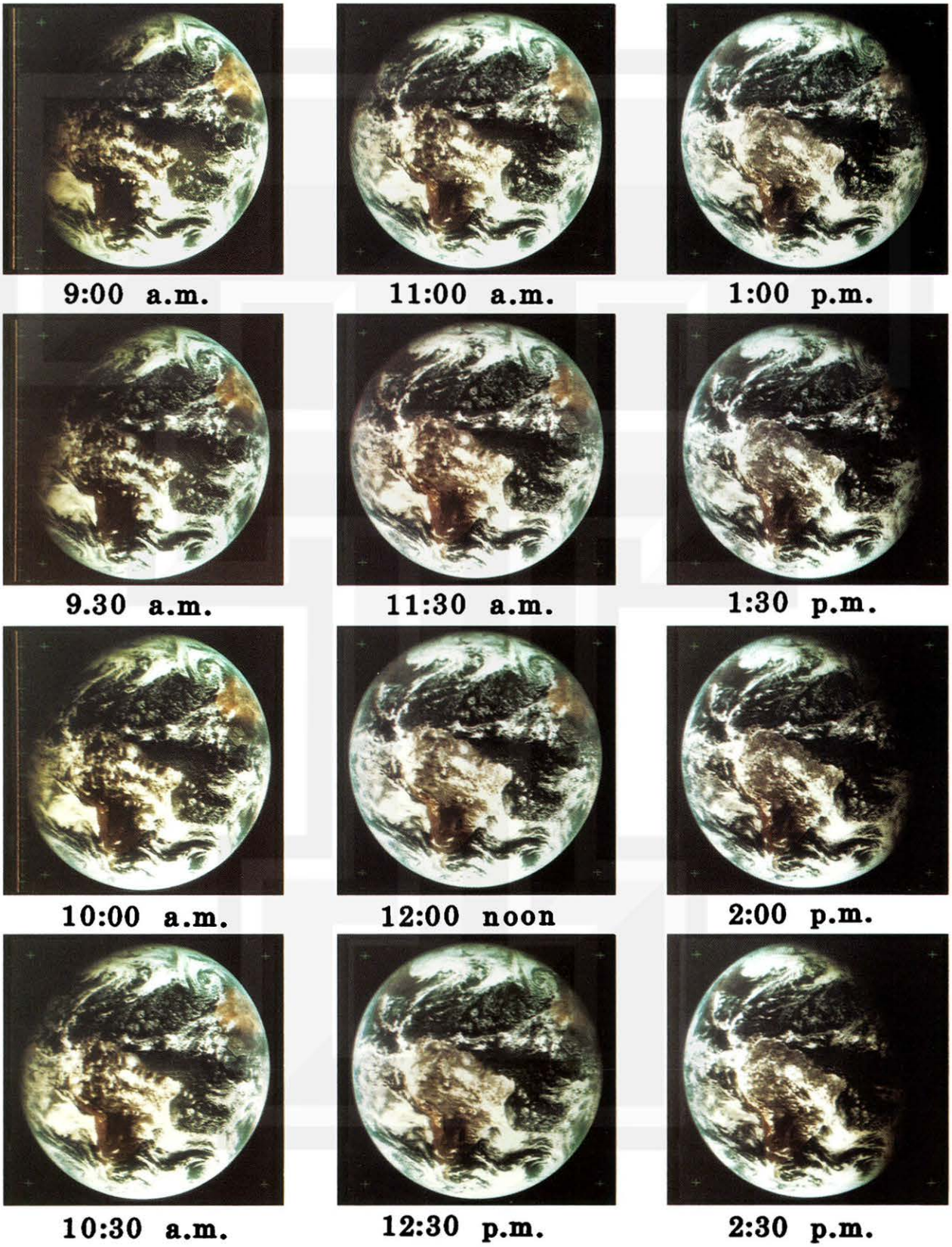

Fig. 5.1-4 After the first color pictures at 30 min. intervals were obtained successfully, I constructed a time-lapse movie camera for producing the first color movie of the earth seen from the geostationary altitude above Brazil.

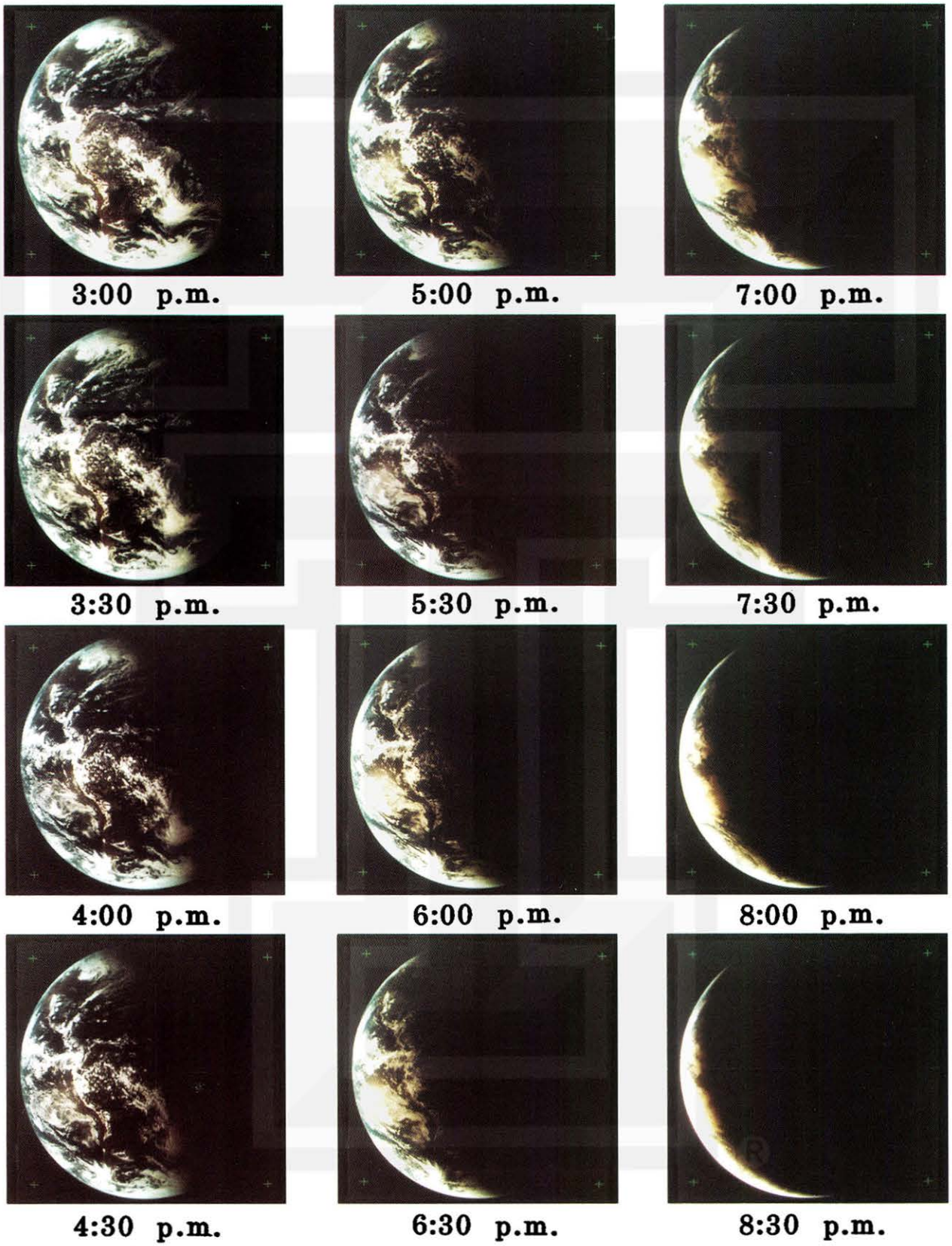

Fig. 5.1-5 The 34 color pictures identified by the local standard time (LST) at the subsatellite point shows the change in the shape of the earth from new earth, first quarter earth, full earth, last quarter earth, and back to new earth.

Rapid Scan Experiment

As cloud-wind computations increased, it became evident that rapid-scan pictures at 2 to 5-min intervals are very useful in determining motion vectors of short-lived and fast-changing clouds.

On 5 August 1976, 2 to 4-min pictures were taken for computing cloud winds over south Florida. A detailed analysis revealed the stages of thunderstorm activities. During the formation stage, the small anvil expands in all directions. When the anvil gets old, it drifts away from the origin. Finally, the outflow from the decaying storm splashes out, creating a circular arc cloud (Figs. 5.1-6 and 7).

This example shows clearly that short scan intervals will generate more winds. However, there is a limitation on the minimum interval due to the zitter of the spacecraft as well as the error in tracking short vectors. The 5-min rapid scans are used in recent years.

Cloud Winds from 4 Pictures (1242-1250 EST) 5 August 1976

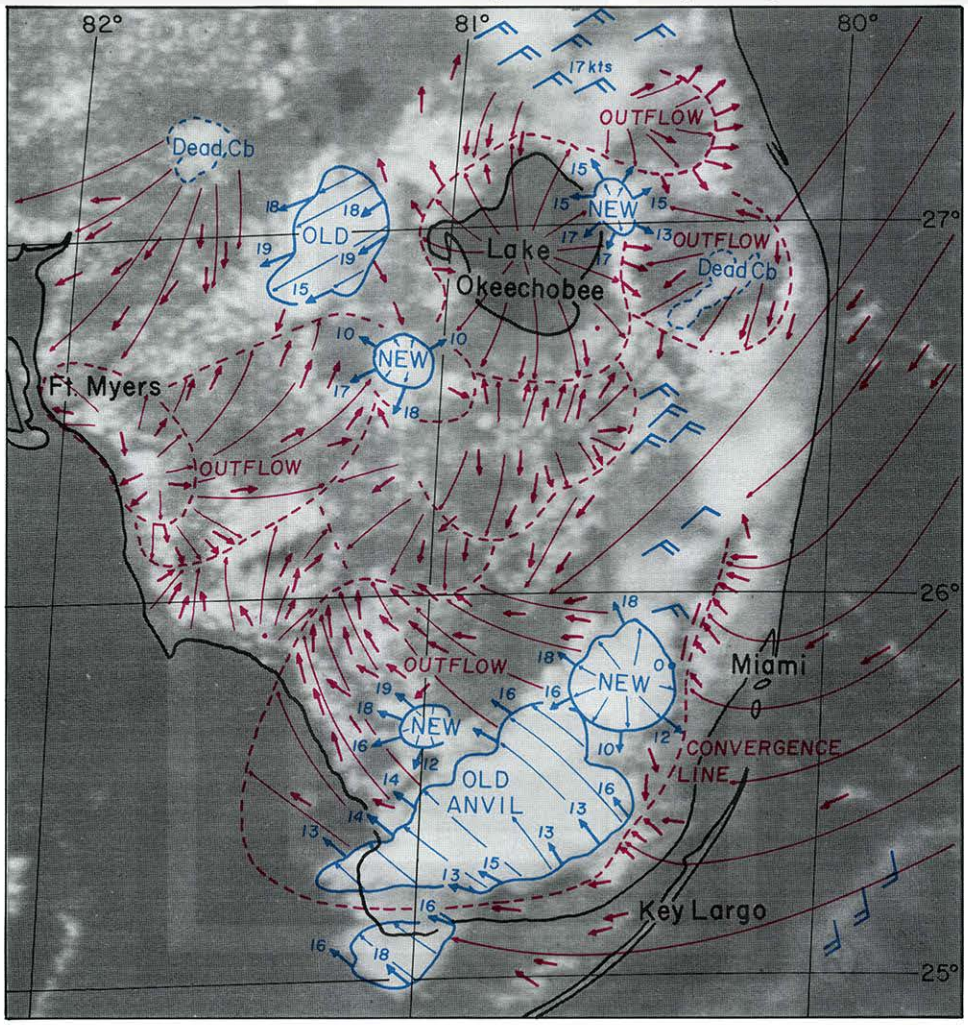

Fig. 5.1-6 High and low cloud winds computed from 2- to 4-min rapid scan pictures on 5 August 1976. Seen in this cloud-wind map are the expansion of new anvils, drifting of old anvils, and circular cloud lines expanding from where an active thunderstorm had been located.

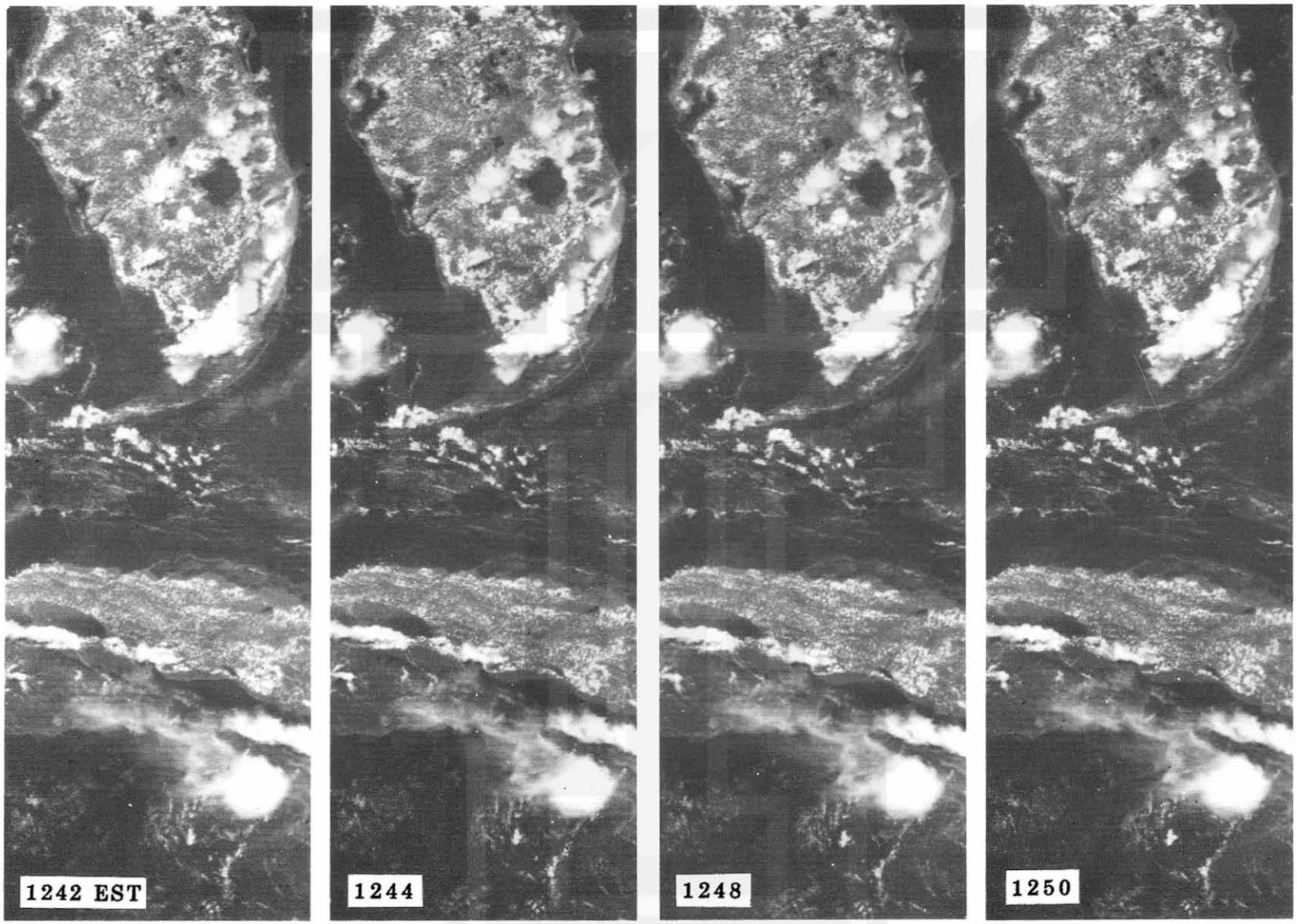

Fig. 5.1-7 A rapid-scan experiment using very short picture intervals. These four pictures were taken at 2-min, 4-min, and 2-min intervals to depict fast-changing clouds over south Florida. Lake Okeechobee with cold water temperature was dark surrounded by small cumulus clouds. Date of experiment: 5 August 1976.

5.2 Pseudocolor Experiments

In 1972, I developed an inexpensive pseudocolor camera capable of multiple-exposing negative and positive images through color transparencies used for Christmas lights as color filters.

The first test was made by combining LANDSAT negatives to generate red-color cities and green forests. Both Chicago (Fig. 5.2-1) and Tokyo (Fig. 5.2-2) were used as test cities. Cloud winds in color were superimposed on the cloud picture to identify tracked clouds (Fig. 5.2-3).

Two typhoons over the Pacific were depicted by combining a moonlight visible picture with corresponding infrared picture in green. Typhoons with infrared green plus visible red became white and cities with visible red only remained red (Fig. 5.2-4).

A combination of visible red and infrared green resulted in white convective clouds, green high clouds, and red low clouds (Fig. 5.2-5).

This technique of color combinations was used in depicting thunderstorms and other types of clouds which cannot be depicted easily by examining visible and infrared pictures separately.

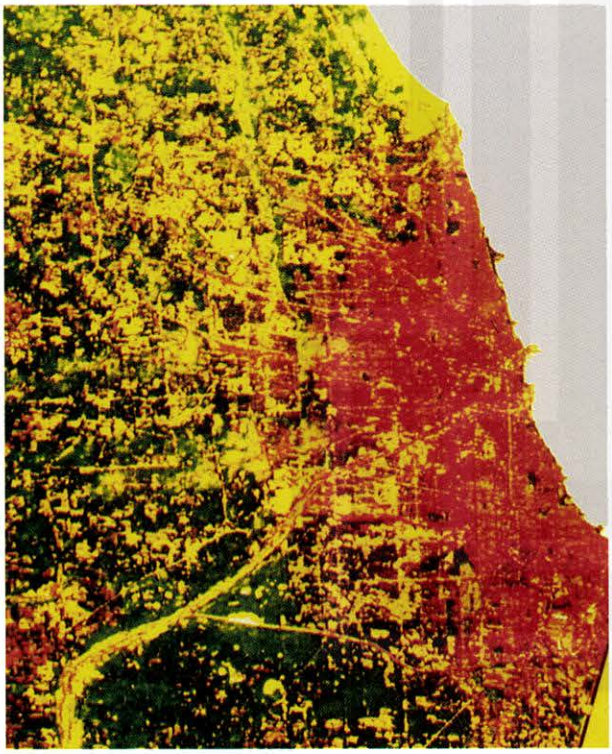

Fig. 5.2-1 Chicago and vicinity on 2 October 1972 seen in a pseudocolor picture.

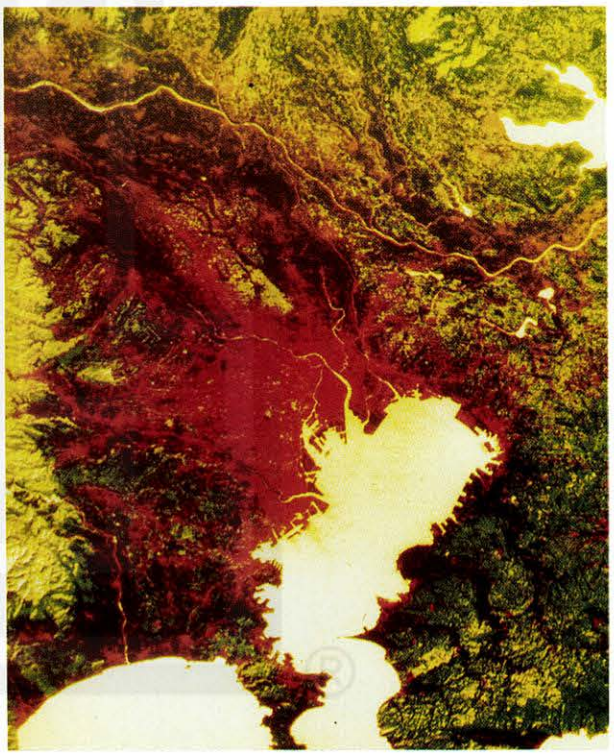

Fig. 5.2-2 Tokyo and vicinity on 26 November 1972 seen in a pseudocolor picture.

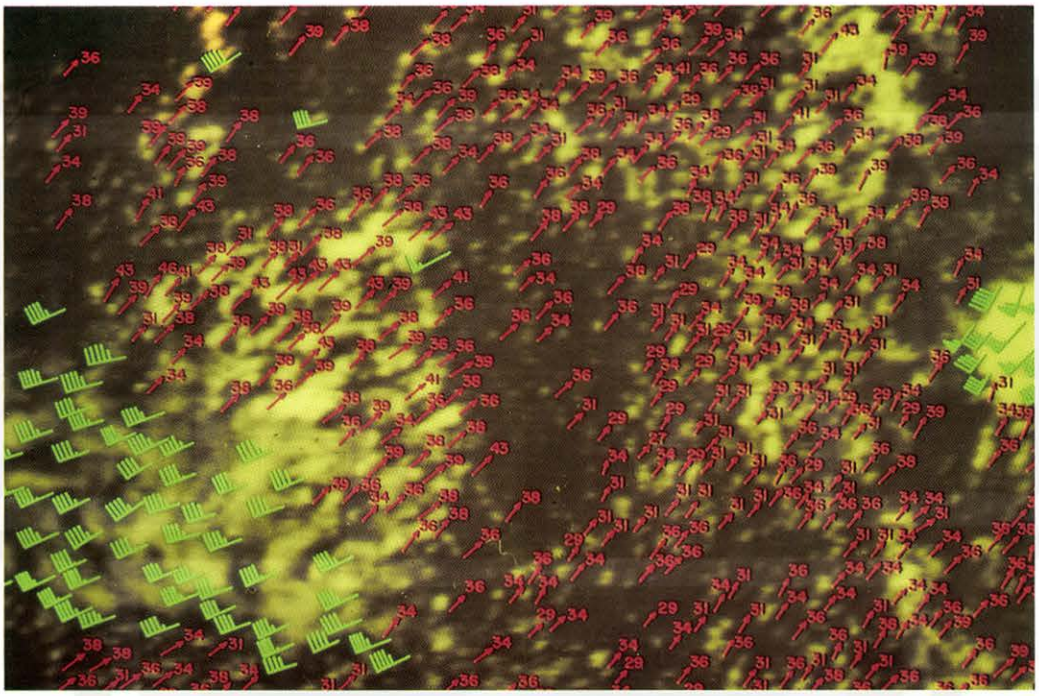

Fig. 5.2-3 High (green) and low (red) cloud winds on 15 May 1977 over southwestern Iowa computed from three pictures at 1939, 1942, and 1945 GMT.

Fig. 5.2-4 Typhoons Rita (left) and Tess under the moonlight at 3 a.m. JST. City lights in Japan are visible. From visible and IR DAPP pictures.

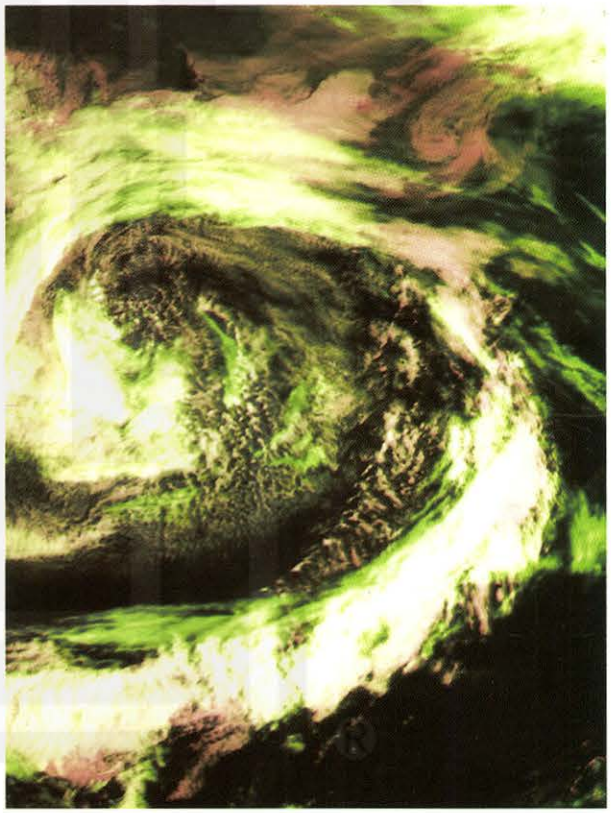

Fig. 5.2-5 An occluded cyclone at 10 a.m. EST on 25 August 1973 over eastern Canada obtained by combining visible and IR pictures from NOAA-2.

5.3 U.S. Hurricanes

Hurricane Camille, 1969

In 1969, monochromatic visible pictures of ATS-III were enhanced by applying my enhancement curves for depicting both eye wall and rainband clouds simultaneously. Finally, hurricane Camille of August 1969 was enhanced successfully (Fig. 5.3-1).

Meanwhile, the land area affected by the hurricane was surveyed by renting a Cessna 172 at Jackson, Mississippi. The purpose of the survey was to map the damage by the Fujita Tornado Scale (F scale) and to compare the damaging winds with enhanced hurricane-top clouds. Unexpectedly, the hurricane maintained the strength for a long time after the landfall. The F-1 isotach extended 800 km inland from the Gulf Coast (Fig. 5.3-2).

The main problem was the time-consuming and tiresome flight to cover the vast area of the hurricane damage. Unlike severe and concentrated tornado damage, it is hard to identify the tornado damage which could be embedded inside the hurricane damage.

Fig. 5.3-1 An enhanced picture of hurricane Camille at 1645 GMT 17 August 1969. This image was produced at Goddard Space Flight Center.

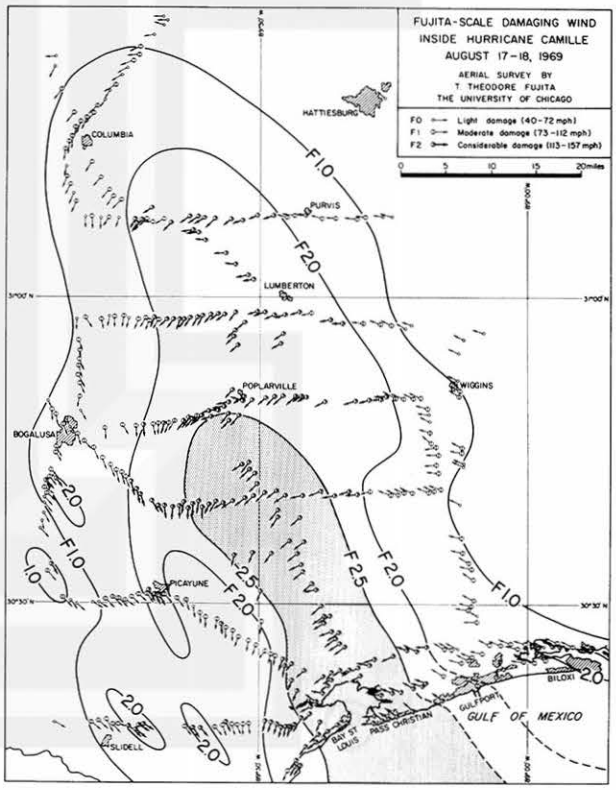

Fig. 5.3-2 My first aerial survey of hurricane damage. A Cessna 172 from Jackson, Mississippi and my car with Susie were used for damage mapping.

Cloud Winds of Hurricane Camille on 17 August 1969

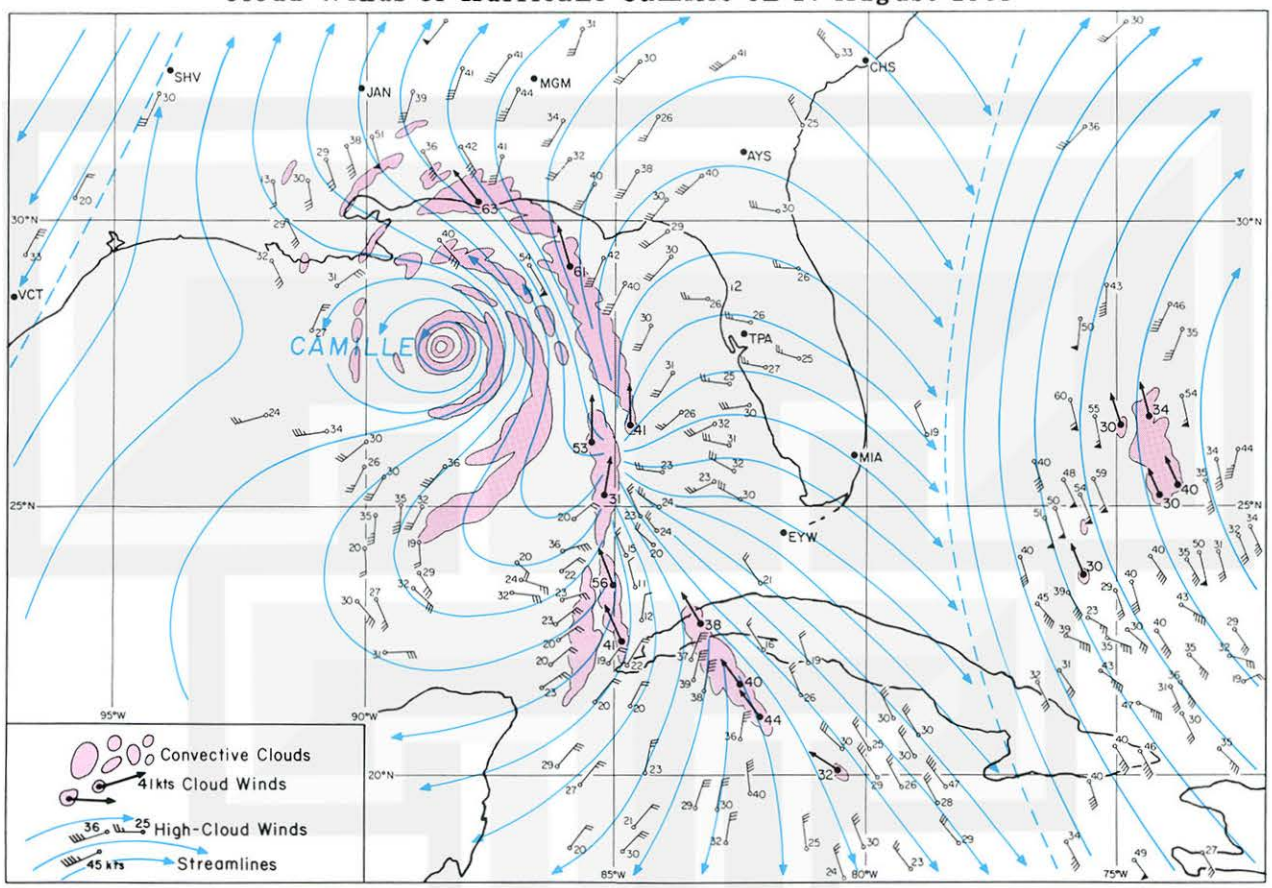

Fig. 5.3-3 High-level airflow in and around hurricane Camille at 1632-1736 GMT on 17 August 1969. Cloud winds were computed by tracking clouds on five enhanced pictures. It is seen that large convective clouds in the outer rainband induced strong divergence fields over the inflow region of the hurricane.

Cloud Winds at Camille Top

Both high cloud and convective cloud winds were computed in determining the outflow at the hurricane-top altitude. The total tracking time was 64 minutes.

There were three separate wind systems depicted by tracking high clouds. They were hurricane-top flow, southerly flow to the east, and northerly flow to the west.

The hurricane-top flow consisted of the hurricane outflow and the rainband outflow. The former consisted of inner rainband circulation and hurricane-scale outflow. The outflow from the outer rainband was very strong, large and dominating, implying that the energy release by outer rainband should not be underestimated.

Hurricane Debbie, 1969

An enhanced picture of Debbie at 1157 GMT, 8 a.m. local time, failed to show an open eye because Debbie was weaker than Camille.

Ten enhanced pictures were used for tracking convective towers embedded inside the hurricane cirrus shield. It was found that the maximum speed on the east side of the hurricane was 40 kts. The convective

tops tracked looked like towering cumuli, rather than anvil tops with strong outflow (Fig. 5.3-4).

The outflow field of the hurricane top was insignificant in the southern sector where the cirrus shield was missing. The inflow winds evidenced by low-cloud winds were also weak both in speeds and cyclonic curvatures.

Although it was unusual to be able to track cloud elements for 142 minutes, I remember that tracked clouds were very stable, maintaining their identities for a long time (Fig. 5.3-5).

As expected, trajectories of clouds for such a long tracking period are curved. In other words, the cloud wind at the beginning and the end of the tracking period could change significantly. For determining instantaneous winds, it would be necessary to use rapid-scan pictures with very short picture intervals.

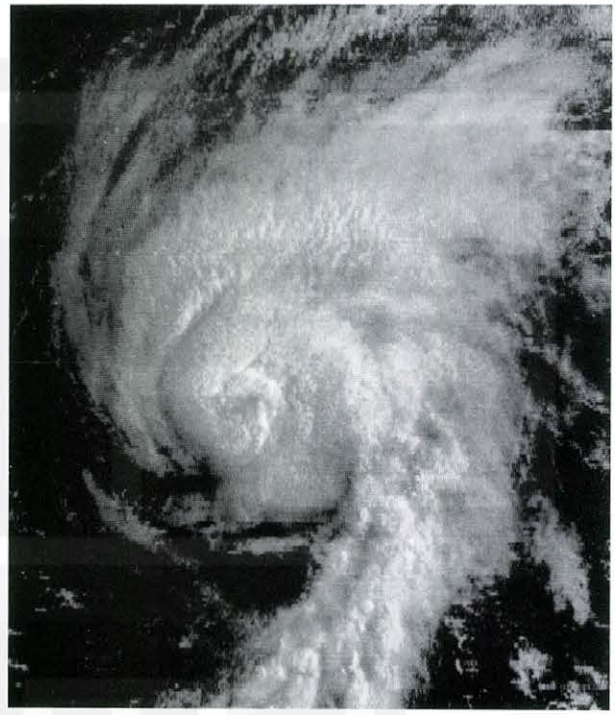

Fig. 5.3-4 An enhanced visible picture of hurricane Debbie at 1157 GMT on 18 August 1969.

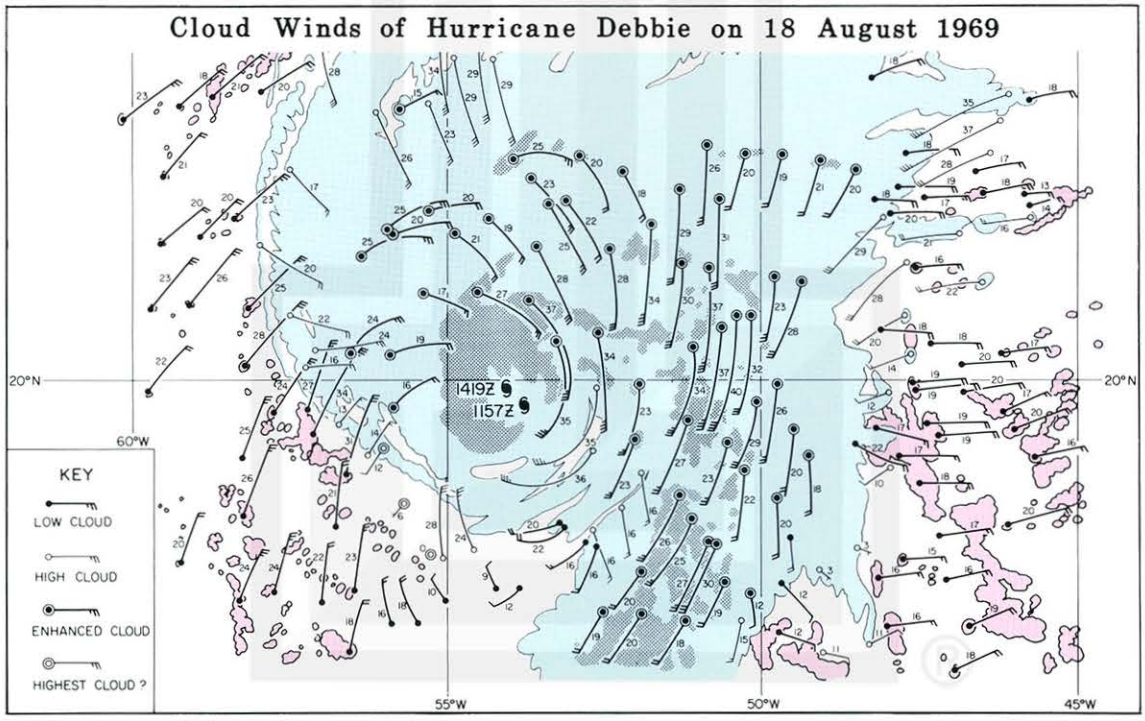

Fig. 5.3-5 High, low, and convective cloud winds of hurricane Debbie obtained by tracking clouds on 10 enhanced pictures for 142 minutes (1157-1419 GMT) on 18 August 1969. Convective clouds were difficult to track without enhancing pictures.

Hurricane Alicia, 1983

This hurricane caused all types of damage to ground structures because the hurricane center headed straight over populated areas toward Houston. In Houston, windows were broken by loose gravel blown off from the gravel roof. The following map was made under the Hurricane Strike Program of NOAA.

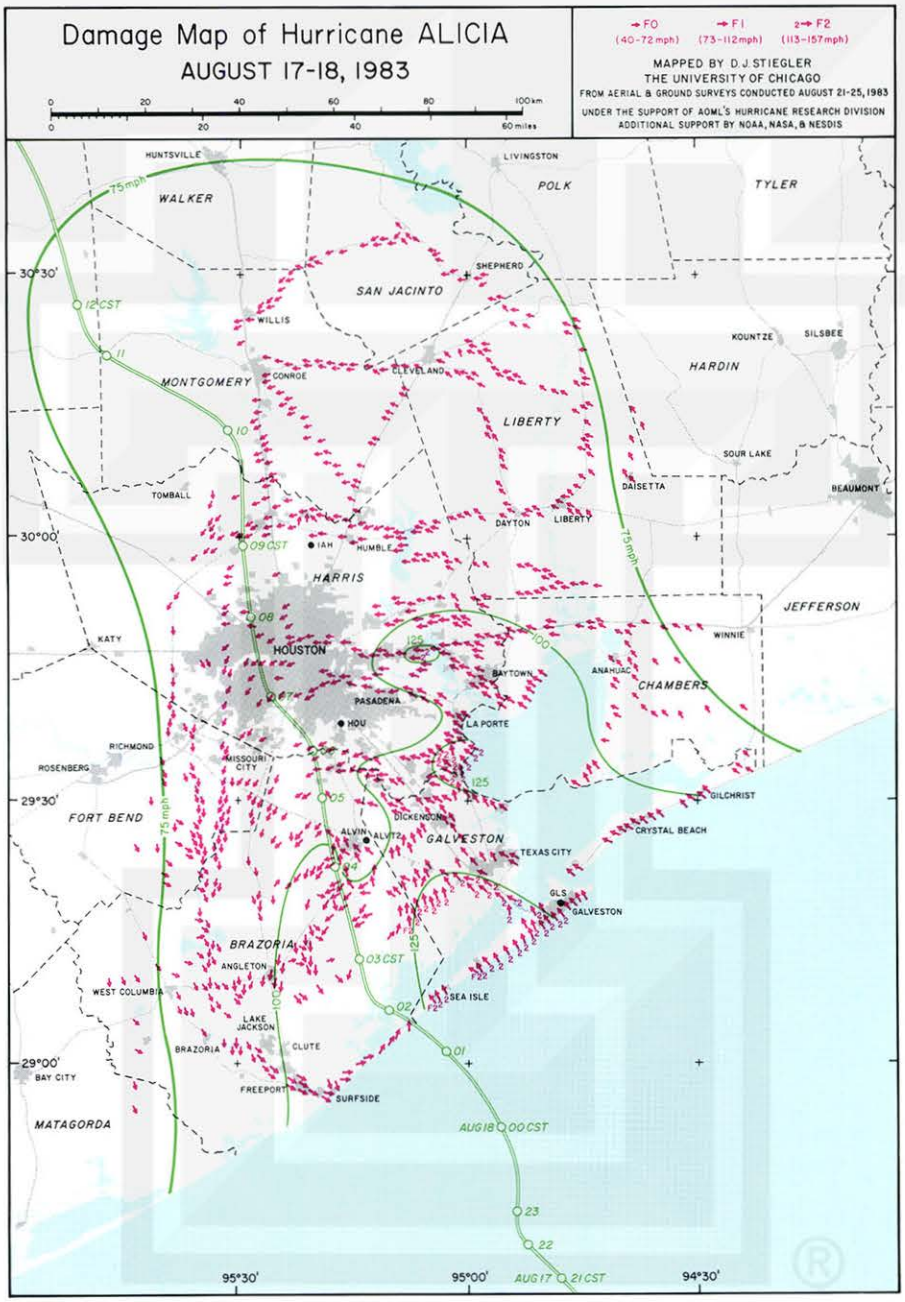

Fig. 5.3-6 Damage map of hurricane Alicia of August 1983 which moved north-northwest through Houston, Texas. The Houston National Weather Service at Alvin recorded the minimum sea-level pressure of 966.7 mb. Aerial survey by Duane Stiegler who became specialized in aerial aurveys of hurricanes and tornadoes.

Hurricane Hugo, 1989

Hurricane Hugo was one of the worst storms which moved deep inland without weakening. The entire coast of South Carolina was affected by high winds and tides.

Under the National Weather Service contract, the vast areas of hurricane damage were flown for generating the following damage map in color. Because of high humidity after Hugo, we experienced frequent rain and low clouds which caused difficulties in mapping and photographing the damage.

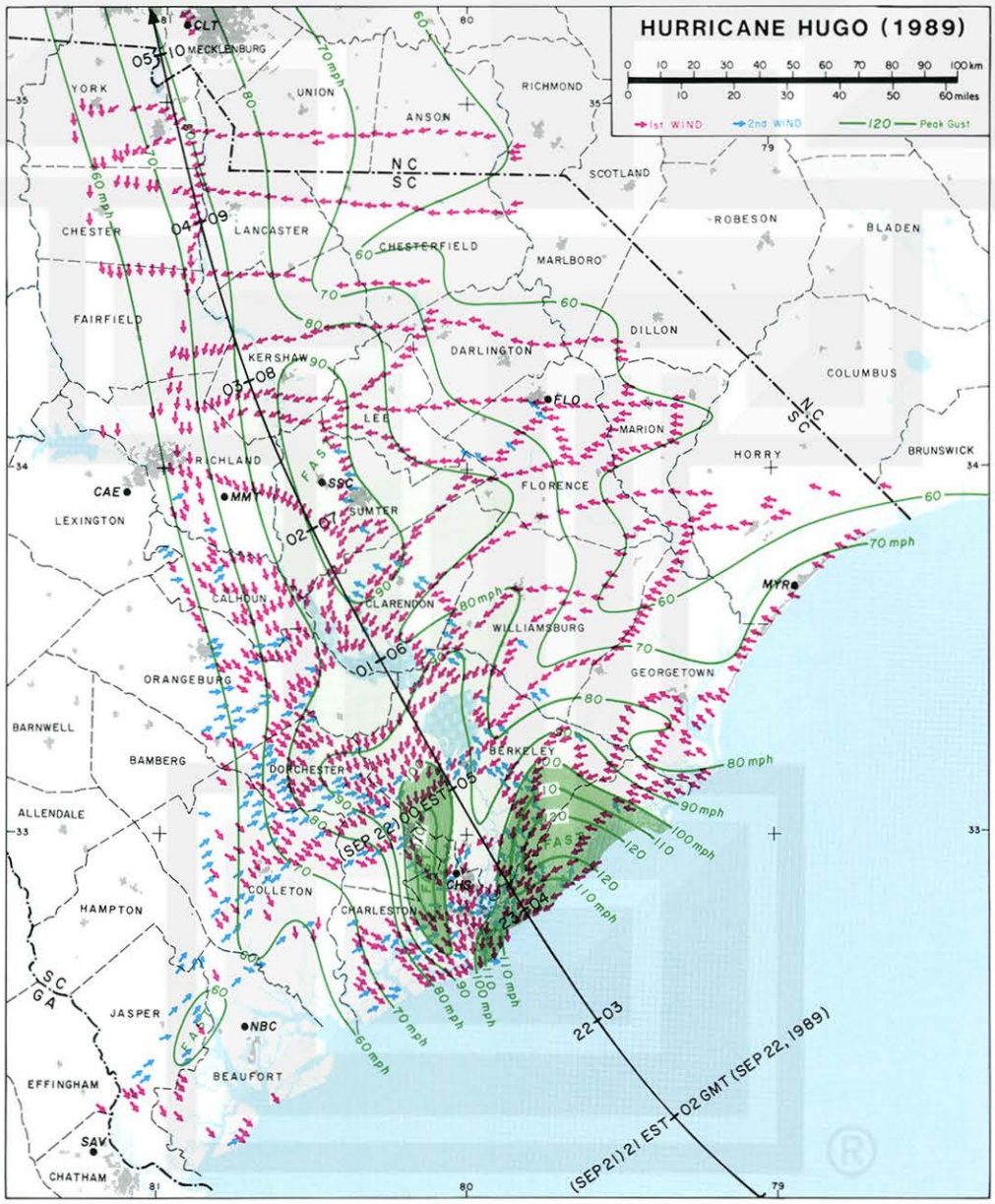

Fig. 5.3-7 Damage map of hurricane Hugo of September 1989. Fujita and Stiegler flew two Cessnas concurrently for four days to map vast areas of the hurricane damage. Damage vectors of the first wind (red) and second wind (blue) were mapped separately. Isotachs denote the windspeeds of the first wind.

A. A pile of boats on Sullivans Island at Intra-coastal Waterway.

B. Uprooted trees in the Francis Marion National Forest northeast of Charleston, South Carolina.

C. A house washed onto the coastal road on Folly Island.

D. A ground view of the house on the road in the aerial photo on the left.

E. A wood-frame roller coaster at Mrytle Beach undamaged by Hugo winds.

F. Hugo-generated sand island in Shallote Inlet, North Carolina.

Fig. 5.3-8 Selected views of the effects of hurricane Hugo as seen from low-flying Cessna. Two Cessnas for the damage survey were based at Savannah, Georgia because no aircraft was available in South Carolina due to the extensive damage. Photos by Ted Fujita.

5.4 Japanese Typhoons

Typhoon Della, 1949

This typhoon was studied for my Sc.D. thesis early in the 1950s. It was an early season typhoon (Fig. 5.4-1) which weakened in northern Kyushu. The most interesting feature of the storm was a "pressure dip" formed in the northwest sector when Della was redeveloping into a middle-latitude

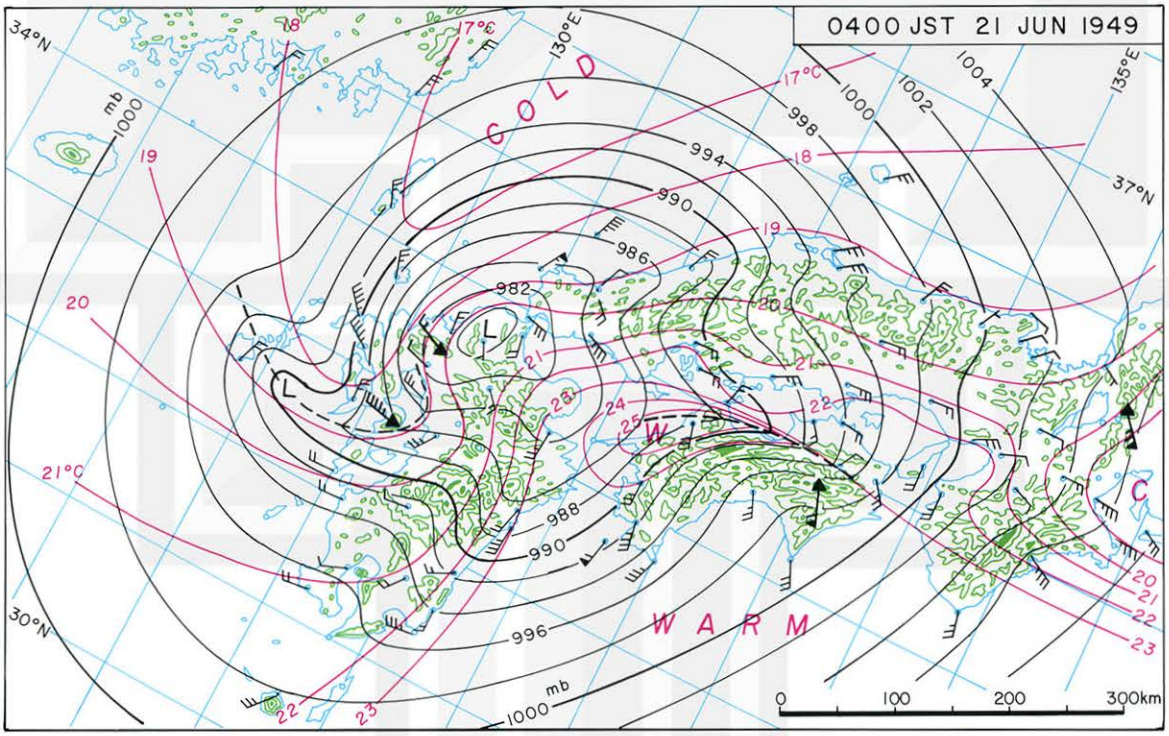

Fig. 5.4-1 The first mesoanalysis of typhoon which I tried in Japan. At that time, data collection was a major problem because all original data were kept at individual stations and no copying machine was available.

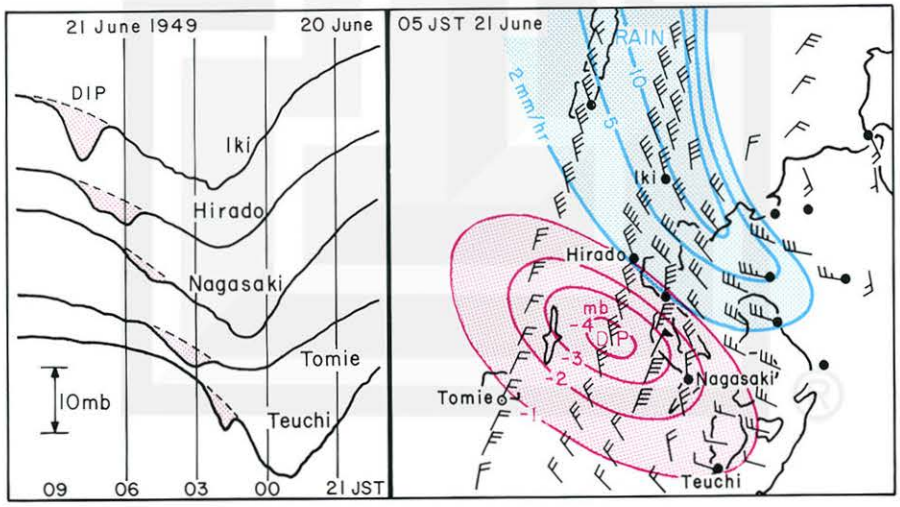

Fig. 5.4-2 A pressure dip formed near the west edge of typhoon Della on 21 June 1949. There was an area of rain ahead of the dip. From Fujita (1952a).

cyclone characterized by an inflow of 17°C cold air from the western Sea of Japan.

Further analyses revealed that there was a band of heavy rain on the advancing side of the dip. Apparently, a combination of the cold-air advection and precipitation created an outflow with significant divergence and anticyclonic curvature (Fig. 5.4-2).

Typhoon Mireille, 1991

About two months after the typhoon, I had a chance to visit my home island of Kyushu, Japan in November 1991. Against my expectation, I could still see damaged trees which were practically untouched since the typhoon.

I asked my brother, Sekiya to perform a makeshift damage survey with me while driving around the damage area mostly in the mountain. After my departure, Sekiya continued his own survey and damage photography (Figs. 5.4-4 and 5) through January 1992. Finally, he charted directions of the tree damage caused by both first and second winds (Fig. 5.4-6).

In some areas, trees were blown down or snapped in opposite directions (Fig. 5.4-5C) due to reversal of typhoon winds. It was learned that most cedar trees in the mountain were afforested after the war to meet the demand for lumber for reconstruction. Japan cultivated the fast-growing cedar trees which were blown down like match sticks due to their weak roots (Fig. 5.4-4, A and B).

Found also in the mountain are distinct upflow and downflow damages (Fig. 5.4-5,

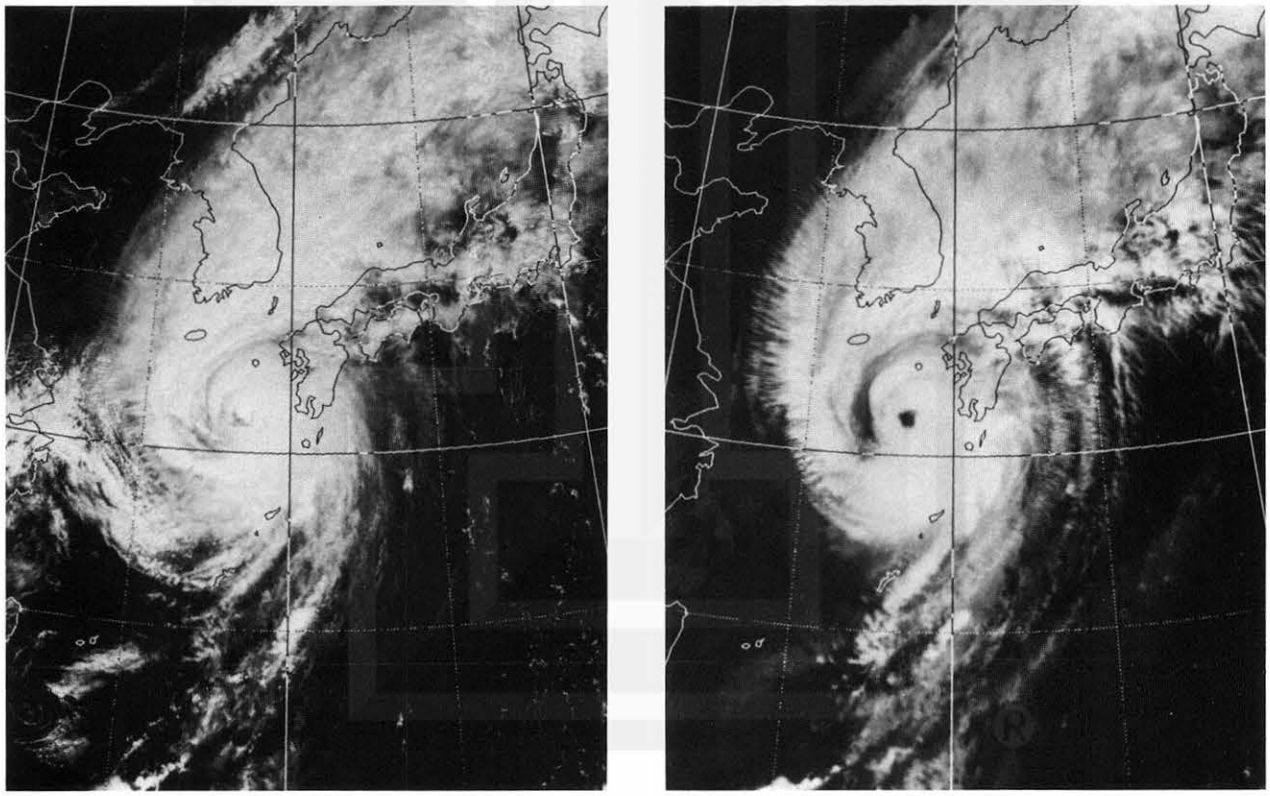

Fig. 5.4-3 Visible (left) and infrared (right) pictures of typhoon Mireille at 1131 JST (0231 GMT) on 27 September 1991. Courtesy of the Meteorological Satellite Center of Japan at Kiyose City.

A. Afforested cedar trees with weak roots and fast growth. Near Hita City.

B. Afforested cedar trees with weak roots blown down like match sticks. In Yabakei Canyon.

C. Slow-growing cedar trees snapped but left standing after the typhoon. Near Bungo Mori.

D. Afforested strong cedar trees with stripped branches off strong trunks. Near Bungo Mori.

Fig. 5.4-4 Two types of cedar trees cultivated in postwar Japan. The fast-growing type of trees are weak-rooted and blown down. The slow-growing trees with strong trunks were snapped after being stripped off branches and leaves. Photos by Sekiya Fujita.

A. Cedar trees blown up by strong upslope winds.

B. Cedar trees blown down by the downslope winds.

C. A forest affected by both first and second winds. Photo looking north.

D. A mountain slope in Yabakei eroded by a huge landslide.

Fig. 5.4-5 Four types of damage caused by typhoon Mireille on 27 September 1991. Photos by Sekiya Fujita, my brother living in the typhoon-affected area.

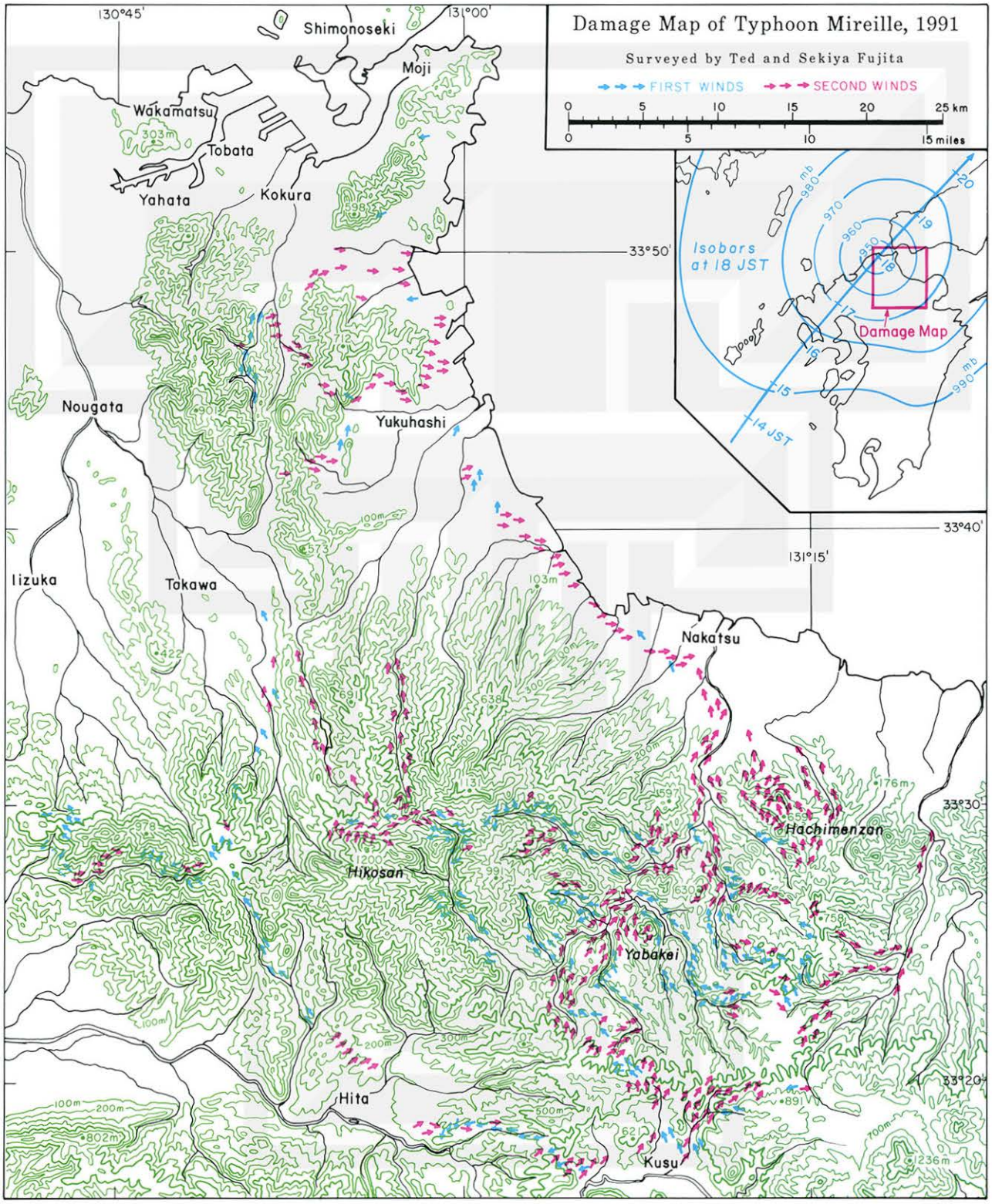

Fig. 5.4-6 Damage directions of trees caused by the first (red) winds and the second (blue) winds on 27 September 1991. The center of the typhoon moved northeast across the northwest corner of this damage map.

A and B). Apparently, these winds were induced locally by a combination of topography and natural up- and downdrafts.

Under my joint research with Mr. Yukio Takemura and other meteorologists of Japan Meteorological Agency, I made a preliminary mesoanalysis of typhoon Mireille at 1800 JST 27 September 1991 when the center was passing over the northern tip of Kyushu Island (Fig. 5.4-7).

It is amazing to learn that the entire area of Japan has been covered by automated meteorological stations which transmit hourly temperature, wind, precipitation and sunshine. These data are mapped automatically along with radar and satellite measurements.

Furthermore, recorded traces of pressure, wind direction and speed, temperature and dew-point temperature, and rainfall amount and rate are excellent. Without exception, all data are recorded on rectangular coordinates with identical length in time. Thus, traces can be placed on top of each other for evaluation and research.

For analyzing typhoon Della in 1949, I visited individual stations to copy recorded traces showing mesoscale disturbances, because no copying machine was available. Thereafter, I had to work with curved coordinates and different time lengths on charts for comparing various meteorological parameters. During the forty years since then, data recording systems in Japan were improved and perfected for better analysis and understanding of mesoscale disturbances.

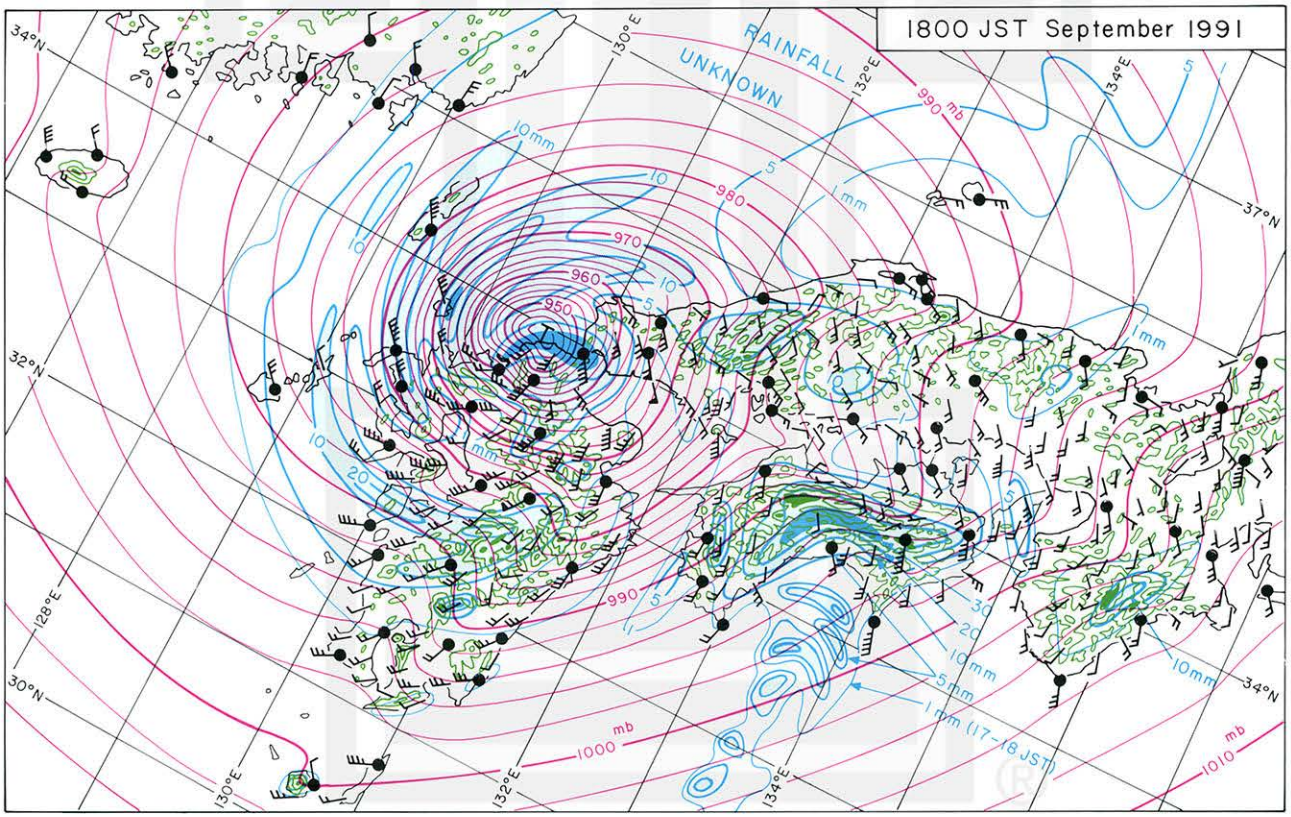

Fig. 5.4-7 Typhoon Mireille over western Japan at 1800 JST 27 September 1991. Shown in this map are: one hour rainfall (17-18 JST) in blue, isobars in red, and winds in knots presented in standard symbols. A band of heavy rain through the eye was caused by the movement of the typhoon during one hour, 17-18 JST. Basic data: Courtesy of Japan Meteorological Agency for joint research on the typhoon.

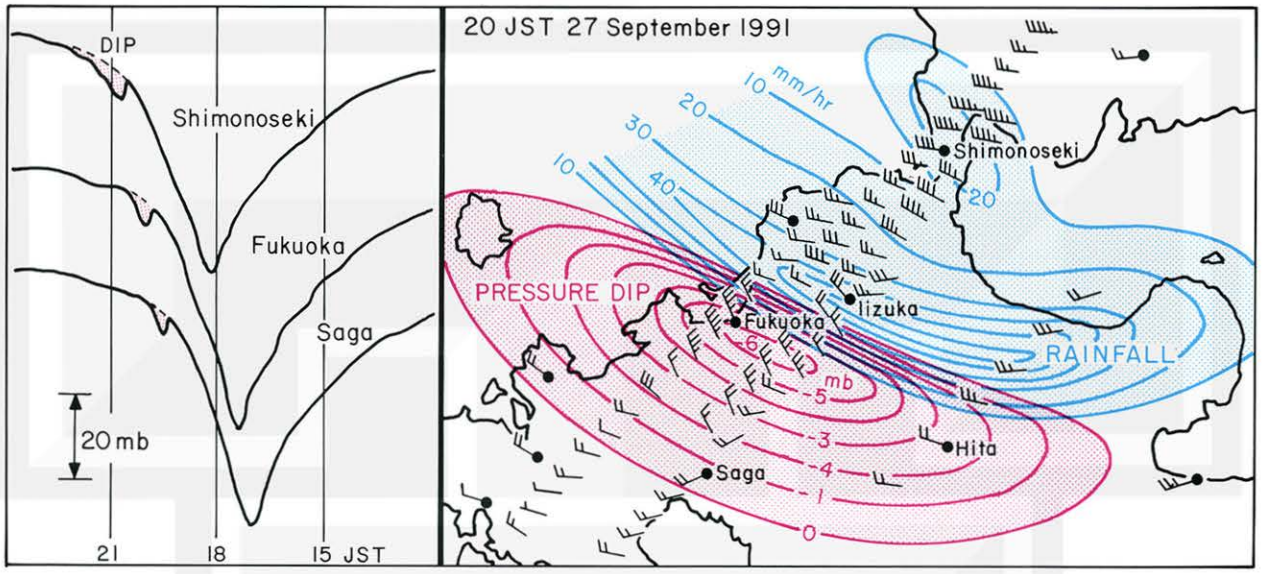

Fig. 5.4-8 Pressure dip which moved from southwest to northeast across this map. Isobars of the dip were drawn in red and rainfall intensity in blue. Similar to the pressure dip in Fig. 5.4-2, a significant diverging flow was located on the advancing (northeast) side of the dip.

Pressure Dip in Mireille

I was excited to find a pressure dip in Mireille which was similar to that in typhoon Della 44 years ago. This time, also, the dip was preceded by a band of heavy rain which moved from southwest to northeast when the typhoon was redeveloping into a subtropical cyclone.

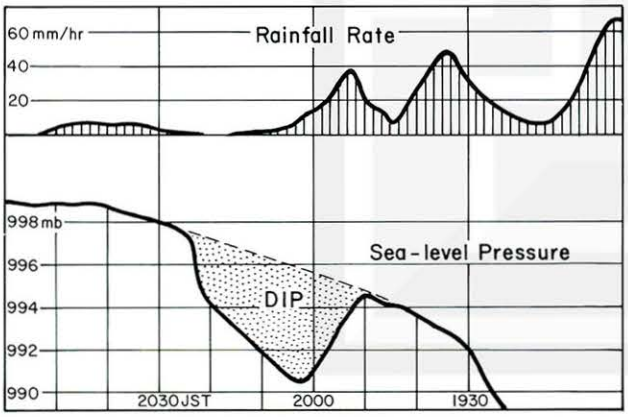

Fig. 5.4-9 Time section of the rainfall rate and pressure dip recorded at Fukuoka Weather Station between 1900 and 2100 JST 27 September 1991.

In analyzing U.S. hurricanes and Japanese typhoons, I noticed that there were two types of pressure dips: (a) cold-sector dip which forms in the wake of a rainband in the northwest sector, and (b) warm-sector dip which forms in any sector of storms free from cold-air inflow.

It should be noted that not all rainbands are accompanied by pressure dips. Naturally, more analyses with high quality mesoscale data are required in solving the structure of the dip.

5.5 Rapidly Intensifying Cyclones

For studying the climatological variation of northern hemisphere cyclones, 5539 cyclones in 7 years on NMC maps were characterized by the following seven (7) parameters:

P_o -- Central pressure
a -- Minimum radius of P_o+8 mb isobar
A -- Shape factor of the isobar
b -- Minimum radius of P_o+16 mb isobar
B -- Shape factor of the isobar
L_a - Latitude of cyclone center
L_o - Longitude of cyclone center

After completing the cyclone tape including these parameters at 00, 06, 12, and 18 GMT map times, cyclone paths were mapped in two colors: Paths of slowly intensifying (0.2-0.6 mb/hr) cyclones in blue color and those of rapidly intensifying (0.7 mb/hr or larger) cyclones in red. The 0.7 mb/hr threshold was used, instead of 1.0 mb/hr because the rates computed from 6-hourly maps are expected to be smaller than those from hourly maps.

	Year	JUN	JUL	AUG	SEP	OCT	NOV	DEC	JAN	FEB	MAR	APR	MAY
Number of CYCLONES by Month	1981	60	60	51	72	82	94	86	-	-	-	-	-
	1982	57	60	44	56	68	75	64	72	55	61	62	56
	1983	53	55	54	55	57	71	78	66	70	70	64	63
	1984	57	47	56	50	64	64	71	63	70	74	76	64
	1985	58	55	60	49	69	73	73	63	67	67	70	63
	1986	62	55	60	49	69	73	73	63	67	67	70	63
	1987	62	54	59	67	63	77	76	93	71	82	83	74
	1988	-	-	-	-	-	-	-	71	65	76	82	79
7 yr Total by Month		409	380	385	417	465	522	515	502	468	499	511	469
		JUN	JUL	AUG	SEP	OCT	NOV	DEC	JAN	FEB	MAR	APR	MAY
7 yr Total by Season		1174 SUMMER			1404 AUTUMN			1485 WINTER			1476 SPRING		

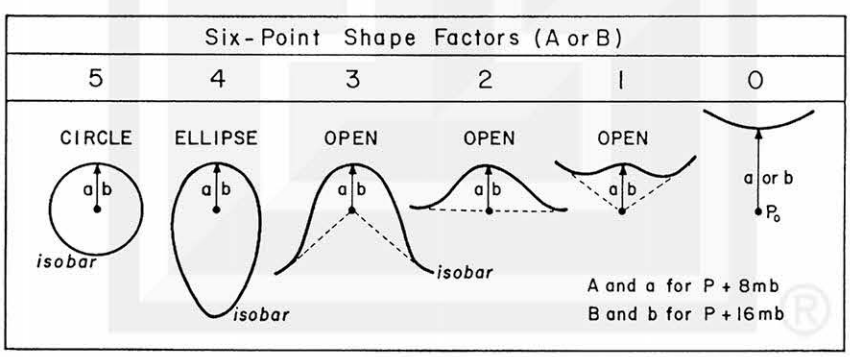

Fig. 5.5-1 Six-point (0 to 5) factors in describing the shape of the isobars with pressures, 8 mb and 16 mb higher than the central pressure. These factors are used in computing the maximum windspeed induced by cyclones.

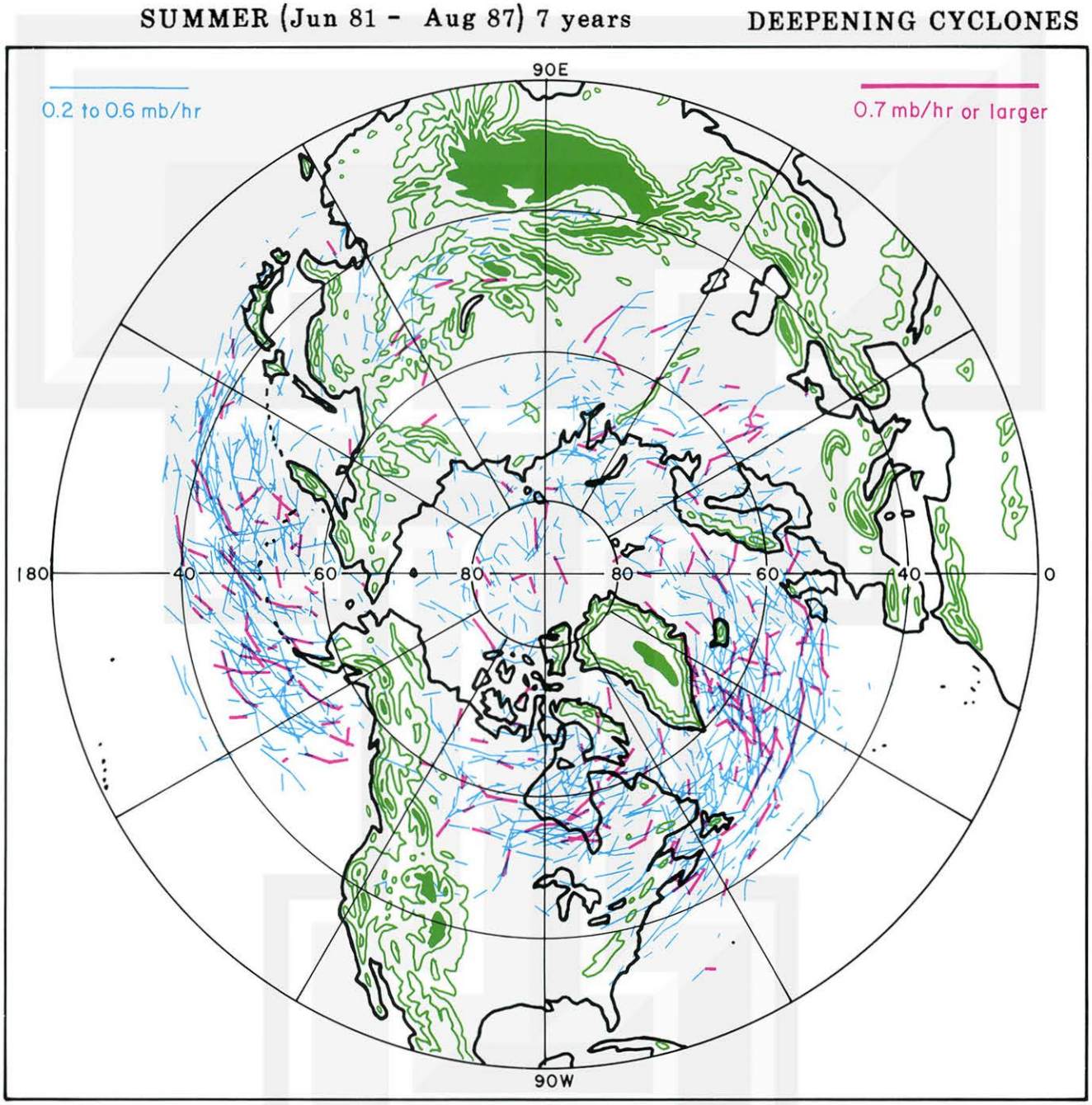

Fig. 5.5-2 Deepening cyclones in seven summer seasons between June 1981 and August 1987. Rapidly intensifying cyclones are seen over the Atlantic and Pacific Oceans north of 35° latitude. The Hudson Bay area and northern Russia are favorable locations of developing polar cyclones. Minor development takes place in the lee of the Mongolian mountains.

AUTUMN (Sep 81 - Nov 87) 7 years DEEPENING CYCLONES

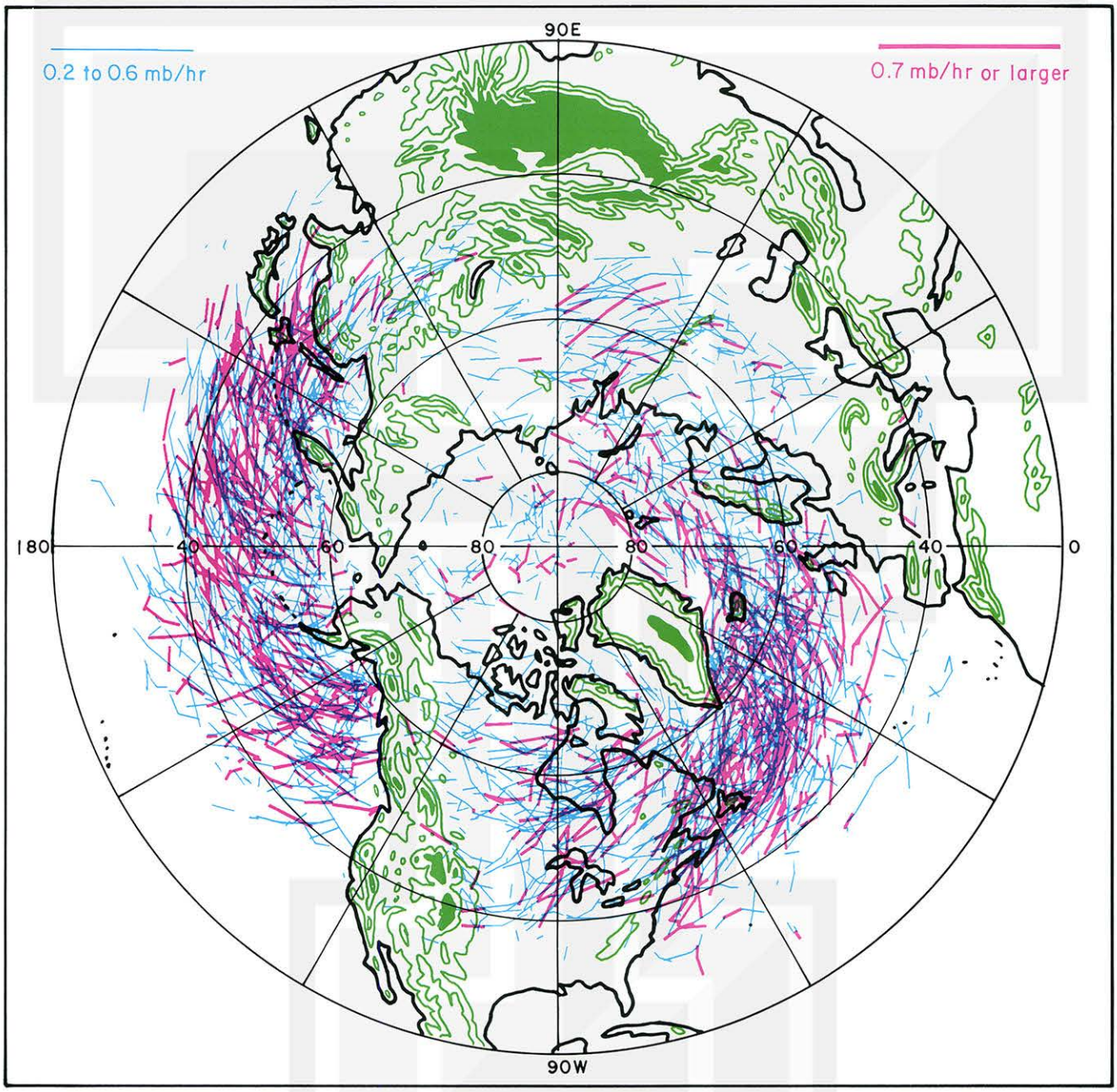

Fig. 5.5-3 Deepening cyclones in seven autumn seasons between September 1981 and November 1987. Cyclone development over both Atlantic and Pacific Oceans becomes more pronounced as the polar air begins to spread out from the arctic. However, the Siberian mountains extending from Lake Baikal to Bering Strait hold back the arctic air mass, preventing cyclone development on the arctic side of the mountains. A significant development takes place to the east of Greenland where the Atlantic and Arctic Oceans are connected, allowing the polar waves to develop rapidly into deep cyclones.

WINTER (Dec 81 - Feb 88) 7 years DEEPENING CYCLONES

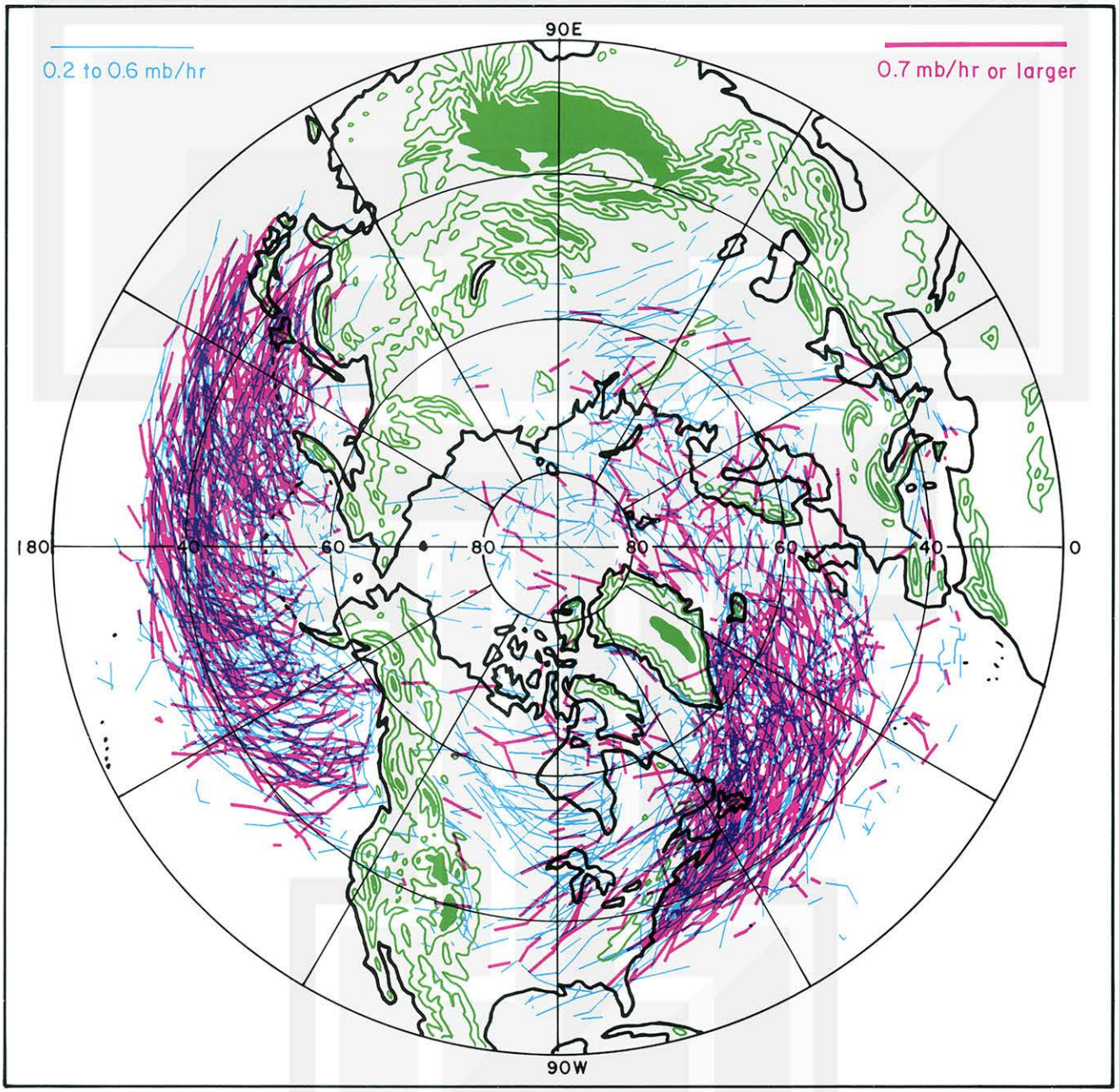

Fig. 5.5-4 Deepening cyclones in seven winter seasons between December 1981 and February 1988. The most significant area of cyclone development extends from off Cape Hatteras to Iceland, where a large temperature gradient exists on the northwest side of the Gulf Stream. This area corresponds to the ERICA area.

Two zones of intensification extend from the Sea of Japan and from the south of the main islands of Japan eastward toward the west-central Pacific. Cyclone intensification decreases gradually from the date line eastward. While no cyclone develops on the west side of the Rockies, some development occurs on the leeward side and move toward the southeast. On the other side of the Atlantic, minor development takes place on the lee side of the Iberian plateau and European Alps.

SPRING (Mar 82 - May 88) 7 years DEEPENING CYCLONES

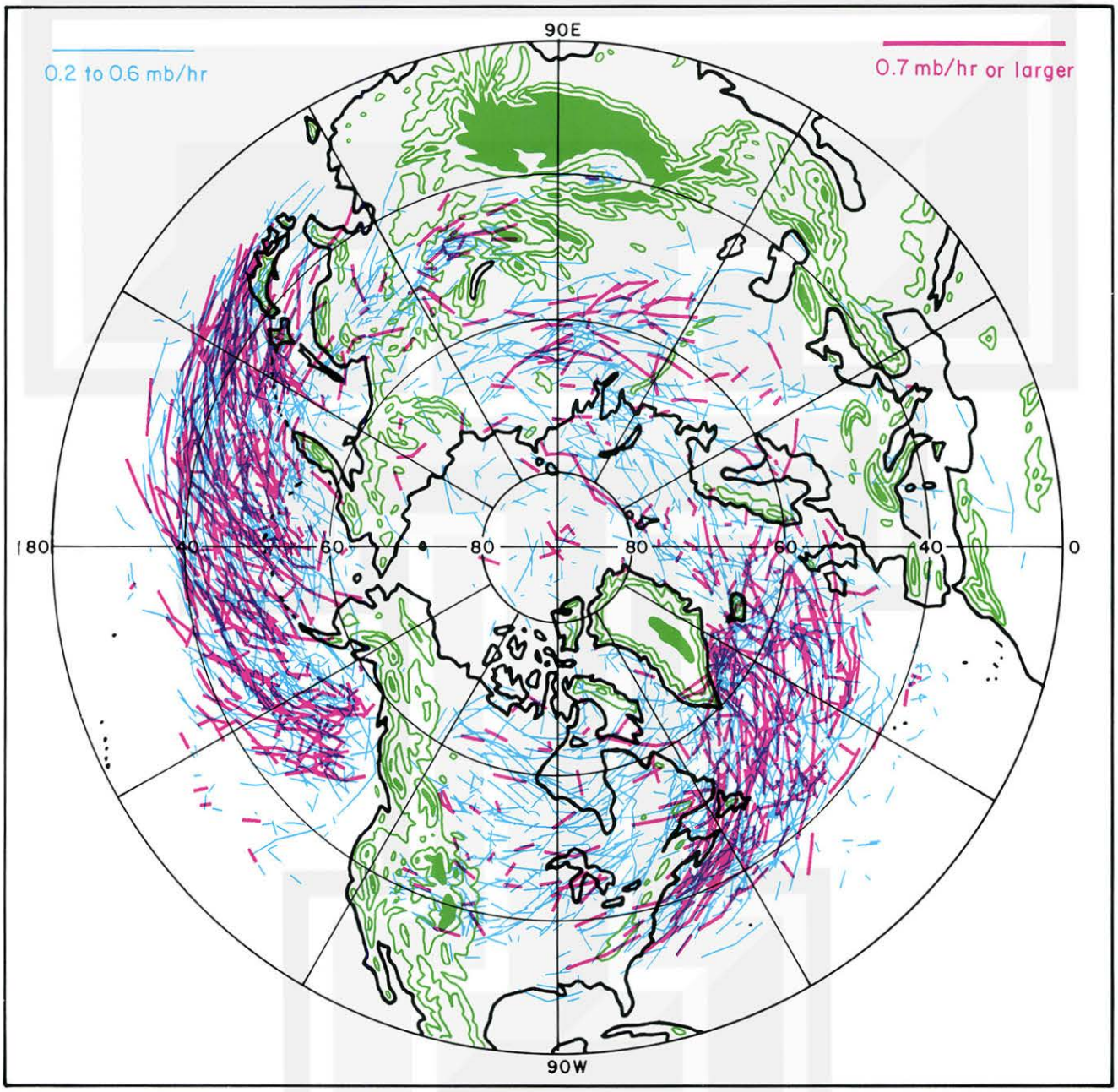

Fig. 5.5-5 Deepening cyclones in seven spring seasons between March 1982 and May 1988. Tornado-inducing cyclones form on the lee side of the Rockies and move toward the northeast. Meanwhile, cyclone intensification in the ERICA area subsides.

Periodic surge of the arctic front induces intensifying cyclones over the large area extending from the Ural mountains to Mongolia.

Significant deepening occurs on the Pacific side of the islands of Japan, resulting in the cyclone deepening over the entire Pacific Ocean.

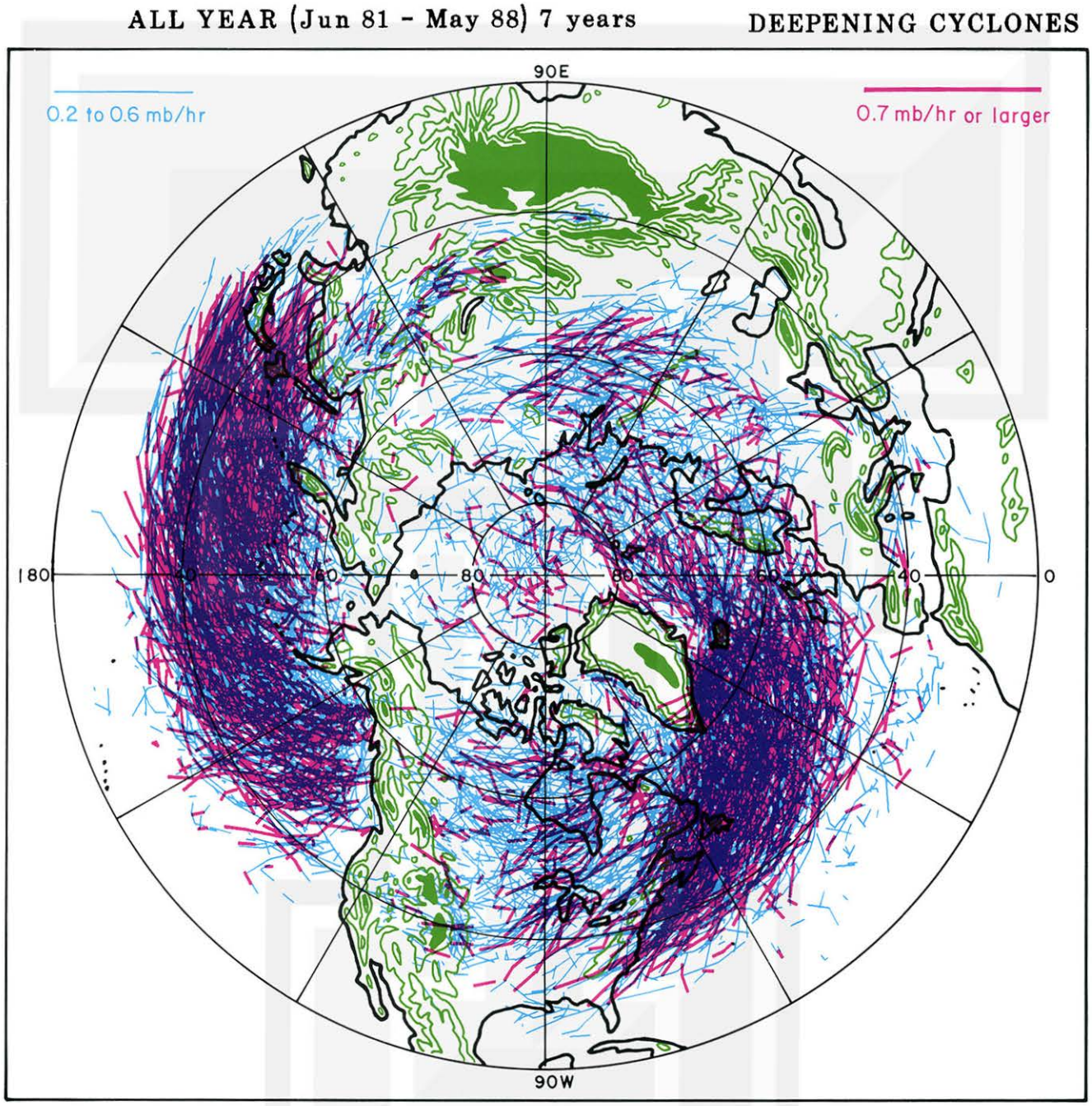

Fig. 5.5-6 Deepening cyclones in seven years or 84 months between June 1981 and May 1988. This climatological map including 5539 cyclones reveals two concentrations of deepening cyclones over the Atlantic and Pacific Oceans. Over the Atlantic, the deepening area fans out from the Carolina coast toward the northeast. Whereas, the deepening area over the Pacific Ocean extends from two areas, Korean peninsula and the Pacific just to the south of the islands of Japan. These two areas merge into a wide band extending eastward across the date line, ending abruptly along the west coast of the Gulf of Alaska.

Chapter Six

Personal History and Footsteps

6.1 Childhood and Schoolboy Years

On October 23, 1920, I was born in northern Kyushu, the southernmost island of Japan adorned with two active volcanoes, Aso volcano near the center of the island and Sakurajima volcano on Cherry Island in Kagoshima Bay far to the south. I visited these volcanoes during eruptions, observing the angry face of our living planet. Kyushu, as seen in a LANDSAT picture, is my wonder island where I spent my childhood, and schoolboy and adulthood years before coming to the United States in 1953.

My father Tomojiro, a grammar-school teacher gave me the first name, "Tetsuya."

Fig. 6.1-1 The Fujita Family on December 16, 1934. Back row from left: grandmother Hatsu (63), mother Yoshie (32), Tetsuya Ted (14); Front row: sister Sizuko (8), father Tomojiro (42), and brother Sekiya (6).

In Chinese character, "Tetsu" denotes philosophy and "ya," a suffix to a boy's name. My father, deceased on January 17, 1939, used to tell me that nothing in this world will remain unchanged. "Look up at the full moon in the sky," he said, "it will have to turn into the new moon."

Moon Over the Ruined Castle

荒 城 の 月

My mother Yoshie, deceased on July 24, 1941, taught me the song "Kohjo no Tsuki" (Moon over the Ruined Castle). I was deeply impressed by the song which reiterates my father's philosophy of ever-changing human life. On 9-13 September 1974, I participated in the US-Japan Seminar on Winds at Kyoto, organized by Prof. Hatsuo Ishizaki of Kyoto University and Prof. Arthur Chiu of the University of Hawaii. During the Japanese-style dinner party, a "geisha" sang the song "Kohjo no Tsuki,"

I. Haru kohro no hana no en
Meguru sakazuki kage sashite
Chiyo no matsugae wakeideshi
Mukashi no hikari ima izuko

While my mother's image was coming to my eyes, our U.S. participants, impressed by the delightful melody ending with a sad tone, requested me to translate the song into English. I hastily grabbed a paper napkin and wrote:

Fig. 6.1-2 A LANDSAT view of Kyushu Island, 330 km (205 mi) long and 235 km (145 mi) wide.

1. Flower parties in the Springtime of my life
   I exchanged SAKE CUPs with my honored guests
   Under eternal pine trees on my castle ground
   But now, where are my days of Glory?
2. Deep frosted encampment in Autumn
   Looking up at the lines of crying geese
   Once, the moon shined upon my lines of swords
   But now, where is my light of Glory?
3. Midnight moon over the ruined castle
   For whom has it been shining bright?
   Clung to the fence are withered vines
   Singing for the pine trees are stormy winds
4. While celestial bodies remain unchanged
   Rises and falls are the way of human life
   Attempting to portray ever changing world
   The moon still shines over the ruined castle

Fig. 6.1-3 A music hostess playing for me the song "Kohjo no Tsuki" (Moon over the Ruined Castle) with her string instrument "Koto."

Fig. 6.1-4 The landmark mountain, Nuki-san 712 m (2335') tall, 6 km to the south of my birthplace. This picture was taken in July 1953 prior to my departure to the University of Chicago as a visiting research associate.

The most beautiful melody of "Kohjo no Tsuki" was played by a music hostess at a restaurant in Kyoto in 1971 while my wife and I were enjoying a shabu-shabu dinner at the restaurant. She brought along a ready-to-request music book, asking me, "Which melody do you wish me to play for you?" I requested "Kohjo no Tsuki" and the young lady in kimono dress played her koto (Fig. 6.1-3).

My Good Old Days

I remember that my childhood life was by no means rationalistic, but I enjoyed the good old days. The population of my native village, Nakasone was about 1,000. I could buy things at local stores by charging to my father's account without using a check or a credit card which he never had anyway. All my father had to do was to pay up all debts before midnight of December 31 of each year.

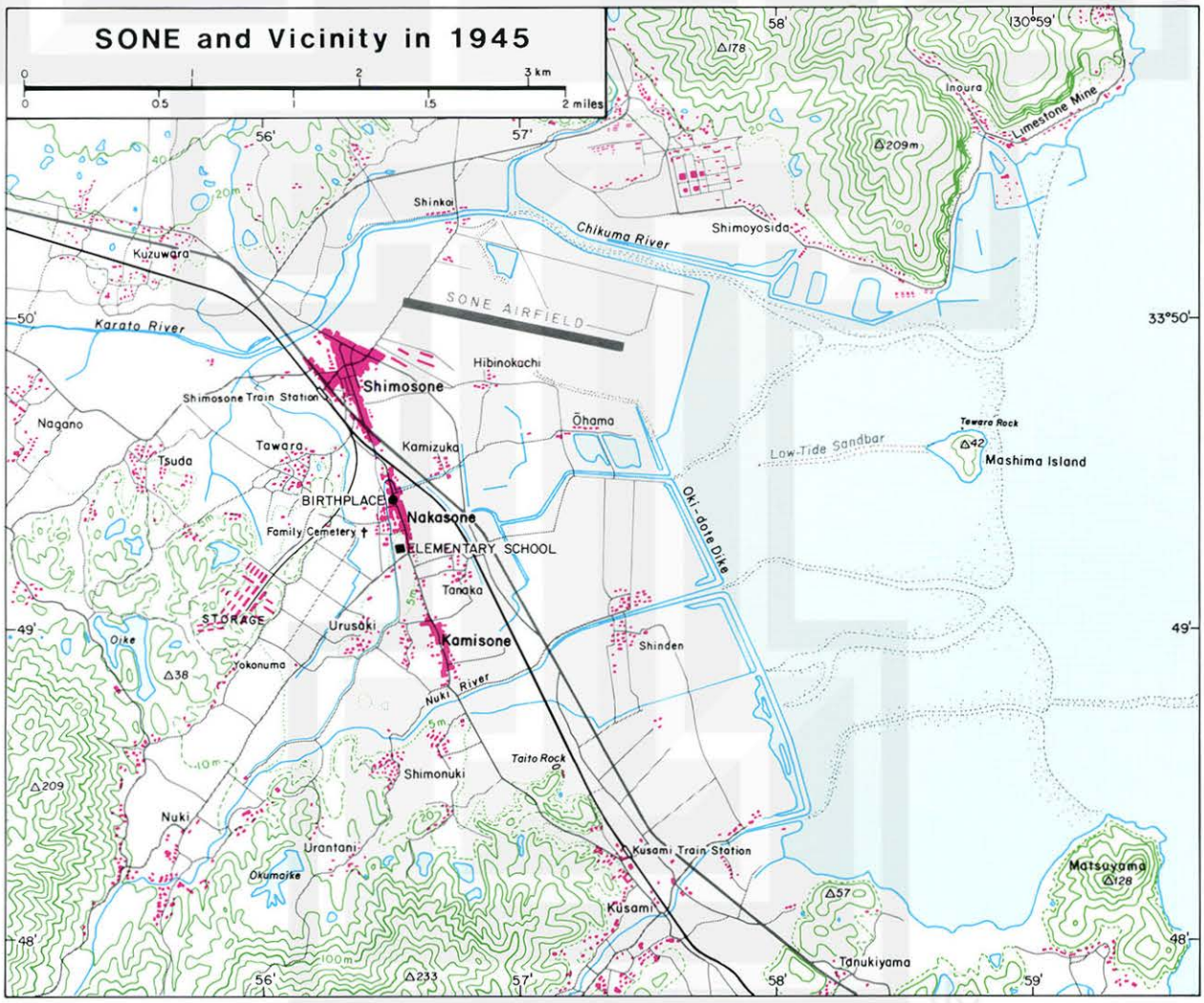

Fig. 6.1-5 My birthplace, Sone-machi (town) in 1945. The town and vicinity remained practically unchanged since 1920 when I was born. Major development took place during the postwar years after 1955. Sone-machi in 1945 consisted of three major villages, Simo (lower) sone, Naka (mid) sone, and Kami (upper) sone. A shallow inland sea to the east was decorated by a long and narrow sandbar exposed during the low tide.

No debt should be carried on beyond New Year's Day, a significant day to all of us. We used the calendar age which increased by one on New Year's Day. My parents never celebrated individual birthdays. Instead, every member of the family celebrated the first day of the year when everybody became one year older simultaneously.

In those good old days, we never locked the front door. Visitors, after entering the house, used to speak in a loud voice, "Mr. Fujita, I am here, where are you?"

Fig. 6.1-6 A distant view of Mashima Island from a helicopter flying 500 m above my birthplace house at Nakasone. This photo was taken in June 1989.

Fig. 6.1-7 A picture of a shako fish and a mate clam I used to catch with my father back in the 1930s. During the low-tide period they hide inside 10-inch deep holes in the muddy sea floor. Shako fish is very rare now due to water pollution. Mr. Masaomi Fujii, my relative caught this fish in 1990 and my brother took this picture for this book.

Fig. 6.1-8 A close-up view of Mashima Island. Seen on the right side of the island is the east end of the sandbar extending 1 km toward the coastline.

Fig. 6.1-9 A panoramic view of Mashima Island and the sandbar I walked with my father during my boyhood years. I took this picture in December 1974 during the low-tide period when the muddy sea floor spread out on both sides of the sandbar. Numerous shako fish and mate clams were found at that time, but not now.

Catching Shako Fish and Mate Clam

In my boyhood days, I walked 2 km across rice fields to the Oki-dote (dike) located along the shoreline of the Inland Sea to watch the tidal change of the sea surface. It was usual to experience a 3 to 5 m (10 to 15') drop of the sea surface, resulting in an exposure of the sea floor as far as 2 km away from the dike.

During the receding phase of the sea water, the moment after the sea floor in front of the dike had been exposed, I departed the dike toward the west end of the sandbar (Fig. 6.1-5). Upon reaching the sandbar, I rushed to Mashima Island before the sand temperature became as hot as 55°C (130°F) under the bright sunlight.

I had to return to the dike before the island would again become completely surrounded by the rising sea water which isolates the island for over six hours.

Naturally, the return trip was very tricky. My father predicted the departure time for me in order to be able to reach the dike in advance of the oncoming tidal water, which often closed in very fast. My father told me that he was once nearly drowned in the fast-rising water. At that time, I was interested in astronomy because the variation of the sea surface was closely related to the relative position of the sun and the moon.

On the muddy sea floor during the low tide, I used to catch pencil-shaped mate clams hiding inside a vertical hole in the sea floor. When the sea water returns, these clams come out of their holes looking for food. My father taught me his method of catching the clam, simply by dropping grains of salt into the clam hole. If the clam responds, it shoots straight up out of the hole under the assumption that the sea water has returned. A quick action, like that of a praying mantis, holds the key to a successful catch, because a clam will never come out again once it realizes that I cheated it.

Catching the shako (squill) fish (Fig. 6.1-7) was the other game my father had taught me. Inside the dry sea floor, the shako digs a U-shaped hole, approximately 15 mm in diameter, with its two openings on the muddy surface. For the fish, one is the entrance hole and the other, the escape hole. Apparently, the shako is by no means a smart fish, because it crawls out of its escape hole when I push a clump

Fig. 6.1-10 An aerial photo of the village of Hishakuda, my mother's birthplace. (1989 photo)

Fig. 6.1-11 A helicopter view of my brother's house at my birthplace in Nakasone. (1989 photo)

Fig. 6.1-12 A ground view of my brother's house with green roofs and white side walls. (1990 photo)

Fig. 6.1-13 Sone Primary School (distant) and Sone Middle School (near). (1989 photo)

Fig. 6.1-14 Kokura High School photographed looking south. (1989 photo)

Fig. 6.1-15 The steep cliff on the east bank of the Yabakei Rapid. (1978 photo)

of mud into its entrance hole. If I push mud into its escape hole, it comes out of the entrance hole. In either case the shako fish is the loser.

Another hobby I enjoyed in Autumn was to search for the matsu-take (pine mushrooms) which grow beneath red pines. Although other mushroom hunters kept their findings secret, I found myself a number of hidden spots where mushrooms grew every year. Due to the air pollution in recent years, mushrooms have become hard-to-find objects in Kyushu, costing 4,000 yen ($30) a pound in 1989.

According to my family roots, three generations of the Fujita family lived at the lot purchased by my grandparents Yasukichi and Hatsu. The old original house had been replaced by a new house which I designed and built in 1956. In June 1987, my brother constructed a modern block house on the inherited family lot. A helicopter photo taken in 1989 (Fig. 6.1-11) and a ground photo in 1990 (Fig. 6.1-12) show the house, which has flat green roofs and white side walls.

My father was an elementary school teacher who married my mother Yoshie while teaching at a school at Hishakuda, a small and quiet fishing village on an inlet of the Inland Sea (Fig. 6.1-10). My mother, born on January 11, 1902 was 32 years old when the family picture (Fig. 6.1-1) was taken.

When I entered the Sone Elementary School in April 1927, the school consisted of several wooden buildings. Due to the post-war educational reform, the school had been divided into the Primary and Middle Schools characterized by a number of 3-story concrete buildings (Fig. 6.1-13).

Blue Tunnel and Digging Machine

In April 1933, I entered Kokura Middle School and commuted by train from Sone to Kokura. In my student years, the school consisted of single-story wooden buildings. After the school was reorganized into Kokura High School under the Education Reform Act, new concrete structures and a swimming pool were constructed. As seen in the helicopter picture (Fig. 6.1-14) which I took on June 1, 1989, the school and vicinity were changed beyond recognition.

Back in 1937 when I was 16 years old, our middle school teachers took us on an educational trip to Yabakei Rapid (Fig. 6.1-15) where a buddhist monk Zenkai dug the "Aono Domon" (Blue Tunnel) through a cliff overlooking the rapid. A tour guide explained to all of us that the monk spent 30 years in digging the tunnel with a hammer and a chisel.

When I was asked of my admiration of the monk's accomplishment, my unexpected answer to my teachers was "No." I said, "If I were asked to dig a tunnel, I would first invent a digging machine during the first 15 years, so that the tunnel could be completed in only 15 years after the invention. After the 30 years of my total effort, I could leave behind a new digging machine and the Blue Tunnel." Unfortunately, I did not receive a passing grade after all, because I failed to appreciate the monk's spiritual accomplishment.

In 1978, forty years after my initial visit as a schoolboy, my brother drove me to the Yabakei Rapid to learn what had happened to the Blue Tunnel since then. The steep cliff remained unchanged, but the rapid had disappeared, having turned into a dammed-up lake with rental rowboats for vacationers. The Blue Tunnel had been replaced by a large straight tunnel of Highway 212. However, I could still see the broken segments of the tunnel preserved by the local historical society.

There was a Monk Zenkei Memorial on the other side of the cliff, where his hammer, chisel, work clothings, and other memorial items were displayed in showcases. Inside the memorial, I saw a number of schoolchildren, taking notes on their scratch pads. At that time, I wished I could ask them what they would like to do if they were at the site where the monk had been digging the tunnel while reciting a sutra continuously.

Interest in Topo Maps and Sunspots

In 1938, I became interested in the topographic mapping with contour lines. In particular, I wanted to map cliffs and overhangs which I observed in 1937 on my initial visit to the Yabakei Rapid. My geography teacher Ito introduced me to several books on topographic survey and mapping. Thereafter, I practiced several survey methods, using the equipment available at my school. Finally, I completed a map of Kokura Middle School with 50-cm (1.5') interval contour lines. I remember that my map covering the school ground and the environment was displayed in the school.

In Autumn 1938, I purchased a long-focus lens at Optician Matsuda in downtown Kokura City. The largest diameter lens I could obtain there was a spectacle for farsightedness with a 50 mm (2") diameter and 1200 mm focal length. Mounting the lens and a magnifying glass (eyepiece) inside a cardboard tube, I constructed a "one-dollar" telescope of magnification 50. The telescope was then used to make sketches of the sunspots for a period of three months on fine-weather days often experienced in Autumn in Japan.

My history teacher Miyake encouraged me to determine the rotation rate of the sun by tracking the sunspots I had sketched. It turned out that the sunspot motions at the equator was 25 days per rotation, but at high latitudes, the period increased to 27 to 29 days. I asked my teacher, "Why?" and he told me that the sun is not a solid fireball.

Slide Rule Without Logarithms

I learned algebra from teacher Hiyoshi and plane geometry from teacher Nishikubo. Prior to my graduation, I constructed a cardboard slide rule without knowing the existence of the logarithms. All I wanted to do at that time, at age 19, was to achieve multiplications simply by adding two lengths.

My slide rule consisted of two sliding parts separated by a straight center line. Both parts were scaled by numbers, 1, 10, 100, 1000, etc., which were spaced uniformly. I found immediately that multiplications, 1×10, 1×100, 10×1000, etc., can be achieved by adding the respective lengths on the upper and lower parts, but I could not generate the fractional scales, 1,2,3,4,5, . . . required to multiply, 2×30, 3×40, etc.

I worked day and night to determine the scale lengths of these fractional numbers to be placed on both upper and lower parts of my slide rule. I ignored my mathematics homework until a slide rule with fractional numbers had been finished to my satisfaction. I showed the finished slide rule to my teacher Hiyoshi, receiving his comment, "You spent over 10 days to generate the logarithms which you will be learning in less than 10 minutes in your regular class next month." He did not tell me if I wasted my time or not.

In March 1939, I graduated from Kokura Middle School, receiving the first RIKA-SHO (Science Award) during the graduation ceremony. This award was created in recognition of my scientific initiative. I regret that my father died on January 17, 1939, two months before I received the first honor in my life.

Shortly before the death of my father, I applied to and completed the entrance examinations for Hiroshima Kohto-Shihan Gakko (Hiroshima College of High School Teachers) and Meiji Semmon Gakko (Meiji College of Technology) at Tobata City.

The results of the examinations were not announced before my father passed away, but I clearly remember that his final words to me were, "Tetsuya, I want you to enter Meiji College even if you are admitted to the Hiroshima College for Teachers" ("Kohshi ni tohttemo Meisen ni yuke"). His inspired final instruction may have saved my life because, had I attended the Hiroshima College, I could have been in Hiroshima when the first atom bomb exploded over the city on August 6, 1945.

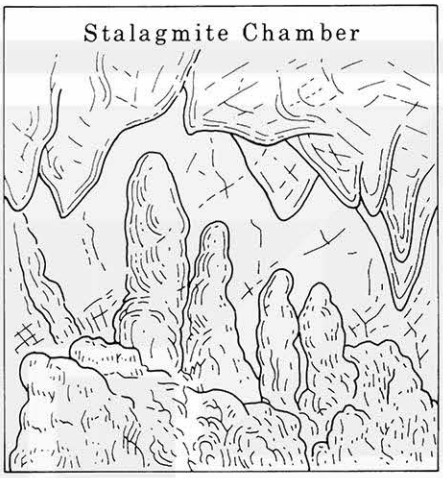

Fujito Cave Found by Two Spelunkers

On March 28, 1939, I walked with my teenage friend, Masayuki Toda, into a large sink hole on the far-side slope of Nuki-san (mountain). While we were climbing a steep limestone cliff covered with a primeval forest of mixed trees, a large opening on a limestone wall appeared in front of us. Although we did not carry a flashlight, we attempted to descend into the cave to confirm what turned out to be a new cave discovered by us, two young spelunkers. We named the cave the FUJITO Cave, combining our family names (FUJIta and TOda).

Three days later we returned to the cave with flashlights and survey chains. Upon entering the cave we were met by a flock of bats. To our surprise, the cave was 50 m (160') long and 20 m (60') tall at the center. There were curtain-shaped, thin rocks with an appearance of aurora borealis. Of the numerous stalagmites, the ones in the Stalagmite Chamber (Fig. 6.1-16) were very beautiful, most likely because they had remained untouched as we found no sign of a previous entry to the cave.

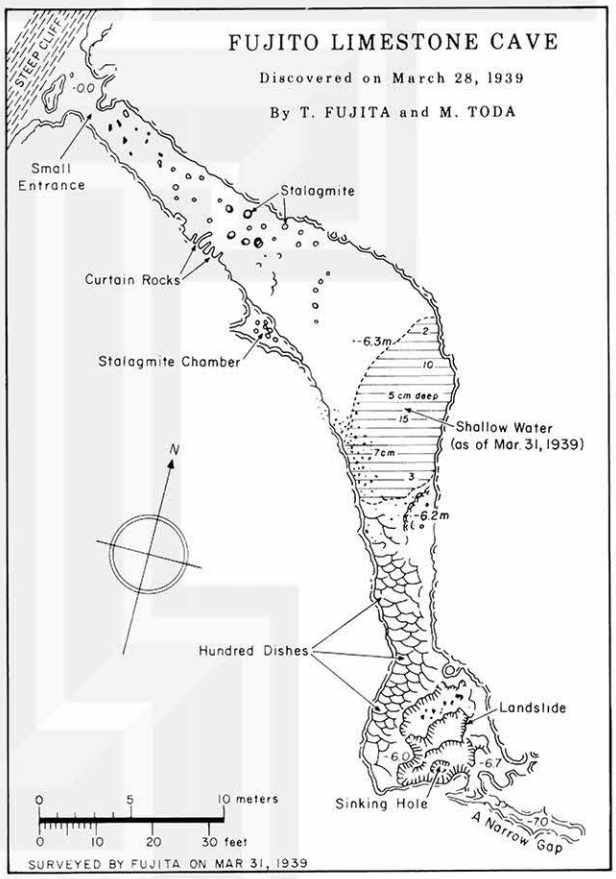

Fig. 6.1-16 The FUJITO Limestone Cave discovered by FUJIta and TOda. The cave has been confirmed by the City of Kitakyushu. Because the cave is located at a hard-to-reach location, it has not been damaged by curiousity seekers. Reproduced from: Tetsuya Fujita (1941) Geological Features of Kitakyushu. Science Magazine of Meiji College of Technology, Vol. 8, 79-88.

Fig. 6.1-17 The location of FUJITO Limestone Cave discovered in 1939 by two young spelunkers, Tetsuya FUJIta and Masayuki TOda. There was no service road in the picture when we walked around. Photo by Ted on June 1, 1989.

Fig. 6.1-18 A view of the cave area from the opposite direction, looking toward Nuki-san mountain. The cave is hidden behind the limestone hill in the foreground.

In June 1989, I was given an opportunity to fly around my hometown Kitakyushu in a Mainichi News helicopter. I really wanted to find the location of the FUJITO cave at the north edge of the Hirao-dai limestone plateau. When the helicopter approached the suspected area, I spotted the exact location of the cliff (Figs. 6.1-17 and 18). Although the cave could not be seen from the air, my 50-year-old memory of climbing the tree-covered cliff came back to my eyes.

Changes in my Birthplace

To the best of my knowledge as told by grandmother Hatsu, the birthplace lot with old structures was purchased in 1895 by my grandfather. The small lot on the west side of Prefectural street was 12 m by 36 m (40' by 120'). The street was not paved at that time but it was a major road connecting three Sone villages, Shimosone, Nakasone, and Kamisone (Fig. 6.1-5).

A plan view of the Fujita residence in 1945 was reconstructed with my brother (Fig. 6.1-19). Although the lot was small, there were four structures used for multiple purposes. Because my father loved flowers and trees, he planted both pink and white magnolias, a black pine, a persimmon, and an orange tree which yielded annually a large number of fruits for the family. He also planted fig trees and nandin bushes which bear red berries in winter. We also had a tall 100-year-old muku tree with a large trunk. We saw large mushrooms called "chairs of monkey" growing up on the tree which was cut down in 1950 due to old age and rotten trunk.

The prefectural street had been built along the ridge of a pre-historic sandbar extending over 2 km from Shimosone to Kamisone (Fig. 6.1-5). Due to sandy soil, the ground water on both sides of the street was clear and tasty. In the absence of running water, we used two wells, the one for the kitchen in the two-story house and the other for the family bath (Fig. 6.1-19).

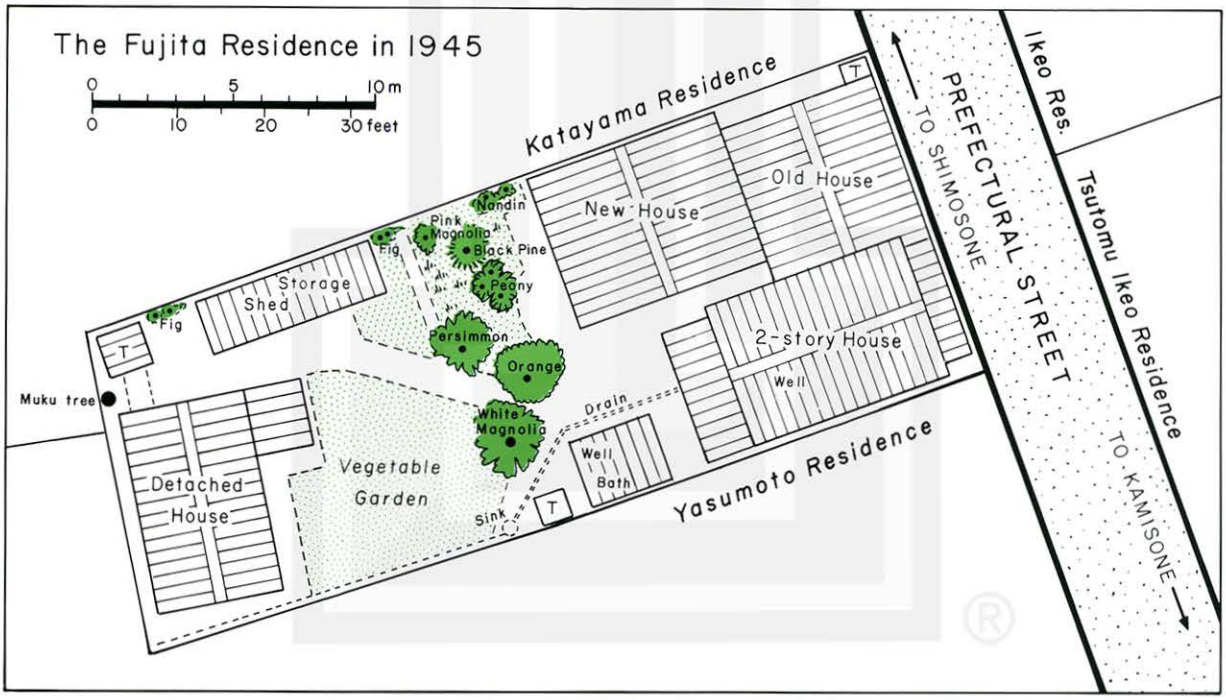

Fig. 6.1-19 The Fujita residence in 1945 located in the Ichiba Section of Nakasone. I walked on Prefectural street to Sone Elementary School and to the Sone train station, taking approximately 3 min and 10 min, respectively.

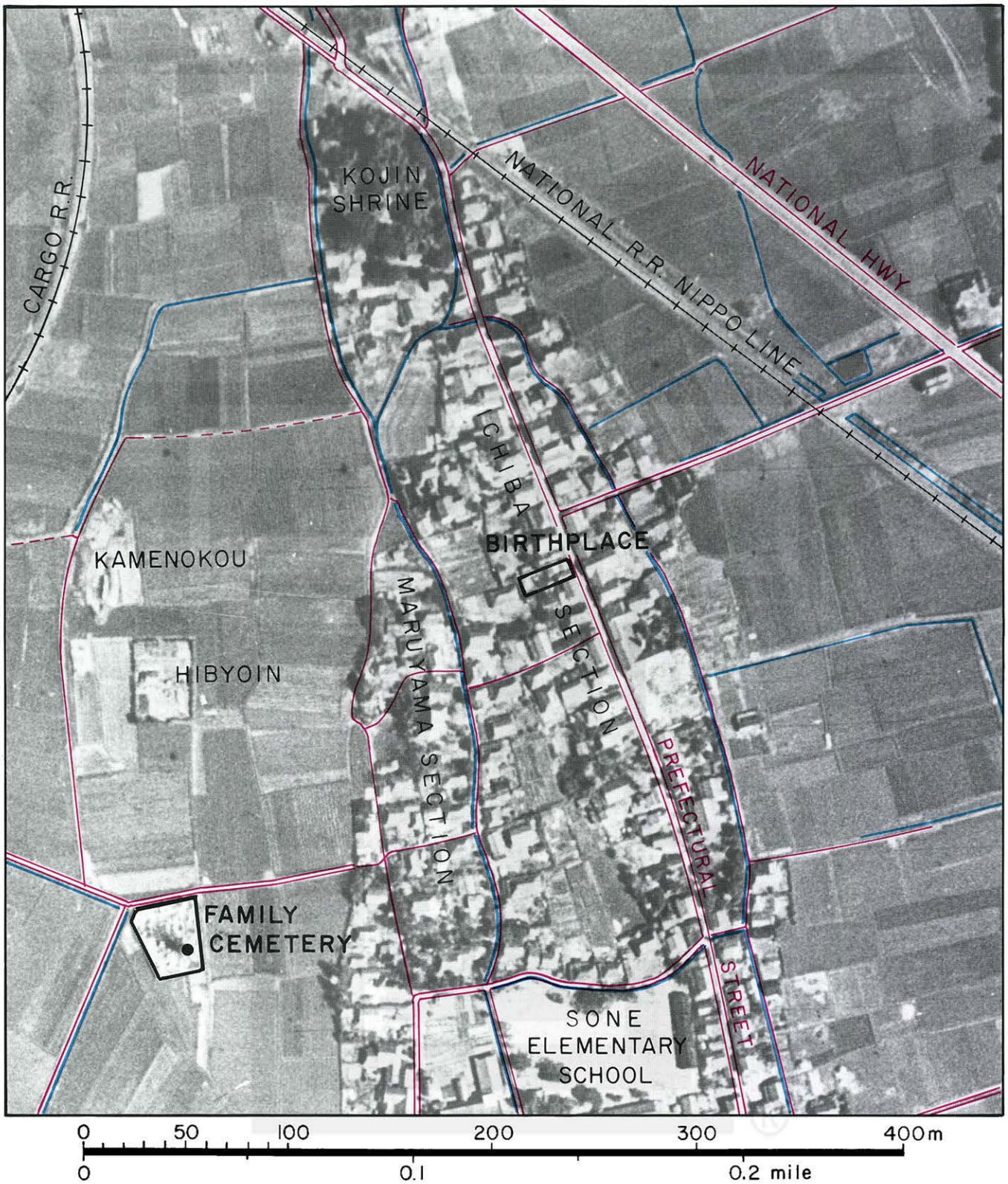

Fig. 6.1-20 Roads and brooks around my birthplace superimposed upon an aerial photo taken in 1948.

Fig. 6.1-21 The identical area as seen in an aerial photo taken in 1989 when I took detailed aerial photos from a Mainichi News helicopter.

Fig. 6.1-22 The overall Sone area in 1948 when I was a 28-year-old faculty member of the Kyushu Institute of Technology.

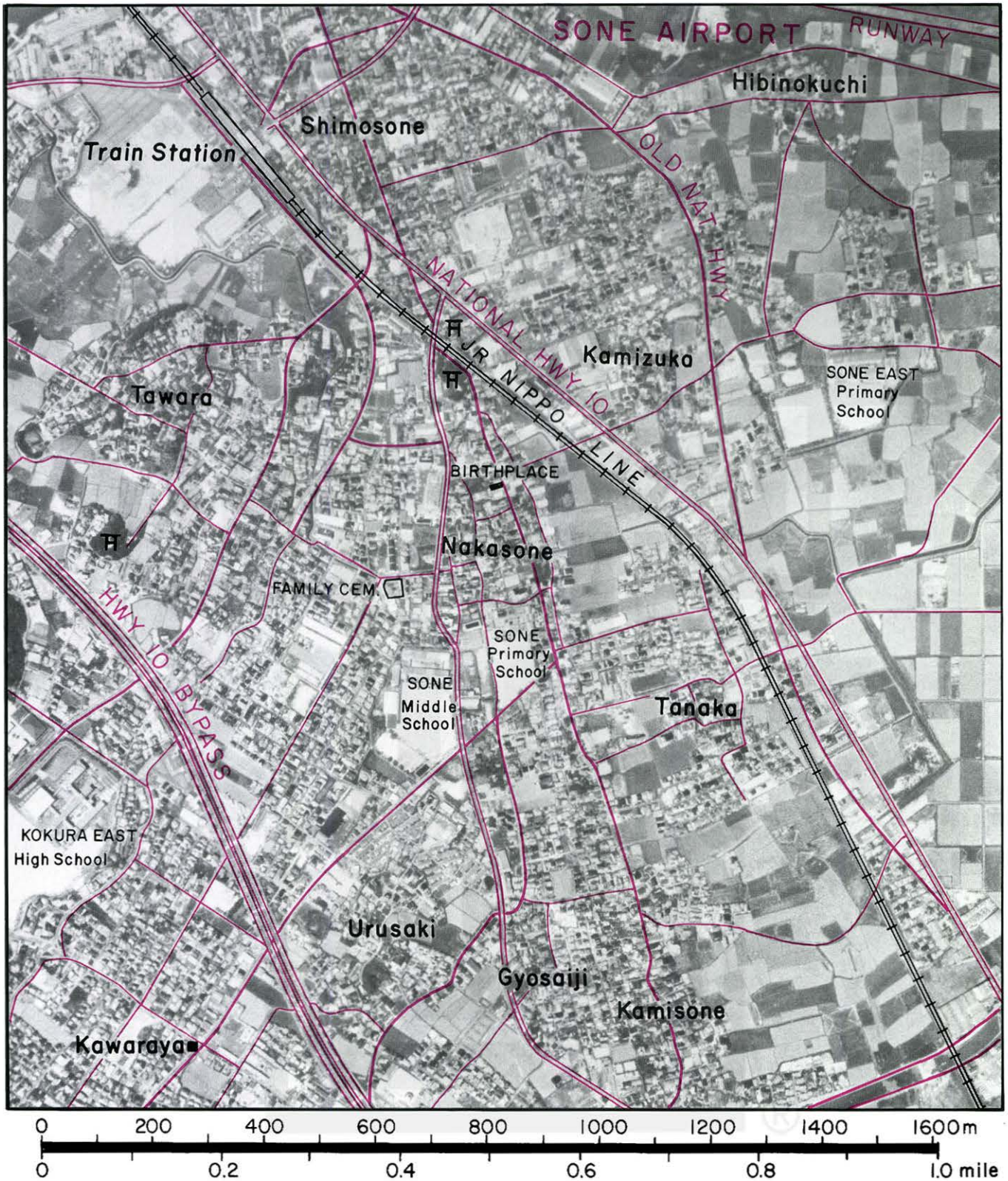

Fig. 6.1-23 Changes in my hometown in the left map depicted by an aerial photo in 1989 when I returned to Japan for an aerial survey.

Fig. 6.1-24 Kitakyushu in 1945, consisting of five separate cities, Moji, Kokura, Tobata, Wakamatsu, and Yahata. In May 1942, my birthplace Sone-machi was annexed to Kokura City, the largest of the five cities located along the northernmost coast of Kyushu Island.

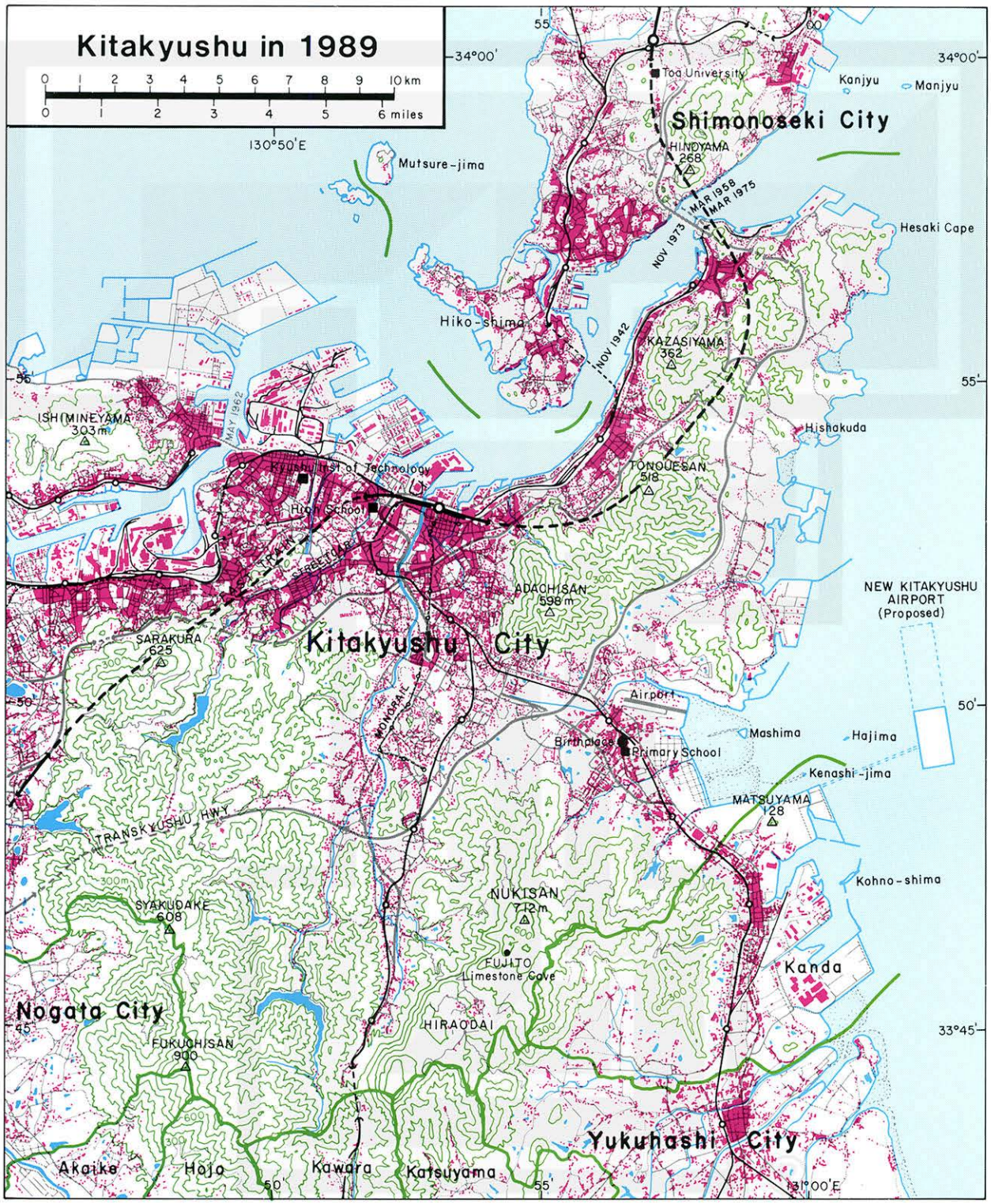

Fig. 6.1-25 Kitakyushu City in 1989, 44 years after the end of World War II. The city of one million population is connected to Honshu, the mainland of Japan, by one highway tunnel, two railroad tunnels, and one highway bridge similar to the Golden Gate Bridge in San Francisco.

The bath was not a bathtub but a large iron pot heated by a fire underneath. The bathpot was about 1 m (3 ft) in diameter, somewhat like an oversized pot for cooking rabbit stew. The pot was called Goemon-buro (Goemon bath). My father told me a story that a skilled burglar, Goemon, was boiled to death in a large pot. My job was to fill the pot by scooping the well water by a roped bucket. Firewood purchased at a local sawmill was used to heat the bathpot.

It is of interest to recall a strange custom that the bath was taken by men first, in the order of age followed by women. When we had an old-age guest, he was the first one to take the Goemon bath.

In my childhood years, Nakasone village was divided into two parts, Ichiba (Market) section and Maruyama (Round Mountain) section. Ichiba was located along Prefectural street where a dozen stores were selling daily necessities.

Unlike the United States, individual farm (rice) fields were too small to build residences inside. Most farming houses were located in a group within the commuting distance to their rice fields. Maruyama, on the west side of Nakasone, consisted of several dozens of farming houses. Although no mountain existed in Maruyama, there was a small sand dome called Kamenokou (Turtle Shell). In the early days, it could have been a large sand hill or mountain. Although I was not allowed to come close, there was a Hibyoin (Isolation Hospital) in the open field for keeping the patients with contagious diseases.

Spectacular Changes Since 1970

Since the 1970s, Nakasone expanded rapidly toward the west. Both Kamenokou and Hibyoin were gone, replaced by modern houses with colored roofs. My family cemetery was surrounded by residential houses, somewhat like an old cemetery in Boston. A large post office was built near Maruyama, and a wide north-south road, parallel to the Prefectural street was constructed, resulted in a significant reduction of automobile traffic in front of my birthplace (Fig. 6.1-21).

In my boyhood days, we could clearly identify three separate Sone villages, Shimosone, Nakasone, and Kamisone (Fig. 6.1-22). My family cemetery, surrounded by rice fields (Fig. 6.1-4), was an excellent location to view the rice fields extending to the foot of Nuki-san mountain. We could see Kawaraya (roof-tile factory) 900 m south-southwest.

The 1989 map (Fig. 6.1-23) shows an extensive housing development which virtually eliminated the rice fields. Kawaraya, being surrounded by new houses, could no longer produce roof tiles. Nakasone became an integral part of the greater Sone housing development. An attempt was made to place the names of the original villages in the 1948 map on the 1989 map so that we can identify the growth of each village.

The single-track Nippo Line, a steam locomotive railroad, was modernized into the double-track electric railroad. The heavy traffic on National Highway 10 was rescued by the construction of Highway 10 Bypass. Three new schools were built in and around Nakasone to accomodate explosive growth in the Sone area for years to come.

Kitakyushu in 1945 and 1989

Kitakyushu is located at the northern tip of Kyushu Island. A narrow channel called Kanmon Kaikyo (Straits) separates Kyushu from Honshu, the main island of Japan. In 1945, there was one undersea train tunnel (finished in 1942) and an undersea highway tunnel under construction since 1937. Moji and Shimonoseki cities were connected by ferry (Fig. 6.1-24).

Both highway and railroad systems in Kitakyushu were improved significantly.

The highway under construction was finished in 1958, taking 21 years due to the war. In November 1973, Trans-Kyushu and Trans-Honshu superhighways were joined by a 6-lane suspension bridge over the straits. Then the fast (bullet) train from Tokyo was extended to Kyushu through a modern undersea tunnel completed in March 1975. Because the runway of the existing Sone Airport is short, a New Kitakyushu Airport on the landfill of the Inland Sea has been proposed (Fig. 6.1-25).

As seen in the 1989 map, coast lines of Kitakyushu changed markedly due to the continuous growth of the landfills on the west side of Kanmon Straits and along the coast of the Inland Sea.

I am pleased to see the growth of my homeland. Meanwhile, I hope that an excessive growth does not damage the traditional environment which I enjoyed during my childhood days.

6.2 Kyushu Institute of Technology

Shortly after my father passed away, I received admission letters from both Hiroshima College of High School Teachers in Hiroshima City and Meiji College of Technology in Tobata City. In accordance with my father's desire, I entered Meiji College of Technology in April 1939. The school was founded in 1909 in Tobata as a four-year private college. As shown in the map surveyed in 1900, Tobata was thinly populated some 90 years ago (Fig. 6.2-1). In 1921, the private college was transferred to the Japanese Government. Under the Education Reform Act after the end of the Second World War, the college was reorganized into Kyushu Institute of Technology in May 1949. After graduating from the Meiji College of Technology, I was appointed as an assistant professor of the school in 1943 and of Kyushu Institute of Technology in 1949.

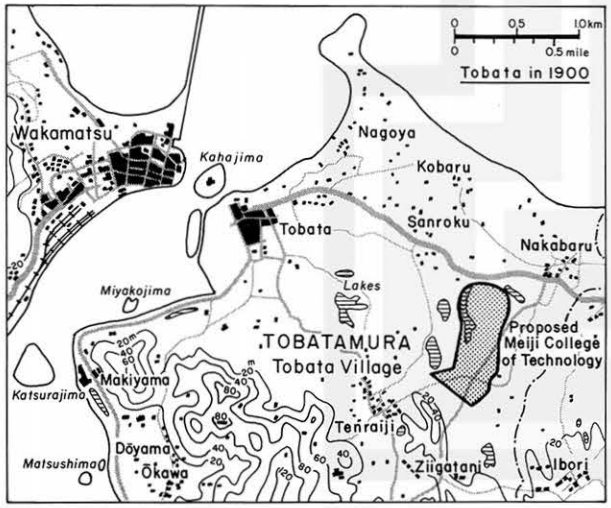

Fig. 6.2-1 The location of Meiji College of Technology placed on a map surveyed 9 years before the school was founded.

Meiji College of Technology

Student Years: 1939-43

Fig. 6.2-2 Tetsuya Fujita (age 19) a first year student in cap and uniform of Meiji College of Technology.

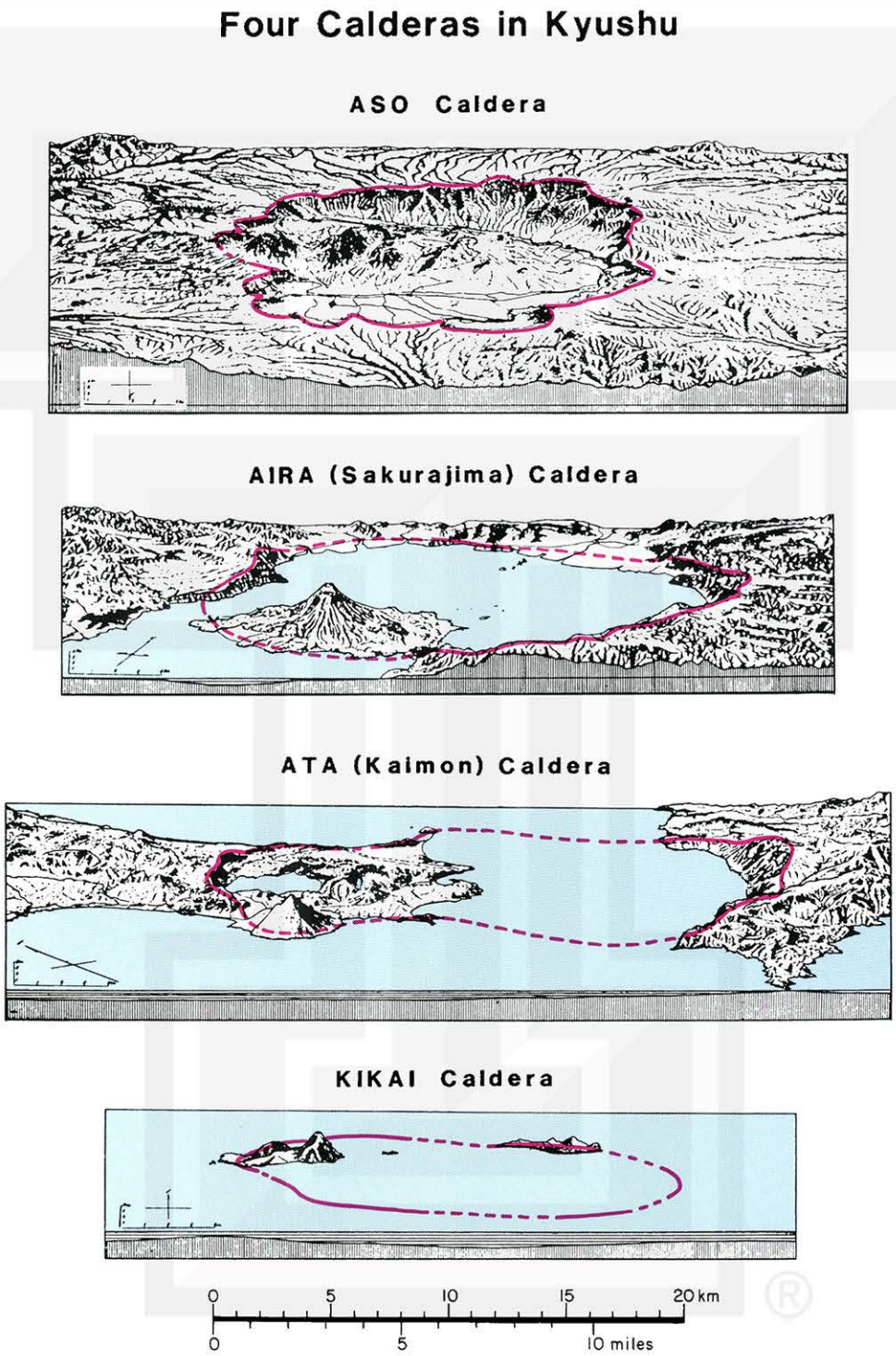

Fig. 6.2-3 Bird's-eye views of the four Calderas which I computed and drafted in 1940 for Professor Matsumoto's ScD thesis. Water areas in light blue and caldera boundaries in red were added for this book.

Because my father died in 1939, three months before I entered Meiji College of Technology, I obtained a no-interest student loan from the Buzen Ikueikai (Scholarship) Funds established by the Buzen Daimyo (Feudal Lord) who had ruled the region of my birthplace. I also worked as a part-time assistant of Professor Tadaichi Matsumoto in the Geology Department. Although my declared major was mechanical engineering, I was deeply impressed by his philosophy, approach, and effort in studying four calderas, ASO, AIRA (Sakurajima), ATA (Kaimon), and KIKAI, all located in my wonder island of Kyushu.

My task assigned by Prof. Matsumoto in 1940 was to generate bird's-eye views of the four calderas based on the given topographic maps of 1:50,000 scale. After he gave me the viewing angle, he never taught me how to convert topographic maps into 3-D views. He simply furnished me with reference books in English and German. Reading these books with the help of dictionaries was very useful in learning my first and second languages, English and German, respectively.

After working on his project for several months, my eyes began seeing contour maps as if they were three dimensional mountains. It was an excellent training in learning how to visualize 3-D topo maps. I was twenty years old (Fig. 6.2-2) when I completed the bird's-eye views of four calderas which were included in his thesis for receiving the ScD degree from the University of Tokyo in 1943.

Since completing the bird's-eye views (Fig. 6.2-3) he took me along to a number of geological field trips. At one time he suggested that I change my major from mechanical engineering to geology, but I could not do so because my mother was seriously ill and I could not stay away from home for extended geological field trips.

My academic sponsor on mechanical engineering was Professor Hajime Nakagawa. He taught the course on "tensile strength" dealing with the theory of stress and strain, including plastic flows of materials. For receiving the "Meisen Kohgakushi" (BS-equvalent degree certified by the school), we had to complete (1) a thesis on a mechanical engineering topic, and (2) participation in an operational practice.

Fig. 6.2-4 Professor (2nd from right) and Mrs. Nakagawa in Winter 1956 sitting around a space heater "Hibachi" in the living room of the official residence inside the college. In my student days, all professors were housed in the campus so that students were able to visit their professors for evening get-togethers.

Fig. 6.2-5 Moji Railroad Station where I departed for Beppu in 1943 for an operational practice of a steam locomotive. (1989 photo)

Fig. 6.2-6 Professor (2nd from right) and Mrs. Matsumoto (center) in July 1971 standing in front of the main office of Kumamoto University.

Fig. 6.2-7 A welcoming get-together at the Tokyo Alumni Club of Meiji College of Technology on May 23, 1988 when I had an emotional meeting with Professor Otsuka, my physics teacher in 1940-41.

Fig. 6.2-8 Scenes of my speech (left) and singing the college song during a cheerful get-together on May 16, 1988 with my former colleagues and students following the dinner at the Meiji College Club.

My thesis dealt with the measurement of impact forces. Under Professor Nakagawa, I worked on the time-dependent force of impact induced by free-falling steel balls. By changing the size and height of the balls, time-dependent impact forces were measured by piezoelectricity which was amplified and recorded by a high-speed optical oscillograph in the Physics Department. My thesis, Über den Stoβ, written in German and English combined was completed for my graduation.

To fulfill the second requirement, I spent one week at a train depot of the National Railroad at Moji City where I learned how to operate steam locomotives. My instructor, Mr. Houshiyama gave me a chance to work as an assistant to the locomotive engineers on a roundtrip passenger train between Moji and Beppu, a 252 km (157 mi) roundtrip distance. Our steam locomotive pulling eight passenger cars departed from Moji station (Fig. 6.2-5). Shortly thereafter, two engineers gave me a chance to practice shoveling coal into the furnace while on level tracks where the steam pressure does not have to be very high. I was thrilled by continuously shoveling water-sprinkled coal into the furnace while standing on the open-ended, small floor of the fast-moving locomotive. It was certainly an unforgettable experience in my life.

Some thirty years later in July 1971, Prof. Matsumoto invited me to give a seminar at Kumamoto University when he was the President of the school. I accepted his invitation and gave a presentation before his faculty and students. A picture of the smiling group in Fig. 6.2-6 was taken after the presentation. Persons in the picture from left to right are: my brother Sekiya, his wife Yaeko, Susie, Mrs. Ranko Matsumoto, Ted, President Matsumoto, and his staff. All of us went to a local restaurant for a get-together dinner. It was an emotional moment when Mrs. Matsumoto was in tears of joy while looking at me sitting next to her husband, my mentor professor.

In 1940-41, I took physics courses taught by Professor Haruo Otsuka who used either English or Romanized Japanese in his lecture notes. He never used Chinese characters. He taught us how to look at the world of physics with the help of his unique silhouette figures, rather than conventional visual aids. After his class, I used to imagine the invisible phenomena which are hidden behind the silhouette images. Unfortunately, he left our school to accept a special professorship at the University of Seoul in Korea, a part of Japan at that time.

At the Alumni Club of the Meiji College of Technology, I had an unexpected meeting with Prof. Otsuka in May 1988 in Tokyo. His first word to me was, "Fujita-kun (dear), you have turned exactly into the person I wanted you to be." Fig. 6.2-7 shows a group picture and my picture with Prof. Otsuka.

During my final two years, I was a part-time assistant to Prof. Hironobu Shibahashi of the Physics Department. My assignment was to prepare his physics laboratory of 30 experiments consisting of thermocouple, adiabatic expansion, Wheatston's bridge, oscillograph, etc.

During my homecoming to Kitakyushu City in May 1988, I gave a talk on my research in the United States. Thereafter, a welcoming party was given at Meisen Kaikan (Meiji College Club) where former students and colleagues talked about our student years. Everybody was happy and emotional, being given the opportunity to recall our memories (Fig. 6.2-8).

Faculty Years: 1943-53

Due to the successive retreats of the Japanese military force from the Pacific Front early in 1943, the Department of Education shortened the school year of colleges by six months. Meanwhile, the military draft age was lowered to nineteen and students were no longer exempt from the military service. Under these new rules, I graduated from Meiji College of Technology on September 26, 1943, six months in advance of the scheduled graduation in March 1944.

On September 27, the day after graduation, I was appointed an assistant in the Physics Department with a full-time salary of 75 yen per month. At the exchange rate of 4.25 yen to a dollar in 1943, the starting salary was $17.64 per month. Less than a month thereafter, I was promoted to assistant professor with an assignment to teach elementary physics and physics lab. My teaching load of 15 hours a week at that time was rather heavy, turning me into a full-time college teacher.

Three-Dimensional Triangulation

In July 1944, U.S. Marines landed on Saipan, Guam, and Tinian islands in succession, signaling the onset of air raids from the Mariana air bases. At that time I received a small Navy contract to generate nomograms to be used in determining aircraft positions by three-dimensional triangulations. Both azimuth and elevation angles of multiple searchlight beams were the main input parameters. Foreseeing applications to the radio-locator (present radar) being developed in Japan at that time, I was told to include the curvature of the earth and the bending of the beams under various weather conditions in the calculations.

The tasks of this basic research gave me an opportunity to study equations and applications of spherical trigonometry, along with the vertical gradient of the index of refraction. At this time I became very interested in the meteorological aspect of the global atmosphere.

In spite of my heavy teaching schedule, I happened to be in Tokyo in March 1945 when several waves of B-29s firebombed the city, burning down 230,000 houses overnight. I was at the house of my middle-school classmate, Dr. Hideo Minato (currently professor emeritus of Tokyo University) at Denen Chofu in west central Tokyo. Upon hearing a series of air-raid alarms we went out of the house and witnessed smoke-filled reddish skies to the southeast. Then we heard a bang from a close distance, after which we noticed that distant houses were on fire. Early next morning we walked around the neighborhood and found unexploded cyclinders of incendiary bombs stuck deep into the gravel road near his house.

Several days later, while on the train from Tokyo back to Kyushu, I began to think about a mechanical/electrical analog computer operated by converting mechanical quantities into electric signals defined by corresponding equations,

$$F = ma \text{ (force = mass x acceleration)}$$

$$E = ir \text{ (voltage = current x resistance).}$$

While I was working on the practical solution of the analog system, I was assigned to visit coal mines where my students had been sent to work for increasing the output of domestic coal.

At the coal mines, I was unexpectedly able to carry out a meteorological experiment on hydrostatic pressure. I brought along a barometer and a thermometer to measure both temperature and air pressure while descending mine shafts with known elevations at a number of check points. Subsequent analysis on adiabatic charts revealed that pressure inside coal mines is far from hydrostatic. This is due to the forced air circulation induced by powerful electric fans. Several pressure/temperature diagrams drawn from the data obtained inside the mine shafts gave me a golden opportunity to understand the non-hydrostatic pressure gradients in both horizontal and vertical directions. As a result of the coal mine experiment, along with my research on searchlight triangulation for determining aircraft locations, I decided to pursue meteorological research that can be achieved with inexpensive instruments. Several years later, I applied the concept of non-hydrostatic pressure in speculating on a downward current in a thunderstorm atop Seburi-yama (mountain).

Nagasaki and Hiroshima Atom Bombs

The Second World War ended on August 15, 1945, six days after the explosion of the second atom bomb over Nagasaki. We were informed later that the initial target of the second bomb was the Kokura Arsenal, 4.3 km (2.7 mi) east-southeast of our college. I clearly remember hearing a series of air-raid sirens on the day of the bombing, but the aircraft was not visible due to a thick layer of stratus clouds. Evidently the bomber flew away to Nagasaki while we were hiding in a bomb shelter next to the physics building.

In September 1945, several weeks after the Nagasaki bombing, President Heihachi Kamura of our college sent a group of

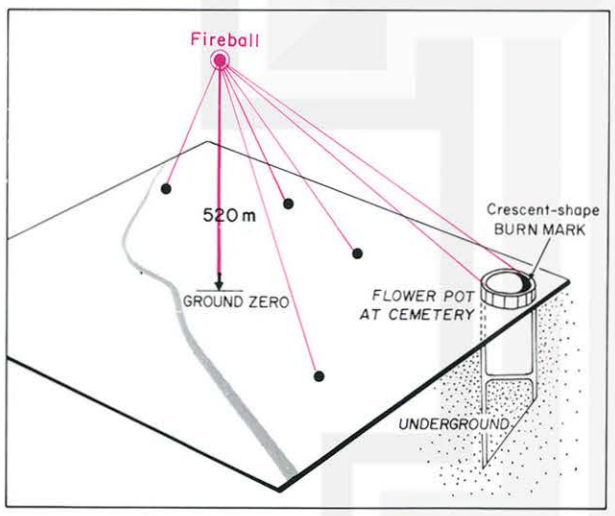

Fig. 6.2-9 Position of the Nagasaki Fireball obtained by measuring the direction of radiation from the crescent-shaped burn marks on bamboo flower pots in cemeteries. A number of burned bodies were still lying on the hillside.

our faculty and volunteer students on a ground-truth mission to Nagasaki and then to Hiroshima where the first atom bomb exploded on August 6. I visited both Nagasaki and Hiroshima, noticing that the train fares to these two cities were identical. In fact, the railroad distances to Nagasaki and Hiroshima from Tobata, the city of our college, are 216.0 km (134.2 mi) and 219.7 km (136.5 mi), respectively. Our college is therefore located halfway between Nagasaki and Hiroshima.

Because damage areas were still radioactive, I told my students, "Do not sit on or touch anything in the bomb area." In spite of our precaution, some suffered diarrhea, nausea, and headache.

I attempted to determine the position of the fireball in each city based on the technique of locating aircraft illuminated by multiple beams of searchlight which I developed under the Navy contract earlier. Against my expectation, reconstructed beams of radiation connecting objects with their burn marks at Nagasaki did not converge into a small volume because the

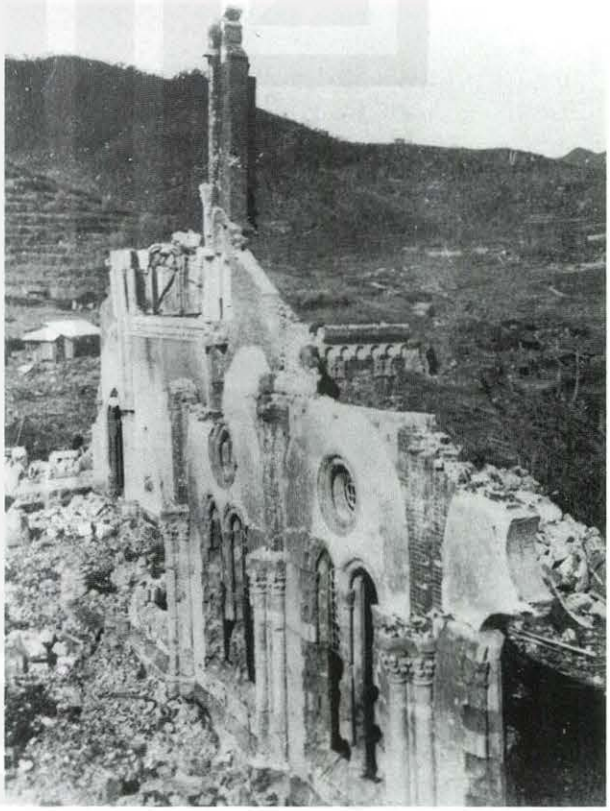

Fig. 6.2-10 A view of the damaged Urakami Cathedral. Trees behind the structure were flattened, while weak houses beyond the 700-m range were not damaged. Photo by Tetsuya Fujita.

Fig. 6.2-11 The Urakami Tenshudo (Cathedral) in Nagasaki smashed open by the shock wave from the fireball. The horizontal component of the shock wave was strongest near the 500-m range circle where this cathedral was located. Photo by Tetsuya Fujita, looking northwest.

shock-wave which arrived after the flash dislocated both objects and burn marks. Shortly thereafter I found a cemetery flower pot with a crescent-shaped burn mark on the bamboo surface (Fig. 6.2-9). Encouraged by this finding, I hopped around from one cemetery to another on the hillsides north, east, and south of ground zero. With a high degree of accuracy, I estimated the fireball height to be 520-m AGL.

After my ground-truth visit to Hiroshima, I computed the height of the fireball to be 530 m. Thus, the heights of both explosions were very close to each other. I thought at that time that the USAF must have known the pressure distribution above these cities accurately, in spite of the complete blackout of weather reports throughout Japan. We learned later that an observation aircraft departed from Tinian one hour in advance of the bomber and used a dropsonde for pressure and temperature measurements in each bombing.

The force of the shockwave pointing outward from ground zero at Nagasaki was devastating at the 400- to 600-m range. The pre-bomb landmark Uragami Tenshudo (Cathedral) at a 500-m range was literally broken into pieces. At ground zero on the other hand, most trees were blackened by radiation but standing upright. I saw a small, weak-looking stone bridge over a shallow creek near ground zero that was left without visible damage. I thought that the shockwave which propagated straight downward was reflected back upward at the creek bed directly beneath the fireball.

Forty-five years have passed since my research visits to the bombed cities, located equidistant from where I was teaching at that time. I am glad that I have not been adversely affected by the remnant radiation to which I had been exposed during those two research visits in September 1945.

Fig. 6.2-12 A scale model of the Urakami Tenshudo (Cathedral) showing the destruction by both radiation and the shock wave which smashed the structure into pieces.

Fig. 6.2-13 A broken portion of the Urakami Cathedral transported to the Ground Zero Park.

Fig. 6.2-14 Four of my former students who visited Sakurajima Volcano during the height of the eruption in April 1946. This photo was taken in the garden of the New Tagawa Hotel after our get-together dinner in May 1989. From left: Hayao Nasu, Takeshi Ohtaka, Ted, Kaoru Kushida, and Masato Yoshida.

On June 7, 1990 I visited the ground zero location in Nagasaki. The whole area had been rebuilt beyond recognition and the Ground Zero Memorial Park and Atom Bomb Museum were added. A scale model (Fig. 6.2-12) of the cathedral after the bomb in a museum showcase demonstrates the power of the bomb 500 m from ground zero. A piece of the cathedral wall transported to the Ground Zero Park (Fig. 6.2-13) has been viewed by visitors from all over the world.

Approaching an Unapproachable Volcano

During my homecoming in 1989 to Kitakyushu City, four students (Fig. 6.2-14) in my physics class in 1946 organized a dinner meeting for me to talk about our visit to Sakurajima volcano, the 1118-m tall central cone of Aira Caldera in Fig. 6.2-3. The volcano erupted violently on March 9 during our Spring break, generating two new lava flows, one toward the east to Kurokami village and the other, south to Arimura village on the island coast. Evacuation from these villages began immediately.

Fig. 6.2-15 My group of volcano researchers sitting on an evacuation boat returning to the volcano island to pick up the remaining refugees. Photo by Tetsuya Fujita on April 8, 1946.

Fig. 6.2-16 An advancing edge of the south lava flow made visible by a 60-sec time exposure. Photo taken from the south slope of Nabeyama on April 9, 1946.

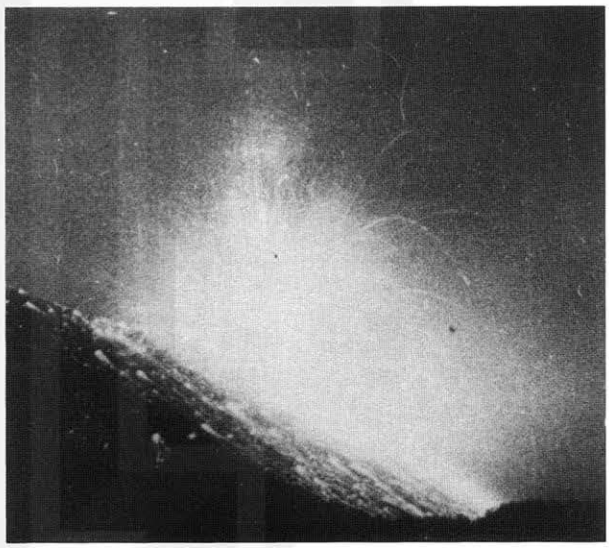

Fig. 6.2-17 A nocturnal view of the trajectories of the red-hot volcanic bombs erupting from the new crater. Photo by Fujita and Yoshida.

Less than one month after its initial explosion and while it was still erupting and spewing lava, I organized a field trip to the volcano, seen in the bird's-eye view in Fig. 6.2-3. On April 7, 1946, I departed our college with four students, Kaoru Kushida, Takeshi Ohtaka, Hayao Nasu, and Masato Yoshida along with two research assistants, Hiroshi Kawaguchi and Tatsuko Hatano.

First we took a train to Kagoshima City, then a returning evacuation boat (Fig. 6.2-15) to Yumoto village on the volcano island. After walking in the steady fall of volcanic ash, being protected by umbrellas overhead, we reached Arimura, a post-eruption semi-ghost town. I tried to rent a room from Mr. Takahashi, but he did not understand my Japanese because of his strong Kagoshima dialect. Thereafter, student Nasu who was raised in Kagoshima negotiated beautifully, renting a house from him practically free of charge.

On April 9 when the eruption calmed down somewhat, I climbed the 358-m (1175') Nabeyama mountain with Mr. Yoshida. Meanwhile, six others walked to Kurokami village where the tip to the east lava flow had already reached the shoreline for some time. They measured the sea surface temperatures, 58°C (135°F) 5 meters off the beach and 29.5°C (85°F) just off the beach. I walked into the sea water next to the lava flow, returning quickly to the shore with two red rings on my legs where the thin surface layer of hot water contacted my skin.

When the eruption intensified again, the brave students and I climbed Nabeyama to take time-exposure pictures of the red-hot lava flow (Fig. 6.2-16) and the parabolic trajectories of volcanic bombs (Fig. 6.2-17). On April 10, the coastal road was cut off by the south lava flow. In the afternoon, my interpreter rented a fishing boat to observe the lava flow from the sea. The boat was large enough to hold everybody, but I was the only person who was able to row and steer the boat with a single oar attached to the stern. Fortunately, I had used the stern oar at my mother's fishing port (Fig. 6.1-10). I took my group around the steaming edge of the submerged lava flow which from time-to-time crumbled, spewing tons of steam clouds up into the air. Another attraction was a number of lava devils, tall, brown-colored rotating columns standing on the south lava flow. After learning a lot from the volcanic eruption, we boarded an evacuation boat from Arimura to Kagoshima City.

Four decades have passed since I visited the active volcano in 1946 with my four brave students, all of whom majored in electronic communication at Meiji College of Technology. After the graduation, however, each of them found his own way of success in life. Kushida utilized his inherited wealth, becoming the founder of Toa University (University of East Asia) in Shimonoseki City (Fig. 6.2-19); Nasu became a nuclear scientist and a faculty of Toa University. Ohtaka became an award-winning design artist, and Yoshida, President of the Yoshida Printing Company.

While in Kitakyushu in 1973, four months before the completion of the Kanmon Suspension Bridge (Fig. 6.2-18), I asked Kushida if he would be able to obtain a permit to walk on the bridge under construction. Thanks to his quick action to get a permit, we were able to walk on the bridge (Fig. 6.2-19) in the hard-hat section and to look down at the blue water underneath (Fig. 6.2-20). It was an unforgettable experience.

Although I enjoyed the visit to the active volcano in 1946, my daily life under the postwar inflation was miserable. The rate of inflation, as measured by the price of rice, rose 260% (1945-46), 220% (1946-47), and 210% (1947-48) (See Fig. 6.2-21). Our college gave us resting days from time to time to compensate for the high costs of food we could not purchase. It was not possible to pay for new research out of my salaries. Meanwhile, I did not want to remain as a full-time college teacher.

Early in 1946, I applied for a Department of Education grant for re-educating grade school teachers in the science field of my choice. I thought that "weather science" was an excellent topic to choose, because it could be studied rather cheaply with pencil and paper. Furthermore, a lot of grade school teachers were interested in weather, reports of which had been blacked out during the Second World War.

Upon receiving a two-year grant on March 16, 1946, I visited Shimonoseki Weather

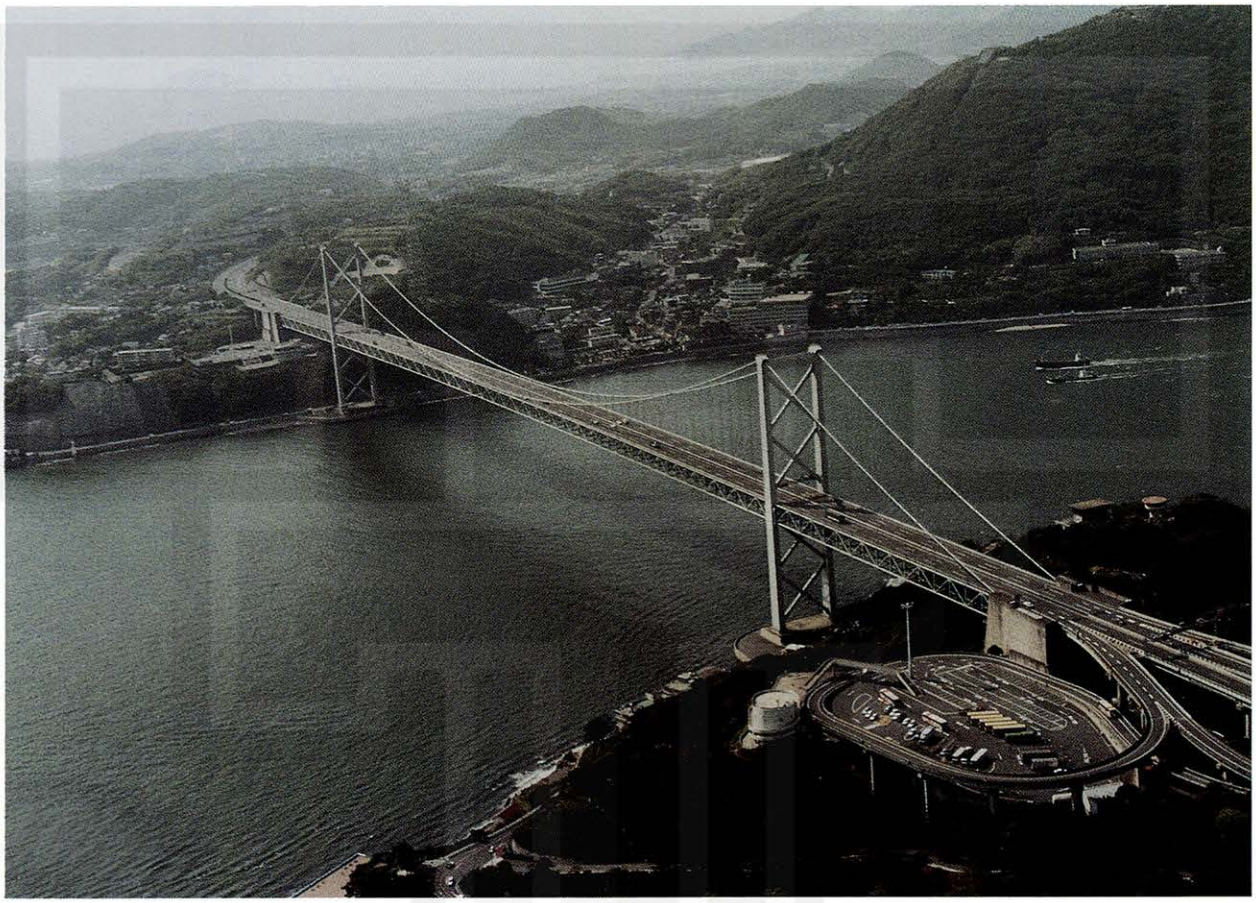

Fig. 6.2-18 The Kanmon Bridge connecting the northern tip of Kyushu (foreground) with the western end of Honshu, the main island of Japan. Photo by Ted Fujita in June 1989.

Fig. 6.2-19 Ted Fujita and his former students Kaoru Kushida (left) and Masato Yoshida (right) standing on the Kanmon Bridge under construction.

Fig. 6.2-20 Ted Fujita and Masato Yoshida looking down from the Kanmon Bridge being constructed in 1973.

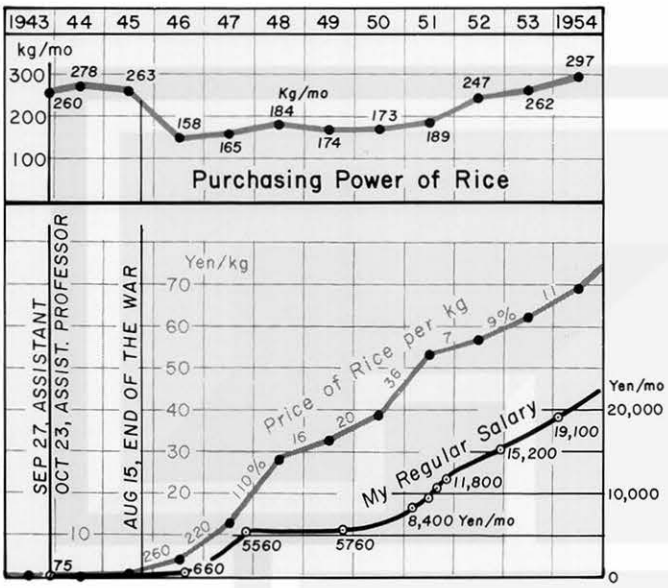

Fig. 6.2-21 The very low standard of living between 1946 and 1951 expressed by the purchasing power of rice, the primary food in postwar Japan. Now, the purchasing power is 800 kg/mo (5 times that of 1946).

Station frequently to collect current and old weather data on wind, temperature, pressure, etc. to be used in explaining the daily weather events experienced in northern Kyushu. The first booklet under the grant was completed on April 6 and 193 copies were distributed under the name, Gakko no Kagaku (Science for Schools). Thereafter, 200 to 300 copies were sent to science teachers every month.

Most teachers wanted me to print weather maps in color. In Spring 1947, I learned the Tosha-Ban (Silk Screen) method of multiple color printing. Shortly thereafter, a number of color maps were added to the "Science for Schools" booklets which became popular among science teachers in Kitakyushu City.

While collecting local weather data at various weather stations, I became interested in analyzing local weather maps based on the analysis methods in Japanese textbooks. Very soon I noticed that it was easy to analyze large-scale synoptic charts based on the basic equations of motion. However, the direction and speed of local winds during convective storms were entirely different from what I expected from the pressure field.

The Seburi-Yama Thunderstorm on 24 August 1947

Fig. 6.2-22 The U.S. Air Force radar installation atop Seburi-yama where a copy of "Nonfrontal Thunderstorms" (1942) by Horace R. Byers was found in a wastepaper basket and picked up outside the base in July 1950. After reading the paper, I sent my research papers to Dr. Byers, Institute of Meteorology, University of Chicago, U.S.A. I would not be at the University of Chicago today if not for the timely finding of this paper in a most unlikely place.

In solving the mystery of unbalanced local winds at the surface, I decided to observe weather at a mountaintop station. In June 1947, I was informed that a weather substation was located at the top of the 1054 m (3457') Seburi-yama (mountain). I contacted the Fukuoka Weather Service, explaining what I intended to observe. After talking to Dr. Yukio Kawabata, director of the service, Mr. Kazuo Otani told me that he was interested in assisting my data collection at the substation.

On August 24, 1947 Otani and I took a bus from Fukuoka to Wakiyama village at the foot of the mountain. We backpacked at the bus terminal and climbed the steep slope while watching fast-growing towering cumuli. Shortly after reaching the summit substation, dark clouds moved in from the southwest accompanied by frequent cloud-to-mountain lightning.

While we were in cloud, strong, cold winds with a 22 m/s (49 mph) gust began shaking the frame building of the substation. In spite of a minor rain leak, we obtained complete records of wind, temperature, and pressure traces. We were very lucky to have had an opportunity to be in the heart of a severe thunderstorm at the mountaintop.

Since my coal mine experiment, I was interested in the nonhydrostatic pressure inside the real atmosphere. This time, I attempted to compute the nonhydrostatic pressure by subtracting the hydrostatic pressure from the static pressure measured at the mountaintop. The static pressure was obtained first by correcting the suction effects of the substation building which was by no means airtight. Second, the hydrostatic pressure was computed by reducing the mean sea-level pressure between the Fukuoka and Saga weather stations located on opposite sides of the mountain to the 1054-m level, the height of the Seburi-yama substation.

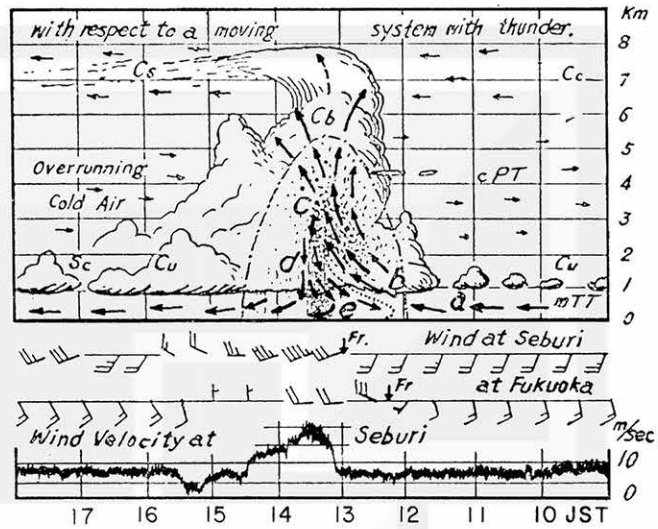

Fig. 6.2-23 A model of the Seburi-yama thunderstorm of August 24, 1947. This model was produced in March 1949, leading to a presentation in Japanese on May 6, 1949. An English translation was sent to Dr. Byers on December 5, 1950. From Fujita (1951b) Micro-analytical study of thunder-nose, Geophysical Mag., 22, 71-88.

The hydrostatic pressure computed from these two pressures turned out to be -0.3 mm Hg or -0.4 mb, indicating that the thunderstorms at the summit were associated with a negative nonhydrostatic pressure. Based on this evidence, I hypothesized the existence of a downward current of 7 m/s which would induce a conservative 0.2 mm Hg dynamic pressure upon reaching sea level.

This magnitude of the descending current, along with the 22 m/s horizontal gust results in an 18° angle of descent at the 1-km height of the substation. I thought that the angle was too steep to be realistic. Furthermore, nobody in Japan in 1948 thought about a downward current (present downdraft) in a thunderstorm.

In spite of my skepticism on the proposed downdraft, I wrote a paper entitled "Raiu-no-hana" (Thunder-nose) in Japanese and presented the paper before the Nishi Nihon Kisho Kenkyukai (Western Japan Meteorology Research Meeting) held in Kyushu on May 6, 1949. As anticipated, I received no comment on my downdraft concept.

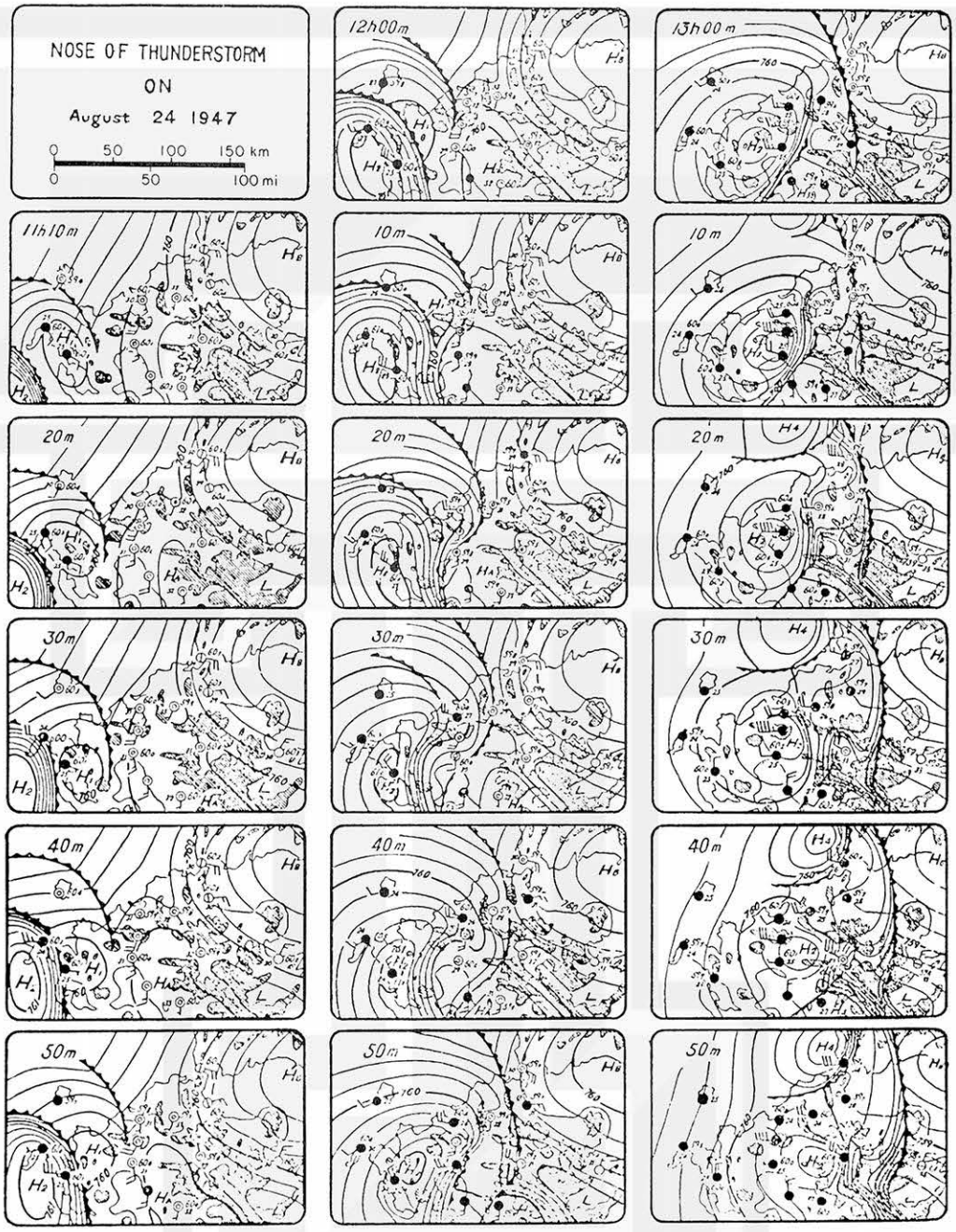

Fig. 6.2-24 Micro-analysis of the thunder-nose of August 24, 1947. This is the first sequence of micro-analysis maps I ever produced. These 10-min interval maps reveal that the parent weather system of the thunder-nose (a quick rise and fall of pressure beneath a severe thunderstorm in progress) is a small-scale dome of high pressure. In order to create these maps, I had to visit individual weather stations to hand copy recorded traces on tracing paper. No center for national data archive nor copying machine was available in Japan in the 1940s. Reproduction of Fig. 12 of the thunder-nose (1951b) paper.

The second half of my presentation in the meeting was a series of local maps showing the variation and movement of the "Nose of Thunderstorm", a nose-shaped rise and fall of the surface pressure during a severe thunderstorm. These local maps (Fig.6.2-24) were analyzed at 10-min intervals between 1110 and 1350 JST during the time of my observations at the summit. Participants were very pleased to identify the thundernose as being a miniature dome of high pressure only 20 to 100 km in horizontal dimension.

At the conclusion of the meeting, I decided to analyze more cases of local weather systems which cannot be depicted by regular synoptic analysis. I identified my local analysis, "Microanalysis" and began collecting necessary data from local stations.

At that time, I never thought that the microanalysis would be the dawn of the "Mesoanalysis" which I developed in 1953 to 1955 at the University of Chicago in cooperation with Dr. Morris Tepper of the U.S. Weather Bureau at Washington, D.C. (Refer to Chapter One).

Solar Eclipse Observation Mesonet on 9 May 1948

An 88% solar eclipse was predicted to occur on May 9, 1948 in Kitakyushu. Taking advantage of the golden opportunity to study the effect of the eclipse on local changes of wind and temperature, I proposed to operate a micro-network (present MESONET). Because no funds for the network were available, I decided to collect the necessary data at 46 surface stations manned by 98 volunteers consisting of my students, their friends and relatives. Students of both Meiji College of Technology and Kokura Middle School participated. They were assigned to take observations at 15-min intervals for an eight hour period between 0800 and 1600 JST on the day of the eclipse.

Available for the observations were 52 thermometers, 3 thermocouples, 3 barometers, and 50 hand-made wind socks. Sea-surface temperature was measured

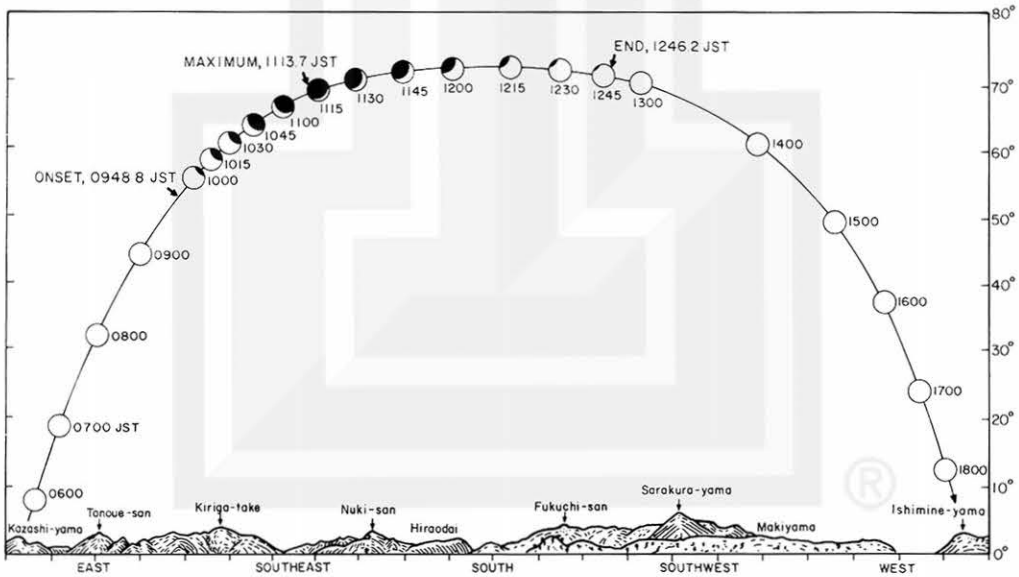

Fig. 6.2-25 Azimuth and elevation angles of the sun viewed from Meiji College of Technology at Tobata City on May 9, 1948.

at 3 coastal stations and ground-surface temperature at 7 selected stations. Because no anemometers were available, wind speeds were estimated in the Beaufort Force, and directions, by wind socks. In view of rather complicated topography, 5 stations were placed on waterbreaks, 4 at building tops, and 9 at mountain and hilltops. Along with three volunteer observers, I was at the top of the 625 m (2050') Sarakura-yama (mountain) overlooking the network. Three eager students climbed up an NHK (Japan Broadcasting Association) tower to the 1, 30, and 50-m levels to determine vertical distributions of wind and temperature.

The eclipse began at 0948 JST, reaching its peak at 1113 JST, and ended at 1246 JST (Fig. 6.2-25). It was cloudy when we began climbing the north slope of Sarakura-yama. Upon reaching the top, however, I saw a narrow band of blue sky approaching us very rapidly. The blue sky spread from our zenith to the northwest horizon when the maximum eclipse occurred. Because of the unexpected clearing, our

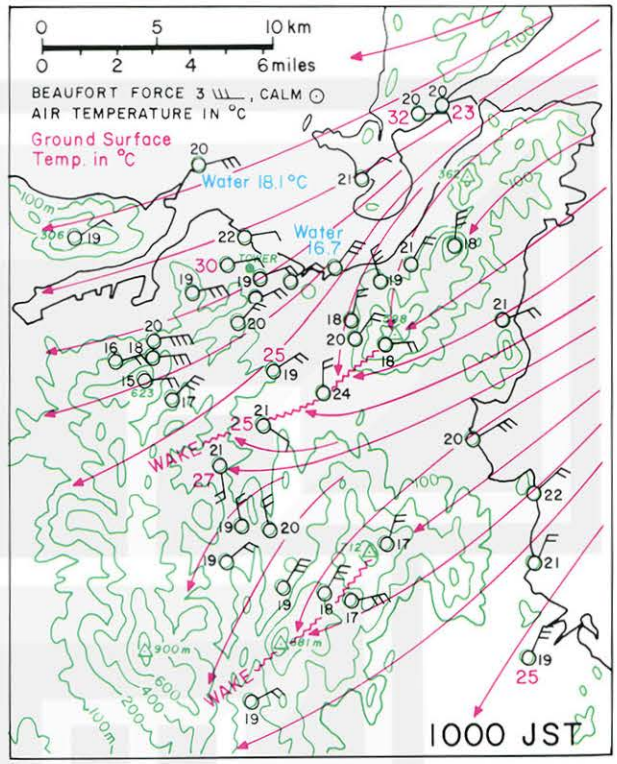

Fig. 6.2-26 Wind and temperature at 1000 JST, 11 minutes after the onset of the eclipse.

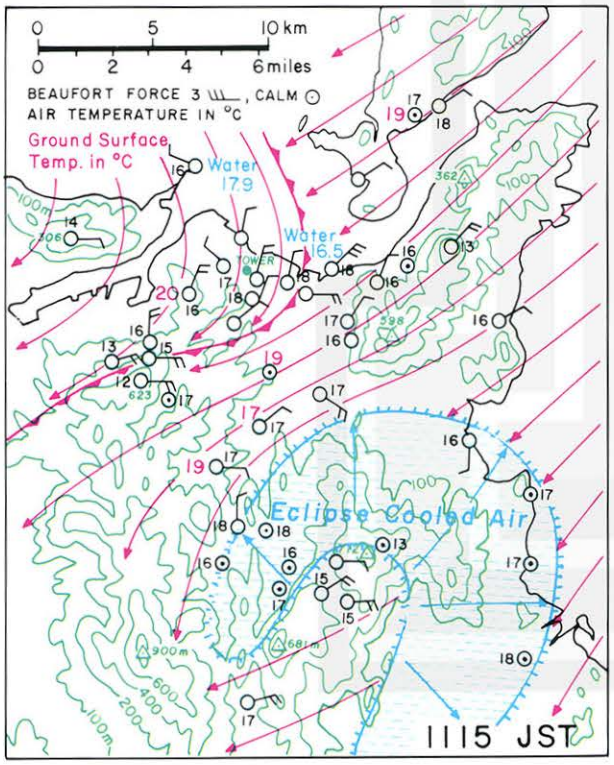

Fig. 6.2-27 Wind and temperature at 1115 JST, near the time of the maximum eclipse of 88%.

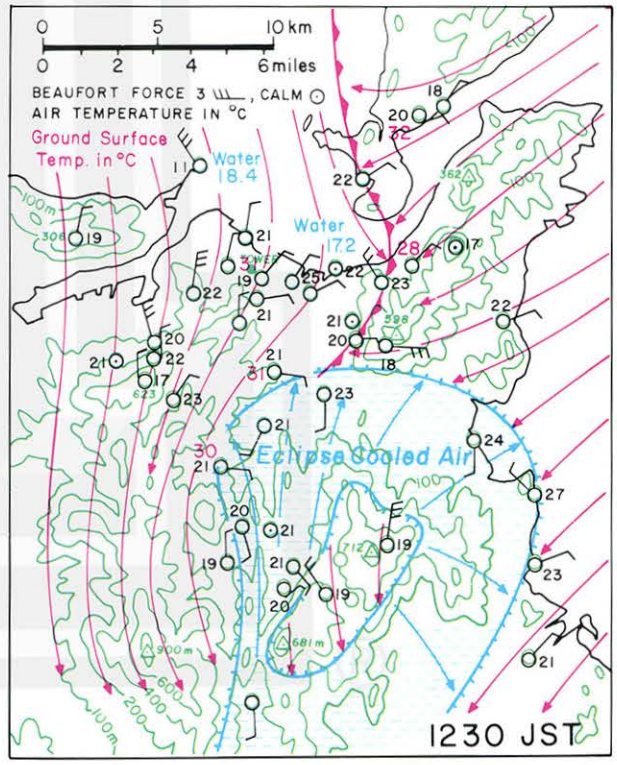

Fig. 6.2-28 Wind and temperature at 1230 JST, 15 minutes before the end of the eclipse.

Fig. 6.2-29 The solar eclipse network consisting of 46 surface stations. Number of stations by elevation are: 27(0-99m), 6(100-199m), 2(200- 299m), 3(300-399m), 3(400-499m), 2(500-599m), and 1(600-699m). This color map was printed with silk screen.

Fig. 6.2-31 My homecoming talk in 1988 on "Tornado and I" before the participants of the 1948 solar eclipse observations some 40 years ago.

Fig. 6.2-32 The participants and their children who came to my homecoming talk sponsored by Kitakyushu City.

Fig. 6.2-30 Twin towers of the NHK Kokura City station. Platforms at 1m, 30m, and 50m AGL were used to measure wind and temperature at 15-minute intervals on the day of the eclipse.

Fig. 6.2-33 A get-together with a group of the participants who were up to 20 years old when they participated in the network operations.

eclipse field experiment turned out to be successful.

At the onset of the eclipse at 10:00 a.m., the entire network area was dominated by northeasterly winds (Fig. 6.2-26) blowing over flat land and water areas. Two distinct wakes were seen in the lee of the 598 m and 712 m mountains. When the eclipse reached its maximum at 11:15 a.m., a shallow pool of cold air extending to about 300 m MSL became visible. However, little air motion was measured inside the eclipse-induced cold air (Fig. 6.2-27)

After the maximum eclipse had passed, the pool of cold air still kept building slowly until 12:30 p.m., 15 minutes before the eclipse ended (Fig. 6.2-28).

My silk screen was very useful in printing copies of color base maps used in analyzing the change in the local atmosphere during the 88% eclipse (Fig. 6.2-29). Most stations were located on the ground. However, one of the NHK Kokura towers was used in measuring winds and temperatures at three levels (Fig. 6.2-30).

A vertical cross section of temperature at the tower revealed that the temperature field was characterized by diurnal and eclipse scales of temperature variation. The eclipse scale temperature reached the minimum on the ground at 11:15 a.m., the peak eclipse time. At 30 m, the minimum temperature time was 11:30 a.m., and at 50 m, 11:45 a.m. The time lag between the ground and the 50-m level was 30 minutes. Wind variations as estimated using the Beaufort Force were also interesting. At the minimum temperature time at each level, the wind force decreased by two, resulting in calm periods on the ground and 30-m height.

After collecting exciting data for both research and teaching, I completed a silk-screen report in Japanese and sent copies to all participants. Because all participants wanted to exercise the "Kagakusuru Kokoro" (Spirit of Pursuing Science) which prevailed in postwar Japan, everybody donated their own time and

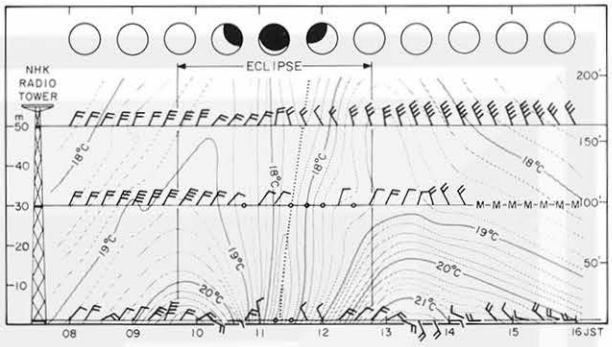

Fig. 6.2-34 Variation of winds at the NHK tower expressed by the Beaufort Force. Three barbs denote Beaufort 3, for example. Isotherms are drawn every 0.2°C.

effort without asking for travel expenses. The only expense incurred was 2,800 yen which was $10.37 at the 270 yen per dollar exchange rate at that time.

It should be mentioned that the "Kagaku Gumi" (Science Group) of Kokura Middle School played an important role in observing the eclipse weather at the 46 surface stations. The Science Group, consisting of a number of students such as Morifumi Fukami, Toshiaki Hayashida, Hiroshi and Takashi Nakamura, and Akira Tani, began conducting their extracurricular scientific activities during the final years of the War. Their organized activities began after I became a faculty of Meiji College in 1944. I assisted in their activities and they, in turn, helped in weather-data collections for the publication of the "Science for Schools."

During the lunar eclipse on June 14, 1946 the Science Group students and I conducted a lunar-eclipse study with a 100-power telescope mounted on the school ground. Since then, they began showing interest in both lunar and solar eclipses. My observational experiment for the 88% solar eclipse was received with enthusiasm by the science group students along with their friends and relatives.

In May 1988, the month of the 40th anniversary of the 88% solar eclipse, Kitakyushu City made arrangements for my homecoming

talk on "Tornado and I" at Chisan Hotel in Kokura. I gave a popular talk (Fig. 6.2-31) on my 35 years of research life in the United States. I was pleased to identify in the audience a number of participants of the solar eclipse network. Some were with their children (Fig. 6.2-32). In a get-together party after the meeting (Fig. 6.2-33), Mr. Morifumi Fukami, now retired from high school teaching, spoke of the unforgettable venture to satisfy our scientific interest in those early years.

The First Tornado Damage Survey

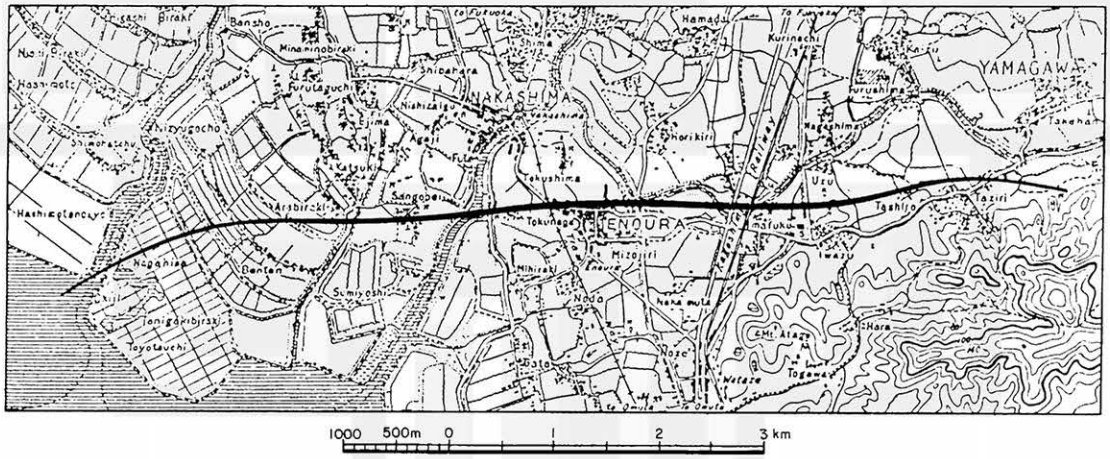

Fig. 6.2-35 Path of the Enoura Tornado of September 26, 1948 in northern Kyushu. To witness the first tornado damage in my life, I recall walking the entire swath in very hot and humid weather. Reproduction of Fig. 1, from Fujita (1951c) Micro-analytical study of cold front, Geophysical Mag., 22, 237-277.

The tornado which I surveyed for the first time in my life occurred on September 26, 1948. After learning that a damaging "Tatsu Maki" (Dragon Swirl) destroyed the Enoura community, my fiancee Tatsuko wanted to come along to witness an act of god rarely experienced in Kyushu.

Upon arrival at the damage site, we were shocked to see roofs blown off residential houses and rice crops flattened in rice fields. At first we walked west to confirm that it originated as a waterspout which landed from Ariake Bay, a shallow-water inlet with large tidal variations. Apparently the tornado intensified after landing, reaching its maximum intensity (F2, according to my memory) after traveling 5 km over rice fields. It left behind a 9.8 km (6 mi) path before disappearing in a bamboo forest on a hillside.

Rain began at 12:20 p.m. at Saga weather station accompanied by a pressure fall. Heavy rainshowers, as high as 85 mm/hr occurred at 1:10 p.m. shortly after the pressure fall ended. Evidently the tornado was associated with a prefrontal shower.

Because local newspapers reported that the squall line after the tornado caused widespread wind damage, I decided to collect meteorological data. In Japan at that time, one had to visit individual weather stations to hand copy surface observations and recorded traces. Since our marriage late in October 1948, both of us spent considerable time visiting weather stations in Kyushu and western Honshu. After one year of effort in collecting the data, a 41-page report on "Micro-analytical study of cold front" was completed in English and submitted to the Geophysical Magazine,

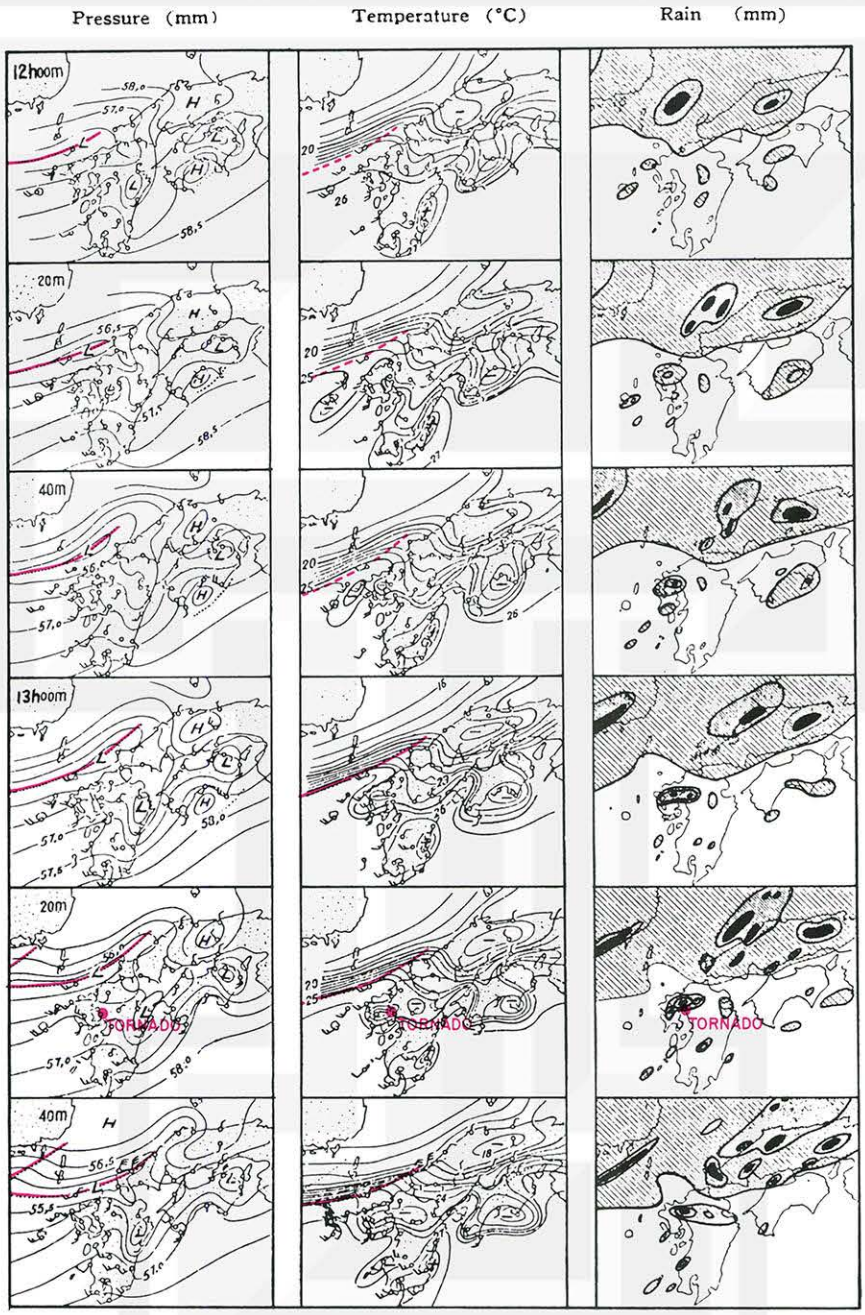

Fig. 6.2-36 An example from the series of 60 micro-analytical maps of pressure, temperature, and rainfall reproduced from Fujita (1951c), in which a series of 20-minute interval maps were analyzed for a 20-hour period from 4:00 p.m. JST to midnight. The Enoura tornado occurred at 1:40 p.m.

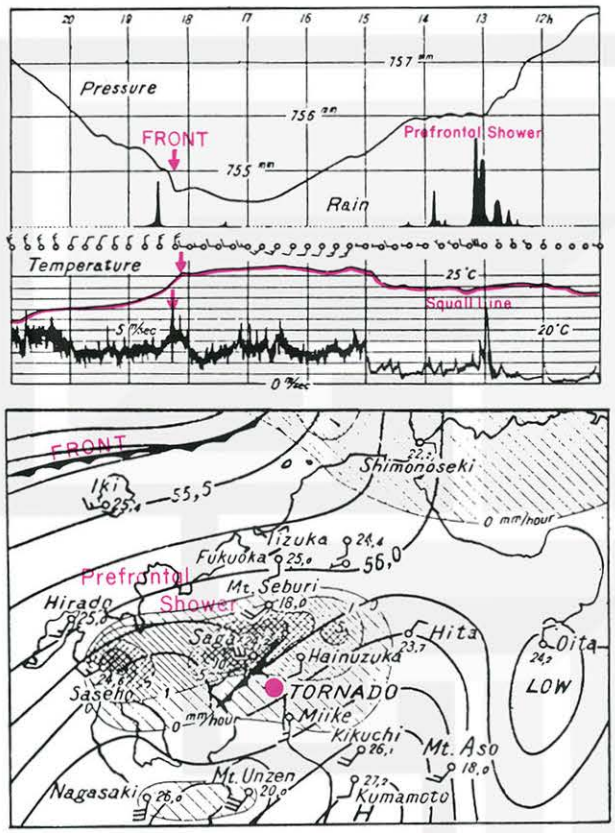

Fig. 6.2-37 Pressure, temperature, and wind traces from Saga weather station, nearest to the Enoura tornado. The tornado occurred at 1:40 p.m. 25 km (16 mi) southeast of the station. This surface map at 1:00 p.m. presents 0, 1, 5, 10, and 20 mm/hr isohyets and isobars for every 0.25 mm Hg. Reproduction of Fig. 12 from Fujita (1951c).

Central Weather Observatory in Tokyo. The paper included a series of 60 surface maps analyzed at 20-min intervals (Fig. 6.2-36).

After mapping the damage of the Enoura tornado, I became interested in determining the pattern of high winds based on the characteristics of damaged rice crops. In September 1949, when numerous rice crops were blown down by gusty high winds behind a cold front, I mapped the damage directions of rice crops in the area all around the 598-m tall Adachi-yama (mountain). Because I spent a lot of time and effort in completing the damage map (Fig. 6.2-38), I wished I could fly over a

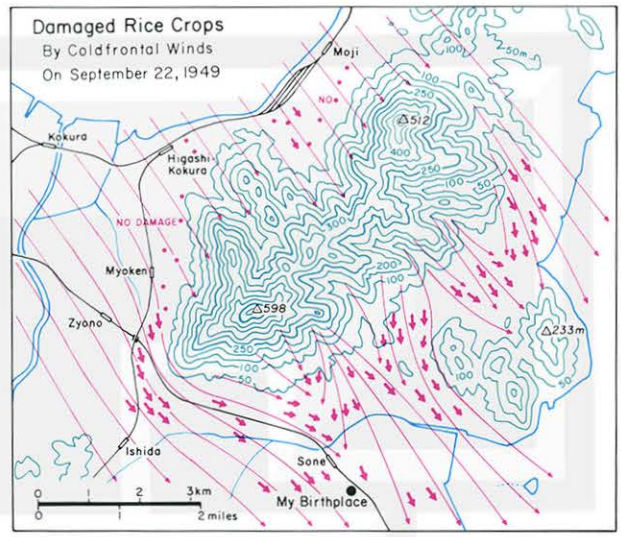

Fig. 6.2-38 Damage directions of the cold front winds in the morning of September 22, 1949 evidenced by damaged rice crops. I surveyed the damage areas on foot, three days after the storm.

damage area to determine wind effects. My dream did not come true until I began flying over cornfields in the Midwest after coming to the United States.

Financial Hardship, 1949-50

Although the postwar inflation in 1946 and 1947 exceeded 200%, my salary increased by 9 to 10 times in these two years, resulting in a temporary relief in 1948 when the rate of inflation was only 16%. As a result, the cost of living adjustment in 1949-50 was 3.5% (Fig. 6.2-21). When the inflation flared up again to 20% (1949-50) and to 36% (1950-51), my small savings were wiped out.

We received pay in cash (not checks) twice a month in brown, sealed envelopes, because nobody had a bank account to cash checks. It is interesting to reexamine the breakdown of my semimonthly payroll stubs (Fig. 6.2-39) of September 1949 when the rate of conversion was $1 to 360 yen. At that time my regular pay was $16.00. In addition, I received a "dependent

昭和24年9月分上		
藤田哲也殿		
俸給	2,880	00
臨時家族手當	500	00
勤務地手當	1,014	00
計	4,394	00
恩給法納金	57	60
官舍料		
電燈料		
瓦斯料		
明月會費		
賣善會費		
藥價		
教職員組合費	50	00
水道料		
共濟組合費	72	00
分類所得稅	521	50
計	701	100
差引渡額	3,692	90

昭和24年9月分下		
藤田哲也殿		
俸給	2,880	00
臨時家族手當	500	00
勤務地手當	1,014	00
計	4,394	00
恩給法納金	57	60
官舍料		
電燈料		
瓦斯料		
明月會費	23	00
賣善會費	14	40
藥價		
教職員組合費		
水道料		
共濟組合費	72	00
分類所得稅	521	50
計	688	50
差引渡額	3,705	50

Pay in September 1949 Tetsuya Fujita, Mr.		
Regular Pay	¥5,760.00	$16.00
Dependent Allowance	1,000.00	2.78
Regional Allowance	2,028.00	5.63
Total Pay (month)	¥8,788.00	$24.41
Pension Reduction	115.20	0.32
School Membership Dues	23.00	0.06
College Alumni Dues	14.40	0.04
Teachers Union Dues	50.00	0.14
Cooperative Union Dues	144.00	0.40
Income Tax (month)	¥1,043.00	$2.90
Total Reduction	¥1,389.50	$3.86
Take-home Cash	¥7,398.40	$20.55

Fig. 6.2-39 My payroll stubs for September 1949, paid on the 15th and the 30th of the month. The total take-home cash was $20.55.

allowance" of $2.78 per head (wife and children) and a "regional allowance" of $5.63 for living in the city. The total pay was $24.41.

They deducted $2.90 in income tax, $0.32 pension fund contribution (social security tax), etc., with a total reduction of $3.86. The total take-home pay was $20.55 in September, $10.26 on the 15th and $10.29 at the end of the month.

Prior to the completion of my paper on the Seburi-yama thunderstorm of August 24, 1947, I presented the outline of the paper at Fukuoka Kanku Kishodai (Fukuoka District Weather Service) on March 4, 1949. At the conclusion of my talk, an employee of the weather service informed me that a copy of "Nonfrontal Thunderstorms" (1942) written by a University of Chicago professor was found in a wastepaper basket inside the U.S.

Fig. 6.2-40 Tetsuya Fujita and Kozo Ohta, professor of physics, standing at the side entrance to the Physics Department on April 1, 1950 when we became faculty of the Kyushu Institute of Technology created under the Education Reform Act.

Air Force installation atop Seburi-yama, and that the paper was picked up later when it was brought out of the installation mixed with trash. I was delighted to learn the professor's identity: Dr. Horace R. Byers, Institute of Meteorology, The University of Chicago, U.S.A.

Late in 1949, after returning from the Western Japan Meteorological Research Meeting at Beppu City, Kyushu on November 25, I felt that it was absolutely necessary to translate my thunder-nose and cold front papers into English. First, I tried to use a typewriter belonging to my Physics Department, but it had been broken for some time.

I decided to purchase a used typewriter from someone because I could not find any in downtown stores. Fortunately, Mrs. Tomi Egami, owner of Egami Cooking School and mother of my student Tanekazu Egami, found an excellent used typewriter for me. On January 25, 1950 I bought the typewriter for 20,000 yen ($55.56), paying 10,000 yen in cash and borrowing the rest, interest-free from Mrs. Egami. The cost of the typewriter was 2.7 times my take-home monthly pay. Nevertheless, I was very pleased to own a typewriter which turned out to be the most expensive item I had ever purchased to that point in my life.

Although I do not remember how Tatsuko and I survived for several months thereafter, I was busy translating my papers into English and typing with a single finger. Upon the completion of these translations, I sent the thunder-nose paper to the Central Meteorological Observatory in Tokyo first, followed by the cold front paper.

ScD From University of Tokyo

The Japanese doctoral system in 1949 (the old system) was under the Imperial Guideline No. 200 issued in 1920 in which a doctoral degree is awarded, upon approval by the Education Minister, to a candidate whose thesis passed the evaluation and examination by the board of faculty in one of the five specific fields, Science, Engineering, Law, Literature, and Medicine. The candidacy requirements are either those who completed more than two years of research at universities or those whose ability has been determined to be equal or higher than the former. In either case, one must complete an acceptable thesis under the guidance of a professor in either a national or private university.

The new doctoral system under the Postwar Education Act is almost identical to the PhD program in the United States. The new graduate program at national universities began as late as April 1953. Since then a PhD candidate has been given the freedom to choose either the new or old system in consultation with the sponsoring professor.

After learning the Japanese doctoral system, I began thinking about the future research that would lead to my ScD thesis. On July 4, 1949 Tatsuko and I visited the Fukuoka Kanku Kishodai (Fukuoka District Weather Service) to discuss my plans with Dr. Yukio Kawabata, director of the weather service. At the conclusion of our meeting, Dr. Kawabata recommended that I pursue more case studies of local weather situations using my micro-analysis technique.

On August 1, 1950 I airmailed my cold front paper to Dr. Byers under the assumption that this paper would be more interesting than the thunder-nose paper. In his October 25, 1950 reply, Dr. Byers responded with this concluding paragraph, "You are to be congratulated on a very careful analysis of the small scale features in a cold front. This problem is attracting a great deal

of attention in the United States at the present time, and the U.S. Weather Bureau has a special project to investigate these smaller disturbances. It is known that they lead to the formation of tornadoes which, as you know, are very common in the west-central and southern United States."

Shortly after receiving Dr. Byers' letter, I airmailed him the thunder-nose paper, which appeared to be less important in Japan. In spite of my pessimism, Dr. Byers sent me a surprising reply dated January 30, 1951 with the first paragraph quoted below.

"I have looked over your paper, Micro-analytical Study of Thunder-Nose, and note that in view of the fact that you were not familiar with the work of the U.S. Thunderstorm Project on this subject your conclusions are highly valuable and really represent an independent discovery of some of the factors derived from our work. In particular you deserve credit for noting the importance of the thunderstorm downdraft and outflowing cold air."

His letter continued, "Under separate cover I am sending you a copy of the book THE THUNDERSTORM which is the principal report of the Thunderstorm Project carried out under my direction." Early in March 1951, I received the book, signaling the onset of my micro-scale research in cooperation with the University of Chicago.

On July 7, 1950 shortly before I sent my paper to Dr. Byers, I visited my family physician, Dr. Masaru Otani in Tobata City. After a physical examination, he and his wife informed me that they would like to render financial support to my ScD program. Upon discussing their kind offer with Tatsuko, I made up my mind to work hard toward my ScD and accepted their offer.

Encouraged by the financial support and Dr. Byers' letter of January 30, 1951, I contacted Dr. Kawabata who had been giving me his advise on my ScD. Since then he moved to Tokyo, becoming Chuou

Fig. 6.2-41 Dr. and Mrs. Otani in 1950 when they offered the financial support toward my ScD degree. They were pleased when I received the ScD from the University of Tokyo in 1953. Unfortunately, Dr. Otani passed away on March 11, 1984 at age 77.

Kishodai Kansoku Bucho (Director of Observation Division, Central Meteorological Observatory). Dr. Kawabata suggested that I consult with Dr. Sigekata Syono, Professor of Meteorology, University of Tokyo, and he made an appointment for me to meet with Dr. Syono during the Spring meeting of the Meteorological Society of Japan.

On Friday, May 11, 1951 Dr. Kawabata and I went to the University of Tokyo and visited Prof. Takeshi Nagata at the Geophysical Institute. Dr. Nagata told us that Dr. Byers told him about my thunder-nose research when he visited the University of Chicago in January 1951, and that he already informed Dr. Syono of my thunderstorm downdraft which was appreciated by Dr. Byers.

My meeting with Dr. Syono at his office lasted for three hours from 10 a.m. to 1 p.m. A number of his faculty and students participated in the meeting. When I explained my idea of the downdraft current inside the Seburi-yama thunderstorm in 1947, Dr. Syono told me that the Japanese Thunderstorm Project was conducted in 1940 making use of the 21 network stations near Maebashi City, 100 km (60 mi) northwest of Tokyo. Although a number of surface

Fig. 6.2-42 Left: Nonfrontal Thunderstorms (1942) by Prof. Horace R. Byers of the University of Chicago. Right: The Seburi-yama (mountain) radar station of the U.S. Air Force, where a copy of the paper was found in a wastepaper basket and picked up outside the station.

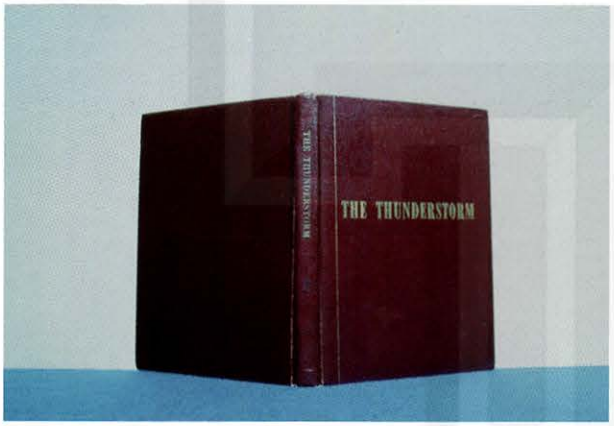

Fig. 6.2-43 A copy of THE THUNDERSTORM from Dr. Byers which was received on March 7, 1951.

Fig. 6.2-44 The "National List of Japanese Doctors" published by the Department of Education.

Fig. 6.2-45 The memorial service of Dr. Masaru Otani (1907-84) in June 1989 at his cemetery on the hillside overlooking Hondo City on Amakusa Island. From right: Yaeko Fujita, Ted, Mrs. Otani, her sister, and the head minister of the Otani Family Temple.

maps revealed the existence of diverging winds on the ground, nobody at that time thought about a downflow to be located above the divergence field at the surface.

At the conclusion of the May 11, 1951 meeting, Dr. Syono recommended that I work on micro-analysis of Japanese typhoons. Meanwhile, he decided to provide me with research funds for data collection and analysis. In several days, I completed all necessary arrangements on my ScD thesis under the sponsorship of Dr. Syono.

I left Tokyo at 10:00 a.m. on May 15, 1951 for my wonder island of Kyushu, arriving at Kokura at 9:10 a.m. on the 16th. The travel time was 23 hr and 10 min, almost 24 hours. Presently, it takes only 6 hours from Tokyo to Kokura via Bullet train.

Three typhoons traversed the island of Kyushu in three consecutive years. They were Typhoon Della of June 20-21, 1949, Typhoon Kezia of September 13, 1950 and Typhoon Ruth of October 14, 1951. Of these, Typhoon Della was the most interesting one, because a number of micro-scale fronts formed inside its central area as it passed across the island. This typhoon was analyzed using hourly observation data and recorded traces from over 180 stations.

My ScD thesis entitled "Analytical Study of Typhoons" was completed and presented to Prof. Syono on August 30, 1952. I remember that I had to submit a police department certificate that I had no criminal record as of that time, in addition to the list of publications consisting of three conference papers and five papers published in English. They were:

Fujita (1948) Meteorological study of the 88% solar eclipse at Kitakyushu on May 9, 1948. A 51 pp report in Japanese.

Fujita (1949a) Fine structure of a cold front and its environment. A 9 pp report in Japanese.

Fujita (1949b) Analytical study of typhoon Della. A preliminary 18 pp report in Japanese.

Fujita (1951a) Disturbances observed in the vicinity of Okhotsh-Sea anticyclone. English Bulletin, Kyushu Institute of Technology, 1, 65-73.

Fujita (1951b) Micro-analytical study of thunder-nose. Geophys. Mag., Central Meteor. Observatory, 22, 71-88.

Fujita (1951c) Micro-analytical study of cold front. Geophys. Mag., Central Meteor. Observatory, 22, 237-277.

Fujita (1952a) A study on pressure dip within typhoon Della. English Bulletin, Kyushu Institute of Technology, 2, 52-61.

Fujita (1952b) Pressure distribution within typhoons. Geophys. Mag., Central Meteor. Observatory, 23, 437-451.

On June 4, 1953 the Board of Faculty of the University of Tokyo passed my ScD thesis. I was requested to submit the certificate of no police record between August 30, 1952 and June 4, 1953 while my thesis was under review and examination. After confirming that the University of Tokyo passed my thesis and that I had no criminal record as of June 4, 1953, the

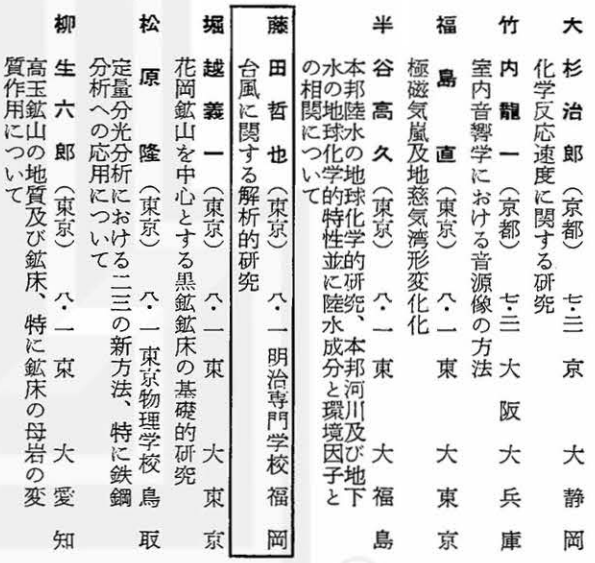
大杉治郎（京都）七・三 京 静岡
化学反応速度に関する研究
竹内龍一（京都）七・三 大阪 大兵庫
室内音響学における音源像の方法
福島直（東京）八・一 東大 東京
極磁気嵐及地磁気湾形変化化
半谷高久（東京）八・一 東大 福島
本邦陸水の地球化学的研究、本邦河川及び地下水の地球化学的特性並に陸水成分と環境因子との相関について
藤田哲也（東京）八・一 明治専門学校 福岡
台風に関する解析的研究
堀越義一（東京）八・一 東大 東京
花岡鉱山を中心とする黒鉱鉱床の基礎的研究
松原隆（東京）八・一 東京物理学校 鳥取
定量分光分析における二三の新方法、特に鉄鋼分析への応用について
柳生六郎（東京）八・一 東 大愛知
高玉鉱山の地質及び鉱床、特に鉱床の母岩の変質作用について

Fig. 6.2-46 The official record of my ScD shown in the National List of Japanese Doctors. The boxed letters in Japanese indicate: TETSUYA FUJITA (ScD from University of Tokyo); August 1, 1953; Graduate of Meiji Semmon Gakko (Meiji College of Technology); Fukuoka Prefecture; Thesis title: Analytical Study of Typhoons.

Education Minister approved my ScD degree on August 1, 1953 and the degree was recorded in the Department of Education publication "National List of Japanese Doctors" (Figs. 6.2-44 and 46).

In retrospect, my research life started as a teenage spelunker in 1939 and reached the first milestone in 1953 when the ScD degree was awarded on August 1. When I looked back at the past 14 years of struggle while enjoying my life as a naturalist, in contrast to a theoretician, I was very lucky. In spite of my visits to Nagasaki and Hiroshima after the atom bombs, I have not been affected by the secondary radiation that prevailed in and around the damaged areas. Then a copy of Prefrontal Thunderstorms found accidentally at the summit of Seburi-yama acted as the matchmaker between Prof. Byers and I, separated by a 6,650 mi (10,700 km) great-circle distance. Finally, Prof. Sigekata Syono directed me toward the completion of my ScD thesis.

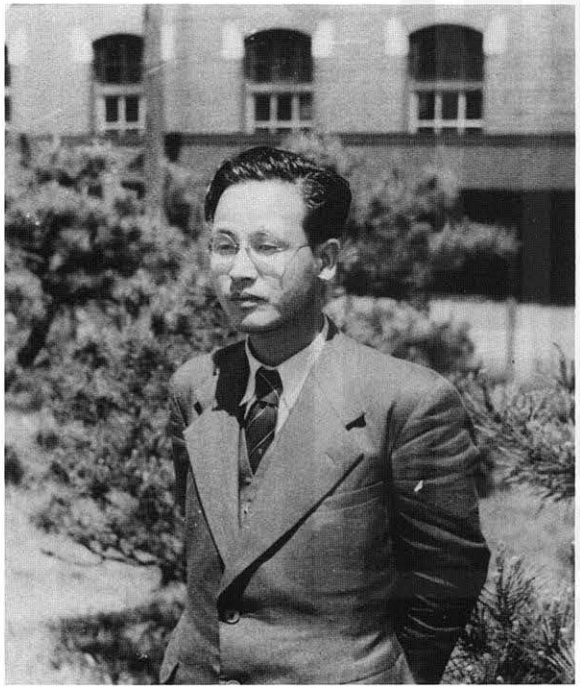

Fig. 6.2-47 Tetsuya Fujita at Kyushu Institute of Technology in May 1950 at age 30. I was nearsighted and required eyeglasses.

Fig. 6.2-48 A family picture of Prof. Shimmachi of Meiji College of Technology. From right: Prof. Kosaku Shimmachi, his brother Kensaku, holding a cat, and niece Takako. They had a male cat, allowing me to perform my cat experiment. My favorite experiment was to put it inside a round basket placed on the turntable of a record player. After a short period of rotation, the cat could not walk straight on the floor. Another experiment was to hold it upside down at various heights above the "tatami" mat to determine the minimum height required to land right-side up. The height varied around 25 cm (12"), always requiring its blitz twist. Prof. Shimmachi's lecture was informative and imaginative. (1963 photo)

During these years, I was assisted and guided by my teachers and students of both Kokura Middle School and Meiji College/Kyushu Institute of Technology. The Fukuoka District Weather Service played the key role in supplying their meteorological data for my micro-analysis. I wish to express my sincere thanks to Mr. Kazuo Otani (1921-71) and Dr. Yukio Kawabata for their personal efforts rendered to my micro-studies.

Most of my research was done during the postwar years of hardship. Without the thoughtful financial support of Dr. and Mrs. Masaru Otani (Fig. 6.2-45) along with the devoted efforts of my family members, wife Tatsuko, brother Sekiya, and grandmother Hatsu, I could not have possibly reached this stage of my life.

6.3 The University of Chicago

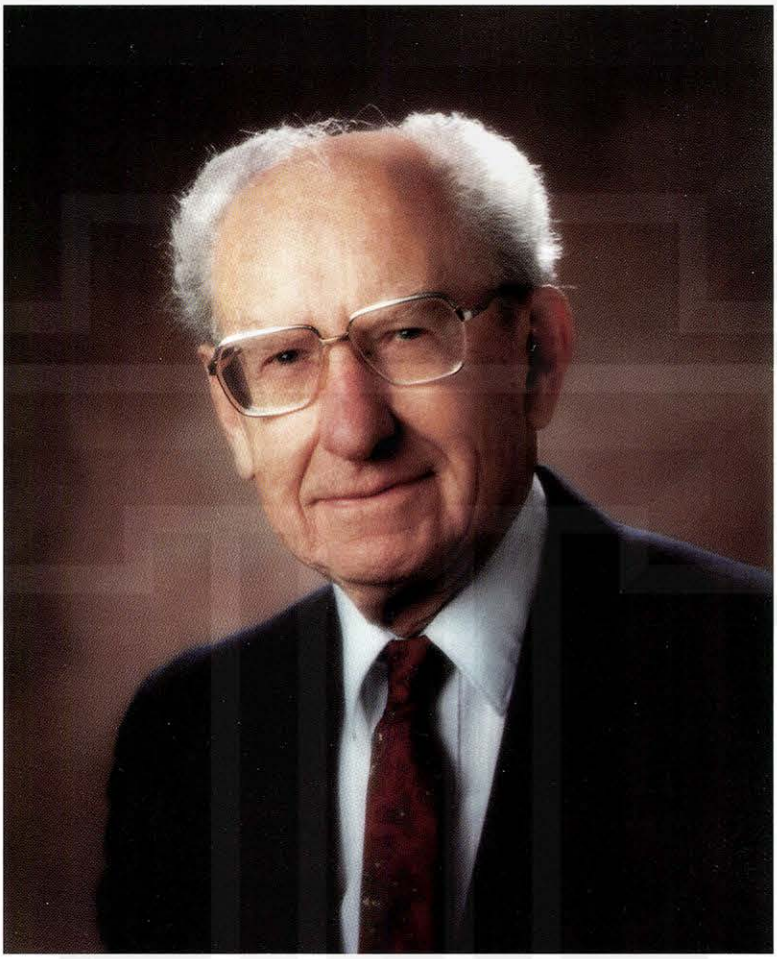

My Mentor Professor Horace R. Byers in Dec. 1988

During the second year of my research associateship, Dr. Byers suggested that I perform severe-storms research at the University of Chicago, obtaining immigrant visas for my family. After discussing the offer with Tatsuko, I decided to come back to Chicago.

I left Chicago for Kyushu in September 1955 to finish up my teaching at the Kyushu Institute of Technology. Upon returning home, I noticed that Kazuya, 14-mo old (Fig. 6.3-1) when I left home, now had become interested in trains (Fig. 6.3-3). I took his pictures sitting on a farm wagon (Fig. 6.3-2), and observing Nuki-san mountain I used to climb (Fig. 6.3-4). I thought that it would be his cultural revolution to move from Japan to the United States.

On 21 July 1956, the three of us with immigrant visas landed the Honolulu International Airport, receiving a warm Aloha welcome. Several days later, we arrived Chicago's Midway Airport where Mr. and Mrs. Jack Kabumoto were waiting for us.

From Kitakyushu, JAPAN to Chicago, U.S.A.

Fig. 6.3-1 My son Kazuya in July 1953 (age 14 mo) when I left home for the University of Chicago.

Fig. 6.3-2 Kazuya in November 1955 (age 3) sitting on the farm wagon of Mr. and Mrs. Tsutomu Ikeo harvesting their rice crops.

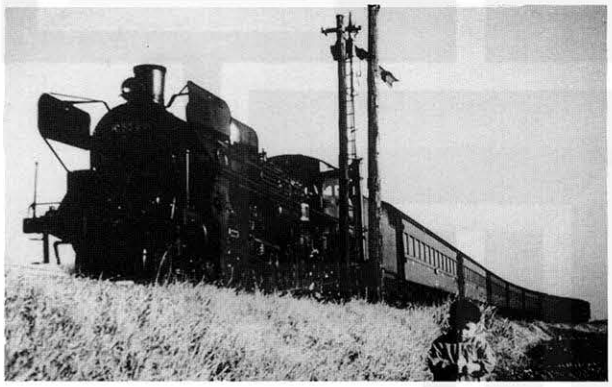

Fig. 6.3-3 Kazuya in October 1955 (age 3) when I returned from the University of Chicago. He liked to watch passing trains.

Fig. 6.3-4 Kazuya in February 1956 standing on a farm road with snow-covered Nuki-san in the background.

They drove us to a pre-arranged apartment at location 3 (Fig. 6.3-6). During my previous visit, I stayed at the International House (location 1) and at an apartment owned by the Chicago Koyasan Buddhist Church (location 2).

On the following day, I reported my permanent return to Prof. Byers (Fig. 6.3-7). He was pleased to see me back after the long trip with my family. Foreseeing the proposed expansion of my severe-storms research, the university purchased for me a private house (Fig. 6.3-7) at 5736 Woodlawn Avenue located one building south of the U.S. Weather Bureau Office then.

I commuted often to Washington, D.C. for joint research with Dr. Morris Tepper (Fig. 6.3-8). Meanwhile, I began receiving my counterpart researchers (Fig. 6.3-9) working under our U.S.-Japan Cooperative Science Program. Although Tatsuko was

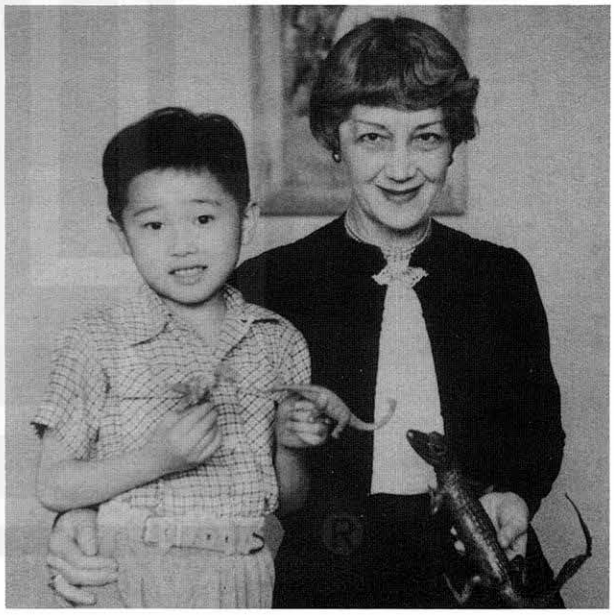

Fig. 6.3-5 Kazuya with his grandmother-like Ms. Babette Becker (deceased in 1987) who taught him English. She received her Ph.D. at U. of Chicago.

Fig. 6.3-6 University of Chicago and vicinity I photographed from Lear Jet at 25,000' (7.6 km) on 14 April 1973 at 1618 CST. My offices: A-Department of Meteorology (1953-57), B-Fujita Laboratory (1958-69), C-Department of the Geophysical Sciences (1969 to present). My residences: 1-International House (1953), 2-Apartment (1954-55), 3-Apartment (1956-59), 4-House (1959 to present). I have always lived within walking distance from work.

New Life at the University of Chicago

Fig. 6.3-7 Dr. Byers and I in 1956 (left). The photo on the right shows my research building on the left side of the U.S. Weather Bureau Chicago Office.

Fig. 6.3-8 Members of the Severe Storms Project at USWB in Washington, D.C. Dr. Morris Tepper, Herman Newstein, and Bill Haas are in the picture.

Fig. 6.3-9 My counterpart researchers from Japan in my backyard. Messrs. Izawa (left), Tsuchiya, and Watanabe are in the front row.

Fig. 6.3-10 A happy hour in February 1967 with Babette, Tatsuko, Kazuya, and Rev. and Mrs. Inouye of the Koyasan Buddhist Church.

Fig. 6.3-11 Three Fujitas in a park at Luján near Buenos Aires, Argentina where I taught in September 1964.

busy in entertaining visitors, we spent a good time with Rev. and Mrs. Chiko Inouye (Fig. 6.3-10) and other ethnic friends, Dr. and Mrs. Henry Inouye, Dr. George Kittaka and his parents, Mr. and Mrs. Mac Kurima, Mr. and Mrs. Jack Kabumoto, Mr. and Mrs. George Iwahashi, and many others. Ms. Babette Becker (Fig. 6.3-5) working on her Ph.D. thesis on Chinese music taught Kazuya English and often corrected my technical papers.

In Summer 1964, I taught satellite meteorology at the University of Buenos Aires where I took my family along (Fig. 6.3-11).

My Research Grants relative to Consumer Price Index

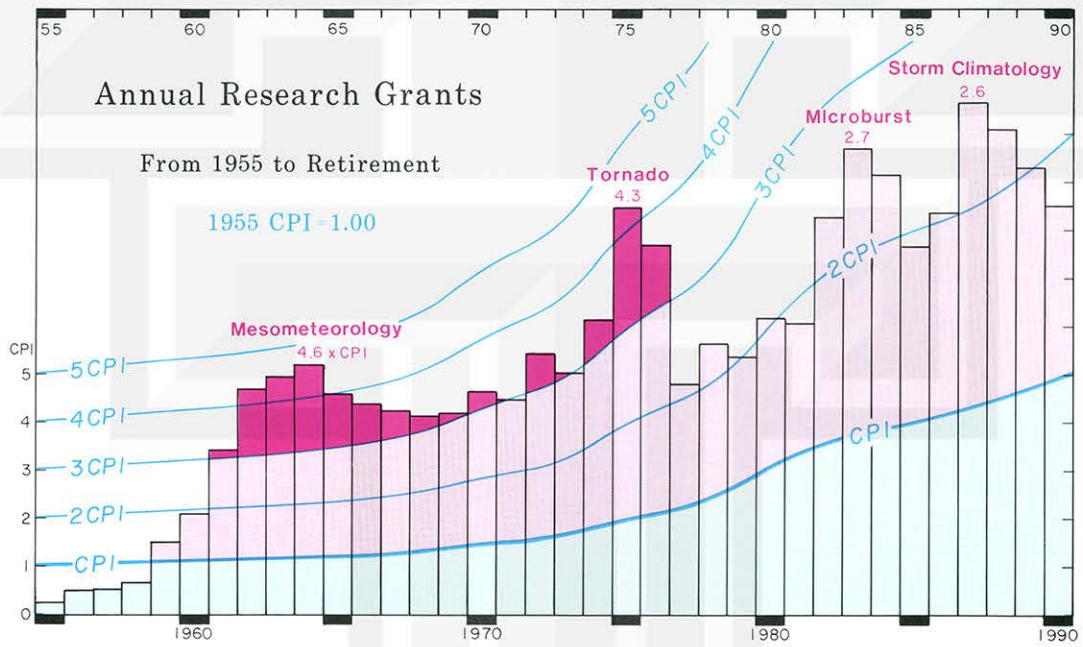

Fig. 6.3-12 Variation in my research grants which increased, on the average, when expressed in dollars but decreased when divided by the Consumer Price Index (CPI) in each year. The CPI increased five times during the 36 years, 1955-1990.

During the 36 years before retirement, I enjoyed my research much more than anything else. I kept feeling that research is my hobby and hobby is my occupation. I learned quickly, however, that I must secure research grants from government agencies in order to continue research in the United States. While in Japan, on the contrary, I received annual basic support from the Kyushu Institute of Technology for maintaining my research activities year after year after year.

At retirement on 31 December 1990, I looked back at my funding history at the University of Chicago, finding that there were four distinct peaks (Fig. 6.3-12) related to my major research subjects: the mesometeorology peak in 1964 during my intensive mesoanalysis of medium-scale disturbances, the tornado peak in 1975, one year after the Superoutbreak tornadoes of 3-4 April 1974, the microburst peak in 1983, the year after JAWS, and the storm climatology peak in 1987 when the effects of Global Warming became an important issue around the world.

It should be noted that each one of these peaks was followed by a decline in funding, because no agency wants to support a project once it has been completed with success. My key words are **"a success in research signals the onset of the funding recession."**

Unless one moves into a new research area, the recession could turn into a depression. Remembering the Japanese song "Kohjo no Tsuki" (Moon over the Ruined Castle) on page 157, I tried hard not to end my research after singing **"where are my Days of Glory? I wonder."**

The longest continuous support for 31 years to retirement (1961 to present) was given by the Meteorological Satellite Laboratory and its successor agencies. The grant began on 1 April 1961, exactly one year after TIROS I sent back the first picture of the earth on April Fools Day, 1960.

The NASA grant continued for 29 years (1962-90) under the identical grant number, NGR 14-001-008. In view of the customary practice that grant numbers change every 2 to 3 years, this was a rather unusual thing to occur.

Four- to 18-year grants were also received from various agencies: U.S. Weather Bureau on mesometeorology (1955-72), Nuclear Regulatory Commission on tornado for protecting nuclear power plants, US Air Force on mesometeorology research (1960-66), US Army Signal Corps on mesoanalysis (1959-62), National Hurricane Research Laboratory on hurricane structure (1970-73) and on damage survey (1980-88). Research on oceanic and land storms has been supported by the Office of Naval Research (1986 to present).

The National Science Foundation supported my specific researches for 38 cumulative years on: mesometeorology (1960-66), U.S.-Japan Science Cooperation (1963-69), Maui, Barbados, and GATE Experiments (1967-76). After my identification of the "downburst," I received supports on Projects NIMROD (1978-79), JAWS (1982-86), MIST (1986-88) and publication of THE DOWNBURST book (1980-83). Basic research on downburst was also supported by FAA through MIT Lincoln Laboratory (1987-90).

At this point, I wish to express my sincere appreciation to these agencies for supporting my continuing research at the University of Chicago. Without these supports, I could not possibly have accomplished the research presented in this book written in appreciation of financial and moral supports rendered by both Japanese and U.S. Governments, as well as my professional friends and the general public who supplied me with important scientific data.

Ph.D and M.S. Students

During my faculty years (1962-90), I sponsored (s) or advised (a) eight Ph.D. students: Yukio Omoto 1964(a), William Bonner 1965(s), Henry Brown 1967(s), Peter Caplan 1970(a), Walter Lyons 1970(s), Ekundayo Balogun 1972(s), Gregory Forbes 1978(s), and Roger Wakimoto 1981(s). They received individual degrees in caps and gowns at convocations (Figs. 6.3-13 and 14).

I also sponsored or advised 15 M.S. students: Rodger Brown 1962(a), Kiyoshi Tsuchiya 1963(a), Jaime Tecson 1964(a), William Winkler 1865(a), Roland Madden 1967(s), Peter Black 1969(s), Yun-Mei Chang 1972(s), Robert Somrek 1972(s), Robert Woronicz 1972(s), Robert Pasken 1974(s), Robert LaPlaca 1974(s), Peter Black 1979(s), Eric Peterson 1986(s), Brian Smith 1986(s), and David Rexroth 1990(s).

Mr. Tornado sees his First

During the JAWS experiment on 12 June 1982, I saw the first tornado in my life. At the conclusion of the tornado meeting at Argonne National Laboratory, we celebrated at the Farmer's Daughter Restaurant (Figs. 6.3-15 right and 16).

My age while at the University of Chicago increased from 33 to 70 at retirement (Fig. 6.3-17). During that time in October 1969, my laboratory at B (Fig. 6.3-6) moved to the 4th floor of the new 5-story building (Fig. 6.3-18) at C. Fortunately, my research went on without interruption.

Mr. Tornado sees his First Tornado

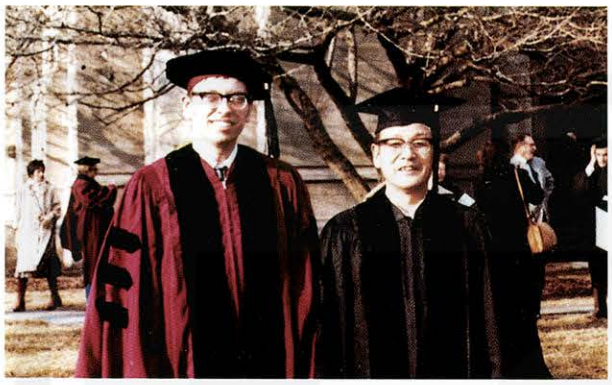

Fig. 6.3-13 Greg Forbes and I after his convocation in Winter Quarter 1978.

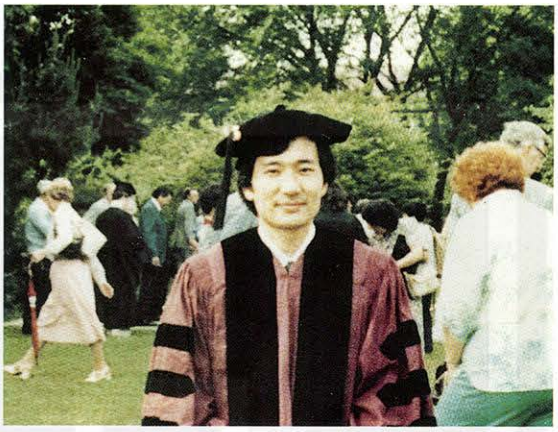

Fig. 6.3-14 Roger Wakimoto after his convocation in Spring Quarter 1981. Sorry, Roger, I was in Spain then.

Fig. 6.3-15 My first tornado sighting on 12 June 1982 (left) and a tornado-sighting decoration cake for the celebration shown below.

Fig. 6.3-16 The tornado-sighting memorable dinner in 1986 participated by Dr. Jim MacDonald (left), Ted, Dr. Bob Abbey, Mr. Tom Grazulis, and Mr. Ron Hadlock.

Age 33 Age 51 Age 60 Age 70

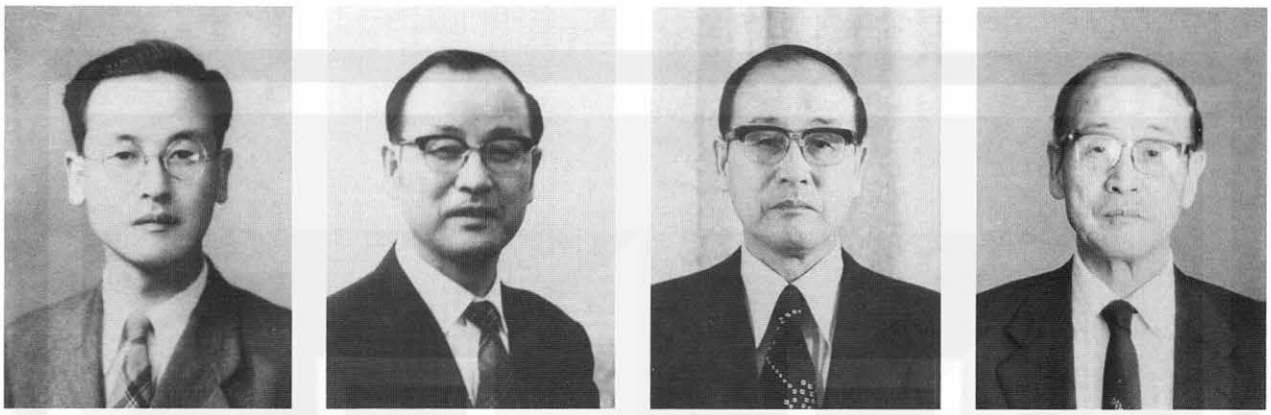

Fig. 6.3-17 Pictures of Ted from 1953, year of the first visit to the University of Chicago to retirement in 1990.

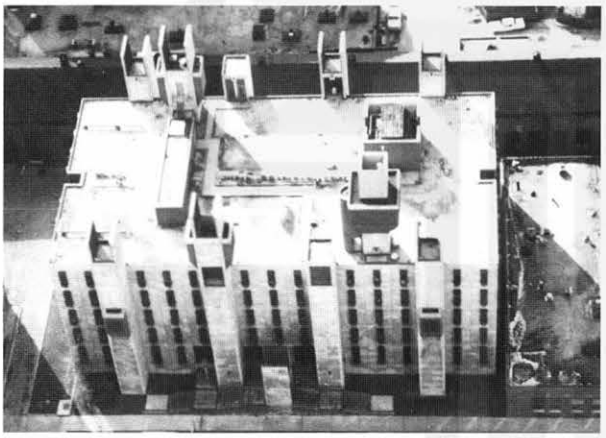

Fig. 6.3-18 New building of the Henry Hinds Laboratory for the Geophysical Sciences opened on 14 October 1969. Photo by Ted in 1973.

Beautiful City of Chicago

Although the city became unsafe at night, I enjoyed nocturnal views of Chicago at various occasions: a view from the 95th-floor restaurant at the 442-m John Hancock Tower (Fig. 6.3-19) and the closely-spaced planets from the Planetarium Point (Fig. 6.3-20). Now, Chicago has become my second home city after Kitakyushu City, Japan.

Publication of The Downburst

The Downburst book was finally completed in Spring 1985 after working closely with Mr. Chuck Stern of the U. of Chicago Printing Department and Mr. Bob Arsenault of the printing company (Figs. 6.3-21 and 22). Both Professors Forbes and Wakimoto (Fig. 6.3-23) joined the celebration at Hatsuhana Restaurant, followed by a Koto music by Mrs. Sugano (Fig. 6.3-23), organizer of the Chicago Koto Group (Fig. 6.3-24) in which Susie practices the string instrument Koto.

My Appreciation at Retirement

It is likely that I would have remained as a college teacher in Japan if I were not acquainted with Dr. Byers through the unexpected and lucky finding of his paper, **Nonfrontal Thunderstorm (1942)** in a wastepaper basket at the USAF radar station atop Seburiyama mountain in Kyushu, Japan.

His broad-minded, warm-hearted guidance at the University of Chicago kept giving me courage and initiative in performing new researches on severe storms. I wish to express my thanks to him again before closing the University of Chicago Section of this book.

Fig. 6.3-19 Chicago after dark seen from the 95th-floor restaurant of John Hancock, the 2nd tallest building in the world. Photo by Ted on 21 May 1981 looking SSE through WSW.

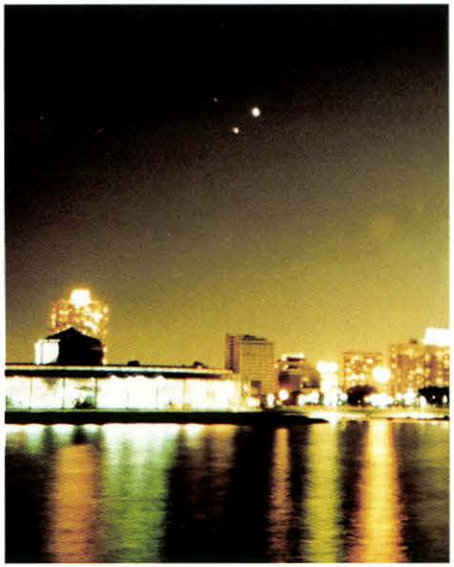

Fig. 6.3-20 A rare view of the three planets, Mars, Venus and Jupiter forming a small triangle above downtown Chicago on 17 June 1991. Right photo taken at 2206 CDT was overexposed to show the planets (left photo).

Publication of THE DOWNBURST

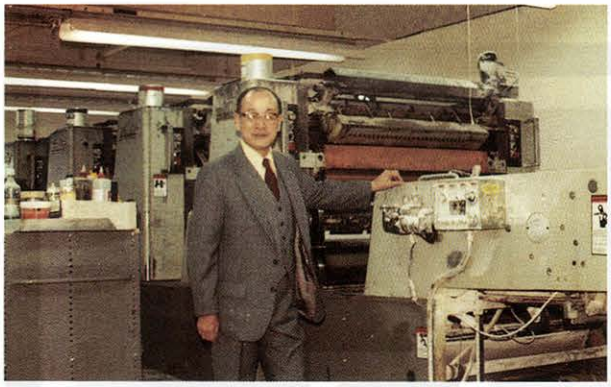

Fig. 6.3-21 Ted standing in front of the 6-color press used for printing "The Downburst" book.

Fig. 6.3-22 Ted Fujita, Chuck Stern, and Bob Arsenault examining the color-printing form.

Fig. 6.3-23 Professors Wakimoto and Forbes (left) at the book publication party. Mrs. Sugano (right) along with Mr. Sugano, receiving a bouquet of flowers from Chuck Stern after her performance with the Japanese string instrument, Koto, for the party.

Fig. 6.3-24 Some members of the Chicago Koto Group organized by Mrs. Sugano. From left to right: Mesdames Motohashi, Sugano, Nagasaka, Ohba, Miura, Fricke, and Fujita.

Many Thanks to Dr. Byers Again

Fig. 6.3-25 Dr. Byers (age 85) and I (age 71) in the backyard of his retirement home in Santa Barbara, California. Photo by Mrs. Byers on 3 October 1991.

Fig. 6.3-26 My "Kanreki" (60th Birthday) celebration wearing red hat and coat. Front row from left: Mr. Morifumi Fukami, Dr. Waichiro Bando, Susie, Ted, brother Sekiya, Dr. Sigenari Hirata. Back row from left: Mrs. Kazue Tsukada, Mrs. Tomoko Harada, Sekiya's wife Yaeko, Mrs. Hideko Otani, Mrs. Tsuneko Nakamura, Mrs. Yoshiko Bando, Mrs. Chieko Nakamura, and Mrs. Mitsuko Hirata.

Fig. 6.3-27 Commemorative picture taken by Mr. Kazuo Watanabe after the decoration ceremony on 8 May 1991 at the Imperial Palace, Tokyo. The Order received was the Kun 2-tou (Level 2) Sacred Treasure Gold and Silver.

6.4 My Hobby Experiments

I have always been interested in conducting observational experiments, large or small, making use of aircraft, radar, satellite, etc. I also like to collect my personal data and analyze them when I am tired of doing scientific research for too long. During the four postwar years in Japan, I experienced a 10,000% inflation rate. Keeping the bitter memory in mind, I worked on my own financial experiment from time to time while drinking glasses of beer. After noticing that my blood pressure goes down with a glass of beer, I kept a record of my blood pressure for several years prior to my retirement. In addition, I enjoy all types of photography both at home and while on travel. Presented in this section are graphical and pictorial records of these hobby experiments.

Financial Experiment

The two-digit inflation we experienced in the U.S. during the 1979-80 period was very bad and costly because it resulted in high interest and mortgage rates. The standard of living decreased accordingly and the value of the lifetime savings of seniors fell much quicker than anticipated.

On the other hand, the three-digit inflation I had gone through in Japan after the war was beyond description. Those who were able to make both ends meet between paydays were very lucky at that time. Because prices increased almost every day, we tried to purchase non-perishable items as soon as possible before the inflation eroded the purchasing power. The value of the yen currency plunged to several hundreths in two years, wiping out the total savings of my family.

Those who still had expensive jewelry and Japanese kimono dresses sold them to purchase food for the family. The word "urigui" (selling for survival) was used widely all over Japan.

Figure 6.4-1 summarizes the variation of several financial parameters during the 70-year period from my birth to retirement. It is remarkable to see that the Consumer Price Index (CPI) of the United States increased by only seven times during this 70-year period. The Dow Jones Industrials increased 30 times from $100 to $3,000 in spite of the Great Depression early in the 1930s. The price of rice in Japanese yen increased by 900 times, or 20 times in U.S. dollars.

The value of U.S. dollars, approximately 2 yen to a dollar, increased to 4 yen after the Great Depression, maintaining its value until the end of the war. Shortly after the war, the dollar gained in value to 360 yen to a dollar. However, as Japan turned gradually into an industrial giant during the 1970s and 80s, the dollar weakened from 360 yen to 120 yen, losing two-thirds of its peak value in the 1950s and 60s. Such an unexpected weakening of the dollar, coupled with the high cost of living in Japan almost prohibits me from retiring in Japan on U.S. pensions. On the other hand, I am pleased to have gone through a period of the most violent changes in economy one can possibly experience in a lifetime.

12-Year Mortgage on Home

In 1959, approximately three years after my permanent employment at the University of Chicago, I purchased my home on the west edge of the campus. It is a brick house with a party wall shared by my friend,

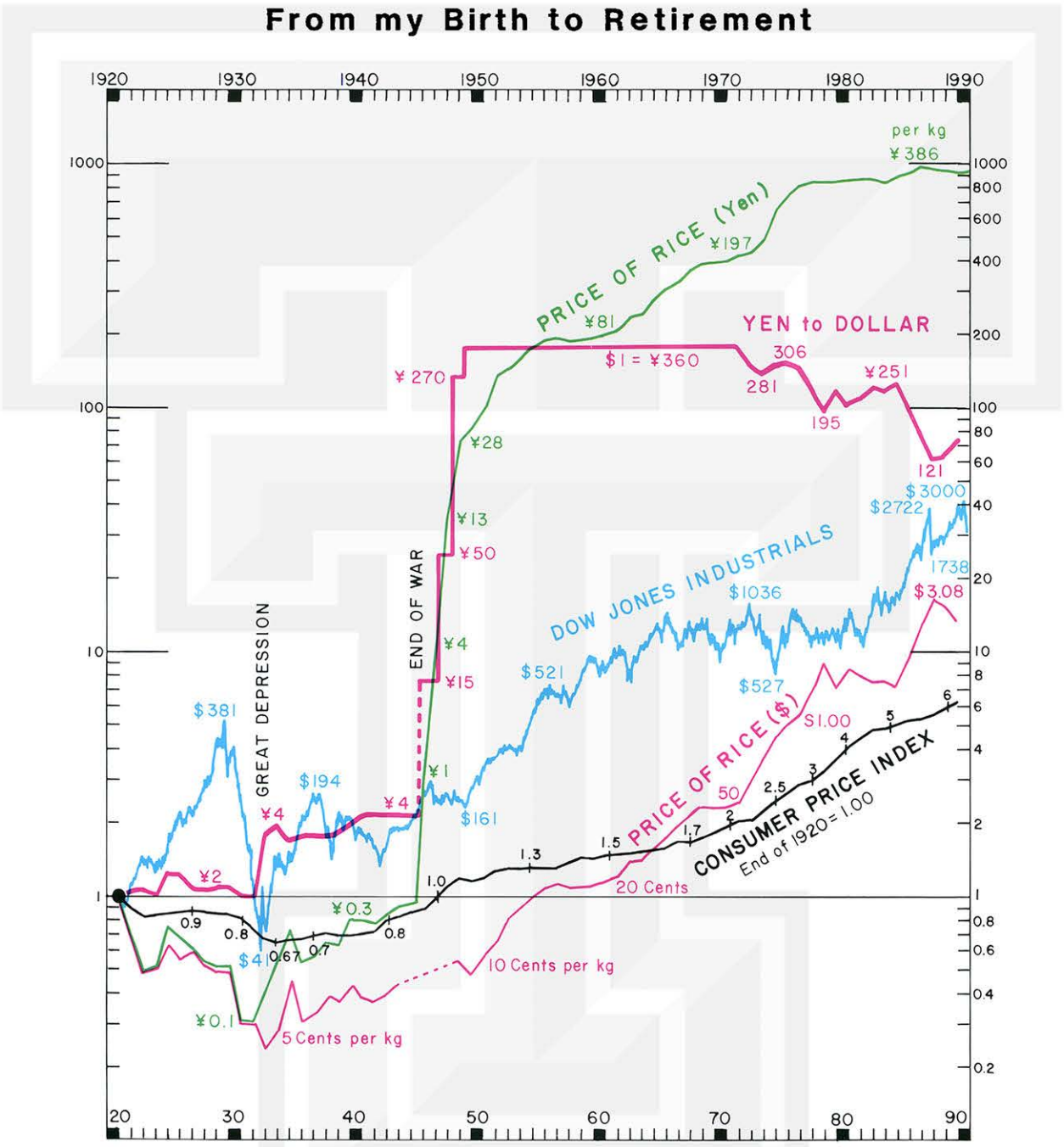

Fig. 6.4-1 A 4-cycle semi-log chart showing changes in financial parameters such as Dow Jones Industrials, U.S. Consumer Price Index (CPI), price of rice in Japanese yen, yen to dollar conversion rate, and the price of rice in U.S. dollars.

Although this logarithmic diagram does not represent the variation on natural coordinates, logarithmic values are excellent in depicting percent changes. The 36% drop in the Dow Jones from $2,722 to $1,736 during the Black Monday Crash was a minor drop in comparison with the 89% drop from $381 to $41 during the Great Depression.

Professor Irving Spergel. The purchase price was $18,000 which was approximately two times my pre-tax annual income at that time.

I paid $3,500 down and got a $10,000 mortgage at 5.5% interest from Hyde Park National Bank and a $4,500 second mortgage at 5.0% from the University of Chicago. Both were 12-year mortgages ending in November 1971.

Upon signing my mortgage contracts, I plotted a simple diagram (Fig. 6.4-2) showing the cumulative values of the payment on principal (blue) and interest (red). At that time, I was surprised to find out that I would have had to pay a total interest of $3,777 if I were to have paid off my mortgage in twelve years. Disturbed by the large sum of the interest, I paid a lump sum of $2,249 to the bank after ten years in order to pay off the $10,000 mortgage.

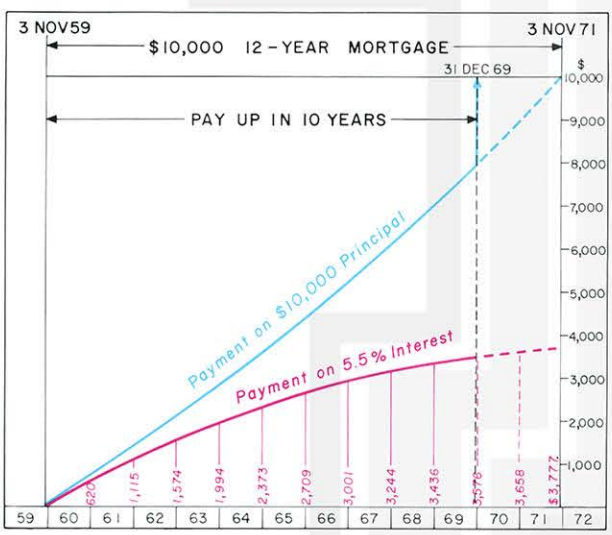

Fig. 6.4-2 Cumulative increase in the mortgage payments on the $10,000 principal and 5.5% interest.

Purchase of a Hypothetical House

In 1969, I decided to continue payments to a bank of my choice in the amount I would pay if I were to purchase a second, hypothetical house at the same location.

The hypothetical mortgage payments computed at that time were:

First mortgage on $10,000 at 5.5 %	$95.02
Second mortgage on $4,500 at 5.0%	$38.87
Interest on down payment	$23.11
TOTAL PAYMENT PER MONTH	$157.00

Unlike the positive mortgage I had paid for ten years, the negative mortgage will pay the interest back to me. This reverse process gives me a chance to recover the interest I had lost for purchasing the house I live in. In fact, this decision worked far better than I had initially anticipated.

After paying $157 a month for eleven years, the total accumulation with an average of 6.7% interest became $29,400, thanks to the higher than 5.5% interest rate I received at that time. Late in 1979, my wife told me that interest rates were rising rapidly and that we should switch our nest egg to a high-yield Certificate of Deposit (CD) at some point. It was April 2, 1980 when we consolidated the negative mortgage into one CD with an unbelievable 17% yield. Since then, we rolled over the CD into a succession of high-yield CDs until 1984 when we deposited them finally into a 10-year CD with a 12.25% compound interest maturing in February 1994, four years after my retirement. The value of the CD at retirement is $110,000 which will increase to $160,000 at maturity (Fig. 6.4-3).

I recall that the rapid fluctutation of high interest rates in 1979-83 (Fig. 6.4-4) was quite unusual. At that time, numerous savings and loans offered high-yield CDs to depositors. Furthermore, they offered higher interest rates for longer term deposits. Susie and I are pleased to have confirmed that my negative-mortgage home returned more interest to me than I had lost while paying for the positive-mortgage home in the 1960s.

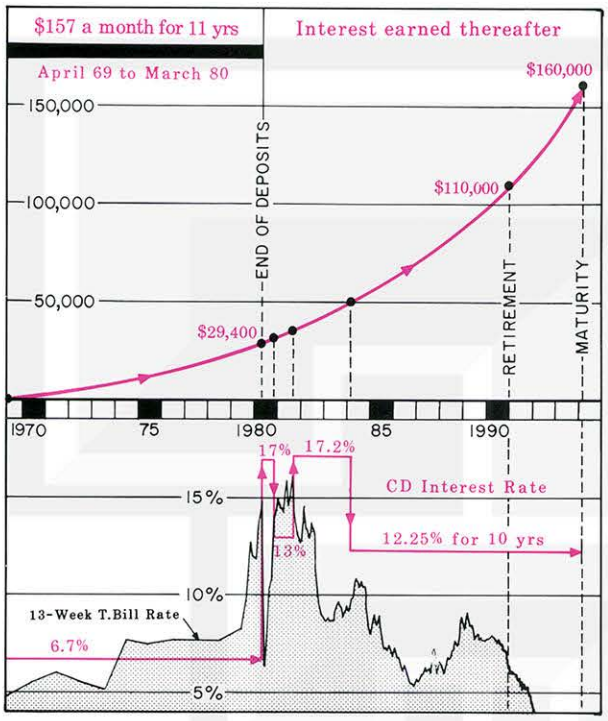

Fig. 6.4-3 My investment on a second (hypothetical) home. $157 was invested monthly assuming that my mortgage on the paid-up house still existed for the next eleven years.

The One-Two-Three Goal

Late in the 1950s, while flying from Washington, D.C. back to Chicago, I read a magazine article stating that we should not rely heavily on our Social Security System which could go bankrupt in the distant future. The article recommended highly that we accumulate our own investment capital and contribute to annuity funds offered by employers. Because I had no reason not to believe the story, I decided to save slowly but steadily in order to retire in Japan upon reaching 65, the retirement age of the University of Chicago at that time.

In 1960, I established a "One-Two-Three Goal" for my post-retirement income. The goal was to receive income from three different sources:—One Unit from Social Security,—Two Units from my personal investment, and—Three Units from TIAA/CREF (Teachers Insurance and Annuity Association/College Retirement Equities Fund).

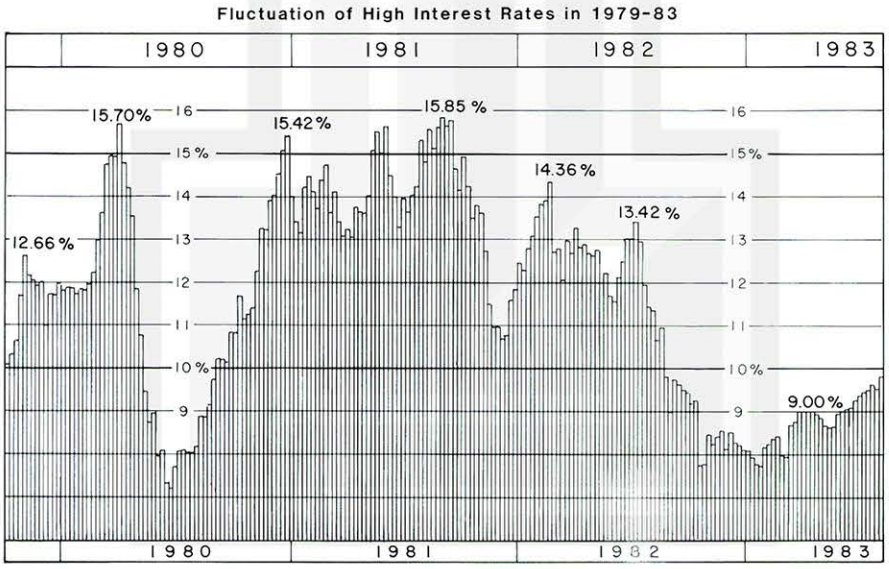

Fig. 6.4-4 A graph of high interest rates which changed once a week. Susie updated the weekly rates and I plotted the values to depict unusual ups and downs of the 6-month T-Bill rates.

Investment in Stock or CD

A number of my ethnic friends advised me to invest in stocks as well as CDs because they had made a lot of money by purchasing the right stocks at the right time. However, I decided to invest solely in high-yield CDs because I found no time to study the stock market. The exponential growth of CDs computed from the n-th power of (1+y), where n denotes the deposit years, and y, the annual yield, increases the initial capital by 10 times when y=8%, by 17 times when y=10%, and 30 times when y=12%. These values apply to 30-year compounds. Based on the concept of exponential growth, I made a simple diagram on my lifetime savings and expenditures.

Naturally, one's savings begin at the first employment and reach a lifetime peak at one's retirement. Thereafter, one enters a spending period. If one could use up one's entire assets upon death, the rate of spending would be ideal. In any event, our investment and spending will follow one of the three curves in Fig. 6.4-5.

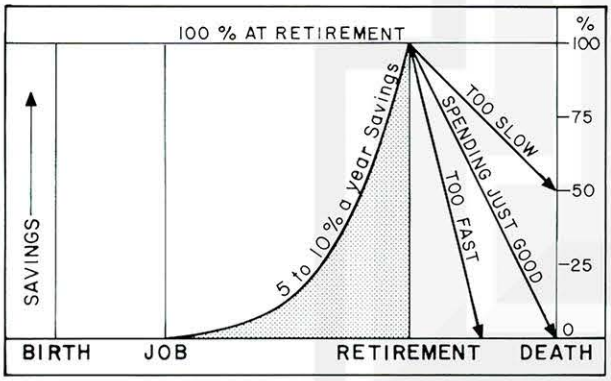

Fig. 6.4-5 Idealized accumulation of the personal investment from the first job to retirement. The post-retirement spendings reduce the accumulated amount. It is ideal to reduce the balance to zero after paying the final expenses.

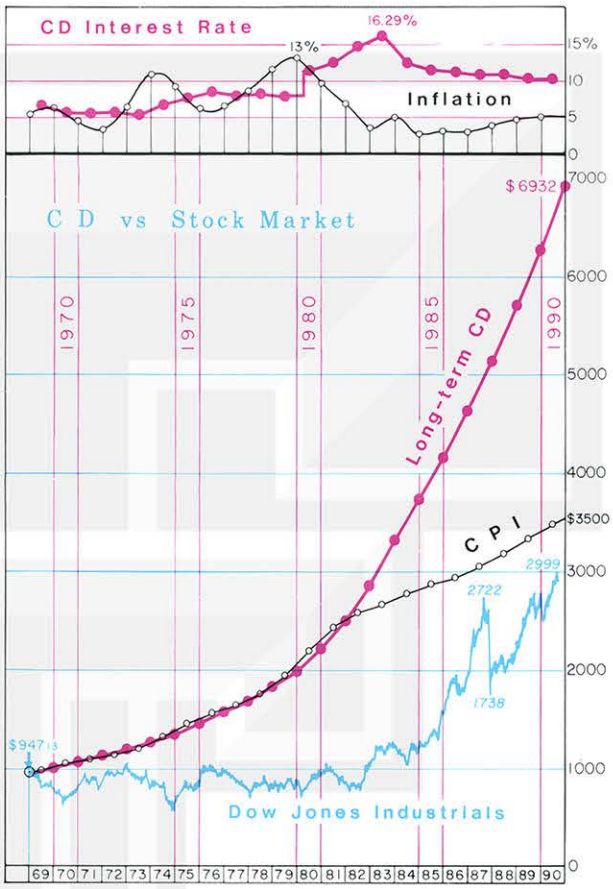

Fig. 6.4-6 A diagram showing the increase in Dow Jones Industrials during the past 22 years which was smaller than that of CPI. On the other hand, the average yield of my long-term CDs increased in cumulative value to $6,932.

A comparison of the curves in Fig. 6.4-6 is very interesting. Since 1969, the Dow Jones Industrials increased by the factor of 3.2 from $947 to $3,000. On the other hand, the CPI originating at $947 in 1969 increased by the factor of 3.7 to $3,500, which is slightly larger than that of the Dow Jones. The curve of the cumulative interest of my long-term CDs during the identical period increased by the factor of 7.3 from $947 to $6,932. This means that the equivalent value of my CDs reached more than twice the value of the Dow Jones, excluding dividends, had I bought these industrial stocks back in 1969.

Due to the availability of the high-yield, long-term CDs during the 20-year period before retirement, my nest egg kept growing exponentially fueled by the compound interest. I have not owned a single stock for investment. All I did in achieving the second goal was to save up to 6% of my salaries and generate additional CDs (Fig. 6.4-7).

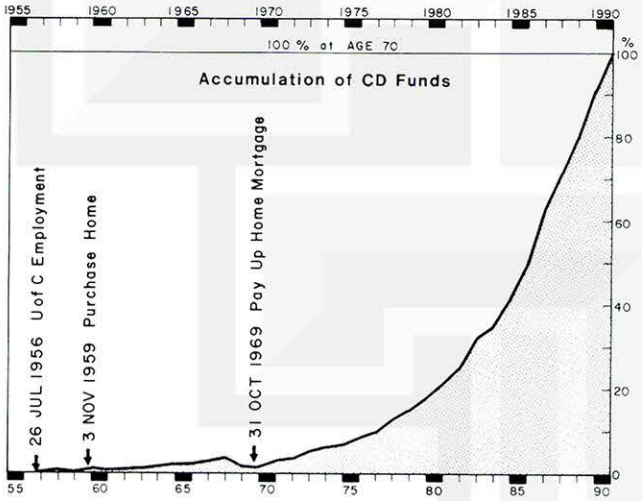

Fig. 6.4-7 Accumulation of my CD fund achieved by selecting long-term CDs and by saving up to 6% of my salaries.

Accumulation of TIAA-CREF

After my permanent employment at the University of Chicago, I was not eligible for the TIAA/CREF Program until becoming a faculty on April 1, 1962. For over 27 years thereafter, 5% of my salaries and 7.5% in matching funds by the university have been contributed every month to my TIAA/CREF funds. A total of 12.5% savings is the largest single accumulation which will generate my post-retirement income. Like most other professors, I made additional contributions to the SRA (Supplemental Retirement Annuity).

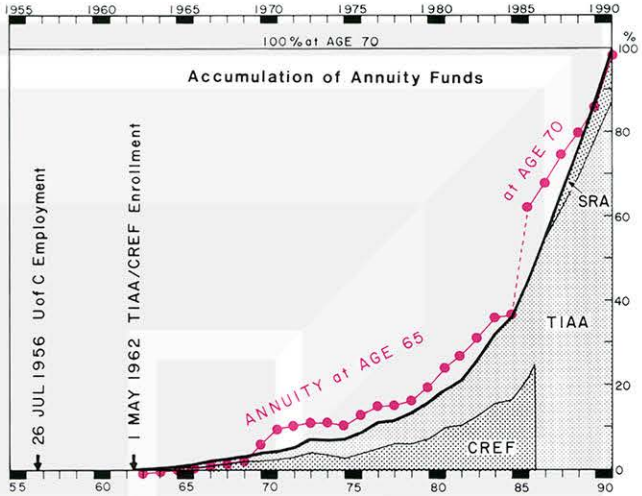

Fig. 6.4-8 Accumulation of my TIAA/CREF funds and the estimates of annuities which nearly doubled when the retirement age changed from 65 to 70.

Because the retirement age at the University of Chicago was changed from 65 to 70, the annuity estimates by TIAA through 1984 were based on the retirement at 65, and from 1985 based on the new retirement age of 70. An amazing thing about the annuity income is the 100% increase caused by the 5-year delay of the retirement year (Fig. 6.4-8).

One mistake I had made was the premature selection of the date of CREF to TIAA transfer. The date of my transfer was April 1986 when I predicted that the Dow Jones Industrials had reached a plateau after a significant climb. Unfortunately, the market began increasing nine months after the transfer and reached $2,722 shortly before the "Black Monday Crash" on October 19, 1987. Following the crash, the market began climbing again, reaching $2,999 before moving down after the Iraqi invasion of Kuwait on August 2, 1990. What I should have done was to have waited until August 1987 before transferring my CREF accumulation to TIAA (Fig. 6.4-9).

What made me happy after all was the fact that I could concentrate my efforts on storm research without worrying about the day-to-day change in the stock market

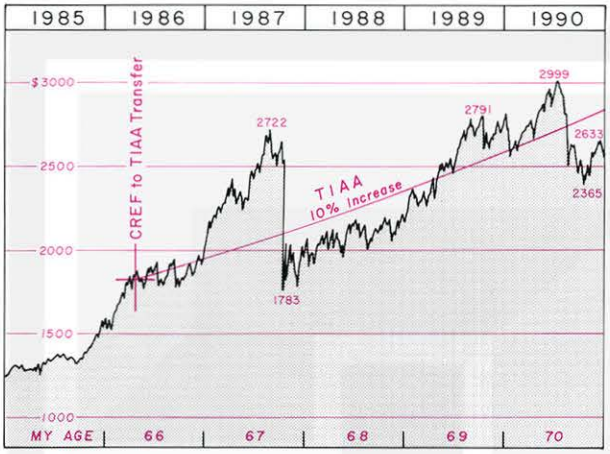

Fig. 6.4-9 Selection of the wrong time (year and date) in transferring from CREF to TIAA. I should have waited until before the Black Monday Crash when the Dow Jones hit the $2,722 mark.

to achieve my retirement goals. In particular, the rapid changes in the Dow Jones after the Black Monday Crash made a lot of investors sick and nervous, because the change was so fast that it can only be depicted in the plot with 30-minute resolution (Fig. 6.4-10). No meteorologist would have had time to follow up and predict future trades.

Although I am not sure if my investment was successful or not, I am pleased to reach my retirement upon achieving the One-Two-Three Goal without causing a financial strain on my family life.

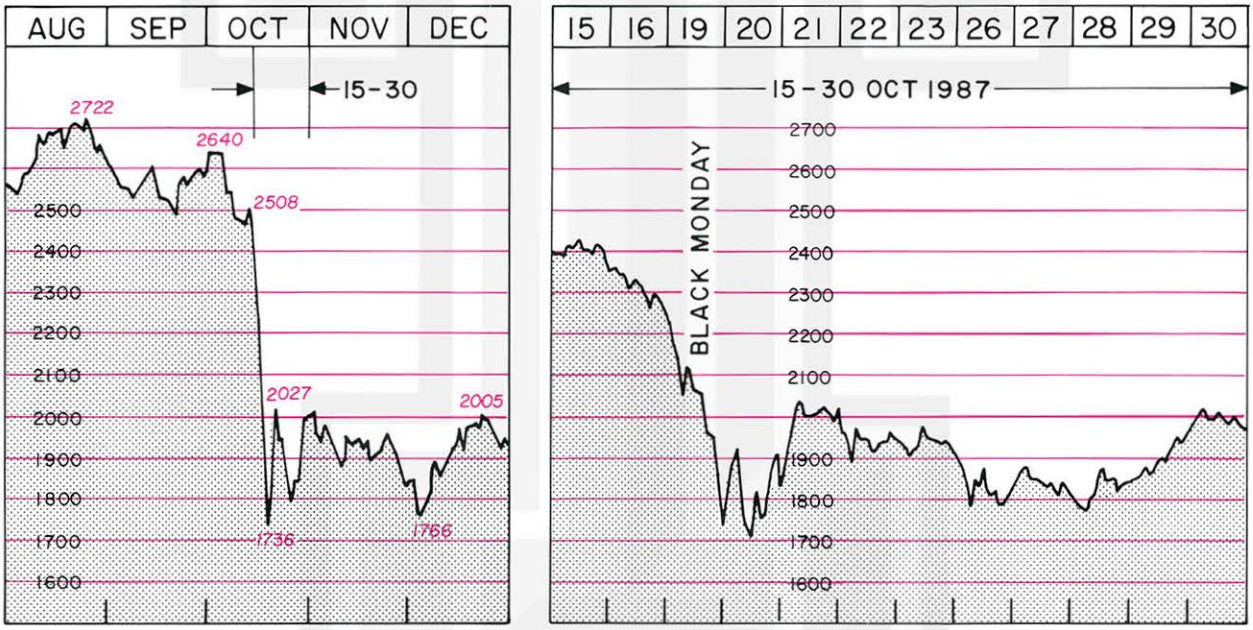

Fig. 6.4-10 The stock market crash of October 19, 1987. Left diagram: Depicted by daily closing values. Right diagram: Revealed by 30-minute interval data.

Blood Pressure Experiment

I was approximately 10-pounds obese in comparison with the standard weight of Japanese men in my age group. Realizing that this magnitude of obesity is a health hazard, I decided to reduce my weight to the standard level, taking one to two months.

In September 1983, I purchased a digital blood-pressure gage for monitoring blood pressure during my weight-reduction experiment. Anticipating diurnal variations of both body weight and blood pressure, I measured my weight once a day at 7:15 a.m. before breakfast. Because blood pressure changes were entirely unknown to me, systolic and diastolic pressures were measured three times a day at 6:30 a.m. before breakfast, at 6:00 p.m. before dinner, and at 11:00 p.m. after nightcap before going to bed.

Within one to two weeks after measurements began, I noticed that the diurnal variation of my systolic pressure was very large, reaching 20 to 40 mm. Surprisingly, it dropped 10 to 20 mm following moderate nightcaps. As my weight decreased gradually, the systolic pressure surged abruptly by 30 mm, while I felt a lack of energy due to malnutrition. Since then, I decided to eat more balanced foods and slow down the rate of weight reduction.

In December 1983, I stopped reducing my weight below 126 pounds after achieving a 14-pound reduction in three months. This magnitude of reduction resulted in the acceptable range of my systolic pressure, between 130 and 150 mm and that of diastolic, between 75 and 85 mm (Fig. 6.4-11).

In 1985, I decided to monitor my blood pressure during pre-retirement years. Because a blood-pressure gage with crystal sensor requires periodic calibrations, I purchased a mercury manometer from Sears Roebuck in order to use the gage for five years or longer without calibration.

On Memorial Day in 1987, I undertook frequent measurements of my health parameters, revealing that the diurnal variation of my body weight was 4.2 pounds (1.9 kg) with a minimum before lunch and a maximum after dinner. As expected, my weight jumped as much as I ate and discharged. However, the rate of weight decrease due to breathing and perspiration was approximately 0.3 pound/hour (Fig. 6.4-12).

The normal range of my pulse was between 60 and 72 per minute. During my stress tests with a stationary bike and a lawnmower, peak rates reached 100 to 120 per minute,

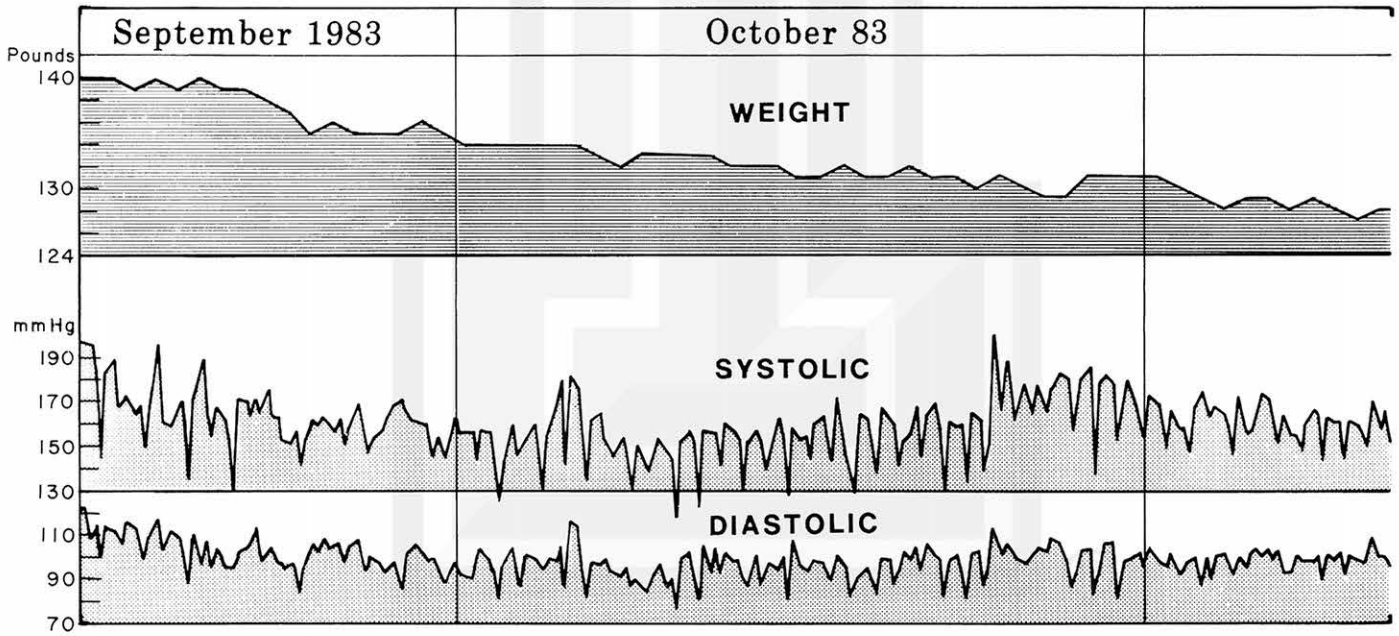

Fig. 6.4-11L My first experiment on weight reduction. Both systolic and diastolic blood pressures decreased with the loss of weight from 140 to 128 pounds.

returning to normal within less than 10 minutes. My systolic pressure dropped by 10 after urination, meal, or nightcap. An exercise with a lawnmower resulted in a significant drop due to body warm-up and perspiration. A drink of a cup of hot tea caused a 20-mm drop, suggesting that a warm-up causes expansion of the blood vessel.

A long-term plot of my weight, systolic and diastolic pressures was generated by measuring the values daily and averaging them three times a month. The result presented in Fig. 6.4-13 reveals a number of significant variations indentified by letters, A, B, C, D, etc. It was found that these variations are related to obesity (A), struggle in research (B and C), relaxed periods (D and E), and sore throat due to weight reduction (F and G).

The first indication of sore throat due to the second experiment of weight reduction occurred on May 2, 1989 accompanied by an increase of my systolic pressure from 145 to 167 mm. Several days later it peaked to 207 mm, resulting in the averaged systolic pressure of 169 mm during the first 10 days of May.

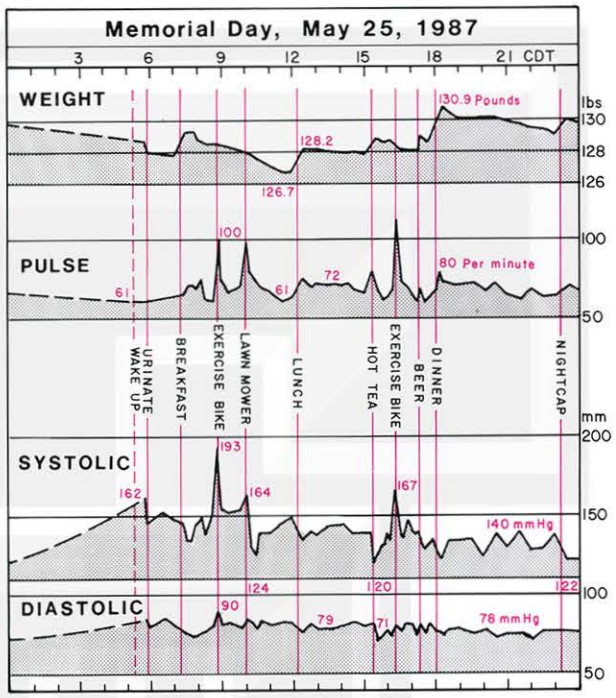

Fig. 6.4-12 Diurnal variation of my weight, pulse, and blood pressure. Three stress tests were conducted by using exercise bike and lawnmower.

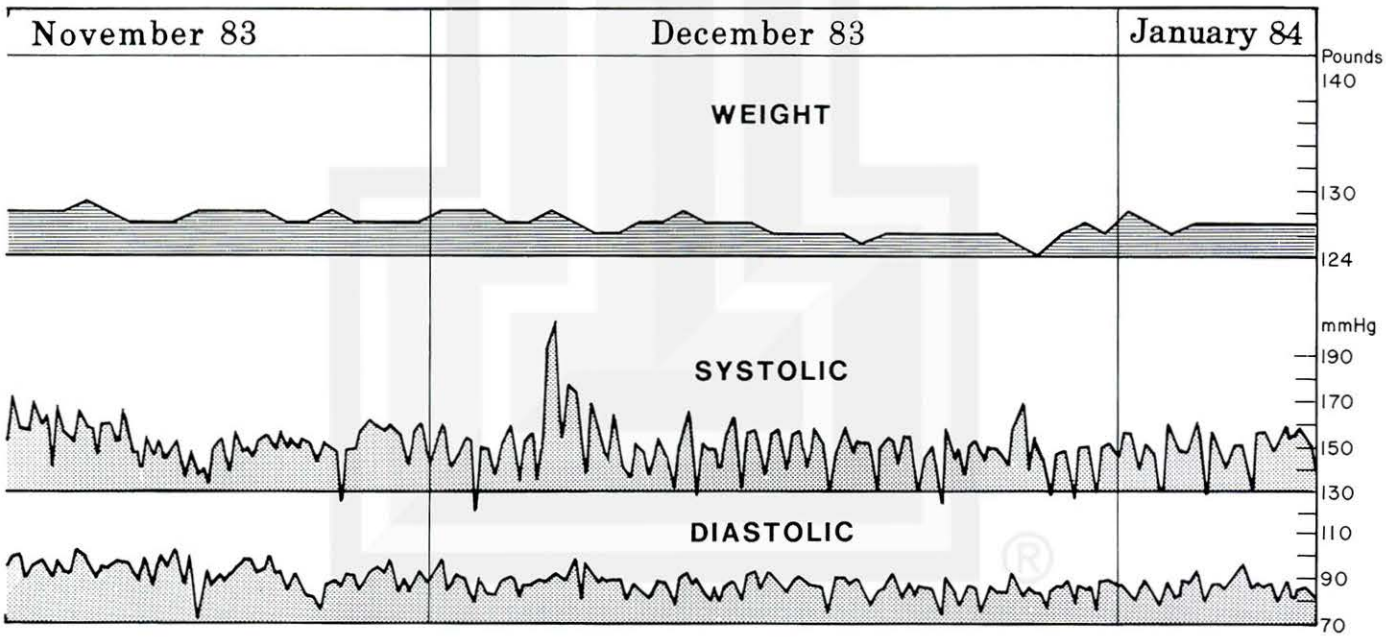

Fig. 6.4-11R Further decrease in my blood pressure when the weight was reduced from 128 to 124 pounds. At this point, I realized that the loss of weight was excessive.

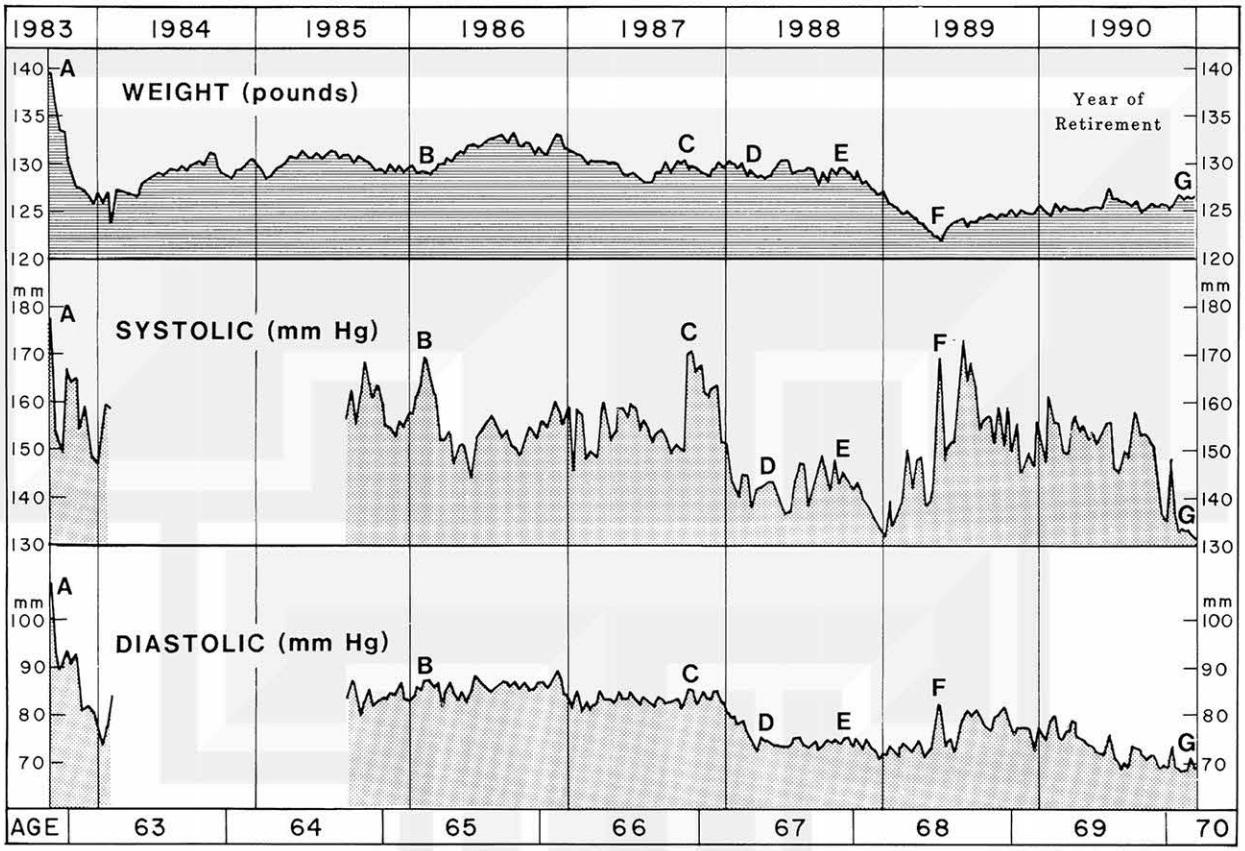

Fig. 6.4-13 My health parameters measured from Autumn 1983 to retirement. I conducted two weight-reduction experiments: the first one in 1983 and the second, in 1988-89. It turned out that my systolic pressure is not correlated to the body weight, but my diastolic pressure decreased with my age.

As a matter of curiosity, I undertook frequent measurements in the weekend of May 14-15 (Fig. 6.4-14) in an attempt to determine the nature of my blood-pressure variation associated with the sore throat during the weight reduction. At 6:00 p.m. on Saturday, my systolic pressure was 172 mm. During the evening hours, it decreased to 132 after relaxation and nightcap. The normal systolic pressure was measured at 7:00 a.m. on Sunday.

Immediately after lunch, my systolic pressure accompanied by a feeling of sore throat reached 202, but I did not feel anything about the high blood pressure. In the evening, I participated in a dinner party and returned home as usual, measuring the 161 mm systolic pressure before bedtime. During the middle of the night when I felt sore throat a couple of times, the pressure was 205 mm at 2:00 a.m. and 200 mm at 6:00 a.m. on Monday, May 16.

What I learned through the weight-reduction experiment was that I should not reduce my weight below the 126-pound threshold, at which I feel lack of energy and vitality, resulting in (1) irritation, (2) sore throat, and (3) transient high blood pressure.

The diurnal variation of my blood pressure was determined by averaging the 105-day measurements at 6:00 a.m. before breakfast, 6:00 p.m. before dinner, and at 11:00 p.m. after nightcap before going to bed (Fig. 6.4-15). The results revealed that my blood pressure is highest at the wake-up time

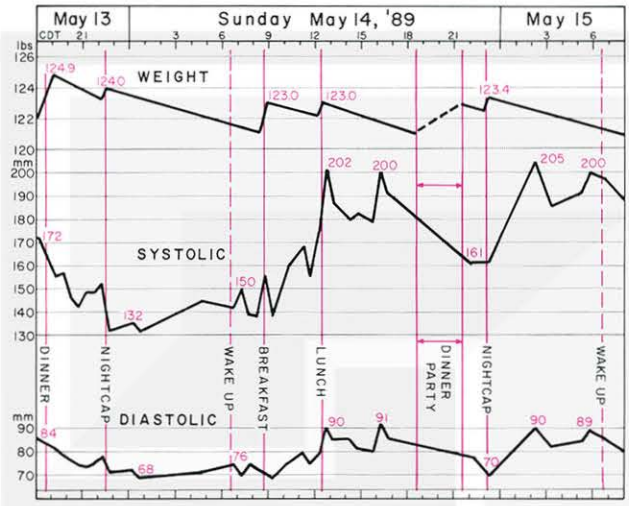

Fig. 6.4-14 Transient increases of my blood pressure induced probably by a feeling of irritation and sore throat associated with weight reduction below the 126-pound threshold.

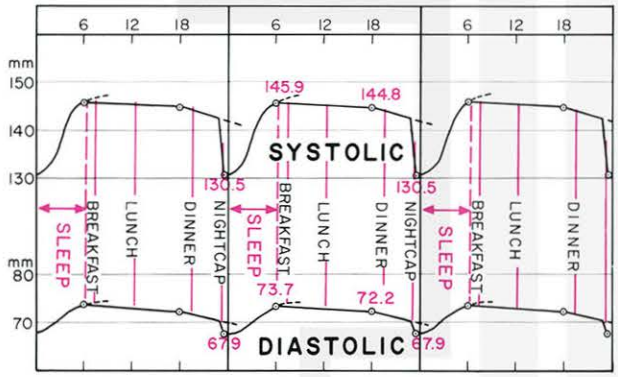

Fig. 6.4-15 Normal diurnal variation of my blood pressure which increases somehow while sleeping in bed and decreases during daily work. A significant drop occurs during a nightcap.

and decreases as my working day wears on. Apparently, my systolic pressure decreases with my activities, wash up, breakfast, walking to my university office on the 4th floor. On the contrary, my blood pressure remains elevated when I stay in bed too long on holidays.

Although I do not understand the reason for my elevated blood pressure in the morning while in bed, other persons may be experiencing similar diurnal variations, because fatal heart attacks are known to occur frequently in the morning hours, 4:00 a.m. to 10:00 a.m., when the systolic pressure is expected to be high. I also hear from my senior friends that those who lose their work incentive after retirement are likely to go under, much quicker than those who keep working regularly after reaching the retirement age.

Photographic Experiment

Explosion of Fuss Volcano

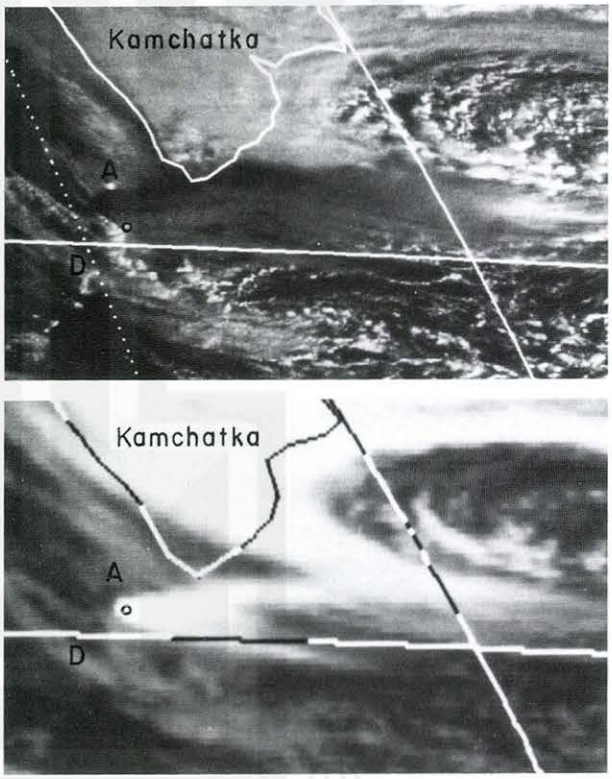

Fig. 6.4-16 Eruption of Fuss Volcano evidenced by the GMS imagery at 00 GMT 20 NOV 1986. Top: Visible photo showing dark, gray volcanic clouds from the volcano indicated by a circle. A denotes Alaid Volcano and D, Onekotan Island. Bottom: Infrared photo of cold volcanic clouds drifting eastward from the volcano.

On November 20, 1986 while flying from Chicago to Tokyo on board Japan Air Lines Flight 009 on the northernmost Pacific route, my wife told me, "I see a huge thunderstorm on the right side of the aircraft." Although it was the unlikely season to see a full-grown thunderstorm in the direction of Kuril Islands, I could clearly identify a huge convective cloud with an overshooting top. It appeared like a giant black cumulonimbus with a black anvil cloud and a dark overshooting dome.

At the Meteorological Satellite Center in Kiyose, I examined both visible and infrared pictures of the Japanese Himawari satellite at 00 GMT on November 20, revealing that the thunderstorm-like cloud was a violent eruption cloud of Fuss Volcano on Paramushir Island (Fig. 6.4-16). The volcano has a long history of violent eruptions of the central cone once every 50 to 100 years. What we saw was a very rare event.

Aerial Photos of Kuril Volcanoes

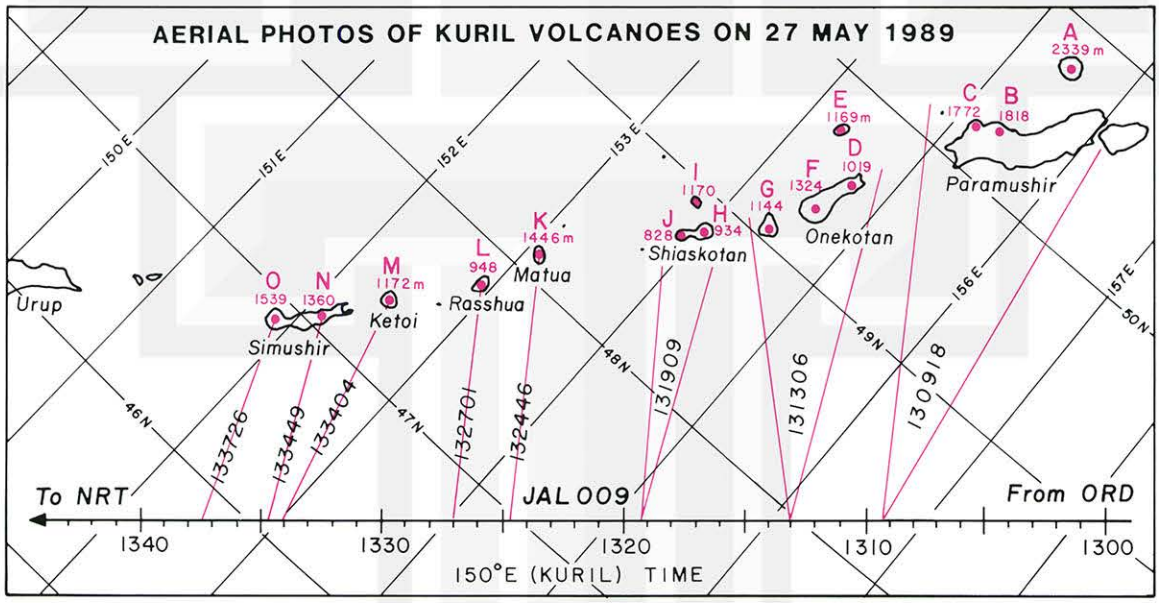

Fig. 6.4-17 Path of JAL 009 on 27 May 1989 on the Northernmost Transpacific Route R-220 when the Kuril Volcanoes were photographed through a right-side window. Photographic data: Minolta camera with Vivitar 105-mm lens, Kodacolor ASA 400 film.

Fig. 6.4-18 A — Alaid Volcano (295-km away) on Atlasov Island. B — Chikurachki Volcano (243 km), and C — Fuss Volcano (249 km) on Paramushir Island.

Fig. 6.4-19 D — Nemo Volcano (207 km), E — Makanrushi Mountain (240 km), F — Krenitsyn Volcano (193 km), and G — Severgin Volcano (178 km) on Kharimkotan Island.

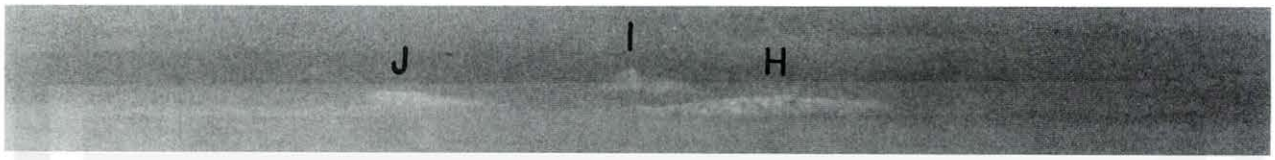

Fig. 6.4-20 H — Sinarka Volcano (180 km), I — Ekarma Volcano (199 km), and J — Kuntomintar Volcano (175 km). H and J are on Shaskotan Island.

Since then I was interested in taking telephoto pictures of Kuril Volcanoes during transpacific flights on clear days. Fortunately, my dream came true on May 27, 1989 while flying on the northernmost Pacific route from Chicago to Tokyo on JAL 009 (Fig. 6.4-17).

After passing far to the south of Kamchatka Peninsula, I could see the conical peak of Alaid Volcano (2339 m), the tallest volcano in the Kuril chain. Seen on the foreground island of Paramushir (Fig. 6.4-18) are Chikurachki Volcano (Chikura Take) and Fuss Volcano (Shiriyajiri Take), the eruption of which on November 20, 1986 was observed as a black thunderstorm. In spite of the long distance to these volcanoes, they are clearly identifiable.

Then I photographed Krenitsyn Volcano (Kuroishi Yama), the central cone of a crater lake and Severgin Volcano on Kharimkotan Island (Fig. 6.4-19). Since then the distance from our aircraft to the volcanoes became less than 200 km. I was beginning to see snow-covered valleys on volcano slopes (Fig. 6.4-20).

The central peak of Matsuwa Island is Sarychev Volcano (Fuyo Yama) with its history of central cone eruptions every 10 to 15 years. The recorded eruption dates back to the 1760s. Thereafter, the volcano erupted in 1878, 1928, 1930, 1946, and 1960, generating hugh scorching clouds and showers of volcanic stones. Seen from the aircraft is a pointed peak of the central cone (Fig. 6.4-21).

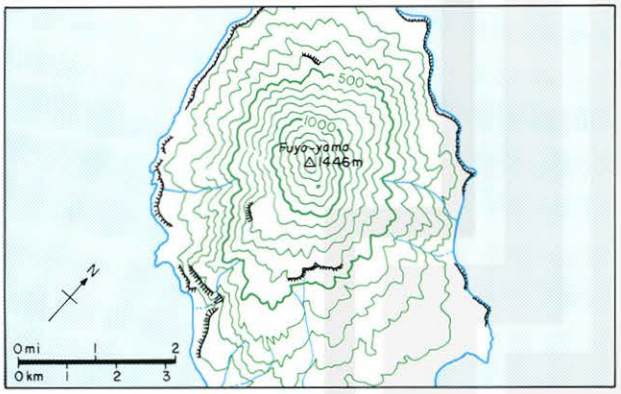

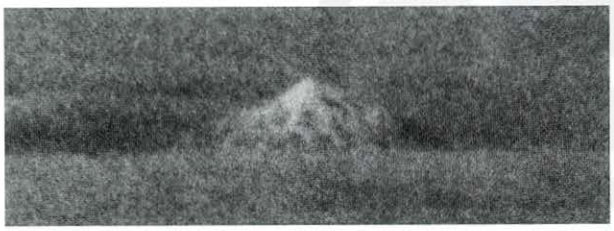

Fig. 6.4-21 K — Sarychev Volcano (Fuyo Yama), the 1446-m center peak of Matsuwa Island, 160 km from the aircraft.

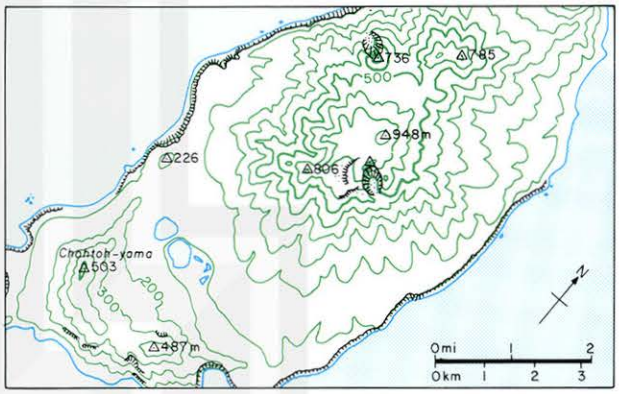

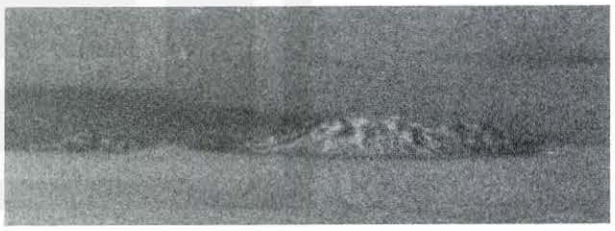

Fig. 6.4-22 L — Rasshua Volcano, the 948-m tall peak, 140 km from the aircraft, on Rasshua Island. Seen on the left side of the peak is Chohtoh Yama.

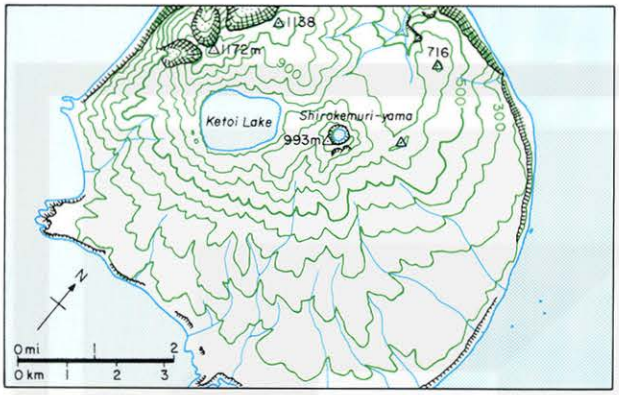

Fig. 6.4-23 M — Pallas Volcano (Shirokemuri Yama), 993-m tall and Ketoi Volcano, 1172-m tall, 140 km from the aircraft, on Ketoi Island. There is a volcanic Ketoi Lake between the two volcanoes.

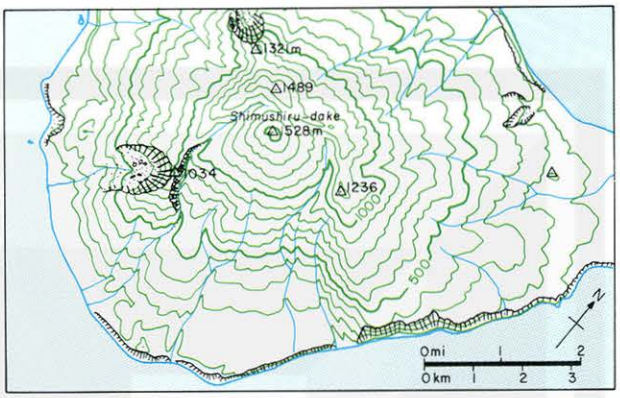

Fig. 6.4-25 O — Goryashchaya Spoka Volcano (Shimushiru Dake), 1528-m tall, 127 km from the aircraft, on the southwest end of Simushir Island.

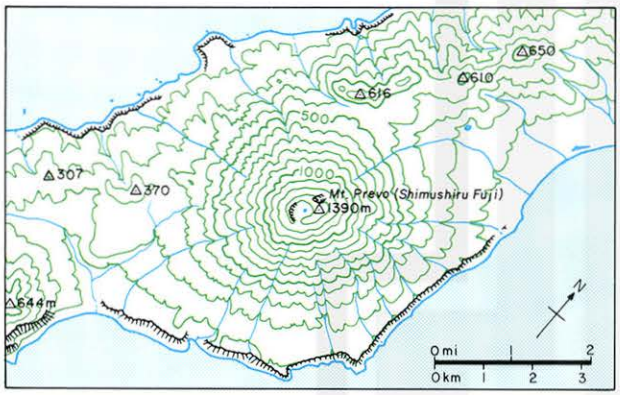

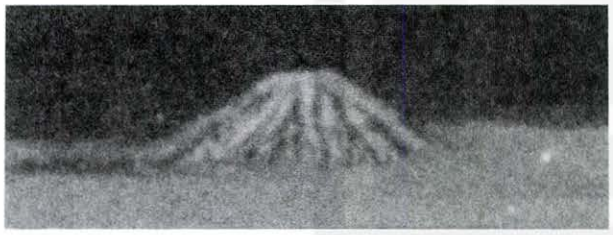

Fig. 6.4-24 N — Prevo Volcano (Shimushiru Fuji) 1390-m tall, 125 km from the aircraft, on Simushiru Island. This volcano appears like Japanese Mt. Fuji.

Eruptions of Rasshua Volcano (Fig. 6.4-22) occurred in 1846 and 1957. Thereafter, the volcano slope has been eroded into snow-covered small valleys. The top of Ketoi Island is characterized by twin peaks, 993 m Pallas Volcano (Sirokemuri Yama) and 1172 m Ketoi Volcano. These peaks with snow-covered slopes and cliffs are visible from a distance of 140 km (Fig. 6.4-23).

The most beautiful volcano I photographed is Mt. Prevo known as Shimushiru Fuji, 1390 m tall (Fig. 6.4-24). Since its eruptions in 1765 and 1825, the volcano has been resting like Mt. Fuji in Japan. Goryashchaya Spoka Volcano (Shimushiru Dake) erupted rather frequently, once every 10 to 40 years, but its mode of eruption has been rather mild, producing lava domes and scorching clouds. The central cone has a gentle slope, giving an impression of a large double crater. (Fig. 6.4-25).

Aerial Photographs of Mt. Fuji on 31 May 1989

Unusually clear views of Mt. Fuji, the 3,776 m (12,358') tall sacred mountain of Japan were photographed through the right-side window of Japan Air Lines Flight 105 from Tokyo to Osaka. The snow-covered mountain was surrounded by scattered cumuli.

For determining the overall cloud cover during the photographic period, 0914 through 0919 JST, both visible and infrared pictures from Himawari, Geostationary Meteorological Satellite of Japan at 0900 scan start-time were received at the Meteorological Satellite Center at Kiyose. Images were then combined into a false-color picture (Fig. 6.4-27) in which cloud-free areas appear dark brown and cold cloud tops, either gray or white.

The first picture (Fig. 6.4-28) shows the snow-covered Akashi Range in the background. As the line of sight of the mountain rotated due to aircraft motion, background mountains moved right to left. The last view of Shirane-san appears near the left edge of the second picture (Fig. 6.4-29) in which snow-covered high peaks in the distant background are those in the Japan Alps, 120 km away.

The explosion crater on the mountain slope in Fig. 6.4-30 was generated in December 1707 (4th year of Hoei), opening up a 0.8 km³ (0.2 mi³) volume of the mountain. As the aircraft flew around, the Hoei Crater turned clockwise around the mountain (Figs. 6.4-31 and 32).

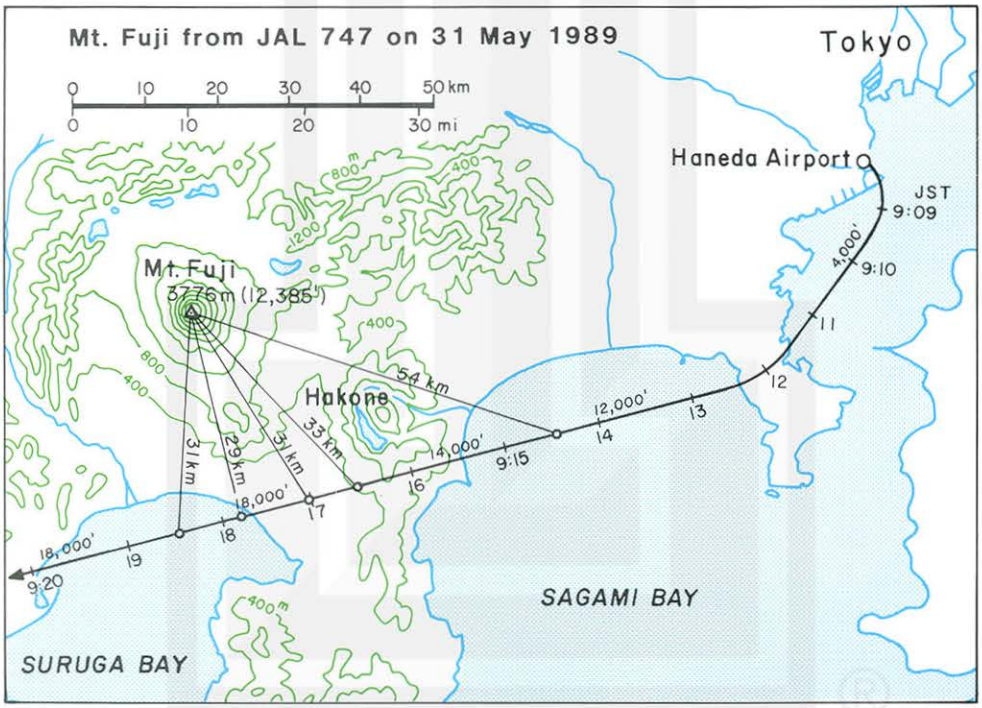

Fig. 6.4-26 The path of JAL Flight 105 from Tokyo to Osaka on 31 May 1989. A sequence of pictures were taken through a right-side window from 4,000 to 5,500 m altitudes.

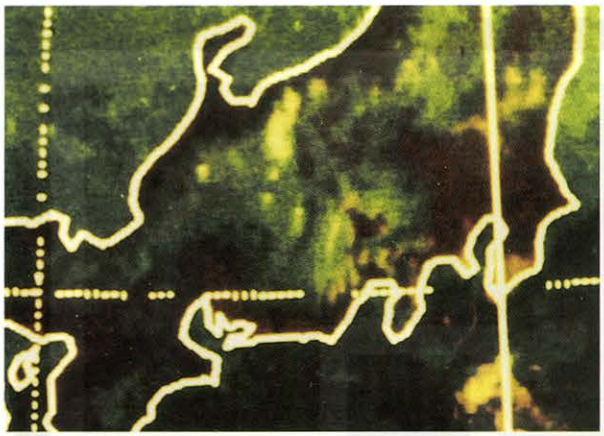

Fig. 6.4-27 A false-color photo generated by double exposed visible and infrared pictures with green and red filters, respectively.

Fig. 6.4-28 Mt. Fuji at 09h14m26s on 31 May 1989 taken from 4,000 m (13,000') toward WNW, 54 km away.

Fig. 6.4-29 Mt. Fuji at 09h16m36s on 31 May 1989 taken from 5,200 m (17,000') toward toward NW, 33 km away.

Fig. 6.4-30 Mt. Fuji at 09h17m04s on 31 May 1989 taken from 5,500 m (18,000') toward NW, 31 km away.

Fig. 6.4-31 Mt. Fuji at 09h17m50s on 31 May 1989 taken from 5,500 m (18,000') toward N, 29 km away.

Fig. 6.4-32 Mt. Fuji at 09h18m28s on 31 May 1989 taken from 5,500 m (18,000') toward NNE, 31 km away.

6.5 Memorable Events

In comparison with the flying range of migrating birds, the traveling distance in my childhood years was extremely short, only less than 50 km (30 miles) from my birthplace. Consequently, my vision of the world was no more than that of a small frog in a deep well.

My first long-distance travel was to an ore mine in Korea, a part of Japan in 1940 when I was 20 years old. The second, and the most exciting and memorable trip, was a transpacific flight in 1953 when I came to the University of Chicago as a visiting research associate. Since then,

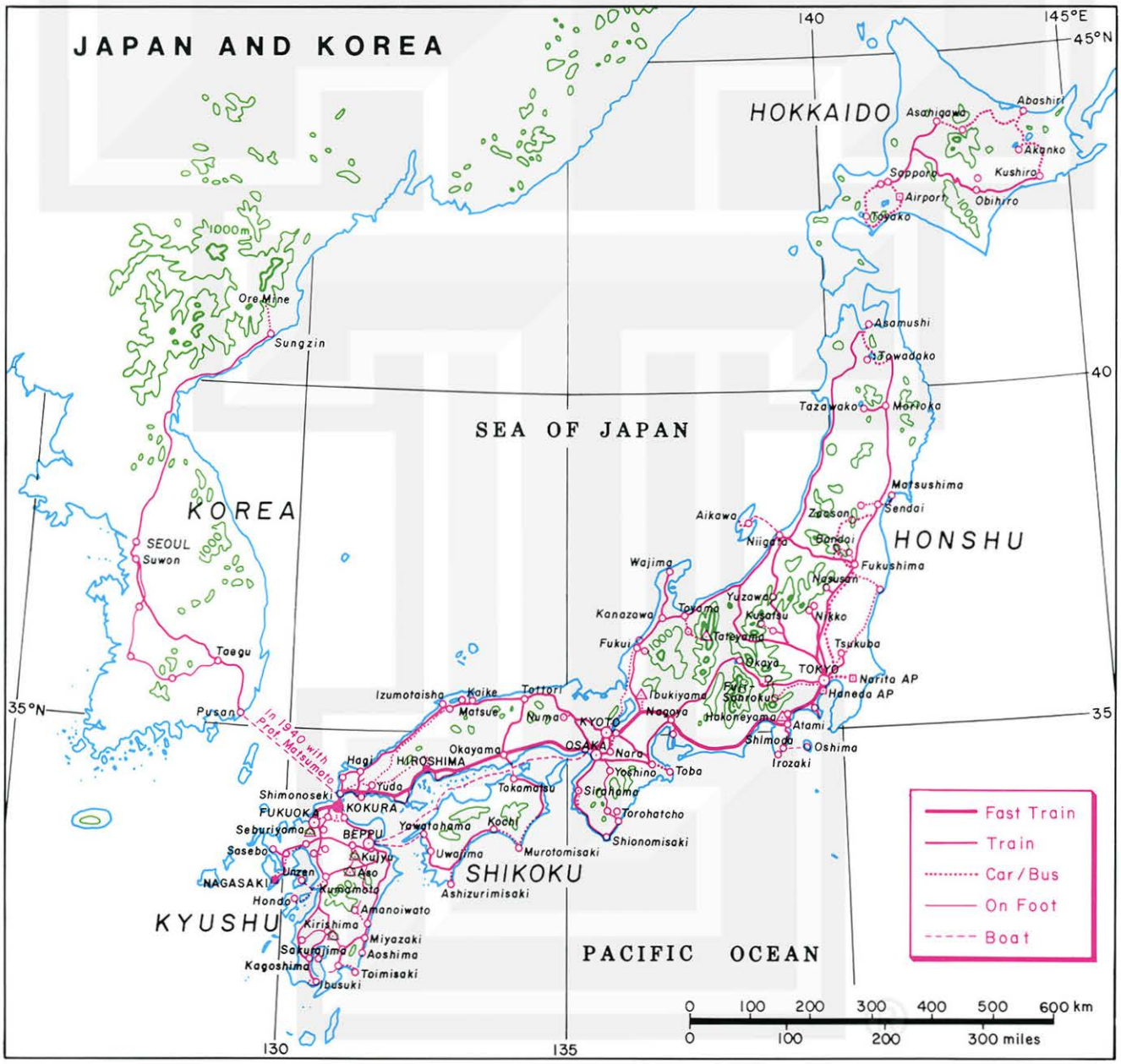

Fig. 6.5-1 My travel routes in Japan and Korea. The first long-distance travel was the geological field trip to Korea in 1940 with Prof. Matsumoto. Thereafter, I traveled all over Japan consisting of the four major islands of Kyushu, Shikoku, Honshu, and Hokkaido.

Aso Volcano

Leaning Smoke Cloud

Initial Explosion

Second Explosion

Falling Ashes

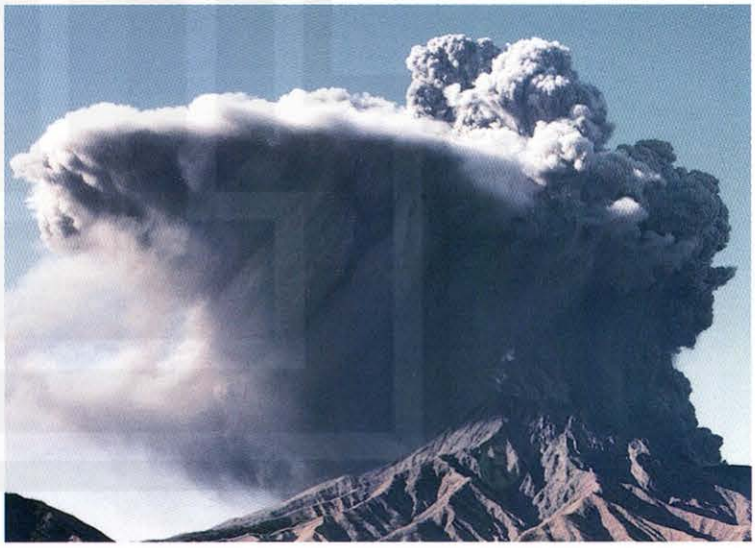

Large Anvil of Ashes

Fig. 6.5-2 A series of photographs showing an eruption of Aso Volcano on 26 November 1989. This rare sequence of photos were taken by my brother, Sekiya Fujita, looking west from the east rim of the Aso Caldera.

I traveled by air, train, boat, automobile, and on foot for conducting all types of researches, large or small scale, official or educational, all around the world except in the communist countries where taking aerial photographs were prohibited. Presented in this section are the memorable events I experienced ever since the small frog leaping in Kitakyushu became airborne in August 1953.

Geological Field Trips

A number of geological field trips guided by my mentor professor Matsumoto enlarged my vision. My 800-km trip to Korea started at Shimonoseki where I took a ferry boat to Pusan and then a train to Taeque (Fig. 6.5-1). A group of our students walked 200 km to Suwon, ending the initial group trip at Seoul, a large city surrounded on all sides by low mountains. Thereafter, Prof. Matsumoto and I took a sleeper train to Sungzin where we stayed in a small Korean inn equipped with a floor-warming device called "ondoru" in Japanese. It consists of a network of smoke tubes laid under the floor. The hot air exhaust generated by cooking, etc., passes through these tubes before escaping through the chimney. It was the most economical system of heat exchange I have ever seen.

Upon reaching an ore mine, 50 km north of Sungzin, we took a narrow-gauge railcar which runs through a dusty straight tunnel. At first, I saw a red light toward the end of the tunnel. As the car approached the red light, the color began changing gradually into orange then yellow and finally to white. The light I observed from the moving railcar was not an artificial light, but rather the bright sunlight outside the other end of the tunnel. What I saw first was the red-light spectrum of the sunlight, which penetrated the dusty air in the tunnel by virtue of its long wavelength.

In 1940 and 1941, until the onset of the Second World War on 7 December 1941, I took a number of field trips with Prof. Matsumoto, learning how to determine dips and strikes, to map hidden layers of lava flows, etc. I was pleased to visit Aso-san volcano, the central cone of Aso Caldera (Fig. 6.2-3). It has been the most active volcano in Kyushu. During the eruptions on 26 November 1989, my brother took a beautiful sequence of color photos looking west toward the central cone of Aso (Fig. 6.5-2).

During another trip, we visited Taketa City, home of the song, "Moon Over the Ruined Castle." We continued to Sobo-san mountain, Obira ore mine, finally to the "Rock Gate of Heaven" (Amano Iwato) where the Japanese legendary goddess (Amateras Ohmikami) was hiding. During the winter recess, he took me to a field trip to the Kushikino gold mine and to Kirishima volcano, ending the trip at the top of Takachiho-no-mine, a 1574-m volcano dormant since 1914. I learned that an early Japanese legendary god descended from heaven to the top of the dormant volcano.

Kyushu, Japan to Chicago

First, I wish to express my sincere appreciation to Prof. Horace R. Byers for providing me with an eye-opening opportunity to study meteorology at the University of Chicago.

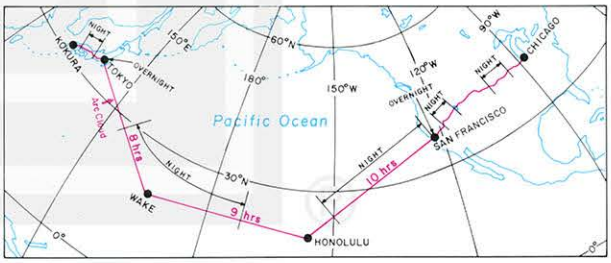

Fig. 6.5-3 My first transpacific flight by Pan American propeller aircraft which took 27 flight hours with refueling stops at Wake Island and Honolulu, Hawaii.

Fig. 6.5-4 Prof. Syono and I standing in front of his residence. Photo by Tatsuko Fujita on 7 August 1953.

Fig. 6.5-5 The tail of the Strato Clipper photographed shortly before departing from Haneda Airport, 1300 Tokyo Time on 8 August 1953.

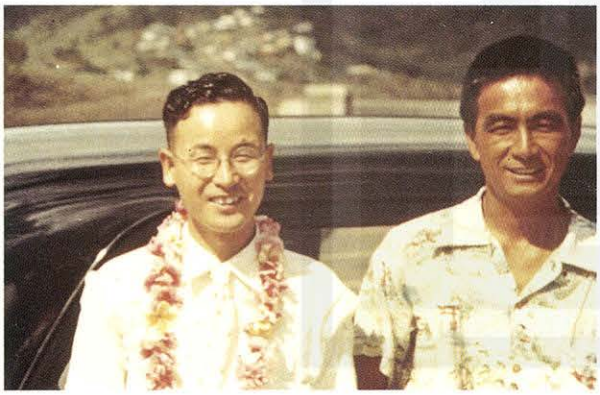

Fig. 6.5-6 An ALOHA welcome at Honolulu Airport with a lei of flowers around my neck, 1500 Hawaii Time on 8 August 1953.

Fig. 6.5-7 A walk toward the International House, the University of Chicago, on 12 August 1953 upon my arrival.

Fig. 6.5-8 Tetsuya Fujita in Room 848, International House with a cup of Coca Cola, 13 August 1953.

Fig. 6.5-9 The Museum of Science and Industry in either 1953 or 54 illuminated by 10,000 Sylvania flash bulbs. Exposure was 3 minutes at F5.6 to include the fireworks following the flash.

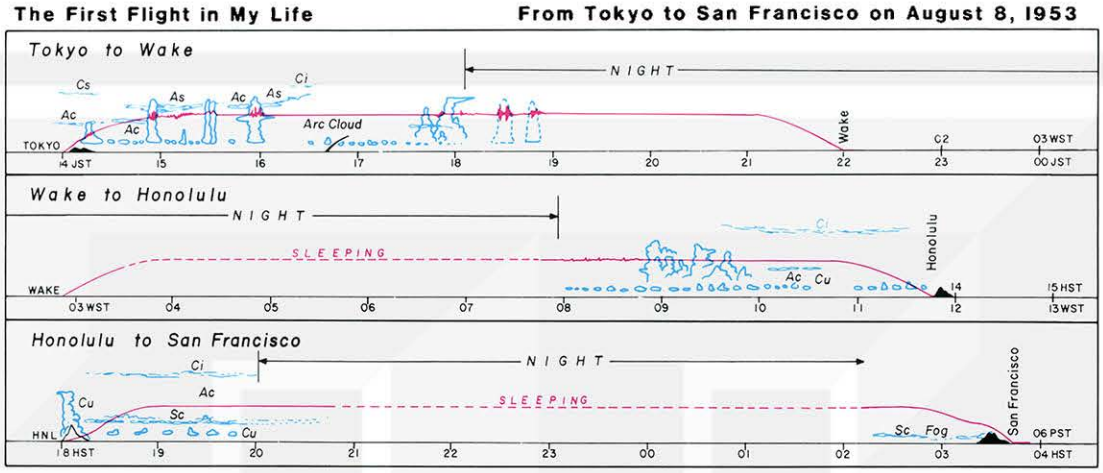

Fig. 6.5-10 Vertical cross sections sketched during my first transpacific flight on 8-9 August 1953. The three cross sections are: 8 hours from Tokyo to Wake; 9 hours from Wake to Honolulu, and 10 hours from Honolulu to San Francisco. Dashed red lines denote lack of observation due to sleep.

Fig. 6.5-11 An arc cloud I photographed at 1640 JST on 8 August 1953, looking south. Estimated location was 31°N and 150°E.

As soon as I received his letter of invitation, I checked the transpacific air fare, learning that Pan American was the only airline with the one-way fare of $650. In 1953, I was receiving a 220,000 yen ($50) per month salary from the Kyushu Institute of Technology. The only air fare available at that time was identical to my 13-month salary. Nevertheless, I was eager to observe clouds from the air for the first time in my life and a decision was made to borrow the air fare. This was my first "fly now, pay later" plan.

On 6 August 1953, I took an overnight train from Kokura to Tokyo with my wife Tatsuko. She wanted to celebrate my first flight with Prof. Syono of the University of Tokyo and to see me off at the Haneda International Airport. Because Prof. Syono was also preparing for his first visit to the United States, we were so happy to discuss foreign trips which had been rare events in post-war years. Tatsuko took our smiling picture in front of his house in Urawa City (Fig. 6.5-4).

At 1300 JST on August 8, Pan American Strato Clipper N1024V (Fig. 6.5-5) left the gate and taxied to the departure end of the runway. It took over 30 minutes in testing the engines for the long over-water flight. While on the ground, they announced two refueling stops at Wake Island and Honolulu, Hawaii (Fig. 6.5-3).

After the brake release at 1400 JST, the Clipper accelerated rapidly and became airborne. I spoke to myself that I was now flying for the first time in my life. Without wasting the expensive flight time, I began sketching the vertical time cross section of clouds along the flight path (Fig. 6.5-10). Shortly before 1600 JST, the aircraft flew into towering cumuli, encountering severe turbulence. I heard crashing sounds of dishes and utensils in the flight kitchen. A moment later, the flight became smooth and I saw a beautiful arc of low clouds (Fig. 6.5-11).

The aircraft landed Wake Island at 2200 JST (0100 Wake Time on 9 August). It was a very humid tropical night when a bus took passengers to the waiting area where tropical drinks were served. At 0250 Wake Time, the Clipper began flying the second leg to Honolulu. In about three hours thereafter, we crossed the International Date Line, turning the date back one day to 8 August. The time and date changes were rather complicated to me, the first-time international traveler.

At about 0800 Wake Time, I began seeing orange-colored tropical cumuli with considerable vertical growth. Without encountering noticeable turbulence, the aircraft descended toward Honolulu Airport. The first attraction of Hawaii was the beautiful tropical flowers. Then, one of the welcoming persons placed a lei around my neck saying "Aloha" (Fig. 6.5-6).

After a four-hour stop for customs and refueling, the clipper departed for San Francisco at 1800 Hawaii Time. It became dark very fast, giving me time to sleep for a while. When I woke up before sunrise, all I could see was a deck of stratus. Very soon, the aircraft began descending over San Francisco Bay, landing at the International Airport at 0340 Hawaii Time (0540 PST).

I was allowed to bring in only $22.00 to the United States due to post-war control of foreign currencies in Japan. Knowing that my money might not last all the way to Chicago, I took a limo to downtown San Francisco and walked to Kusano Hotel, owned by a Japanese. At the front desk I asked the manager George Iseri, how I could stretch the money on board the train to Chicago. Mr. Iseri told me that my money was not enough for the 3-day meals in the overland train to Chicago. All of a sudden he handed me a $20 bill. He did not want me to sign a receipt of appreciation. All I did was to tell him that I will return the money after I receive my first pay check from the University of Chicago.

I went to a small grocery store near the hotel and purchased a 3-day supply of fig bars and Coca Cola. I carried them into the train which departed from the Southern Pacific Station at Oakland. Along with the views of the Bay area, I enjoyed eating the first fig bar lunch with Coca Cola. At the Sacramento Station, I stepped out of the train to feel a 105° heat which was the highest air temperature I ever experienced. After a long sleep, I took a fig bar breakfast when the train was passing over the dike in the Great Salt Lake, followed by a fig bar lunch after departing Green River, Wyoming. At this point, I was tired of eating fig bar dinner while the train was in eastern Nebraska. After drinking Coca Cola, I fell asleep until the train stopped at Cedar Rapids, Iowa early next morning.

After eating fig bar brunch only for survival, I noticed that our train was approaching my destination - Chicago. We arrived at the Chicago Northwestern Railroad Station shortly before noon on 12 August. Mrs. Ethel Pearson, Prof. Byers' secretary, found me walking down the station platform, carrying an aluminum suitcase with a hand-painted white cross for identification. Assisted by Mrs. Pearson, I checked in at the International House in Room 848. The $1.50 meal in the evening at the dining room was my best dinner since departing Tokyo on 8 August.

I liked the International House (Fig. 6.5-7) where I met a number of foreign students. Needless to say, I never ate a fig bar in Chicago anymore, but Coca Cola became my favorite after-dinner drink (Fig. 6.5-8). In the evenings, we could walk safely around the university area. Chicago in 1953 was a crime-free city like Tokyo. I enjoyed strolling along the Lake Michigan shoreline and the Museum of Science and Industry areas to take pictures (Fig. 6.5-9).

Travel Around the World by Air

Because I enjoyed the first transpacific flight on 8-9 August 1953, I asked Prof. Byers if I could fly on my official travels. He told me immediately, "Travel by air is the standard mode of transportation in this country."

Since then, I traveled by air to both domestic and international destinations while keeping records of all flights. During my academic years, I had chances to visit communist countries, but I did not do so because aerial photography was prohibited. My flight routes since 1953, when superimposed upon a topo map, look like a huge spider net centered at Chicago (Fig. 6.5-12). During these flights, I tried to sit by the window in observing both atmospheric phenomena and geological features on planet earth.

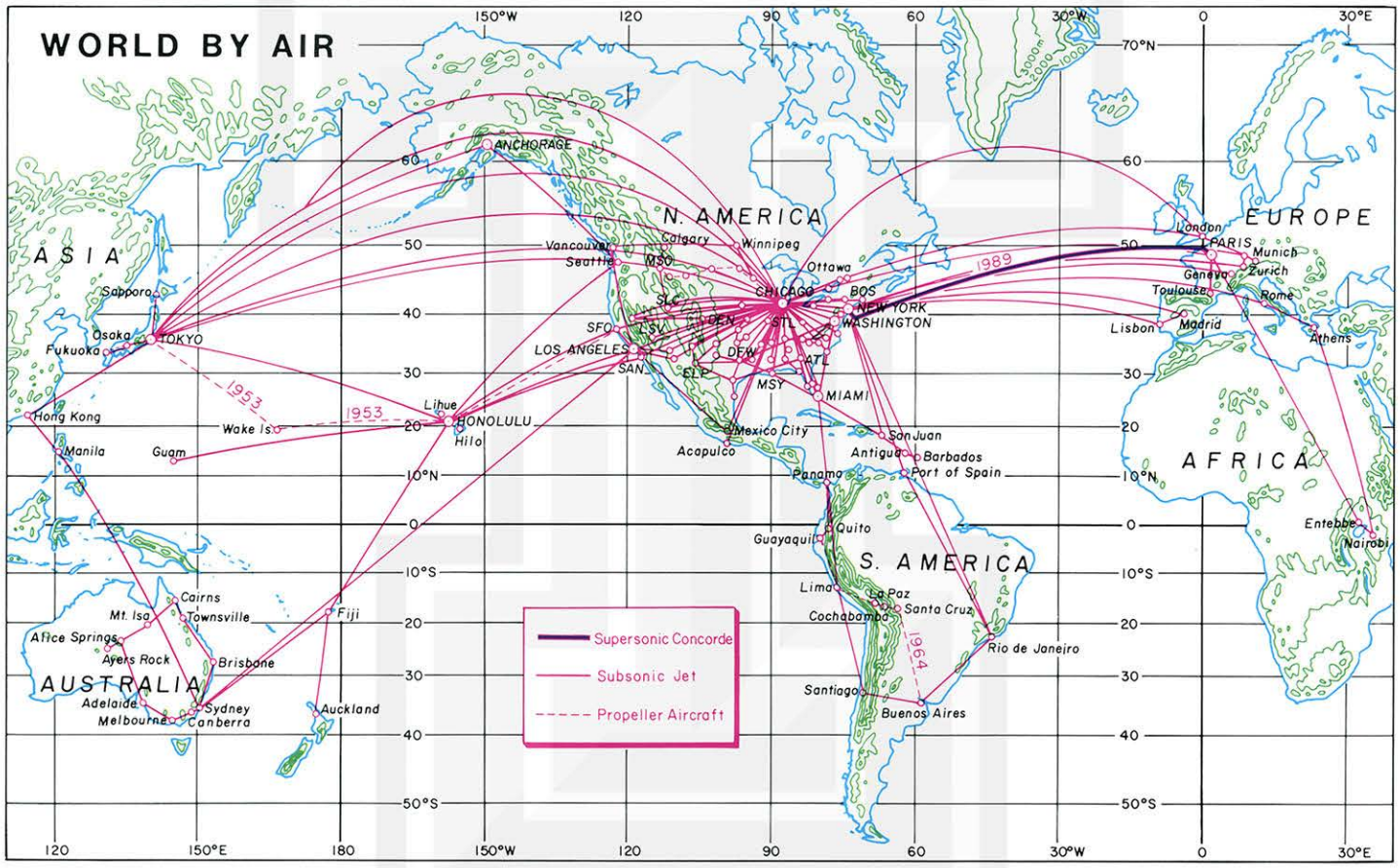

Fig. 6.5-12 A composite map of the air routes which I flew during the 38 years from 1953 to 1990, the year of retirement. I visited Australia twice, New Zealand once, South America twice, Africa twice, and Europe eight times. Noncommercial research flights by Lear Jet and Cessna were not included.

Flight Over the Bolivian Andes

After teaching satellite meteorology at the University of Buenos Aires, Argentina, Tatsuko and I, along with our son Kazuya departed Buenos Aires by air on 12 September 1964 for La Paz, Bolivia, to visit Lake Titicaca which I saw in satellite pictures almost everyday. First, our DC-6 flew in clear air to Santa Cruz airport on the plain, 30 km east of the foothills of the Andes.

From Santa Cruz, the aircraft departed toward the high mountains. About an hour later, the DC-6 encountered light rain without turbulence. When we flew out of the rain, I saw high mountains covered with broken layers of clouds on both sides of the aircraft. I got an impression that we were flying inside a canyon in the Andes. Very soon we were in rain again, resulting in zero visibility. Without telling anything to Tatsuko and Kazuya, I prayed silently for the successful flyout over the high spots likely to exist at the end of the canyon. Although I felt a long passage of time in the fog, the aircraft suddenly broke out of the rain clouds about 2,000' above the mountain at the end of the canyon.

The aircraft began descending toward the Cochabamba airport at 2,550 m (8,367') elevation. The airport area was clear, surrounded on all sides by 4,000 to 4,500 m (13,000' to 15,000') tall mountains. After a short stop, the aircraft headed toward La Paz. They announced that the aircraft was pressurized to the mile-high altitude, but El Alto airport of La Paz, the highest airport in the world, is 4,085 m (13,348') high. In other words, the cabin pressure would be higher than the air pressure outside the aircraft after landing. The use of oxygen mask was advised should anyone feel sick after opening the cabin door. Fortunately, the three of us did not feel too sick to use oxygen at the airport.

I wanted to visit Lake Titicaca next day. After a brief negotiation, a taxi driver offered me a fixed rate of $20 for the 200 km roundtrip to the lake. We were pleased to see the lake shortly before passing the village of Huarina where we saw grass boats made of reed moving slowly over the smooth lake. The dirt road on the north shore of the lake led us to the small village of San Pedro at the tip of a tiny peninsula.

Since no eating place was found in the village, the driver suggested that we take the car ferry to Tiquina on the other side of a narrow channel. When the ferry arrived, his taxi, with the four of us inside, rolled into the boat which crossed the channel in about 20 minutes. We walked up a small hill to the hotel looking for a nice lunch.

While we were eating in the dining room overlooking the channel, winds picked up suddenly and a couple of small boats in the channel began drifting away toward the southeast. The taxi driver began worrying about our return trip and rushed to the ferry station. He came back with bad news saying, "The winds are so strong that the ferry must remain here tonight. If the ferry operates tomorrow, they will accept passengers on first come, first serve basis." The driver returned immediately to his taxi at the ferry station.

As soon as we finished lunch, I went down to the ferry station to find 20 Indios and 10 llamas waiting ahead of the taxicab with our driver waiting inside. He advised me to get a hotel room for the three of us because he had decided to stay in the cab all night. I returned to the hotel to make reservations, but nobody understood English. Fortunately, my broken Spanish did the job. I asked, "Tiene usted una habitación con tres camas para esta noche?" The clerk replied, "Si, señor. Cinco dolares para todos." "Muchas gracias." I was glad to learn that he was willing to accept US dollars. The $5 he quoted was the cheapest room rate ever. We also found out that the hard beds were the worst ever.

As the high winds continued, I began worrying about our trip back to La Paz. At dinner time, three agriculture inspectors checked in after finishing their local job.

A. Kazuya Fujita (age 12) standing in front of the refueling DC-6B of Lloid Aëreo Boliviano (LAB) at the Santa Cruz airport. (Sep. 12)

B. Kazuya at Cochabamba airport after the 60-min flight from Santa Cruz in rain and fog. (Sep. 12)

C. Lake Titicaca seen from a hill by the dirt road to San Pedro. Rolling hills are on the other side of the Tiquina strait. (Sep. 13)

D. Small grass boats made of reed. These boats are used for fishing on the lake at 12,500' elevation in the Andes. (Sep. 13)

E. Indio passengers waiting for an approaching ferry which was not operated during the previous night due to high winds. (Sep. 14)

F. Indio sailors fighting with the wind which began increasing during our sailing from Tiquina to San Pedro. (Sep. 14)

Fig. 6.5-13 Pictures taken in Bolivia on 12-14 September 1964 on the way back from Buenos Aires to Chicago with Kazuya and Tatsuko.

They spoke to me in better-than-nothing English and I responded in my broken Spanish. They told me, in effect, that the Tiquina ferry service was closed for two weeks last month due to high winds. I could not sleep all night while listening to the periodic roar of the unexplainable dry northwest winds at 3.8 km (12,500') elevation in the southern hemisphere, 16° south of the equator.

Unexpectedly, the winds subsided at sunrise. Without breakfast, we checked out of the hotel using my $5 and $20 bills Tatsuko kept in her handbag. When we rushed down to the ferry station, our taxi driver told me that this could be the only ferry for the day. Now we had to be on this ferry. At 8 a.m., they began loading while making the head count; Indios first, llamas next. After all llamas got into the ferry, they resumed head count of the four of us in the taxicab. Many Indios were still waiting in line behind us.

We were happy to say "adiós" to the Tiquina hotel from the ferry moving slowly toward San Pedro on the other side of the 600 m (2,000') wide channel.

Supersonic Concorde Across the Atlantic on 30 November 1989

On the return trip to U.S. after receiving the Vermeil Gold Medal at Toulouse, France, Vice President Marc Pélegrin of the French National Academy of Air and Space, and Monsieur Michel Reddan, director of airline operations of Air France made arrangements for a memorable supersonic flight for Susie and me. The airline gave me a seat in the cockpit behind Captain Robin, while Susie was sitting in the front window seat, 02D. She enjoyed the best steak lunch. I ate nothing because of busy observations.

The Concorde, Air France Flight 001 (Fig. 6.5-14), left the special Concorde gate at Charles de Gaulle Airport on time at 1000 (time in GMT) and taxied to the runway. The aircraft lifted off at 1011 with the outer windshield at the down position. At 1012, I noticed frost on the windshield, but it quickly melted away after raising the windshield. As quickly as possible, I read dials and digital displays and wrote them down. The data I recorded were GMT time, pressure altitude, INS

Fig. 6.5-14 A picture of Air France Concorde taken shortly before departing the Concorde gate at Charles de Gaulle Airport, 24 km northeast of Paris.

wind, Mach Number, static and dynamic air temperature. Meanwhile, I took 107 color pictures during the 3 hrs and 31 min flight. The time section of these flight data (Fig. 6.5-15) was completed after returning to the University of Chicago. The flight path superimposed upon the METEOSAT infrared imagery at 1200 GMT revealed that the Concorde flew over the cold-frontal high clouds extending from Greenland to Bermuda (Fig. 6.5-16).

At 1036, we were climbing over the English Channel at 12.5 km (41,000') north of Cape de la Hague (Fig. 6.5-17) at Mach 1.6. Then we topped a narrow band of tall convective towers at 1121 (Fig. 6.5-18) at 15.4 km (50,500'), Mach 2.00. Although the outside temperature was -61°C, the dynamic temperature at the nose was 112°C. The flight engineer told me that the aircraft stretched due to high temperature, creating a gap between the cabin wall and the instrument panel. I could push my fingers into the gap, but the engineer reminded me that I should pull my fingers out before landing New York.

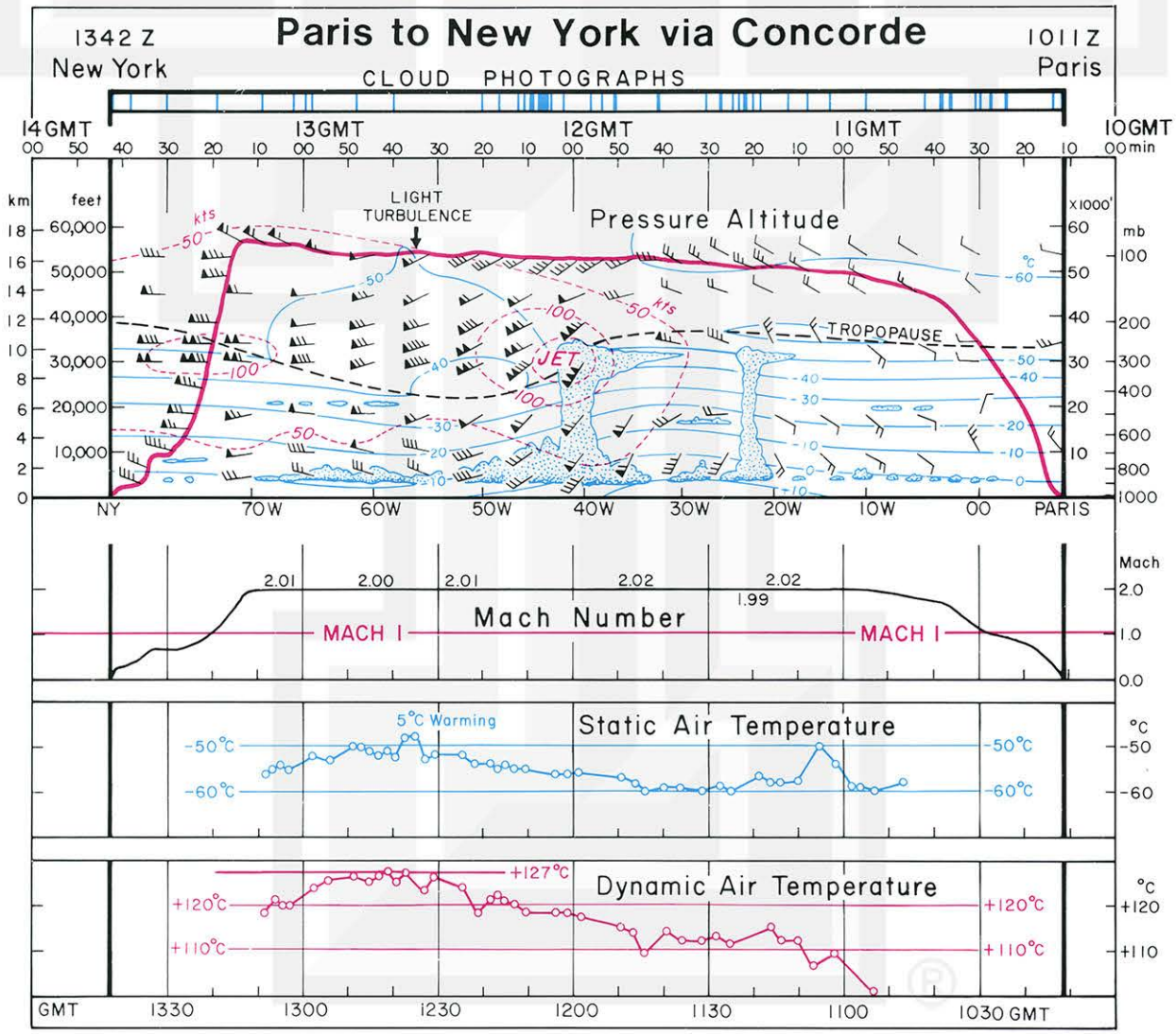

Fig. 6.5-15 The vertical time cross section along the flight path. Flight level winds were read from INS digital display and low-level winds from 1200 GMT synoptic charts.

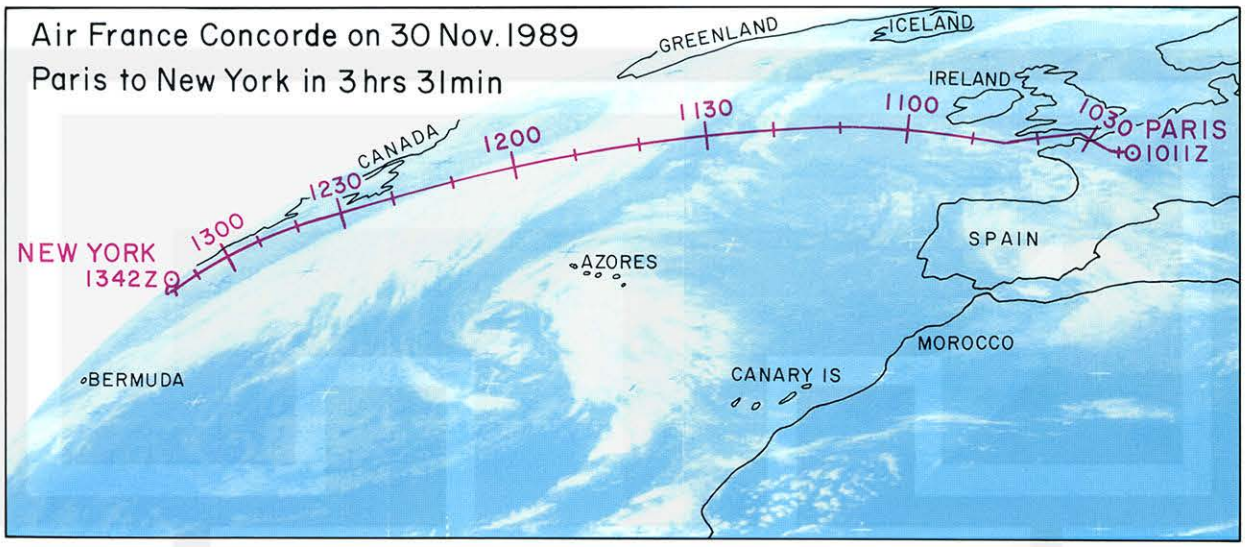

Fig. 6.5-16 The path of the Concorde superimposed upon the infrared imagery of METEOSAT at 1200 GMT.

I had to write down quickly the flight parameters from the numerous dials and displays (Fig. 6.5-19). At 1207, we flew over the cold-frontal high clouds at 16.0 km (53,500') altitude, Mach 2.01 (Fig. 6.5-20). I felt light turbulence shortly after 1235 when the outside temperature jumped 5°C from -53 to -48°C. The cause of the warming could be the descending motion of the stratospheric air.

After burning fuel for over 3 hrs, the aircraft became lighter and the altitude increased progressively, reaching 16.7 km (55,000') at 1300 when the aircraft moved far to the west of the sun. A picture taken at 1259 looking south (Fig. 6.5-21) shows the sun far to the east and dark western clouds.

At 1313, the Concorde reached the highest pressure altitude of 17.4 km (57,000'). Thereafter, both Mach number and altitude decreased rapidly while approaching New York. In spite of the large rate of descent, 6.1 km (20,000') in 10 minutes, I did not feel anything because the cabin was pressurized and the fuselage was kept in horizontal attitude during the descent. The aircraft landed the JFK runway at 1342 (0842 EST) and taxied to the gate area where a ground person guided the Concorde to its precise parking position (Fig. 6.5-22).

We spent practically no time at immigration and customs. At the ground transportation area, a limo was waiting our arrival to take us anywhere in New York City, compliments of Air France. We took the limo to LaGuardia Airport where our tickets were changed to an earlier United Flight 69 scheduled to depart at 1611. The connecting time at New York was 2 hrs 19 min, 66% of the transatlantic flight time.

It is of interest to compute the Fujita-relative position of the sun during this special day. While in Paris, the sun moved from southeast to south due to the rotation of the earth. While crossing the Atlantic at supersonic speed, the Concorde overtook the sun by 20°. While connecting at New York, the sun moved westward to the pre-noon position. The subsonic United flight simply slowed down the solar movement until landing the O'Hare airport where the Fujita-relative sun resumed its daily uninterrupted movement (Fig. 6.5-23).

Fig. 6.5-17 The last landmark of France seen to the south of the Concorde flying over the English Channel. Time 103631 GMT: Altitude 12.5 km: Mach 1.60.

Fig. 6.5-18 A narrow band of tall convective clouds. Time 112142 GMT: Altitude 15.4 km: Mach 2.00.

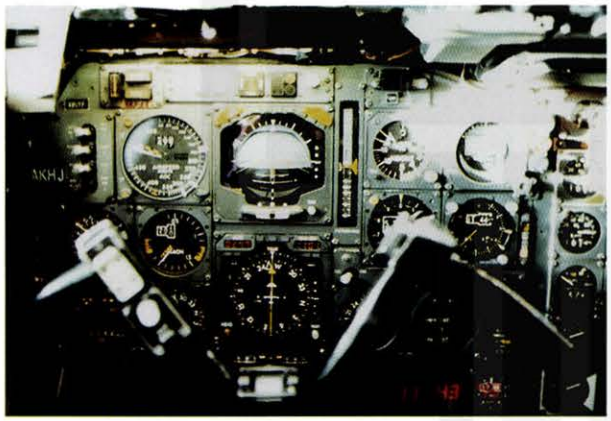

Fig. 6.5-19 Instrument panels inside the cockpit. Picture time 114343 GMT: Instrument readings — Altitude 49,800' (15.18 km): Mach 2.005.

Fig. 6.5-20 The cold-frontal high clouds extending southwest toward Bermuda. Time 120719 GMT: Altitude 16.0 km: Mach 2.01.

Fig. 6.5-21 The sun descending toward the east horizon due to supersonic speed of the aircraft, faster than the rotation of the earth. Time 125913 GMT: Time at 66°W 0835 LST: Altitude 16.7 km: Mach 2.01.

Fig. 6.5-22 Eight minutes after touchdown at JFK when the Concorde was guided to the parking position at the gate. Time 135028 GMT.

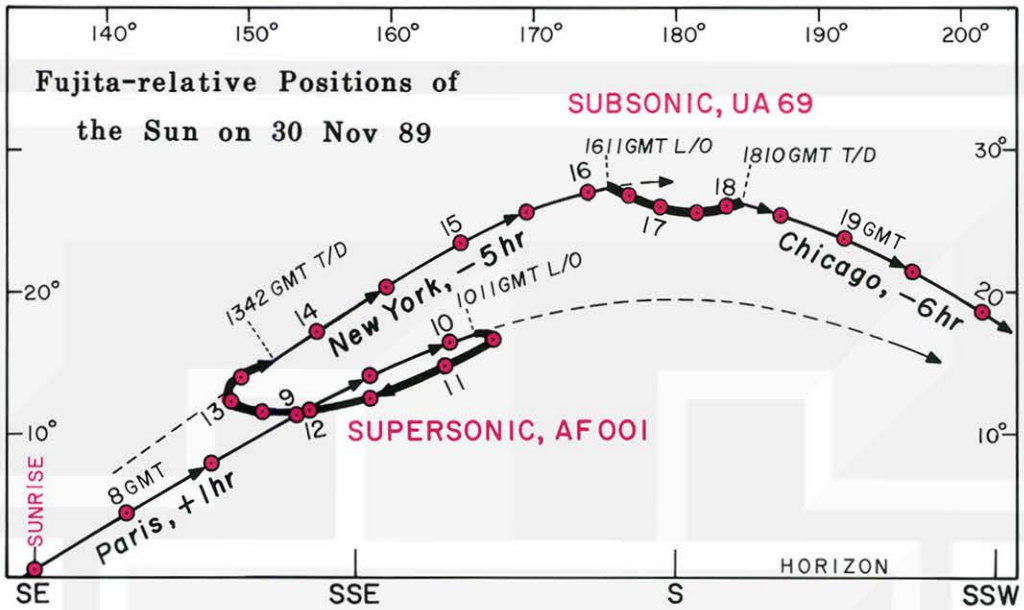

Fig. 6.5-23 Fujita-relative position of the sun, from sunrise at Paris to the afternoon in Chicago on the same day. The sun moved backward during the supersonic flight

The wide-angle composite picture from the cockpit reveals the gentle curvature of the earth (Fig. 6.5-24). The sky above the curvature was dark blue. I also printed stereoscopic cloud pictures taken in the direction perpendicular to the Concorde heading. It was found that the time distance of stereo pairs should be less than 10 seconds because of the supersonic speed. It is interesting to examine three-dimensional cloud patterns through the stereoscope (Fig. 6.5-25).

In comparison with my first transpacific flight by Strato Clipper in 1953, the supersonic flight across the Atlantic in 1989 was entirely different. During the 37 years between 1953 and 1989, aircraft technology advanced. So did my knowledge of meteorology, along with my position in the scientific community. Without these advancements in time, both Susie and I could not have experienced this excitement.

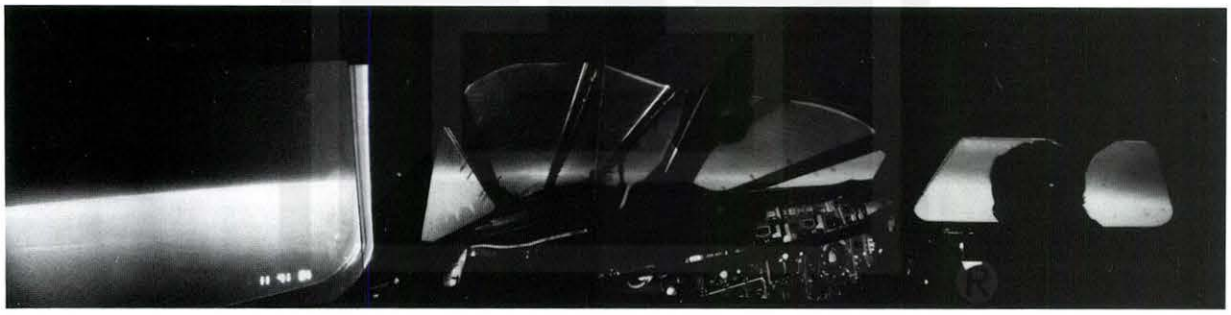

Fig. 6.5-24 The gentle curvature of the earth at 1411 GMT when the Concorde was flying above extensive high clouds extending to the Azores.

6-sec stereo pictures taken from over the band of tall convective clouds. Stereo-pair times 1121 GMT plus 42 sec and 48 sec: Altitude 15.4 km: Mach 2.00.

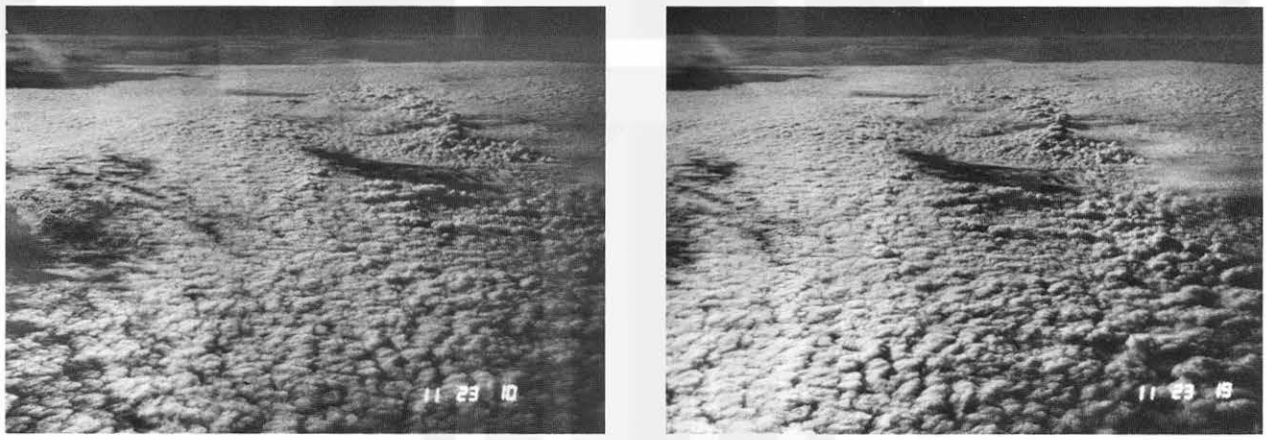

9-sec stereo pictures showing low stratus clouds to the west of the band of tall convective clouds in the above pictures. Stereo-pair times 1123 GMT plus 10 sec and 19 sec: Altitude 15.7 km: Mach 2.01.

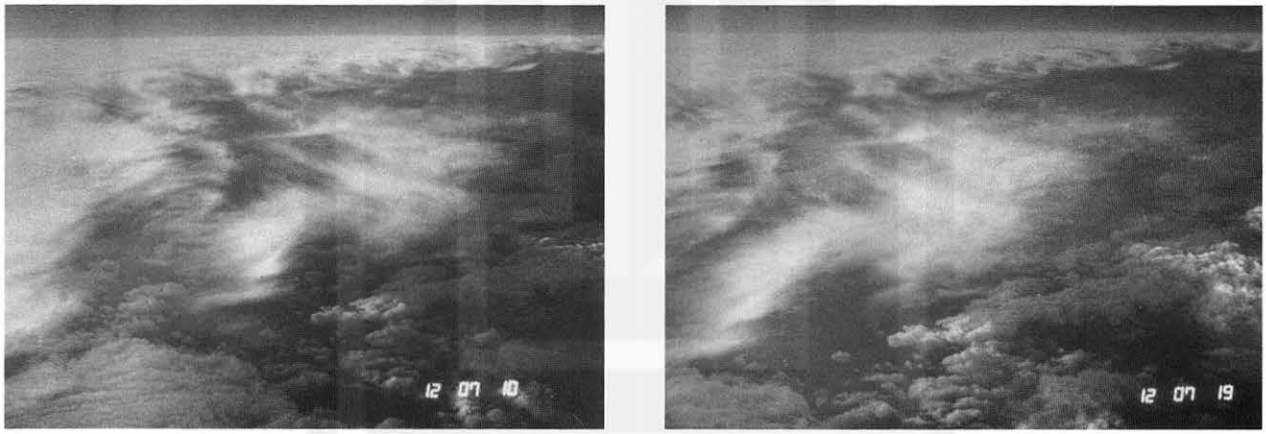

9-sec stereo pictures showing the west edge of the cold-frontal high clouds extending to Bermuda. The cause of the thin cirrus off the west edge of the frontal clouds is still unknown. Stereo-pair times 1207 GMT plus 10 sec and 19 sec: Altitude 16.0 km: Mach 2.01.

Fig. 6.5-25 Three stereo-pair pictures taken from the Concorde while flying over the Atlantic.

Trips to Europe

I visited Europe eight times for meetings and sightseeings (Fig. 6.5-26). During these trips, I tried to study meteorological, climatological, and geological aspects of European countries.

The first trip was to Madrid, Spain in 1966 for a meeting on satellite meteorology. Prof. Giichi Yamamoto of Tohoku University, Japan was in the meeting. Due to his late arrival, however, no hotel room was available and he stayed in an apartment with limited dining facilities. He told me that he had been encountering a number of problems which could have been solved if he spoke Spanish. Fortunately, an apartment next to his was vacant. For our mutual benefit, we decided to rent two adjoining apartments at the fraction of the cost I would pay if I were to stay in my hotel.

Next evening, we had a nice dinner together at a Flamenco theater-restaurant. Although he spoke some Spanish, Prof. Yamamoto wanted me to negotiate. I tried to use my broken Spanish with Argentinian accent which they detected immediately. First, he wanted to sit close to the Flamenco dancers. I asked, "Dos asientos cerca de las señoritas, por favor." They responded immediately. The problem thereafter was that we were too close to the dancers so that it was too dusty to eat a clean dinner.

It was after midnight when we returned to the apartment complex after the show. We could not get in because the front gate was locked. Our keys did not work for the gate. Then I heard someone clapping hands in front of another gate. I did the same in front of ours. A guard suddenly showed up and walked toward us. I told him, "Señor, llave no funcion." With a smile, he opened the gate and let us in. Since then, we did the same hand clapping every night coming home after dinner.

One year later in 1967, I visited Luzern, Switzerland. I had no serious language problems because I took German as a second language. After the Exeter, England meeting in 1971, Susie and I visited Stonehenge and Bath, England and Edinburgh, Scotland. Two Alpine trips in 1977 and 1979 were enjoyable. We cannot forget the Summer 1981 trip to southern Spain and Morroco, crossing the Strait of Gibraltar by boat to Tangier. In the winter of the same year, I spent one week in Lisbon, Protugal with Mr. Vince Oliver of NOAA in teaching satellite meteorology. Finally, the award-receiving trip to Toulouse, France in 1989 followed by the Concorde flight was an unforgettable experience.

Eiger, Mönch and Jungfrau

Since my schoolboy years in Kyushu, I was eager to see the famous mountains in central Switzerland. My dream came true on 4 October 1967 at the conclusion of the IUGG meeting at Luzern, Switzerland. Along with Dr. Michio Yanai, currently a UCLA professor, we took a local train to Interlaken Ost, the transfer station to Kleine Scheidegg, where we began the most interesting climb to Jungfraujoch via steep Zahnrad railroad.

The narrow-gauge train moved slowly on the snow-free slope overlooking the beautiful Lauterbrunnental. The train began climbing inside a long tunnel through the north wall of the 3,970 m (13,022') Eiger. During a brief stop at Eismeer observation station on the sheer rock, I saw the source region of a glacier through the glass windows. There were a lot of bugs clinging on the glass looking inside

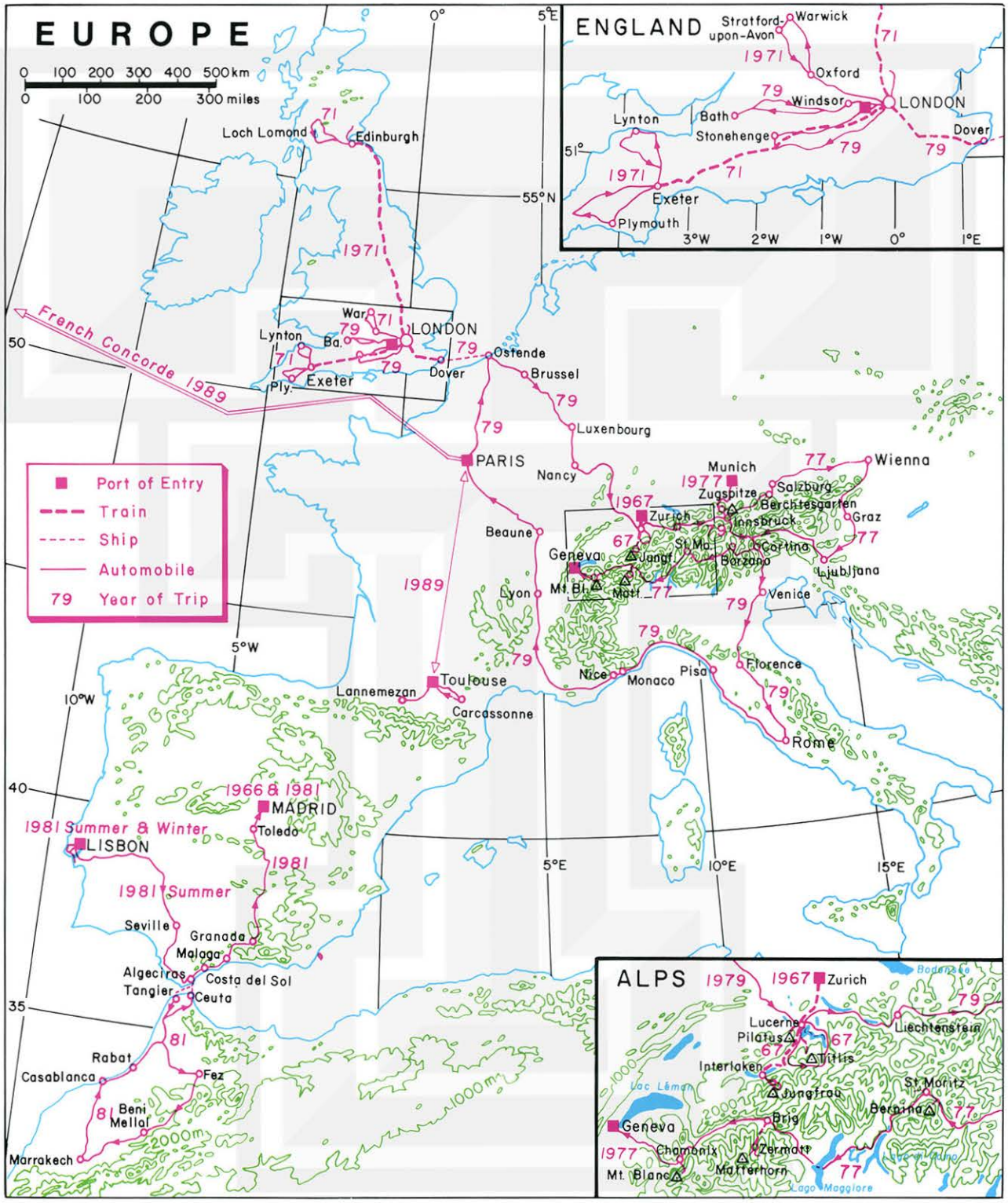

Fig. 6.5-26 Combined routes of my eight European trips between 1966 and 1990. Height contours are 1,000 m intervals.

Fig. 6.5-27 Piz Bernina, the 4,049 m (13,280') peak on the Italian border where the Morteratsh glacier originates.

Fig. 6.5-28 Converging area of Pers (foreground) and Morteratsh glaciers seen from Diavolezza cable station.

Fig. 6.5-29 Morteratsh train station where Susie and I departed toward the edge of the Morteratsh glacier.

Fig. 6.5-30 The Morteratsh glacier photographed while walking from the train station to its receding edge.

Fig. 6.5-31 A vertical crack on the glacier edge. A distant view (left) and two close-up views. I tried to enter the crack as deep as 60 cm standing sideways, feeling cold on both sides of my body.

toward us. The German passengers were saying, "The bugs know that it is warm around this station." Thereafter, the train continued to climb in the tunnel directly beneath the 4,099 m (13,445') top of Mönch, reaching the Jungfraujoch terminal at the 3,454 m (11,329') elevation. I felt dizzy due to the lack of oxygen at high altitude.

Seen from the station to the northeast was the soaring peak of Mönch and to the south, the packed icefield of Jungfraufirn flowing slowly into the Aletsch glacier. The 4,158 m (13,638') tall beauty of Jungfrau was only 2 km from the station across the icefield. The total view was majestic and unforgettable indeed. After our lunch at the station, we took a returning train down to Kleine Scheidegg where we decided to take the long route to Interlaken Ost via Grindelwald to enjoy views of green meadows with cows playing a continuous sound of cowbell music. It was dusk when we stepped out of the Luzern train station.

Receding Morteratsh Glacier

In September 1977, we were at St. Moritz, Switzerland for a couple of days. During that time, I wanted to see the Alpine glaciers which have been receding for some time. The best observation area near St. Moritz was Piz Bernina and vicinity. Along with Mr. and Mrs. Kabumoto of Chicago, we took a local train to the base station of a ropeway. The Diavolezza Zeilbahn lifted us from 2,093 m to 2,973 m (6,865' to 9,751') where the Diavolezza view point was located. It was the best location to see Piz Bernina (Fig. 6.5-27) and the Pers glacier (Fig. 6.5-28) which flows into the Morteratsh glacier.

To inspect the receding edge of the Morteratsh glacier on the 1965 topo map which

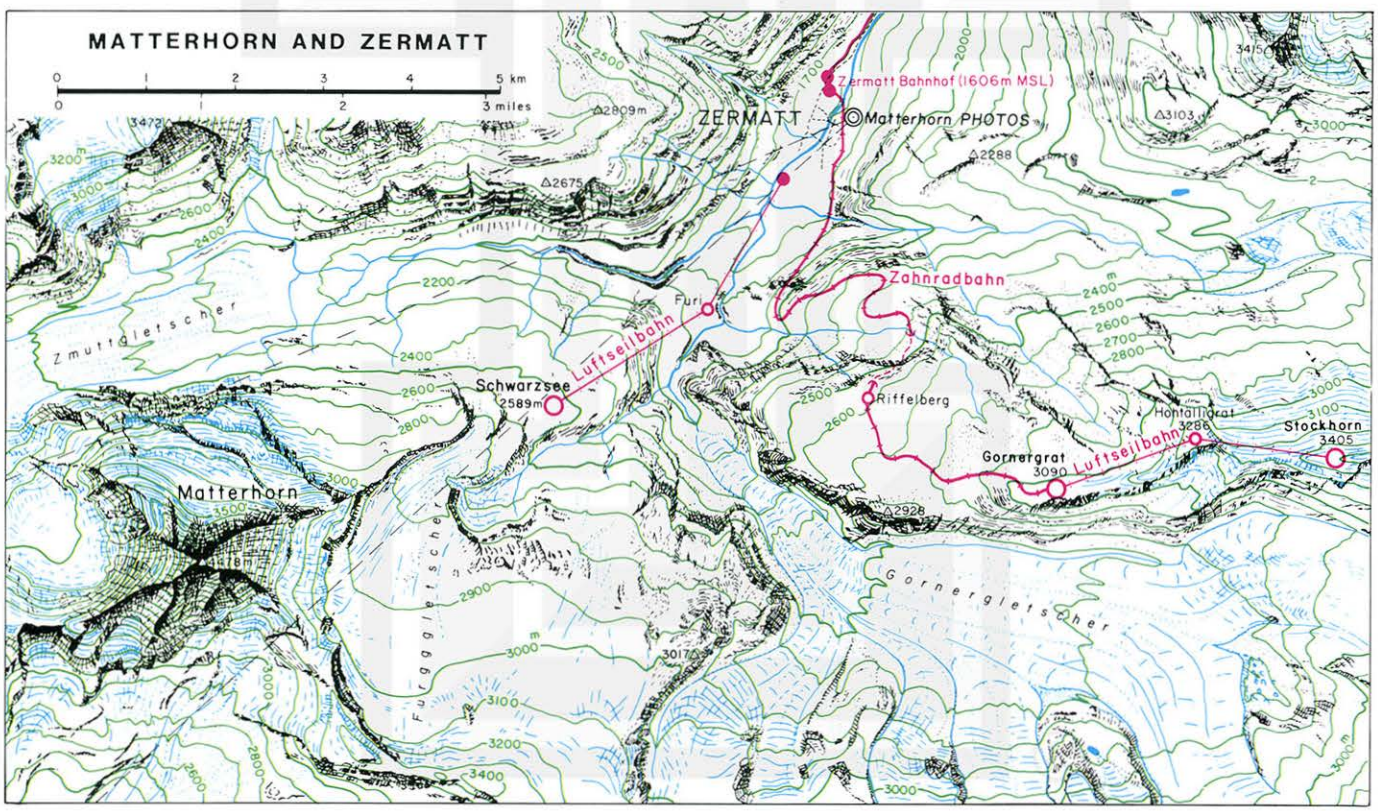

Fig. 6.5-32 Topographic map of the Zermatt, Switzerland area. During the two-night stay in Zermatt, Susie and I took Schwarzsee and Stockhorn Luftzeilbahnen and Gornergrad Zahnradbahn. It was clear and the view under the blue sky was spectacular. We were very lucky.

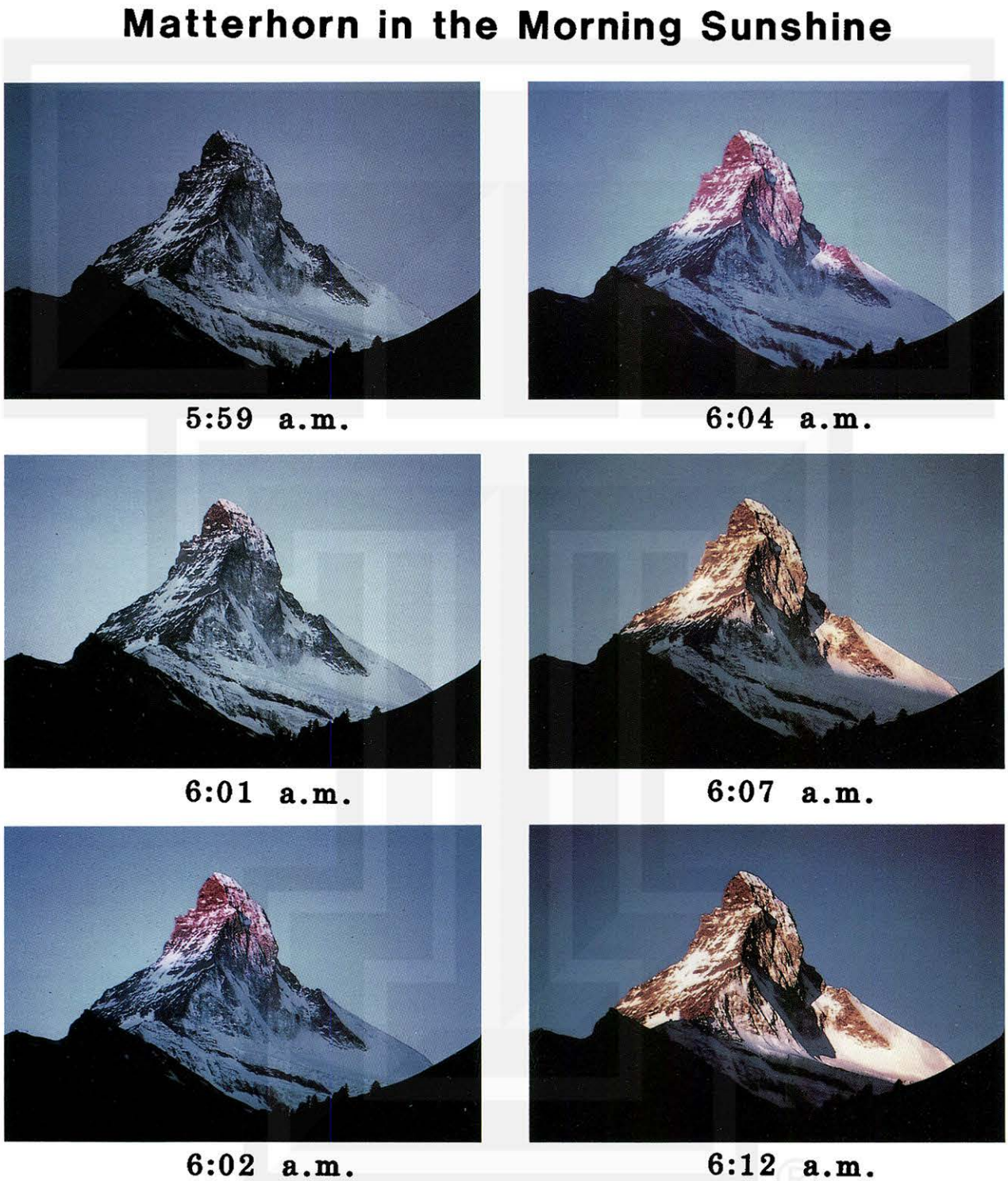

Fig. 6.5-33 A rapid change in the color of Matterhorn after the sunrise on 14 September 1977. Photos by Ted from a meadow on the west slope of the Zermatt valley.

was located 1 km south of the Morteratsh train station (Fig. 6.5-29), Susie and I got off the train and walked from the station toward the edge of the glacier. After walking about 1 km, we were still at the midpoint between the station and the glacier. From there, we had to walk another kilometer before reaching the edge of the glacier (Figs. 6.5-30 and 31). After returning to St. Moritz, I purchased a new map surveyed in 1976, finding that the glacier receded one more kilometer in 11 years. Because of the misjudgment, we missed the returning train. A local resident informed me that the receding phenomenon was a result of lesser precipitation rather than the global warming.

Sunrise at Matterhorn

It was about 5 a.m. on 14 September 1977 when I saw beautiful stars from my hotel room in Zermatt. I thought that this was the ideal morning to photograph Matterhorn during sunrise. I noticed quickly that the east slope of Höhbalmen was blocking the view of the mountain, necessitating the selection of the site for photography somewhere in the meadow on the east side of the Zermatt valley (Fig. 6.5-32).

In the pre-dawn darkness, I walked east across the Mattervispa River and climbed the meadow toward the best spot where I would be able to take good pictures. The most difficult question was to determine quickly the best combination of F stops and shutter speeds when the brightness of the peak was expected to change very rapidly upon the sunrise at the mountaintop.

Although I was rather excited in determining the best exposure for each picture, my best guess turned out to be excellent (Fig. 6.5-33).

Trips in the United States and Canada

I did not own a car during my first visit to the United States in 1953-55. After returning to Chicago with Tatsuko and son Kazuya in July 1956 as immigrants, I bought a 1951 Mercury previously owned by my mechanic friend, Tom Miyata. Then I had to learn "how to drive." Fortunately, my former student, Hayao Nasu (Fig. 6.2-14), a student of Iowa State University at that time came from Ames, Iowa to Chicago to give me driving lessons. Because he was an excellent teacher, I got my driver's license in two days.

Travel by Car with Kazuya

My first long-distance drive was to visit Dr. Vince Schaefer's Project Skyfire at Missoula, Montana. By way of Fargo, North Dakota, we arrived Missoula on 30 July 1957 with Kazuya (age 5) and Tatsuko. During our trip to the 6,400' radar mountain, I noticed that he could locate his position on topographic maps. I thought that he might become interested in the geophysical sciences as he grows up.

Since that time, I took him by car to various places in U.S. and Canada. These trips were: to Key West (1958); Grand Canyon, Dinosaur National Monument (1960); Los Angeles, Bend, Teton (1961); Boston, Arcadia, White Mountain (1962); a long trip to Glacier National Park, Canadian

Rockies, Vancouver, Dinosaur, Denver, Grand Canyon which was, in effect, a geological trip for Kazuya (1965); and a trip to Stone Mountain near Atlanta (1967).

Kazuya became a Geophysicist

During my automobile trips with Kazuya to the western states, we visited a number of national parks. Kazuya enjoyed the large-scale natural beauty of the parks which he had never seen in Japan. While visiting Yellowstone National Park, I asked him, "What do you wish to do when you grow up like me?" After a short pause, he replied, "I want to be a park ranger."

After completing his graduate work at Northwestern University, Kazuya received his PhD in geophysics in 1979. I was pleased to learn that he became interested in teaching geophysics. Shortly thereafter, he became a faculty of the Michigan State

Fig. 6.5-34 Travel routes in the United States and Canada. Trips by car were made after 1956, the year in which I got my first driver's license. Several round trips by car to both east and west coasts were made, driving through every state except Rhode Island.

A. Going-to-the-Sun Highway, Montana

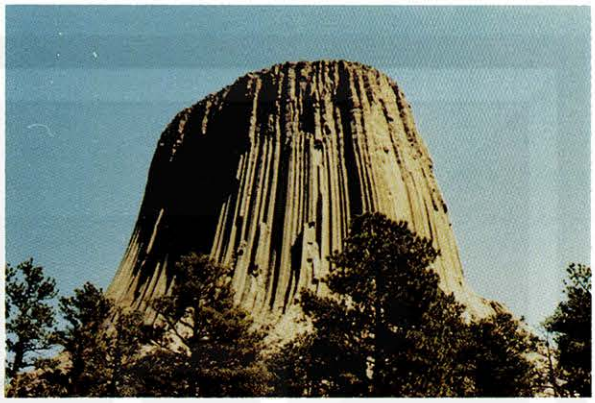

B. Devil's Tower, Wyoming

C. Columbia Icefield, Canada

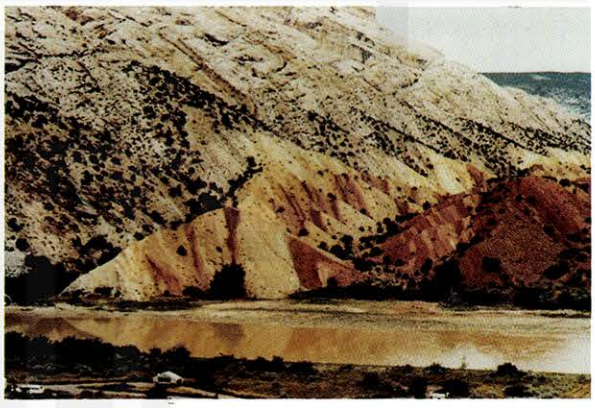

D. Green River at Dinosaur, Utah

E. Goosenecks, Utah

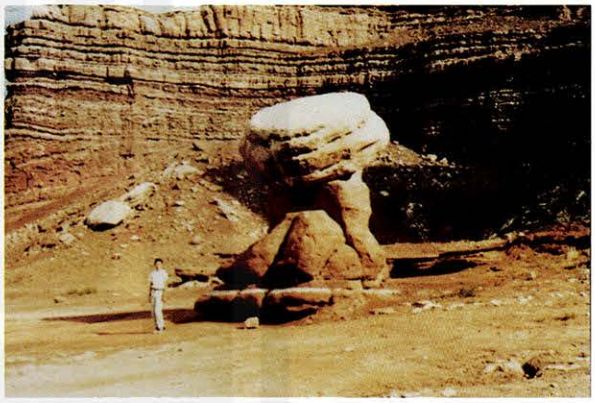

F. Mexican Hat, Utah

Fig. 6.5-35 Geological features of the West visited with Kazuya, Tatsuko and friend, Hamada. The routing was Chicago, Devil's Tower, Glacier National Park, Canadian Rockies, Mt. Rainier, Dinosaur, Rocky Mountain National Park, Grand Canyon, Meteor Crater, and back to Chicago.

University at East Lansing and married Martha Jean Mellon, a native of Fort Wayne, Indiana. He enjoyed both teaching and research, and was promoted to professor in 1988.

In Autumn (Aki in Japanese) 1989 on the 19th day of October, I became a proud grandfather of Elizabeth Fujita with her middle name, Aki. Thanks to Kazuya and Martha for adding a new beautiful family chain to the Fujita roots originated in the Sone village of Kitakyushu, Japan.

Kazuya's Aerial Photos

For years, the boundary between the North American and Eurasian Plates has been known to extend through Siberia. Nonetheless, the exact location of the boundary has remained a mystery.

In an attempt to determine the location more accurately, Kazuya and his colleagues visited Yakutsk in Siberia and performed aerial surveys of geological features on board a Russian helicopter based at Belaya Gora (White Mountain in English).

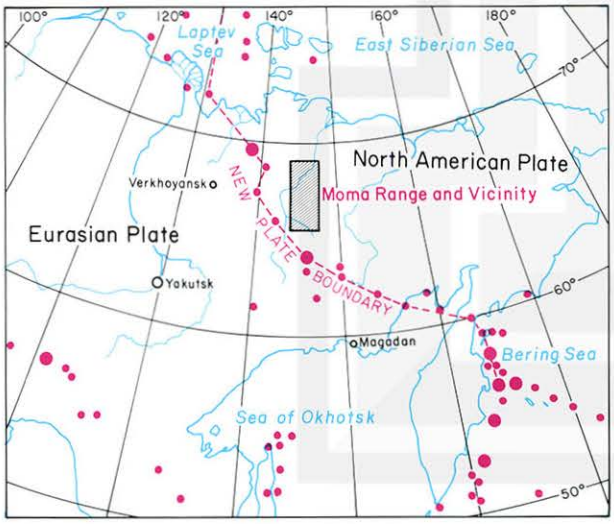

Fig. 6.5-36 The new boundary of the North American Plate being confirmed by Kazuya and his colleagues. Red circles denote epicenters.

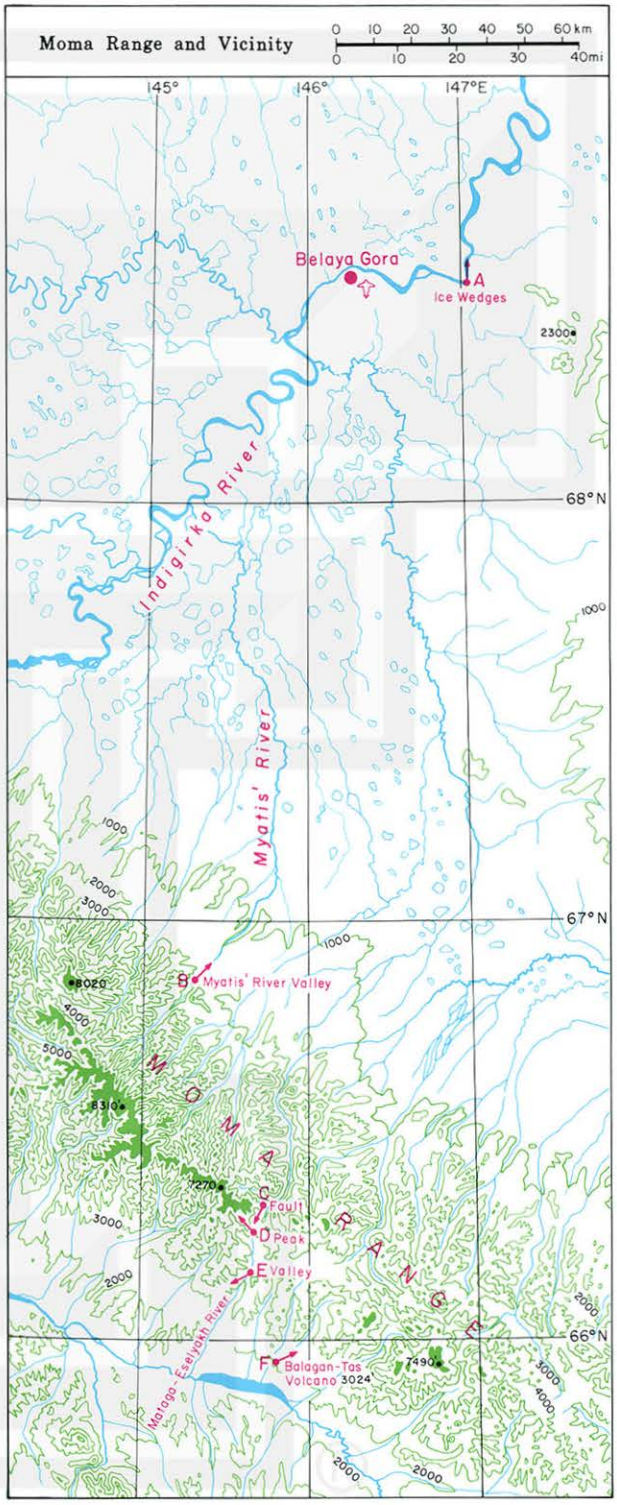

Fig. 6.5-37 A local map showing the six locations of Kazuya's photographs taken inside the rectangular box in the key map to the left.

A. Soil and ice wedges in Quaternary deposits, 29,000-yrs old at the base, along the Indigirka River. Mammoths were found in this layer.

B. Outcrops of Early Cretaceous sandstones of the Ozhogina Suite along the Myatis' River in the thrust faulted northern foothills of the Moma Range.

C. Faulted Late Jurassic argillites and sandstones of the Ust' Aganzhinsky Horizon in the central Moma Range. Note a fault near the center.

D. High mountains of the Moma Range looking northwest. The pyramid-shaped peak on the right side of this picture is 7,270' tall.

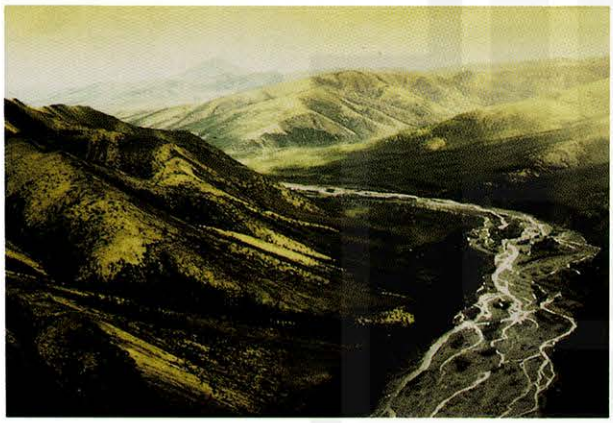

E. The valley of the Mataga-Eselyakh River in the southern foothills of the Moma Range. Uraga Khaya rhyolitic dome is seen in the background.

F. The 200,000-yr old (elevation 3,024') basaltic volcano, Balagan-Tas, in the Pliocene Moma rift zone. This photo was taken looking northeast.

Fig. 6.5-38 Geological features of the Moma Range and vicinity in Siberia photographed by Kazuya from a Russian helicopter in July 1990.

Kazuya's cooperative research with Russian seismologists is changing the current belief of the boundary extending south from the Laptev Sea to Japan. Instead, they are now suggesting an alternative boundary which extends from the Laptev Sea through Chersky mountain range of northeastern Russia, continuing eastward to the northernmost Kamchatka Peninsula, where it turns south toward the Pacific Ocean (Fig. 6.5-36).

I am pleased to learn that Kazuya has been conducting aerial survey and photography (Figs. 6.5-37 and 38) in the remote areas of Siberia for his cooperative research on the boundary between North American and Eurasian Plates.

Coldest Record Temperature in Chicago

The coldest record temperature of -27°F occurred at 5 a.m. on Sunday, 20 January 1985 under a blue sky. At that time, a ridge of surface high pressure extended from the North Pole to the Gulf, bringing the record cold air via western Canada (Fig. 6.5-39). It was the cold wave of the North-Pole Express category which was far more impressive than the Yukon Express and the Alberta Clipper.

The air temperature, above 23°F on the 18th, kept falling the whole day of the 19th, reaching the minimum temperature at sunrise on the 20th (Fig. 6.5-40). A mesoanalysis of isotherms at 0600 CST (Fig. 6.5-41) revealed a significant warming of the cold air, from -27°F to -2°F, as it moved over the water surface of Lake Michigan, over 150 m deep. The lake-effect warming extended east to western New York State. Lake Superior, the largest and the deepest of the Great Lakes, acted as the significant heat and moisture source.

Isobars at 6 a.m. 20 January 1985

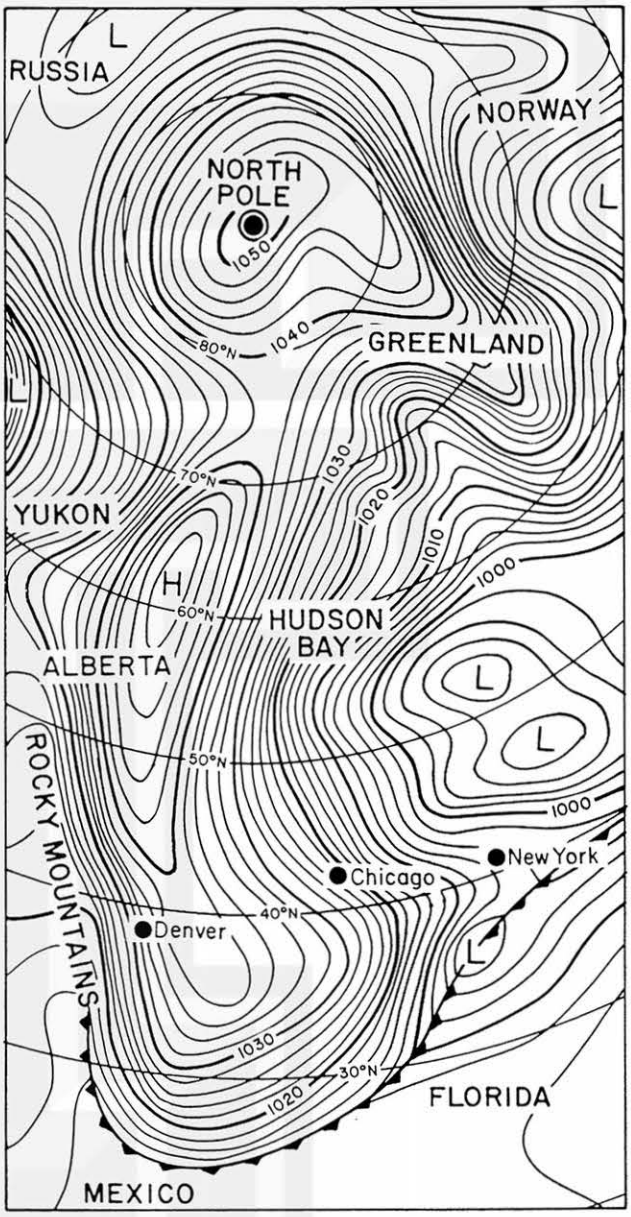

Fig. 6.5-39 Sea-level isobars at 0600 CST on 20 January 1985 one hour after the record cold temperature at Chicago occurred at 0500 CST. A ridge of high pressure at sea level extended from the North Pole to the Gulf Coast. This was the typical situation of the so-called "North-Pole Express."

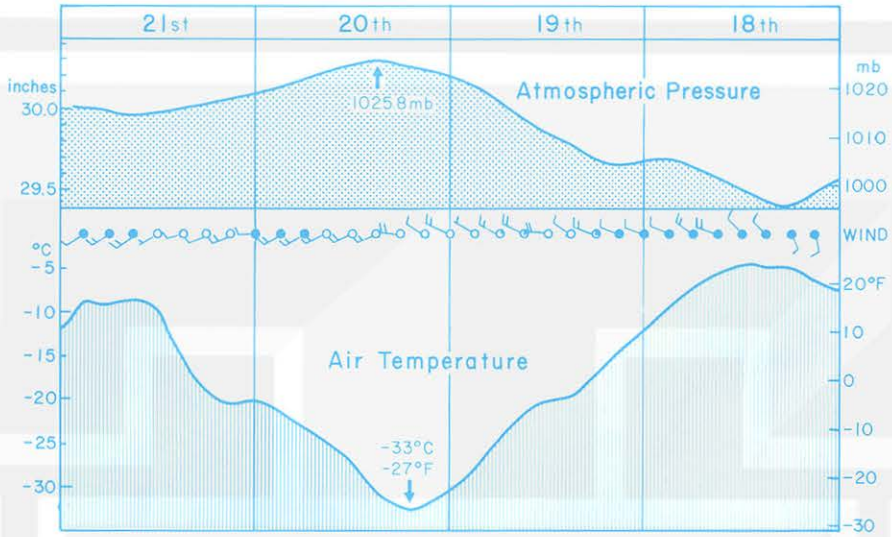

Fig. 6.5-40 Variation of air temperature and atmospheric pressure during the 4-day period, 18 to 21 January 1985. The record cold temperature at Chicago, -27°F (-33°C) occurred at 0500 CST.

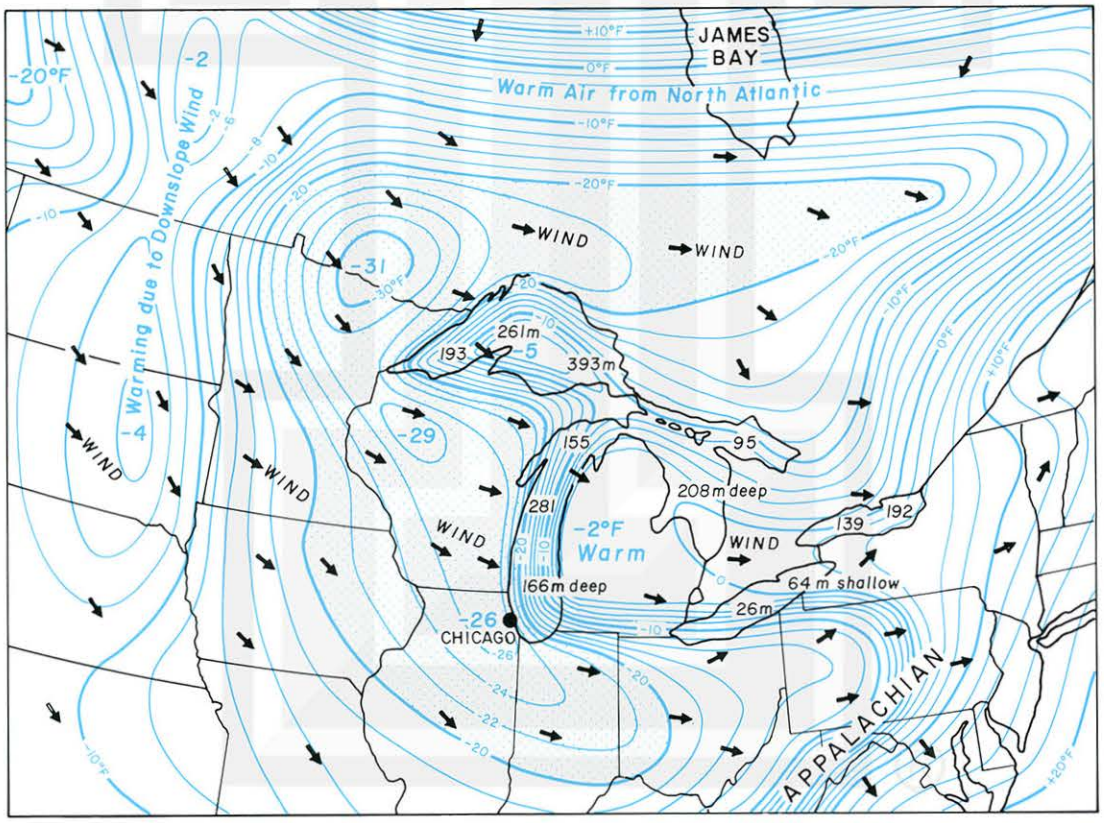

Fig. 6.5-41 Mesoscale pattern of the cold temperature at 0600 CST, one hour after the coldest temperature time. From the surface of the deep Great Lakes, the record cold air received heat and moisture as it moved over the lakes. Note that the difference in air temperature on both sides of Lake Michigan was 24°F (13°C).

Downtown Chicago on the Coldest Day

Fig. 6.5-42 A view of Sears Tower, the world's tallest building and other downtown buildings standing above the ice fog rising from the open water between the shoreline and the Planetarium point. Temperature: -21°F. Photo by Ted at 1030 CST.

Fig. 6.5-43 Ice fog rising from the open water of the downtown shoreline. Photo time: 1045 CST.

Fig. 6.5-44 A dark swirling column of ice fog rising violently from the open water of Lake Michigan.

Record Snowfall in Chicago

The deepest snow in Chicago occurred on 26-27 January 1967 when I was in New York City to receive the Meisinger Award of the American Meteorological Society at the Award Banquet on 25 January.

The next morning, I went to La Guardia Airport where I learned of the onset of the snow in Chicago. Against the initial expectation of the airlines, snow became worse, resulting in the cancellation of all Chicago-bound flights. After returning to the hotel, I kept calling the airlines, learning finally that flights had been booked for five days.

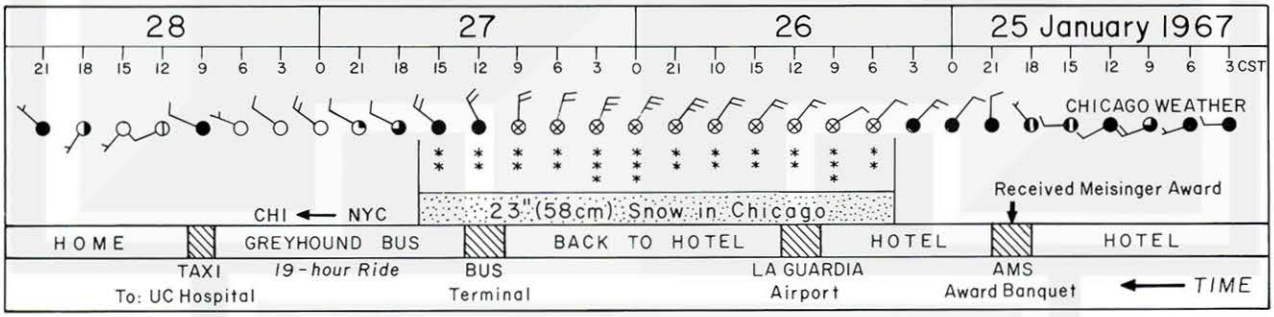

Fig. 6.5-45 Time section of the Chicago weather and my struggle to get back to Chicago from New York. The only mode of transportation was by Greyhound bus.

Finally, I took a Greyhound bus back to Chicago (Fig. 6.5-45) without knowing that nothing was moving on the city streets. After waiting for a long time in front of the bus terminal, a taxi driver asked me, "Are you a doctor?" I replied, "Yes, I am." "Where are you going?" he asked me. My answer was, "The University of Chicago hospital."

Taking two hours, the driver navigated his way to the university and dropped me off at the emergency entrance. After giving reasonable tips, I walked in the knee-deep snow to my home, only one block away. On January 30, I took snow pictures (Fig. 6.5-47) and kept a photographic record of the snow mountain on the campus as it melted away, taking just about two months (Fig. 6.5-48).

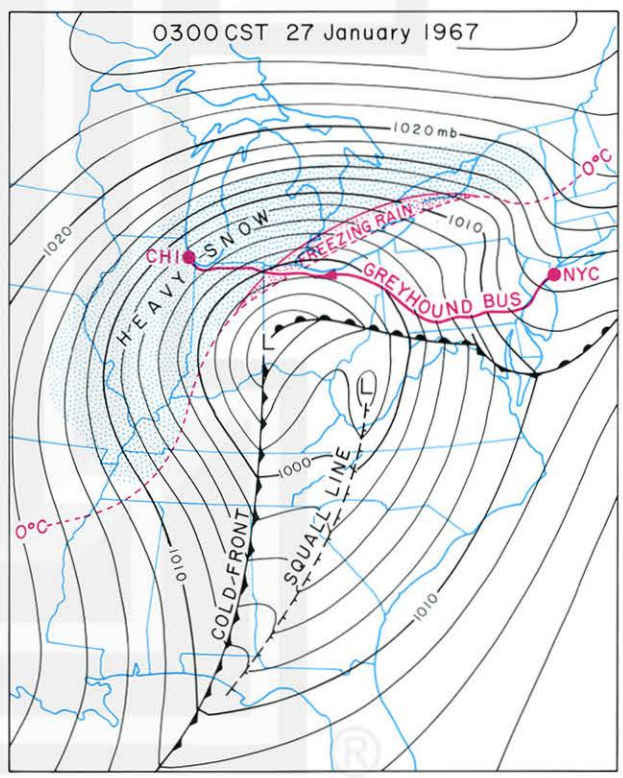

Fig. 6.5-46 Surface map at 0300 CST on the 27th when the O'Hare airport was experiencing the worst snowfall rate. The Greyhound bus I took did not encounter snow until coming close to northern Indiana.

The University of Chicago Area after the Deepest Snow on Record

A. A car parked in front of a NO PARKING sign.

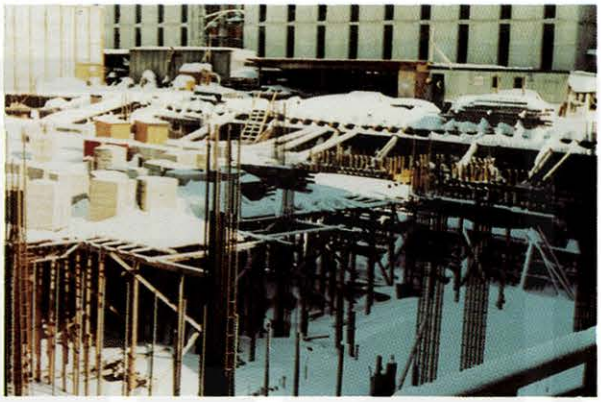

B. Our department building under construction at 5734 Ellis Avenue.

C. Sidewalk in front of my house at 5727 Maryland Avenue.

D. My neighbor's cat "Sam" enjoying the sun while sitting on our fence.

E. Gingiss Brothers Shop where I returned my formal wear for the award.

F. My shadow casting on the snow with small holes beneath tall trees.

Fig. 6.5-47 Six views of the 23" snow on 30 January 1967. All highways except Lake Shore Drive were open on the 28th, but all city streets were not passable due to abandoned cars everywhere.

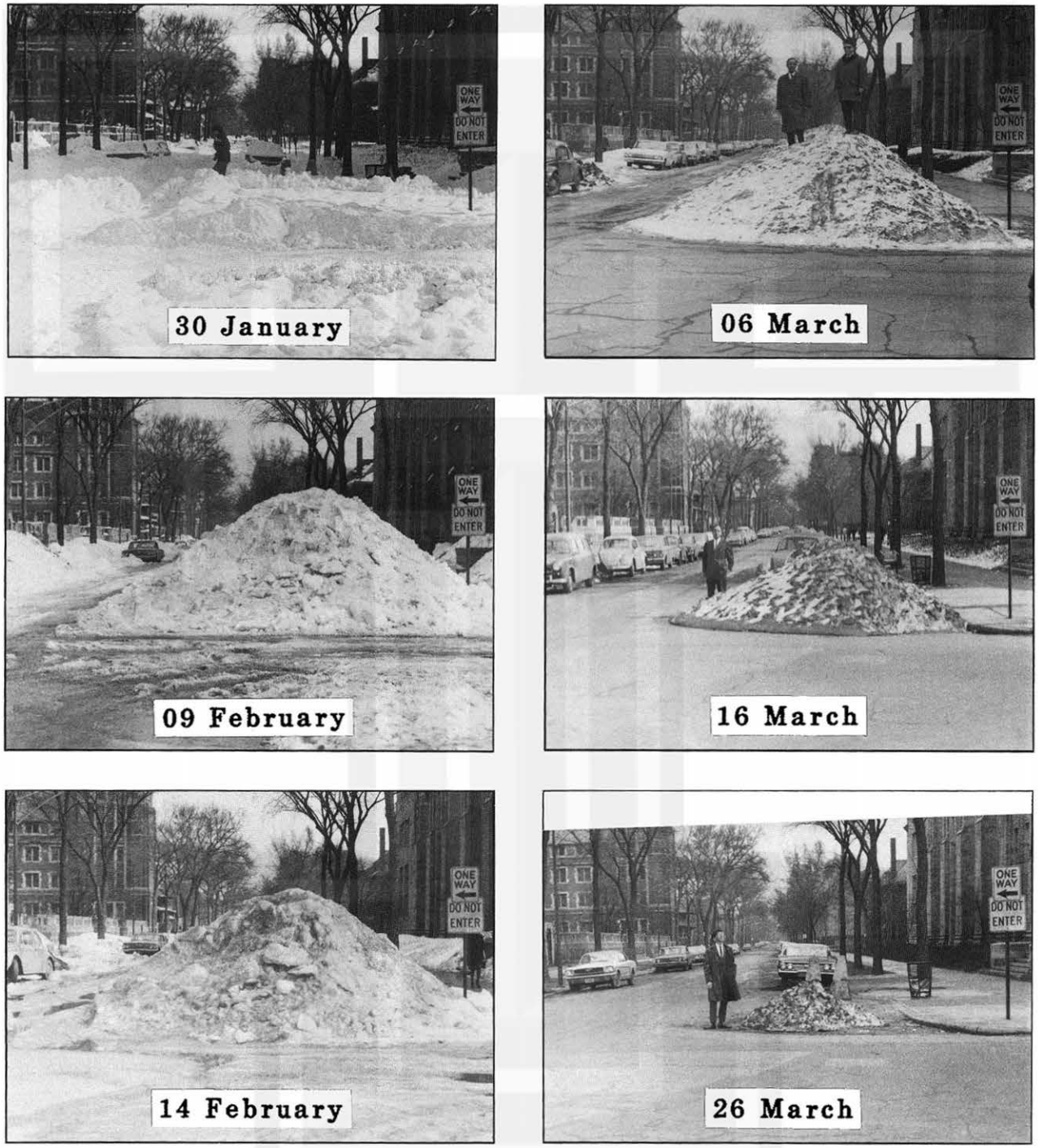

Fig. 6.5-48 Change in the shape of the snow mountain at 58th Street and University Avenue. The first picture was taken on 30 January 1967 before the snow pile was created in front of the Oriental Institute.

6.6 Scientific Awards Received

Seventeen scientific awards were received between 1939 and 1991. The specifications of these awards are grossly categorized into the contribution to the development of mesometeorology (5 awards), appreciation of tornado research leading to public safety and awareness (4 awards), utilization of weather satellites (2 awards), the discovery of the microburst and its application to air safety (5 awards), and scientific achievement in general (3 awards). Presented below are brief descriptions of my memory of each award.

1939 Rika Sho (Science Award) Kokura Middle School

昭和14年　小倉中学　理科賞

This was the first award I ever received in my life. It was presented in March 1939 at graduation from Kokura Middle School, currently Kokura High School. I remember that I liked all types of scientific activities. For about one year prior to graduation, I made sketches of sunspots using my homemade telescope, determining the rotation period of the sun to be 25 days at the solar equator and 27 to 29 days at high latitudes. My first question was, "Why does the sun rotate faster at its equator?" Being encouraged by my middle school teachers, this award became the first milestone on the unpaved road leading to my destination, The University of Chicago.

Fig. 6.6-1 My teachers and classmates gathered at Kokura High School on November 1, 1955 when I returned from the University of Chicago to Japan for immigrant visa to the United States.

A group picture taken on November 1, 1955 at Kokura High School shows my teachers and friends who participated in my homecoming activities which brought back the memories of my schoolboy days from April 1933 to March 1939 at Kokura Middle School.

1959 Okada Award — Meteorological Society of Japan

昭和34年　日本気象学会　岡田賞

The Okada Award was established in 1957 by the Meteorological Society of Japan, commemorating the leadership of Dr. Takematsu Okada (1874-1956), the fourth Director General of the Central Meteorological Observatory from 1934 to 1941. I was honored to be the third recipient of the award. Because I was not able to be at the award ceremony on November 6, 1959, my brother Sekiya received the award on my behalf during the Autumn Meeting of the Meteorological Society held at Fukuoka City, Japan. My brother informed me that Dr. Hisanao Hatakeyama summarized my research on mesometeorology for which the award was presented.

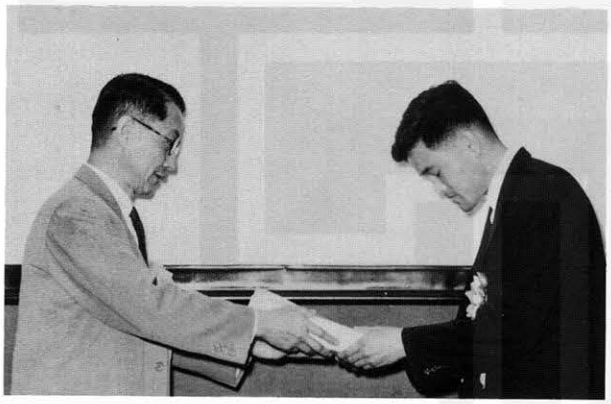

Fig. 6.6-2 My brother Sekiya receiving the Okada Award from Dr. Hatakeyama.

Fig. 6.6-3 The Okada Award Medal, 69 mm in diameter and 8 mm thick. Engraved on the back are: "To Tetsuya Fujita," "Year 1959," and "The Okada Memorial Society."

1965 Kamura Award — Kyushu Institute of Technology

昭和40年　九州工業大学　嘉村賞

嘉村記念賞第2回受賞者

昭和 40 年 5 月 18 日

嘉村記念賞運営委員会委員長

さきに明専会報第 406 号を通じて受賞候補者の推薦方を依頼した嘉村記念賞については，選考委員会においては慎重審議の結果，下記の者が第2回の受賞者に決定したのでお知らせします。

記

1. 受賞者　シカゴ大学地球物理学教室
　　シカゴ大学 Associate Professor
　　藤　田　哲　也
2. 研究題目　メソ気象学の開発ならび人工衛星による気象学の研究

I was the second recipient of the Kamura Award which was created under the name of Dr. Heihachi Kamura, President of the Kyushu Institute of Technology. The announcement of the award in Japanese, dated May 18, 1965, cited that the award was presented for contributions to the development of mesometeorology and meteorological utilization of artificial satellites.

Dr. Kamura was a graduate of LeHigh University. Four weeks after the Nagasaki Atom Bomb in 1945, he authorized my

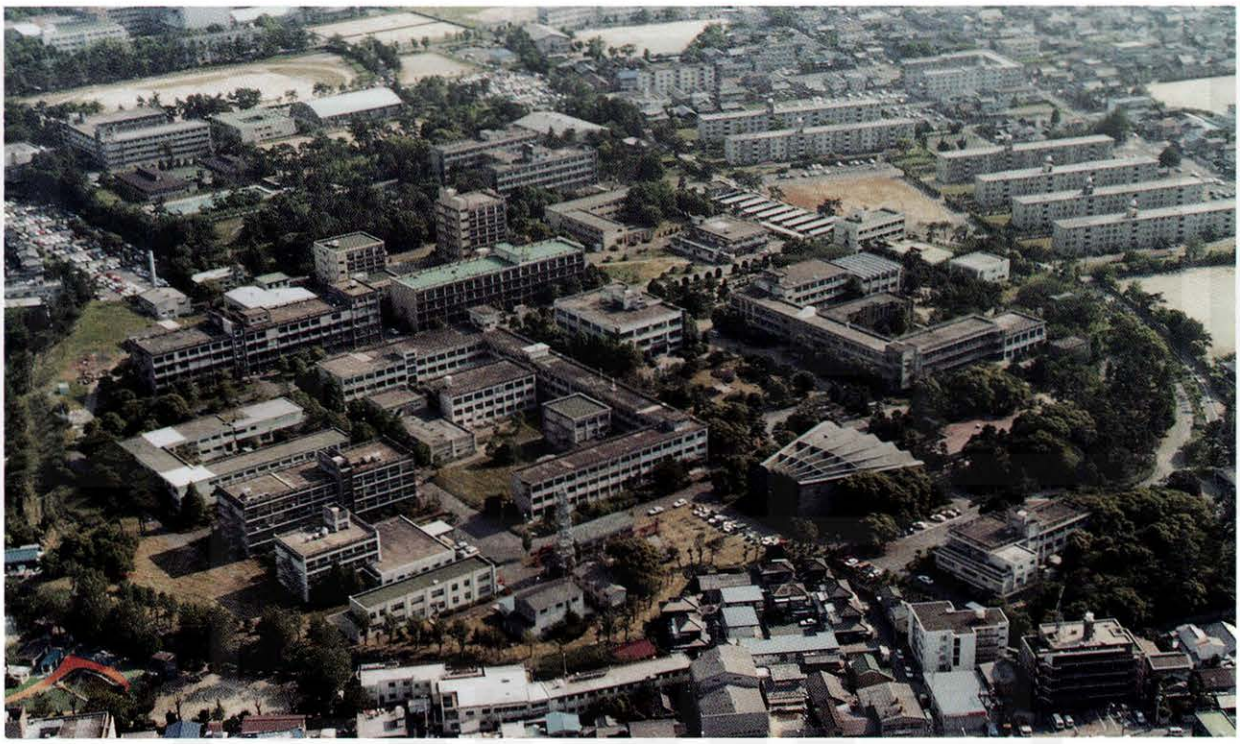

Fig. 6.6-4 Kyushu Institute of Technology photograped in 1989 by Ted from a Mainichi News helicopter.

fact-finding research visits to both Nagasaki and Hiroshima. Since then, he rendered moral support to my research as a faculty of Meiji College/Kyushu Institute of Technology, suggesting that I look for an opportunity to visit the United States of America. Dr. Kamura passed away on September 15, 1970 after I became a faculty of the University of Chicago.

Fig. 6.6-5 The Kamura Award Medal (left), 55 mm in diameter and 4 mm thick. Engraved on the back are: "The second recipient," "Tetsuya Fujita," and "1965." Prof. Kamura and I in his guest room after receiving the medal (right).

1967 Meisinger Award American Meteorological Society

昭和42年　アメリカ気象学会　マイシンガー賞

The citation of my Meisinger Award in the April 1967 issue of the Bulletin of the American Meteorological Society was as follows. The Meisinger Award, the first award established by the Society (1938), honors the memory of a young meteorologist who lost his life in 1924 when his free-flight balloon was destroyed in a thunderstorm. The award is made in recognition of particularly meritorious and outstanding research in aerology and its application to forecasting. This year the award was presented to Tetsuya Fujita, professor of meteorology, University of Chicago, for "pioneering research on the techniques of mesometeorological analysis, for the new insights provided by such method to our understanding of the mechanisms of severe local storms and tornadoes, and for broad contributions to the use of meteorological satellites." In 1953 he came to the United States and later joined the faculty of the University of Chicago, where he is now full professor of meteorology and director of the Satellite and Mesometeorology Project. Dr. Fujita recieved the Okada Award of the Meteorological Society of Japan in 1959 for his contribution to the development of mesometeorology. His many publications on severe storm analysis and mesometeorology are internationally known.

The award was presented on January 24, 1967 during the National Meeting of the American Meteorological Society at the Statler Hilton, New York City. At the conclusion of the meeting, heavy snow in the Chicago area closed down O'Hare Airport for several days, resulting in an overbooking of all trains. I had to return by Greyhound bus, taking 18 hours, and found that the city was digging out of the record-breaking 30-inch snowfall.

1975 Special Commendation and Service Award

Alabama Civil Defense Association

昭和50年　アラバマ州民間防衛局　特別貢献賞

The State of Alabama experienced its worst damage during the Superoutbreak tornadoes of April 3-4, 1974. A series of nine tornadoes left behind a combined damage path of 414 miles or 666 km, killing 88 persons and injuring 1,058 others. This special award was presented to me on July 31, 1975 at Tuscaloosa during the Tornado Preparedness Meeting of the Alabama Civil Defense Association. It cited that my aerial investigation of the tornado damage made a significant contribution to the public education of tornado safety in the State of Alabama.

1975 First Award of Best Visual Aids

Severe Local Storms Conference, AMS

昭和50年　局地性嵐会議　視覚表現最良賞

The program committee of the Ninth Conference on Severe Local Storms, American Meteorological Society held at Norman, Oklahoma decided to vote for the best visual aids paper out of the 86 presentations made during the conference. It was the first attempt by the conference to present the Best Visual Aids Award. Following the award presentation, it was announced that future awards will be presented at the conclusion of the conferences, under the rule that the past winner is not eligible for future contests.

1976 Arkansas Traveler State of Arkansas

昭和51年　アーカンサス州　特別貢献賞

This award, signed by both the Governor and the Secretary of State was presented to me at Little Rock on February 2, 1976 for my contribution to the tornado safety of the State of Arkansas. The award states,

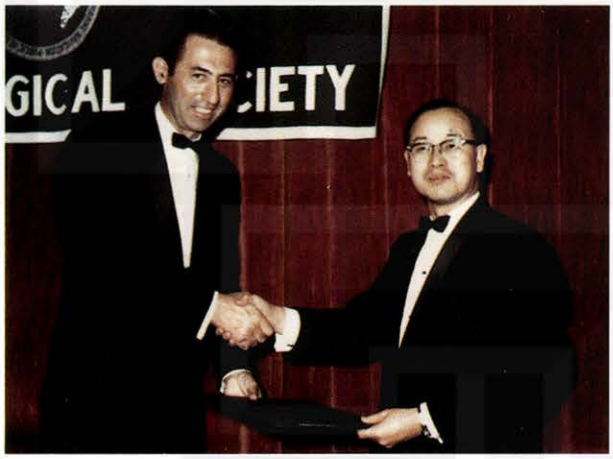

Fig. 6.6-6 Receiving the Meisinger Award from Dr. Louis Battan, President of the American Meteorological Society. (Black tie was required).

"Know Ye, that the Governor of the State of Arkansas, in the name and the authority of the people of said State, as vested in him by the Constitution and Laws of the State of Arkansas, reposing special recognition for the distinguished accomplishments, do hereby appoint and commission Dr. Theodore Fujita ARKANSAS

Fig. 6.6-7 The Special Commendation and Service Award signed by the President and the Secretary of the Alabama Civil Defense Association.

Fig. 6.6-8 The trophy of the Best Visual Aids Award.

Fig. 6.6-9 Certificate of ARKANSAS TRAVELER, an Ambassador of Good Will from Arkansas.

TRAVELER who is authorized and commissioned to serve as an Ambassador of Good Will from Arkansas to the people of other states, the people of other nations beyond the border of the United States or wherever this Ambassador of Arkansas may hereafter travel or reside. In Testimony Whereof, I have hereunder set my hand and caused the Great Seal of the State to be affixed at Little Rock this 2nd day of February in the year of One Thousand Nine Hundred and Seventy Six."

1977 Admiral Luis de Florez Flight Safety Award

Flight Safety Foundation

昭和52年　航空安全財団　アドミラル　ルイス　デ　フロレス賞

The Admiral Luis de Florez Flight Safety Award was received in Ottawa, Canada on September 21, 1977 during the International Conference on Flight Safety. The citation states, "the award is presented to Dr. T. Theodore Fujita, University of Chicago for his research and communications of information regarding thunderstorm phenomena which has provided the foundation for increased awareness and understanding of severe weather-related hazards during aircraft takeoffs and landings. Thus energized, the aviation community has been able to reconsider designs and effect procedures to further advance safety of flights."

Fig. 6.6-10 Certificate of the Admiral Luis de Florez Flight Safety Award received on September 21, 1977.

Fig. 6.6-11 Plaque of the Admiral Luis de Florez Flight Safety Award FOR OUTSTANDING CONTRIBUTIONS TO AVIATION SAFETY, 280 X 340 mm, 20 mm thick.

1977 Aviation Week & Space Technology Distinguished Service Award Flight Safety Foundation

昭和52年　航空安全財団　特別貢献賞

The Aviation Week and Space Technology Distinguished Service Award was received following the previous award. The citation states, "the award is presented to Dr. T. Theodore Fujita, University of Chicago for distinguished service in achieving safer utilization of aircraft through significant weather research identifying low-level downburst wind shears of previously unidentified severity and intensity."

Twelve years later in 1989, I was told, "You may not realize that you are the only person who has ever been selected for both the de Florez and the Distinguished Service Award at the same time when they were presented to you in Ottawa, Canada in September 1977. And you were selected by two separate and independent award boards, not connected with the Flight Safety Foundation. But the Flight Safety Foundation was especially proud to provide the forum at which they were presented."

Fig. 6.6-12 Certificate of the Aviation Week & Space Technology Distinguished Service Award received on September 21, 1977.

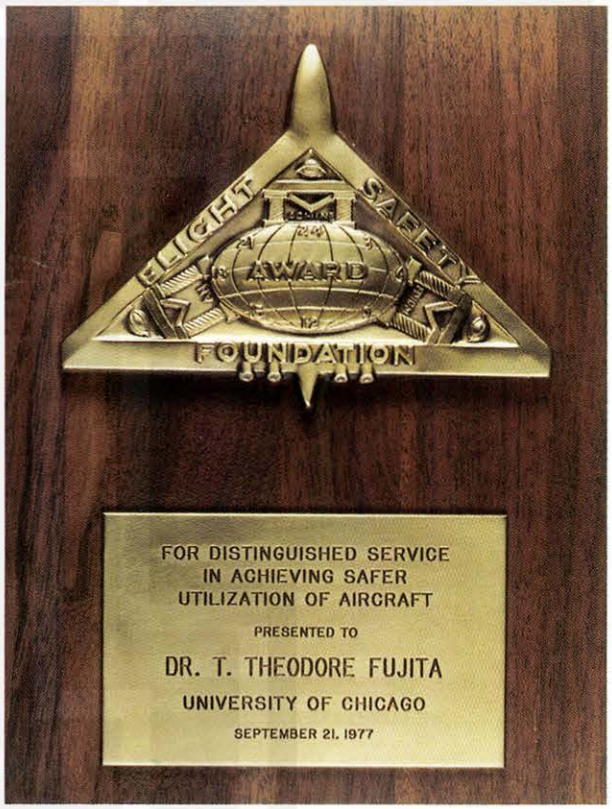

Fig. 6.6-13 Plaque of the Award FOR DISTINGUISHED SERVICE IN ACHIEVING SAFER UTILIZATION OF AIRCRAFT, 205 X 280 mm, 20 mm thick.

1978 Applied Meteorology Award

National Weather Association

昭和53年　アメリカ気象協会　応用気象学賞

This award was received in 1978, the year of the Northern Illinois Meteorological Research on Downburst (NIMROD) Project, the first fact-finding field program of the controversial downburst at that time. In spite of the controversy which prevailed, I was able to detect a number of small but strong downbursts called the "microburst." This award was timely, as it encouraged my further effort in studying the low-altitude wind shear which endangers aircraft during takeoffs and landings.

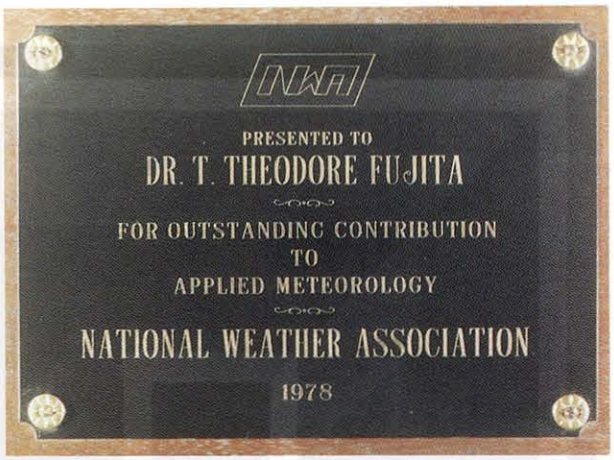

Fig. 6.6-14 The plaque of the Applied Meteorology Award of the National Weather Association received in December 1978.

1979 Distinguished Public Service Medal

National Aeronautics and Space Administration

昭和54年　アメリカ航空宇宙局　特別貢献賞

As the citation reads, "The National Aeronautics and Space Administration awards to Tetsuya T. Fujita, University of Chicago, the NASA Distinguished Public Service Medal for his significant and imaginative utilization of the measurements from low orbiting and geosynchronous meteorological satellites for nearly two decades, resulting in major advances in our understanding of the structure and evolution of severe storms."


The National Aeronautics and Space Administration
Awards to
Tetsuya T. Fujita
UNIVERSITY OF CHICAGO
the
NASA
Distinguished Public Service Medal
For his significant and imaginative utilization of the measurements from low orbiting and geosynchronous meteorological satellites for nearly two decades, resulting in major advances in our understanding of the structure and evolution of severe storms.
Signed and sealed at Washington, D.C. this twentieth day of November Nineteen Hundred and Seventy-Nine

Fig. 6.6-15 NASA Distinguished Public Service Award dated November 20, 1979 (left) and the Medal (right) received at Washington, D.C.

1982 Losey Atmospheric Sciences Award

American Institute of Aeronautics and Astronautics

昭和57年　アメリカ航空宇宙学会　ローシー大気科学賞

The American Institute of Aeronautics and Astronautics presented the Losey Atmospheric Sciences Award "in recognition of outstanding contributions to the science of meteorology as applied to aeronautics to T. Theodore Fujita for his contributions to the understanding of the development and characterization of tornadoes and for studies on the aeronautical consequences of wind shear and downbursts. January 12, 1982" at Orlando, Florida.

Fig. 6.6-16 The Losey Atmospheric Sciences Award dated January 12, 1982 (left) and the Medal, 64 mm in diameter and 6 mm thick.

1985 25 Years of Weather Satellites Award

United States Department of Commerce

昭和60年　アメリカ商務省　気象衛星25周年記念メダル

This Certificate of Appreciation signed by the Secretary of the United States Department of Commerce states, "For creative scientific leadership as an enthusiastic pioneer in the use of satellite imagery to analyze and predict mesoscale weather phenomena and to understand severe thunderstorms, tornadoes, and hurricanes."

On April 1, 1960, the United States weather satellite, TIROS 1 sent back to earth the first sequence of cloud photographs. On the 25th anniversary date, April 1, 1985 a certificate of appreciation and a silver medal were presented to a dozen contributors.

Fig. 6.6-17 The 25 Years of Weather Satellites Medal. The front side (left) of the sterling silver medal, 76 mm in diameter and 7 mm thick. The back side states,"TIROS 1, FIRST WEATHER SATELLITE, APRIL 1, 1960. FIRST GEOSTATIONARY ENVIRONMENTAL SATELLITE GOES 1, OCTOBER 16, 1975."

UNITED STATES
DEPARTMENT of COMMERCE

Certificate of Appreciation

Presented to

Mr. T. Theodore Fujita
University of Chicago (1961 - Present)

For creative scientific leadership as an enthusiastic pioneer in the use of satellite imagery to analyze and predict mesoscale weather phenomena and to understand severe thunderstorms, tornadoes and hurricanes.

SECRETARY OF COMMERCE

Fig. 6.6-18 Certificate of Appreciation signed by the United States Secretary of Commerce, Mr. Malcolm Baldridge who sent me a separate letter of congratulations.

Fig. 6.6-19 Award ceremony at the Space Museum in Washington, D.C. preceded by a military honor.

1988 Applied Meteorology Award

American Meteorological Society

昭和63年　アメリカ気象学会　応用気象学賞

The Award for Outstanding Contribution to the Advance of Applied Meteorology of the American Meteorological Society was received "for pioneering studies of damaging storms on the mesoscale." Since 1953, when I began studying mesoscale severe storms, I introduced the new terms being used in applied meteorology and storm warnings as follows: mesohigh, mesolow, mesocyclone, tornado-related wall cloud, collar cloud, tail cloud, Fujita tornado scale, suction vortex, downburst, macroburst, and microburst.

1989 Vermeil Gold Medal

French National Academy of Air and Space

平成元年　フランス航空宇宙アカデミー金メダル

The notification of the Vermeil Gold Medal Award from Dr. Michel Bignier, President of the French National Academy of Air and Space states in French, "J'ai le plaisir de vous faire connaitre que lors de sa derniere seance tenue le 6 Juin a Paris, l'Academie Nationale de l'Air et de l'Espace, sur la proposition de Monsieur Marc Pelegrin, a decide a l'unanimite de vous attribuer sa Medaille de Vermeil en reconnaissance de la contribution eminente que vous avez apportee a l'etude des phenomenes meteorologiques dangereux pour l'aviation."

Fig. 6.6-20 The Vermeil Gold Medal received on November 24, 1989 at Toulouse, France. The medal is 70 mm in diameter, 15 mm thick at the center and 5 mm thick around its edge.

Fig. 6.6-21 Front and back sides of the medal with convex surfaces which are hard to photograph under artificial illumination.

Fig. 6.6-22 The award ceremony at the Capitol Building in Toulouse. From left: Vice-President Marc Pelegrin, President Michel Bignier, Ted Fujita, and an Academy official.

Fig. 6.6-23 Ted Fujita seated behind Captain Robin during the 3 hr 31 min flight of the French Concorde from Paris to New York on November 30, 1989. (Photo by Susie Fujita)

1990 Fujiwara Award

Meteorological Society of Japan

平成 2 年　日本気象学会　藤原賞

It was a great honor to be selected as the recipient of the 1990 Fujiwara Award of the Meteorological Society of Japan. Dr. Sakuhei Fujiwara was the fifth Director General of the Central Meteorological Observatory of Japan. I visited his house in 1949 when I was working on my doctoral thesis on typhoons. Without showing me

Fig. 6.6-24 The Fujiwara Award Medal, 110 mm in diameter and 9 mm thick, received on May 24, 1990 during the Spring Meeting of the Meteorological Society of Japan.

any sign of his deteriorating health, he taught me his concept of cyclonic storms of all types and the Fujiwara Effect of typhoon motions. My keen interest in studying U.S. tornadoes was brought forth during the brief but imaginative meeting with him, only one year before he passed away on September 22, 1950.

The citation for the Fujiwara Award was "for the pioneering research and development of mesometeorology." The reason for the award selection as published in the April 1990 issue of Tenki (Weather) is reproduced.

業　績：メソ気象学の開拓

選定理由：藤田会員は，地域気象観測・航空機観測・写真観測・レーダー観測・高層観測・気象衛星観測とあらゆる観測手段で得られた気象データを巧妙精緻に解析して，気象擾乱のメソないしマイクロ構造を世に示すことにより，全く新しいメソ気象学と呼ばれる分野を開拓し，その研究成果はトルネードの解明や航空保安対策などに大きな貢献をした．

藤田会員は，戦後間もない時期に，雷雨の解析から雷雲中に下降気流が存在することを提唱し，また寒冷前線や台風の細かい解析を行ってメソ解析の道を開いた．

シカゴ大学に移ってからはスコールラインとトルネードの調査研究を精力的に進め，新しいメソ気象解析法を確立すると共にメソ気象学を体系づけた．トルネードの研究においては，航空機を使った調査や実地踏査においてその鋭い洞察力は他の追随を許さぬものがあり，その結晶である被害状況からトルネードの強さを判定する藤田スケールはアメリカ国内で広く使われている．また，トルネードの渦には複数の漏斗が存在しうることや，大きな破壊力を持った吸上渦の存在を実証した．さらに藤田会員はトルネード調査の過程で，竜巻きによるスパイラルな被害物散乱パターンの他に放射状の被害物散乱パターンが存在することを発見し，積雲活動の一過程で，従来の気象観測網にはかかりにくい小規模ながら強い垂

直噴流が現れることがあることを発見し，これをマイクロバーストと命名した．その存在は NIMROD 計画や JAWS 計画，COHMEX 計画等の特別観測で明らかとなり，従来はとかくパイロットの操縦ミスとされた離着陸時の事故の多くがマイクロバーストに伴うウインドシアによることが裏づけられ，それへの安全対策も進められている．同会員は衛星気象の分野でも多くの業績があり，また日米間の気象研究の橋渡しや共同研究においても多くの貢献を果している．

以上のとおり，藤田会員の功績は誠に大きいものがある．よって日本気象学会は同会員に藤原賞を贈呈するものである．

1991 Kun-nito Zuihosho

Government of Japan

平成 3 年　日本国政府　勲二等瑞寶章

Dr. Tetsuya (Theodore) Fujita, 70, Charles E. Merriam Distinguished Service Professor Emeritus of the University of Chicago, was honored April 29 by the Japanese government for his life-long contributions to the science of meteorology and public safety. He attended the Joint National Awards Ceremony at the Imperial Palace in Tokyo where he was decorated by Prime Minister Kaifu and blessed by Emperor Akihito on May 8. He received the Order of the Sacred Treasure, Gold and Silver Star.

Born and educated in Japan, Dr. Fujita began his career as a member of the Physics Department at the Kyushu Institute of Technology, where he began his research on severe storms. A turning point in his career came in 1953 when the University of Chicago offered him a position as a research associate. He became a faculty member of the Department of Geophysical Sciences in 1962 and was named the Director of the Severe Storms Project.

Among Dr. Fujita's many accomplishments is his development of the Fujita Tornado Scale, which is now the internationally accepted standard to measure the severity of tornadoes. During the past 27 years he and his staff have flown over the damage areas of more than 400 tornadoes all over the world, taking high-quality aerial photographs for his study of tornadoes. These works have earned him the nickname of "Mr. Tornado."

The development, in 1976, of his hypothesis regarding "microbursts," a simultaneous downflow and outflow of winds, was a significant milestone in his career. Dr. Fujita hypothesized that the crash of a commercial airliner in 1975 was due to a microburst. At the time, many meteorological experts disagreed with him, but his continued research, using Doppler radar, led to the discovery of a microburst windshear. His research on this subject convinced aviation authorities to install Doppler radar, which is recognized as a step in improving aviation safety.

Dr. Fujita has served as an important link between American and Japanese meteorologists. His profound work, coupled with his frequent visits to Japan have inspired numerous meteorologists, scholars and officials. He also initiated a joint U.S. Japan research project 1962-1968, which is credited with greatly improving the study of meteorology in Japan.

The government of Japan is pleased to recognize Dr. Fujita for his work as a pre-eminent meteorological scholar.

The Consulate General of Japan at Chicago

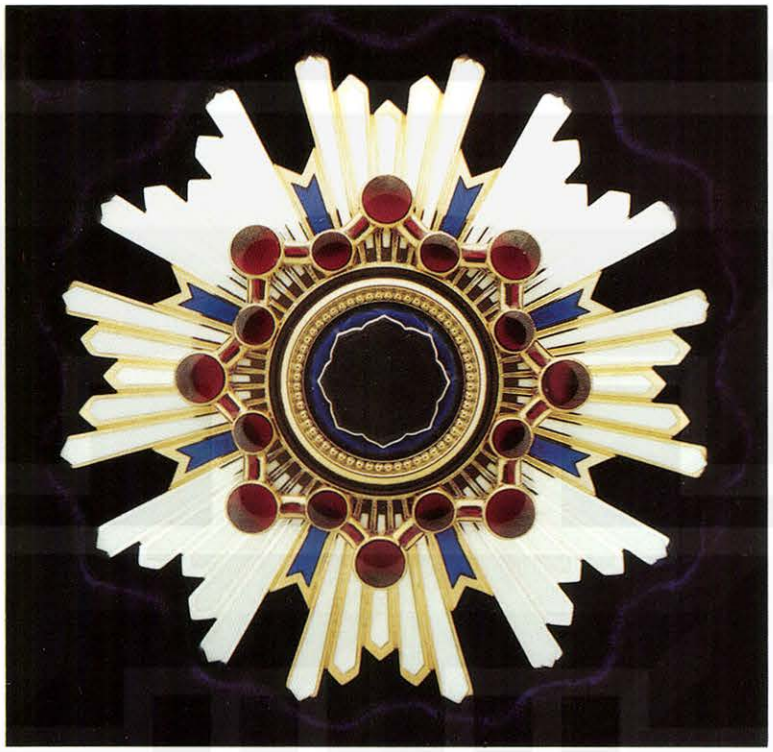

日本国天皇はアメリカ合衆国人
藤田哲也を勲二等に叙し
瑞寶章を贈与する
平成三年四月二十九日皇居において
璽をおさせる

平成三年四月二十九日
内閣総理大臣 海部俊樹
総理府賞勲局長 稲橋一正
第一〇六〇四号

Fig. 6.6-25 Kun-2tou Zuihosho, the Level 2 Order of the Sacred Treasure, Gold and Silver Star (above) and Kunki, the Certificate of Order (below) with the Seals of the State of Japan, Prime Minister Toshiki Kaifu, and Director Kazumasa Inehashi, Bureau of Decoration, affixed at the Imperial Palace on the 29th of April in the 3rd year of Heisei. Certificate Number 10604.

Two GOES pictures showing the Monrovia microburst cloud (circled) in northern Alabama at 1400 CDT (above) and at 1430 CDT. The microburst wind began at 1421, reaching the peak wind of 30 m/s at 1425 CDT (p122).

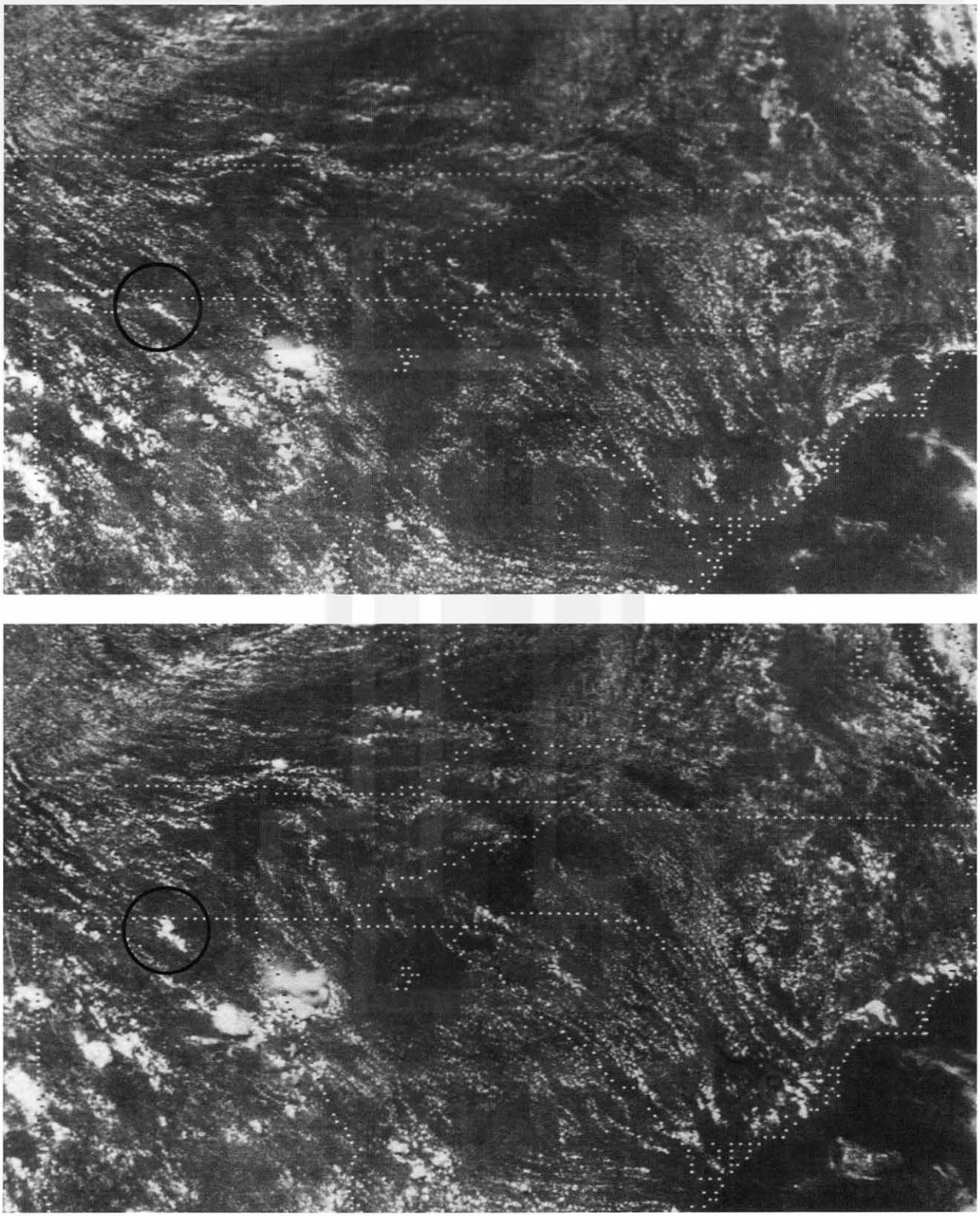

The Monrovia cloud I photographed from NOAA P-3 at 140934 CDT when the high reflectivity core began sinking from near the cloud top (p123) and at 141539 CDT, the time of constriction (p125).

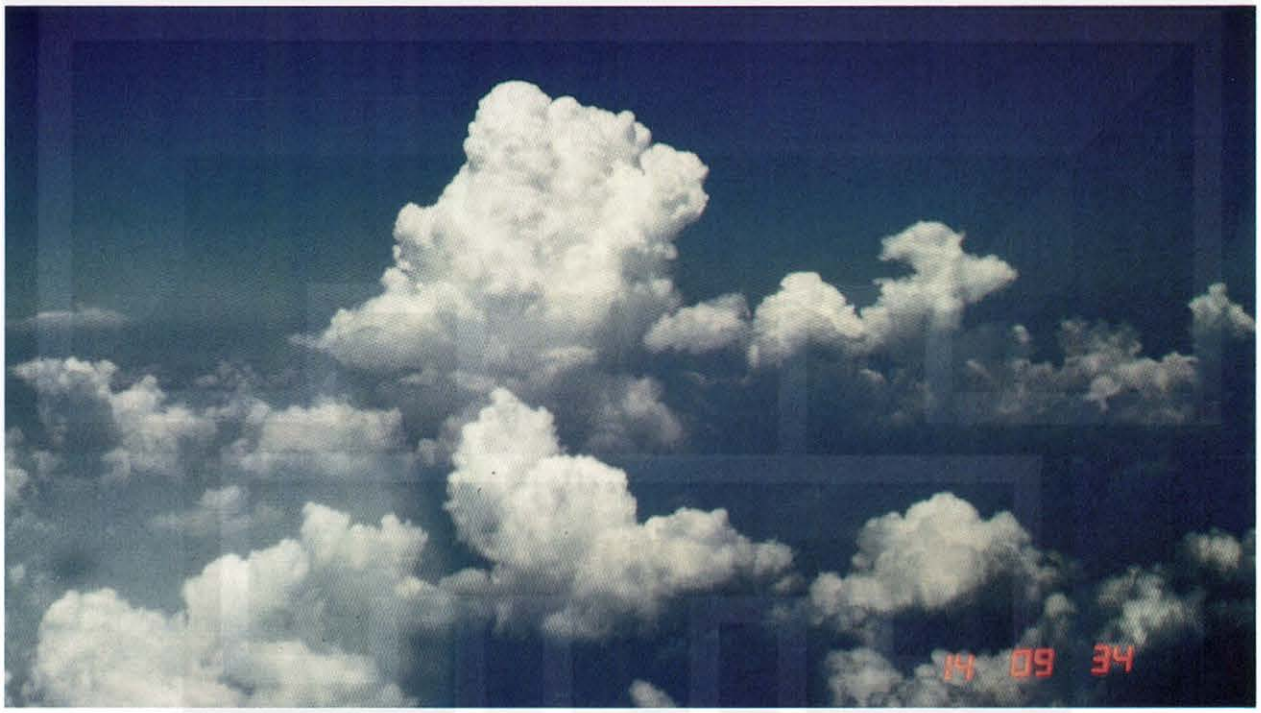

The Monrovia cloud at 142505 CDT when the 30 m/s peak winds (p122) were in progress. The reflectivity core was already on the ground, giving an impression of little wind shear at low altitudes beneath the cloud.

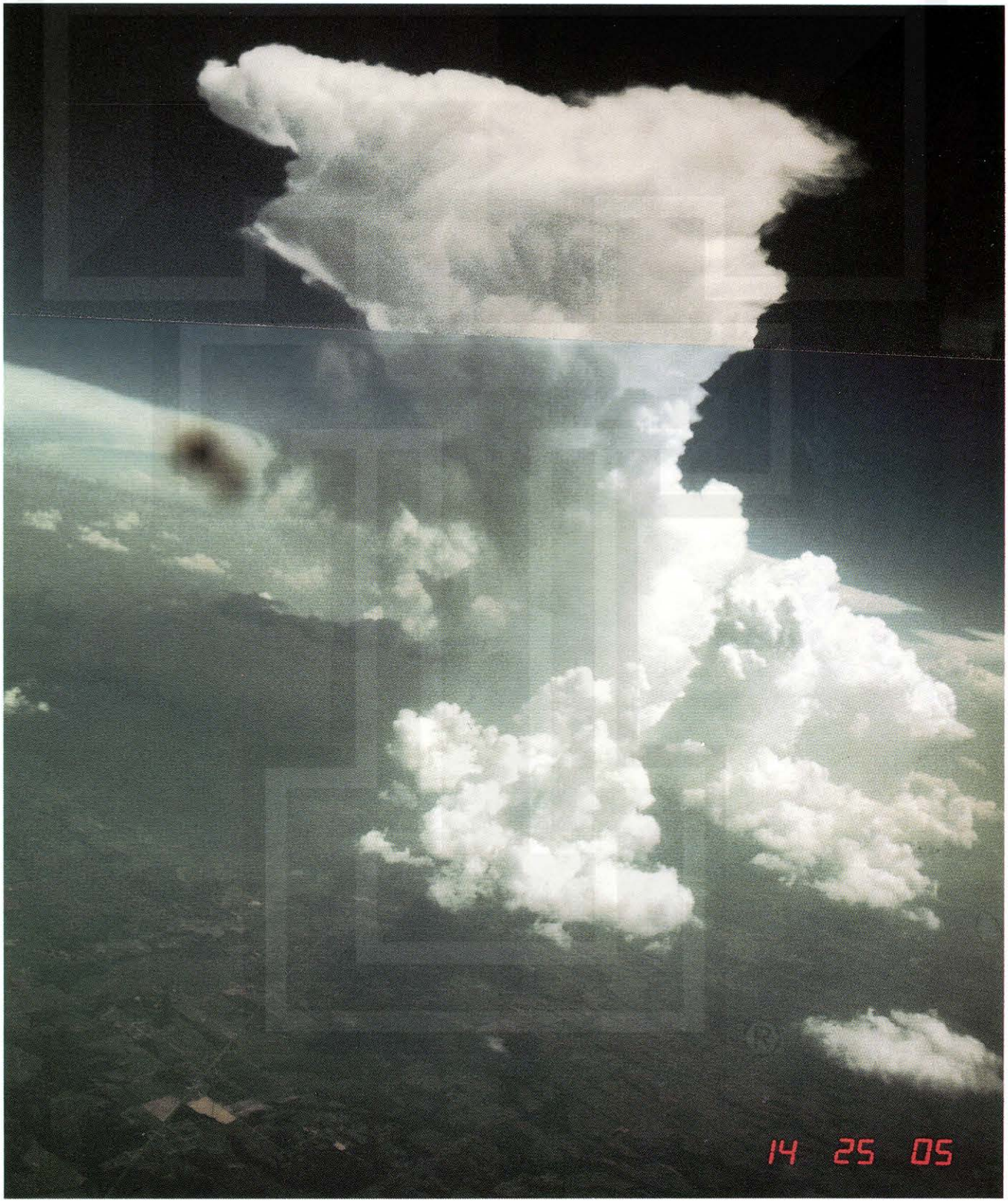

The industrial section of Streamwood near the O'Hare airport damaged by an early morning microburst occurring at 0809 CDT on 29 June 1990. Photo by the Streamwood Police Department.

Brandenburg, Kentucky before and after the F5 tornado on 3 April 1974. The tornado touched down in western Breckenridge county at 3:30 p.m. and moved northeast. After reaching the F5 intensity, Brandenburg was hit at 4:07 p.m. In the wake of the incredible tornado, 31 persons were killed injuring 270 others. Three days after the storm, three more persons died of injuries and one person suffering from injuries died five years after the tornado.

After the 3-4 April 1974 superoutbreak tornadoes, I flew over 10,000 miles in Cessna, noticing that the damages in Xenia, Ohio and Brandenburg, Kentucky were the worst as seen from the air. Since then, I visited Brandenburg and interviewed Ms. Jane Willis, then the owner and editor of the Meade County Messenger newspaper on Main Street seen in the middle of this aerial picture which I received at that time. Before completing this manuscript, I called Jane to refresh our memories of the tornado 18 years ago. We sincerely hope that Brandenburg is free from tornado forever.

Brandenburg after the 3 April 1974 tornado photographed by the Kentucky Air National Guard. The areas of the two pictures were selected as similar as possible.

Path of the Guin, Alabama tornado (above) of 3 April 1974 photographed by NASA's Earth Resources Technology Satellite (ERTS) on 28 April 1974 and an aerial photo (below) of William B. Bankhead National Forest by the Alabama National Forest Service.

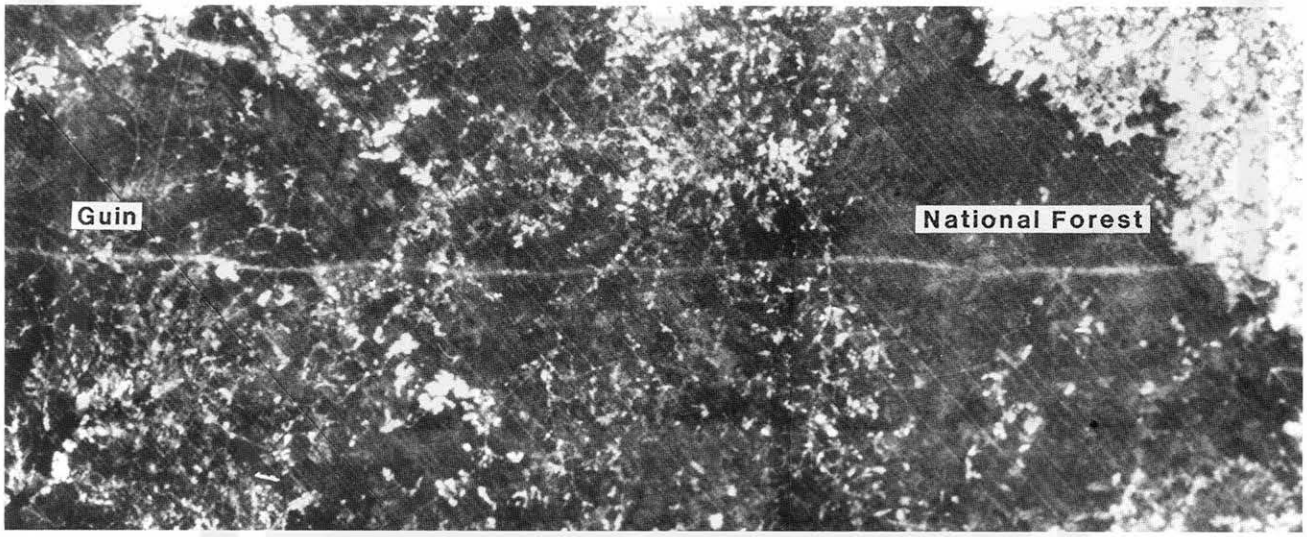

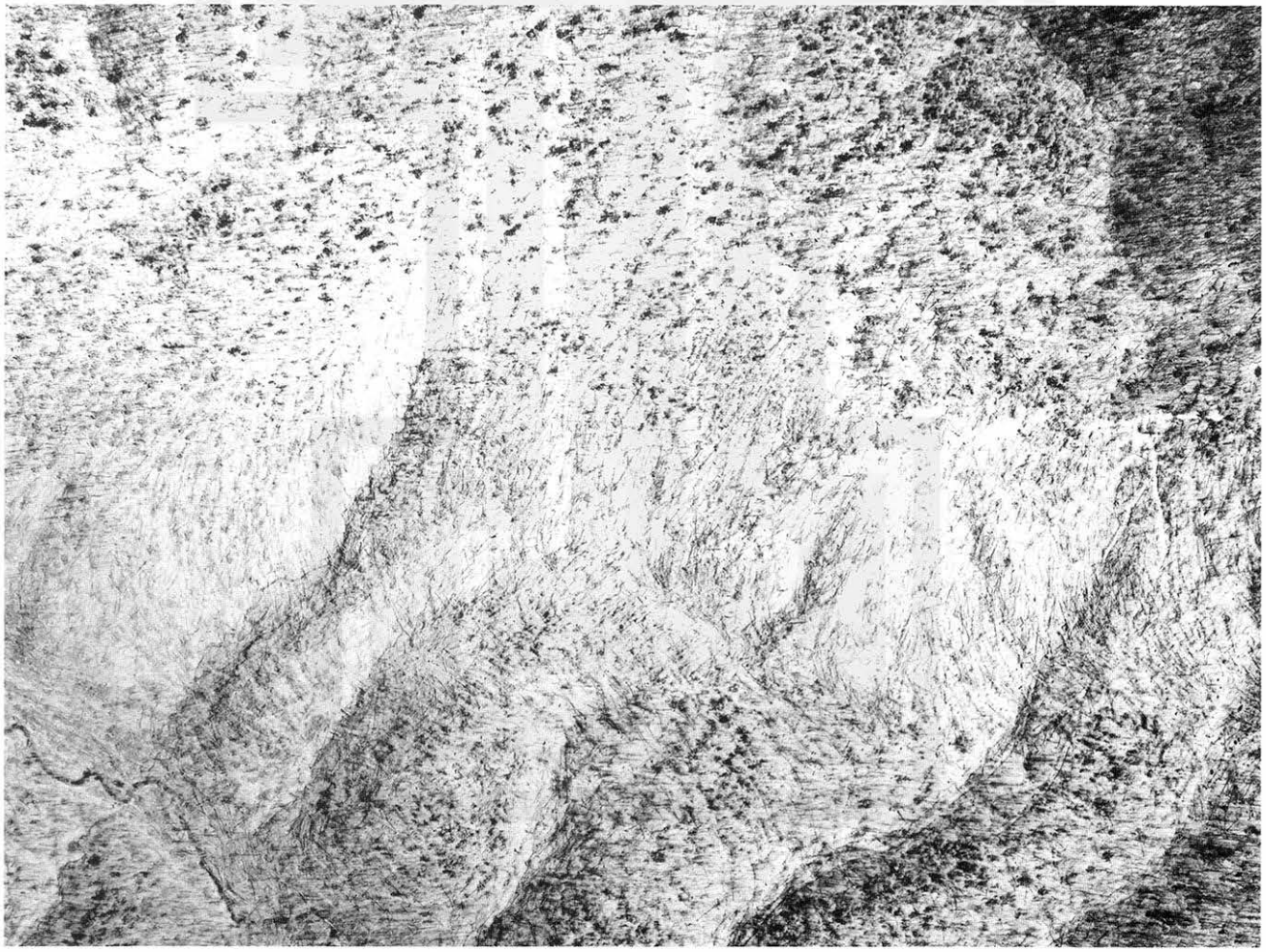

An F5 forest damage southwest of Murphy, South Carolina (above) and uprooted trees on the steep slope in Kentucky (below) by the 3 April 1974 tornadoes.

A laboratory model tornado at the Wind Research Laboratory, the University of Chicago. I designed the machine which was constructed by Mr. Vincent Ankus.

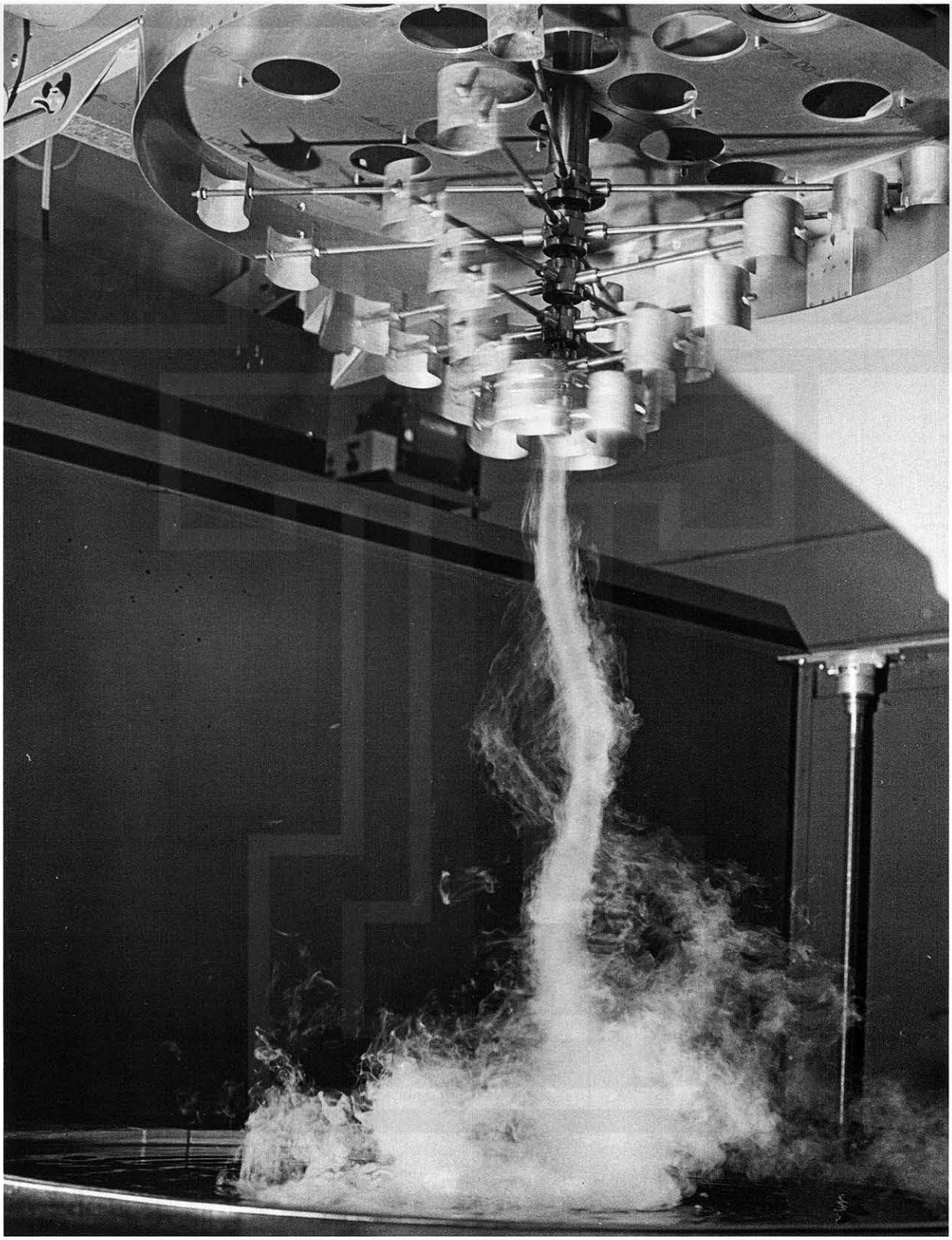

A model tornado moving from right to left along with the casing of rotating cups traveling toward the left. Unlike idealized tornado models elsewhere, students are allowed to play with the vortex generated by the casing (or cloud) which is designed to travel at various speeds while changing the height above the surface with numerous holes which release dry ice smokes.

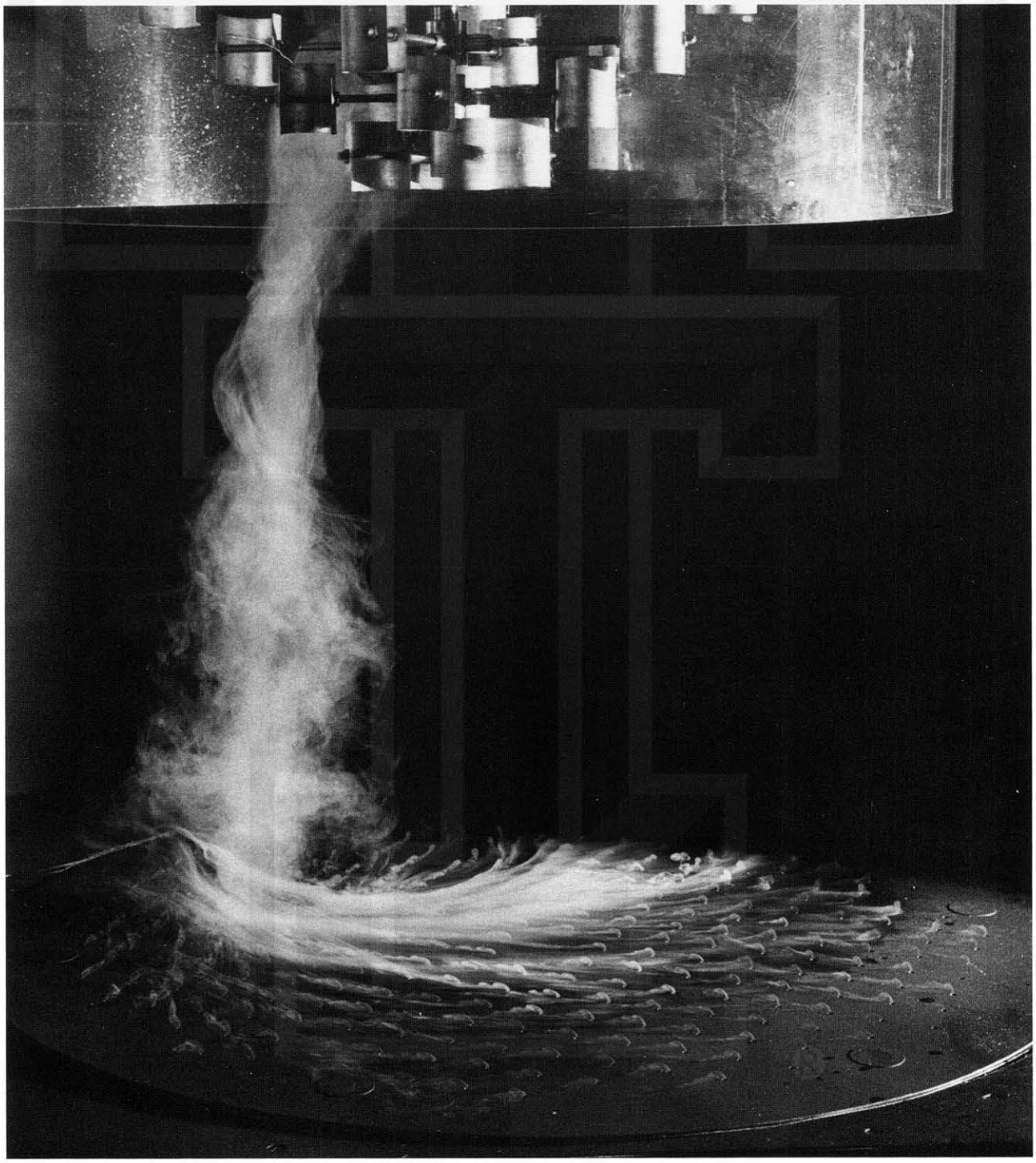

Multiple suction vortices formed beneath the Wichita Falls, Texas tornado of 10 April 1979. This is the most dramatic picture in proving the existence of suction vortices which I proposed in 1971 (p36) based on the ground marks before seeing a picture such as this. Courtesy of Mr. Floyd Styles who took me around his photographic sites.

Positions of the Sayler Park tornado in segments A through I of the 8-mm movie taken by Mrs. Pat Berding on 3 April 1974. Tornado centers were determined by combining tornado azimuths with my damage photographs.

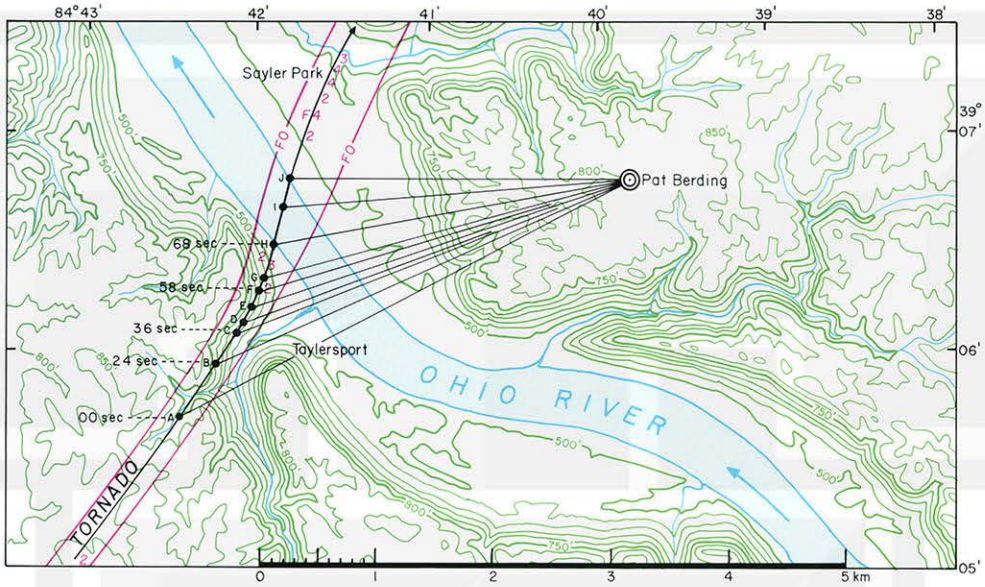

Airflow of the Sayler Park tornado at location "F" estimated by tracking the cloud fragments in Berding's movie for one second. Found unexpectedly was an upburst wind of 63 m/s (141 mph) which eroded the funnel cloud.

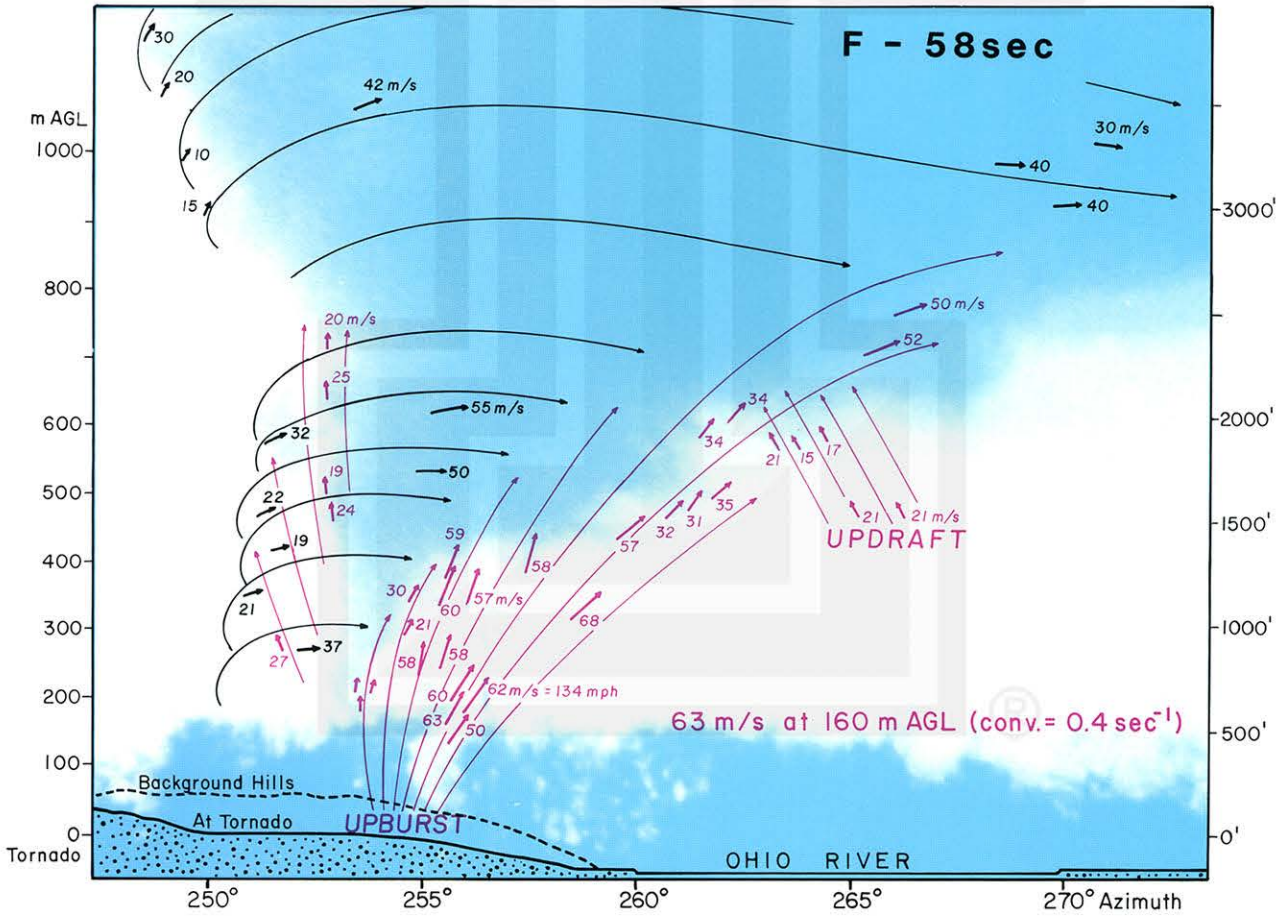

The tornado at location "C" on the slope of the plateau. The speed of the upburst was 56 m/s (125 mph) when the tornado was descending the steep slope.

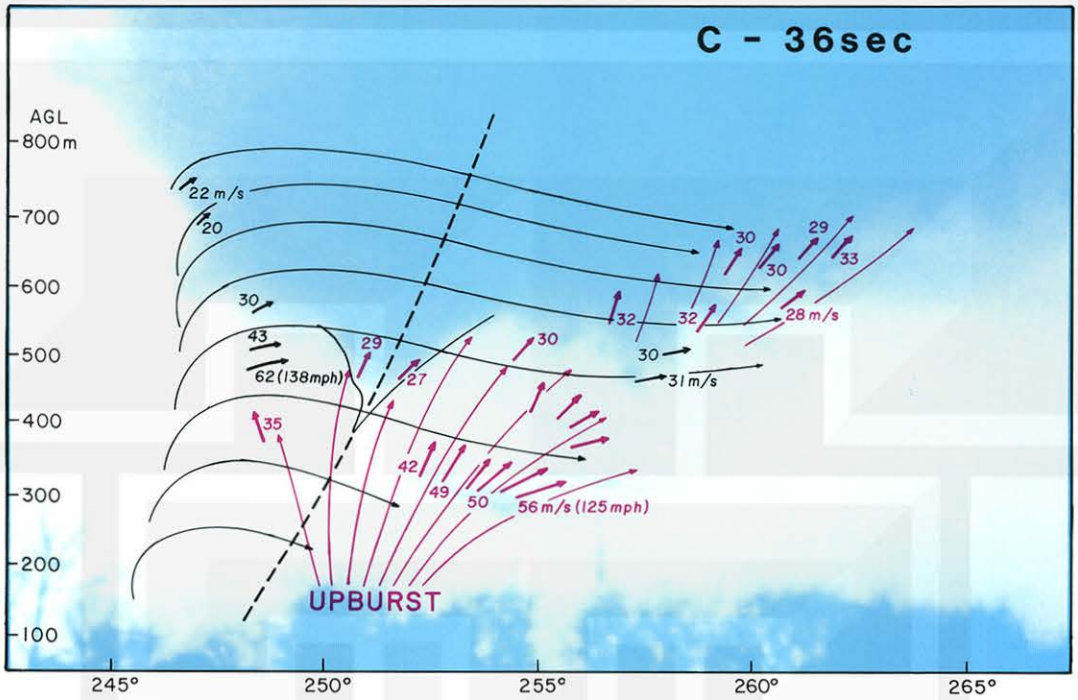

The tornado at location "H" on the flat valley of the Ohio River. The maximum swirling speed of 76 m/s (170 mph) was measured at 300 m AGL. These motion computations revealed a rapid change in the flow fields within a very short time.

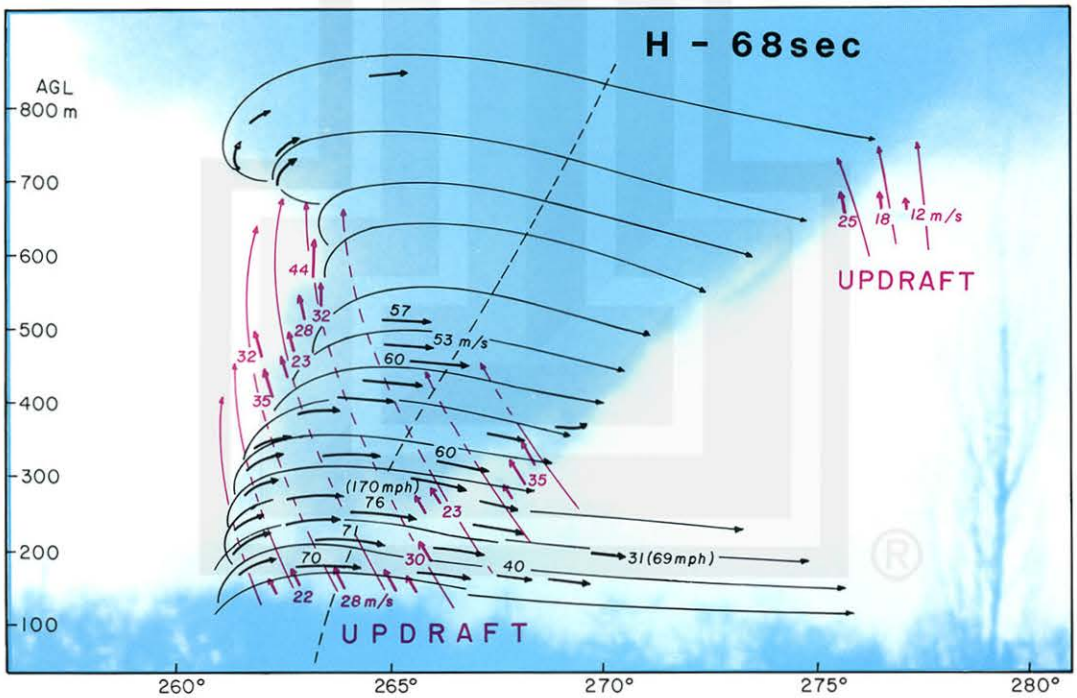

An experiment conducted during the laboratory session of my undergraduate course in general meteorology. In this experiment, a matrix of 20 pictures was taken by changing the rotation rate of the cups in the overhead casing and the suction speed of the air drawn through the multiple holes in the casing (p284). The rotation is supposed to simulate mesocyclone while the suction simulates the updraft beneath the rotating cloud.

In general, the induced vortex intensifies with increasing rotation rate, suggesting that a fast-rotating mesocyclone is likely to spawn strong vortices. When a strong updraft is applied to a rotation-induced vortex, the vortex either weakens or even disappears, suggesting that strong subcloud updraft could destroy a tornado by forcing the air swirling on the surface to rise prematurely before entering the vortex. I was pleased to have provided my students with unsolved problems regarding the mystery of complicated vortices (pp287 and 288).

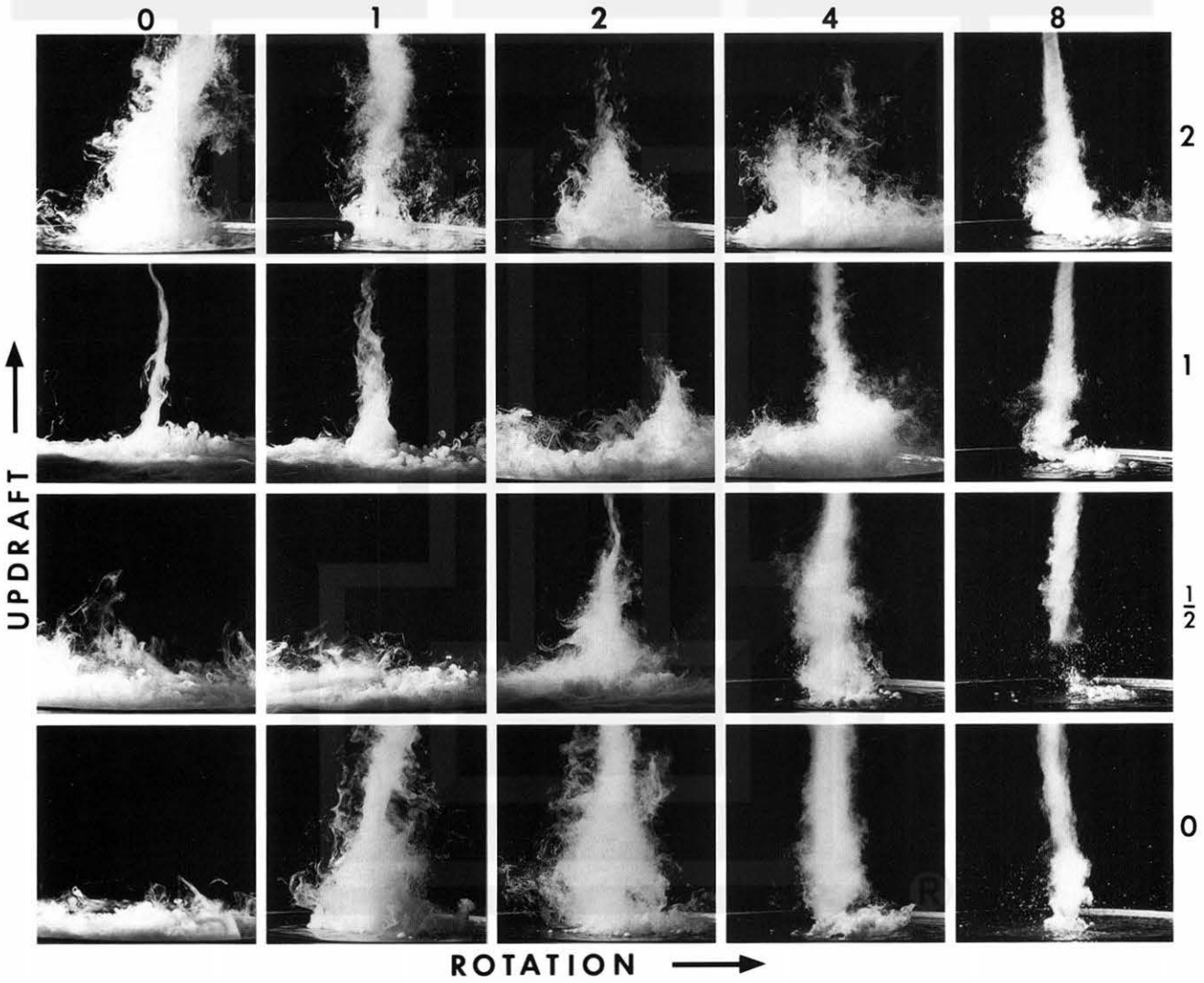

A planet-scale view of the earth in color obtained by NASA's Applications and Technology Satellite (ATS) III at local noon on 19 November 1967. From the geosynchronous altitude of 37,000 km (23,000 miles) above the surface, the earth is a beautiful and peaceful planet we live in.

City-scale views of my birthplace which I photographed on 1 June 1989. The birthplace area (below) became congested while the view toward the Inland Sea (above) is still full of green rice fields untouched by developers.

EDUCATION AND EMPLOYMENT

1920	OCT	23	Born at 1258 Sone-machi, Kiku-gun, Fukuoka-ken (3-3-5 Nakasone, Kokuraminami-ku, Kitakyushu City now), JAPAN
1927	APR	01	Enter Sone Elementary School (Sone Primary/Middle School now), Sonemachi
1932	APR	01	Transfer to Komemachi Elementary School, Kokura City
1933	MAR	25	Graduate Komemachi Elementary School
	APR	01	Enter Kokura Middle School (Kokura High School now), Kokura City
1939	MAR	25	Graduate Kokura Middle School
	APR	10	Enter Meiji College of Technology (Kyushu Institute of Technology now), Tobata City
1943	SEP	26	Graduate Meiji College of Technology with B.S. equivalent in Mechanical Engineering. Thesis: On the force of impact
	SEP	27	Research Assistant of Physics, Meiji College of Technology
	OCT	23	Assistant Professor of Physics, Meiji College of Technology
1949	MAY	31	Meiji College of Technology was reorganized into Kyushu Institute of Technology under the Education Reform Act.
	JUN	30	Assistant Professor, Kyushu Institute of Technology
1950	AUG	01	Doctor of Science (ScD) from Tokyo University. ScD Thesis: Analytical study of typhoons
	AUG	13	Visiting Research Associate, University of Chicago, Chicago, Illinois, U.S.A.
1955	OCT	04	Back to Japan for immigrant visa
1956	JUL	21	Return to U.S. as an immigrant
	JUL	26	Research Professor/Senior Meteorologist, University of Chicago
1962	JUL	01	Associate Professor of Meteorology, University of Chicago
1965	OCT	01	Professor of Meteorology, University of Chicago
1968	NOV	12	Become a U.S. citizen
1989	FEB	01	Charles E. Merriam Distinguished Service Professor, University of Chicago
1990	DEC	31	Retire at age 70
1991	JAN	01	Charles E. Merriam Distinguished Service Professor Emeritus

List of Publications

MRP Mesometeorology Research Project (1961-63)

SMRP Satellite and Mesometeorology Research Project (1964-87)

WRL Wind Research Laboratory (1988-)

1948 Meteorological study of the 88% solar eclipse at Kitakyushu on May 9, 1948. 51 pp. (Japanese)

1949 a Fine structure of a cold front and its environment. 9 pp. (Japanese)

b Analytical study of typhoon Della. 18 pp. (Japanese)

1951 a Disturbances observed in the vicinity of the Okhotsk Sea anticyclone. Bull. Kyushu Inst. Technol., 1, 65-73.

b Microanalytical study of thunder-nose. Geophys. Mag. Japan, 22, 78-88.

c Microanalytical study of cold front. Geophys. Mag. Japan, 22, 237-277.

1952 a A study on pressure dip within typhoon Della. Bull. Kyushu Inst. Technol., 2, 52-61.

b Pressure distribution within typhoon. Geophys. Mag. Japan, 23, 437-451.

1955 Results of detailed synoptic studies of squall lines. Tellus, 7, 405-436.

1957 a Mesoanalysis: An important scale in the analysis of weather data. U.S. Wea. Bur. Res. Paper 39, 83 pp. (Fujita, Newstein, and Tepper)

b Recent studies in mesometeorology. 75th Anniv. Vol. J. Meteor. Soc. Japan, 256-261.

c A revised method of pressure reduction. U.S. Wea. Bur. Tech. Report 4, 8 pp. (Fujita and Brown)

d Three-dimensional mesoanalysis of a squall line. Rep. of Investigation, Illinois State Water Survey, 36 pp.

1958 a A study of mesosystems and their radar echoes. Bull. Amer. Meteor. Soc., 39, 538-554. (Fujita and Brown)

b Structure and movement of a dry front. Bull. Amer. Meteor. Soc., 39, 574-582.

c Mesoanalysis of the Illinois tornadoes of 9 April 1953. J. Meteor., 15, 288-296.

d Tornado cyclone: The bearing system of tornadoes. Proceedings, 7th Weather Radar Conference, Miami Beach, K 31-38.

1959 a Precipitation and cold air production in mesoscale thunderstorm systems. J. Meteor., 16, 454-466.

b Study of mesosystems associated with stationary radar echoes. J. Meteor., 16, 38-52.

1960 a A detailed analysis of the Fargo tornadoes of June 20, 1957. U.S. Wea. Bur. Res. Paper 42, 67 pp.

b Mesometeorological study of pressure and wind fields beneath isolated radar echoes. Proceedings, 8th Weather Radar Conference, San Francisco, 151-158.

c Mother cloud of the Fargo tornadoes of 20 June 1957. Monogr. No. 5 Amer. Geophys. Union, Cumulus Dynamics, Pergamon Press, 175-177.

d Structure of convective storms. Proceedings, Cloud Physics Conference, Woods Hole, 61-66.

1961 a Investigation of squall lines with the use of radar and satellite photographs. Proceedings, 9th Weather Radar Conference, Kansas City, 186-192. (Fujita and Ushijima)

1961 b A method of combining radar, aerial, and satellite photographs taken during hurricanes. 2nd Technical Conference on Hurricanes, Miami Beach.

c Report on the Chicago tornado of March 4, 1961. MRP Res. Paper 1, Univ. of Chicago, 13 pp. (Brown and Fujita) #1

d Outline of a technique for precise rectification of satellite cloud photographs. MRP Res. Paper 3, Univ. of Chicago, 25 pp. #3

1962 a Index to the NSSP surface network. U.S. Wea. Bur., NSSP Report 6, [NTIS No. PB-168212], 32 pp. #2

b A review of researches on analytical mesometeorology. MRP Res. Paper 8, Univ. of Chicago, 114 pp. #8

c On the mesometeorological field studies near Flagstaff, Arizona. J. Appl. Meteor., 1, 26-42. (Fujita, Styber, and Brown)

d Meteorological interpretation of convective nephsystems appearing in TIROS cloud photographs. Proceedings, 1st International Symposium on Rocket and Satellite Meteorology, Washington, D.C., 357-387. (Fujita, Ushijima, Hass, and Dellert) #9

e Numerical study of a mesohigh of June 26-27, 1953 over the United States Midwest. Proceedings, International Symposium on Numerical Weather Prediction, Tokyo, 501-519.

f Model of a hail cloud as revealed by photogrammetric analysis. Nubila, 1, 85-105. (Fujita and Byers)

1963 a A technique for precise analysis of satellite data: Volume I-Photogrammetry. U.S. Wea. Bur., Meteor. Sat. Lab. Report 14, 106 pp.

b Analysis of selected aircraft data from NSSP operation, 1962. U.S. Wea. Bur. NSSP Report 16, 29 pp. #11

c Radar and photogrammetric study of the Illinois tornadoes of April 17 and 22, 1963. Preprints, 3rd Conference on Severe Local Storms, Urbana, 19 pp. (Goldman and Fujita) #24

d Development of a cumulonimbus under the influence of strong vertical wind shear. Proceedings, 10th Weather Radar Conference, 178-186. (Fujita and Arnold)

e Outline of a theory and examples for precise analysis of satellite radiation data. MRP Res. Paper 15, Univ. of Chicago, 33 pp. #15

f Preliminary result of analysis of the cumulonimbus cloud of April 21, 1961. MRP Res. Paper 16, Univ. of Chicago, 16 pp. (Fujita and Arnold) #16

g A technique for precise analysis of satellite photographs. MRP Res. Paper 17, Univ. of Chicago, 50 pp. #17

h Cloud distribution over the Great Lakes observed by TIROS meteorological satellite. 224th Natl. Mtg., Amer. Meteor. Soc., Cleveland. (Fujita, Mendez, and Gargard)

i Detection of hurricanes using TIROS infrared data. Proceedings, Symposium on Tropical Meteorology, New Zealand, 582-589. (Fujita and Arnold)

j Evaluation of limb darkening from Tiros III radiation data. MRP Res. Paper 18, Univ. of Chicago, 19 pp. (Larsen, Fujita, and Fletcher) #18

k Analytical mesometeorology: A review. Meteor. Monogr., Amer. Meteor. Soc., 5, 77-125.

l Synoptic interpretation of Tiros III measurements of infrared radiation. MRP Res. Paper 19, Univ. of Chicago, 39 pp. (Pedersen and Fujita) #19

m Tiros III measurements of terrestrial radiation and reflected and scattered solar radiation. MRP Res. Paper 20, Univ. of Chicago, 11 pp. (Larsen, Fujita, and Fletcher) #20

1963 n Use of Tiros pictures for studies of the internal structure of tropical storms. MRP Res. Paper 25, Univ. of Chicago, 25 pp. (Fujita and Ushijima) #25

o Proposed mechanism of hook echo formation. MRP Res. Paper 27, Univ. of Chicago, 35 pp. (Fujita and Stuhmer) #27

p The decaying stage of hurricane Anna of July 1961 as portrayed by Tiros cloud photographs and infrared radiation from the top of the storm. MRP Res. Paper 28, Univ. of Chicago, 13 pp. (Fujita and Arnold) #28

1964 a Meteorological interpretation of satellite data. WMO Seminar, Tokyo.

b A technique for precise analysis of satellite data, Volume II-Radiation analysis. SMRP Res. Paper 29, Univ. of Chicago, 20 pp. #29

c A study of cumulus clouds over the Flagstaff research network with the use of U-2 photographs. SMRP Res. Paper 33, Univ. of Chicago, 25 pp. (Bradbury and Fujita) #33

d The scanning printer and its application to detailed analysis of satellite radiation data. SMRP Res. Paper 34, Univ. of Chicago, 29 pp. #34

e Synoptic study of cold air outbreak over the Mediterranean using satellite photographs and radiation data. SMRP Res. Paper 35, Univ. of Chicago, 33 pp. (Rabbe and Fujita) #35

f Proposed operation of instrumented aircraft for research on moisture fronts and wake depressions. SMRP Res. Paper 37, Univ. of Chicago, 31 pp. (Fujita and Bradbury) #37

1965 a Evaluation of errors in the graphical rectification of satellite photographs. J. Geophys. Res., 70, 5997-6007. #30

b Resolution of the Nimbus high resolution infrared radiometer. J. Appl. Meteor., 4, 492-503. (Fujita and Bandeen) #40

c A study of factors contributing to dissipation of energy in a developing cumulonimbus. SMRP Res. Paper 42, Univ. of Chicago, 65 pp. (Brown and Fujita) #42

d Death Valley temperature analysis utilizing NIMBUS 1 infrared data and ground-based measurements. SMRP Res. Paper 45, Univ. of Chicago, 19 pp. (Reap and Fujita) #45

e Formation and steering mechanism of tornado cyclone and associated hook echoes. Mon. Wea. Rev., 93, 67-78.

1966 a Accurate calibration of Doppler winds for their use in the computation of mesoscale wind fields. Mon. Wea. Rev., 94, 19-35. #36

b Aerial survey of the Palm Sunday Tornadoes of April 11, 1965. SMRP Res. Paper 49, Univ. of Chicago, 35 pp. #49

c Early stage of tornado development as revealed by satellite photographs. SMRP Res. Paper 50, Univ. of Chicago, 15 pp. #50

d Features and motions of radar echoes on Palm Sunday, 1965. Preprints, 12th Conference on Radar Meteorology, Norman, 319-324. (Bradbury and Fujita) #51

e A proposed explanation of deviate paths of echo couplets. Preprints, 12th Conference on Radar Meteorology, Norman, 347. (Fujita, Wilk, and Fankhauser)

f Stability and differential advection associated with tornado development. SMRP Res. Paper 52, Univ. of Chicago, 17 pp. (Fujita and Bradbury) #52

g Results of the computation of cloud heights, emissivity, and cover from long- and short-wave radiation data. Proceedings, XVII Congress of International Astronautical Federation, Madrid, 155-162.

1966 h Use of wet-beam Doppler winds in the determination of the vertical velocity of raindrops inside hurricane bands. SMRP Res. Paper 59, Univ. of Chicago, 39 pp. (Fujita, Black, and Loesch) #59

i Mesoscale motions in oceanic stratus as revealed by satellite data. Mon. Wea. Rev., 96, 304-314. (Lyons and Fujita) #66

1967 a A proposed method of estimating cloud-top temperature, cloud covers, emissivity, and cloudiness from short- and long-wave radiation data obtained by medium-resolution scanning radiometers. SMRP Res. Paper 48, Univ. of Chicago, 48 pp. (Fujita and Grandoso) #48

b Estimated wind speeds of the Palm Sunday Tornadoes. SMRP Res. Paper 53, Univ. of Chicago, 25 pp. #53

c A satellite meteorological study of evaporation and cloud formation over the Western Pacific under the influence of the winter monsoon. J. Meteor. Soc. Japan, 45, 232-250. (Tsuchiya and Fujita) #55

d A proposed mechanism of snowstorm mesojet over Japan under the influence of the winter monsoon. J. Meteor. Soc. Japan, 45, 96-110. (Fujita and Tsuchiya) #56

e A model of typhoons accompanied by inner and outer rainbands. J. Appl. Meteor., 6, 3-19. (Fujita, Izawa, Watanabe, and Imai) #60

f Mesoscale aspects of orographic influences on flow and precipitation patterns. Proceedings, Symposium on Mountain Meteorology, Colorado State University, 132-146. #67

g Estimation of tornado wind speed from characteristic ground marks. Preprints, 6th Conference on Severe Local Storms, Chicago, 38-45. (Fujita, Bradbury, and Black) #69

h Result of the computation of cloud heights, emissivity, and cover from long- and short-wave radiation data. Proceedings, General Assembly of IUGG, Lucerne, 155-162.

1968 a Split of a thunderstorm into anticyclonic and cyclonic storms and their motion as determined from numerical model experiments. J. Atmos. Sci., 25, 416-439. (Fujita and Grandoso) #62

b A mesometeorological study of a subtropical mesocyclone. SMRP Res. Paper 68, Univ. of Chicago, 28 pp. (Arakawa, Watanabe, Tsuchiya, and Fujita) #68

c Computation of height and velocity of clouds from dual, whole-sky, time-lapse picture sequences. SMRP Res. Paper 70, Univ. of Chicago, 17 pp. (Bradbury and Fujita) #70

d A study of mesoscale cloud motions computed from ATS-1 and terrestrial photographs. SMRP Res. Paper 71, Univ. of Chicago, 25 pp. (Fujita, Bradbury, Murino, and Hull) #71

e Aerial measurement of radiation temperatures over Mt. Fuji and Tokyo areas and their application of the determination of ground- and water-surface temperatures. J. Appl. Meteor., 7, 801-816. (Fujita, Baralt, and Tsuchiya) #72

f Relationship between observed winds and cloud velocities determined from pictures obtained by the ESSA III, ESSA V, and ATS-I satellites. Proceedings, 11th Plenary Meeting of COSPAR, Tokyo. (Izawa and Fujita)

g Present status of cloud velocity computations from ATS-I and ATS-III satellites. Proceedings, 11th Plenary Meeting of COSPAR, Tokyo, 557-570.

h The first color movie of the planet Earth viewed from 22,300 miles over Brazil. A 400-ft film made from the 18 November 1967 color pictures televised by ATS-III. (Suomi, Parent, and Fujita)

1969 a Formation and structure of equatorial anticyclones caused by large-scale cross-equatorial flows determined by

ATS-I photographs. J. Appl. Meteor., 8, 649-667. (Fujita, Watanabe, and Izawa) #78

1969 b Application of enhanced ATS pictures. 6th Hurricane Conference, Miami.

c Determination of mass outflow from a thunderstorm complex using ATS-III pictures. Preprints, 6th Conference on Severe Local Storms, Chicago, 38-43. (Fujita and Bradbury) #79

1970 a Aircraft, spacecraft, satellite and radar observations of hurricane Gladys, 1968. J. Appl. Meteor., 9, 837-850. (Gentry, Fujita, and Sheets) #83

b Basic problems on cloud identification related to the design of SMS-GOES spin scan radiometers. SMRP Res. Paper 84, Univ. of Chicago, 33 pp. #84

c Palm Sunday Tornadoes of April II, 1965. Mon. Wea. Rev., 98, 29-69. (Fujita, Bradbury, and Van Thullenar) #86

d The Lubbock Tornadoes: A study of suction spots. Weatherwise, 23, 160-173.

e Lubbock tornadoes of 11 May 1970. SMRP Res. Paper 88, Univ. of Chicago, 23 pp. #88

f Estimate of areal probability of tornadoes from inflationary reporting of their frequencies. SMRP Res. Paper 89, Univ. of Chicago, 23 pp. #89

g Estimate of maximum wind speeds of tornadoes in three northwestern states. SMRP Res. Paper 92, Univ. of Chicago, 27 pp. #92

h In- and outflow field of hurricane Debbie as revealed by echo and cloud velocities from airborne radar and ATS-III pictures. Preprints, 14th Radar Meteorology Conference, Tucson, 353-358. (Fujita and Black) #93

1971 a Application of ATS III photographs for determination of dust and cloud velocities over the northern tropical Atlantic. J. Meteor. Soc. Japan, 49, 813-821. #90

b Proposed characterization of tornadoes and hurricanes by area and intensity. SMRP Res. Paper 91, Univ. of Chicago, 42 pp. #91

c Preliminary results of tornado watch experiment 1971. Preprints, 7th Conference on Severe Local Storms, Kansas City, 255-261. (Fujita, Tecson, and Schaal) #99

d Proposed mechanism of suction spots accompanied by tornadoes. Preprints, 7th Conference on Severe Local Storms, Kansas City, 208-213. #102

1972 a Tornado occurrences related to overshooting cloud-top heights as determined from ATS pictures. SMRP Res. Paper 97, Univ. of Chicago, 32 pp. #97

b F-scale classification of 1971 tornadoes. SMRP Res. Paper 100, Univ. of Chicago, 16 pp. #100

c Typhoon-associated tornadoes in Japan and new evidence of suction vortices in a tornado near Tokyo. J. Meteor. Soc. Japan, 50, 431-454. (Fujita, Watanabe, Tsuchiya, and Shimada) #101

d Estimate of maximum windspeeds of tornadoes in southernmost Rockies. SMRP Res. Paper 105, Univ. of Chicago, 47 pp. #105

e Use of ATS pictures in hurricane modification. SMRP Res. Paper 106, Univ. of Chicago, 31 pp. #106

f Analisis tropical en mesoescala sobre Latino America. SMRP Res. Paper 107, Univ. of Chicago, 30 pp. #107

g A mesometeorological study of a subtropical mesocyclone. Papers in Meteorology and Geophysics, Meteor. Res. Inst., Tokyo, 23, 163-181. (Arakawa, Watanabe, Tsuchiya, and Fujita)

h Fotografias y movemiento de nubes de la Haracane Camille, Agosto 15-20, 1969. Joint UN/WMO Panel and Training Seminar on the Uses of Meteorological Satellite Data, Mexico, D.F.

1972 i Use of ATS pictures for gulf-stream research. Preprints, 4th Annual Offshore Technology Conference, Houston, I 760-764. (Fujita and Tecson)

1973 a Experimental classification of tornadoes in FPP scale. SMRP Res. Paper 98, Univ. of Chicago, 15 pp. #98

b Tornadoes around the world. Weatherwise, 26, 56-83. #108

c METRACOM system of cloud-velocity determination from geostationary satellite pictures. SMRP Res. Paper 110, Univ. of Chicago, 29 pp. (Chang, Tecson, and Fujita) #110

d Proposed mechanism of tornado formation from rotating thunderstorm. Preprints, 8th Conference on Severe Local Storms, Denver, 191-196. #111

e Results of FPP classification of 1971 and 1972 tornadoes. Preprints, 8th Conference on Severe Local Storms, Denver, 142-145. (Fujita and Pearson) #113

f General and local circulation of mantle and atmosphere toward prediction of earthquakes and tornadoes. SMRP Res. Paper 115, Univ. of Chicago, 19 pp. (Fujita and Fujita) #115

g Cloud motion field of hurricane Ginger during the seeding period as determined by the METRACOM system. 8th Technical Conference on Hurricanes and Tropical Meteorology, Key Biscayne. (Tecson, Chang, and Fujita) #116

h Thermal and dynamical features of a thunderstorm with a tilted axis of rotation. SMRP Res. Paper 118, Univ. of Chicago, 15 pp. #118

1974 a Overshooting thunderheads observed from ATS and learjet. SMRP Res. Paper 117, Univ. of Chicago, 29 pp. #117

b Jumbo tornado outbreak of 3 April 1974. Weatherwise, 27, 116-126. #120

c Superoutbreak tornadoes of April 3-4, 1974 as seen in ATS pictures. Preprints, 6th Conference on Aerospace and Aeronautical Meteorology, El Paso, 165-172. (Fujita and Forbes) #124

d A kinematic analysis of tropical storm based on ATS cloud motions. SMRP Res. Paper 125, Univ. of Chicago, 20 pp. (Fujita and Tecson) #125

1975 a Superoutbreak tornadoes of April 3-4, 1974. Final edition color map with statistics of April 3-4 tornadoes. Univ. of Chicago.

b Satellite-tracked cumulus velocities. J. Appl. Meteor., 14, 407-413. (Fujita, Pearl, and Shenk) #114

c New evidence from April 3-4, 1974 tornadoes. Preprints, 9th Conference on Severe Local Storms, Norman, 248-255. #127

d Long-term fluctuation of tornado activities. Preprints, 9th Conference on Severe Local Storms, Norman, 417-423. (Fujita, Pearson, and Ludlum) #128

e Detection of severe storms by satellites. Preprints, 3rd Symposium on Meteorological Observations and Instrumentation, Washington, D.C., 5-9. #131

f Cloud-motion vectors over the GATE area computed by McIDAS and METRACOM methods. SMRP Res. Paper 136, Univ. of Chicago, 23 pp. (Tecson and Fujita) #136

g Use of tornado path lengths and gradations of damage to assess tornado intensity probabilities. Preprints, 9th Conference on Severe Local Storms, Norman, 286-293. (Abbey and Fujita) #138

h Theory for the drift of severe local storms with application to the storm of April 21, 1961, near Topeka, Kansas. Preprints, 9th Conference on Severe Local Storms, Norman, 124-130. (Costen and Fujita)

1976 a Spearhead echo and downburst near the approach end of a John F. Kennedy Airport runway, New York City.

SMRP Res. Paper 137, [NTIS No. PB-254009], Univ. of Chicago, 51 pp. #137

1976 b Close-up view of 20 March 1976 tornadoes: Sinking cloud tops to suction vortices. Weatherwise, 29, 116-131. (Fujita, Forbes, and Umenhofer) #139

c Photogrammetric analyses of tornadoes. Proceedings, Symposium on Tornadoes, Texas Tech Univ., 43-88. #140

d Old and new concept of tornadoes. Preprints, ASCE Annual Convention and Exposition, Philadelphia, 9 pp. #141

e Graphic example of tornadoes. Bull. Amer. Meteor. Soc., 57, 401-412. #142

f History of suction vortices. Proceedings, Symposium on Tornadoes, Texas Tech Univ., 78-88.

g Recent concepts of tornado winds. Proceedings, 2nd U.S.-Japan Research Seminar on Wind Effects on Structures, Kyoto, Univ. of Tokyo Press, 3-14.

1977 a An analysis of three weather-related aircraft accidents. Bull. Amer. Meteor. Soc., 58, 1164-1181. (Fujita and Caracena) #145

b Anticyclonic tornadoes. Weatherwise, 30, 51-64. #146

c Spearhead echo and downburst in the crash of an airliner. Mon. Wea. Rev., 105, 129-146. (Fujita and Byers) #147

d Mesoanalysis of record Chicago rainstorm using radar, satellite, and raingauge data. Preprints, 10th Conference on Severe Local Storms, Omaha, 65-72. (Fujita, Hjelmfelt, and Changnon) #148

e Great Bend tornadoes of August 30, 1974. Preprints, 10th Conference on Severe Local Storms, Omaha, 457-462. (Umenhofer, Fujita, and Dundas) #149

f Thunderstorm-associated cloud motions as computed from 5-minute SMS pictures. Preprints, 10th Conference on Severe Local Storms, Omaha, 22-29. (Tecson, Umenhofer, and Fujita) #151

g Common denominator of three weather-related aircraft accidents. Preprints, 10th Conference on Severe Local Storms, Omaha, 135-142. (Fujita and Caracena) #152

h Regionalization of the tornado hazard. Preprints, 10th Conference on Severe Local Storms, Omaha, 526-531. (Abbey and Fujita)

i Mesoscale wake clouds in Skylab photographs. Skylab Explores the Earth, NASA SP-380, 463-477. (Fujita and Tecson) #158

1978 a A site-specific study of wind and tornado probabilities at the WIPP site in southeast New Mexico. SMRP Res. Paper 155, Univ. of Chicago, 43 pp. #155

b Manual of downburst identification for Project NIMROD. SMRP Res. Paper 156, [NTIS No. PB-286048], Univ. of Chicago, 104 pp. #156

c Wind shear at Dulles Airport on 18 May 1977. SMRP Res. Paper 159, Univ. of Chicago, 19 pp. #159

d Tornado damage at the Grand Gulf, Mississippi nuclear power plant site: Aerial survey. NUREG/CR-0383, 1-18. #162

e An omni-directional, tilt insensitive, wind speed threshold detector. Preprints, 4th Symposium on Meteorological Observations and Instrumentation, Denver, 83-86. (Bedard and Fujita) #163

f Workbook of tornadoes and high winds for engineering applications. SMRP Res. Paper 165, Univ. of Chicago, 142 pp. #165

1979 a Preliminary report of the Bossier City tornado of December 3, 1978. SMRP Res. Paper 169, Univ. of Chicago, 33 pp. #169

b Wind loading and missile generation in tornado. Preprints, International Conference on Environmental Forces on Engineering Structures, Imperial College, London, 14 pp. #170

1979 c Objectives, operation, and results of Project NIMROD. Preprints, 11th Conference on Severe Local Storms, Kansas City, 259-266. #171

d Vertical cross section through a rotating thunderstorm by Doppler radar. Preprints, 11th Conference on Severe Local Storms, Kansas City, 447-452. (Wilson and Fujita) #173

e Statistics of U.S. tornadoes based on the DAPPLE (Damage Area Per Path LEngth) tornado tape. Preprints, 11th Conference on Severe Local Storms, Kansas City, 227-234. (Tecson, Fujita, and Abbey) #174

f The effect of side lobes upon measured Doppler velocities in weak echo regions. Preprints, 11th Conference on Severe Local Storms, Kansas City, 509-514. (Stiegler, Fujita, and Wakimoto) #175

g The DAPPLE method for computing tornado hazard probabilities: Refinements and theoretical considerations. Preprints, 11th Conference on Severe Local Storms, Kansas City, 241-248. (Abbey and Fujita) #177

h A site-specific evaluation of tornado and high-wind risks at West Valley site, New York. SMRP Res. Paper 178, Univ. of Chicago, 21 pp. (Fujita, Tecson, and Levine) #178

1980 a Downbursts and microbursts — An aviation hazard. Preprints, 19th Conference on Radar Meteorology, Miami, 94-101. #179

b Mesoscale damage patterns of hurricane Frederic in relation to enhanced SMS imagery. Preprints, 19th Conference on Radar Meteorology, Miami, 48-55. (Fujita, Wakimoto, and Stiegler) #180

c Miso-scale structure of downbursts depicted by Doppler radar. (Supplement to downbursts and microbursts — an aviation hazard). SMRP Res. Paper 181, Univ. of Chicago, 19 pp. #181

d Diabatic analysis: A new method for predicting tornado outbreaks. SMRP Res. Paper 183, Univ. of Chicago, 15 pp. [NASA Science Review] #183

e Severe weather events of 10 April 1979. Bull. Amer. Meteor. Soc., 61, 1033-1034. (Alberty, Burgess, and Fujita)

f In search of mesoscale wind fields in landfalling hurricanes. Preprints, 13th Technical Conference on Hurricanes and Tropical Meteorology, Miami Beach, 43-57. #189

1981 a Five scales of airflow associated with a series of downbursts on 16 July 1980. Mon. Wea. Rev., 109, 1438-1456. (Fujita and Wakimoto) #184

b Tornado wind effects on the Grand Gulf cooling tower. Proceedings, 2nd Conference on Dynamic Response of Structures, Amer. Soc. Civil Engr., Atlanta, 555-566. #187

c Microbursts as an aviation wind shear hazard. Preprints, 19th Aerospace Sciences Meeting, St. Louis, AIAA-81-0386, 9 pp. #188

d Tornadoes and downbursts in the context of generalized planetary scales. J. Atmos. Sci., 38, 1511-1534. #190

e Mesoscale aspects of convective storms. Proceedings, IAMAP Symposium, Hamburg, 3-10. #191

f The tornado outbreak of 3-4 April 1974. The Thunderstorm in Human Affairs, NOAA/ERL, 47-84. (Abbey and Fujita)

1982 a Principle of stereoscopic height computations and their applications to stratospheric cirrus over severe thunderstorms. J. Meteor. Soc. Japan, 60, 355-368. #192

b Climatological mapping of U.S. tornadoes during 1916-1980. Preprints, 12th Conference on Severe Local Storms, San Antonio, 38-41. (Tecson, Fujita, and Abbey)

1982 c Meteorological and engineering analyses of the Bossier City, Louisiana, tornado of 3 December 1978. Preprints, 12th Conference on Severe Local Storms, San Antonio, 135-138. (Abbey, Fujita, and McDonald)

d Infrared, stereo-height, cloud-motion, and radar-echo analysis of SESAME-day thunderstorms. Preprints, 12th Conference on Severe Local Storms, San Antonio, 213-216. #193B

e A detailed analysis of the San Marcos, Texas tornado induced by hurricane "Allen" on 10 August 1980. Preprints, 12th Conference on Severe Local Storms, San Antonio, 371-374. (Stiegler and Fujita) #193C

f Anticyclonic tornadoes in 1980 and 1981. Preprints, 12th Conference on Severe Local Storms, San Antonio, 401-404. (Fujita and Wakimoto) #193D

g Effects of miso- and mesoscale obstructions on PAM winds obtained during the Project NIMROD. J. Appl. Meteor., 21, 840-858. (Fujita and Wakimoto) #195

1983 a Applications of stereoscopic height computations from dual geosynchronous satellite data/Joint NASA-Japan stereo project. Adv. Space Res., 2, 153-160. (Fujita and Dodge) #198

b Microburst wind shear at New Orleans International Airport, Kenner, Louisiana on July 9, 1982. SMRP Res. Paper 199, Univ. of Chicago, 39 pp. #199

c Microburst in JAWS depicted by Doppler radars, PAM, and aerial photographs. Preprints, 21st Conference on Radar Meteorology, Edmonton, 638-645. (Fujita and Wakimoto) #200

d JAWS microbursts revealed by triple-Doppler radar, aircraft, and PAM data. Preprints, 13th Conference on Severe Local Storms, Tulsa, 97-100. (Fujita and Wakimoto) #201

e Statistical analyses of U.S. tornadoes based on the geographic distribution of population, community, and other parameters. Preprints, 13th Conference on Severe Local Storms, Tulsa, 120-123. (Tecson, Fujita, and Abbey) #202

f Analysis of storm-cell hazards to aviation as related to terminal Doppler radar siting and update rate. SMRP Res. Paper 204, Univ. of Chicago, 90 pp. #204

g Andrews AFB microburst. SMRP Res. Paper 205, Univ. of Chicago, 38 pp. #205

1984 a Review of the history of mesoscale meteorology and forecasting, Chapter 1. SMRP Res. Paper 208, Univ. of Chicago, 42 pp. #208

b Mesoscale structure of Hurricane Alicia. Proceedings, Specialty Conference, Hurricane Alicia: One Year Later. Amer. Soc. Civil Engr., Galveston, 21-39. (Stiegler and Fujita) #209

1985 a The Downburst: Microburst and macroburst. SMRP Res. Paper 210, Hardbound color book. [NTIS No. PB 85-148880], [Library of Congress Catalogue No. 85-50115], Univ. of Chicago, 122 pp. #210

b Detailed analysis of the tornado outbreak in the Carolinas by using radar, satellite, and aerial survey data. Preprints, 14th Conference on Severe Local Storms, Indianapolis, 271-274. (Fujita and Stiegler) #211

c Automated mapping of maximum tornado windspeeds in the United States as a function of occurrence probabilities. Preprints, 14th Conference on Severe Local Storms, Indianapolis, 21-24. (Tecson and Fujita) #212

d Low-altitude wind shear characteristics in the Memphis, TN area based on Mesonet and LLWAS data. Preprints, 14th Conference on Severe Local Storms, Indianapolis, 322-327. (Wolfson, DiStefano, and Fujita) #216

1986 a DFW microburst on August 2, 1985. SMRP Res. Paper 217, Hardbound color book. [NTIS No. PB 86-131638], [Library of Congress Catalogue Card No. 85-52386], Univ. of Chicago, 154 pp. #217

b Mesoscale classifications: Their history and their application to forecasting. Mesoscale Meteorology and Forecasting, Amer. Meteor. Soc., 18-35.

1987 a U.S. Tornadoes, Part One, 70-year statistics. SMRP Res. Paper 218, Hardbound color book. [NTIS No. PB 87-127742], [Library of Congress Catalogue Card No. 86-51637], Univ. of Chicago, 122 pp. #218

b Correcting wind speed measurements for site obstructions. Preprints, 6th Symposium on Meteorological Observations and Instrumentation, New Orleans, 358-363. (Wolfson and Fujita)

1988 a Monrovia microburst of 20 July 1986: A study of "SST." Preprints, 15th Conference on Severe Local Storms, Baltimore, 380-383. (Fujita and Black) #219

b A method of correcting PAM winds based on obstructions and measured windspeed. Preprints, 15th Conference on Severe Local Storms, Baltimore, 339-342. (Smith, Fujita, and Partacz) #220

c In-depth evaluation of Doppler and anemometer data for detecting wet microbursts at Huntsville airport. WRL Res. Paper 222, Univ. of Chicago, 68 pp. #222

d Northern hemisphere cyclones, Jun 81-May 82. WRL Res. Paper 223, Univ. of Chicago, 92 pp. #223

e Northern hemisphere cyclones, Jun 82-May 83. WRL Res. Paper 224, Univ. of Chicago, 92 pp. #224

f Northern hemisphere cyclones, Jun 83-May 84. WRL Res. Paper 225, Univ. of Chicago, 92 pp. #225

1989 a The Teton-Yellowstone tornado of 21 July 1987. Mon. Wea. Rev., 117, 1913-1940. #226

b Northern hemisphere cyclones, Jun 84-May 85. WRL Res. Paper 228, Univ. of Chicago, 92 pp. #228

c Correcting wind speed measurements for site obstructions. J. Atmos. Ocean Technol., 6, 343-352. (Wolfson and Fujita)

1990 a The application of weather radar to aviation meteorology. Radar in Meteorology: Battan Memorial and 40th Anniversary Radar Meteorology Conference, Boston, Amer. Meteor. Soc., 657-681. (Fujita and McCarthy)

b Downbursts: Meteorological features and wind field characterisitcs. J. Wind Eng. Ind. Aerodyn., 36, 75-86. #227

c Northern hemisphere cyclones, Jun 85-May 86. WRL Res. Paper 229, Univ. of Chicago, 92 pp. #229

1991 a Cloud height and motion experiment: CHAMEX. WRL Res. Paper 230, Univ. of Chicago, 39 pp. #230

b Northern hemisphere storms—Cyclones, typhoons, and tornadoes: Final Report ONR N00014-86-K-0374. WRL Res. Paper 231, Univ. of Chicago, 152 pp. #231

c Northern hemisphere cyclones, Jun 86-May 87. WRL Res. Paper 232, Univ. of Chicago, 92 pp. #232

d Interpretation of cloud winds. Proceedings, Wind Extraction Workshop, EUMETSAT, NOAA and WMO, Washington, D.C., 99-104. #233

e Plainfield tornado of 28 August 1990. WRL Res. Paper 234, Univ. of Chicago, 16 pp. #234

f Aerial survey and photography of tornado and microburst damage. Tornado Symposium III, Norman. (Fujita and Smith) #235

g Streamwood microburst of 29 June 1990. WRL Res. Paper 236, Univ. of Chicago, 29 pp. #236

1992 An overview of mesoscale prediction. Preprints, Symposium on Weather Forecasting and 5th Conference on Mesoscale Processes, Atlanta, J49-58.

Silent Friends in our Backyard (Praying Mantes)

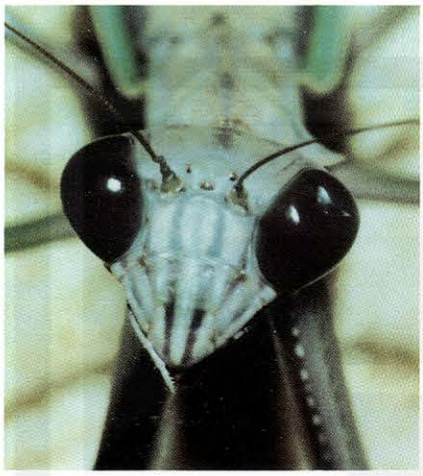

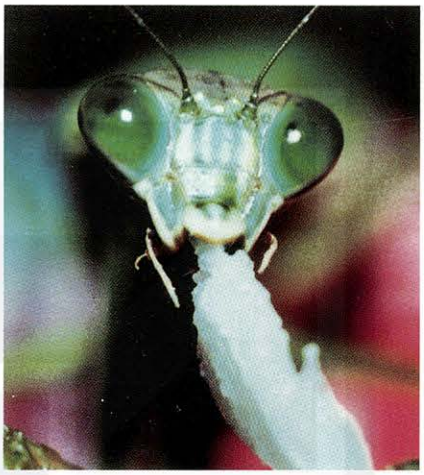

Look at me! I change the color of my eyes three times a day.

I am scared, do not come close.

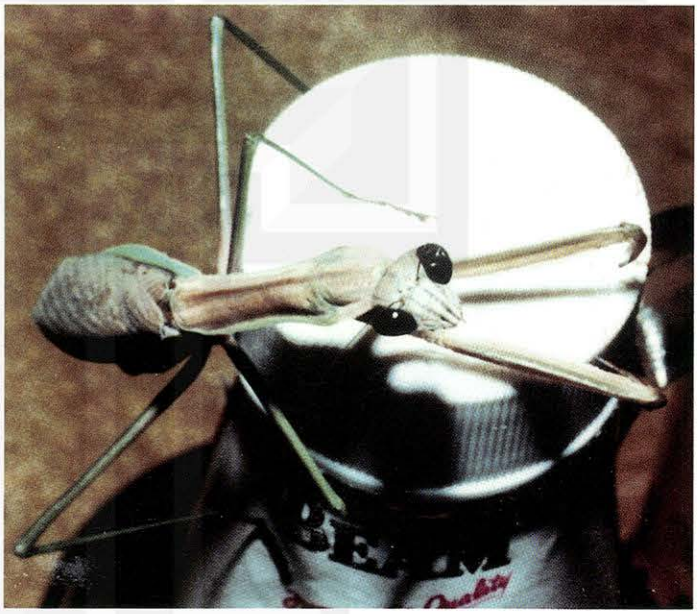

No more JIM BEAM, my lord.

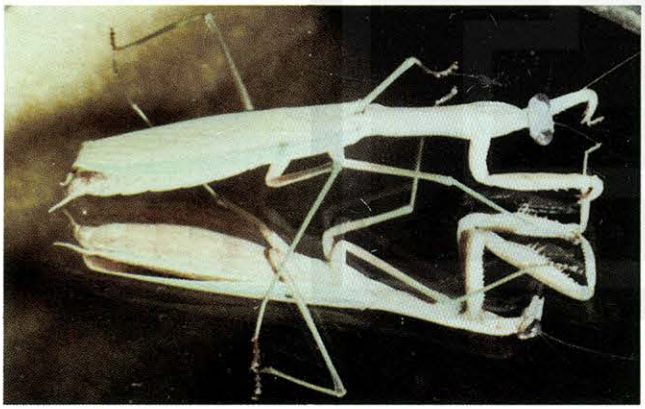

I am playing with my mirror image.

I wish I were your human friend.